

Target-Guided synthesis of metalloenzyme ligands with therapeutic potential

Dissertation

Zur Erlangung des akademischen Grades
des Doktors der Naturwissenschaften
der Naturwissenschaftlich-Technischen Fakultät
der Universität des Saarlandes

vorgelegt von

M.Sc. Virgyl Camberlein

Saarbrücken, Januar 2022

Tag des Kolloquiums: 10.Jan.2022

Committee Chair:

Prof. Dr. Nicolas LEBEGUE, Lille University

Rapporteurs:

Prof. Dr. Myriam SEEMANN, Strasbourg Institute of Chemistry

Prof. Dr. Christian DUCHO, Saarland University

Examiner:

Dr. Matthias ENGEL, Saarland University

Thesis advisors:

Prof. Dr. DEPREZ-POULAIN Rebecca, Lille University

Prof. Dr. HIRSCH Anna, Saarland University

Die vorliegende Arbeit wurde von Oktober 2018 bis Dezember 2021 unter Anleitung von Frau Prof. Dr. Anna KH. Hirsch in der Universität des Saarlandes sowie am Helmholtz Institut für Pharmazeutische Forschung Saarland (HIPS) in der Abteilung Drug Design and Optimization (DDOP) angefertigt, und Frau Prof. Dr. Rebecca Deprez-Poulain in der Lille Universität sowie am Pharmazeutische Fakultät in der Abteilung INSERM U1177.

Acknowledgements

Je remercie tout d'abord l'Université de Lille, l'Université de la Sarre, ainsi que l'école doctorale biologie santé et l'Helmholtz Center for Infection Research de m'avoir permis d'effectuer ce travail.

Monsieur Nicolas Lebègue,

Je suis très honoré de l'intérêt que vous portez à mes travaux, de ceux de Master à ceux de thèse. Merci d'avoir accepté de présider ce jury de thèse.

Madame Myriam Seemann, Messieurs Christian Ducho et Matthias Engel,

Je vous suis très reconnaissant d'avoir accepté de faire partie de ce jury et de juger de mes travaux.

Mesdames Rebecca Déprez-Poulain et Anna Hirsch,

Sachez que je suis profondément reconnaissant pour l'ensemble de notre parcours commun et votre participation à ce jury.

Je tiens également à exprimer mes sincères remerciements à tous ceux qui ont contribué à la réussite de ce projet.

Je tiens tout d'abord à remercier le Professeur Benoit Déprez, directeur de l'unité U1177. Merci de m'avoir accueilli dans votre laboratoire, de m'avoir suivi, guidé et fait grandir depuis ma 3^{ème} année de pharmacie jusqu'à cette thèse. Merci pour vos enseignements incroyables et passionnants, merci de m'avoir épaulé durant les nombreuses répétitions pour le concours de l'EDBSL, merci pour vos remarques et conseils durant toutes ces années.

A mes deux directrices de thèse, Anna et Rebecca, merci indéfiniment pour vos connaissances, vos disponibilités, vos connaissances, et votre soutien durant ces années. Rebecca, merci de m'avoir donné l'opportunité d'avoir pu évoluer tant scientifiquement qu'humainement au sein du laboratoire à Lille, de m'avoir suivi de la 3^{ème} année jusqu'à aujourd'hui et de m'avoir transmis ta passion pour la chimie médicinale et cette envie de continuer en thèse. Sans toi, je n'aurais pas suivi cette voie et tout ça n'aurait pas été possible. Anna, je te suis profondément reconnaissant de m'avoir donné l'opportunité de découvrir un autre pays, un autre environnement de travail ainsi que pour ta gentillesse, ta patience, ton empathie et ton aide précieuse. Je vous remercie profondément de m'avoir accompagné durant ces années et notamment lors de la rédaction.

Un énorme merci au Dr Damien Bosc pour ton encadrement sans faille durant ces trois années. J'ai pris plaisir à travailler avec toi-même si ce fût difficile durant la méthodo. Je tiens également à te dire quand sans toi, ce travail n'aurait pas été possible. Tu as su être disponible et trouver la solution à chacun de mes problèmes rencontrés. Tu as été un parfait conseillé et tu as une part importante dans la réussite de ce projet. Je te serai indéfiniment reconnaissant pour tout ce que tu m'as apporté.

Merci au Drs Ronan Gealageas et Jelena Konstantinovic. Ronan, ça fait bizarre de t'appeler « Docteur », tout a commencé avec toi lors de mon premier stage. Je tenais également à souligner que tu as grandement participé quant à ma décision de poursuivre vers la chimie médicinale. Tu fus mon premier encadrant et tu as su me transmettre ta passion et ta motivation. Merci pour ton aide précieuse durant ces 7 années, les KTGS, les analyses RMN, les idées de chimie, tes conseils à la paillasse, tes méthodes de travail... Je n'oublie pas nos interminables débats footballistiques, nos paris ainsi que les séances du mardi midi ; Paris n'a toujours pas gagné de ligue des champions... Ce fût un réel plaisir d'avoir pu partager tous ces moments avec toi. Jelena, merci pour ton accueil lorsque je suis arrivé à Saarbrücken ainsi que pour ta disponibilité, ta patience, tes remarques et tes corrections durant la rédaction de cette thèse.

Merci à l'ADME team de Lille, Alex et Catherine. Vous avez grandement participé à ce projet grâce à votre incroyable travail. Sans vous, je pense que je serais mort devant les analyses ! Merci pour ces moments de partage scientifique et humain, sans oublier les dégustations de cookies, chocolat...

Aux teams ERAP et LasB pour les tests effectués sur les composés synthétisés ainsi que pour les différentes discussions. Merci au Dr Jörg Haupenthal d'avoir assuré toute la partie bio du projet LasB et de m'avoir accueilli au sein de la team LasB. Merci au Dr Andreas Kany pour ton travail remarquable concernant la partie ADME sur le projet LasB.

Au Dr Emmanuelle Lipka, merci pour ces moments de partage, de m'avoir fait découvrir la SFC, de m'avoir transmis tes connaissances sur cette technique et ainsi d'avoir participé au travail de méthodologie.

Au Dr Fanny Roussy et Pr Eric Deniau pour votre participation à mes comités de suivi de thèse et vos conseils.

Au professeur Nathalie Azaroual et son équipe pour les analyses RMN à Lille.

A l'équipe enseignante du Master Conception, Synthèse, Evaluation et Sélection des principes actifs à Lille, merci pour vos enseignements de qualité qui ont permis de renforcer mes connaissances dans le domaine des sciences du médicament.

Aux secrétaires des deux laboratoires, Nathalie, Annette et Bahareh. Merci pour votre aide précieuse et d'avoir assuré tout le côté administratif de cette thèse. Je tiens également à remercier Mr François Delcroix, coordinateur de l'EDBSL pour son aide précieuse et sa réactivité.

Aux post-docs, camarades thésards et autres rencontrés durant cette thèse Mélissa, Aurore, Léo, Charlotte, Chris, Andreas K, Ahmed, Mostafa, Gwen, Alex, Samira, Selina, Marine, Laetitia, Kevin, Atanaz... La liste est longue. Merci à Tony et Andreas Klein pour votre aide sur la crystallo ! Merci à Eleonora, Ioulia, Tony, Daan pour tous ces moments de partage. Un énorme merci à Lucile ! Enfin merci à Federica, Cansu et Alaa de m'avoir accueilli à Saabrücken. Merci également à mes anciens collocs Thomas, Toufik et mes anciens camarades de pharma notamment Sabrina pour ton soutien incroyable durant ces années.

Enfin, merci à ma famille et en particulier mes frères Allan et Matthias et à mes parents de pour votre soutien, votre écoute et vos sacrifices pour je puisse suivre ces études.

Publications and communications

Publications

Bosc Damien, Camberlein Virgyl, Gealageas Ronan, Castillo-Aguilera Omar, Deprez Benoit, Deprez-Poulain Rebecca.

Kinetic Target-Guided Synthesis: reaching the age of maturity. *J. Med. Chem.* **2020**, 63, 8, 3817–3833.

Laura Medve, Ronan Gealageas, Bao Vy Lam, Valentin Guillaume, Omar Castillo-Aguilera, Virgyl Camberlein, Melissa Rossel, Charlotte Fléau, Sandrine Waremghem, Julie Charton, Julie Dumont-Ryckembusch, Damien Bosc, Florence Leroux, van Endert Peter, Benoit P Deprez.

Modulators of hERAP2 discovered by High-Throughput Screening. *Eur J. Med. Chem.*, **2021**, Vol.211, p.113053.

Camberlein Virgyl, Kraupner Nicolas, Bou Karroum Nour, Lipka Emmanuelle, Deprez-Poulain Rebecca, Deprez Benoit, Bosc Damien.

Multi-component reaction for the preparation of 1,5-disubstituted 1,2,3-triazoles by in-situ generation of azides and nickel-catalyzed azide-alkyne cycloaddition. *Tetrahedron letters*, **2021**, Vol.73, p.153131.

Poster communication

V. Camberlein, D. Bosc, R. Gealageas, B. Deprez, R. Deprez-Poulain.

1,2,3-triazoles ring : a scaffold of high interest for medicinal chemistry. Drug Discovery Day, **Lille**, France, January 18th, 2019.

V. Camberlein, D. Bosc, E. Lipka, R. Gealageas, B. Deprez, R. Deprez-Poulain.

New Methodology to Access 1,5-Disubstituted 1,2,3-triazole. 2nd Molecules Medicinal Chemistry Symposium: Facing Novel Challenges in Drug Discovery, **Barcelona**, 15-17th May, 2019.

V. Camberlein, C. Tabey-Fleau, R. Gealageas, S. Waremghem, V. Guillaume, D. Bosc, B. Deprez, R. Deprez-Poulain. **Discovery of hERAP2 inhibitors by in situ click chemistry and hit-optimization.** 27th SCT Young Research Fellows Meeting, **Caen**, 29-31th January, 2020.

Oral communication

V. Camberlein, R. Gealageas, C. Tabey-Fleau, S. Warengem, V. Guillaume, D. Bosc, B. Deprez, R. Deprez-Poulain. **Discovery of hERAP2 inhibitors by in situ click chemistry and hit optimization.** Drug Discovery Day, **Lille**, France, December 17th, 2019.

Summary

Target-guided synthesis of protein ligands is an innovative strategy to discover bioactive compounds. In particular, the Kinetic Target-Guided Synthesis (KTGS) and the Dynamic Combinatorial Chemistry (DCC) have allowed, in recent years, the discovery of novel ligands for poorly explored therapeutic targets, which has enabled drug-discovery projects. This thesis project aims at using KTGS to discover and optimize ligands for two classes of metalloenzymes, namely endoplasmic reticulum aminopeptidases (ERAPs) and elastase LasB from the bacterium *Pseudomonas aeruginosa*.

ERAPs (1 and 2) are involved in the process of antigen maturation. These enzymes cleave peptide precursors into mature antigenic peptides so that they have an optimal size for their complexation to the major histocompatibility complex of class I and thus initiate or not the adaptive immune response. The expression levels of these proteases as well as single nucleotide polymorphisms have been associated with the development of cancers and autoimmune diseases. Thus, the modulation of these enzymes would allow to fight against pathologies associated with the immune system.

P. aeruginosa is a Gram-negative bacterium with remarkable virulence and antimicrobial resistance. Today, antibiotic resistance represents a major public health issue and there is an urgent need for new therapeutics. In order to meet this need, new strategies have emerged such as targeting the virulence of bacteria to "disarm" them. LasB represents a therapeutic target of choice due to its extracellular localization and its physiopathological implications (colonization, invasion, evasion of immune response, biofilm formation, etc.).

Although there is a clear unmet medical need in these two therapeutic areas, no modulator of ERAPs or LasB has reached the market.

Thus, the use of the KTGS strategy followed by optimization phases allowed us to identify and optimize new families of ligands for these enzymes. These compounds can be considered as promising lead compounds since they present nanomolar affinities for their respective targets, selectivity and toxicity profiles as well as remarkable physicochemical properties.

Keywords: metalloenzymes, ligand, ERAP, immune system, LasB, antimicrobial resistance, inhibitor, selectivity.

Résumé

La synthèse guidée par la cible de ligands protéiques est une stratégie innovante pour découvrir des composés bioactifs. En particulier, la Kinetic Target-Guided Synthesis (KTGS) and the Dynamic Combinatorial Chemistry (DCC) ont permis, ces dernières années, de découvrir des ligands originaux pour des cibles thérapeutiques mal explorées, ce qui a permis de lancer des projets de découverte de médicaments. Ce projet de thèse vise à utiliser la KTGS pour découvrir, puis optimiser des ligands de deux classes de métalloenzymes que sont les aminopeptidases du réticulum endoplasmiques (ERAP) et l'élastase LasB de la bactérie *Pseudomonas aeruginosa*.

Les ERAPs (1 et 2) participent au processus de maturation des antigènes. Ces enzymes clivent les précurseurs peptidiques en peptides antigéniques matures afin que ceux-ci disposent d'une taille optimale pour leur complexation au complexe majeur d'histocompatibilité de classe I et ainsi initient ou non la réponse immunitaire adaptative. Les niveaux d'expression de ces protéases ainsi que des polymorphismes d'un seul nucléotide ont été associé au développement de cancers et de maladies auto-immunes. Ainsi, la modulation de ces enzymes permettrait de lutter contre les pathologies associées au système immunitaire.

P. aeruginosa est une bactérie Gram négative dotée d'une virulence et d'une résistance aux antimicrobiens remarquable. Aujourd'hui, la résistance aux antibiotiques représente un enjeu de santé publique majeur et il y a un besoin urgent en nouvelles thérapeutiques. Afin de satisfaire ce besoin, de nouvelles stratégies sont apparues comme celle consistant à cibler la virulence des bactéries afin de « désarmer » celles-ci. LasB représente une cible thérapeutique de choix de par sa localisation extracellulaire et ses implications physiopathologiques (colonisation, invasion, évasion à la réponse immunitaire, formation de biofilm, etc.).

Bien qu'il y ait un besoin médical évident non satisfait dans ces deux aires thérapeutiques, aucun modulateur des ERAPs ni de LasB n'a atteint le marché.

Ainsi, l'utilisation de la stratégie KTGS suivie de phases d'optimisation nous ont permis d'identifier et optimiser de nouvelles familles de ligands de ces enzymes. Ces composés peuvent être considérés comme des leads prometteurs puisqu'ils présentent des affinités nanomolaires pour leurs cibles respectives, des profils de sélectivité et de toxicité ainsi que des propriétés physicochimiques remarquables.

Mots-clés : KTGS, ligand, métalloenzymes, ERAP, système immunitaire, LasB, résistance antimicrobienne, inhibiteur, sélectivité.

Zusammenfassung

Die Target-Guided Synthese von Proteinliganden ist eine innovative Strategie zur Entdeckung bioaktiver Verbindungen. Insbesondere die kinetische Target-Guided Synthese (KTGS) und die dynamische kombinatorische Chemie (DCC) haben in den letzten Jahren die Entdeckung neuartiger Liganden für schlecht erforschte therapeutische Ziele ermöglicht, was Projekte zur Entdeckung von Arzneimitteln ermöglicht hat. Im Rahmen dieses Forschungsprojekts sollen mithilfe der KTGS Liganden für zwei Klassen von Metalloenzymen entdeckt und optimiert werden, nämlich die Aminopeptidasen des endoplasmatischen Retikulums (ERAPs) und die Elastase LasB aus dem Bakterium *Pseudomonas aeruginosa*.

Die ERAPs (1 und 2) sind am Prozess der Antigenreifung beteiligt. Diese Enzyme spalten Peptidvorläufer in reife antigene Peptide, so dass diese eine optimale Größe für ihre Komplexbildung mit dem Haupt histokompatibilitätskomplex der Klasse I haben und somit die adaptive Immunantwort einführen oder nicht. Die Expressionsniveaus dieser Proteasen sowie Einzelnukleotid-Polymorphismen wurden mit der Entwicklung von Krebs und Autoimmunkrankheiten in Verbindung gebracht. Die Modulation dieser Enzyme würde es also ermöglichen, Pathologien zu bekämpfen, die mit dem Immunsystem zusammenhängen.

P. aeruginosa ist ein Gramnegatives Bakterium mit bemerkenswerter Virulenz und antimikrobieller Resistenz. Die Antibiotikaresistenz stellt heute ein großes Problem für die öffentliche Gesundheit dar, und es besteht ein dringender Bedarf an neuen Therapeutika. Um diesem Bedarf gerecht zu werden, wurden neue Strategien entwickelt, die auf die Virulenz der Bakterien abzielen, um sie zu "entwaffnen". LasB ist aufgrund seiner extrazellulären Lokalisierung und seiner physiopathologischen Auswirkungen (Kolonisierung, Invasion, Umgehung der Immunantwort, Biofilmbildung usw.) ein therapeutisches Ziel der Wahl.

Obwohl in diesen beiden therapeutischen Bereichen eindeutig ein ungedeckter medizinischer Bedarf besteht, ist bisher kein Modulator von ERAPs oder LasB auf dem Markt.

Durch die Anwendung der KTGS-Strategie, gefolgt von Optimierungsphasen, konnten wir neue Familien von Liganden für diese Enzyme identifizieren und optimieren. Diese Verbindungen können als vielversprechende Leitverbindungen betrachtet werden, da sie.

Schlüsselwörter: KTGS, ligand, metalloenzymen, ERAP, Immunsystem, LasB, antimikrobieller Resistenz, Hemmstoff, selektivität.

Abbreviations

AA: Amino acid

ACC: Adrenocortical carcinoma

ACE: Angiotensin-converting enzyme

AChE: Acetylcholinesterase

AML: Acute myeloid leukemia

AMR: Antimicrobial resistance

APC: Antigen-presenting cell

APN: Aminopeptidase N

AST: Antimicrobial susceptibility testing

bRo5: Beyond rule-of-five

CF: Cystic fibrosis

COX-1: Cyclooxygenase 1

DCC: Dynamic Combinatorial Chemistry

DTPA: diethylenetriaminepentaacetic acid

EAOC: Elimination azide-olefin cycloaddition

ECDC: European Centre for Disease Prevention and Control

ECM: Extracellular matrix

ERAP: Endoplasmic reticulum aminopeptidase

EU: Europe

FRET: Fluorescence Resonance Energy Transfer

HBA: Hydrogen bond acceptor

HBD: Hydrogen bond donor

hCAII: human carbonic anhydrase

HLA: Human leucocyte antigen

HNE: Human neutrophil elastase

HRMS: High Resolution Mass Spectrometry

IDE: Insulin-degrading enzyme

IC₅₀: half maximal inhibitory concentration

IFN- γ : Interferon- γ

Ig: Immunoglobulin

IL: Interleukine

IRAP: Insulin-regulated aminopeptidase

KIRC: Kidney renal clear cell carcinoma

KTGS: Kinetic Target-Guided Synthesis

L-AMC: L-leucine-7-amino-4-Methylcoumarin
LE: Ligand Efficiency
LC: Liquid Chromatography
LLE: Ligand Lipophilicity Efficiency
LUSC: Lung squamous cell carcinoma
MBL: Metallobetalactamase
MHC: Major Histocompatibility Complex
MMP: Matrix metalloprotease
MRM: Multiple Reaction Monitoring
MS: Mass spectrometry
MW: Molecular Weight
NEP: Neprilysin
NiAAC: Nickel-catalyzed azide alkyne cycloaddition
NK: Natural Killer
NdK: Nucleoside-diphosphate kinase
NMR: Nuclear Magnetic Resonance
PAAD: Pancreatic adenocarcinoma
PAMP: Pathogen-associated molecular pattern
PRR: Pattern Recognition Receptors
PDB: Protein Data Bank
PSA: Polar Surface Area
QS: Quorum Sensing
R-AMC: L-arginine-7-amino-4-methylcoumarin
Ro3: Rule-of-three
Ro5: Rule-of-five
RuAAC: Ruthenium-catalyzed azide alkyne cycloaddition
SAR: Structure-Activity Relationship
SFC: Supercritical Fluid Chromatography
SNP: Single-nucleotide polymorphism
STAD: Stomach adenocarcinoma
TACE: Tumor necrosis factor-alpha-converting enzyme
TGCT: Testicular germ cell carcinoma
UPLC: Ultra Performance Liquid Chromatography
US: United States
UVM: Uveal melanoma
ZBG: Zinc Binding Group

Table of Contents

GENERAL INTRODUCTION	- 1 -
CHAPTER 1: PROTEIN-TEMPLATED STRATEGIES: THE KTGS	- 3 -
I. INTRODUCTION	- 3 -
1. Principle	- 3 -
History and Recent Achievements	- 4 -
2.....	- 4 -
II. DESIGN & PRACTICAL ASPECTS	- 4 -
1. Chemical reactions used.....	- 4 -
2. Warhead-bearing reagent.....	- 5 -
3. Formats, Sizes, Hit Rates and Detection Methods.....	- 7 -
III. RELEVANCE OF KTGS FOR MEDICINAL CHEMISTRY AND DRUG DISCOVERY	- 8 -
1. Therapeutic Areas and Protein Targets.....	- 8 -
2. Protein Pockets and Conformation	- 9 -
3. Chemical Space and Ligand Efficiency of KTGS Ligands.....	- 9 -
IV. CASE STUDIES	- 11 -
1. <i>Mycobacterium tuberculosis</i> transcriptional repressor <i>EthR</i>	- 11 -
2. <i>Insulin Degrading Enzyme (IDE)</i>	- 12 -
<i>Endothiapepsin</i>	- 13 -
3.....	- 13 -
V. CONCLUSION	- 14 -
CHAPTER 2: KTGS LEADS TO THE IDENTIFICATION OF THE FIRST POTENT AND SELECTIVE ERAP2 INHIBITORS	- 16 -
INTRODUCTION.....	- 16 -
I. Overview of the immune system.....	- 16 -
1. Immune system and defense mechanisms	- 16 -
2. Immune system and antigen presentation.....	- 17 -
II. The ERAPs as pharmaceutical targets implicated in the antigen processing.....	- 20 -
1. Classification, structure and organization	- 20 -
2. Catalytic mechanism, substrate recognition and mechanism	- 22 -
3. Physiopathological implications.....	- 24 -
4. ERAPs modulation in therapy	- 26 -
III. ERAPs modulators.....	- 28 -
1. Aminobenzamide	- 28 -
2. Phosphinic pseudopeptides.....	- 30 -
IV. Objectives and strategy	- 33 -
RESULTS.....	- 34 -
I. Design and results of KTGS experiment to identify ERAP2 inhibitors.....	- 34 -
1. Design and synthesis of the starting building blocks	- 34 -
2. Protein-templated reaction and controls	- 34 -
3. Hits selection	- 35 -
4. Biochemical evaluation of selected hits	- 35 -
5. Conclusions	- 37 -
II. Preliminary Structure – Activity Relationships	- 38 -
1. 1,5-Disubstituted 1,2,3-Triazoles	- 38 -
2. Sulfonamide “linker”	- 39 -
3. Homologation n-1: switch to α -amino acid series	- 41 -
III. Extended Structure – Activity Relationships.....	- 44 -
1. Family 1: 1,4-disubstituted 1,2,3-triazoles in α -configuration	- 44 -
2. Family 2: 1,5-disubstituted 1,2,3-triazoles in β -configuration	- 50 -
IV. Selectivity-profile studies.....	- 51 -
V. Binding mode study	- 52 -
CONCLUSION & PERSPECTIVES	- 55 -

CHAPTER 3: KTGS LEADS TO THE IDENTIFICATION OF POTENT AND SELECTIVE LASB INHIBITORS	- 57 -
INTRODUCTION.....	- 57 -
I. <i>Pseudomonas aeruginosa</i> and resistance	- 58 -
II. <i>P. aeruginosa</i> and virulence.....	- 59 -
III. <i>P. aeruginosa</i> elastase LasB as a therapeutic target.....	- 61 -
4. Therapeutical solutions to inhibit LasB.....	- 68 -
IV. <i>Strategy of the PhD project</i>	- 71 -
RESULTS.....	- 72 -
I. <i>KTGS Las B</i>	- 72 -
1. Design and synthesis of the starting building blocks	- 72 -
2. Protein-templated reaction and controls	- 75 -
3. Hit selection	- 75 -
4. Chemical synthesis of the selected hits	- 76 -
5. Biochemical evaluations of selected hits.....	- 79 -
II. <i>SAR studies</i>	- 81 -
1. The amide.....	- 82 -
2. The linker part.....	- 83 -
3. The nature of the sulfonamide.....	- 86 -
4. The malonic position.....	- 89 -
5. 1,5-Triazole regioisomer synthesis.....	- 91 -
6. The ZBG	- 93 -
III. <i>Toxicity and selectivity profile studies</i>	- 95 -
IV. <i>Binding mode study of hydroxamic acid inhibitor-LasB</i>	- 96 -
CONCLUSION & PERSPECTIVES	- 98 -
CHAPTER 4: DEVELOPMENT OF AN EFFICIENT ONE POT METHODOLOGY FOR THE PREPARATION OF 1,5-DISUBSTITUTED 1,2,3-TRIAZOLES.....	- 100 -
INTRODUCTION.....	- 100 -
RESULTS.....	- 105 -
I. <i>Screening of reaction conditions</i>	- 105 -
II. <i>Substrate scope</i>	- 106 -
1. With various alkynes	- 106 -
2. With various bromides	- 108 -
CONCLUSION	- 109 -
GENERAL CONCLUSION	- 110 -
EXPERIMENTAL PART	- 114 -
I. CHEMISTRY	- 114 -
1. <i>General information</i>	- 114 -
2. <i>General procedures</i>	- 115 -
3. <i>Synthesis of chapter 2 compounds (1–75)</i>	- 118 -
4. <i>Synthesis of chapter 3 compounds (Z7–Z10 and 76–196)</i>	- 155 -
5. <i>Synthesis of chapter 4 compounds (3aA–3aH and 3bA–3l)</i>	- 213 -
II. BIOLOGY	- 221 -
REFERENCES.....	- 225 -

General introduction

For a drug-discovery team, the ligand identification represents a key step in the drug-discovery process. The choice of the method to identify ligands is dependent on multiple factors such as the overall costs, the technical demands or the nature of the disease or of the target. Several hit-identification strategies have been reported (Figure 1). Knowledge-based programs, High-Throughput Screening or High-Content Screening have been commonly used in recent years. Progress in IT and natural sciences (biophysics, chemistry and structural biology) has led to the development of new technologies such as biophysical strategies (e.g., Nuclear Magnetic Resonance (NMR), Surface Plasmon Resonance, virtual screening, fragment screening, DNA-encoded library screening and protein-templated synthesis.

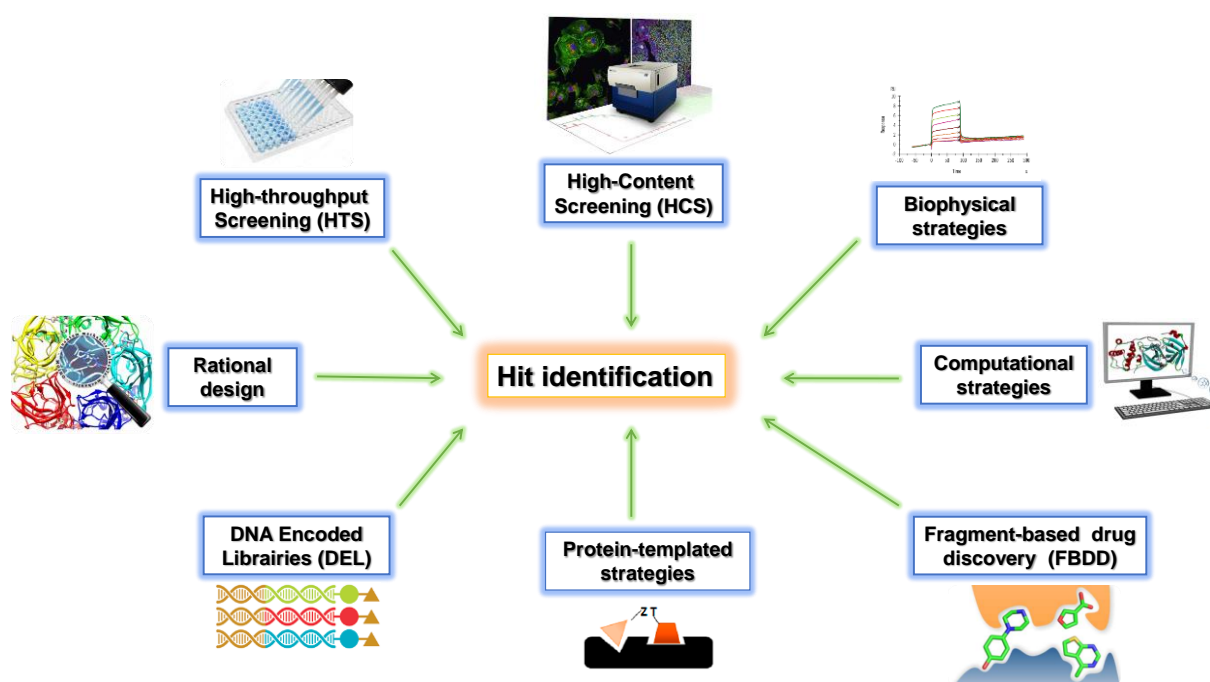


Figure 1: Hit identification strategies in drug discovery

In the present work, we were interested in the identification of metalloenzymes ligands. As their name suggests, metalloproteins are proteins containing metal ions; the metal ion having a structural and/or functional role. If this ion is present in the active site and promotes the catalytic mechanism, we talk about metalloenzymes.

Metalloenzymes account for almost 50% of all enzymes and carry out a diverse range of biological processes like inflammation, cell proliferation, hormonal signaling or pathogen growth, depending on the nature of the reaction in which the metal ion is involved (zinc, copper, calcium, magnesium, manganese or iron).⁽¹⁾

In particular zinc metalloenzymes are an important subclass of metalloenzymes. Some of them led to pharmacological drug classes used in major therapeutic indications:

- Angiotensin-converting enzyme (ACE) inhibitors for the treatment of high blood pressure,
- Histone deacetylase (HDAC) inhibitors for the treatment of cancer and inflammatory diseases,
- Neprilysin (NEP) inhibitors for the treatment of heart failure.

In addition, many compounds targeting these enzymes are in development like TNF- α converting enzyme (TACE) inhibitors and metallo β lactamase (MBL) inhibitors to fight against inflammation and antimicrobial resistance (AMR), respectively.^{(2),(3)}

The teams of Prof. Deprez-Poulain and Prof. Hirsch target such metalloenzymes: Insulin-degrading enzyme (IDE) and the Endoplasmic reticulum Aminopeptidases (ERAP) in Lille and Clostridial collagenases (ColH and ColQ1) and *Pseudomonas aeruginosa* elastase (LasB) in Saarbrücken, respectively.^{(4),(5),(6),(7)}

The objectives of this project are to use innovative protein-templated strategies, which use the target protein itself to form its own ligands^{(8),(9)} to identify and optimize new ligands of metalloenzymes of interest in both labs (Figure 2). We will focus on the discovery of ERAP inhibitors for application in the modulation of the immune response, and LasB inhibitors to block the virulence process in *P. aeruginosa* infection. These ligands will serve as pharmacological tools to explore the role of these enzymes and as leads for therapeutic applications. More specifically, amongst the different target-guided synthesis approaches, dynamic combinatorial chemistry (DCC), which is thermodynamically controlled and kinetic-target guided synthesis (KTGS) which is kinetically controlled,⁽¹⁰⁾ we have chosen to use KTGS exclusively in this work.



Figure 2 : Objectives of the PhD project

Chapter 1: Protein-templated strategies: the KTGS

I. Introduction

1. Principle

Even if the focus is focused on KTGS, it is important to compare the principle of the two protein-templated approaches (Figure 3).

In DCC, the target protein assembles ligands via a reversible process. The reagents and products interact continuously (dynamic combinatorial library, Figure 3A) and the thermodynamic equilibrium is displaced by the target in favor of ligands, which display the highest affinity for the protein and therefore the production of those is amplified.^{(11),(12)}

In KTGS, the target catalyzes the reaction between the most affine pair of reagents for its active site and templates the formation of the ligand by an irreversible link (Figure 3B). Thus, DCC is based on the product affinity whereas KTGS is based on the reagents affinity and their proper orientation in the active site.

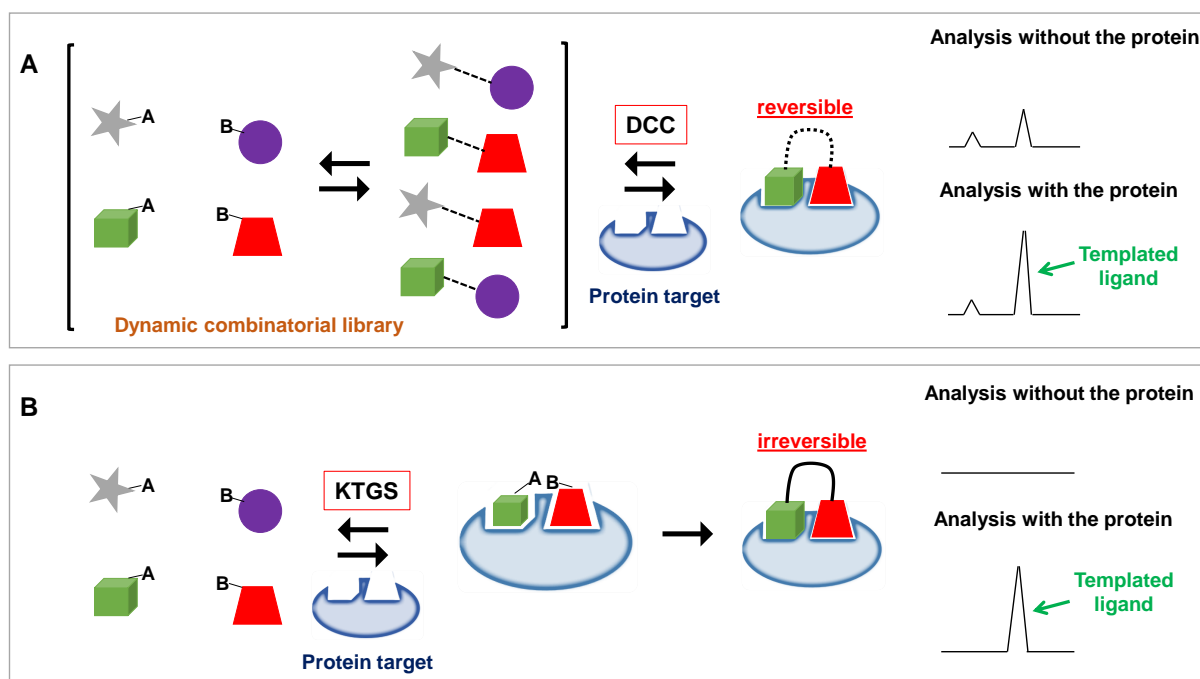


Figure 3 : Principles of target-guided synthesis. (A) Principle of DCC, the target protein displaces the equilibrium toward the most affine ligand. (B) Principle of KTGS, the target protein stabilizes a pair of reagents in reacting relative configurations and accelerates the irreversible formation of the ligand, which is finally detected. Adapted from Deprez-Poulain *et al.*⁽¹³⁾

2. History and Recent Achievements

Although the first intentional example of KTGS was reported by Huc *et al.* in 2001 with the use of the human carbonic anhydrase II (hCAII) to catalyze thiol alkylations,⁽¹⁴⁾ a previous unexpected use of this strategy was disclosed by Inglese *et al.* in 1991 using the glycinamide ribonucleotide transformylase.⁽¹⁵⁾ The 2000s can be considered as an important date in the development and use of this strategy thanks to the work of the Sharpless, Meldal and Fokin groups who reported the copper-catalyzed azide-alkyne 1,3-dipolar cycloaddition. Subsequent to this discovery, the term “in situ click chemistry” was created; the most popular example was carried out with the acetylcholinesterase (AChE).⁽¹⁶⁾

Noteworthy, KTGS has greatly evolved in a short time. First, apart from the Huisgen 1,3-dipolar cycloaddition between alkynes and azides, it is possible to use other templated reaction such as the sulfo-click reaction,⁽¹⁷⁾ hydrolysis/thio-Michael coupling,⁽¹⁸⁾ amidation,⁽¹⁹⁾ Mannich reaction and more recently four-components Ugi reaction.^{(20),(21)} Although the majority of KTGS experiments are performed using enzymes, some experiments were published using transcriptional factors, channels and protein–protein interactions. Finally, Deprez-Poulain *et al.* have demonstrated that KTGS experiments can be performed in multicomponent formats.⁽⁴⁾

Thus, the increasing variety of targets, the chemical reactions diversity, the evolving of the KGTS format and the biological characterization of the templated ligands have contributed to the evolution of this approach, demonstrating that KTGS has undeniable potential for hit identification.

II. Design & practical aspects

1. Chemical reactions used

Among the reported reaction, the in situ click reaction between alkynes and azides is the most employed and represents around 80% of the published KTGS experiments; eight other reactions accounting for the remaining percentage ($\approx 20\%$).⁽¹³⁾ The high interest for the Huisgen 1,3-dipolar cycloaddition comes both from the fact that the azides and alkynes are biocompatible and that a broad range are commercially available or can be synthesized easily.

2. Warhead-bearing reagent

The selection and/or design of warhead-bearing reagents represent the most important step for the achievement of a KTGS experiment. Deprez *et al.* have analyzed the origin and nature of those in Figure 4.⁽¹³⁾

In the majority of cases ($\approx 63\%$), the warhead-bearing reagents come from known Structure–Activity Relationship (SAR) or previously described modulators (Figure 4A). In more than 12% of cases, the warhead-bearing reagents derive from substrates or cofactors like biotin. Interestingly, marketed drugs can also be used to design warheads ($\approx 9\%$).

Strikingly, around 16% of cases concern warheads, which were discovered by fragment screening; demonstrating that KTGS can be complementary to other strategies for ligand identification.

Although for all ligands, the majority of warhead-bearing reagents ($\approx 77\%$) are synthetic compounds, a non-negligible proportion derived from natural product ($\approx 24\%$) (Figure 4B). Finally, regarding the binding of the templated ligands, non-covalent compounds were templated in almost all cases ($\approx 95\%$, Figure 4C).

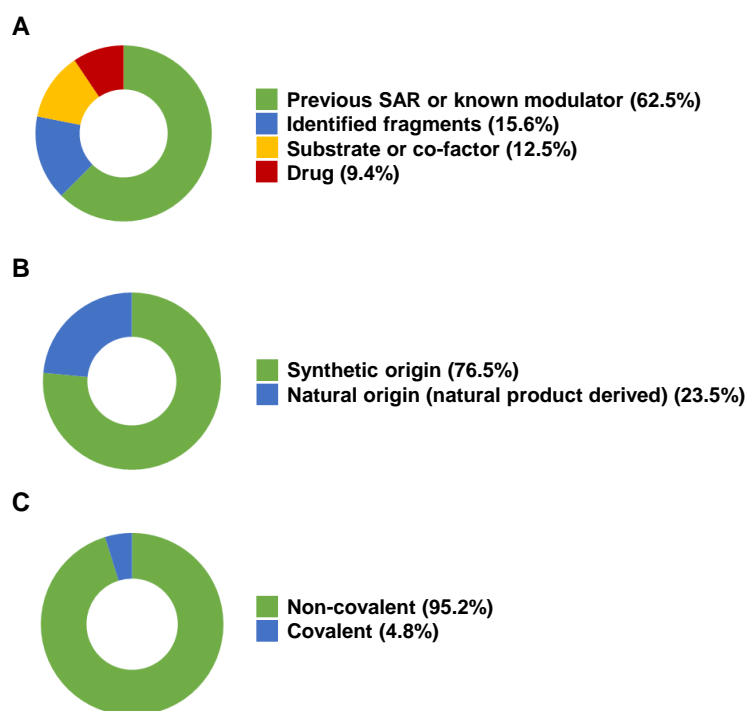


Figure 4 : Origin and nature of the warhead-bearing reagents. (A) Inspiration sources for the design of the warhead-bearing reagents. (B) Nature of the warhead-bearing reagents. (C) Character of the templated ligand–protein binding, adapted from Deprez-Poulain *et al.*⁽¹³⁾

Sometimes, there is a confusion between protein-templated and fragment approaches; the protein-templated being wrongly considered as an extension of fragment approaches. In order to discriminate the two strategies, Deprez-Poulain *et al.* have also studied the features of

the warhead-bearing reagents and compared these characteristics with those in fragment approaches.

According to the rule of 3 (Ro3), a reagent can be considered as a fragment if it has a molecular weight (MW) lower than 300 g/mol, no more than 3 hydrogen-bond donors (HBD), no more than 3 hydrogen-bond acceptors (HBA) and a clogP of less than 3.⁽²²⁾

If the majority of the warheads used in KTGS respect the Ro3 for the clogP (70%) and HBD (76%) criteria, the analysis is not the same for the MW and HBA criteria (Figure 5A–D). Indeed, 62% have a MW higher than 300 g/mol (Figure 5A) and 71% display a number of HBA above 3 (Figure 5D). In conclusion, most of the reagents used in KTGS are not in accordance with the Ro3.

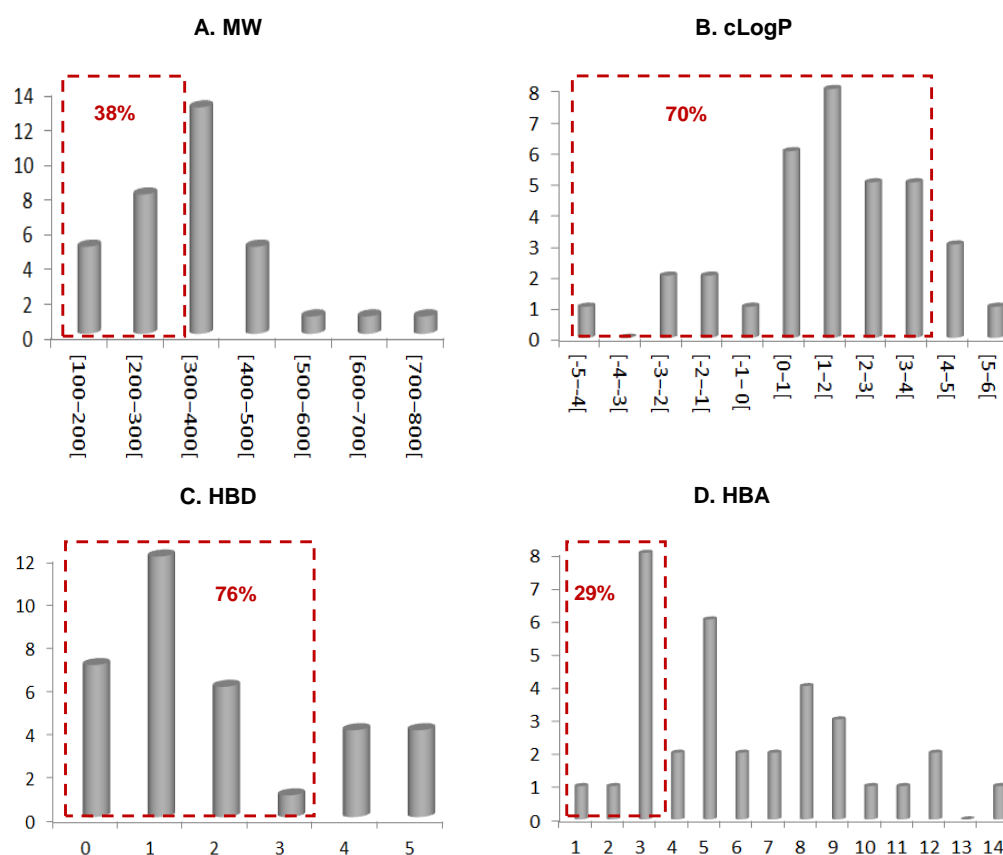


Figure 5 : Distribution of the structural features of the warhead-bearing reagents. (A) MW, (B) cLogP, (C) HBA and (D) HBD. The proportions of warhead-bearing reagents that comply with the Ro3 are presented in red dotted lines, Adapted from Deprez-Poulain *et al.*⁽¹³⁾

The analysis of Deprez-Poulain *et al.*, concerning the structural features of reagents used in KTGS, showed that the number of heavy atoms differs significantly between fragments. Indeed, the majority of fragments have between 10 and 16 heavy atoms, whereas the majority of KTGS reagents have between 10 and 30 heavy atoms.

However, the reagents in KTGS and fragments differ slightly concerning the fraction of sp^3 -hybridized carbon atoms; both displaying a limited fraction: < 0.6 in KTGS and < 0.5 for

fragments. Then, 50% of the KTGS reagents contain more rotatable bonds (between 2 and 6) and rings (> 2) compared to fragments.

Although the main proportion of these reagents (KTGS and fragments) are neutral compounds ($\approx 60\%$ in KTGS and $\approx 70\%$ for fragments), an important percentage of the remaining proportion of the KTGS warheads are positively charged ($\approx 30\%$) whereas, the proportion of positively charged fragments is lower ($\approx 10\%$); fragments with negative charge represents around 20%.

Noteworthy, these reagents can be distinguished by their potency or affinity for the protein target as, usually, fragments display potency in a millimolar range, whereas KTGS warheads display potency in a micromolar range ($\leq 500 \mu\text{M}$). Thus, KTGS strategy cannot be considered as an extension of the fragment linking approach since many differences exist, in particular, regarding the potency of the “starting building block”.

3. Formats, Sizes, Hit Rates and Detection Methods

Apart from the binary format, Kolb *et al.* and Deprez-Poulain *et al.* have demonstrated that KTGS experiments can be performed in multicomponent or orthogonal multicomponent formats, respectively^{(23),(4)}. Therefore the number of templated ligands increases and thus the chances of success are maximized as the pair of reagents is replaced by clusters. However, the binary format is still the most employed format in the published KTGS assays (67%, Figure 6A), partly explaining that in only one quarter of the disclosed examples, the authors investigated the formation of more than 50 putative ligands (Figure 6B).

Deprez-Poulain's group has unsurprisingly reported that the hit rate is high in KTGS. This can be explained by the fact that the majority of assays were performed with limited pools of reagents, which were derived from known SARs or modulators. They have disclosed that 50% of KTGS experiments, in which a minimum of 30 ligands can be templated, displayed comparable hit rates to random screening (1–5%, Figure 6C).

Finally, the team has reported that mass Spectrometry (MS) methods are used in 85% of cases to detect the templated ligands (Figure 6D); X-ray, NMR or thermal shift assay can be mentioned as other methods.

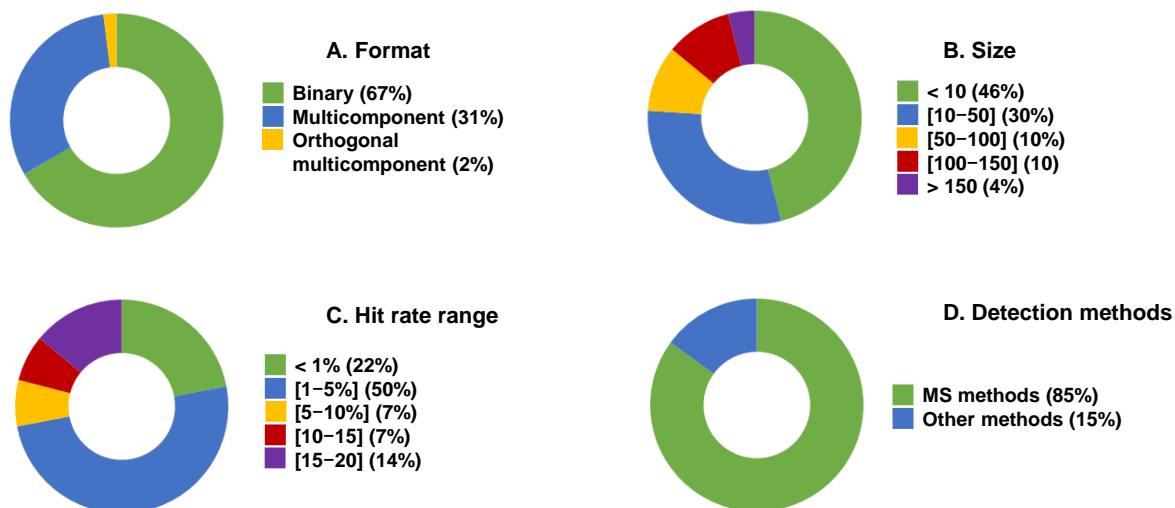


Figure 6 : Format (A), size (B), hit rate (C) and detection methods (D) in disclosed KTGS experiments adapted from Deprez-Poulain *et al.*⁽¹³⁾

III. Relevance of KTGS for medicinal chemistry and drug discovery

1. Therapeutic Areas and Protein Targets

A significant number of therapeutic areas were targeted by the published KTGS experiments, in particular infectiology and cancerology, which account for around 55% (Figure 7A).

In the published review by Deprez-Poulain's team, KTGS experiments were performed using 26 different proteins; the most used protein family being the enzymes (73%, Figure 7B). Among the enzymes used, we can find hydrolases, ligases, oxydoreductases, lyases and transferases. Interestingly, the team has also revealed that around 60% of the used proteins do not have marketed drugs or clinical candidates.⁽¹³⁾

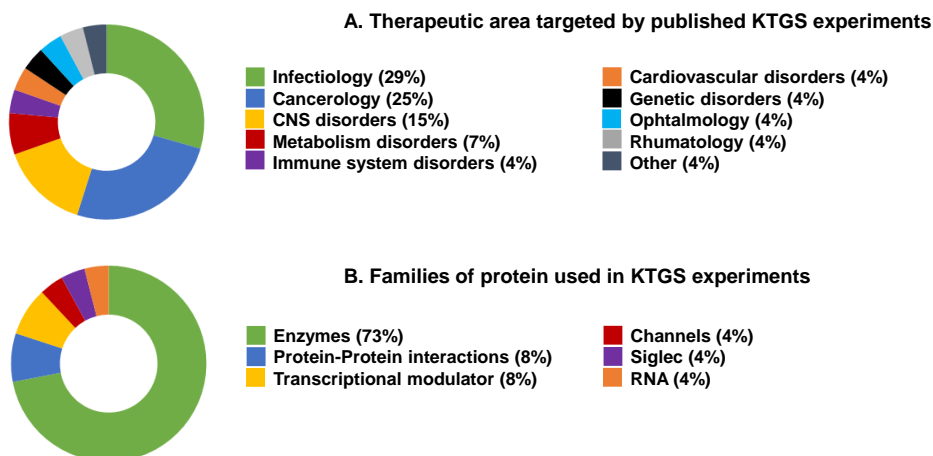


Figure 7 : (A) The therapeutic areas with at least one published KTGS example and theirs respective proportions. (B) The protein families used in KTGS experiments and theirs respective proportions adapted from Deprez-Poulain *et al.*⁽¹³⁾

2. Protein Pockets and Conformation

In Hirsch's and Deprez-Poulain's published studies, the different pockets were scored according to their size, depth, enclosure and fraction of apolar residues. They did not observe significant differences for the depth of pockets but KTGS pocket are a bit wider and contain a higher fraction of apolar amino acids (Table 1).

Table 1 : Characteristics of the KTGS Pockets adapted from Hirsch *et al.*⁽²⁴⁾ and Deprez-Poulain *et al.*⁽¹³⁾

	Volume (Å ³)	Depth (Å)	Enclosure	Fraction of apolar amino acids
KTGS pockets	1445	26	0.11	0.4
reference set of drug pockets	1338	26.5	0.08	0.5

In case of enzymes, it is quite “easy” to target the active site with the templated ligands, using warheads which can bind it. For example, Deprez-Poulain *et al.* used hydroxamate-bearing warheads to coordinate the zinc of IDE and therefore allow the binding of the templated ligands in the active site.⁽⁴⁾ Thus, unsurprisingly, almost all templated ligands by enzymes target and bind the active site.

Additionally, protein-templated strategies have demonstrated that they can allow the identification of new binding pockets and/conformations, which cannot be discovered through conventional methods like X-ray crystallography or computational strategies.^{(4),(25)}

3. Chemical Space and Ligand Efficiency of KTGS Ligands

Deprez-Poulain's team was interested in the behavior of KTGS ligands with respect to the Lipinski–Weber rules and the Doak chemical space (Figure 8). The Lipinski–Weber rules (Rule of 5 (Ro5)) are employed to evaluate if a drug can be used as an oral drug. To comply with the Ro5, the compound must have fewer than 5 HBA and 10 HBD, a MW less than 500 g/mol and an octanol-water partition coefficient (cLogP) not greater than 5.⁽²⁶⁾ The Doak space corresponds to the “possible to be oral” chemical space, the compound must display fewer or equal to 15 HBA and 6 HBD, a MW less or equal to 1000, a cLogP ranging from less or equal to -2 to less or equal to 10, a Polar Surface Area (PSA) less or equal to 250 Å² and a number of rotatable bounds less or equal to 20.⁽²⁷⁾

According to analyses, although the majority of the KTGS ligands do not comply with the with the Lipinski–Weber rules (72%), most of them display values allowing them to be in the Doak space (82%, Figure 8). Thus, thanks to the KTGS method, it is possible to explore larger chemical spaces than the one defined by Lipinski–Weber.⁽¹³⁾

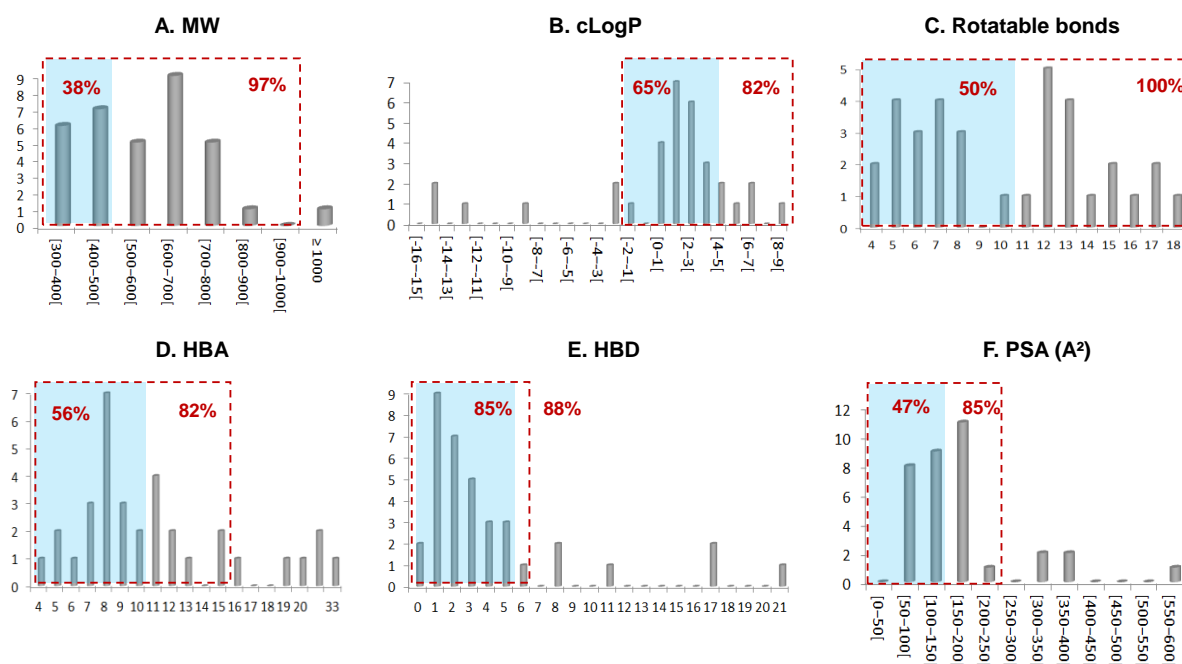


Figure 8 : Structural characteristics distribution of KTGS ligands and their behavior regarding the Ro5 and the Doak chemical space. (A) MW, (B) cLogP, (C) number of rotatable bonds, (D) number of HBA, (E) number of HBD, and (F) PSA. The proportions of templated ligands which comply with the Ro5 are in blue box and these for those in the Doak chemical space are in red dotted lines, adapted from Deprez-Poulain *et al.*⁽¹³⁾

Finally, Deprez-Poulain *et al.* have also compared the properties of the templated ligands and those of the FDA-approved drugs (Figure 9). These comparisons revealed that FDA approved drugs are lighter, less polar and less flexible than the KTGS ligands.

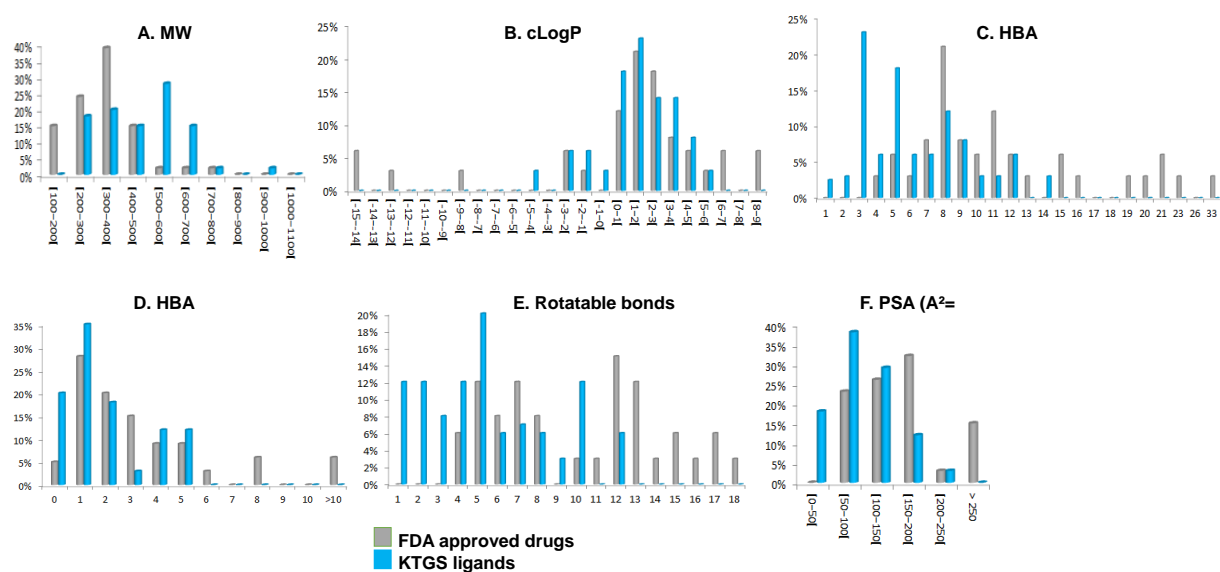


Figure 9 : Comparison of the structural and physicochemical properties of KTGS ligands and FDA approved drugs. (A) MW, (B) cLogP, HBA (C), HBD (D), (E) rotatable bonds and (F) PSA. FDA-approved drugs are in grey and KTGS ligands in blue; N=34 for KTGS and N=751 for FDA, adapted from Deprez-Poulain *et al.*⁽¹³⁾

Noteworthy, as presented on Figure 10, around 70% of templated ligands can be considered as good medchem starting points as they display a Lipophilic Ligand Efficiency (LLE) higher than 3 and, strikingly, one quarter of them can be considered as promising drug candidates as they display LLEs higher than 6 (Figure 10A). Noteworthy, in most cases, KTGS experiments led to an increase of the LLE (Δ LLE, Figure 10B).⁽¹³⁾

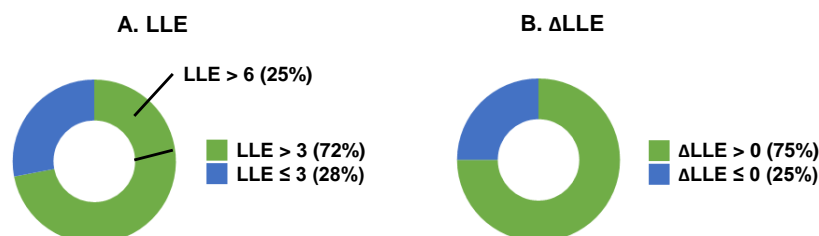
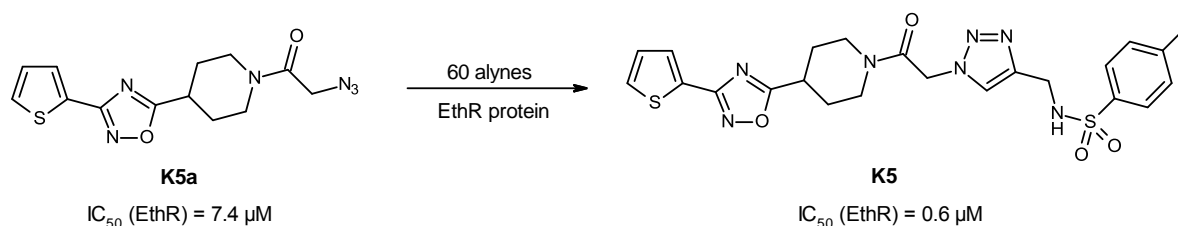


Figure 10 : LLE (A) and ALLE (B) of the KTGS ligands adapted from Deprez-Poulain *et al.*⁽¹³⁾

IV. Case studies

1. *Mycobacterium tuberculosis* transcriptional repressor EthR

Willand's team performed a KTGS experiment using an in situ click chemistry reaction from one azide and sixty alkynes to identify inhibitors of EthR (Scheme 1), a mycobacterial transcriptional regulator involved in the sensitivity control of *Mycobacterium tuberculosis* to several antibiotics. The starting azide **K5a** displayed an activity in micromolaire range and was derived from an EthR inhibitor, which was previously discovered by screening. The KTGS experiment led to the identification of the templated ligand **K5**, increasing the potency by a factor of 10 (0.6 μ M vs 7.4 μ M).⁽²⁵⁾



Scheme 1 : *Mycobacterium tuberculosis* EthR-templated formation of **K5**

Surprisingly, the binding of **K5** to EthR led to structural modifications at the level of the deeper portion of the pocket to accommodate the bulky iodophenylsulfonamide motif (Figure). In fact, in presence of the azide **K3a**, EthR adopts a “closed-gate” conformation, whereas the binding of **K5** to the protein forces it to adopt an “open-gate” conformation

unveiling a deeper hydrophobic through the displacement of two phenylalanine residues (Phe114 and Phe184) (Figure 11).

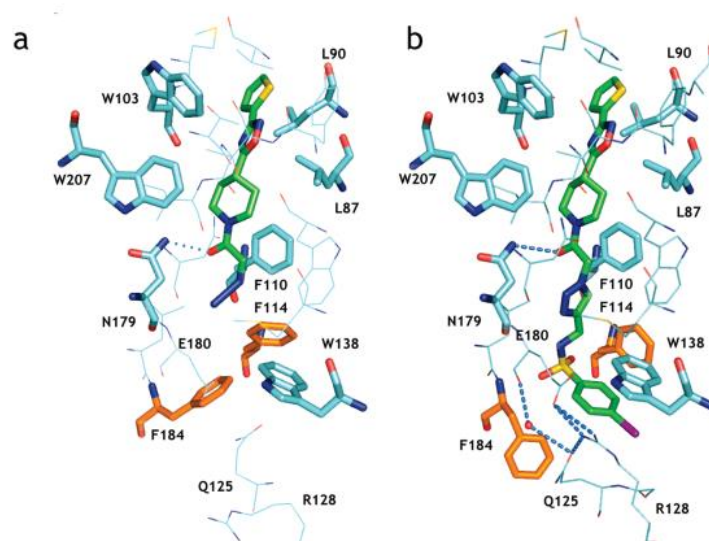
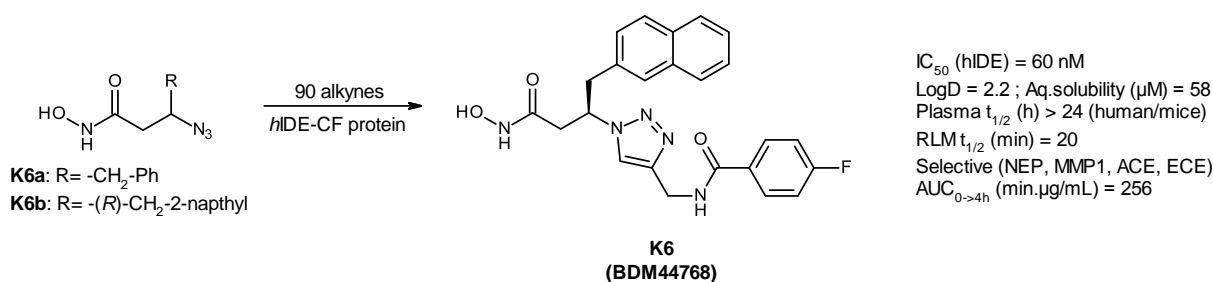


Figure 11 : X-ray structure representations of the ligand-binding pocket of EthR. a) K5a–EthR complex (PDB code: 3O8G). b) K5–EthR complex (PDB code: 3O8H). Colors legend: green (ligand) and light blue (EthR) = carbon, blue = nitrogen, red = oxygen, yellow = sulfur, dotted lines = hydrogen bonds. Key flexible residues are highlighted in orange. Adapted from Willand *et al.*⁽²⁵⁾

2. Insulin Degrading Enzyme (IDE)

Deprez-Poulain's team applied KTGS strategy to identify inhibitors of IDE, a zinc-metalloprotease (member of the M16 group) which cleaves insulin and other bioactive peptides like amyloid- β and glucagon.⁽⁴⁾ They performed an orthogonal multicomponent experiment from two azides (**K6a** and **K6b**) and ninety alkynes (Scheme 2). They used the information available on substrate preference and inhibition of human IDE (*hIDE*) to design two azides-bearing hydroxamate warheads to coordinate the zinc ion in the N-terminal part of the enzyme (**K6a** and **K6b**) while the alkynes were chosen as potential binders to the C-terminal extremity of the active site.⁽⁴⁾ 66 hits were identified, the most promising hit **K6** displaying good potency, good ADME properties and selectivity over other zinc metalloenzymes (Scheme 2).



Scheme 2 : *hIDE*-CF-templated formation of **K6**

Interestingly, they observed that **K6** has an influence on the open/closed equilibrium of *hIDE* by shifting it toward closed conformations (Figure 12).

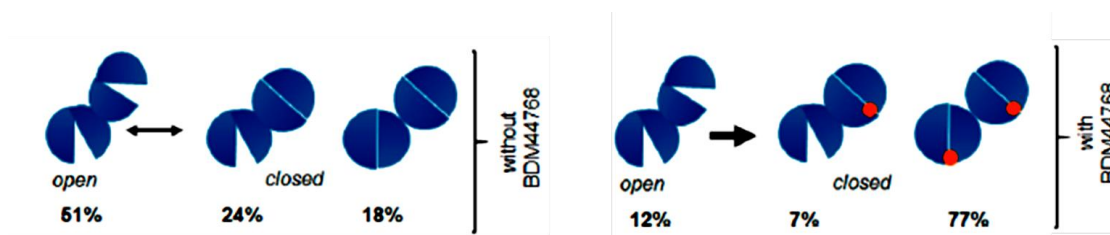
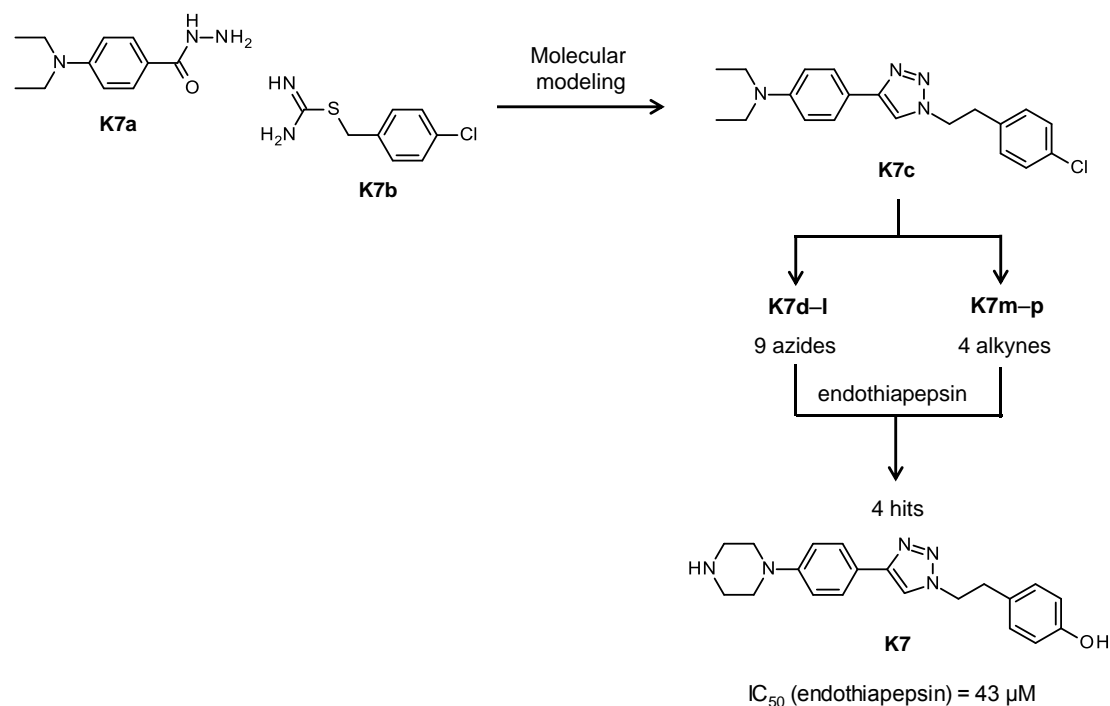


Figure 12 : Shift of the conformation equilibrium of *hIDE* by **K6** adapted from Depez-Poulain *et al.*⁽⁴⁾

3. Endothiapepsin

Hirsch *et al.* combined the fragment-linking approach with the protein-templated strategy to identify inhibitors of endothiapepsin (Scheme 3), a model enzyme for the studies of aspartyl proteases.⁽²⁸⁾



Scheme 3 : Combination of fragment linking approach and KTGS strategy to identify endothiapepsin inhibitors

The starting fragments **K7a** and **K7b** were previously identified by Klebe *et al.*⁽²⁹⁾ They make H-bonds with two aspartate residues (Asp35 and Asp219) of the catalytic dyad through their hydrazide (**K7a**) and amidine groups (**K7b**) (Figure 13). As they display good physicochemical properties, promising inhibitory potency ($\approx 85\%$ inh at 1 mM) and interesting occupancy in the active site, these fragments were chosen by Hirsch *et al.* as good starting points for fragment linking strategy. Thanks to molecular modeling, they linked the fragments through a triazolyl moiety (**K7c**, Figure 13). Interestingly, the triazole ring seems to

be in close proximity to the two aspartate residue and thus could interact with the catalytic dyad (Figure 13).

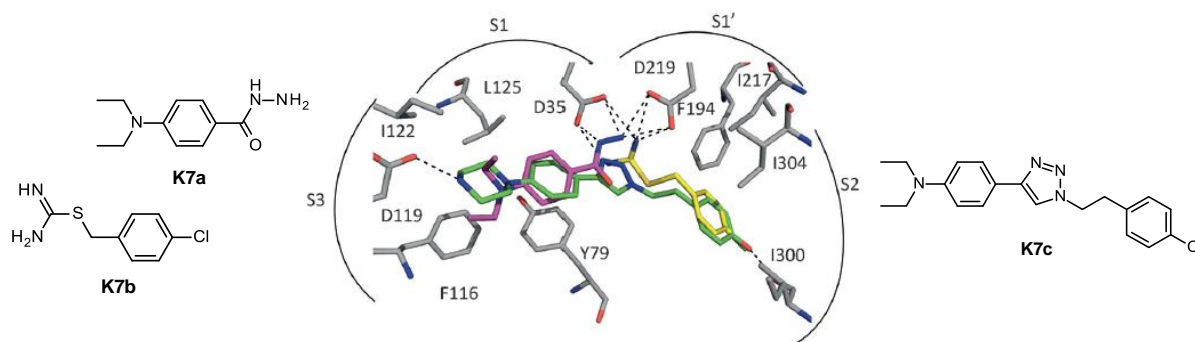


Figure 13 : X-ray crystal structure of endothiapepsin–K7a and –K7b complexes (PDB code: 3PBZ and 3PLD, respectively) and modeled potential triazole inhibitor K7c. Colors legend: purple (K7a), yellow (K7b), green (K7c) and grey (protein) = carbon, blue = nitrogen, red = oxygen and dashed lines = hydrogen bonds. Adapted from Hirsch *et al.*⁽²⁸⁾

Following the molecular modeling, they performed the KTGS through in situ click from four alkynes and nine azides which were identified by retrosynthesis of the modeled triazoles. Four hits were identified, the most potent displaying an IC_{50} in the micromolaire range (**K7**, Scheme 3). Docking of the hit **K7** showed H-bonding interactions: the triazole ring–Asp35 residue, the NH group of the piperazine–Asp119 and phenol–isoleucine 300 (Ile300), and hydrophobic interactions of the piperazine with the S3 pocket (Ileu122, Leu125 and Phe116) (Figure 14).

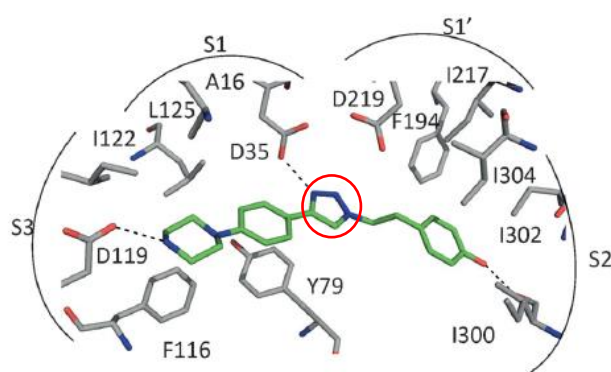


Figure 14 : Docking of K7. Colors legend: green (K7) and grey (protein) = carbon, blue = nitrogen, red = oxygen and dashed lines = hydrogen bonds and triazole is circled in red. Adapted from Hirsch *et al.*⁽²⁸⁾

V. Conclusion

KTGS has proved that it can be employed as a hit identification/optimization strategy. So far, more than 50 examples were published leading to the discovery of ligands in different

therapeutic areas, especially in infectiology, cancerology and CNS disorders domains. Several target families were explored like enzymes, receptors, channels, protein–protein interactions and RNA.

Strikingly, this protein-templated strategy has the capacity to provide, in most cases, ligands which can be considered as interesting starting points for medchem programs (LLE > 3) or promising drug candidates (LLE > 6).

Additionally, KTGS allows the exploration of unknown protein conformations and therefore the discovery of new binding sites, which cannot be captured by computational strategies or NMR, showing that this strategy can be used as a valuable tool in context of drug discovery to explore the conformational space of a ligand-binding pocket.

Although this strategy presents drawbacks and limitations such as the use of biocompatible reagents or large amounts of the protein target, most of these limitations have been solved in particular through the use of multicomponents formats and development of in cellulo experiments.⁽¹³⁾

Thus, the KTGS strategy appears as an attractive and promising approach to find ligands, and for all mentioned reasons, we decided to use it to discover new ligands of two zinc metalloenzymes, nameley the Endoplasmic Reticulum Aminopeptidases (ERAPs) and the elastase LasB of the bacterium *P. aeruginosa*. The next chapters of this thesis will be dedicated to the presentation of my PhD work on the ERAPs and LasB, which will be followed by a final chapter about the description of a new methodology to access 1,5-disubstituted 1,2,3-triazoles, developed during my thesis.

Chapter 2: KTGS leads to the identification of the first potent and selective ERAP2 inhibitors

Introduction

I. Overview of the immune system

1. Immune system and defense mechanisms

The immune system displays two cooperative defense mechanisms which are the innate and the adaptive immune responses (Figure 15).

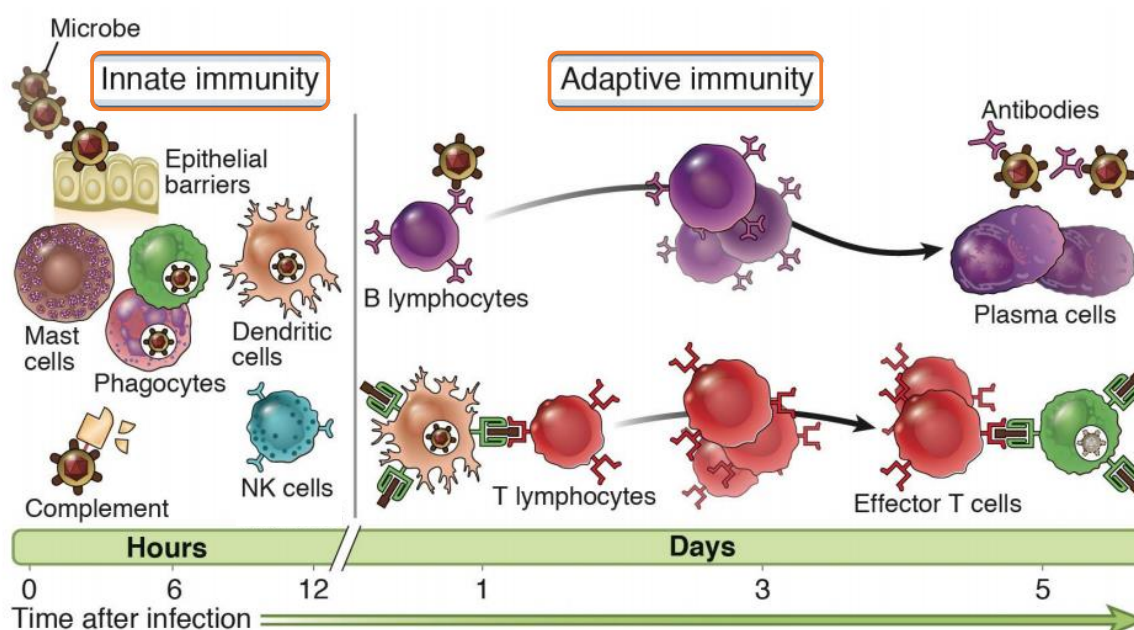


Figure 15 : Innate and adaptive immunity time line with their respective main actors adapted from Abbas, Lichtman and Pillai. Basic Immunology, 5th edition, 2016, Elsevier

A- Innate immunity

Innate or “non-specific” immunity is defined as the early line of defense against pathogens and is organized around constitutive and induced responses.⁽³⁰⁾

The constitutive immune mechanisms refer to the chemical and physical barriers of the body (skin, saliva, lacrimal secretions, stomach acid, etc.), which allow an immediate response to a danger signal. However, they do not have the capacity to amplify the response and are therefore, in some cases, insufficient to eliminate the pathogen.⁽³¹⁾

Once the pathogen is in the body, the induced immune mechanisms take over from the constitutive systems allowing the recognition and destruction of the pathogen. The Pattern Recognition Receptors (PRRs), immune sensors, which discriminate self from non-self, detect

Pathogen-Associated Molecular Patterns (PAMPs) (non-self-molecules) and initiate the immune response. Cellular effectors such as Antigen-Presenting cells (APCs), macrophages, phagocytes and Natural Killer lymphocytes (NK) are thus recruited, facilitating the set-up of the defense mechanisms (inflammation, phagocytosis and complement activation here).⁽³⁰⁾

In cases where pathogen eliminations require more powerful mechanisms, the innate immune response stimulates its collaborative system, which is the adaptive immunity.

B- Adaptive immunity

Adaptive immunity is referred as the “specific” immunity by its ability to respond selectively to numerous non-self-materials.⁽³²⁾ Although the APCs are innate immunity actors, they play a key role in the specific immunity in interacting and stimulating the main self-defensive weapons of the adaptive response, which are the T (CD4⁺ and CD8⁺) and B lymphocytes.⁽³³⁾

The CD4⁺ T-cells, also named helper T-lymphocytes, coordinate the adaptive response in secreting key proteins like cytokines and interleukines.⁽³⁴⁾ The CD8⁺ T-cells, also named cytotoxic or killer T-lymphocytes, eliminate the infected cells and are thus the effectors of the adaptive cellular response.⁽³⁵⁾

Once activated by the CD4⁺ T-lymphocytes, the B-cells differentiate into plasmocytes, which are responsible for the adaptive humoral response through the immunoglobulin secretion.⁽³⁶⁾

Thus, when innate immunity is not sufficient to eliminate pathogens, the immune system displays a second line of defense where these pathogens are presented to more specific mechanisms; the presentation or recognition step being fundamental to initiate the response.

2. Immune system and antigen presentation

An antigen is a natural (protein, carbohydrate or lipid residues) or synthetic macromolecule, which, when introduced into an organism, has the capacity to stimulate the immunocompetent cells. An antigen has two main properties: its antigenicity and its immunogenicity. Antigenicity is the ability of the antigen to be recognized by the immune system and immunogenicity is its potential to induce an immune response.

The presentation or recognition step is a fundamental principle of the immunity. Numerous immune cells have the capacity to pick up these antigens and associate them with APC, thus initiating the immune response.

A- The Human Leucocyte Antigen (HLA) system

Before initiating the immune response, the immune system has to do the distinction between self-antigens and non-self-antigens. The HLA system, found on the surface of the cells, allows us to make this distinction. These HLA antigens, also named Major Histocompatibility Complex (MHC), are divided in three groups: MHC class I (MHC-I), MHC class II (MHC-II) and MHC class III (MHC-III). Only the MHC-I and MHC-II are involved in the antigenic presentation. It should be noted that these MHC systems only present protein molecules, although some polysaccharides can still be presented through this system.⁽³⁷⁾

The MHC-I (Figure 16A) is composed of two polypeptide chains α and β . The polymorphic α -heavy chain, composed by three subunits (α_1 , α_2 and α_3) and encoded by the HLA genes (A, B and C), spans the membrane. The non-polymorphic β -light chain, composed of a β_2 -microglobulin subunit and encoded by a non-HLA gene, maintains the MHC-I conformation with the α_3 subunit. The α_1 and α_2 subunits delimit the peptide (antigen) binding region and are thus referred to the recognition region. The β_2 microglobulin and α_3 bind the CD8 glycoprotein.

The MHC-II (Figure 16B) is also composed of two polypeptide chains α and β , each chain being composed of two subunits (α_1/α_2 and β_1/β_2), encoded by the HLA genes (HLA-DP, HLA-DQ et HLA-DR) and spanning the membrane. The α_1 and β_1 subunits delimit the peptide binding region. The α_2 and β_2 bind the CD4 glycoprotein.

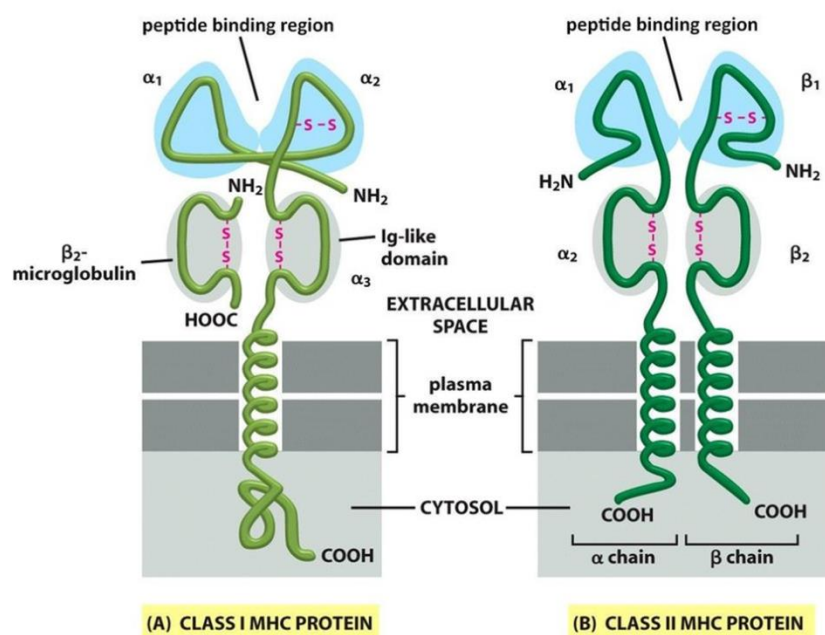


Figure 16 : Structural characteristics of the MHC-I (A) and MHC-II (B) adapted from molecular biology of the cell 5e Garland science

As they display different structural characteristics, they do not have the same specificities and therefore do not bind the same antigens. Here we will focus on the HLA-I system and the implication of the ERAP enzymes in the processing and presentation of antigenic peptides.

B- Antigen-presentation process mediated by the MHC-I

The MHC-I molecules are ubiquitously expressed contrary to the MHC-II, all the nucleated cells and platelets (thrombocytes) have MHC-I complexes on their surface. The MHC-I presents the endogenous antigens. The endogenous antigens are initially present in our cells as their name suggests and are the result of protein degradation in the cytoplasm by the proteasome.

The generation of antigen–MHC-I complexes results in a multistep process (Figure 17). The proteasome, here the immunoproteasome, degrades cytoplasmic proteins further to its ubiquitination and generates peptides, which have a size from 4 to 20 amino acids.⁽³⁸⁾ As the optimal size to be complexed with the MHC-I is between 8 and 11 residues,⁽³⁹⁾ the extended peptides are translocated to the ER through the TAP transporter and their sizes are adjusted by the endoplasmic reticulum aminopeptidases: the ERAP enzymes. Chaperones (tapasin, calreticulin and ERp57) bind the MHC-I, maintaining its conformation and allowing an optimal binding between the peptide and MHC-I. The peptide–MHC-I complex is then transported via the Golgi to the plasma membrane where the antigenic peptide is presented to the CD8⁺ T-cells or NK cells, also named cytotoxic T-lymphocytes, through an interaction MHC-I–TCR.

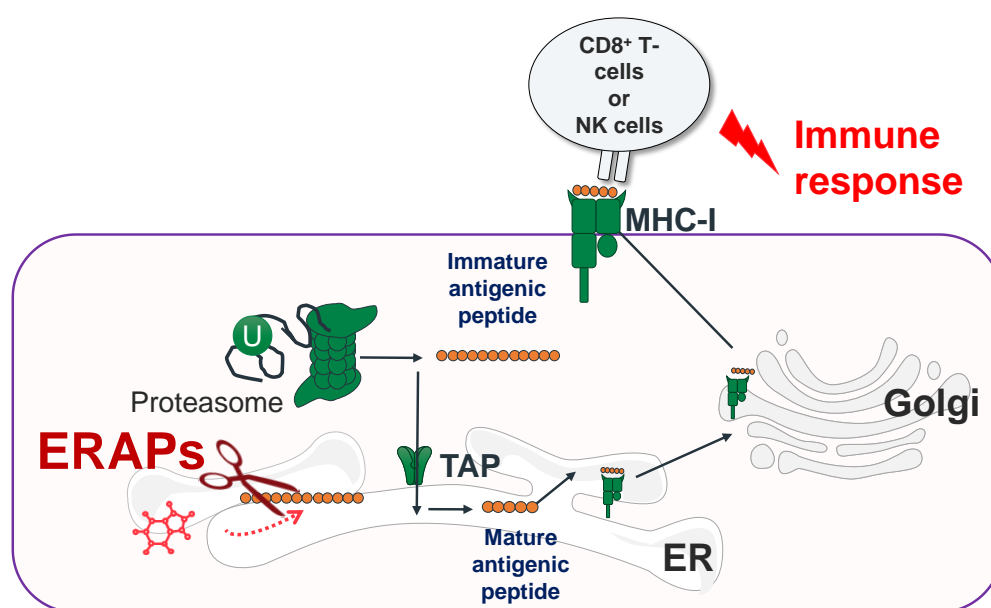


Figure 17 : The basic MHC-I antigen presentation pathway

However, nothing is perfect and the process of loading antigen peptides on the MHC-I can be disrupted at different steps, in particular at the level of the ERAPs.

As seen on Figure 17, the ERAPs play a key role in the process by trimming peptide precursors into mature antigenic epitopes of appropriate size for presentation on the cell surface through the MHC-I. Disruptions of their proteolytic activities can modify the presented antigenic peptide repertoire, also named immunopeptidome, altering therefore the adaptive immune response both qualitatively and quantitatively. Indeed, firstly, the non-generation of the specific immunodominant epitopes by the ERAPs can lead to a non-presentation to the immunocompetent cells and therefore to a suppression of existing cytotoxic responses mediated by the CD8⁺ T-cells resulting in an immune evasion. On the other hand, these enzymes can produce truncated peptides which, once presented, cause an abnormal stimulation of the immunocompetent cells and therefore to unusual cytotoxic responses, resulting in an over-activation of the immune system. Thus, the ERAPs appear as attractive targets to fight against the immune system associated diseases like cancer and autoimmune disorders.

II. The ERAPs as pharmaceutical targets implicated in the antigen processing

1. Classification, structure and organization

The ERAPs (ERAP1 and ERAP2) are zinc metalloproteases belonging to the oxytocinase subgroup of M1 zinc metallopeptidases and are localized in the ER as their name suggests.⁽⁴⁰⁾ Both isoforms share almost 50% sequence similarity.⁽⁴¹⁾ Endoplasmic Reticulum Associated with Antigen Processing (ERAAP) is an ERAP1 homolog in mouse, while ERAP2 does not have any homolog in rodents.⁽⁴²⁾

The human ERAP genes are encoded in a short arm of the chromosome 5q15 in the opposite direction (Figure 18). The isoform 1 contains 20 exons and the other 19; both enzymes being segmented in 4 domains. The active site, containing HEXXH(X)₁₈E and GAMEN motifs, which are characteristics of the M1 zinc metallopeptidases group,⁽⁴³⁾ are located in the domain II for each ERAP.

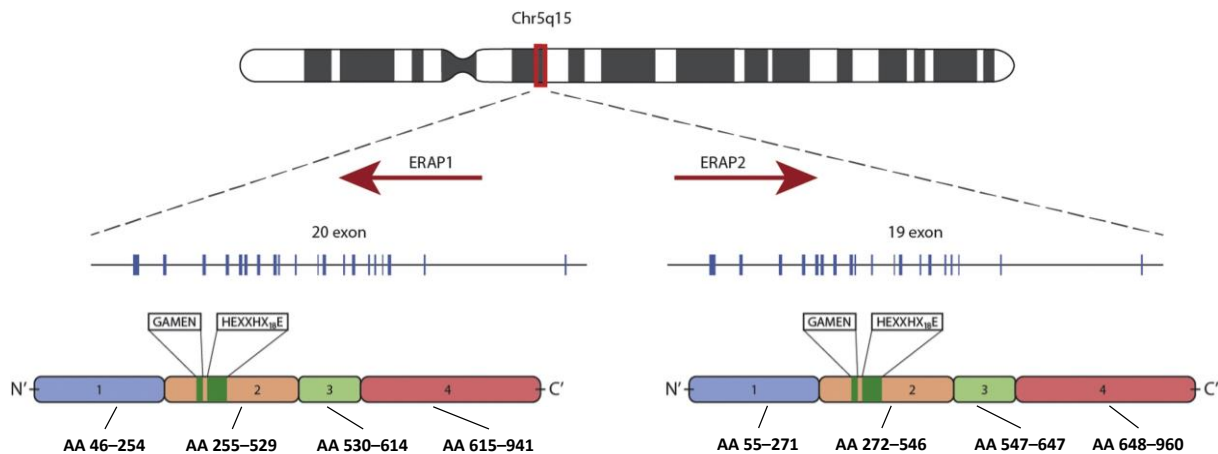


Figure 18 : Genomic organization of the human chromosome 5q15 containing the ERAPs and their respective schematic organization in four domains adapted from Babaie et al.⁽⁴⁴⁾

The HEXXH(X)₁₈E motif, containing two histidine (H), two glutamic acid and other (X) residues, is referred as a zinc-binding motif.⁽⁴⁵⁾ The first glutamic acid residue is also involved in the catalytic activity by polarizing a catalytic water molecule.⁽⁴⁶⁾ The residue positions are not similar between the two ERAPs (Figure 19).

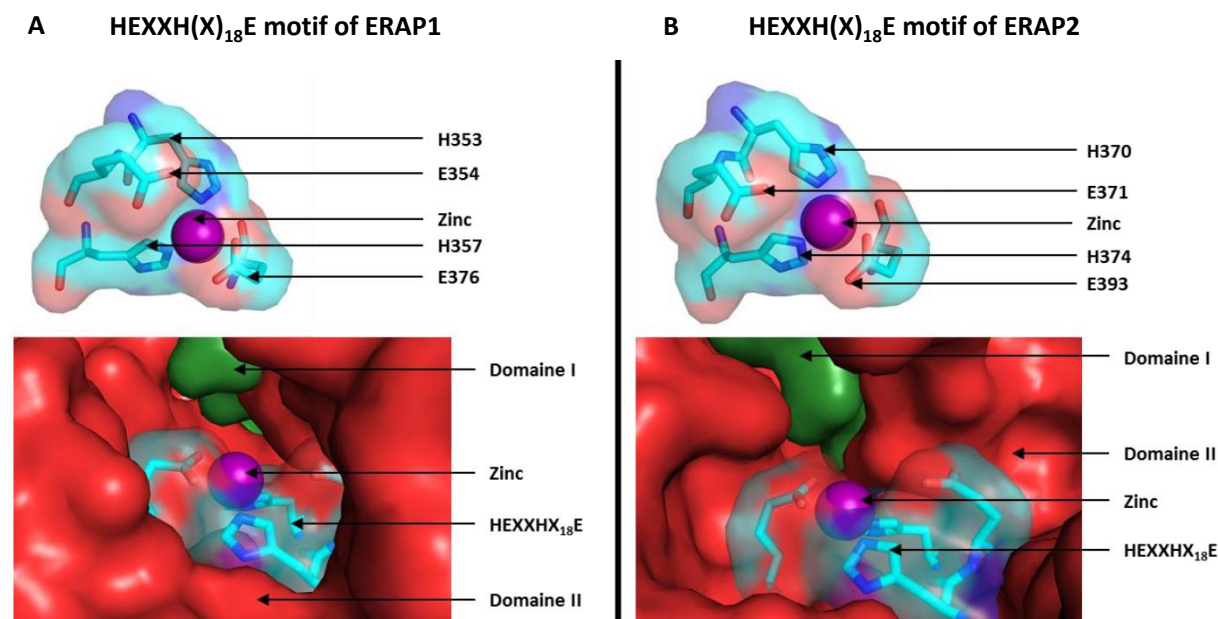


Figure 19 : Comparison of the HEXXH(X)₁₈E motif between the two ERAPs. (A) Illustration of the HEXXH(X)₁₈E motif in ERAP1 (PDB 3MDJ). (B) Illustration of the HEXXH(X)₁₈E motif in ERAP2 (PDB 3SE6). From Paul Hermant's PharmD thesis⁽⁴⁷⁾

The GAMEN motif, containing a glycine (G), an alanine (A), a methionine (M), a glutamic acid (E) and an asparagine (N), is crucial for the enzymatic activity in interacting with the *N*-terminal part of substrates.⁽⁴⁸⁾ As previously, the residue positions are different between the two isoforms (Figure 20).

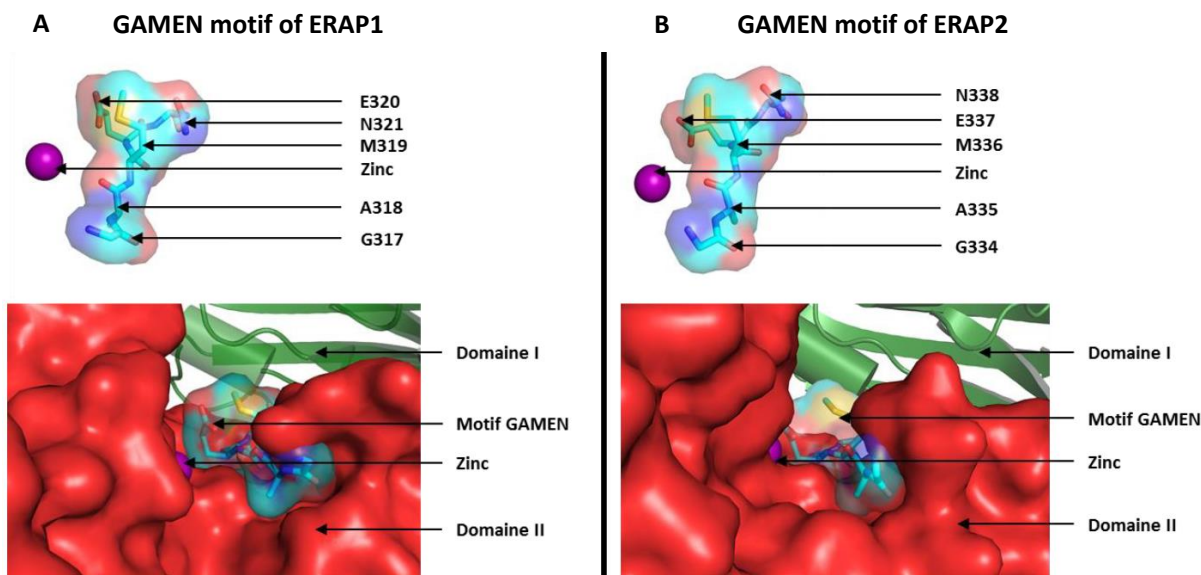


Figure 20 : Comparison of the GAMEN motif between the two ERAPs. (A) Illustration of the GAMEN motif in ERAP1 (PDB 3MDJ). (B) Illustration of the GAMEN motif in ERAP2 (PDB 3SE6). From Paul Hermant's PharmD thesis⁽⁴⁷⁾

2. Catalytic mechanism, substrate recognition and mechanism

The catalytic site contains a zinc ion, which is coordinated by two histidine residues (H353 and 357 for ERAP1, H370 and 373 for ERAP2) and a glutamate residue (E376 for ERAP1 and E393 for ERAP2), forming the first coordination sphere (Figure 19). The second coordination sphere is formed by a tyrosine residue (Y438 for ERAP1 and Y455 for ERAP2) and the first glutamate residue of the HEXXH(X)₁₈E motif (E354 for ERAP1 and E371 for ERAP2), the tyrosine participating in the stabilization of the tetrahedral intermediate during the catalytic mechanism and the glutamate polarizing a catalytic water molecule.^{(49),(46)}

The Zn (II) is crucial for the catalytic activity. It interacts with a hydrolytic water molecule which, once polarized by a glutamate residue, initiates the nucleophilic attack on the substrate amide group resulting in the formation of tetrahedral intermediate. Subsequent to a proton rearrangement, this intermediate is degraded regenerating the ground-state enzyme and releasing an inactivated substrate (amine and carboxylic acid moieties).

The ERAPs display different substrate specificities and thus complement each other in shaping the immunopeptidome.

Chang *et al.* have analyzed ERAP1 substrate specificity and preference.⁽⁵⁰⁾ First, they observed that ERAP1 prefers long substrates with a length between 10 and 16 residues

(Figure 21A); ERAP1 quickly cleaving 13-residue peptides but not 9- and 5-residue peptides (Figure 21B).

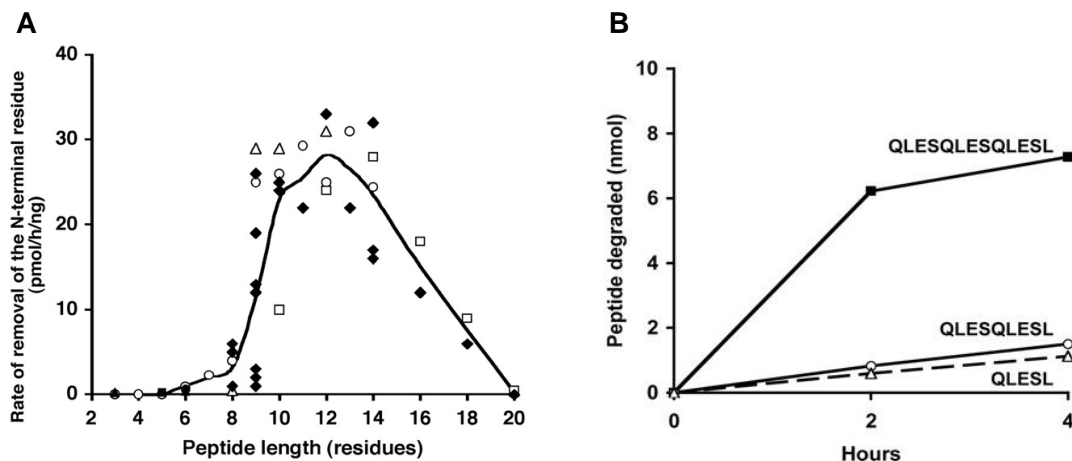


Figure 21 : ERAP1 substrate preferences length adapted from Chang et al.⁽⁵⁰⁾

Then, they demonstrated that ERAP1 prefers peptides, which contain a hydrophobic or aromatic C-terminal residue (Figure 22).

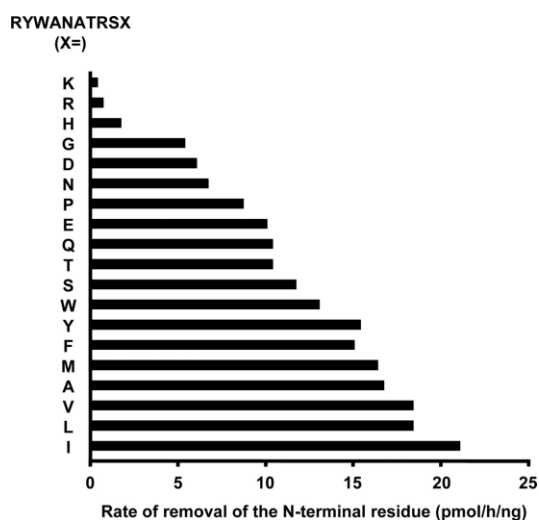


Figure 22 : ERAP1 substrate preferences nature from Chang et al.⁽⁵⁰⁾

Thanks to their studies, they demonstrated that ERAP1 cleaves preferentially long and/or hydrophobic peptides thanks to a hydrophobic pocket close to the active site. They have described a “molecular ruler” mechanism for ERAP1 (Figure 23). In cases where peptides contain between 9 and 16 residues, the peptides bind optimally ERAP1 by interacting with the N- and C-terminal sites and ERAP1 trims the peptides in N-terminal direction, releasing therefore mature antigens (Figure 23A). In cases where peptides display a length below 9 residues (Figure 23A) or contain charged residues (Figure 23B), ERAP1 cannot trim them.

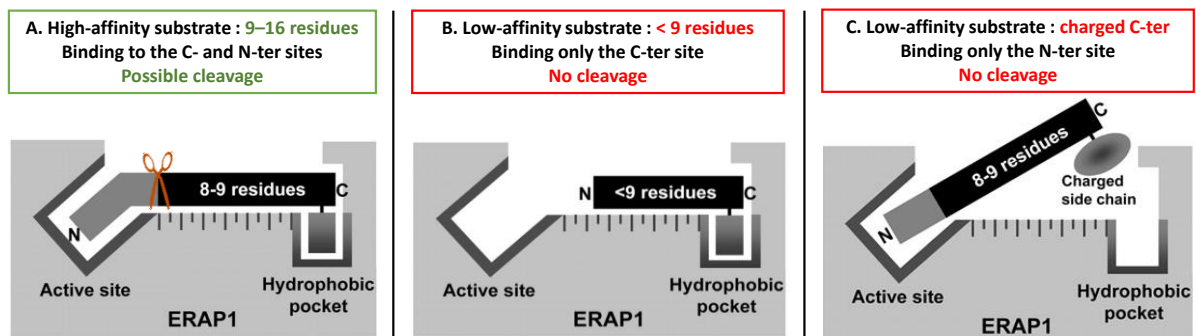


Figure 23 : Schematic representation of the proposed ERAP1 cleavage model. (A) Cleavage occurs further to the binding of a substrate with an optimal length. (B) Cleavage does not occur due to the binding of a too smaller substrate. (C) Cleavage does not occur due to the presence of charged C-ter residues. Adapted from Chang et al.⁽⁵⁰⁾

Contrary to ERAP1, Chang and Stratikos groups have reported that ERAP2 does not follow the “molecular ruler” mechanism described on Figure 23. Indeed, through crystal structure studies, they observed that the peptides access to the substrate cavity of ERAP2 with difficulty as the interactions with this cavity appear shallow and opportunistic. This isoform showed preferences for short and/or positively charged peptides, ERAP2 activity being maximal on octameric substrates and lower on longer peptides. The ERAP2 selectivity for positively charged amino acids is due to the presence of a glutamate residue, which lines the side of the selectivity pocket of the enzyme (S1).^{(42),(50),(51)}

3. Physiopathological implications

During a physiological process (Figure 24A), the ERAPs shape the immature peptides into mature epitopes. In cases where these antigens are immunogenic, they are complexed to the MHC-I to be presented to the CD8⁺ T-lymphocytes and finally activate the immune response. Otherwise, they are not complexed to the MHC-I and no immune response is activated.

Disruptions of these aminopeptidases result in an abnormal antigen processing. First, the ERAP trimming can result in the formation of immunogenic epitopes, which normally are not formed and therefore cause unsuitable immune responses further to the exportation of peptide–MHC-I complexes to the surface of the cell (Figure 24B). Secondly, the ERAPs can either shape immature peptides into non-immunogenic epitopes, which normally are or destroy the “right” immunogenic epitopes leading their accumulation in the ER as they are not complexed to the MHC-I (Figure 24C). Thus, these antigens are not presented to the CD8⁺ T-cells with potential escape from the immune system. Consequently to their accumulation in the ER, they are finally exported to the extracellular media, provoking a local inflammatory response.

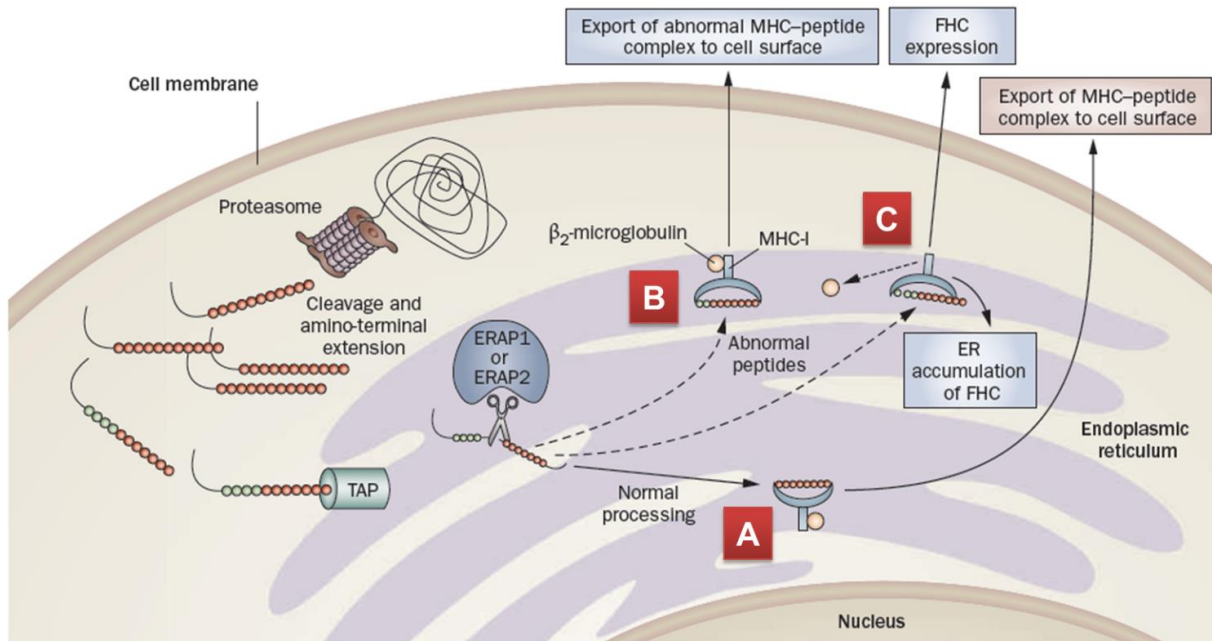


Figure 24 : ERAPs and antigen processing. [A] Normal processing of the antigens. [B] Abnormal processing resulting in the exportation of abnormal peptide-MHC-I complexes to the surface cell when antigens are taken in charge by the MHC-I. [C] Abnormal processing resulting in their accumulation in the ER since the antigens are not taken in charge by the MHC-I. Adapted from Haroon *et al.*⁽⁵²⁾

It is important to understand that this mechanism does not only concern one antigen but the whole antigenic repertoire (immunopeptidome). The ERAPs thus exert qualitative and quantitative control on the immunopeptidome. Their expression levels and enzymatic activity are strongly linked with its composition and can therefore affect the adaptive immune response by trimming the “wrong” and/or destroying the “right” epitopes.

Two opposite consequences are linked with disruptions of these enzymes. Either the “wrong” epitopes are shaped and presented to the CD8⁺ T-cells, causing an excessive stimulation of the immune system, which finally leads to autoimmune disease appearances, or, the “right” epitopes are destroyed and therefore cannot be recognized, escaping from the immune system with cancer or infectious disease developments as consequences.

Single Nucleotide Polymorphisms (SNPs) of the ERAPs, which affect enzymatic activity or protein expression, have been associated with diseases.⁽⁵²⁾

4. ERAPs modulation in therapy

A- Oncology

Stratikos *et al.* have reported that defects in the expression of the ERAP were detected in several tumors such as leukemias, lymphomas, melanomas and carcinomas of skin, breast, lung, colon, chorion, cervix, prostate, bladder and kidney.⁽⁵³⁾

Fruci *et al.* have analyzed the mRNA expression of ERAP1 and ERAP2 in around 9000 cancer samples of various origin from The Cancer Genomic Atlas and they found that the expression levels of these enzymes were altered in several tumors (Figure 25).

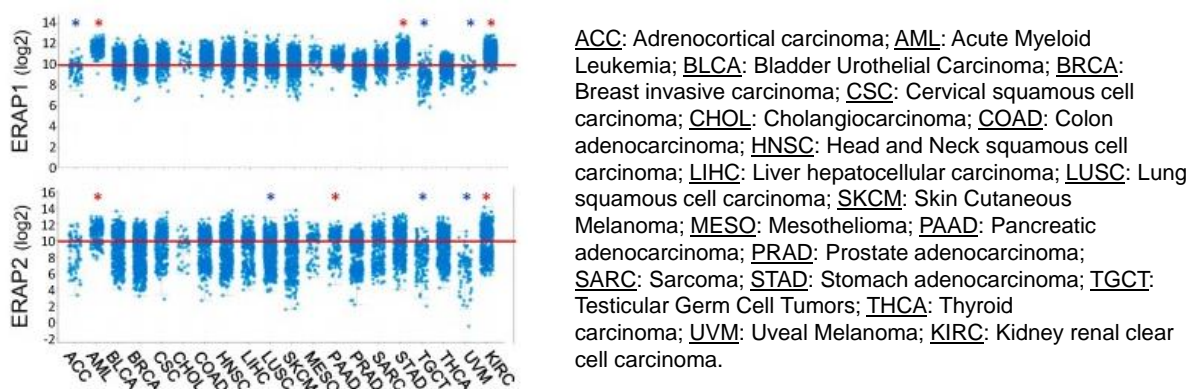


Figure 25 : Expression of ERAP1 and ERAP2 across The Cancer Genomic Atlas tumor tissues. Red bars are used to compare ERAP1 and ERAP2 expression levels. Red and blue asterisks respectively indicate the higher and the lower ERAP1 and ERAP2 expressing tumor types from adapted from Fruci *et al.*⁽⁵⁴⁾

ERAP1 is more expressed in acute myeloid leukemia (AML), stomach adenocarcinoma (STAD) and kidney renal clear cell carcinoma (KIRC), but less expressed in testicular germ cell carcinoma (TGCT), uveal melanoma (UVM) and adrenocortical carcinoma (ACC). ERAP2 is more expressed in acute myeloid leukemia (AML), pancreatic adenocarcinoma (PAAD) and kidney renal clear cell carcinoma (KIRC), but less expressed in lung squamous cell carcinoma (LUSC), testicular germ cell carcinoma (TGCT) and uveal melanoma (UVM).

Thus, alteration of ERAP expression levels can result in a defect in the production or degradation of tumor antigens, leading to tumor escape from the immune system (Figure 26). At physiological level, the ERAPs shape the tumor-specific antigen peptide, resulting in an activation of the cytotoxic T-cells (Figure 26A). However, when the ERAPs are altered, they do not “correctly” trim the tumor-specific mature antigens not allowing the cytotoxic T-cells activation and therefore facilitating immune evasion (Figure 26B).^{(53),(55)} Modulation of the ERAP pathway would therefore allow the “right” shaping of the immature antigens and therefore the production of the mature tumor-specific antigens which, once complexed to the

MHC-I would activate the immunocompetent cells; which then would lead to the tumor suppression.

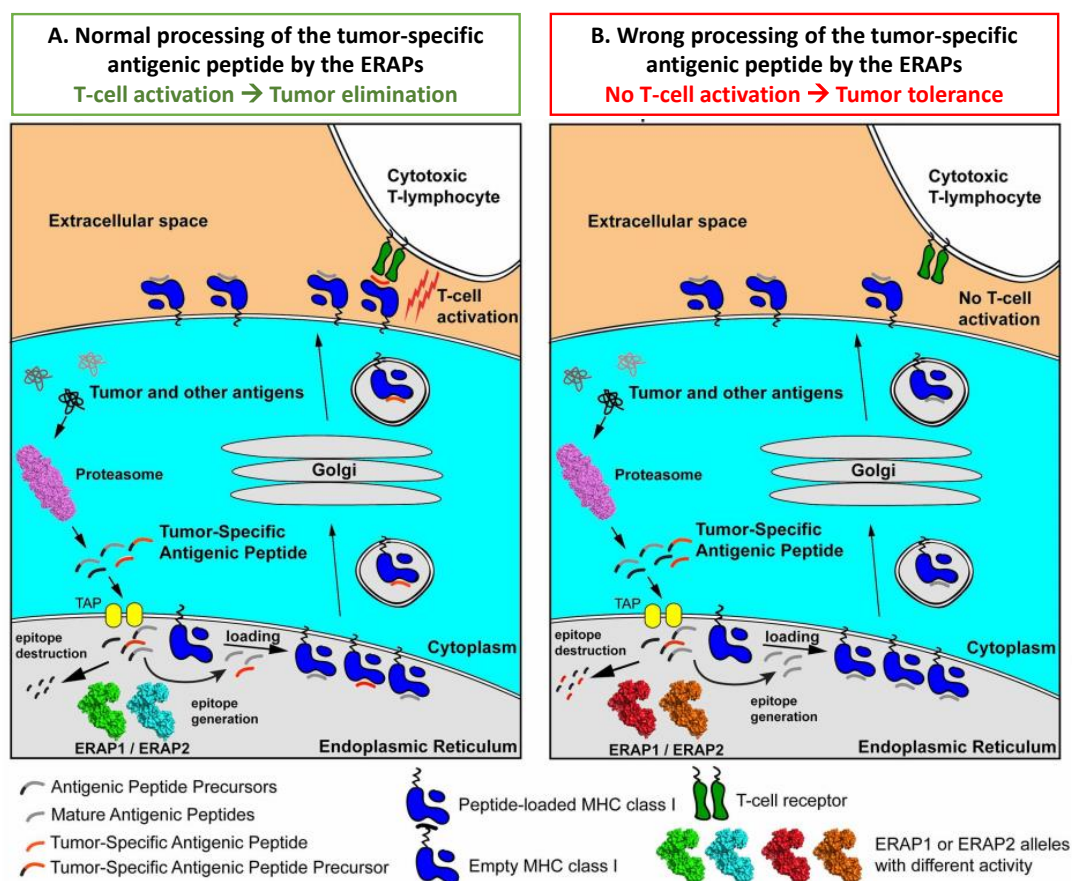


Figure 26 : Schematic representation of the normal processing resulting in effective cytotoxic responses against tumor antigens (A) and of the abnormal processing resulting in an immune evasion consequently to the altered ERAPs (B). Adapted from Stratikos *et al.*⁽⁵³⁾

Thus, Cifaldi *et al.* have shown that the ERAP1 knockout induced the tumor rejection (lymphoma) in mice through a mechanism involving the NK cells,⁽⁵⁶⁾ supporting the idea that ERAPs modulation represents a promising pathway for cancer immunotherapy.

Besides, Lim *et al.* have demonstrated that low levels of ERAP2 were associated with improved response to anti-PD-L1 therapy, in patients with luminal bladder cancers.⁽⁵⁷⁾ So, ERAP2 inhibitors could help to reverse resistance to checkpoint inhibitors and therefore increase the overall survival.

B- Autoimmunity

As seen previously, SNPs of the ERAPs are linked with pre-disposition to autoimmune diseases. Indeed, these SNPs modify the expression and/or the enzymatic activity of the aminopeptidases, leading in non-desired immune responses.

ERAP1 is associated with Ankylosing Spondylitis,⁽⁵⁸⁾ a chronic inflammatory rheumatopathy of the lower spine; the HLA-B27 being known as a high risk factor. This isoform is also associated with Behçet disease that results in inflammation of the blood vessels; the HLA-B51 being known as a high risk factor.⁽⁵⁹⁾ ERAP2 is associated with Ankylosing Spondylitis, Birdshot chorioretinopathy which results in a uveitis, psoriasis and Crohn disease.^{(60),(44)} Thus, inhibition of mutated ERAPs would reduce the production of the pro-inflammatory antigens and therefore restore a normal immune response.

III. ERAPs modulators

In order to develop ERAP modulators, two possibilities can be envisaged: use a compound that mimics the transition state or use a compound containing a zinc Binding Group (ZBG). Several groups have the capacity to coordinate this ion like as amide, carboxylic acid, hydroxamic acid, thiol, phosphinate or phosphonate. We will focus on the ZBG strategy here.

Although some molecules display modulation of ERAPs such as leucinethiol and bestatin, these can also modulate other zinc metalloenzymes, in particular other aminopeptidases,⁽⁶¹⁾ and will therefore not to be discussed here.

So far, only two families of inhibitors have been reported in the literature: aminobenzamide and phosphinic compounds; both developed by Stratikos and colleagues.^{(62),(63)}

1. Aminobenzamide

As their name suggests, these compounds contain a central aminobenzamide core. Regarding their binding mode (Figure 27), with the isoform ERAP1 here, the 2-amide group coordinates the zinc ion monodentally. The aniline interacts with a glutamate residue (Glu354), which participates in the polarization of a water molecule involved in the catalytic activity. The free amine strongly interacts with two glutamate residues (Glu 183 and 320) through an ionic interaction. Finally, the α -substitution (Pn' groups) of the 4-amide and of the 2-amide (P1 groups) allow the interaction with other pockets and therefore maximize the binding in the active site.

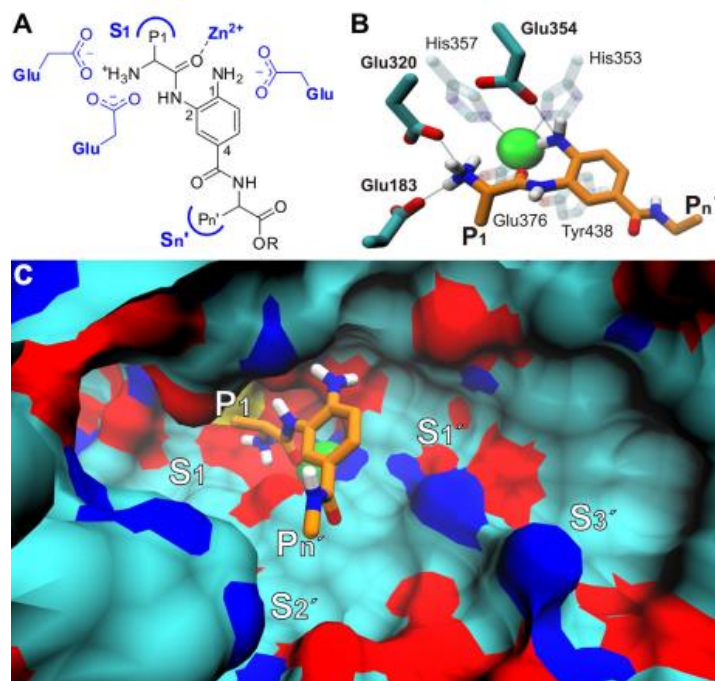
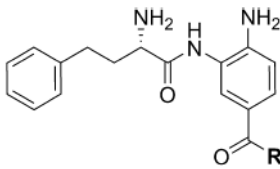


Figure 27 : (A) Schematic representation of an aminobenzamide compound indicating the key interacting residues in blue. (B) Molecular model of the scaffold with carbon atoms shown in orange. The zinc-coordinated residues (His-353, His-357 and Glu-376) and the catalytically important Tyr-438 are shown transparent. The three key interacting glutamic residues (Glu-183, Glu-320 and Glu-354) are shown in dark green and Zn²⁺ with a green sphere. All oxygen and nitrogen atoms are red and blue respectively. (C) Surface representation of the active site of ERAP1 showing the S1 and the putative S1'–S3' subsites. Adapted from Stratikos et al.(62)

Stratikos's team has previously explored the selectivity profile of the S1 pocket using a library of fluorogenic substrates. This study suggested that ERAP1 exhibits selectivity for long, aromatic or hydrophobic substrates, whereas ERAP2 displays higher selectivity for positively charged substrates.⁽⁶⁴⁾ Based on these analyses and docking studies, they introduced an L-homo-phenylalanine moiety in S1 and they explored the flexibility of the Pn' position to obtain an acceptable selectivity for the isoform 1 (Table 2). The L-lysine-containing compounds (carboxylic acid and methyl ester) are the most potent ERAP1 inhibitors ($\approx 2 \mu\text{M}$). Interestingly, the L-tryptophan benzyl ester is fully selective for isoform 2; no ERAP1 inhibition was recovered. However, these aminobenzamide compounds exhibit limited ERAP1/ERAP2 selectivity ratios (> 10 -fold for ERAP1 with respect to ERAP2) and display moderate levels of activity, in the micromolar range. These limited activities can be explained by the fact that the zinc coordination by the amide group is monodentate and therefore weak.

Table 2 : Biochemical evaluation of the synthesized analogs adapted from Stratikos *et al.*⁽⁶²⁾



R	ERAP1	ERAP2
L-Ala-OMe	NI	NI
L-Val-OBn	95.5 ± 3.3	11.5 ± 0.6
L-Val-OH	NI	NI
L-Thr-OMe	NI	NI
L-Lys-OMe	2.0 ± 0.6	24.9 ± 1.2
L-Lys-OH	2.6 ± 0.2	8.9 ± 0.5
L-Arg-OMe	NI	NI
L-Tyr-OMe	7.7 ± 0.4	>100 ^a
L-Trp-OBn	NI	23.9 ± 0.8
OMe	NI	>100 ^a
OH	NI	>100 ^a

NI = No inhibition observed at 50 μ M.

^a Limited inhibition (up to 20%) was evident in the 50–100 μ M range indicating an IC_{50} value >100 μ M.

2. Phosphinic pseudopeptides

The second family of ERAPs inhibitors are phosphinic pseudopeptides (Figure 28A) and was developed by rational design. In order to attain an acceptable selectivity, they replaced the amide by a phosphinic group as a ZBG. Indeed, the phosphinic group is known as a weak ligand of the ion zinc, and therefore the binding affinity arises mainly from specific interactions between the side chains of the peptides and the active site specificity pockets of the enzyme. As seen previously, the L-homo-phenylalanine side chain interacts with the S1 pocket through a π - π stacking interaction between the phenyl and a phenylalanine residue (Phe-450). Introduction of an isobutyl group in β -position of the phosphinic allows for interactions with the small hydrophobic S1' pocket and introduction of a tryptophan moiety in C-terminal position enables a π - π stacking interaction between the indole and a tyrosine residue (Tyr-892) of the S2' pocket (Figure 28B).

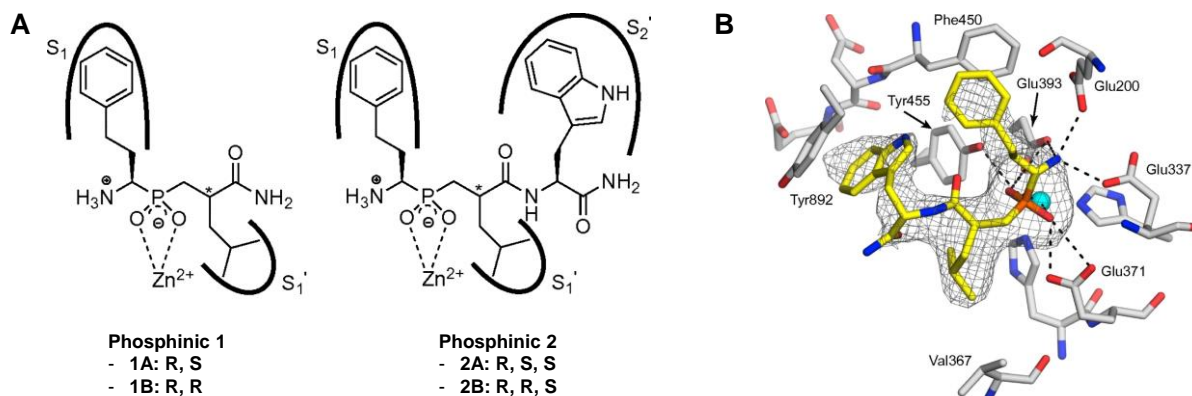


Figure 28 : (A) Schematic representation of phosphinic compounds indicating their key interacting residues. (B) Schematic representation of the crystal structure of phosphinic 2A bound inside the ERAP2 catalytic site. The mesh indicates the $jF_o - F_ej$ unbiased electron density at 2.5σ calculated before ligand addition to the structure. Phosphinic 2A is shown in yellow sticks. ERAP2 residues within 4 \AA of the inhibitor are shown in gray sticks. Oxygen are shown in red, nitrogen in blue, phosphorus in orange, and Zn(II) in cyan. Hydrogen bonding interactions which stabilize phosphinic 2A are indicated as dashed lines. Adapted from Stratikos *et al.* (63)

The phosphinic compounds (**1A**, **1B**, **2A** and **2B**) display micromolar to nanomolar activities (Table 3). Introduction of a tryptophan residue on phosphinic **1A** increases significantly the potency (phosphinic **2A**, ≈ 16 -fold for ERAP1, ≈ 50 -fold for ERAP2). For compounds containing the tryptophan residue (phosphinic **2A** and **2B**), the stereogenic carbon bearing isobutyl group displays a high influence on the potency; the (*S*)-compound (phosphinic **2A**) being more potent than the (*R*)-compound (phosphinic **2B**) (≈ 110 -fold for ERAP1 and 155-fold for ERAP2). Although exhibiting a significant increase in potency, the phosphinic compounds suffer from a lack of selectivity; the compounds demonstrate same activities on both isoforms. Additionally, they display a low bioavailability, which limits their uses in vivo.

Table 3 : Biological activity of the phosphinic **1A**, **1B**, **2A**, **2B** adapted from Stratikos *et al.* (63)

Compound	hERAP1	hERAP2
	IC ₅₀ , nM	IC ₅₀ , nM
Phosphinic 1A [R,S]	520 ± 75	547 ± 110
Phosphinic 1B [R,R]	513 ± 51	571 ± 95
Phosphinic 2A [R,S,S]	33 ± 5	11 ± 2
Phosphinic 2B [R,R,S]	3,600 ± 500	1,700 ± 200

Although working cooperatively and being structurally quite close, the ERAP enzymes do not present the same properties in particular regarding the substrate cleavages and therefore have different biological functions. Thus, effective and selective inhibition and in particular of one

isoform with respect to the other must be developed to explore the respective roles of each ERAP and therefore to better understand the biological phenomena attributable to ERAP1 and ERAP2.

Unfortunately, there are no promising pharmacological tools yet available as the published aminobenzamide and phosphonic compounds suffer from a lack of potency and/or selectivity.

In order to develop inhibitors of the ERAPs, Deprez-Poulain's team used HTS screening and rational design approaches. The HTS screening allowed the discovery of selective ERAP2 inhibitors, which bear a carboxylic acid as ZBG (Figure 29).⁽⁶⁵⁾ Although providing a high selectivity for the isoform 2, these compounds display a limited potency with activities in the micromolar range.

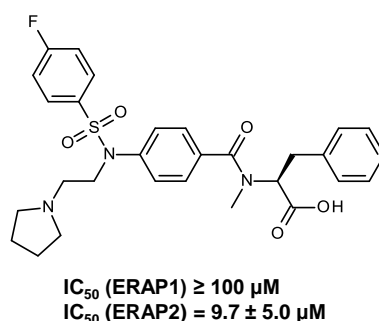


Figure 29 : Chemical structure of one carboxylic acid selective ERAP2 inhibitor

On the other hand, the team has also designed hydroxamate-bearing inhibitors of the ERAPs inhibitors by rational design. The hydroxamate function, known as a strong zinc ligand through a bidentate coordination, is notably present in potent and selective inhibitors of a large number of metalloenzymes like matrix metalloproteinases, cyclooxygenases or HDACs;⁽⁶⁶⁾ vorinostat and panobinostat being two approved HDAC inhibitors containing this ZBG. Interestingly, the designed hydroxamates for the ERAPs inhibition by Deprez-Poulain's team display different selectivity profiles. Indeed, the team has developed equipotent inhibitors of both isoforms, inhibitors of both isoforms with preference for one with respect to the other and selective ERAP1 inhibitors; both with submicromolar activities. Unfortunately, they do not have potent selective ERAP2 inhibitors so far.

IV. Objectives and strategy

In this specific area, the goal of this work is to use KTGS to identify and optimize potent (submicromolar) and selective (in particular towards ERAP1 and IRAP) ERAP2 inhibitors that will serve to decipher ERAP2 role in cancer and autoimmune disease and as starting points for drug discovery (Figure 30).

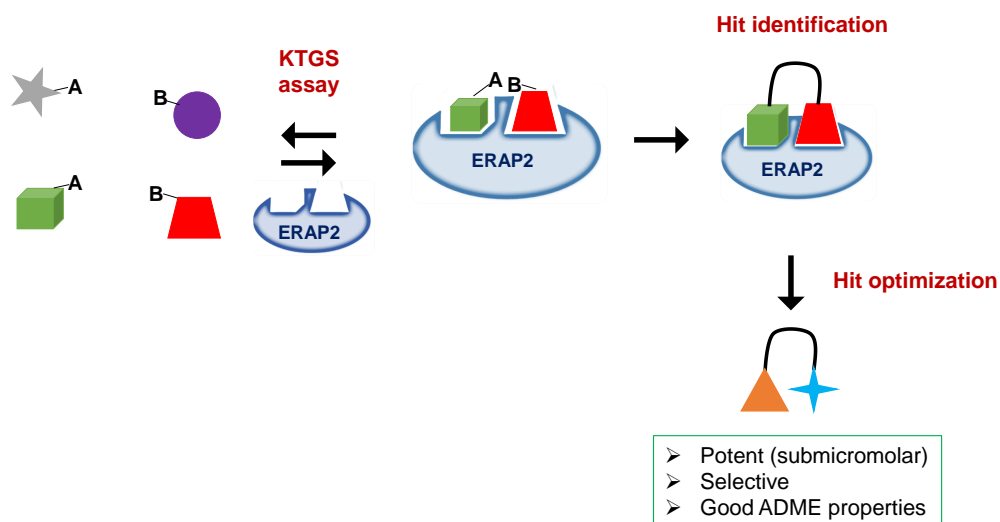


Figure 30 : objective and strategy for the ERAP2 PhD project

Results

I. Design and results of KTGS experiment to identify ERAP2 inhibitors

1. Design and synthesis of the starting building blocks

To identify new ERAP2 inhibitors, we chose to apply the KTGS strategy using the Huisgen [1,3] dipolar cycloaddition. Our six azides were from the U1177 laboratory's azide library and were derived from β -amino acids (Figure 31), which contained a hydroxamate allowing us to place the ligands in the active site using zinc coordination. The alkynes were from the U1177 laboratory's alkyne library and brought the chemical diversity.

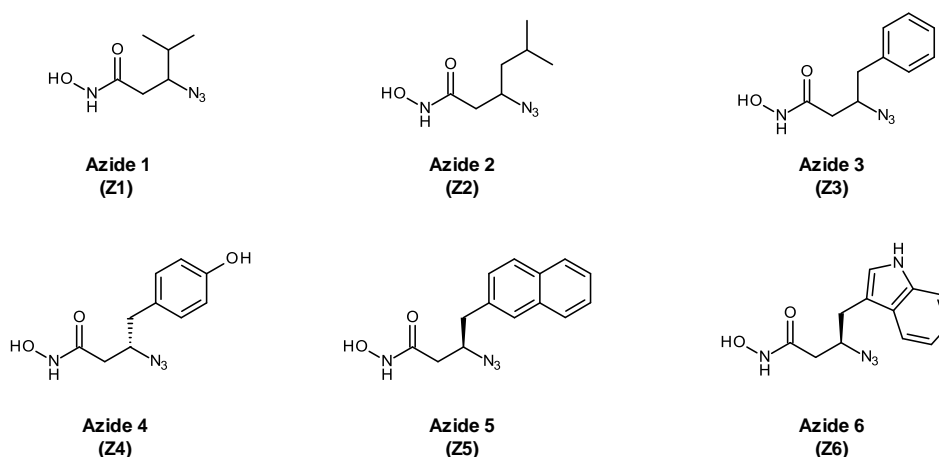


Figure 31: Chemical structures of the starting azides for the KTGS with ERAP2

2. Protein-templated reaction and controls

Regarding the assay, we used ERAP2 at 1.02 μ M, the azides and the alkynes at 100.0 μ M. The experiment was performed in 96-wells plate, each well containing one or two azides for ten alkynes (**Z1 + Z3**, **Z2 + Z5** and **Z4, Z6**).

Two control experiments were done, one without the enzyme buffer (“blank experiment”) and the other with copper in place of the enzyme solution (“chemical catalysis experiment”). The blank experiment did not contain the enzyme and allowed us to identify the unspecific couplings during the protein-templated reaction and the chemical catalysis experiment allowed us to afford the 1,4-disubstituted 1,2,3-triazole controls.

In order to validate the hits, a UPLC–MS–MS analysis using a multi MRM-method was performed after three and seven days. The hits were thus identified in each cluster by mass

and retention time and compared to both incubation with buffer in place of the enzyme (blank plate) and synthetically prepared triazoles (chemical catalysis plate).

3. Hits selection

The MS analysis led to the identification of forty six hits. An additional analysis by LC–HRMS using a time-of-flight method was performed to search for the exact mass of the expected triazoles and therefore refine the hit selection. Thus, this second HRMS analysis allowed us to confirm nineteen hits and three of these were prioritized for the chemical synthesis; these hits bearing a phenylthiophene motif (Figure 32). As the MS analysis showed perfect mass and retention time correlations between the protein-templated and copper experiments for the selected hits, we supposed that the enzyme templated the formation of the 1,4-regioisomers. Thus, we started with the chemical synthesis of the 1,4-disubstituted 1,2,3-triazoles.

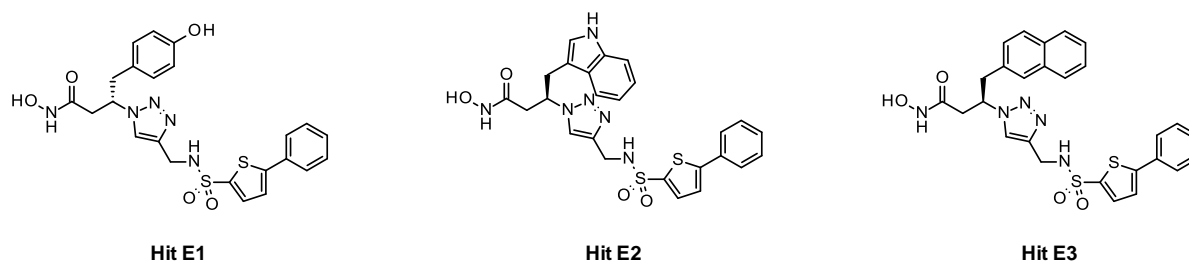


Figure 32: Chemical structures of the selected hits for the chemical synthesis

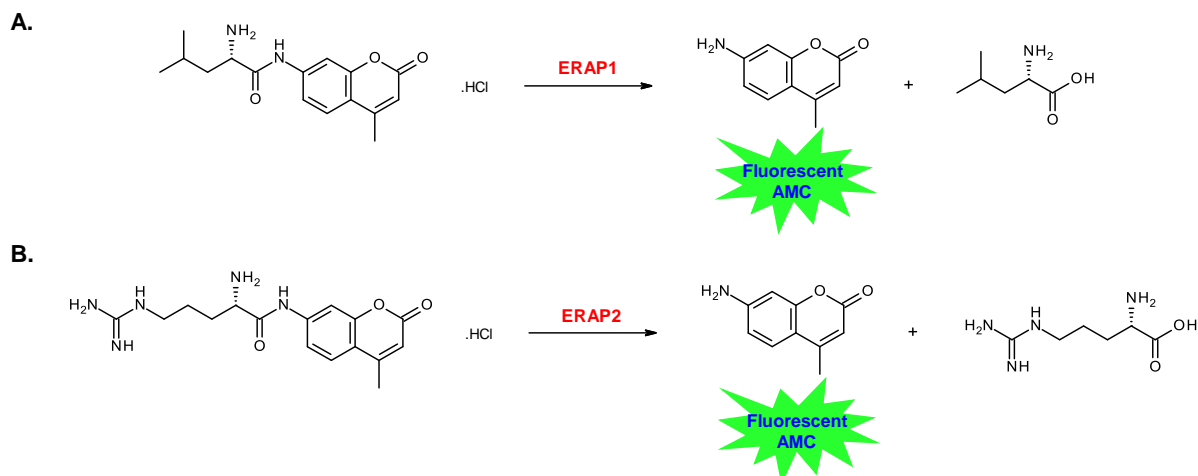
To synthesize these 1,4-triazoles (**Hit 1–3**), a copper-catalyzed click reaction was performed between the starting azides and the corresponding alkynes. Given that, I did not take part in the synthesis of these 1,4-triazoles; their chemical synthesis will not be presented and discussed here.

4. Biochemical evaluation of selected hits

A- Principle of the enzymatic assay

The enzymatic activity of our ERAP inhibitors was determined using fluorogenic peptide substrates.⁽⁶⁷⁾ L-Leucine-7-amino-4-methylcoumarine hydrochloride (L-AMC) was used for ERAP1 enzymatic activity, whereas L-Arginine-7-amino-4-methylcoumarin hydrochloride (R-AMC) was used for ERAP2 enzymatic activity. Under the action of the ERAPs, these peptides are cleaved, which releases the fluorescent AMC part (Scheme 4).

Enzyme inhibition leads to reduced substrate cleavage and consequently to reduced fluorescence.



Scheme 4: Principle of the ERAP enzymatic assay. (A) Use of L-AMC for ERAP1. (B) Use of R-AMC for ERAP2.

B- Biochemical evaluation

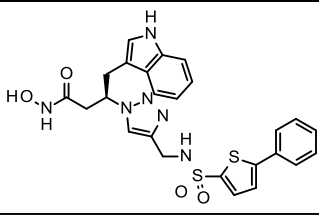
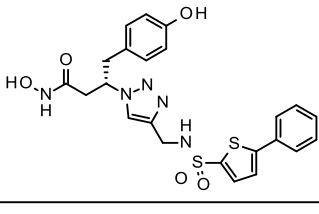
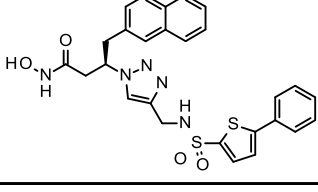
Before starting the KTGS experiment, the inhibitory activity of starting azides ERAP2 activities were determined (Table 4). Only two azides (**Z4** and **Z6**) have shown a low level of inhibition: IC_{50} = 59.0 and 64.0 μ M, respectively; the others having no activity.

Table 4 : Biochemical activities of the starting azides Z1–Z6

Compound	Chemical structure	IC_{50} ERAP2 (μ M)	Compound	Chemical structure	IC_{50} ERAP2 (μ M)
Z1		> 300	Z4		59.0
Z2		> 300	Z5		> 300
Z3		> 300	Z6		64.0

Concerning the selected, even if the aim of the KTGS was to discover new ERAP2 inhibitors, their activities on the isoform ERAP1 were also measured (Table 5).

Table 5 : Biochemical activities of the selected hits on ERAP1 and ERAP2

Compound	Chemical structure	IC ₅₀ (hERAP2) (μ M)	IC ₅₀ (hERAP1) (μ M)
Hit E2		> 100	> 100
Hit E1		3.0	> 100
Hit E3		2.3	> 100

The selected hits showed IC₅₀ values in the micromolar range. Surprisingly, no ERAP2 inhibition was observed with **hit E2**, whereas activities were found for **hit E1** and **E3**, which have the same sulfonamide moiety as **hit E2** (IC₅₀ = 3.0 and 2.3 μ M, respectively). Interestingly, no activity on ERAP1 was observed for each compound, which means the KTGS has afforded selectivity for ERAP2.

5. Conclusions

Although most of our warhead-bearing reagents (azide) displayed no ERAP2 activity (Table 4), the KTGS strategy allowed us to identify templated ligands with a selectivity for ERAP2 (no activity on ERAP1) and low micromolar activity, making them promising hits.

Thus, these results constitute good starting points and SARs have been carried out.

II. Preliminary Structure – Activity Relationships

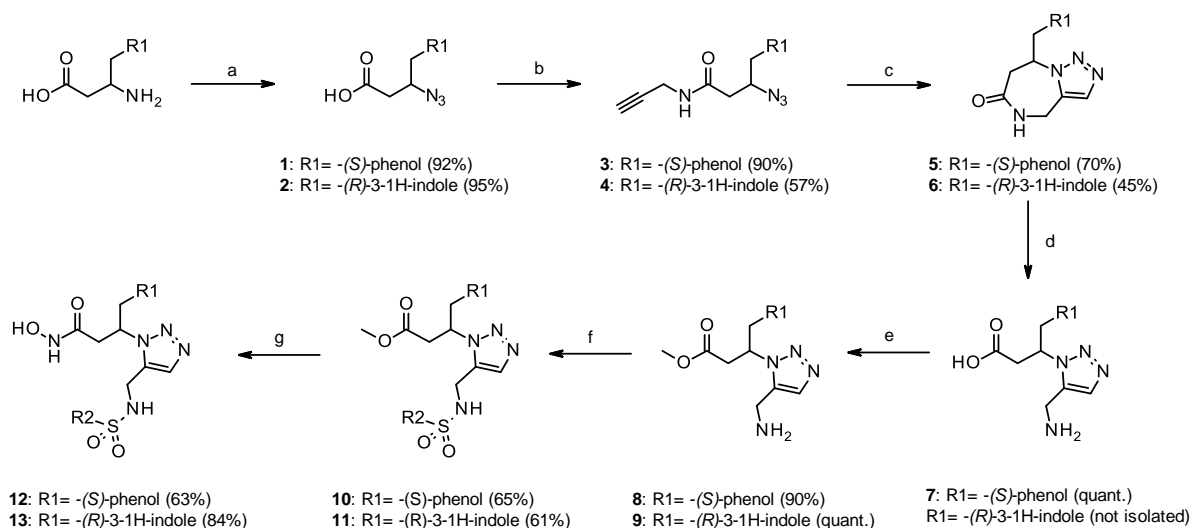
After being interested in the 1,4-regioisomers, we then synthesized the 1,5-triazoles to know if they would display activity values in the same range as the other regioisomers.

1. 1,5-Disubstituted 1,2,3-Triazoles

Compared to the 1,4-triazole, the access to the 1,5-regioisomer is difficult; that is why only the β -tryptophan and β -tyrosine analogs were synthesized. The β -naphthylalanine analog was not synthesized for solubility reasons; we supposed that its solubility would be lower than the others and could be a problem for the future.

A- Chemical synthesis

The 1,5-triazoles were obtained by a succession of seven steps (Scheme 5): diazo transfer (a), amide coupling using propargylamine (b), intramolecular Huisgen cycloaddition (c)⁽⁶⁸⁾, lactam hydrolysis (d) followed by esterification (e), sulfonamide formation by nucleophilic substitution (f) and aminolysis (g); the intramolecular Huisgen cycloaddition being the key step to form the 1,5-triazole by cycle constraint.



Reagents and conditions: (a) azide-*N*-diazoimidazole-1-sulfonamide hydrogen sulfate, K_2CO_3 , $ZnCl_2$, DIPEA, MeOH, 0 °C to rt., overnight, 92–95%; (b) propargylamine, HBTU, Et_3N , DMF, rt., overnight, 57–90%; (c) DMF, reflux, overnight, 45–70%; (d) HCl, H_2O , 85 °C, MW, 1 h, quant. yield; (e) $SOCl_2$, MeOH, 0°C to rt., overnight, 90–quant. yield; (f) sulfonyl chloride, DIPEA, DMF, 0°C to rt., overnight, 61–65%; (g) KCN, NH_4OH/H_2O (1/1 : w/w), MeOH, rt, overnight, 63–84%.

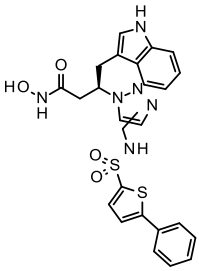
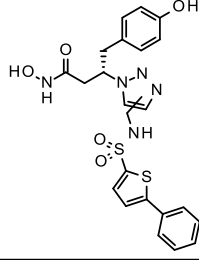
Scheme 5 : Seven-step synthesis of 1,5-triazoles

B- Biochemical evaluations

A “slight” increase of ERAP2 inhibition was observed with the 1,5-regioisomers (**12**) compared to the 1,4-: $IC_{50} = 0.8$ vs 3.0 μM . Unfortunately, no ERAP2 inhibition was detected

for the beta-homo-tryptophan 1,5-triazole analog (**13**) by analogy to the 1,4-regioisomer. Interestingly, the selectivity for the isoform 2 was kept for the 1,5-triazole (Table 6).

Table 6: Comparison of ERAP activities between 1,4- and 1,5-triazoles

Chemical structure	Compound	Regioisomer	IC ₅₀ (hERAP2) (μM)	IC ₅₀ (hERAP1) (μM)
	Hit E2	1.4	> 100	> 100
	13	1.5	> 100	> 100
	Hit E1	1.4	3.0	> 100
	12	1.5	0.8	> 100

C- Conclusion

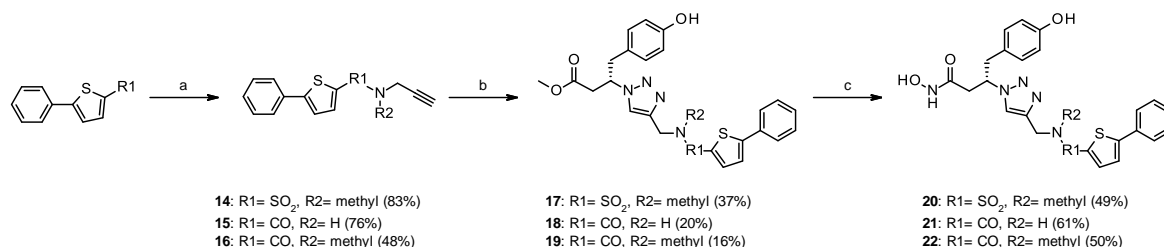
Based on these results, the 1,5-disubstituted 1,2,3-triazole seems slightly more potent than the 1,4-analog. The β-tryptophan analog, in 1,5-configuration did not show activity as the 1,4-regioisomer.

2. Sulfonamide “linker”

After focusing on 1,5-triazoles, we replaced the sulfonamide to know if ERAP2 could support other linkers. *N*-methylsulfonamide, amide with a spacer methylene and *N*-methylamide analogs were synthesized, using β-homo tyrosine. These compounds were synthesized in 1,4-configuration for chemical accessibilities reasons.

A- Chemical synthesis

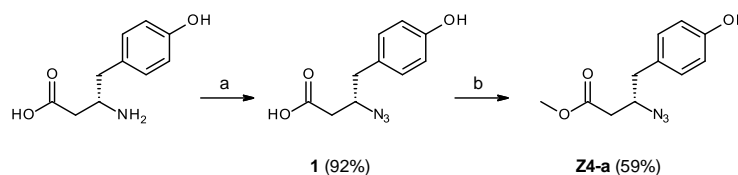
The final compounds were synthesized in three steps (Scheme 6): alkyne formation (a), copper-catalyzed click reaction (b) and aminolysis (c).



Reagents and conditions: (a) R1=sulfonyl chloride: *N*-methylpropargylamine, DIPEA, CH₂Cl₂, 0 °C to rt., overnight, 83% or R1=carboxylic acid, propargylamine or *N*-methylpropargylamine: HBTU, Et₃N, rt., overnight, 48–76%; (b) **Z4-a**, CuSO₄ (5H₂O), sodium ascorbate, DMF/H₂O, rt., overnight, 16–37%; (c) KCN, NH₂OH/H₂O (1/1 : w/w), MeOH, rt., overnight, 49–61%.

Scheme 6: Chemical synthesis of the hydroxamic acids 30–31 in three steps

The needed azide (**Z4-b**) for the click reaction was previously synthesized in two steps: diazo transfer (a) and esterification (b) (Scheme 7).



(a) azide-*N*-diazoimidazole-1-sulfonamide hydrogen sulfate, K₂CO₃, ZnCl₂, DIPEA, MeOH, 0 °C to rt., overnight; (b) SOCl₂, MeOH, 0 °C to rt, overnight; (c) KCN, NH₂OH/H₂O (1/1 : w/w), MeOH, rt, overnight.

Scheme 7: Chemical synthesis of the azide Z4-a

B- Biochemical evaluation

Regarding the sulfonamide linker (**hit E1**), its *N*-methylation (**20**) did not affect the activity significantly, whereas its replacement by amide (**21**) and *N*-methylamide (**22**) led to a loss of the activity. Surprisingly, an ERAP1 activity was retrieved with the amide linker (**21**). The selectivity for ERAP2 was also maintained with the *N*-methylsulfonamide linker (**20**) (Table 7).

Table 7: Biochemical activities of ERAP2 hit 1 and 20–22

Compound	R	IC ₅₀ (hERAP2) (μM)	IC ₅₀ (ERAP1) (μM)
Hit 1		3.0	> 100
20		6.0	> 100
21		> 100	28.0
22		> 100	> 100

C- Conclusions

Firstly, as the sulfonamide replacement by amide or *N*-methanamide leads to a loss of activity on ERAP2, and secondly, as its methylation decreases the solubility, the sulfonamide linker has been kept for the other modulations.

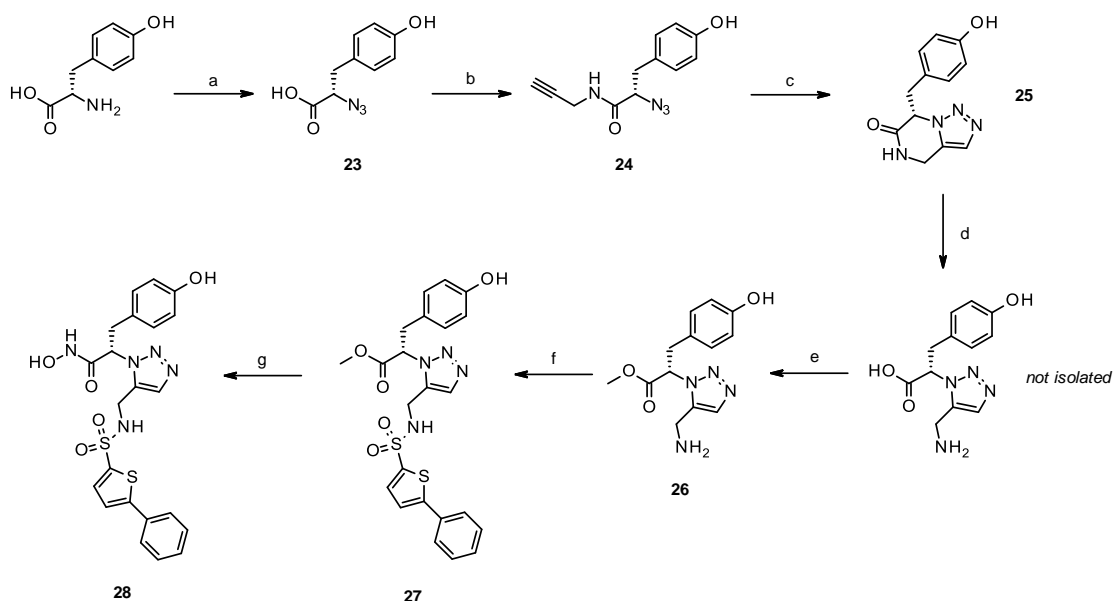
3. Homologation n-1: switch to α -amino acid series

The KTGS experiment was performed from β -amino acids. We therefore decided to switch to α -amino acids, in 1,4- and 1,5-configuration.

A- For 1,5-triazoles

- Chemical synthesis

The α -analog, from the L-tyrosine was synthesized using the route described in the Scheme 2 (Scheme 8). Due to lack of time, the tryptophan analog could not be synthesized.



Reagents and conditions: (a) azide-*N*-diazoimidazole-1-sulfonamide hydrogen sulfate, K_2CO_3 , $ZnCl_2$, DIPEA, MeOH, 0 °C to rt., overnight, 94%; (b) propargylamine, HBTU, Et_3N , DMF, rt, overnight, 50%; (c) DMF, reflux, overnight, 48%; (d) HCl, H_2O , 85–100 °C, MW, 3h; (e) $SOCl_2$, MeOH, 0 °C to rt, overnight, 89%; (f) sulfonylchloride, DIPEA, DMF, 0 °C to rt., overnight, 29%; (g) KCN, NH_2OH/H_2O (1/1 : w/w), MeOH, rt, overnight, 25%.

Scheme 8: Chemical synthesis of 28

- Biochemical evaluation

Deletion of the methylene group (**28**) was tolerated, but with a decrease in potency compared to the β -compound (**12**); ERAP2 selectivity was maintained in α -configuration (Table 8).

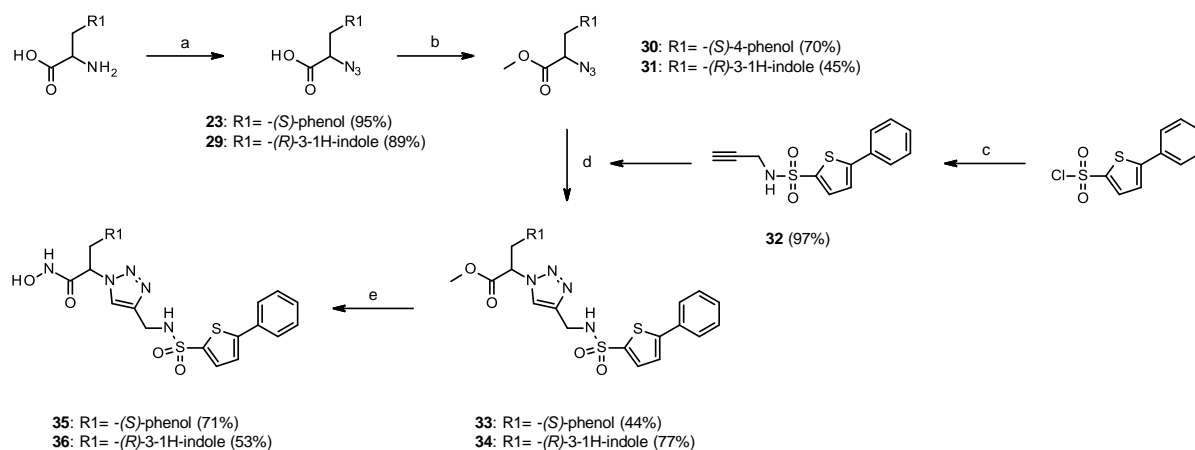
Table 8: Comparison of ERAP activities between β - and α - 1,5-triazoles

Chemical structure	Compound	n	IC ₅₀ (hERAP2) (μ M)	IC ₅₀ (hERAP1) (μ M)
	12	1	0.8	> 100
	28	0	3.3	> 100

B- For 1,4-triazoles

- Chemical synthesis

The 1,4-disubstituted 1,2,3-triazoles were synthesized in four steps from the corresponding α -amino acid (Scheme 9): diazo transfer (a), esterification (b), copper-catalyzed click reaction (d) and aminolysis (e). The needed alkyne for the click reaction was also synthesized using a nucleophilic acyl substitution of the propargylamine on the sulfonyl chloride (c).



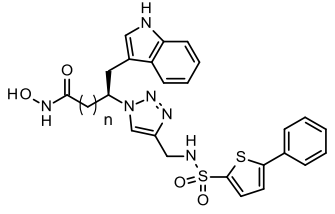
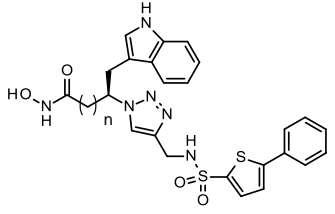
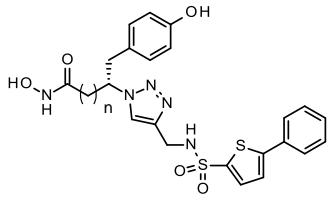
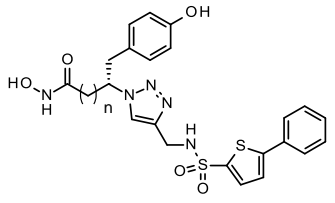
Reagents and conditions: (a) azide-*N*-diazoimidazole-1-sulfonamide hydrogen sulfate, K₂CO₃, ZnCl₂, DIPEA, MeOH, 0 °C to rt., overnight, 89–95%; (b) SOCl₂, MeOH, 0 °C to rt., overnight, 45–70%; (c) propargylamine, DIPEA, CH₂Cl₂, 0 °C to rt, overnight, 97%; (d) **32**, CuSO₄, sodium ascorbate, DMF/H₂O, rt., overnight, 44–77%; (e) KCN, NH₂OH/H₂O (1/1 : w/w), MeOH, rt, overnight, 53–71%.

Scheme 9 : Chemical synthesis of the compound 35–36 in four steps

- Biochemical evaluation

In the D-tryptophan series, deletion of the methylene group did not restore the activity on ERAP2 (**36**), while it led to a four-fold gain in ERAP2 activity in the L-tyrosine (**35**) series: $IC_{50} = 0.8$ vs $3.0 \mu\text{M}$; ERAP2 selectivity being maintained in α -1,4 series (Table 9).

Table 9 : Comparison of ERAP activities between β - and α -1,4-triazoles

Chemical structure	Compound	n	IC_{50} (hERAP2) (μM)	IC_{50} (hERAP1) (μM)
	Hit E2	1	> 100	> 100
	36	0	> 100	> 100
	Hit E1	1	3.0	> 100
	35	0	0.8	> 100

C- Conclusions

For the 1,5-triazoles, deletion of the methylene group is tolerated in the tyrosine series but decreases ERAP2 inhibition by a factor of 4 (**12**, $IC_{50} = 0.8$ vs $3.3 \mu\text{M}$ for **28**). Thus, the 1,5-disubstituted 1,2,3-triazole are more potent in β -configuration than in α -configuration (Table 10).

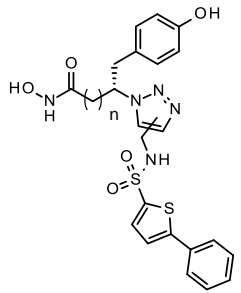
For the 1,4-triazoles, although deletion of the methylene group does not allow to retrieve ERAP2 inhibition in the D-tryptophan series, it is beneficial in the tyrosine series. Indeed, in the tyrosine series, this switch to α -configuration increases the ERAP2 activity by almost 4-fold (**35**, $IC_{50} = 0.8$ vs $3.0 \mu\text{M}$ for **Hit E1**). Thus, the 1,2,3-triazole 1,4-disubstituted are more potent in α -configuration than in β -configuration (Table 10).

The ERAP2 selectivity is kept in the α -series, as in β -series for the 1,4- and the 1,5-triazoles.

Thus, regarding these results, two families of ERAP2 inhibitors can be distinguished:

- Family 1: 1,4-disubstituted 1,2,3-triazoles in α -configuration
- Family 2: 1,5-disubstituted 1,2,3-triazoles in β -configuration

Table 10 : Comparison of ERAP activities between 1,5- and 1,4-triazoles in β - and α -configuration for the tyrosine analogs

Chemical structure	Compound	n	Regioisomer	IC ₅₀ (hERAP2) (μ M)	IC ₅₀ (hERAP1) (μ M)
	12	1	1,5	0.8	> 100
	28	0	1,5	3.3	> 100
	Hit E1	1	1,4	3.0	> 100
	35	0	1,4	0.8	> 100

Subsequent to the KTGS assay and the preliminary SARs, two families of selective ERAP2 inhibitors were identified with activity values in the submicromolar range; which makes them interesting starting points for further SARs.

III. Extended Structure – Activity Relationships

1. Family 1: 1,4-disubstituted 1,2,3-triazoles in α -configuration

Three parts on **22** were identified for the pharmacomodulations in this family (Figure 33): the configuration (yellow), the “south-part” corresponding to the phenylthiophene group (blue), the “north-part” corresponding to the phenol group (green).

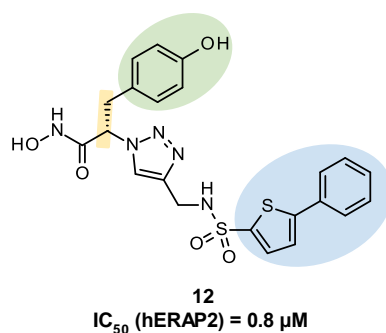


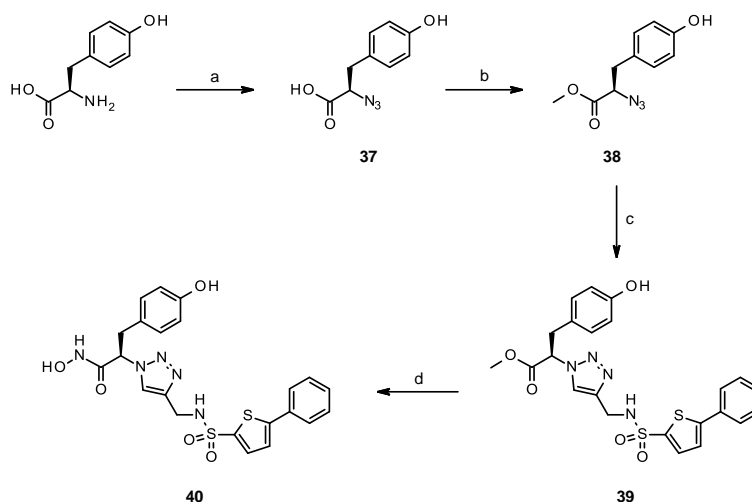
Figure 33 : Identified parts of compound 12 for the pharmacomodulations concerning the family 1

A- Configuration

To know if the configuration would be a key element for the activity and selectivity, the *R*-analog was synthesized from D-tyrosine.

- Chemical synthesis

The *R*-compound was synthesized in four steps, following the route described previously for the 1,2,3-triazole 1,4-disubstituted: diazo transfer (a), esterification (b), copper-catalyzed click chemistry (c) and aminolysis (e) (Scheme 10).



Reagents and conditions: (a) azide-*N*-diazoimidazole-1-sulfonamide hydrogen sulfate, K_2CO_3 , $ZnCl_2$, DIPEA, MeOH, 0 °C to rt., overnight, 76%; (b) $SOCl_2$, MeOH, 0 °C to rt, overnight, 60%; (c) **32**, $CuSO_4 \cdot (5H_2O)$, sodium ascorbate, DMF/ H_2O , rt., overnight, 73%; (e) KCN, NH_2OH/H_2O (1/1 : w/w), MeOH, rt., overnight, 74%.

Scheme 10 : Chemical synthesis of the *R*-analog 40 in four steps

- Biochemical evaluation

The switch to *R*-configuration did not affect the ERAP2 activity significantly: IC_{50} for **40** = 1.3 vs 0.8 μM for **35** and it was the same for the selectivity: no hERAP1 activity was observed in *R*-configuration.

- Conclusions

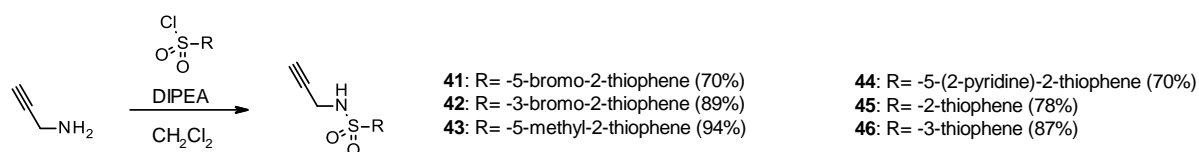
No significant effects on the activity and selectivity were observed with the *R*-analog; we decided to continue with the *S*-compound. The racemic mixture has to be synthesized for comparison.

B- South-part

After demonstrating that *S*- and *R*-configurations are equipotent, we continued with the modification of the phenylthiophene moiety and synthesized six corresponding analogs.

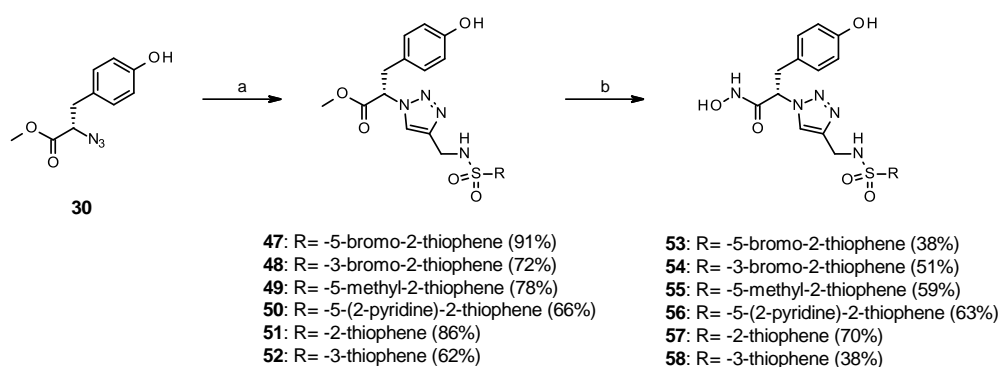
- Chemical synthesis

Before to start the synthesis of the final analogs, the alkynes needed for the triazole formation were synthesized using a nucleophilic acyl substitution by propargylamine on the corresponding sulfonyl chlorides (Scheme 9, step c), as described previously (Scheme 11).



Scheme 11 : Synthesis of alkynes 41–46

The final compounds were synthesized using a copper-catalyzed click reaction and aminolysis (Scheme 12), as also described previously.



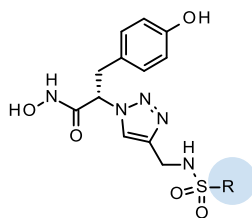
Reagents and conditions: (a) alkyne (**41–46**), CuSO₄ (5H₂O), sodium ascorbate, DMF/H₂O, rt., overnight, 62–91%; (b) KCN, NH₂OH/H₂O (1/1: w/w), MeOH, rt., overnight, 38–70%.

Scheme 12 : Synthesis of the final compounds 53–58 and their respective intermediate 47–52

- Biochemical evaluation

First, the replacement of the phenyl by 5-(2-pyridine) did not have an influence on the activity (**56**, IC₅₀ = 0.5 μM). Next, its replacement by 5-methyl (**55**), 5- or 3-bromine (**53** and **54**) led to a decrease in the IC₅₀; 2 to 6-fold drop compared to **35**. Surprisingly, the phenyl removal (**57**) proved to be in the same range of activity as the initial compound **35** (IC₅₀ = 0.6 vs 0.8 μM). Then, based on this result, the 2-thiophene was replaced by 3-thiophene (**58**) reducing the activity by a factor of six. In each case of active compound, the ERAP2 selectivity was kept (Table 11).

Table 11 : Biochemical activities of the compounds 45 and 63–68



Compound	R	IC ₅₀ (hERAP2) (μ M)	IC ₅₀ (hERAP1) (μ M)
35	-5-phenyl-2-thiophene	0.8	> 100
56	-5-(2-pyridine)-2-thiophene	0.5	> 100
55	-5-methyl-2-thiophene	4.9	> 100
53	-5-bromo-2-thiophene	1.6	> 100
54	-3-bromo-2-thiophene	2.7	> 100
57	-2-thiophene	0.6	> 100
58	-3-thiophene	3.7	> 100

- Conclusions

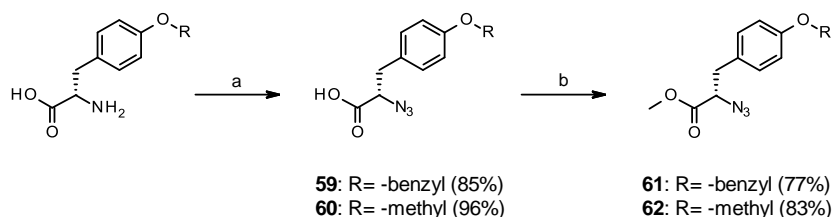
The phenyl replacement did not allow us to increase significantly the potency; **56** and **57** displaying activity values in the same range as **35**.

C- Northern part

After changing the southern part, we explored the chemical space around the phenol moiety by hydroxyl substitutions: *O*-benzyl, *O*-*tert*-butyl and *O*-methyl.

- Chemical synthesis

The needed methyl ester azides for the triazole formation were synthesized according to the routes described on Scheme 9, from commercial tyrosine analogs (Scheme 13).

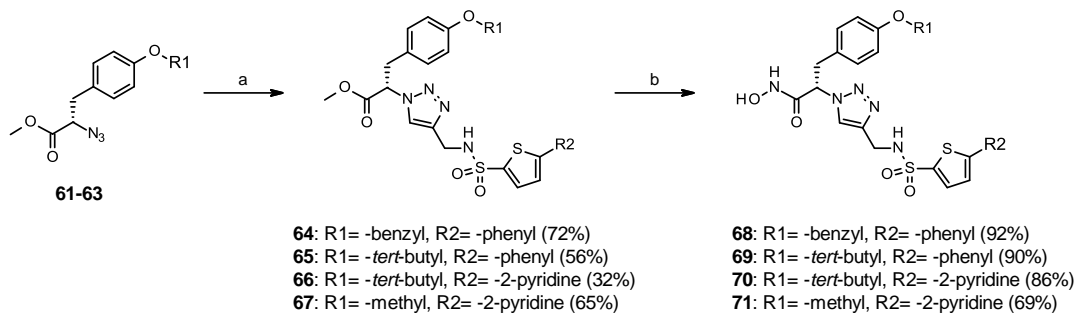


Reagents and conditions: (a) azide-*N*-diazoimidazole-1-sulfonamide hydrogen sulfate, K₂CO₃, ZnCl₂, DIPEA, MeOH, 0 °C to rt., overnight, 85–96% ; (b) SOCl₂, MeOH, 0 °C to rt., overnight; 77–83%

Scheme 13 : Synthesis of the azides 61–62

Unfortunately, in case of the *tert*-butyl derivative, we observed de-*tert*-butylation during the esterification; that is why we decided to perform the diazo transfer directly from the azide to get the needed methyl ester azide (**63**, 50% yield).

The final compounds were synthesized in two steps (Scheme 14) using the routes described previously.



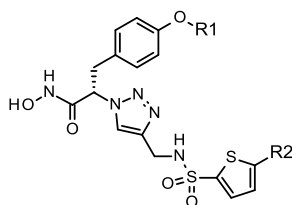
Reagents and conditions: a) alkyne (**32** or **44**), CuSO₄ (5H₂O), sodium ascorbate, DMF/H₂O, rt., overnight, 32–72%; b) KCN, NH₂OH/H₂O (1/1: w/w), MeOH, rt., overnight, 69–92%.

Scheme 14 : Synthesis of the final compounds 78–81 and their respective intermediates 74–77

- Biochemical evaluation

The *O*-benzylation (**68**) was deleterious for the IC₅₀, the activity being completely lost in this case whereas the *O*-*tert*-butylation (**69**) was beneficial, increasing the potency by more than two compared to **35** (IC₅₀ = 0.3 vs 0.8 μM for **35**). As seen before, for the southern part exploration, the phenyl replacement by a 2-pyridine (**56**) led to a “slight” increase in the IC₅₀ (0.5 vs 0.8 μM for **35**). We therefore decided to “combine” the southern part results with the northern part results (phenyl replacement by 2-pyridine and *O*-*tert*-butylation) to synthesize **70**. It resulted in a seven-fold gain of activity compared to **56** (IC₅₀ = 0.07 to 0.5 μM) and 11-fold gain compared to **35** (IC₅₀ = 0.07 to 0.8 μM). Finally, as the *tert*-butyl group has shown instability, it was replaced by a methyl (**71**) increasing the potency by a factor of eighteen compared to the *tert*-butyl analog **70** (IC₅₀ = 4 vs 70 nM). In each case, interestingly, no ERAP1 activity was observed (Table 12).

Table 12 : Biochemical activities of the compounds 35, 56 and 68–71

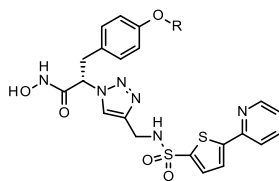


Compound	R1	R2	IC ₅₀ (hERAP2) (μ M)	IC ₅₀ (hERAP1) (μ M)
35	-H	-phenyl	0.8	> 100
56	-H	-2-pyridine	0.5	> 100
68	-benzyl	-phenyl	> 100	> 100
69	- <i>tert</i> -butyl	-phenyl	0.3	> 100
70	- <i>tert</i> -butyl	-2-pyridine	0.07	> 100
71	-methyl	-2-pyridine	0.004	> 100

- Conclusions

The *O*-substitution, in particular with non-bulky groups, is beneficial for the activity and, noteworthy, did not affect the selectivity for the isoform 2. However, it drastically decreases the solubility (Table 13). Interestingly, the compounds are stable in plasma and display intermediate metabolic stability values in mouse.

Table 13 : comparison between the compounds 56 and 81 according to their activity, LogD, solubility, plasma (mouse) and microsomal stabilities



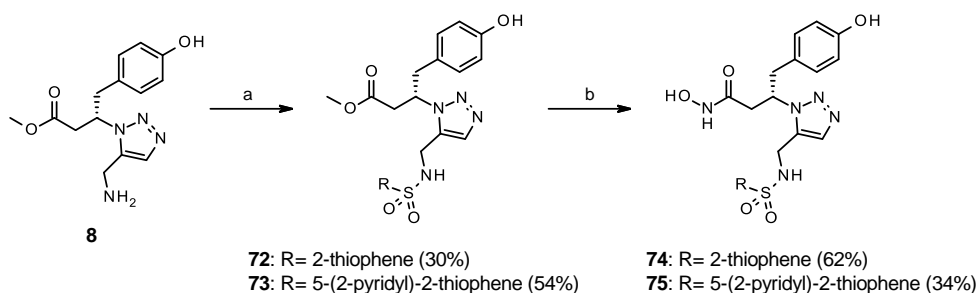
Compound	R	IC ₅₀ (hERAP2) (μ M)	LogD	Solubility (μ M)	Plasma Stab <i>t</i> _{1/2} [h]	Microsomal stab <i>t</i> _{1/2} [min]
56	-H	0.5	1.3	154	> 6	23.9
71	-methyl	0.004	1.8	11	> 24	40

2. Family 2: 1,5-disubstituted 1,2,3-triazoles in β -configuration

After studying the α -1,4-family, we continued with the exploration of the β -1,5-family. A focused SAR from the β -tyrosine compound (**12**, $IC_{50} = 0.8 \mu M$) was performed, in particular on the phenylthiophene moiety.

A- Chemical synthesis

The final analogs were obtained using the routes described earlier in Scheme 2 using a nucleophilic acyl substitution and aminolysis (Scheme 15).



Scheme 15 : Synthesis of the compounds 74–75 and their respective intermediates 72–73

B- Biochemical evaluation

Surprisingly, contrary to the α -1,4-family, the phenyl removal (**74**) was deleterious for the activity ($IC_{50} > 100 \mu M$). As the phenyl replacement by 2-pyridyl was beneficial for the IC_{50} in α -series, we reproduced the same replacement (**75**), which did not improve the activity here ($IC_{50} = 1.2$ vs $0.8 \mu M$ for **12**) (Table 14).

Table 14 : Biochemical activities of the compound 12 and 74–75

Compound	R	IC_{50} (hERAP2) (μM)	IC_{50} (hERAP1) (μM)
12	5-phenyl-2-thiophene	0.8	> 100
74	2-thiophene	> 100	> 100
75	5-(2-pyridyl)-2-thiophene	1.2	> 100

Due to a lack of time, only two analogs were synthesized; exploring the phenylthiophenyl group. Therefore, more analogs must be synthesized to extend our scope of investigation

concerning this part. Then, as in α -1,4-series, the phenol moiety needs to be investigated to know if it could have a positive impact on the activity and physicochemical properties; **12** displaying acceptable ADME profile: LogD = 2.7, solubility = 179 μ M, plasma stability (mouse) $t_{1/2}$ > 6 h and microsomal stability $t_{1/2}$ = 15.8 min.

IV. Selectivity-profile studies

One compound of each family was selected for a selectivity profiling (Table 15). Each compound has been tested against eight other zinc metalloproteases included ERAP1, IRAP (Insulin-Regulated Aminopeptidase), APN (Aminopeptidase N), TACE and the MMPs -1, -2 and -3. Strikingly, each compound is selective for the isoform 2 of the ERAPs. **71** displays IRAP and APN inhibition but is still selective for ERAP2 (by 50-fold compare to IRAP and -250 compared to APN); these two enzymes being involve in the hormone and hormone peptide degradations (e.g. oxytocin, vasopressin or angiotensin III). **71** did not exhibit inhibition of the MMPs -1, -2 and -3 but showed activity on TACE.

Concerning **12** (β -1,5 series), no ERAP1 inhibition was observed but it showed activities on IRAP and APN and, in particular, a lower IC_{50} on IRAP than on ERAP2 (0.1 μ M for IRAP vs 0.8 μ M for ERAP2).

Table 15 : Selectivity profiles of 12 and 71

Compound	ERAP2	ERAP1	IRAP	APN	TACE	MMP -1, -2, -3
71	IC_{50} = 0.004 μ M	IC_{50} > 100 μ M	IC_{50} = 0.2 μ M	IC_{50} = 1.0 μ M	88% inh @ 20 μ M	< 30% inh @ 20 μ M
12	IC_{50} = 0.8 μ M	IC_{50} > 100 μ M	IC_{50} = 0.1 μ M	IC_{50} = 5.0 μ M	To be measured	To be measured

Thus, further SAR studies are required to refine and enhance the selectivity profile of our ERAP2 inhibitors, in particular on IRAP.

V. Binding mode study

To elucidate the binding mode of our compounds in the active site of ERAP2, co-crystallizations were performed with **56** (1.4-triazole) and **12** (1.5-triazole) by Prof. Stratikos in Athens; their chemical structures are presented below together with their IC_{50} values (Figure 34).

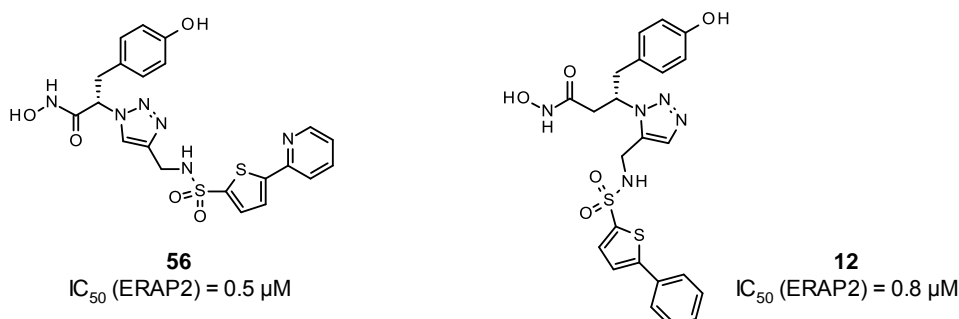


Figure 34 : Chemical structures of **56** and **12** and their IC_{50} values on ERAP2

Concerning the binding of **56** in ERAP2, we observed a surprising folding of **56** in the active site, which can probably be explained by the flexibility provided by the methylene spacer between the triazole and the nitrogen of the sulfonamide (Figure 35).

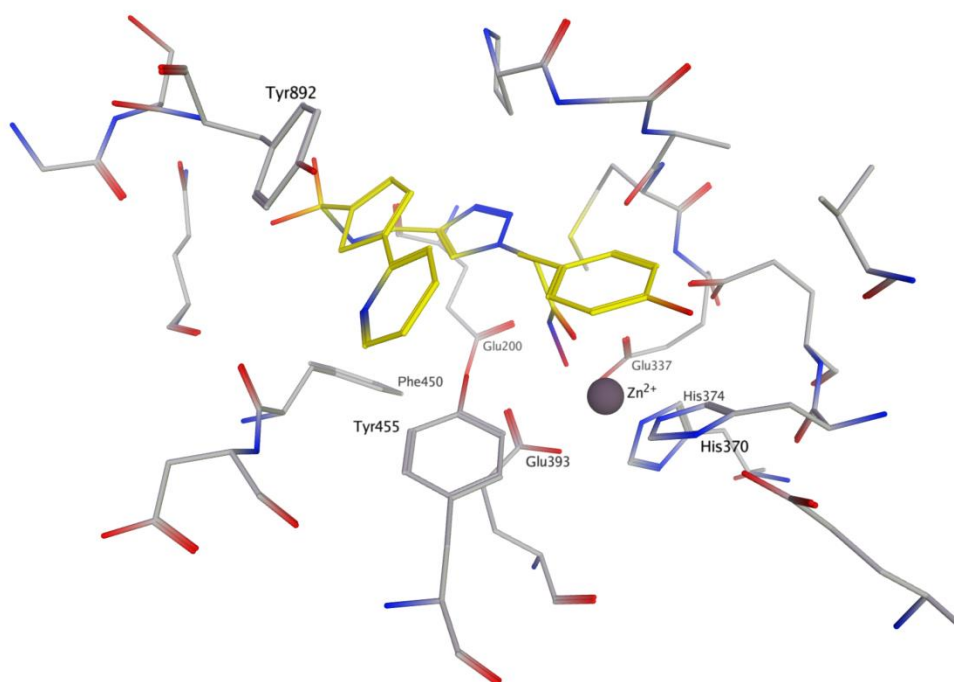


Figure 35 : Binding mode of **56** in ERAP2. **56** is represented in yellow, the active site residues of ERAP2 in gray, the zinc as a gray sphere, oxygen and nitrogen are in red and blue, respectively.

The hydroxamate coordinates the zinc and the nitrogen of it interacts with a glutamate residue (Glu200) through a hydrogen bond. The pyridine thiophene moiety lines a hydrophobic

pocket, which contains two important tyrosine residues for the binding of **56** (Tyr892 and 455); the thiophene interacting with the tyrosine 892 and the pyridine with the tyrosine 455 through π - π interactions. Interestingly, a valine residue (Val367) is close to the phenol moiety of **56**. The presence of this residue could be explained why the *O*-substitution of the phenol by methyl or *tert*-butyl increases significantly the activity (Figure 36).

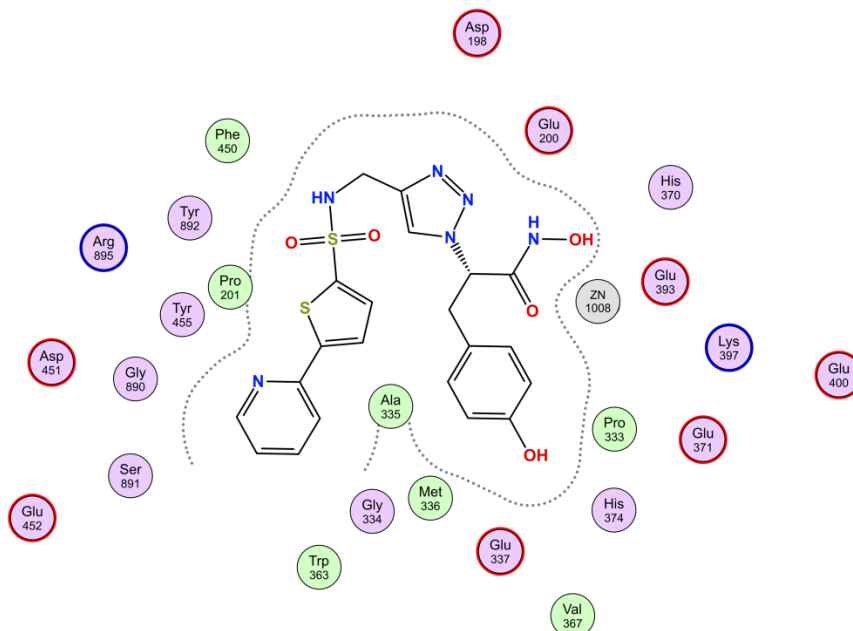


Figure 36 : 2D representation of the binding mode of **56 in ERAP2.**

For the 1,5-triazole **12**, unsurprisingly, the binding of **12** in ERAP2 is totally different as for **56** (Figure 37).

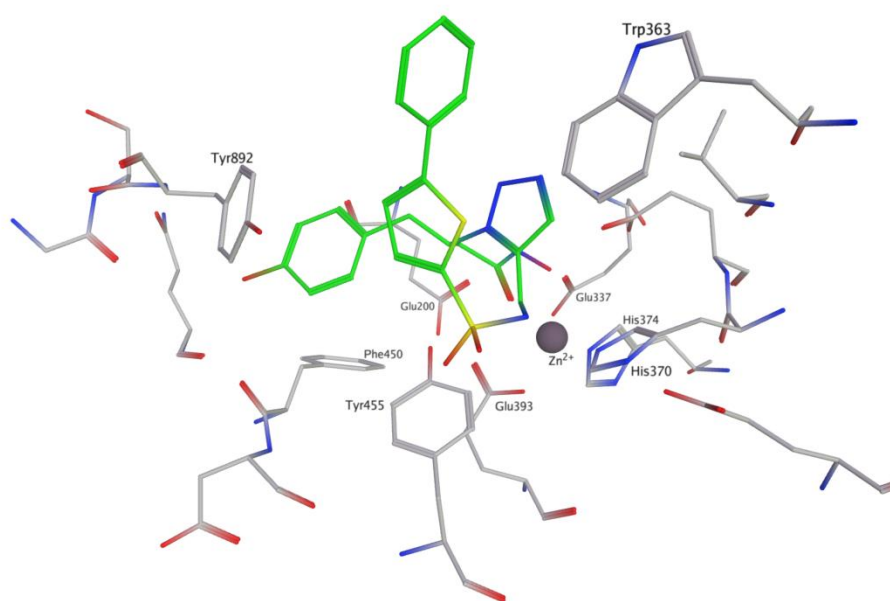


Figure 37 : Binding mode of **12 in ERAP2. **56** is represented in green, the active site residues of ERAP2 in gray, the zinc as a gray sphere, oxygen, sulfur and nitrogen are in red, yellow and blue, respectively.**

We also observed a fold of the compound in the active site allowing an interaction between the triazole and the thiophene of **12**, and between the phenol and the phenyl of **12**. The phenol moiety interacts with a tyrosine residue through a π - π interaction. Additionally, the phenyl interacts with a tryptophan residue (Trp363) through a π - π interaction also (Figure 38).

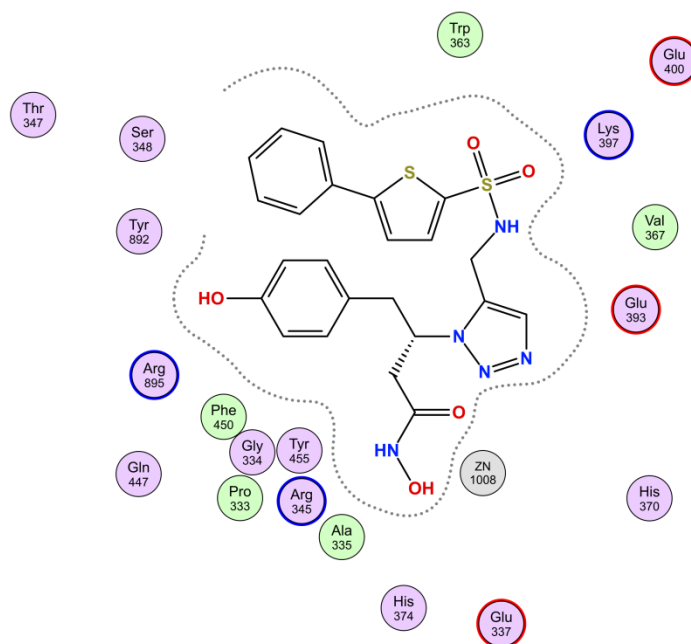


Figure 38 : 2D representation of the binding mode of 12 in ERAP2.

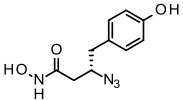
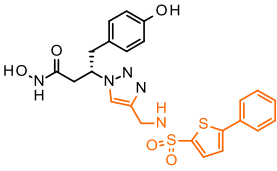
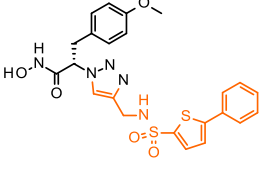
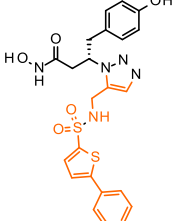
Conclusion & perspectives

Thus, the use of the KTGS approach allowed us to discover two new families of selective ERAP2 inhibitors, one with nanomolar activities (α -1,4 family) and the other with submicromolar activities (β -1,5 family); these compounds are the first selective ERAP2 inhibitors with submicromolar activities.

Strikingly, the triazole formation allowed us to increase the activity by 20-fold and 70-fold in 1,4- and 1,5-substitution respectively compared to the starting azide (**Z4**); the 1,5-regioisomer being more potent than the 1,4. Hit **E1** and **12** exhibited a LLE higher than 3 and thus represented promising starting points for the hit optimization step. SAR studies, in the α -1,4 family, led to a high increase in the potency ($IC_{50} = 3.0 \mu M$ for hit **E1** vs $0.004 \mu M$ for **71**) especially through *O*-substitution of the phenol and increasing therefore the LLE (3.2 vs 7.1) (Table 16).

Concerning the β -1,5 family, due to a lack of time, only a limited number of compounds were synthesized and they displayed higher IC_{50} values than the initial hit (**12**).

Table 16 : IC_{50} , LE and LLE comparisons between the starting azide, the most potent hit (1,4 and 1,5-regioisomers) and a optimized compound in α -1,4 family. LE and LLE were calculated using Datawarrior software from the IC_{50}

Compound	Chemical structure	IC_{50} (hERAP2)	Ligand Efficiency (LE)	Lipophilic Ligand Efficiency (LLE)
Z4		59.0 μM	0.3	3.8
Hit E1		3.0 μM	0.2	3.2
71		0.004 μM	0.3	7.1
12		0.8 μM	0.2	3.7

Further SAR studies are required to continue the exploration and in particular to enhance the selectivity profile of our compounds in both families.

In α -1,4 family, as the *O*-substitution drastically decreases the solubility (11 μ M), polar groups must be introduced to solve this problem.

In β -1,5 family, more analogs have to be synthesized in order to refine the selectivity profile of this family. We have to continue the exploration about the thiophene substitution and the *R*-compound has to be synthesized to judge its impact on the activity and the selectivity. Moreover, the linker sulfonamide has not yet been explored and thus can be replaced through *N*-methylsulfonamide, amide or *N*-methanamide linkers as we did in 1,4-configuration.

Finally, for each family, if the hydroxamic acid becomes a problem for the selectivity in the future, it is possible to replace it by other ZBGs such as sulfamate, boronate or phosphonate.

Chapter 3: KTGS leads to the identification of potent and selective LasB inhibitors

Introduction

Along with the vaccines, antibiotics are considered as one of the greatest advances in modern medicine. These drugs are used to fight bacterial infections, potentially fatal in some cases, and are extensively used in medical procedures which expose us to bacteria: surgery, transplants, and therapies affecting the immune system. The overuse and misuse of antibiotics in human or veterinary medicine and poor hygiene conditions and practices in healthcare settings or in the food chain, facilitate the transmission of resistant microorganisms, which boost the resistance development, therefore making the antibiotics less effective and finally useless. The spread of resistant bacteria, particularly Gram-negative bacteria, has increased to the point where, today, AMR represents a major global public health problem.

According to the European Centre for Disease Prevention and Control (ECDC), AMR is defined as “the inability or reduced ability of an antimicrobial agent to inhibit the growth of a bacterium, which, in the case of a pathogenic organism, can lead to therapy failure”.⁽⁶⁹⁾ Based on the ECDC reports, in 2019, AMR was responsible for more than 670,000 infections and 33,000 deaths in Europe (EU).⁽⁷⁰⁾ The associated cost to the health care systems was around 1.1 billion euros.⁽⁷¹⁾ The World Health Organization (WHO) indicates that 10 million deaths can be expected by 2050 as a direct consequence of AMR (Figure 39).

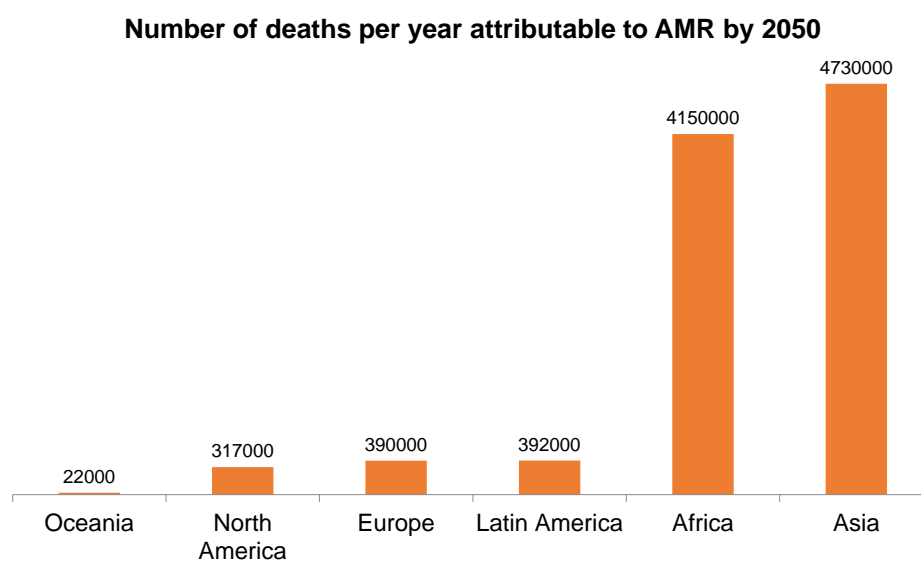


Figure 39: Number of deaths per year attributable to AMR by 2050 by continent adapted from O'Neill⁽⁷²⁾

According to the WHO, several bacteria are of special importance; in particular the pathogens grouped under the acronym ESKAPE – *Enterococcus faecium*, *Staphylococcus aureus*, *Klebsiella pneumoniae*, *Acinetobacter baumannii*, *Pseudomonas aeruginosa* and some Enterobacteria. For three of them, which are classified as a critical priority, there is an urgent need to develop new antimicrobial drugs: *A. baumannii*, some extended-spectrum β -lactamase-producing *Enterobacteriaceae* and *P. aeruginosa*.

Within the scope of this PhD work, we focused on *P. aeruginosa*.

I. *Pseudomonas aeruginosa* and resistance

P. aeruginosa is an opportunistic Gram-negative bacterium, which has remarkable host persistence and virulence. *P. aeruginosa* infections are the leading cause of morbidity and mortality in cystic fibrosis (CF) patients and one of the leading causes of nosocomial infections.⁽⁷³⁾ Its ability to adopt a biofilm growth mode, in which the bacterium can survive the antimicrobial agents, makes its elimination even more difficult and therefore leads to the emergence of resistant strains.

Based on the ECDC study, in 2019, 30 countries in Europe have reported 20,356 isolates of *P. aeruginosa*. The AMR results are reported in (Table 17) according to their antimicrobial susceptibility testing (AST). The highest EU population-weighted mean resistance percentage was reported for fluoroquinolones (18.9%), followed by piperacillin + tazobactam (16.9%), carbapenems (16.5%), ceftazidime (14.3%) and aminoglycosides (11.5%). The authors also observed that the resistance to two or more antimicrobial groups was frequent and seen in around 18.0% of all tested isolates.

Table 17: Total number of invasive isolates of *P. aeruginosa* tested and % of isolates with resistant phenotype in 2019 adapted from the ECDC⁽⁷⁰⁾

Antimicrobial group	Total number of invasive isolates tested	% with resistant phenotype
Piperacillin + tazobactam resistance	19 355	16.9
Ceftazidime resistance	19 849	14.3
Carbapenem (imipenem/meropenem) resistance	20 127	16.5
Fluoroquinolone (ciprofloxacin/levofloxacin) resistance	20 273	18.9
Aminoglycoside (gentamicin/netilmicin/tobramycin) resistance	20 109	11.5
Combined resistance to >3 antimicrobial groups (among piperacillin + tazobactam, ceftazidime, carbapenems, fluoroquinolones and aminoglycosides)	20 296	12.1

Important inter-country variations were observed for all antimicrobial groups; with higher resistance percentages in Southern and Eastern Europe (Figure 40).

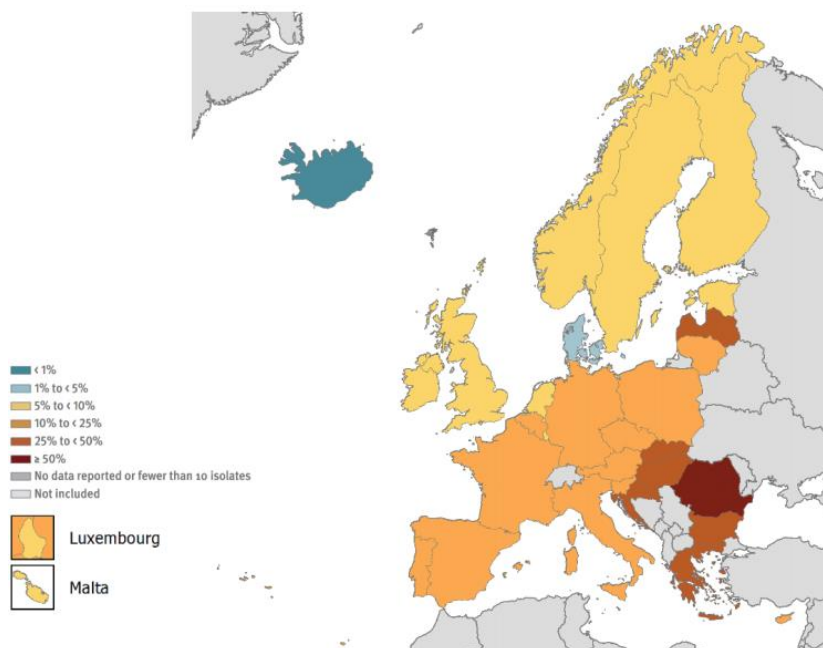


Figure 40: Percentage of invasive isolates with resistance to carbapenems (imipenem or/and meropenem) by country in Europe in 2019 from the ECDC⁽⁷⁰⁾

AMR is conducive to the appearance of bacterial superinfections and to the installation of chronicity. For *P. aeruginosa*, this phenomenon of chronic bacterial infections is commonly encountered in CF patients because this bacterium has preference for the respiratory tract.⁽⁷⁴⁾ In Europe and the US, *P. aeruginosa* infections are among the most common in CF patients. In Europe, 29.1% of people with CF had chronic *P. aeruginosa* infection in 2017.⁽⁷⁵⁾ In US, 27.7% of people with CF were chronically infected with this bacterium in 2019.⁽⁷⁶⁾

II. *P. aeruginosa* and virulence

As mentioned previously, apart from its resistance, this bacterium has remarkable virulence. The virulence allows bacteria to cause host damage, to adapt to hostile situations and to evade the host immune system leading to their persistence within its host.⁽⁷⁷⁾

Most of virulence factors are under the control of quorum sensing (QS). QS is a communication system, which is based on the diffusion of small molecules and depends on the bacterial density and various environmental signals. These small molecules are essential because, based on their quantities; they lead to the activation or repression of genes and thus allow the bacteria to coordinate their behavior.⁽⁷⁸⁾

In *P. aeruginosa*, four pathways form the QS: LasI-LasR, RhlI-RhIR, PqsABCDE-PqsR and AmbCDE-IqsR. Each pathway contains an enzyme with synthase activity which, depending on various environmental signals (low levels of iron, oxygen, phosphate or phospholipids in the host surfactant...), leads to the production of an auto-inducer (signaling molecule) and a transcriptional receptor protein. When the auto-inducer concentration reaches a certain threshold, it activates the transcriptional receptor protein, allowing the network to control the production of many factors which are important for the bacterial growth and virulence (Figure 41).

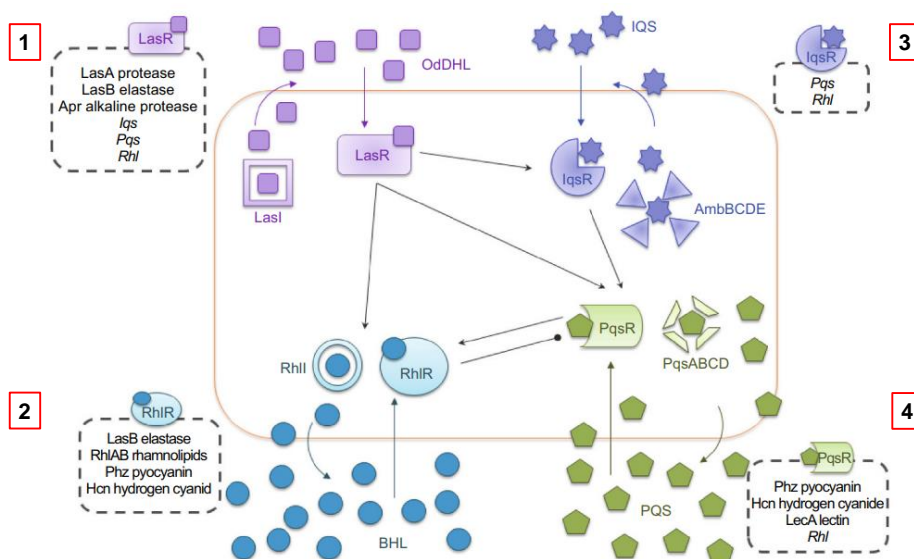


Figure 41: Schematic representation of the four QS signaling network in *P. aeruginosa* and their respective regulation adapted from Lee et al.⁽⁷⁹⁾

P. aeruginosa is known for its capacity to produce numerous virulence factors, which enable the bacteria to promote their survival by playing specific roles in the pathogenesis (Figure 42).

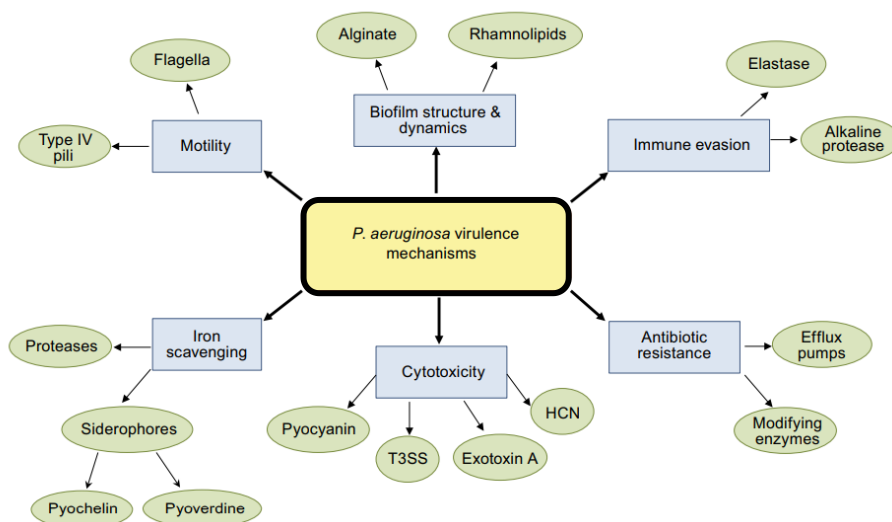


Figure 42: Produced virulence factors by *P. aeruginosa* adapted from Lee et al.⁽⁷⁹⁾

Thus, by their broad scope of harmful actions, these mechanisms appear as attractive drug targets to fight *P. aeruginosa*, with the idea to “disarm” bacteria rather than killing them.

In my PhD work, we focused on LasB, which is the most abundant protein in the *P. aeruginosa* secretome and one of the major virulence factors due to its capacity to hydrolyze a broad spectrum of substrates.

III. *P. aeruginosa* elastase LasB as a therapeutic target

1. Production and regulation

LasB elastase (or pseudolysin) is a metallo-type (Zn^{2+}/Ca^{2+} cofactors) protease, which belongs to the thermolysin group (M4), a large group of zinc metalloproteases. It is synthesized as a preproelastase formed by three peptide domains: an N-terminal prepeptide (AA 1–23 = signal prepeptide), a propeptide (AA 24–197) functioning as an intramolecular chaperone for the C-terminal domain (IMC) (AA 198–498), encoding the mature elastase (33 kDa) (Figure 43).

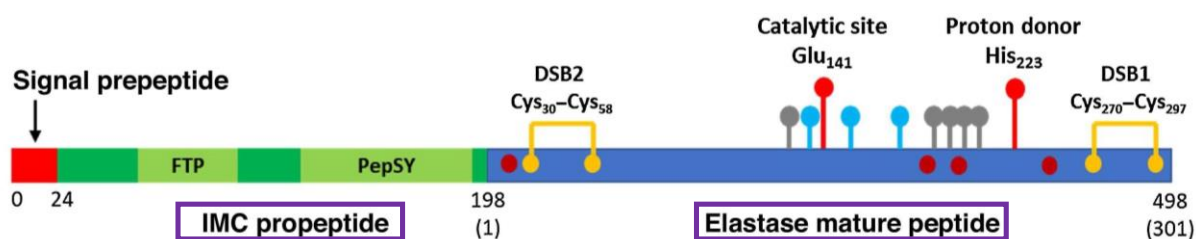


Figure 43: Representation of the preproelastase. The signal prepeptide is in red, IMC propeptide with the chaperone (FTP) and elastase inhibitor subdomains (PepSY) in green and the mature enzyme in blue. The lysine residues subject to post-translational modification are represented in dark-red dots, the positions of the involved cysteine in the two disulfides bridges (DSB1 and DSB2) in yellow dots, the calcium-binding sites in gray, zinc-binding sites in turquoise blue and catalytic site and proton donor sites in red markers. Adapted from Everett et al.⁽⁸⁰⁾

As shown previously, the regulation of LasB expression is under the control of the QS system. Located on top of *P. aeruginosa* QS, LasR is able to activate the three other systems and could represent a promising target. However, these systems communicate and have the capacity to activate each other and, thus, can counteract LasR inhibition. For example, LasB production can be done by a second direct pathway: the RhlR-RhII network (Figure 41). In addition, other QS systems can indirectly influence LasB expression such as IqsR and PqsR, IqsR regulating PqsR, which, in turn, regulates RhlR (Figure 41).

2. Activity and biological role

A. Structure

Belonging to the M4 group, LasB is structurally close to thermolysin (Figure 6), with a difference in the active site; it is more open for LasB with a preference for hydrophobic amino acids in P1' position of the substrate. Its secondary structure consists of two antiparallel β -sheets and seven α -helices. The active site is formed by the connection of two α -helices and a loop, which connects them. Key actor of the catalytic activity, the zinc ion is tetrahedrally coordinated by the side chain of two histidines (His₁₄₀ and His₁₄₄) and a glutamic acid (Glu₁₆₄); the remaining coordination site is being occupied by the catalytic water molecule (Figure 44).⁽¹⁾

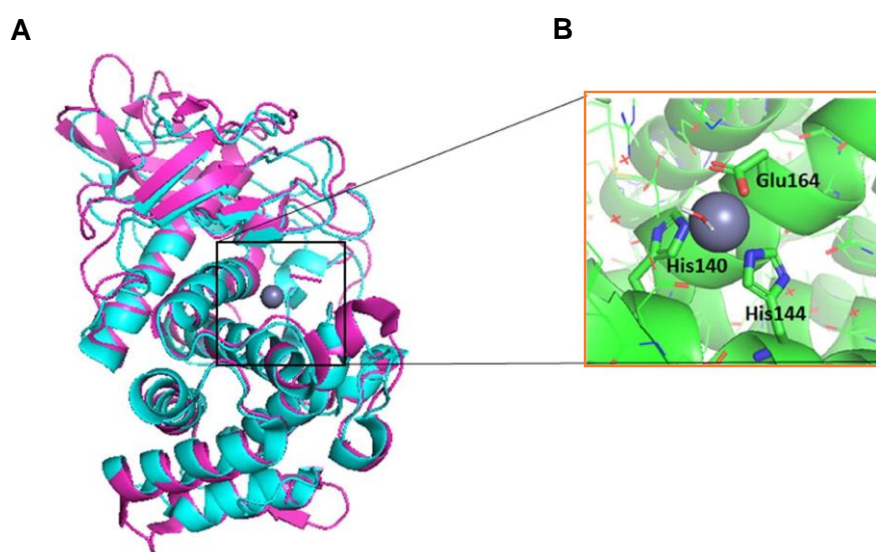


Figure 44: (A) superposition of tertiary structures of LasB (turquoise blue, PDB entry 1EZM) and thermolysin (pink, PDB entry 1KEI), the zinc ion is represented in gray. (B) tetrahedral zinc coordination in LasB active site (PBD entry 1EZM). Adapted from Everett et al.⁽⁸⁰⁾

B. Catalytic mechanism

Regarding the catalytic mechanism (Figure 45), the carboxylic group of the glutamic acid binds to the hydrolytic water molecule by hydrogen-bonding interactions and activates it (A), facilitating its nucleophilic attack on the substrate amide group (B). This attack leads to the formation of an oxyanionic intermediate, which is stabilized by zinc coordination (C). Subsequent to a proton rearrangement, this intermediate is degraded (D), which regenerates the ground-state enzyme and liberates the amine and carboxylic acid from the amide bond, leading to substrate inactivation €. Using this mechanism, this enzyme cleaves a large variety of host as well as bacterial substrates.

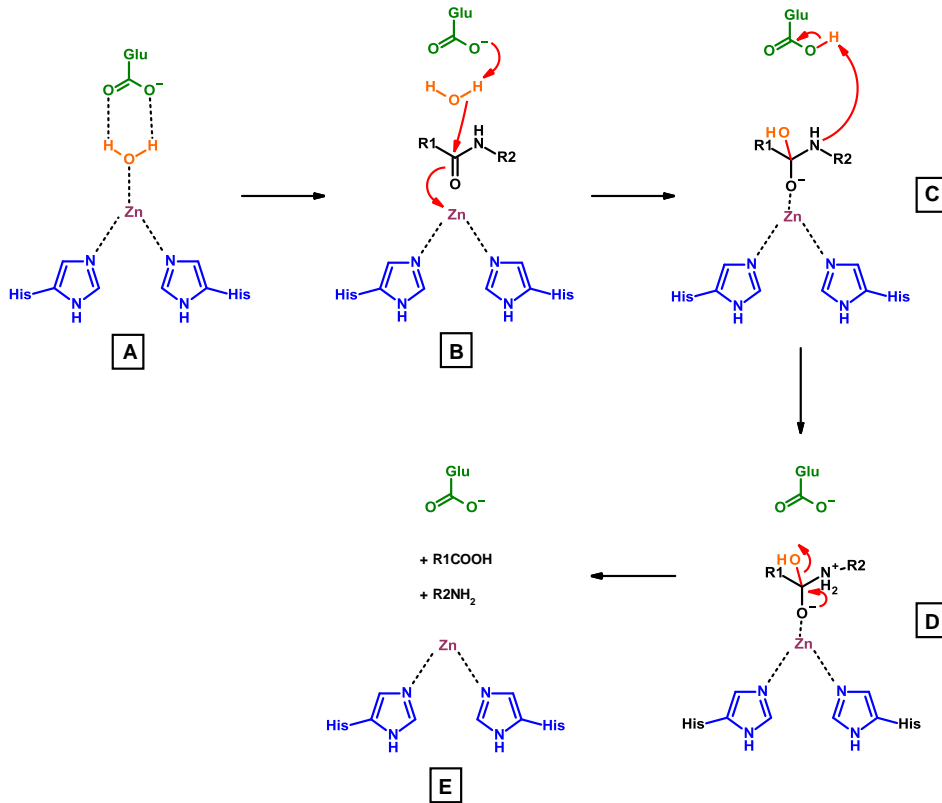


Figure 45: Proposed catalytic mechanism of hydrolysis of substrates by the elastase LasB adapted from Everett *et al.*⁽⁸⁰⁾

C. Substrates cleaved by LasB

- Host substrates

Concerning the host substrates cleaved by LasB, we can classify them in three categories: structural components, components of the immune system and others.

➤ Structural components

LasB has the ability to cleave three major components of the extracellular matrix (ECM): elastin, collagens III–IV and laminin with various consequences for the host. In fact, elastin destruction leads to the loss of tissue integrity, releasing elastin fragments able to inhibit phagocytosis.⁽⁸¹⁾ Moreover, collagen and laminin degradation also takes part in the loss of tissue integrity by ECM lysis.⁽⁸²⁾

Apart from ECM components, this enzyme can also damage the uPar–vitronectin complex and the VE–cadherin which, respectively, participate in cell adherence and tight-junction establishment. The detachment-induced cell apoptosis (anoikis) is a result of the loss of cell adherence while the degradation of cadherins increases the epithelial permeability.^{(83),(84)}

Thus, by damaging structural components, LasB promotes the invasion and the colonization.

➤ Immune system components

Besides the structural components, this elastase can degrade numerous actors of the immune system.

LasB is able to neutralize certain immunoglobulins such as IgA and IgGs,^{(85),(86)} reducing the opsonization and, thus, the bacterial phagocytosis. It is also capable of impairing the cell-mediated immunity (TNF- α , IFN- γ) and the cellular immune response (CD4).^{(87),(88)}

Moreover, it participates in the inflammatory terrain installation by activating the IL-1 β interleukin, an early proinflammatory molecule.⁽⁸⁹⁾

Other interleukins can be inactivated by LasB such as IL-2, IL-6, and IL-8 leading, respectively, to inhibition of lymphocyte proliferation, inactivation of epithelial cell repair and disruption of neutrophil recruitment to inflammatory sites (neutrophil chemotactism).^{(90),(91)}

Regarding the chemotactism, the elastase is able to cleave epithelial chemokines such as MPC-1, ENA-78 and RANTES.⁽⁹²⁾

Another ability of this enzyme is to target antimicrobial substrates such as the complement system (C1, C3, C5, C8 and C9),⁽⁹³⁾ the pulmonary surfactant collectins SP-A/SP-D,^{(94),(95)} and the LL-37 peptide.⁽⁹⁶⁾

Finally, LasB can impair the human neutrophil elastase (HNE), by targeting the α 1-antiprotease, which normally fights against bacterial virulence.⁽⁹⁷⁾

Thus, by targeting various immune components, LasB leads to immune evasion.

➤ Others

Among the other substrates, we find blood components including the transferrin, lactoferrin and hemoglobin, whose degradation is responsible for a release of iron and a generation of cytotoxic radicals.^{(98),(99),(100)} Coagulation factors such as the fibrin-fibrinogen-thrombin triad can also be degraded leading to hemorrhages (fibrin and fibrinogen) and inflammation (thrombin).^{(101),(102)} While the inflammation and the hemorrhages are deleterious for the host, the iron acquisition is favorable for bacterial growth.

Then, some matrix metalloproteinases are targeted by LasB (MMP-1, -2, -3, and -9), causing ECM and α 1-antiprotease degradation.⁽¹⁰³⁾

- Bacterial substrates

In addition to hydrolysis of host substrates, LasB plays an essential role in the cleavage and the activation of bacterial components. It can activate the ExoS-ExoT exotoxins

and the flagellin which, respectively, increases the invasion of epithelial cells and decreases the recognition of the flagellum by the immune system.^{(104),(105)} Furthermore, it is involved in biofilm formation by activating the Ndk kinase; Ndk activation being essential for the initiation of alginate synthesis and the expression of a mucoid phenotype.⁽¹⁰⁶⁾

In conclusion, regarding the deleterious consequences of the LasB actions, this enzyme plays a crucial role in the pathogenesis of *P. aeruginosa* by disrupting the host response.

In order to establish a causal effect of the LasB elastase activity on the virulence, various studies on animal models of *P. aeruginosa* infection were performed.

3. Impact of LasB on virulence in animal models of *P. aeruginosa* infection

Gi and colleagues demonstrated that a *lasB* mutant was avirulent in a model of acute lung infection in mouse.⁽¹⁰⁷⁾ In this study, the mice were separated in three groups: mice infected with the *lasB* mutant and treated with a saline solution ($\Delta lasB$, saline), mice infected with the *P. aeruginosa* PAO1 strain and treated with a saline solution (PAO1, saline) and mice infected with PAO1 and treated with a broad-spectrum metalloprotease inhibitor such as the DTPA (diethylenetriaminepentaacetic acid) (PAO1, Ca-DTPA).

The mice from the $\Delta lasB$ group treated with a saline solution remained viable during five days whereas the mice from the PAO1 group treated with a saline solution died within the five days (Figure 46A). Moreover, the mice from the PAO1 group treated with the DTPA showed a significantly higher survival rate than saline-treated mice (PAO1, saline) (Figure 46A); demonstrating that inhibition of the enzyme LasB can lead to mouse survival. Lung sections for mice infected with the *lasB* mutant showed normal lung architecture after hematoxylin and eosin staining (Figure 46B). In contrast, an infiltration of inflammatory cells was visible for mice infected with the PAO1 strain and not receiving DTPA. This inflammatory response was less visible in mice treated with DTPA (Figure 46B).

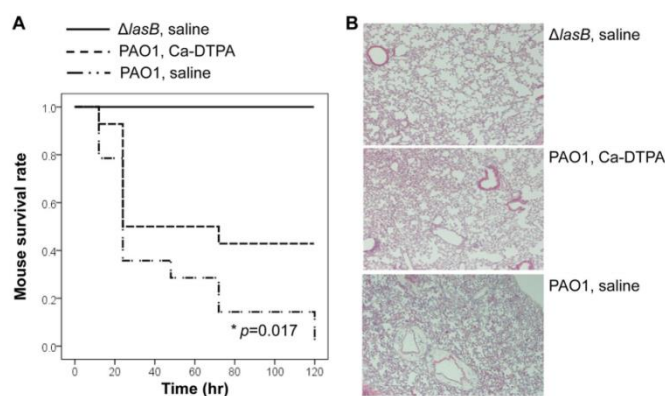


Figure 46: (A) Kaplan–Meier survival plot of each mice group. (B) Representative images of lung tissue of each group of mice group adapted from Gi et al.⁽¹⁰⁷⁾

Cigana and colleagues studied the role of LasB in a model of chronic pulmonary *P. aeruginosa* infection using clinical isolates from CF patients (PAO1, RP45 and RP73).⁽¹⁰⁸⁾ Interestingly, the RP45 isolate is found in seventeen-year old and the RP73 is found at twenty-four-year old patients.

Firstly, they investigated the elastase activity in different groups: wild-type PAO1 (wt PAO1) and $\Delta lasB$ PAO1, wt RP45 and $\Delta lasB$ RP45, wt RP73 and $\Delta lasB$ RP73, and a Leria-Bertani growth medium used as a negative control (LB). The RP45 isolate showed a strong elastolytic activity, whereas RP73 showed no activity despite the presence of the LasB enzyme (Figure 47). This absence of elastolytic activity for the RP73 isolate is consistent with the *P. aeruginosa* patho-adaptation previously observed in the development of chronic infection in CF;⁽¹⁰⁹⁾ RP73 clearly does not have a functional LasB enzyme. As shown, not all *lasB* mutants ($\Delta lasB$) showed elastolytic activity (Figure 47).

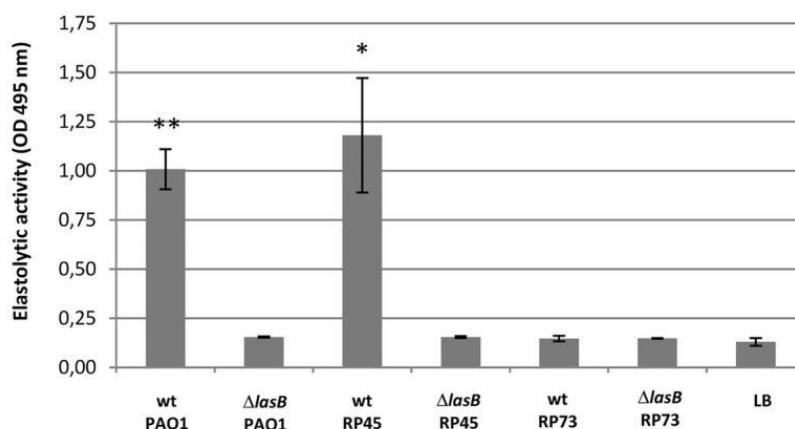


Figure 47: LasB elastolytic activity in culture supernatants from each group presented previously adapted from Cigana *et al.*⁽¹⁰⁸⁾

Secondly, they wanted to test the hypothesis that LasB promotes lung colonization during chronic *P. aeruginosa* infections. For the RP45 strain, at day two after the infection, the lung bacterial load did not differ between wt RP45 and $\Delta lasB$ RP45 whereas, at day seven, the $\Delta lasB$ RP45 mice had significantly lower lung bacterial loads than wt RP45 (Figure 48A). This reduced lung bacterial loads are a consequence of the less virulent $\Delta lasB$ RP45 strain, making clearance by the host easier in comparison to the wt RP45 strain (Figure 48B).

Regarding the later isolated RP73 strain, the lung bacterial load was the same as $\Delta lasB$ RP73 after seven days (Figure 48C). No difference in the incidence of colonization was observed between the two groups (Figure 48D); probably due to the absence of elastolytic activity for RP73 strains as seen previously.

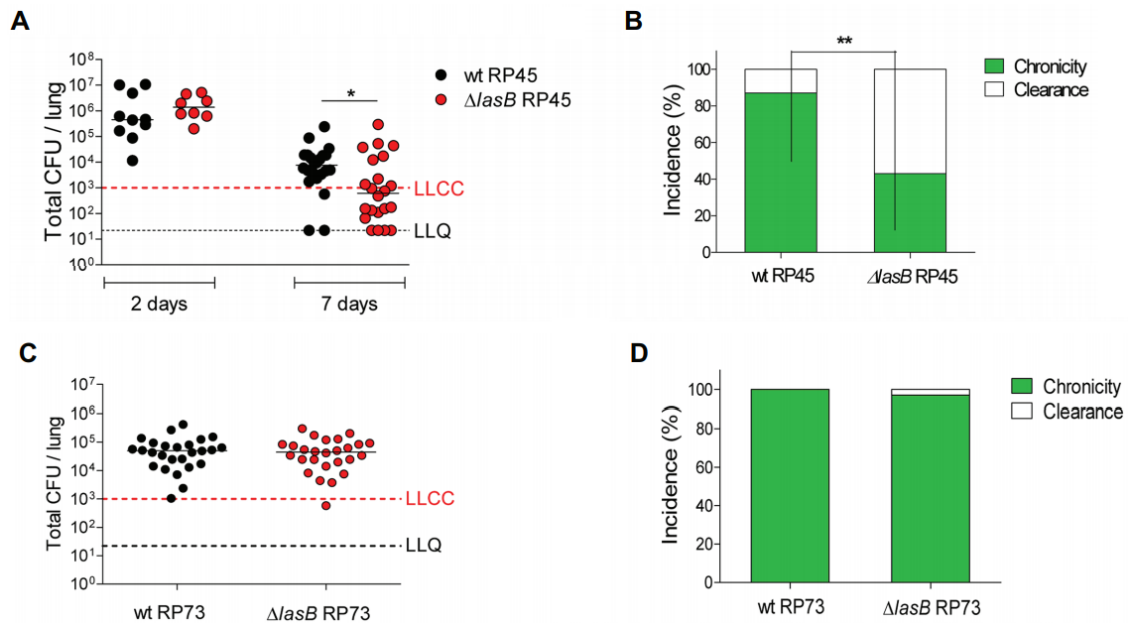


Figure 48: (A) Measure of the lung CFUs after two and seven days for wt RP45 and $\Delta lasB$ RP45; LLCC (Lower Limit of Chronic Colonization) and LLQ (Lower Limit of Quantification) are indicated. (B) Incidence of clearance and capacity to establish chronic infection for wt RP45 and $\Delta lasB$ RP73. (C) Measure of the lung CFUs after two and seven days for wt RP73 and $\Delta lasB$ RP73. (D) Incidence of clearance and capacity to establish chronic infection for wt RP45 and $\Delta lasB$ RP73. Adapted from Cigana *et al.*⁽¹⁰⁸⁾

Finally, they investigated the role of LasB in inflammation. Levels of chemokines, cytokines, and some growth factors were measured seven days after infection for wt and $\Delta lasB$ RP45 strains (Table 18). The absence of LasB ($\Delta lasB$ RP45) led to significantly higher levels of IL-1 α , IL-1 β , IL-3, IL-12p70, IL-17A, eotaxin, G-CSF, macrophagic inflammatory proteins MIP-1 α and 1 β , RANTES. This indicates that LasB can reduce inflammation.

Table 18: Cytokine and chemokine concentrations following chronic infection by wt RP45 and $\Delta lasB$ RP45 adapted from Cigana *et al.*⁽¹⁰⁸⁾

Cytokine/Chemokine	Concentration (mean pg/700 μ g lung protein \pm SEM)	
	wt RP45 strain	$\Delta lasB$ RP45 strain
IL-1 α	7,36 \pm 1,12	14,66 \pm 1,53***
IL-1 β	3,08 \pm 0,33	5,35 \pm 0,33****
IL-2	6,26 \pm 0,28	6,20 \pm 0,37
IL-3	0,92 \pm 0,05	1,11 \pm 0,05*
IL-4	0,52 \pm 0,03	0,60 \pm 0,04
IL-6	3,75 \pm 0,06	3,54 \pm 0,16
IL-9	18,47 \pm 0,51	19,78 \pm 0,69
IL-12p40	34,05 \pm 2,37	38,89 \pm 1,82
IL-12p70	18,21 \pm 1,19	24,71 \pm 1,42***
IL-17A	11,37 \pm 1,00	15,73 \pm 1,29*
Eotaxin	574,0 \pm 23,22	640,6 \pm 18,07*
G-CSF	10,36 \pm 0,95	21,10 \pm 2,00****
IFN- γ	20,59 \pm 0,80	22,29 \pm 0,43
KC	63,71 \pm 5,08	73,22 \pm 6,69
MCP-1	169,0 \pm 11,38	169,9 \pm 6,84
MIP-1 α	14,64 \pm 2,45	40,57 \pm 4,21****
MIP-1 β	36,08 \pm 3,80	76,55 \pm 7,44****
RANTES	248,0 \pm 21,83	392,4 \pm 40,96*
TNF- α	31,58 \pm 1,12	34,91 \pm 1,15

To summarize, in this study, the authors demonstrated that:

- The production and the activity of LasB differ depending on the strain, these being important during earlier stages of the infection (RP45 strain)
- LasB promotes chronic lung colonization because the lung bacterial load was lower in the $\Delta lasB$ RP45 strain after seven days
- LasB is able to decrease the inflammation, which can lead to immune evasion

So, this enzyme plays an essential role in the establishment of a chronic context at the early stage of the infection.

Thus, through different studies, a causal effect between LasB and virulence has been demonstrated. Moreover, this enzyme has an extracellular localization. All these arguments make it a promising therapeutic target.

4. Therapeutical solutions to inhibit LasB

The main strategy to inhibit LasB is to target the zinc cation in its active site using a zinc binding group (ZBG). Various ZBGs are used and will be presented below.

A- Phosphoramidon and analogs

Phosphoramidon (**IL1**) is the first reported inhibitor of LasB. It is a natural dipeptide isolated from *Streptomyces tanashiensis* with LasB $K_i = 1.0 \mu\text{M}$.⁽⁸⁰⁾

Powers and colleagues used this as a starting point for further medicinal-chemistry optimization.⁽¹¹⁰⁾ Tryptophan replacement by a phenylalanine and removal of the glycosidic moiety led to a compound with a $K_i = 0.2 \mu\text{M}$ (**IL2**), demonstrating that the glycosidic moiety was not essential for the activity (Figure 49).

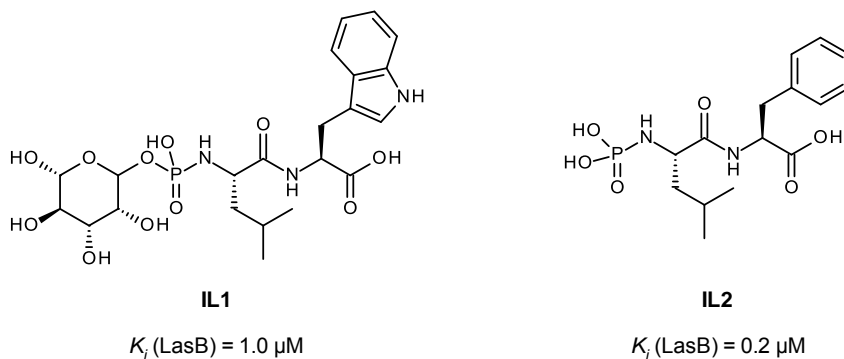


Figure 49 : Chemical structures of IL1 and IL2 with their K_i values

B- Thiol inhibitors

Later, Kessler and colleagues replaced the phosphoramidate group by a thiol as an alternative ZBG and reversed the phenylalanine and the leucine moiety leading **IL3** with $K_i = 0.2 \mu\text{M}$ (Figure 50).⁽¹¹¹⁾ Then, Cathcart and colleagues investigated the carboxylic acid in the C-terminal position and replaced it by an amide.^{(112),(113)} 1,600 dipeptides were synthesized with K_i values of 1.0 to 0.04 μM (**IL4** and **IL5**) (Figure 50).

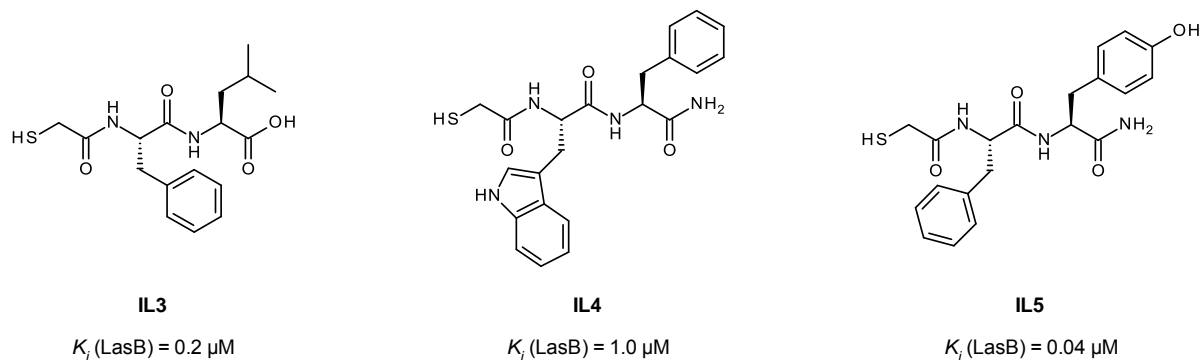


Figure 50 : Chemical structures of **IL3**, **IL4** and **IL5** with their K_i

Recently, several thiol families have been developed in Prof. Hirsch's and Hartmann's group. These inhibitors are not built around a dipeptide skeleton; these are thiobenzamides (**IL6**) and *N*-aryl-3-mercaptosuccinimides (**IL7**) with $\text{IC}_{50} = 6.6$ and $3.5 \mu\text{M}$, respectively (Figure 51).^{(114),(115)}

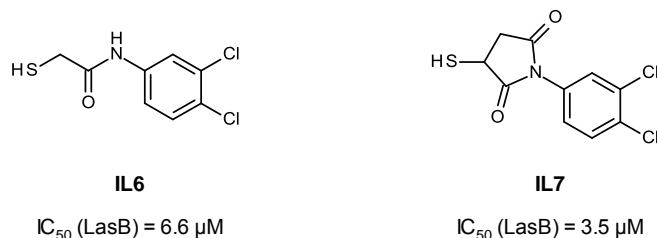


Figure 51: Chemical structures of **IL6** and **IL7** and their IC_{50}

Unfortunately, these thiols lack potency and some of them are sensitive to oxidation. In order to solve these problems, the thiol moiety was replaced by other ZBGs such as hydroxamic acids.

C- Hydroxamic acid inhibitors

Taking inspiration from phosphoramidon and its derivatives, Dickens and colleagues designed inhibitors bearing a hydroxamic acid function as ZBG, including one with a K_i value of $0.05 \mu\text{M}$ (**IL8**).⁽¹¹⁶⁾ In Prof. Hartmann's team, one hydroxamic acid was synthesized. Based on the chemical structure of thiols developed previously (**IL 6** and **IL7**), this hydroxamic acid

is presented on a malonic skeleton (**IL9**).⁽¹¹⁷⁾ Hydroxamate avoids the risk of oxidation observed with some thiols but it suffers from a lack of selectivity.

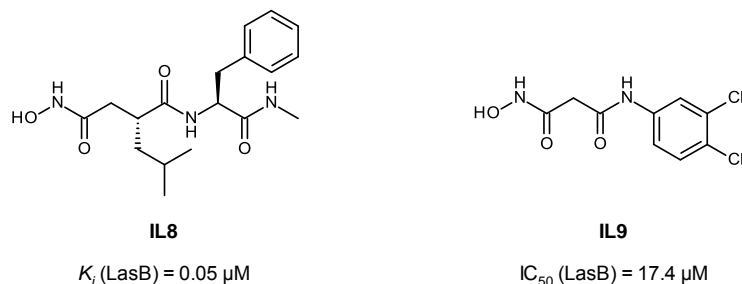


Figure 52: Chemical structures of IL8 and IL9 and their LasB activities

D- Carboxylic acid inhibitors

Carboxylic acid is another ZBG reported in the literature. A family of carboxylic acids was identified by virtual screening (**IL10**) and, following structure–activity relationship studies (SAR), the activity was improved by a factor of 100 (**IL11**) (Figure 53).⁽¹¹⁸⁾

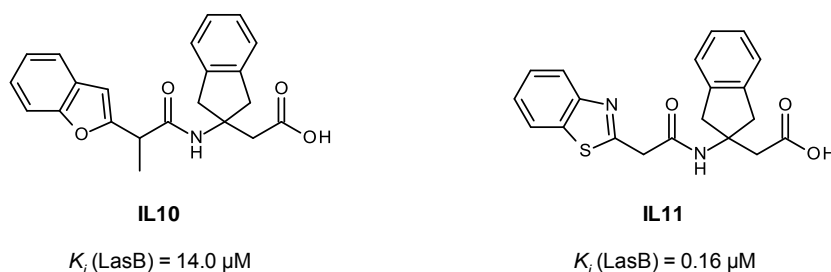


Figure 53: Chemical structures of IL10 and IL11 and their K_i

E- Other inhibitors

A screening of a library of fragments containing different ZBGs was performed, and the results were followed by SAR studies to identify new thiopyridone and tropolone inhibitors with activities in the micromolar range (**IL12** and **IL13**) (Figure 54).^{(119),(120)}

Galdino and colleagues showed that the copper complex of 1,10-phenanthroline-5,6-dione has a K_i of 0.09 μ M (**IL14**) (Figure 54).⁽¹²¹⁾

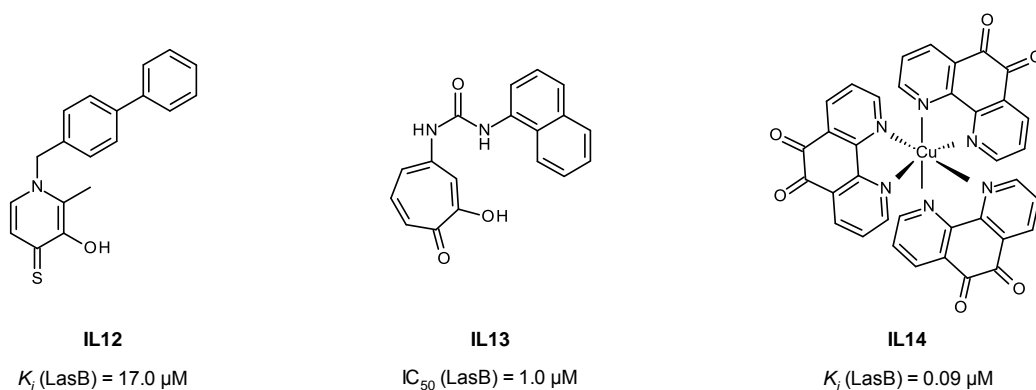


Figure 54: Chemical structures of LasB inh 12, 14 with K_i and LasB inh 14 with its IC_{50}

Thus, many chemical classes have been described in the literature but no LasB inhibitor has reached the clinic due to chemical stability, selectivity or physicochemical properties issues so far. Despite these problems, these inhibitors are very good starting points for further medicinal-chemistry programs.

As seen previously, thiols and hydroxamic acids have been developed in Prof. Hirsch's and Hartmann's teams. While the thiols have been studied in detail and several subfamilies have been identified,⁽¹²²⁾ the hydroxamates have not been widely studied and their numbers are consequently limited.

IV. Strategy of the PhD project

In this specific area, as for ERAP2 project, the goal of this work is to use KTGS strategy to identify and optimize potent and selective LasB inhibitors (Figure 55).

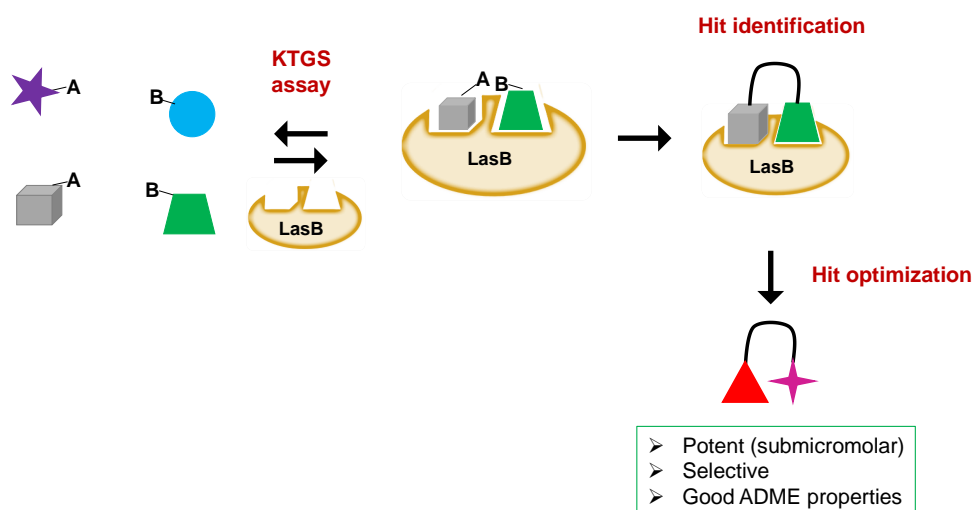


Figure 55 : Strategy for the LasB PhD project

Results

I. KTGS Las B

1. Design and synthesis of the starting building blocks

To identify new hydroxamic acid inhibitors, we chose to apply the KTGS strategy using the Huisgen [1,3] dipolar cycloaddition. The four azides (Figure 56), which bear a hydroxamate, allowed us to direct the ligands towards the active site using zinc coordination, while the alkynes introduce the chemical diversity. The alkynes come from the U1177 laboratory's alkyne library and the azides were designed specifically for this project.

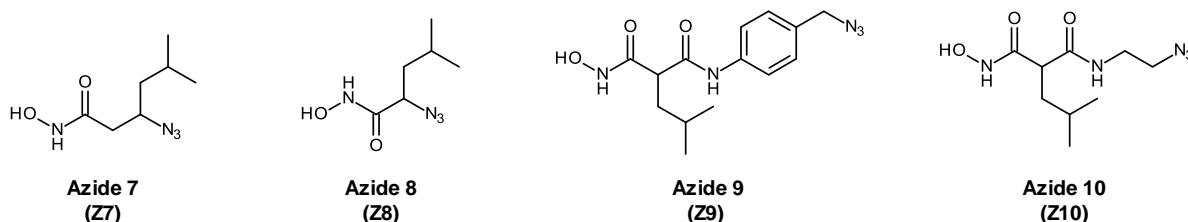


Figure 56: Chemical structures of the starting azides for the KTGS with LasB

Regarding the design of the azides **Z7** and **Z8**, we used the specificities of LasB for the cleavage of substrates. In fact, in a protease, there are sites and pockets for the peptide binding as described in Figure 57.

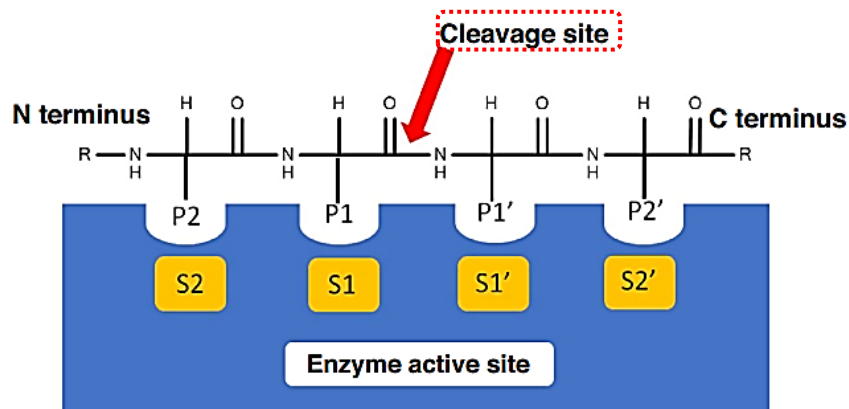
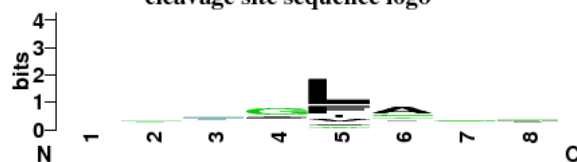


Figure 57: Schematic representation of peptidyl side-chains and corresponding enzyme-binding sites adapted from Everett et al.⁽⁸⁰⁾

The peptide cleavage takes place between S1 and S1', and at these positions, LasB has a glycine at P1 and leucine at P1' as preferences (Table 19). For these reasons, we decided to introduce an azide on the β -leucine (**Z7**) and on the leucine (**Z8**).

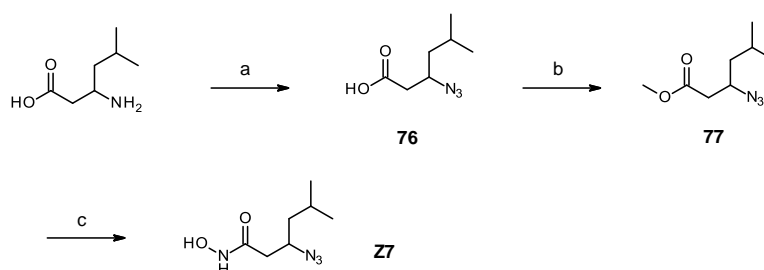
Table 19: Table of LasB specificities according to the amino acids adapted from MeROPs base cleavage site sequence logo



Amino acid	Specificity matrix							
	P4	P3	P2	P1	P1'	P2'	P3'	P4'
Gly	3	8	7	26	0	8	10	6
Pro	2	0	2	3	0	0	5	6
Ala	3	6	6	8	4	21	2	2
Val	2	3	3	1	6	5	1	1
Leu	3	4	1	1	35	2	1	0
Ile	3	1	1	0	6	3	1	1
Met	0	0	0	1	1	0	2	0
Phe	1	5	5	7	12	2	1	1
Tyr	1	1	1	2	4	2	3	0
Trp	0	0	0	0	1	0	0	0
Ser	3	2	3	5	0	3	2	3
Thr	2	1	0	2	0	6	1	3
Cys	0	1	0	0	0	0	0	0
Asn	0	1	1	2	0	2	0	1
Gln	1	1	5	1	0	1	1	1
Asp	1	1	0	1	0	0	2	1
Glu	4	2	2	1	0	2	3	4
Lys	2	2	4	4	0	2	1	3
Arg	5	2	7	2	0	2	3	3
His	0	0	0	3	0	0	0	0

Concerning the design of the azides **Z9** and **Z10**, we took our inspiration from the hydroxamic acid inhibitor synthesized by Prof. Hartmann's team, which was described previously (**IL9**, Figure 52). For **Z9**, based on LasB's preferences for the substrate cleavage, we introduced an isobutyl group in the malonic position (α -position) and we put a methylazide in position 4 to explore the ligand-growing direction. For **Z10**, the azidobenzyl motif of **Z9** was replaced by an ethyl chain for an enhanced flexibility.

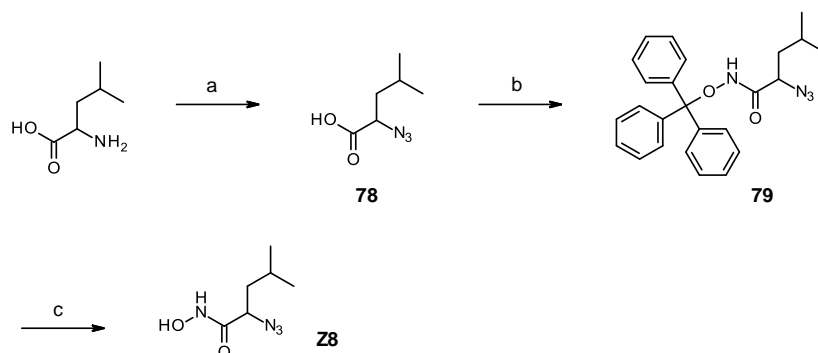
The four azides were synthesized using more or less different synthetic pathways. The azide **Z7** was prepared in three steps: diazo transfer (a), esterification (b) and aminolysis (c) (Scheme 16).



Reagents and conditions: a) azide-*N*-diazimidazole-1-sulfonamide hydrogen sulfate, K_2CO_3 , $ZnCl_2$, DIPEA, MeOH, 0 °C to rt., overnight, quantit. Yield; b) $SOCl_2$, MeOH, 0 °C to rt., overnight, 77%; c) aq. Hydroxylamine (50% in water w/w), KCN (cat.), MeOH, rt., overnight, 48%.

Scheme 16 : Three-step synthesis of Z7

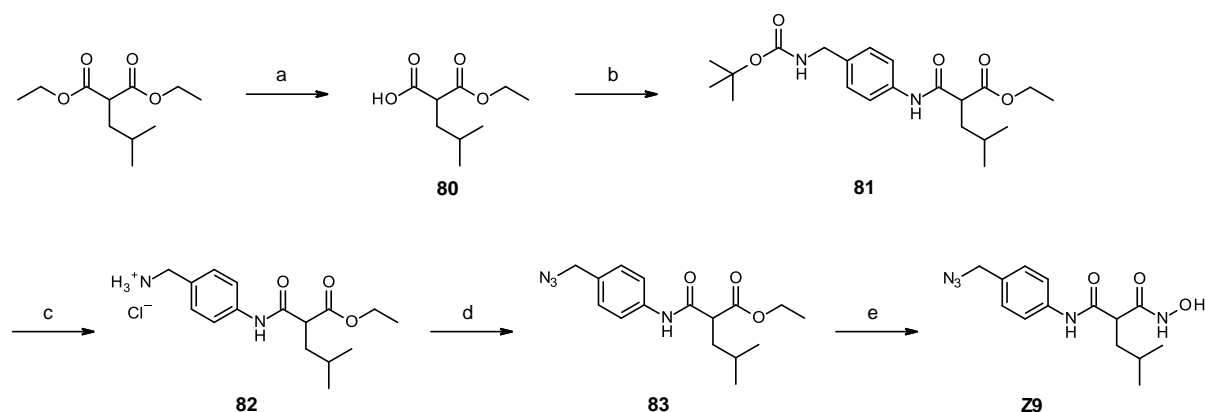
The azide **Z8** was also synthesized in three steps: diazo transfer (a), coupling with the *O*-tritylhydroxylamine (b) and deprotection (c) (Scheme 17). The synthetic pathway was changed compared to the previous one for safety reasons because the azidoleucine ester could be volatile.



Reagents and conditions : a) azide-*N*-diazoimidazole-1-sulfonamide hydrogen sulfate, K_2CO_3 , $ZnCl_2$, DIPEA, MeOH, 0 °C to rt., overnight, quantit. Yield ; b) *O*-tritylhydroxylamine, EDC·HCl, HOBt, *N*-methylmorpholine, DMF, rt., 48 h, 19% ; c) TFA, TMS, CH_2Cl_2 , 0 °C to rt., 20 min, 39%.

Scheme 17 : Three-step synthesis of Z8

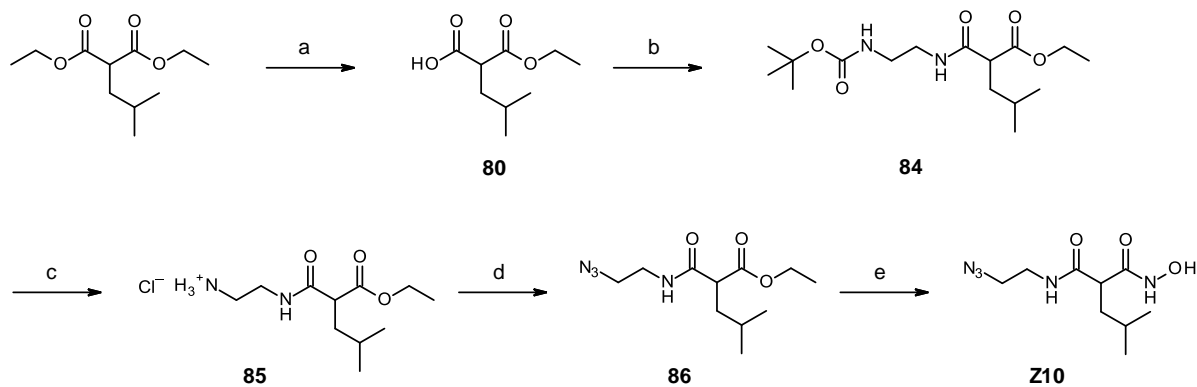
Five steps were necessary for the synthesis of **Z9**: monosaponification (a), amide formation (b), Boc removal (c), diazo transfer (d) and aminolysis (e) (Scheme 18).



Reagents and conditions : a) NaOH, EtOH/ H_2O (4 : 1), rt., overnight, 77% ; b) tert-butyl *N*-[(4-aminophenyl)methyl]carbamate, HBTU, Et_3N , DMF, rt., overnight, 47% ; c) HCl 4M in dioxane, EtOH, 0 °C to rt., overnight, quantit. Yield ; d) azide-*N*-diazoimidazole-1-sulfonamide hydrogen sulfate, K_2CO_3 , $ZnCl_2$, DIPEA, MeOH, 0 °C to rt., overnight, 58% ; e) aq. Hydroxylamine (50% in water w/w), KCN (cat.), MeOH, rt., overnight, 38%.

Scheme 18 : Five-step synthesis of Z9

Finally, for **Z10**, the synthetic route was the same as before; only the amine and the conditions for the amide formation were different (b) (Scheme 19).



Reagents and conditions : a) NaOH, EtOH/H₂O (4 :1), rt., overnight, 77% ; b) tert-butyl N-(2-aminoethyl)carbamate, EDC, HOBT, DIPEA, CH₂Cl₂, rt., overnight, 80% ; c) HCl 4M in dioxane, EtOH, 0 °C to rt., overnight, quantitative yield ; d) azide-*N*-diazoimidazole-1-sulfonamide hydrogen sulfate, K₂CO₃, ZnCl₂, DIPEA, MeOH, 0 °C to rt., overnight, 19% ; e) aq. hydroxylamine (50% in water w/w), KCN (cat.), MeOH, rt., overnight, 51%.

Scheme 19 : Five-step synthesis of Z10

2. Protein-templated reaction and controls

In this assay, we used LasB at a concentration of 4.08 μM and the azides and the alkynes at 100 μM.

The experiment was performed in low-binding 96-wells plate, each well containing one azide and ten alkynes. As for ERAP2 KTGS, two experiment controls were done, one without the enzyme buffer (“blank experiment”) and the other with copper in place of the enzyme solution (“chemical catalysis experiment”). The blank experiment did not contain the enzyme and allowed us to identify the unspecific couplings during the protein templated reaction and the chemical catalysis experiment allowed us to afford the 1,4-disubstituted 1,2,3-triazole controls.

In order to validate the hits, an UPLC–MS–MS analysis using a multi MRM-method was performed after three and six days. The hits were thus identified in each cluster by mass and retention time and compared to both incubation with buffer in place of the enzyme (blank plate) and synthetically prepared triazoles (chemical catalysis plate).

3. Hit selection

The MS analysis led to the identification of 264 hits. An additional analysis by LC–HRMS using a time of flight method was performed to search for the exact mass of the expected triazoles and therefore refine the hits selection. Thus, this second analysis allowed us to confirm 43 hits and ten of these were prioritized for the chemical synthesis; five from **Z9** and **Z10**.

The identified hits from **Z7** and **Z8** were chemically very close to the identified hits from the KTGS with ERAP2 and we did not therefore select those for intellectual property reasons.

Among the five selected hits from **Z9**, three were bearing a sulfonamide “linker” (**Hit L1-L3**), one was having a thiazolidine “linker” (**Hit L4**) and the last a phenol “linker” (**Hit L5**) (Figure 59).

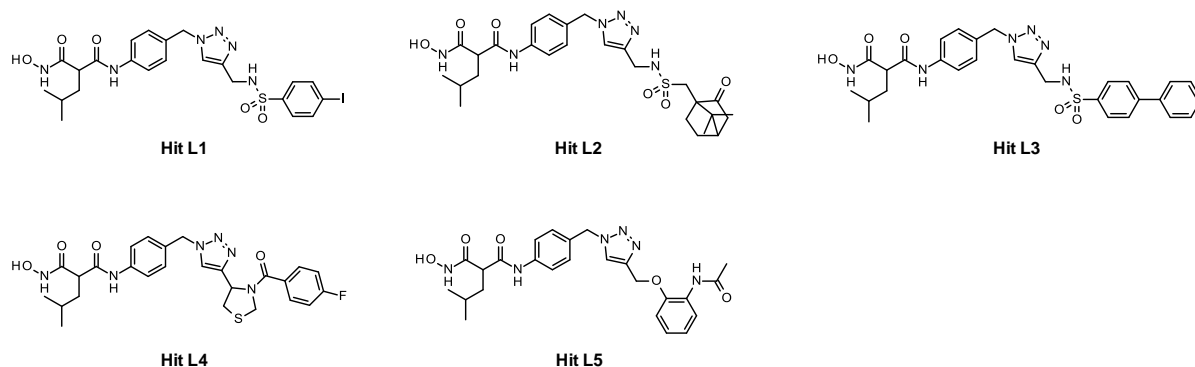


Figure 58 : Chemical structure of the selected hits from **Z9**

Concerning the chosen hits from **Z10**, three were with a sulfonamide function (**Hit L6-L8**), one with the same phenol “linker” as before (**Hit L9**) and the last one with an amide (**Hit L10**) (Figure 59).

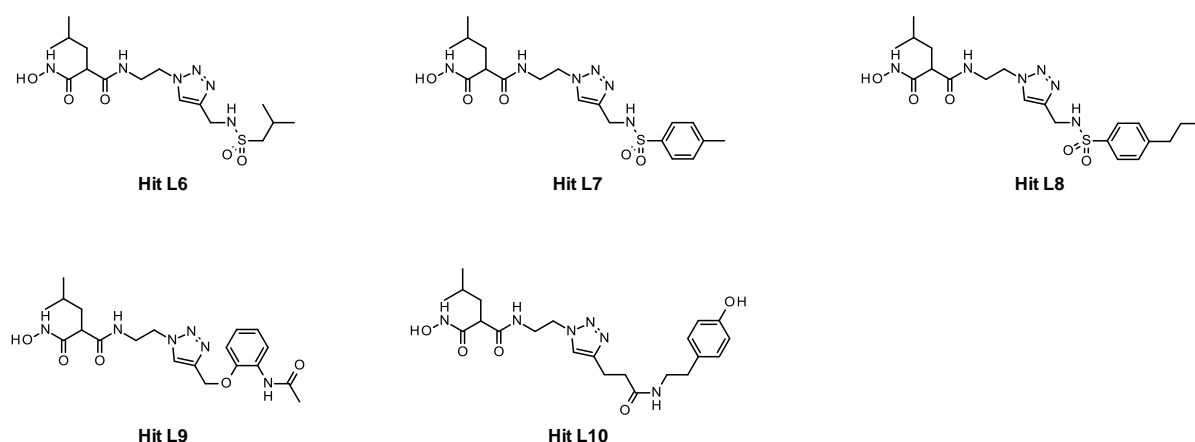


Figure 59: Chemical structures of the selected hits from **Z10**

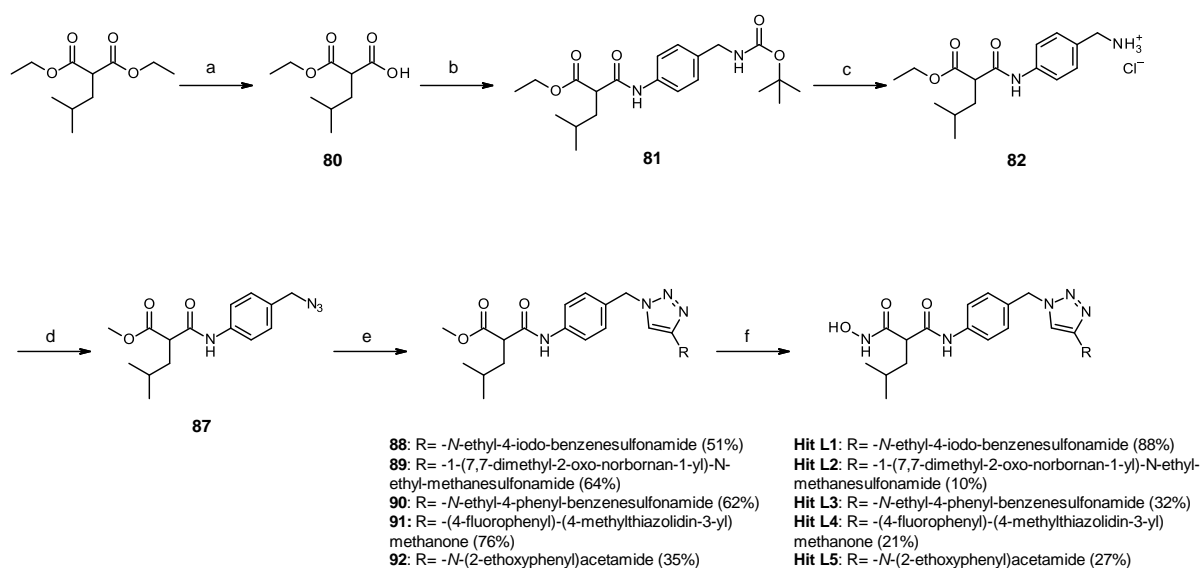
4. Chemical synthesis of the selected hits

All the mentioned hits were synthesized in six identical reaction steps, with the only difference in the coupling step, as seen previously for the synthesis of the azides **Z9** and **Z10** (Scheme 18 and Scheme 19). As the MS analysis showed perfect mass and retention time correlations between the protein templated and copper experiments for the selected hits, we

supposed that the enzyme templated the formation of the 1,4-regioisomers. Thus, we started with the chemical synthesis of the 1,4-disubstituted 1,2,3-triazoles.

A- Chemical synthesis of the selected hits from Z9

The first step consists of a monosaponification of the diethylmalonate to get the mono carboxylic acid (a). This one is activated using HBTU, in DMF with trimethylamine, to form the desired amide by reaction with the aniline (b). Then, an addition of hydrochloric acid (4N in dioxane) afforded the free amine (c) and this one reacts with the diazo transfer reagent to form the azide (d). During this step, transesterification was observed and the methyl ester was isolated. This azide engages in a copper-catalyzed [1,3] dipolar Huisgen cycloaddition to synthesize the desired 1,2,3-triazole 1,4-disubstituted (e). The final step is a KCN-catalysed aminolysis reaction of the ethyl ester, leading to the formation of the hydroxamic acid (f) (Scheme 20).

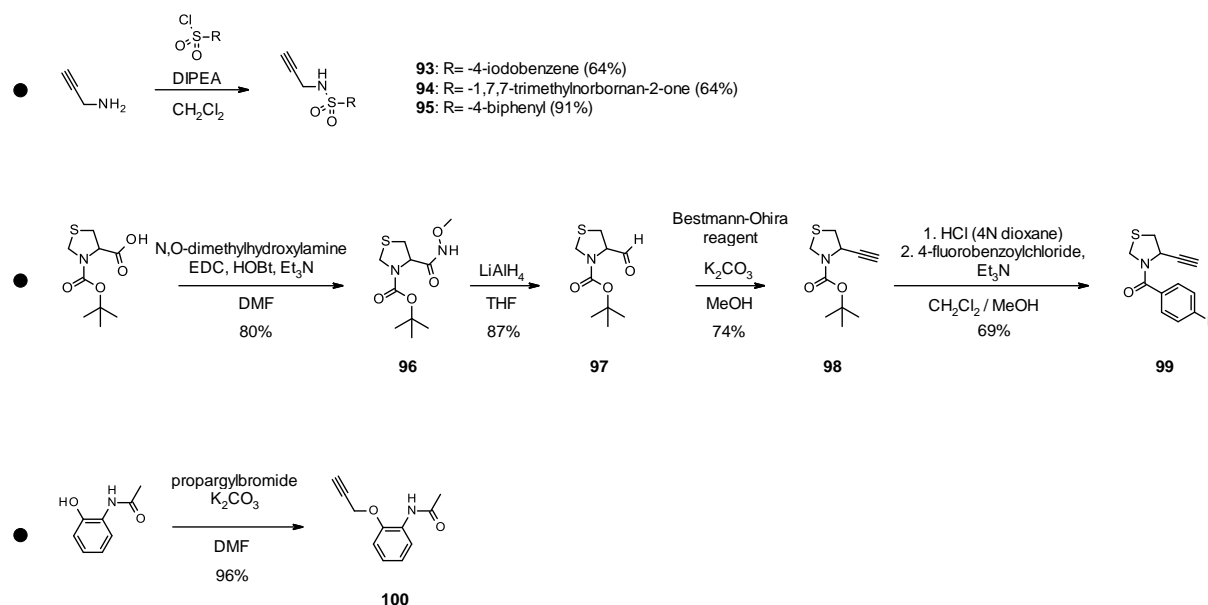


Reagents and conditions: a) NaOH, EtOH/H₂O (4:1), rt., overnight, 77%; b) tert-butyl *N*-[(4-aminophenyl)methyl]carbamate, HBTU, Et₃N, DMF, rt., overnight, 47%; c) HCl 4M in dioxane, EtOH, 0 °C to rt., overnight, quantitative yield; d) azide-*N*-diazoimidazole-1-sulfonamide hydrogen chloride, K₂CO₃, ZnCl₂, DIPEA, MeOH, rt., overnight, 58%; e) alkyne (**93**, **94**, **95**, **99** or **100**), CuSO₄ (5H₂O), sodium ascorbate, DMF/H₂O (1.2:1), rt., overnight, 35–76%; f) aq. hydroxylamine (50% in water w/w), KCN (cat.), MeOH, rt., overnight to 76 h, 10–88%.

Scheme 20 : Chemical synthesis of the selected hits from Z9

The alkynes were synthesized according to the routes described in Scheme 6. In case of the sulfonamide linkers, the alkynes (**93–95**) are formed by reacting propargylamine with the corresponding sulfonyl chlorides. Thiazolidine alkyne **99** was obtained in five reaction steps: preparation of the Weinreb amide (**96**), the reduction to aldehyde (**97**), a Seyferth–Gilbert homologation (**98**), and finally, Boc removal followed by nucleophilic acyl substitution with

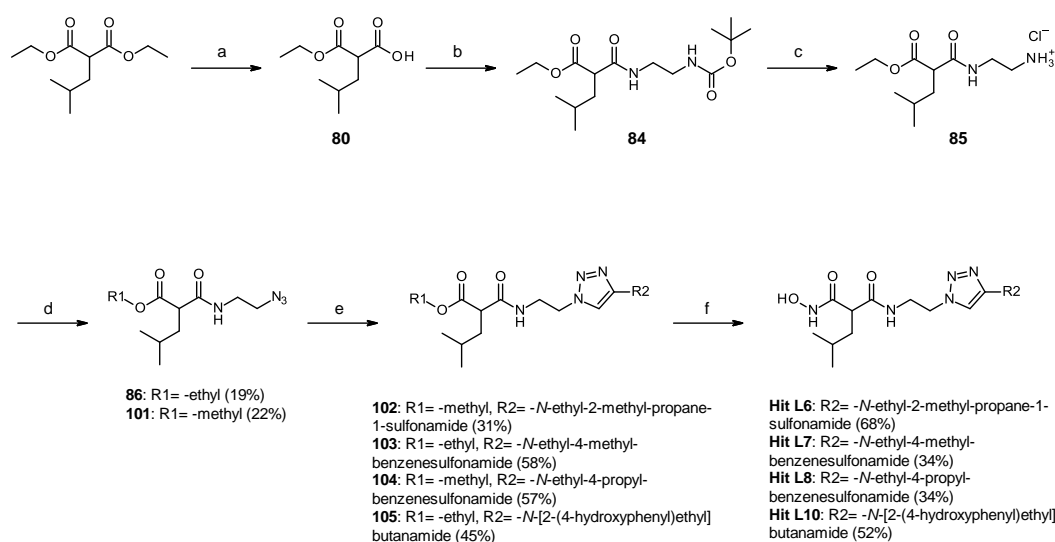
the 4-fluorobenzoyl chloride (**99**). Finally, for the phenol derivative, the alkyne was synthesized by nucleophilic substitution of phenol on the propargylbromide (**100**) (Scheme 21).



Scheme 21 : Synthesis of the alkynes for the click step (e)

B- Chemical synthesis of the selected hits from LasB Z4

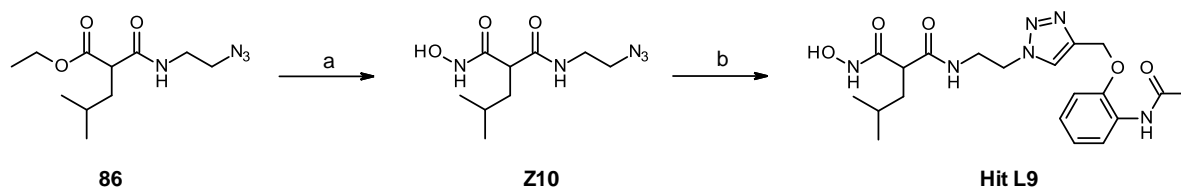
Concerning the amide formation (**84**), the mono carboxylic acid is activated by a mixture of EDC/HOBT in dichloromethane with DIPEA.



Reagents and conditions: a) NaOH, EtOH/H₂O (4:1), rt., overnight, 77%; b) tert-butyl N-(2-aminoethyl)carbamate, EDC.HCl, HOBT, DIPEA, CH₂Cl₂, rt., overnight, 80%; c) HCl 4M in dioxane, EtOH, 0 °C to rt., overnight, quantit. yield; d) azide-N-diazoimidazole-1-sulfonamide hydrogen chloride, K₂CO₃, ZnCl₂, DIPEA, MeOH or EtOH, 0 °C to rt., overnight, 19% (if MeOH: **86**), 22% (if EtOH: **101**); e) alkyne (**106**, **107**, **108** or **109**), CuSO₄ (5H₂O), sodium ascorbate, DMF/H₂O (1.2:1), rt., overnight, 31–58%; f) aq. hydroxylamine (50% in water w/w), KCN (cat.), MeOH, rt., overnight, 34–68%.

Scheme 22 : Chemical synthesis of the selected hits from Z10

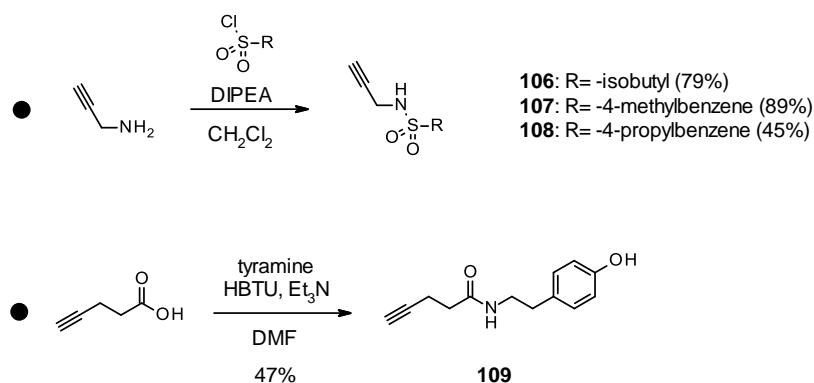
Unlike previously described for **Hit L6–L8** and **Hit L10**, in case of **Hit L9**, the click reaction and the aminolysis were inverted (Scheme 23). In this way, we avoided the cleavage of the acetamide functional group, which took place when the aminolysis was used as the last step.



Reagents and conditions: a) aq. hydroxylamine (50% in water w/w), KCN (cat.), MeOH, rt., overnight, 86%; (b) **100**, CuSO₄ (5H₂O), sodium ascorbate, DMF/H₂O (1.2:1), rt., overnight, 51%.

Scheme 23 : Chemical synthesis of Hit L9

The alkynes necessary for the click reaction with the azide **Z10** were synthesized according to the routes described in Scheme 9. For the sulfonamides (**106–108**), the reaction was performed using the same conditions as described previously. In case of the alkyne **109**, we performed the coupling between the 4-pentynoic acid and tyramine (Scheme 9).



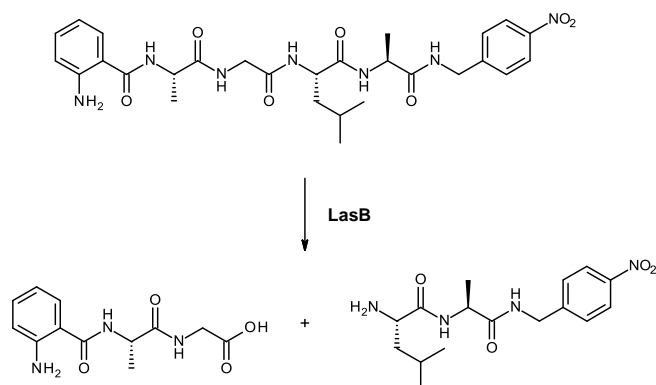
Scheme 24 : Synthesis of the alkynes for the click step (e)

5. Biochemical evaluations of selected hits

A- Principle of the enzymatic assay

To measure the enzymatic activity of our LasB inhibitors, we use a FRET-based proteolytic assay. In this assay, active LasB cleaves a quenched substrate, which produces an increase of fluorescence.⁽¹²³⁾ Enzyme inhibition leads to reduced substrate cleavage and consequently to reduced fluorescence (Figure 60). Phosphoramidon, a known LasB inhibitor, is used as a positive control.⁽¹¹⁷⁾

A. Fluorogenic substrate Abz-Ala-Gly-Leu-Ala-Nba



B. Concentration-dependent inhibition of the enzymatic reaction

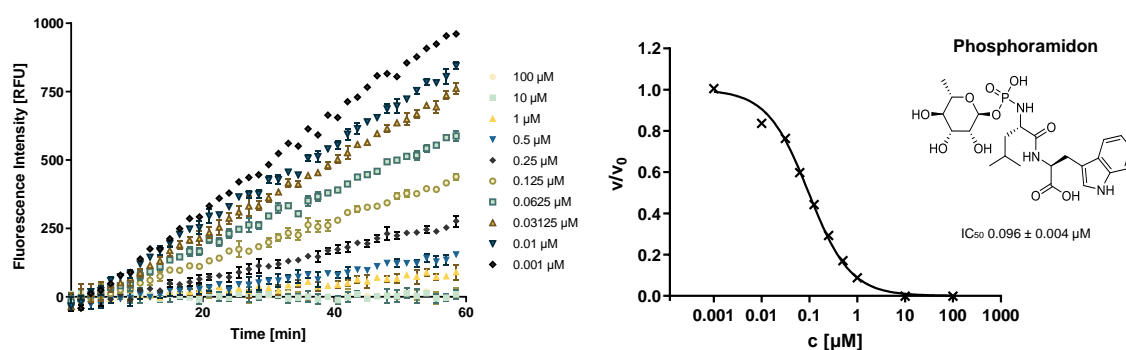


Figure 60: (A) Cleavage of the fluorogenic substrate by LasB. (B) Concentration-dependent inhibition of the enzymatic reaction, phosphoramidon used as a positive control

B- Biochemical results from the KTGS

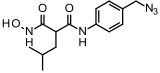
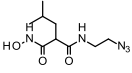
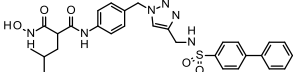
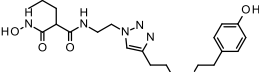
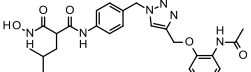
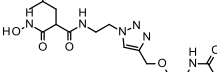
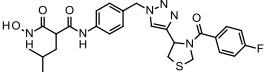
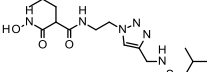
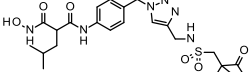
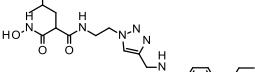
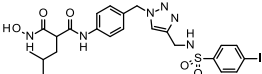
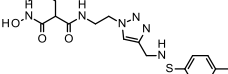
The biological results for the previously described LasB hits are highly promising and they are reported in Table 20.

The hits derived from **Z9** are particularly interesting, showing IC_{50} values in the range of 2.4–14 nM (**Hit L1–Hit L5**). Surprisingly, the starting azide is quite potent itself, with an IC_{50} of 17 nM. We assume that the potency of this azide comes from the introduction of the isobutyl group in the malonic position. It is difficult to judge the impact of the KTGS strategy only by looking at the IC_{50} values as for the most potent compound, it only led to a slight increase of the activity (17 nM to 2.4 nM, ≈ 7 -fold). However, it is important to note that this strategy does not only improve the biological activity; it can also improve other parameters such as the selectivity profile of the hits or the ADME properties.

Concerning the hits derived from the starting azide **Z10**, the results are less promising, showing the activities in micromolar range, e.g., $\text{IC}_{50} = 1.3 \mu\text{M}$ for **Hit L8**. Strangely, the starting azide is more potent than the obtained KTGS hits: $0.2 \mu\text{M}$ vs $1.3 \mu\text{M}$ (≈ 6.5 -fold). We

suppose that the introduction of the ethyl linker caused the flexibility of the hit structures, which turned out to be detrimental for the binding to the active site. Therefore, we decided to focus our efforts on the hits obtained from the azide **Z9** and especially to further optimize the **Hit L1** using conventional medicinal-chemistry strategies.

Table 20: Biochemical activities of the selected hits

Compound	Chemical structure	IC ₅₀ LasB (nM)	Compound	Chemical structure	IC ₅₀ LasB (μM)
Z9		16.9 ± 0.6	Z10		IC ₅₀ = 0.2 ± 0.1
Hit L3		13.9 ± 0.3	Hit L10		20.4 ± 0.1% @ 1μM
Hit L5		13.8 ± 0.3	Hit L9		21.9% @ 1μM
Hit L4		6.6 ± 0.2	Hit L6		31.8 ± 1.8% @ 1μM
Hit L2		5.3 ± 0.1	Hit L7		49.2 ± 0.1% @ 1μM
Hit L1		2.4 ± 0.1	Hit L8		IC ₅₀ = 1.3 ± 0.1

II. SAR studies

Six parts on the **LasB hit 1** were identified for the pharmacomodulation (Figure 61):

- the amide (gray)
- the “linker” sulfonamide (orange)
- the nature of the sulfonamide (blue)
- the malonic position (red)
- the triazole (green)
- the ZBG (purple)

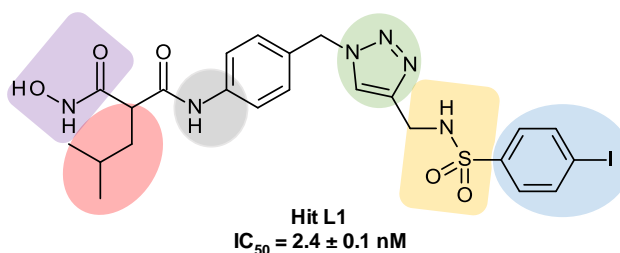
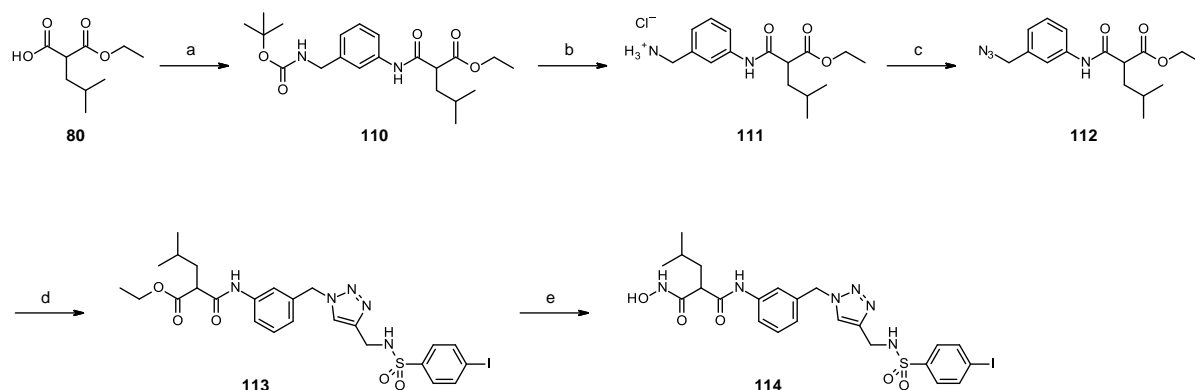


Figure 61: Identified parts of the Hit L1 for the pharmacomodulations

1. The amide

Concerning this part, we modified the amide position and synthesized the analog with the *meta*-substitution on the phenyl ring. The synthesis followed the same pathway described previously for **Z9** (Scheme 25).



Reagents and conditions : a) tert-butyl *N*-[(3-aminophenyl)methyl]carbamate, HBTU, Et₃N, DMF, rt., overnight, 74%; b) HCl 4M in dioxane, EtOH, 0 °C to rt., overnight, quantit. yield; c) azide-*N*-diazoimidazole-1-sulfonamide hydrogen chloride, K₂CO₃, ZnCl₂, DIPEA, EtOH, 0 °C to rt., overnight, 31%; d) **93**, CuSO₄ (5H₂O), sodium ascorbate, DMF/H₂O (1.2:1), rt., overnight, 86%; e) aq. hydroxylamine (50% in water w/w), KCN (cat.), MeOH, 48 h, overnight, 7%.

Scheme 25 : Synthesis of the meta-analog 114

This modification did not affect the activity significantly, with compound **114** showing an IC₅₀ value = 9.37 ± 0.27 nM. However, this derivative proved to be chemically less stable during the last step of the synthesis, with observed degradation leading to the release of the free aniline (Figure 62).

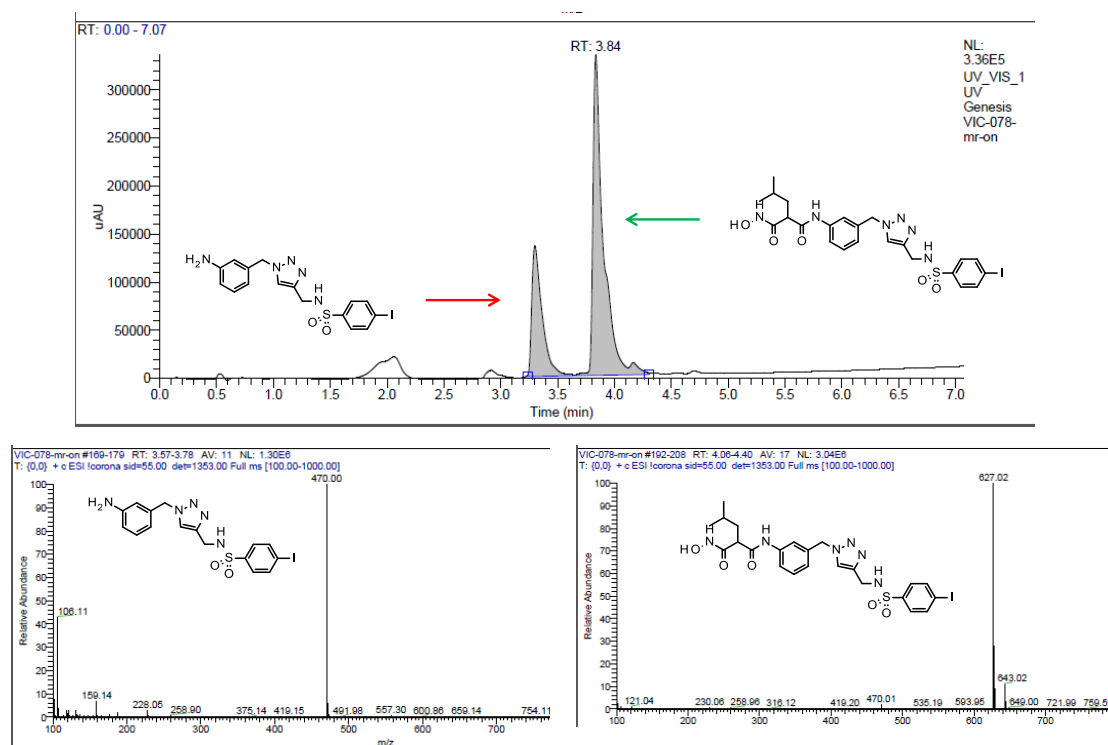


Figure 62 : LC UV-spectra at 254nm of the last step crude showing the degradation of the desired compound 114 and ESI⁺ ionization MS-spectra.

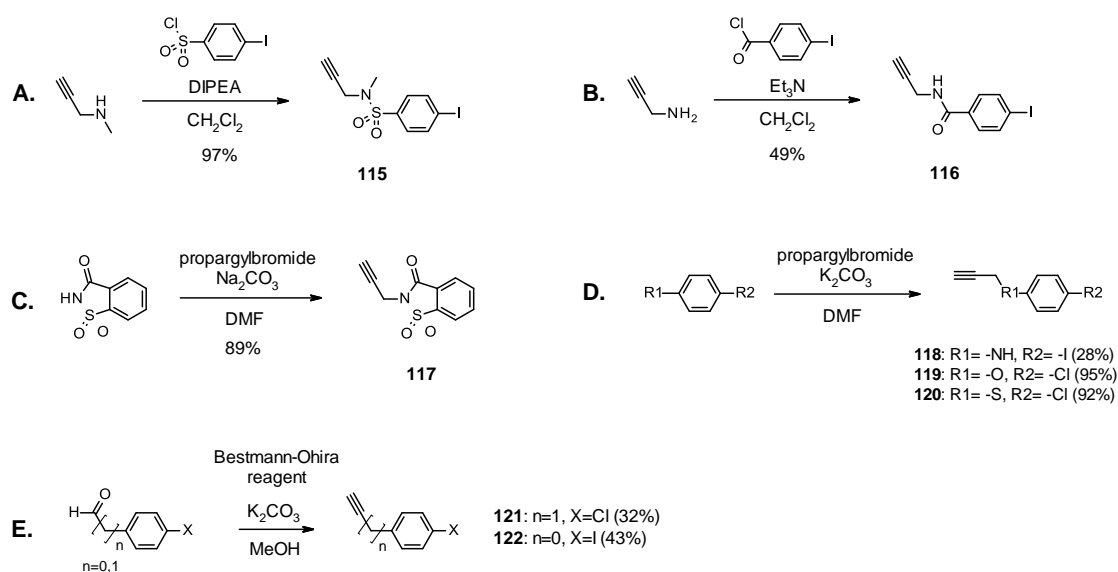
This cleavage was also observed sometimes during the synthesis of the initial KTGS hits, but less pronounced. Therefore, we decided to keep the amide in *para*-position to the triazole moiety.

2. The linker part

Concerning the linker part, we synthesized ten analogs of the **Hit L1** to explore the chemical space and determine which linker is most favorable for the activity. We replaced the sulfonamide linker with a *N*-methylsulfonamide, a cyclic sulfonamide, an amide, a carbamate, a free amine, an aniline, a ether a thioether and we also simplified it by directly linking the triazole to a benzyl or a phenyl.

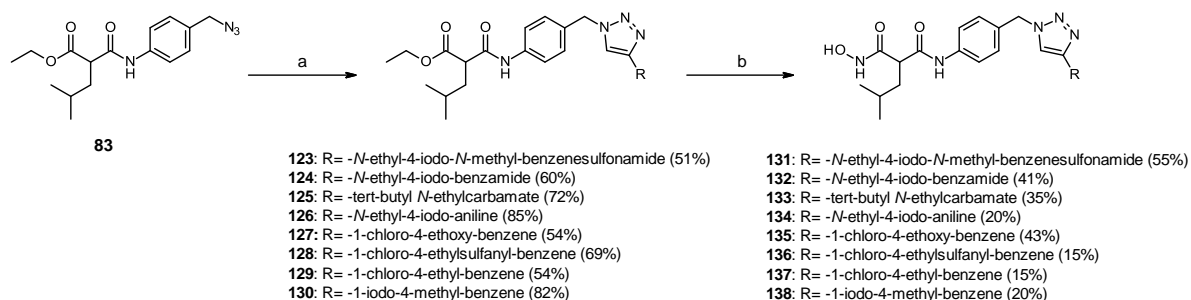
A- Chemical synthesis

The alkynes needed for the synthesis of the final compounds were synthesized as described previously (Scheme 24). For the *N*-methylsulfonamide alkyne (**115**) and the amide alkyne (**116**), we used the same reaction as before: nucleophilic acyl substitution of *N*-methylpropargylamine and propargylamine on the desired sulfonylchloride and acyl chloride, respectively (Scheme 26, A and B). In case of, to get the cyclic sulfonamide alkyne (**117**), we used the reaction of the saccharin and propargylbromide (Scheme 26C). Concerning the aniline, the ether and the thioether (**118–120**), the corresponding aniline, ether and thioether reacted with the propargylbromide to afford the desired alkynes (Scheme 26D). Finally, to simplify the linker, we formed the alkynes **121** and **122** by a Seyferth–Gilbert homologation (Scheme 26E).



Scheme 26 : (A) Nucleophilic acyl substitution (SN) of the *N*-methylpropargylamine on the sulfonylchloride and reagents/conditions/yield. (B) SN of the propargylamine on the acyl chloride and reagents/conditions/yield. (C) SN of the saccharin on the propargylbromide and reagents/conditions/yield. (D) SN on the propargylbromide and reagents/conditions/yield. (E) Seyferth–Gilbert homologation and reagents/conditions/yield.

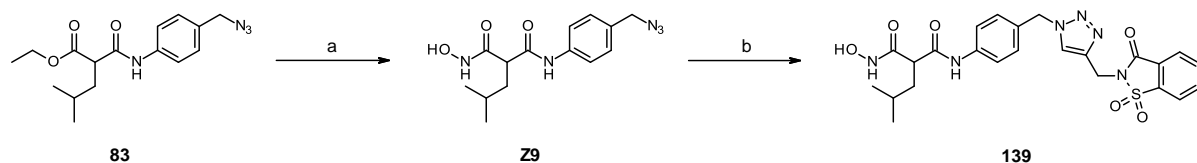
Eight compounds were synthesized using the same synthetic pathway described for the hits derived from **Z9** (Scheme 20), a copper-catalyzed click reaction followed by aminolysis (Scheme 27).



Reagents and conditions: a) alkyne (**115**, **116**, **118–122**, *N*-Boc-propargylamine), CuSO₄ (5H₂O), sodium ascorbate, DMF/H₂O (1.2:1), rt., overnight, 51–85%; b) aq. hydroxylamine (50% in water w/w), KCN (cat.), MeOH, rt., overnight–96 h, 15–55%.

Scheme 27 : Synthesis of the final compounds 131–138 and their respective intermediates 123–130

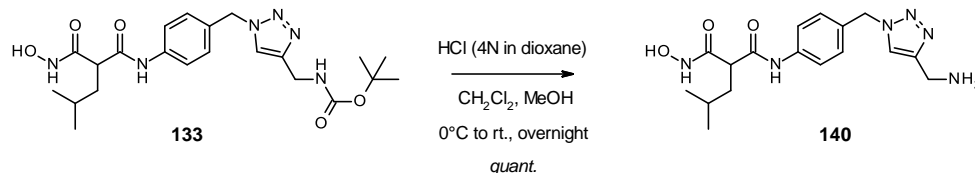
For the saccharin derivative, we reversed the click reaction and the aminolysis step to prevent the cleavage between the nitrogen and the sulfur of the sulfonamide (Scheme 13). Unfortunately, the yield of the click reaction was very low. We can explain this by the difficulties encountered during the purification; it was difficult to separate the starting azide and the final compound.



Reagents and conditions: a) aq. hydroxylamine (50% in water w/w), KCN (cat.), MeOH, rt., overnight, 38%; (b) **117**, CuSO₄ (5H₂O), sodium ascorbate, DMF/H₂O (1.2:1), rt., overnight, 15%.

Scheme 28 : Synthesis of compound 139

Finally, the free amine **140** was obtained by Boc-deprotection from the carbamate **133** using hydrogen chloride in dioxane (Scheme 29).



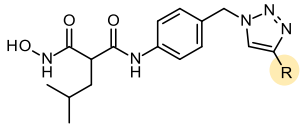
Scheme 29 : Synthesis of compound 140

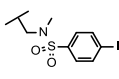
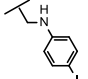
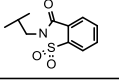
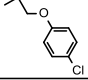
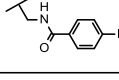
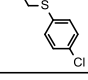
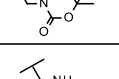
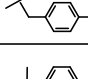
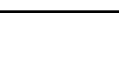
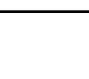
B- Biochemical evaluation

First, we wanted to know if the secondary sulfonamide is essential for the activity, and therefore, we synthesized compound **131** with an *N*-methyl sulfonamide linker. This modification did not affect the activity ($IC_{50} = 2.3 \pm 0.1$ nM). Then, we replaced the sulfonamide by a cyclic sulfonamide and amide, which led to a decrease of the IC_{50} by a factor of 10 (**139** and **132**). Introduction of the free amine with an aim to form stronger ionic interactions with the active site proved to be detrimental for the activity of the compound **140** ($IC_{50} = 55.9 \pm 2.3$ μ M, 23-fold drop compared to **Hit L1**) (Table 21).

The carbamate intermediate (**133**) was also tested, showing better activity compared to the free amine analog ($IC_{50} = 9.8 \pm 0.4$ nM). Comparable activity was observed for the aniline (**134**) or ether (**135**). Surprisingly, the introduction of a thioether linker demonstrated a significant increase in activity compared to *NH*- and *O*-analogs; the compound **136** proved to be even more active than the **Hit L1** ($IC_{50} = 1.4 \pm 0.1$ nM). Finally, we simplified the linker by directly connecting the triazole with a benzyl (**137**) or a phenyl (**138**) group. These modifications decreased the activities compared to the **Hit L1** by factors of eight and sixteen, respectively (Table 21).

Table 21: Biochemical activities of the compounds 131-140



Compound	R	IC_{50} LasB (nM)	Compound	R	IC_{50} LasB (nM)
131		2.3 ± 0.1	134		8.4 ± 0.5
139		19.3 ± 0.6	135		9.8 ± 0.3
132		22.8 ± 0.1	136		1.4 ± 0.1
133		9.8 ± 0.4	137		16.9 ± 1.3
140		55.9 ± 2.3	138		37.8 ± 2.9

C- Conclusions

The compounds **131** and **136** looked equally promising as the initial **Hit L1** and, for this reason; we decided to do the further profiling by exploring other properties such as the solubility and the metabolic stability (Table 22). Firstly, compared to **Hit L1**, the introduction of a tertiary sulfonamide decreases the solubility (**131**) and does not change significantly the metabolic stability. More importantly, the derivative with the thioether linker (**136**) has a poor

metabolic stability in mouse microsomes ($t_{1/2} = 3.3 \pm 0.2$ min). Therefore, the sulfonamide linker was kept for the other modulations.

Table 22: Comparison study between Hit L1, 131 and 136 according to their activity, solubility and metabolic stability in mouse

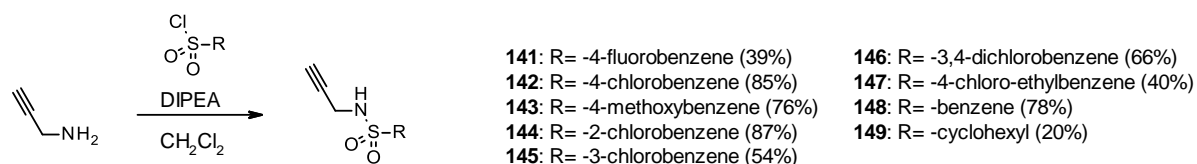
Compound	Structure	IC ₅₀ LasB (nM)	Solubility (μM)	Met Stab in mouse liver S9 t _{1/2} [min]
Hit L1		2.4 ± 0.1	106 ± 19	30.1 ± 1.5
131		2.3 ± 0.1	< 200	37.5 ± 2.5
136		1.4 ± 0.1	< 200	3.3 ± 0.2

3. The nature of the sulfonamide

After demonstrating that the sulfonamide linker is the most promising, we continued with the modification of the *para*-iodophenyl moiety and synthesized ten corresponding analogs.

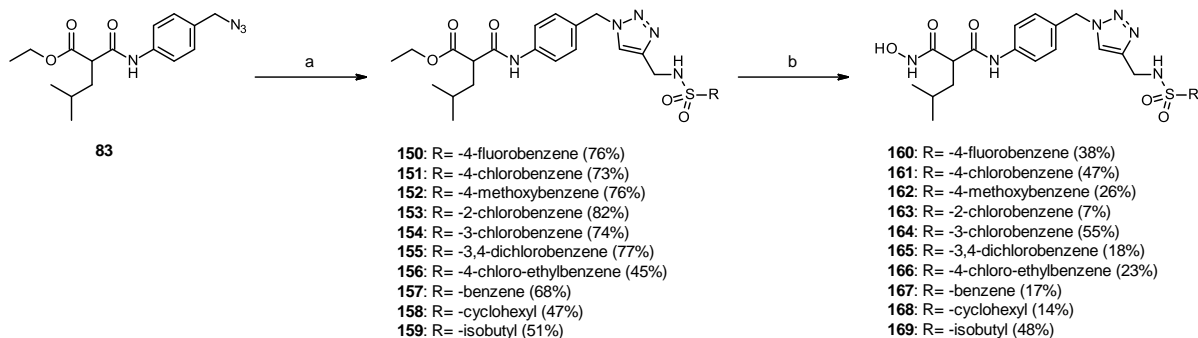
A- Chemical synthesis

The alkynes needed for the triazole formation were synthesized using a nucleophilic acyl substitution by propargylamine on the corresponding sulfonyl chlorides (Scheme 30), as described previously (Scheme 21).



Scheme 30 : Synthesis of alkynes 141–149

The final compounds were synthesized using a copper-catalyzed click reaction and aminolysis (Scheme 31), as described previously (Scheme 20 and Scheme 27).



Reagents and conditions: a) alkyne (**106**, **141–149**), $\text{CuSO}_4 \cdot 5\text{H}_2\text{O}$, sodium ascorbate, $\text{DMF}/\text{H}_2\text{O}$ (1.2:1), rt., overnight, 47–82%; b) aq. hydroxylamine (50% in water w/w), KCN (cat.), MeOH, rt., overnight–72 h, 7–55%.

Scheme 31 : Synthesis of the final compounds 160–169 and their respective intermediates 150–159

B- Biochemical evaluations

First, the replacement of the 4-iodine by 4-fluorine or 4-chlorine (**160** and **161**) did not significantly affect the activity. Introduction of an electron-donating group, such as methoxy (**162**) did not affect the inhibitory activity either. Variations in the halogen position from *para*- (**161**) to *meta*- (**164**) and *ortho*- (**163**) resulted in comparable IC_{50} s values.

Next, we decided to modify the electronic density of the phenyl ring by introduction of an additional chlorine substituent in position 3 (**165**), which also did not have an influence on the activity. Finally, we continued our investigations by increasing the chain length (**166**), removing the substituent (**167**) and replacing the aromatic moiety by a cyclohexyl (**168**) and an isobutyl (**169**). In each case no improvement of the IC_{50} value was observed (Table 23).

Table 23: Biochemical activities of the compounds 160–169

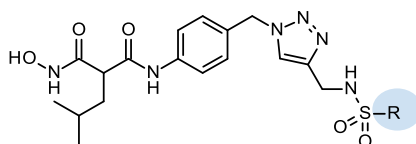
Compound	R	IC_{50} LasB (nM)	Compound	R	IC_{50} LasB (nM)
160		3.8 ± 0.1	165		1.6 ± 0.1
161		1.7 ± 0.1	166		5.2 ± 0.3
162		1.9 ± 0.1	167		5.5 ± 0.3
163		4.3 ± 0.1	168		2.7 ± 0.2
164		2.4 ± 0.1	169		5.2 ± 0.2

C- Conclusions

As a conclusion, the nature of the substituent on the sulfonamide linker has no significant impact on the activity and a broad list of substituents is tolerated in this part of the structure. We decided to carry out further investigations, in particular regarding the ADME properties. We selected the compounds **160**, **161**, **165** and **169** and measured their solubility and the metabolic stabilities in mouse and human liver microsomes, as well as calculated the corresponding cLogP values (Table 24).

The replacement of 4-iodine in **Hit L1** by 4-chlorine (**161**) increased the solubility without affecting the metabolic stability. The introduction of an additional chlorine in position 3 (**165**) decreased the solubility as well as the metabolic stability by a factor of three. At the same time, we managed to improve the solubility and the metabolic stability by replacing the 4-iodobenzene by 4-fluorobenzene (**160**) and isobutyl group (**169**). In fact, the metabolic stability increased 3- and 4-fold for the 4-fluoro and the isobutyl compounds, respectively, being now in a satisfactory range. The metabolic stability in mouse seems to be nicely correlated with the lipophilicity, based on the calculated cLogP values (Table 24).

Table 24: Comparative study between Hit L1, 160, 161, 165 and L94 according to their activity, solubility, clogP and metabolic stability in mouse. *cLogP values were calculated using Datawarrior.



Compound	R	IC ₅₀ LasB (nM)	cLogP*	Solubility [μM]	Met Stab in mouse liver S9 t _{1/2} [min]
Hit L1		2.4 ± 0.1	1.5	142	30.1 ± 1.5
161		1.7 ± 0.1	1.6	> 200	33.9 ± 1.0
165		1.6 ± 0.1	2.2	117	10.7 ± 0.6
160		3.8 ± 0.1	1.1	> 200	65.5 ± 0.7
169		5.2 ± 0.2	0.9	> 200	> 120

Thus, regarding these results, the compounds **160** and **169** were chosen for *in vivo* pharmacokinetic studies and further biological evaluation.

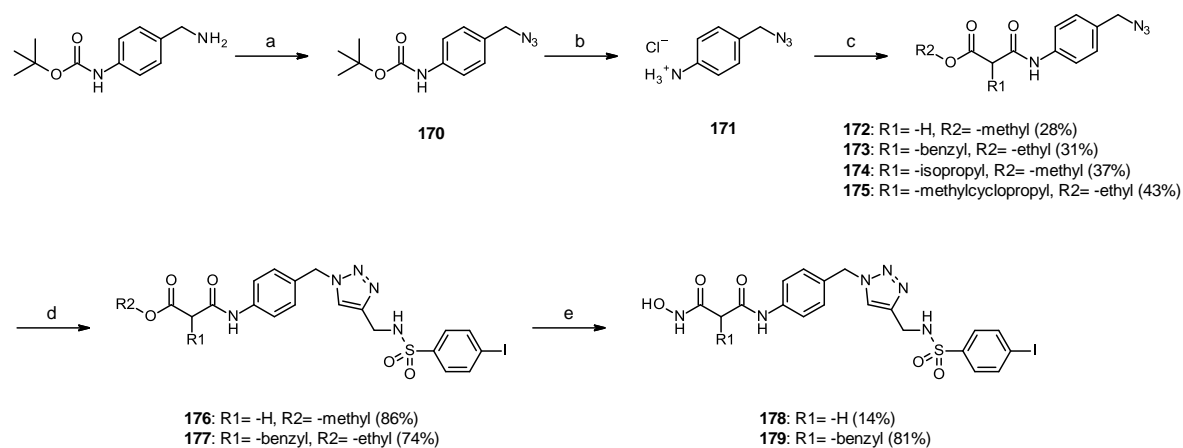
After this small SAR study around the nature of the sulfonamide, we moved to the investigation of the malonic position.

4. The malonic position

For the design of the starting azides for the KTGS, we assumed that the introduction of an isobutyl chain in α -position will have a positive impact on the activity; based on the LasB preferences for the substrate cleavage and known SAR of Hirsch's team.⁽¹²²⁾ This α -substitution could also be a key element to control the selectivity. So, the aim of this study was to verify this hypothesis. We synthesized the derivatives with no α -side chain, with an isopropyl, methylcyclopropyl and benzyl group.

A- Chemical synthesis

For the synthesis of the mentioned analogs, the synthetic pathway had to be slightly adjusted due to the known reactivity of the malonic position, particularly during the diazo transfer. The diazo transfer was performed during the first step with a quantitative yield (**170**). This was followed by Boc deprotection (**171**) and amide formation using an acyl chloride (**172**) or a carboxylic acid (**173–175**). Finally, the last two steps were the click reaction and the aminolysis to get the final compounds without substituent (**178**) or with a benzyl (**179**) in the malonic position (Scheme 32).



Reagents and conditions : a) azide-*N*-diazoimidazole-1-sulfonamide hydrogen sulfate, K_2CO_3 , $ZnCl_2$, DIPEA, MeOH, 0 °C to rt., overnight, quantit. yield; b) HCl 4M in dioxane, CH_2Cl_2 , MeOH, 0 °C to rt., overnight, quant. yield; c) methyl 3-chloro-3-oxo-propanoate, Et_3N , CH_2Cl_2 , 0 °C to rt., 3 h, 29% or carboxylic acids (**173a–175a**), HBTU, Et_3N , DMF, rt., overnight, 28–43%; d) **93**, $CuSO_4 (5H_2O)$, sodium ascorbate, DMF/ H_2O (1.2:1), rt., overnight, 74–86%.; e) aq. hydroxylamine (50% in water w/w), KCN (cat.), MeOH, rt., 16–96 h, 14–81%

Scheme 32 : Chemical synthesis of final compounds 178 and 179

Unfortunately, in case of the isopropyl derivative, we observed deiodination when the aminolysis was used as the last step (Figure 63). We decided not to continue with this route due to the difficult purification and low yields.

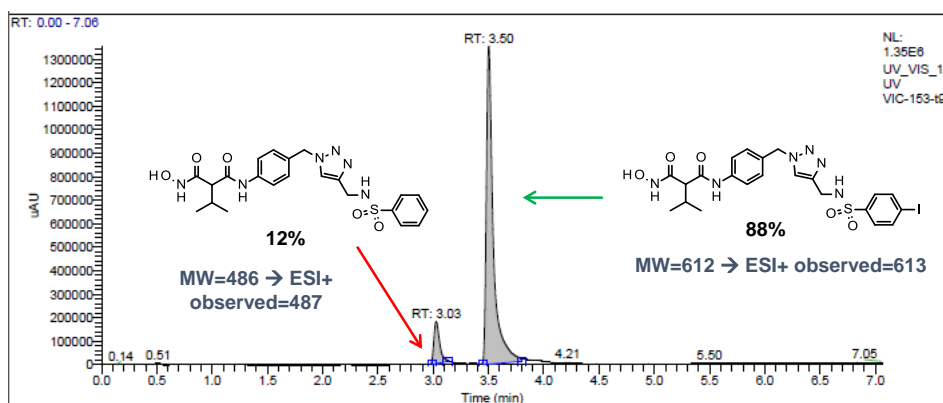
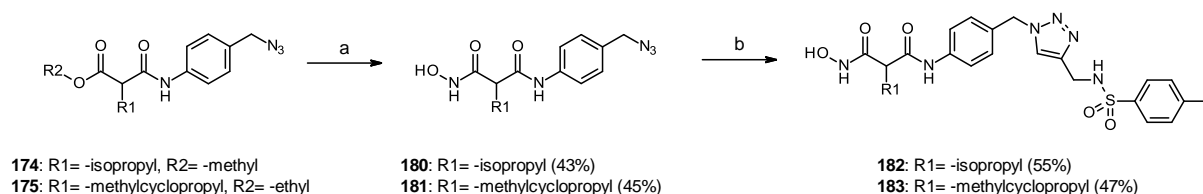


Figure 63: LC-UV spectra of the purified fraction of the isopropyl derivative showing the diiodination (mixture 88:12)

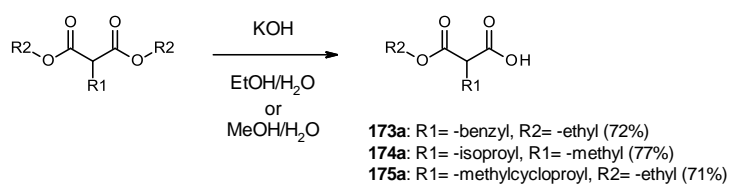
Therefore, we decided to reverse the click reaction and aminolysis steps for both isopropyl and methylcyclopropyl derivatives (Scheme 33).



Reagents and conditions: a) aq. hydroxylamine (50% in water w/w), KCN (cat.), MeOH, rt., overnight, 43–45%; b) **93**, CuSO₄ (5H₂O), sodium ascorbate, DMF/H₂O (1.2:1), rt., overnight, 47–55%.

Scheme 33 : Chemical synthesis of final compounds **182** and **183** by inverting the click reaction and the aminolysis steps

The carboxylic acids needed for the amide formation were synthesized using a monosaponification of the malonic diester (Scheme 34).



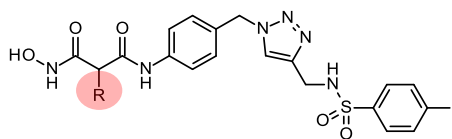
Scheme 34 : Formation of the mono carboxylic acids **173a–175a**

B- Biochemical evaluation

Results of the derivatives with the variations in the malonic position are presented in Table 25. Removal of the isobutyl group resulted in 1log loss of the activity (**178**). The introduction of benzyl (**179**) and methylcyclopropyl side chains (**183**) led to a slight decrease in the IC₅₀, value, suggesting that the corresponding binding pocket is not very deep. The

compound bearing the smaller isopropyl substituent (**182**) proved to be in the same range of activity as the initial **Hit L1** ($IC_{50} = 1.9 \text{ nM}$ vs 2.4 nM).

Table 25: Biochemical activities of the compounds Hit L1, 178–179 and 182–183



Compound	R	IC_{50} LasB (μM)
Hit L1	-isobutyl	0.0024 ± 0.0001
178	-H	14.57 ± 0.69
182	-isopropyl	0.0019 ± 0.0001
183	-methylcyclopropyl	0.0099 ± 0.0003
179	-benzyl	0.0010 ± 0.0006

C- Conclusions

We have demonstrated that the substitution on the malonic position is essential for the activity. However, only four compounds were synthesized. Therefore, more analogs must be explored to extend our scope of investigation and thus establish if the substitution would have an impact on the selectivity profile.

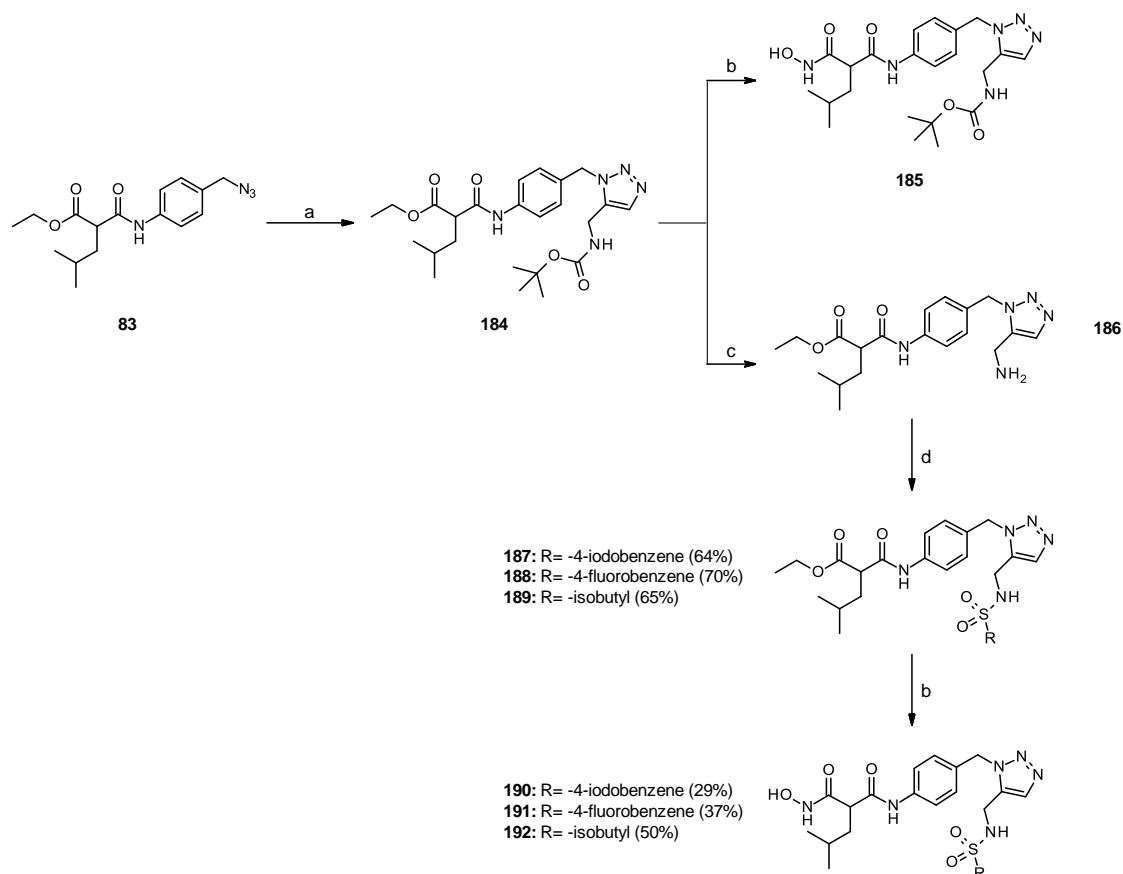
5. 1,5-Triazole regioisomer synthesis

As presented previously, during the KTGS, the enzyme can catalyze the formation of the 1,4-disubstituted or the 1,5-disubstituted 1,2,3-triazole (or both regioisomers). For the selected hits, we supposed that LasB catalyzed the formation of the 1,4-regioisomers. In order to compare the two regioisomers, we synthesized the corresponding 1,5-triazoles.

A- Chemical synthesis

To access the 1,5-regioisomer, ruthenium-catalyzed click reaction was used.⁽¹²⁴⁾ For accessibility reasons, and as the carbamate **133** showed a good activity on LasB ($IC_{50} = 9.8 \pm 0.4 \text{ nM}$), we first decided to perform the ruthenium-catalyzed click reaction using *N*-Boc-propargylamine as an alkyne. During the click reaction, only the 1,5-regioisomer formation was observed and therefore the compound was isolated in a good yield. This reaction was followed by aminolysis to give the final compound **185**. **184** was engaged in a succession of

three steps to afford the desired 1,5-triazoles bearing a sulfonamide linker (**190–192**) (Scheme 35).



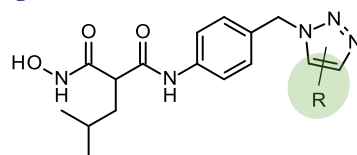
Reagents and conditions: a) *N*-Boc-propargylamine, Cp**Ru*Cl (COD), dioxane, 80 °C, overnight, 73%; b) aq. hydroxylamine (50% in water w/w), KCN (cat.), MeOH, rt., 48 h, 26–50%; c) HCl 4M in dioxane, CH₂Cl₂, EtOH, 0 °C to rt., overnight, quant. yield; d) R-SO₂-Cl, DIPEA, DMF, 0 °C to rt., overnight, 64–70%.

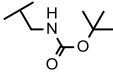
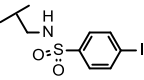
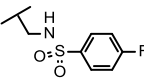
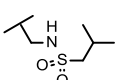
Scheme 35 : Chemical synthesis of the 1,5-disubstituted 1,2,3-triazoles using ruthenium-catalyzed click reaction

B- Biochemical evaluation

Regarding the carbamate linker (**133** and **185**), no significant difference in the activity was observed between the 1,4-triazole **133** and the 1,5-triazole **185** ($IC_{50} = 9.8$ nM vs 6.5 nM, respectively). The observations were the same for the sulfonamide linkers (**190–192**) although the 1,4-triazoles (**Hit L1**, **160** and **169**) display “slightly” higher activity values. As for the 1,4-triazoles, the nature of the sulfonamide did not have a significant impact on the potency; the three 1,5-triazoles displaying the same IC_{50} (**190–192**, $IC_{50} \approx 7–8$ nM) (Table 26).

Table 26 : Comparative study between the biochemical activities of 1,4- and 1,5-disubstituted 1,2,3-triazoles containing carbamate and sulfonamide linkers



R	Compound	IC ₅₀ LasB (nM)
	133 Regioisomer 1,4	9.8 ± 0.4
	185 Regioisomer 1,5	6.5 ± 0.2
	Hit L1 Regioisomer 1,4	2.4 ± 0.1
	190 Regioisomer 1,5	7.8 ± 0.1
	160 Regioisomer 1,4	3.8 ± 0.1
	191 Regioisomer 1,5	7.9 ± 0.1
	169 Regioisomer 1,4	5.2 ± 0.2
	192 Regioisomer 1,5	6.8 ± 0.1

C- Conclusion

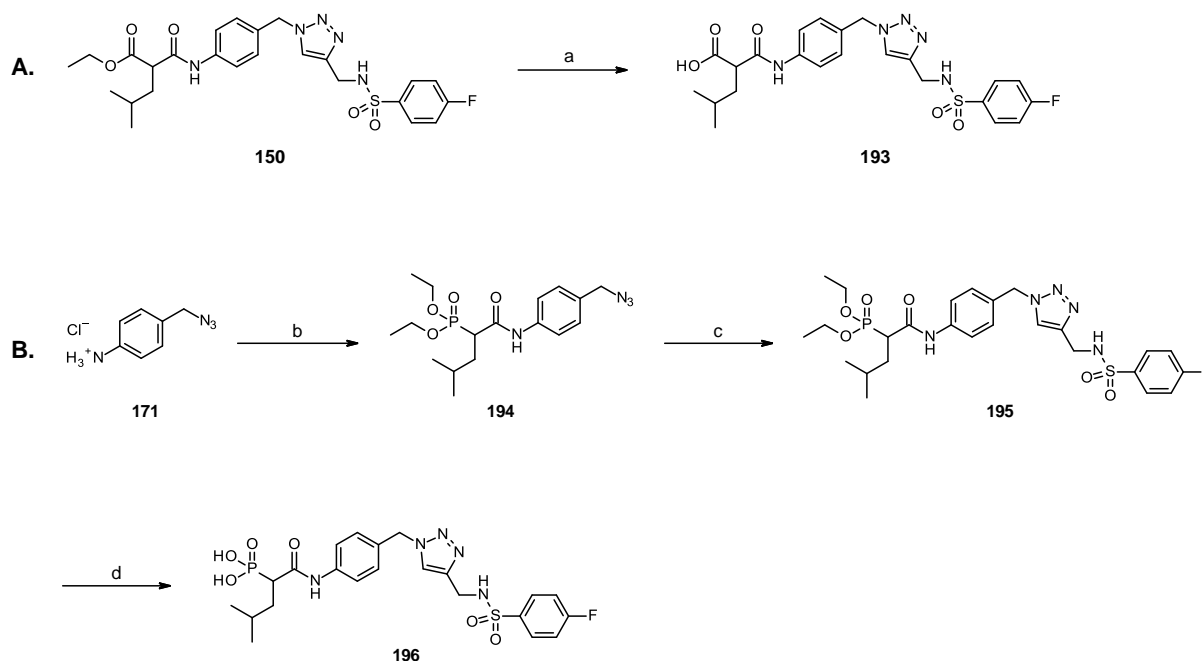
In order to extend our comparison study, the synthesis of 1,5-disubstituted 1,2,3-triazoles with other linkers is planned.

6. The ZBG

In addition to the variety of previously discussed modifications, to get the full picture around the chemical space of the KTGS hits, we investigated the replacement of the hydroxamic acid with alternative ZBGs. In the literature, some cases of zinc coordination by sulfonamides were reported.⁽¹²⁵⁾ As our compounds contain both hydroxamic acid and a sulfonamide group, we wanted to check whether the hydroxamic acid is responsible for the coordination of the zinc cation. To verify our hypothesis, the ethyl ester **150** was tested. Secondly, as the hydroxamic acid is known for its selectivity-related issues, it was replaced by other ZBGs such as carboxylic acid and phosphonate.

A- Chemical synthesis

The carboxylic acid was obtained by saponification of the ethyl ester using sodium hydroxide (Scheme 36A). The phosphonate was synthesized in three steps: amide formation, click reaction and ester deprotection (Scheme 36B).



Scheme 36 : (A) Synthesis of the carboxylic acid 193, (B) Synthesis of the phosphonate 196

Reagents and conditions: a) NaOH, THF/H₂O (1:1), rt., overnight, 54%; b) 2-diethoxyphosphoryl-4-methyl-pentanoic acid, TBTU, NMM, DMF, rt., overnight, 66%; (c) **141**, CuSO₄ (5H₂O), sodium ascorbate, DMF/H₂O (1.2:1), rt., overnight, 77%; d) TMSBr, CH₂Cl₂, 0 °C to rt., 48 h, 35%.

B- Biochemical evaluation

As expected, the ethyl ester (**150**) as well as the corresponding carboxylic acid (**193**) did not show any activity on LasB (IC₅₀ > 100 μM). On the other hand, replacement of the hydroxamic acid with a phosphonate (**196**) resulted in the compound showing the activity in nM range, however, still being 20-fold less active than the corresponding hydroxamate derivative (IC₅₀ = 75.6 ± 2.6 nM).

C- Conclusions

The hydroxamate replacement by ethyl ester led to a loss of activity, which means that the zinc coordination is carried out by the hydroxamic acid and not by the sulfonamide. Known for its poor selectivity, the hydroxamic was then replaced by carboxylic acid or phosphonate but these two ZBG did not show good activities on LasB. Therefore, we can conclude that the hydroxamate is essential for the potency. The toxicity and selectivity studies have been presented below.

III. Toxicity and selectivity profile studies

Four hydroxamic acid derivatives were selected for the selectivity and toxicity profiling: **Hit L1**, **160**, **169**, and **Z9**. Their chemical structures are shown below together with their biological activities on LasB (Figure 64).

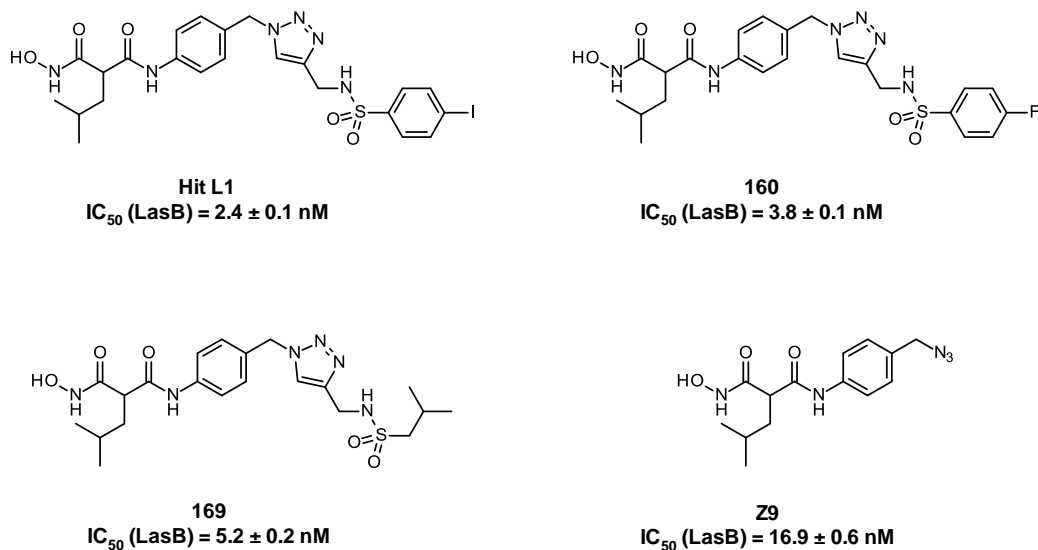


Figure 64: Chemical structures of Hit L1, 160, 169, Z9 and their biological activities on LasB

While identical profiles would be expected for **Hit L1** and **160**, **169** has been included to determine the influence of the sulfonamide nature on the selectivity, the toxicity and the antibacterial activity on *P. aeruginosa*. The starting **Z9** has been included to rationalize the use of KTGS for the synthesis of more complex structures.

Each compound has been tested against seven other zinc metalloproteases including the MMPs -1, -2 and -3, the HDACs -3 and -8, TACE and COX-1. The cytotoxicity has been measured on three different cell-lines: HepG2, HEK293 and A549. The antibacterial activity has been measured using *P. aeruginosa* PA-14 strain. The results are reported in the table below.

Table 27: Selectivity and cytotoxicity profiles of Hit L1, 160, 169 and Z9 with their antibacterial activities against the strain PA-14

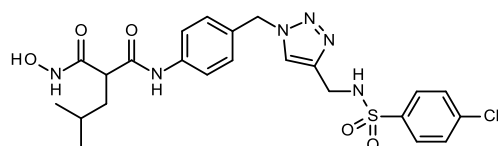
		Hit L1	160	169	Z9
Selectivity IC ₅₀ (μM)	MMP1	> 100	> 100	> 100	> 100
	MMP2	> 100	> 100	> 100	> 100
	MMP3	> 100	> 100	> 100	> 100
	HDAC3	> 100	> 100	> 100	> 100
	HDAC8	> 100	> 100	> 100	> 100
	TACE	> 100	> 100	> 100	1.6 ± 0.2
	COX-1	> 100	> 100	> 100	> 100
Cytotoxicity IC ₅₀ (μM)	HepG2	> 100	> 100	> 100	> 100
	HEK293	> 100	> 100	> 100	> 100
	A549	> 100	> 100	> 100	> 100
Antibacterial activity IC ₅₀ (μM)	PA-14	> 100	> 100	> 100	> 100

To our great pleasure, the profile of the KTGS hit (**Hit L1**) looks very promising: no off-target effects, no cytotoxicity and no antibacterial activity. The analysis is the same for **160** and **169**. So, it would seem that the nature of the sulfonamide does not have an impact on these parameters; but this has to be confirmed with the evaluation of more compounds. Additionally, **160** and **169** have also been tested against the MMPs 7, 8 and 14 without demonstrating residual activities on them (IC₅₀ > 100 μM).

Although the selectivity profile of **Z9** looks promising, the starting azide displays a micromolar activity value on TACE that is not found for **Hit L1** (KTGS templated ligand). Thus, the KTGS strategy allowed us to improve the selectivity profile.

IV. Binding mode study of hydroxamic acid inhibitor-LasB

To elucidate the binding mode of our compounds in the active site of LasB, co-crystallization was performed with **161** (resolution 2.4Å); its structure is presented below together with its IC₅₀ value (Figure 65).



161
 $IC_{50} (LasB) = 1.7 \pm 0.1 \text{ nM}$

Figure 65: Chemical structure of 161 and its IC_{50} value on LasB

Concerning the binding (Figure 66), we observed a surprising folding of **161** in the active site, which can probably be explained by the flexibility provided by the methylene spacers between the phenyl and the triazole and the triazole and the nitrogen of the sulfonamide. The isobutyl chain is nicely accommodated in a small pocket close to the zinc cation, explaining why the α -substitution is essential for the activity; in particular with non-bulky groups. The chlorophenyl moiety lines a cavity, which contains hydrophobic residues such as methionine (Met128) and phenylalanine (Phe129) residues. The phenyl group interacts with a histidine residue (His223) and the oxygen of the amide interacts with an arginine residue (Arg 198) through a hydrogen bond. Interestingly, in the active site, compound **161** seems to have a favorable conformation for macro cyclization.

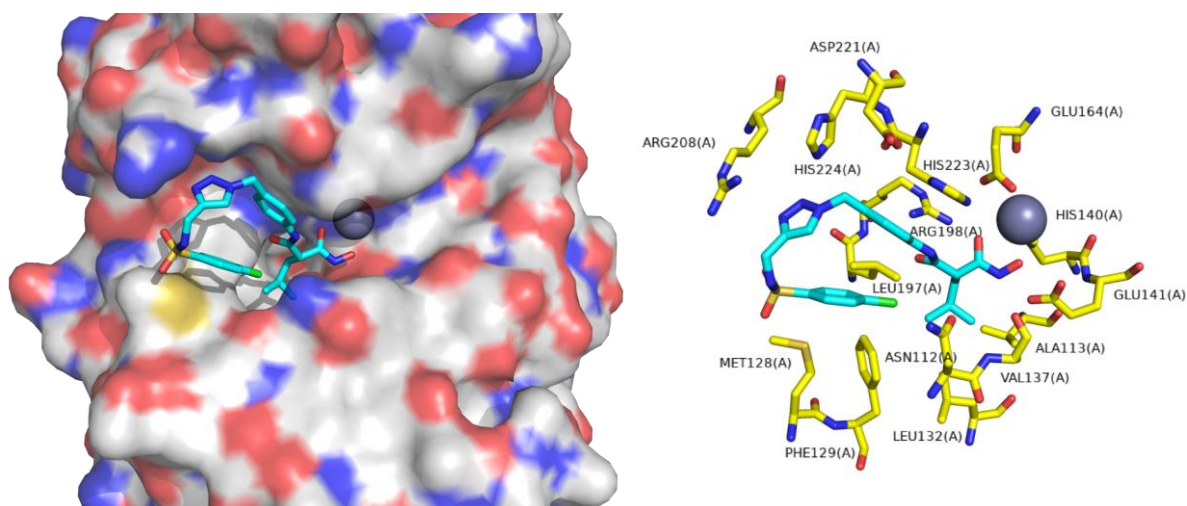


Figure 66 : Binding mode of 161 in LasB. Carbons are indicated in gray, nitrogens in blue, oxygens in red, sulfur in yellow and chlorine in green. The ligand 161 is represented in cyan and the zinc as a gray sphere. (A) Surface representation of LasB bound to 161. (B) Interactions between 161 and the adjacent amino acid side chains of LasB which are represented in yellow stick

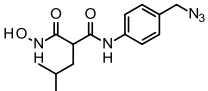
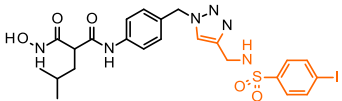
With this folding, the pocket occupancy looks extremely good and offers an explanation for the compound's excellent potency and probably explains the good selectivity profile.

Conclusion & Perspectives

For all the reasons mentioned, the use of the KTGS strategy allowed us to discover two new families of LasB inhibitors, one with nanomolar activities (family from **Z9**: **Hit L1** to **Hit L5**) and the other with micromolar activities (family from **Z10**: **Hit L6** to **Hit L10**). Regarding, the compounds from **Z10**, we supposed that the ethyl linker probably brings a lot of flexibility which could be negative for the binding in the active site. We decided thus to stay focus on the compounds from **Z9** which displayed nanomolar activity values.

Regarding the most potent hit from **Hit L1**, although the starting azide **Z9** was surprisingly potent, a seven-fold gain in the activity was observed with the most potent KTGS hit (**Hit L1**) (17 nM vs 2.4 nM). This gain in the activity comes from the triazole formation (orange part) which maximizes the pocket occupancy and therefore explains the increase of the LLE. The decrease of the LE can be explained by the smaller size of the azide (Table 28).

Table 28: IC₅₀, LE and LLE comparison between Z9 and Hit L1. LE and LLE were calculated using Datawarrior software from the IC₅₀

Compound	Chemical structure	IC ₅₀ LasB	Ligand Efficiency (LE)*	Lipophilic Ligand Efficiency (LLE)*
Z9		16.9 ± 0.6 nM	0.5	6.8
Hit L1		2.4 ± 0.1 μM	0.3	7.1

In **Hit L1**, we identified six parts used for the pharmacomodulation: the amide, the sulfonamide linker, the nature of this sulfonamide, the malonic position, the triazole and the ZBG.

Hit L1 has a perfect profile: nanomolar potency, no off-target effects, no cytotoxicity and no antibacterial activity. Strikingly, compared to **Z9**, **Hit L1** does not display residual activity on TACE. The SAR studies performed on this compound did not lead to a significant increase of the IC₅₀ value but allowed us to improve the physicochemical properties such as the solubility and the metabolic stability. The most promising analogs with enhanced physicochemical properties such as **160** (4-fluorobenzene sulfonamide), and **190** (isobutyl sulfonamide) are also potent, selective, non-cytotoxic and devoid of antibacterial activity which makes them

promising lead compounds. For this reason, we selected these compounds for *in vivo* pharmacokinetic studies and further biological evaluation. We need to investigate their activities in the model systems closer to reality, as for example, in presence of pulmonary surfactant or in the *Galleria mellonella* infection model.

Co-crystallization of **161** (4-chlorobenzene sulfonamide) with LasB was performed to elucidate the binding mode of the KTGS inhibitors. The complex structure demonstrated perfect pocket occupancy, presumably due to the two methylene spacers in the linker. These two CH₂ groups are responsible for the “folding” of the compound, which leads to an optimal occupancy of the pocket. This co-crystallization sets the stage for further structure-based medicinal-chemistry optimization of the initial hits.

Concerning the future modifications, first we plan to modify the two methylene spacers stated above to verify their real impact on the activity. Then, since only four analogs were synthesized with regard to the malonic position; we plan to extend the scope of possible substituents. Regarding the nature of the sulfonamide, we can introduce heterocycles (imidazole, pyridine, thiophene...). Finally, based on the compound folding, we envisage that the synthesis of macrocycles would reduce the flexibility while improving the other parameters (potency, affinity, selectivity...). All mentioned modifications are schematically presented on Figure 67.

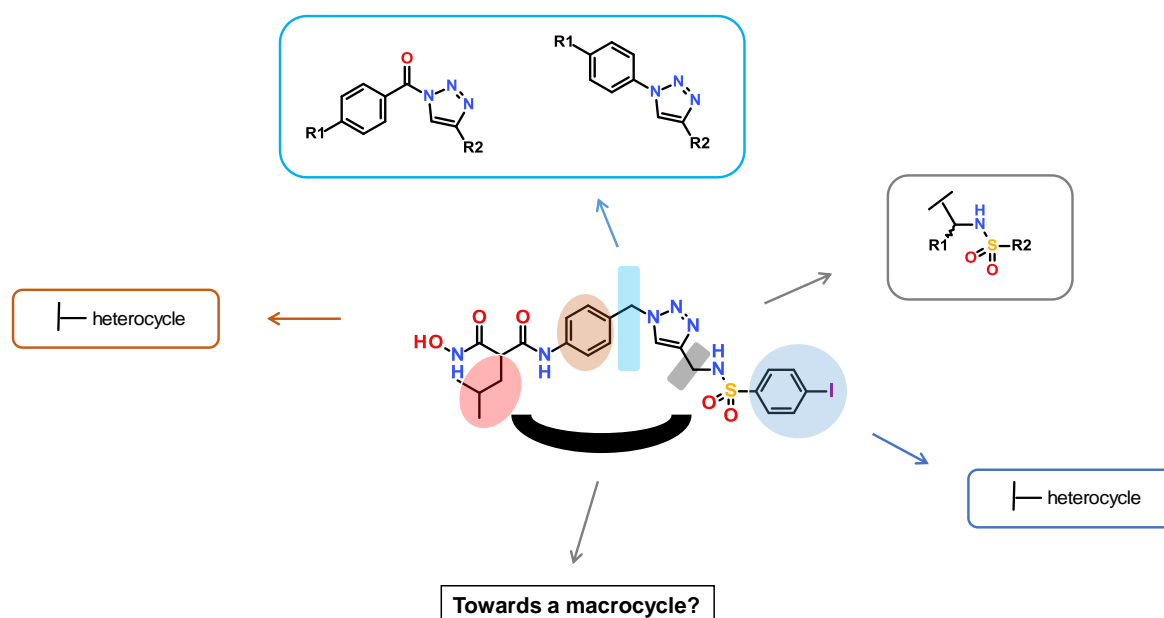
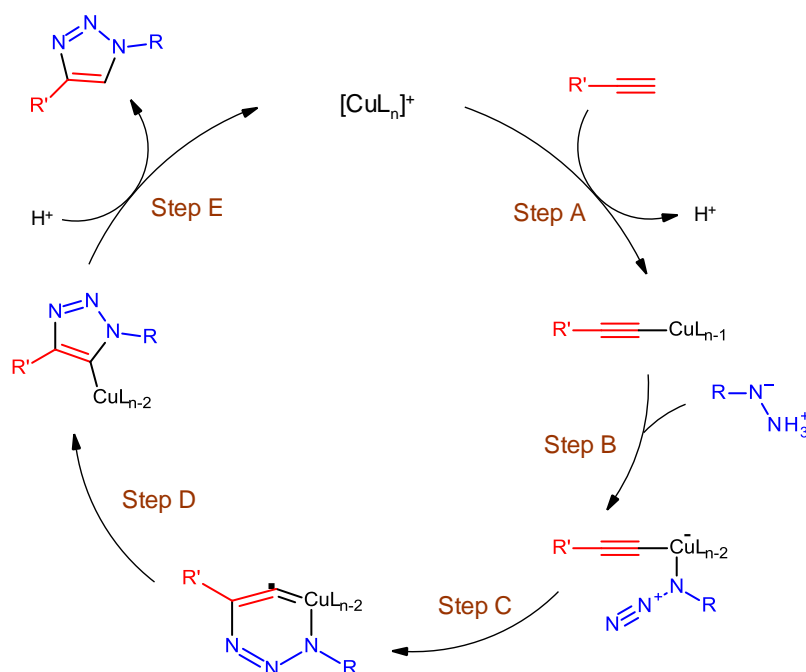


Figure 67: Planned modifications

Chapter 4: Development of an efficient one pot methodology for the preparation of 1,5-disubstituted 1,2,3-triazoles

Introduction

As seen previously, the 1,2,3-triazole is a ring of interest in our projects. Access to the 1,4-disubstituted 1,2,3-triazole is quite easy by using a copper-catalyzed azide-alkyne cycloaddition which has been reported by Meldal, Fokin and Sharpless.⁽¹²⁶⁾ Concerning the mechanism (Scheme 37), the acetylide is firstly formed (step A). Then, the azide is activated by copper coordination (step B) followed by the key bond formation, where the intermediate is converted to a six-membered copper-metallacycle (step C). The metallacycle contraction leads to the formation of a copper-triazole derivative (step D). Finally, proteolysis of the intermediate releases the triazole and regenerates the catalyst (step E).

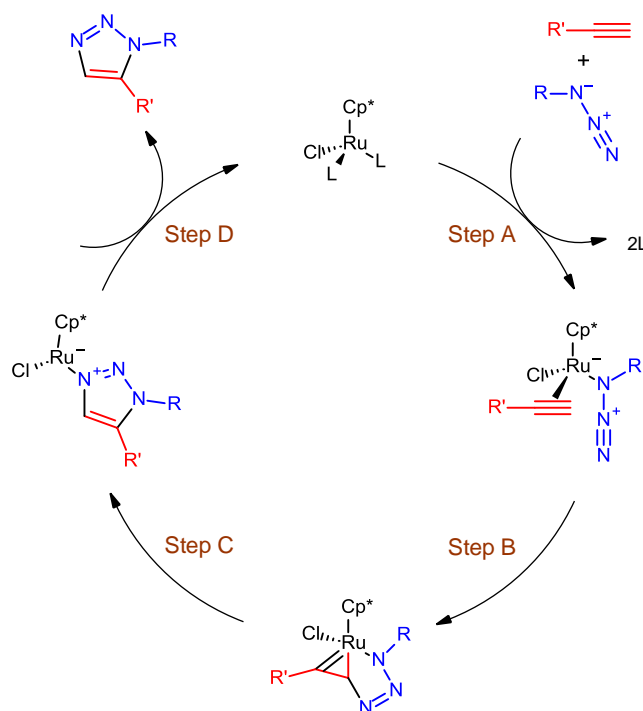


Scheme 37 : catalytic cycle for the 1,4-disubstituted 1,2,3-triazole catalyzed by copper (I) adapted from Worrell et al.⁽¹²⁶⁾

On the other side, the 1,5-regioisomer formation is more difficult. Few methods to access to the 1,5-disubstituted 1,2,3-triazoles have been reported, and for most of them with limited scope.

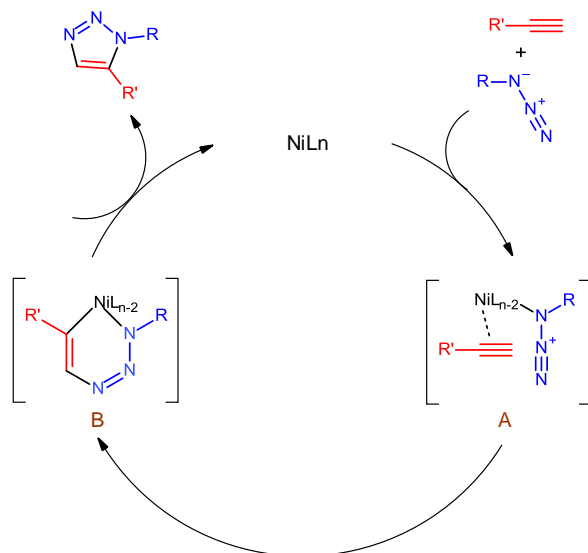
- Metal-catalyzed synthesis of 1,5-disubstituted 1,2,3-triazoles

In most cases, azide-alkyne cycloadditions either mediated by metal acetylide or metal catalysts are used. As metal catalysts, the use of ruthenium complexes is commonly encountered and was reported by Sharpless *et al.* (RuAAC).⁽¹²⁷⁾ Mechanistically (Scheme 38), the displacement of spectator ligands (step A) enables the formation of an activated complex which, through an oxidative coupling, is converted into a ruthenium-metallacycle (step B); the regioselectivity being controlled by this step. Then, a reductive elimination leads to the triazole formation (step C) that is finally released and the catalyst is regenerated (step D).



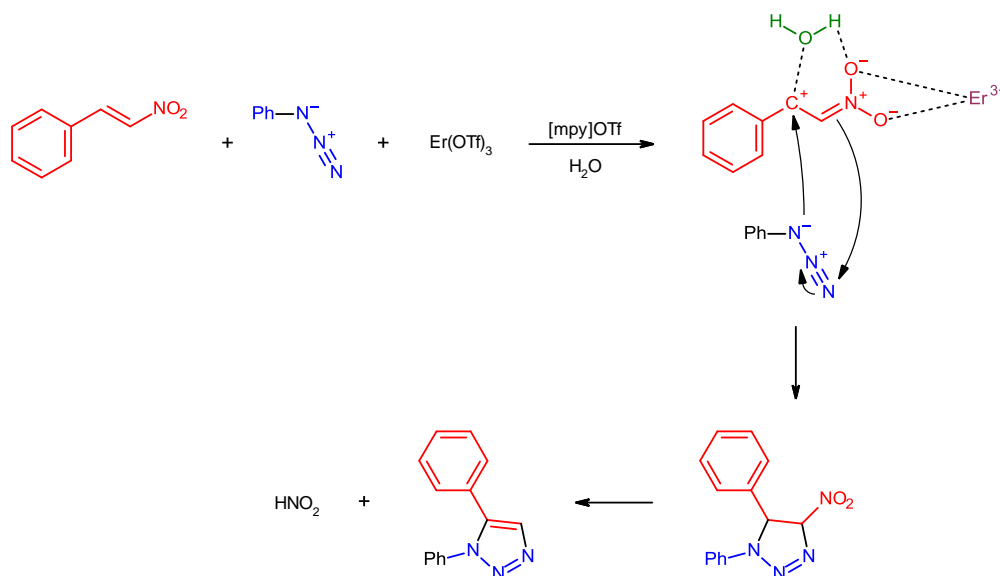
Scheme 38 : catalytic cycle for the 1,5-disubstituted 1,2,3-triazole catalyzed by ruthenium (II) adapted from Boren *et al.*⁽¹²⁷⁾

More recently, Kim *et al.* have shown that nickel complexes can also catalyze the 1,5-regioisomer formation.⁽¹²⁸⁾ In the proposed mechanism (Scheme 39), the intermediate A is forming through nickel coordination by the azide and the alkyne. The 1,5-regioselectivity is determined by intermediate B, which is formed by a C–N bond formation between the azide and the alkyne. Final reductive elimination leads to triazole formation and catalyst regeneration.



Scheme 39 : proposed catalytic cycle for the formation of 1,5-disubstituted 1,2,3-triazoles catalyzed by ruthenium (II) adapted from Kim *et al.*⁽¹²⁸⁾

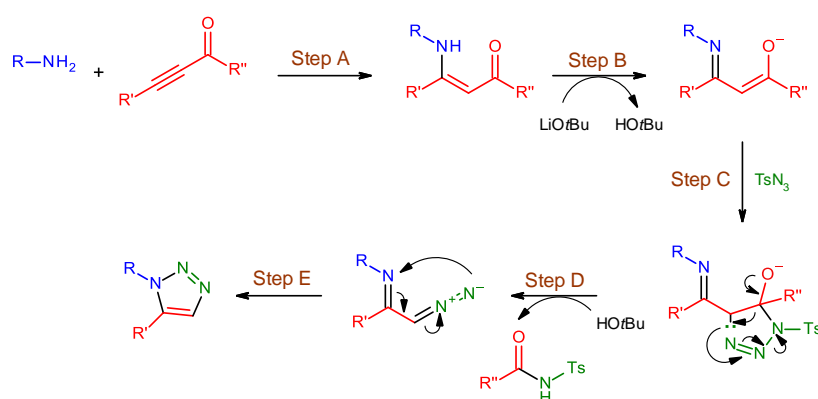
Besides, Maiuolo *et al.* have demonstrated that 1,5-regioisomers can also be obtained by replacing the alkynes with nitroolefins and using metallic additives. This method can be seen as an eliminative azide–olefin cycloaddition (EAOC).⁽¹²⁹⁾ Mechanistically, the nitroolefin may coordinate the erbium (III) triflate forming an activated intermediate which is stabilized by hydrogen bonds with water and electrostatic interactions with the ionic liquid. The azide-olefin cycloaddition affords the triazolene, an unstable compound, which evolves to the 1,5-disubstituted 1,2,3-triazole by a nitrous acid elimination (Scheme 40).



Scheme 40 : proposed mechanism of the 1,5-disubstituted 1,2,3-triazole using nitroolefins adapted from Maiuolo *et al.*⁽¹²⁹⁾

- Metal free-catalyzed synthesis of 1,5-disubstituted 1,2,3-triazole

Cheng *et al.* have described a metal-free procedure using a cascade Michael addition leading to the formation of 1,5-disubstituted 1,2,3-triazoles.⁽¹³⁰⁾ According to the proposed mechanism (Scheme 41), the initial Michael addition between a primary amine and a propynone leads to the formation of the enaminone (step A). Followed deprotonation of the enaminone by lithium tert-butoxide (LiOtBu) affords the iminoenolate intermediate (step B). 1,3-Dipolar cycloaddition (step C) between this intermediate and tosyl azide (TsN₃) followed by deacylative diazo transfer (step D) gives the diazoimine. Finally, cyclization of the diazoimine provides the 1,5-disubstituted 1,2,3-triazole (step E).

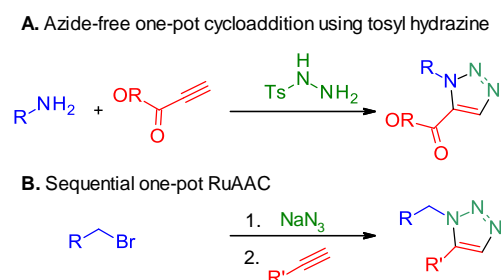


Scheme 41 : proposed mechanism of the 1,5-disubstituted 1,2,3-triazole using a cascade Michael addition adapted from Cheng *et al.*⁽¹³⁰⁾

However, most of these methodologies have restricted scopes. Moreover, most of them require the handling of isolated organic azides, which are not often commercially available and are known to be unstable, in particular those with a low molecular weight.⁽¹³¹⁾

- Synthesis of 1,5-disubstituted 1,2,3-triazole through one pot reactions

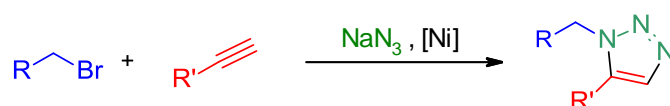
To get around these drawbacks, multicomponent methodologies have been developed.^{(132),(133),(134),(135),(136),(137)} For example, a metal- and azide-free one-pot procedure using tosyl hydrazine (Scheme 42A) and, a one-pot procedure via metal, a RuAAC strategy from bromide was described (Scheme 42B) were described to produce 1,5-disubstituted 1,2,3-triazoles.



Scheme 42 : Examples of one-pot strategies for the synthesis of 1,5-disubstituted 1,2,3-triazoles

These methods have the advantage to be safer by preventing the handling of organic azides. Regrettably, they suffer from a much narrowed substrate scope, often requiring high temperatures, strict inert atmosphere conditions or an inconvenient sequential pattern, all of which have limited their use.

Thus, we investigated the feasibility to implement an efficient and safe one-pot, two-step method. This procedure would enable the *in-situ* conversion of bromides into azides by nucleophilic substitution with sodium azide. The azides react consecutively with alkynes by NiAAC (Scheme 43).



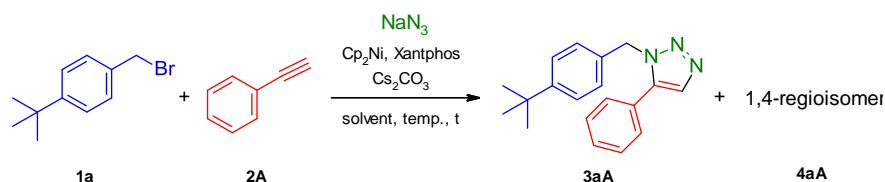
Scheme 43 : Our one-pot NiAAC methodology for the synthesis of 1,5-disubstituted 1,2,3-triazoles

Results

I. Screening of reaction conditions

We started to screen different conditions for the reaction, using 4-*tert*-butylbenzylbromide (**1a**) and phenylacetylene (**2A**) as model substrates (Table 29).

Table 29 : Conditions screening.^a adapted from Camberlein *et al.*⁽¹³⁸⁾



Entry	Solvent	Temperature (°C)	Time (h)	cYield (%) ^c	Ratio 3aA/4aA ^d
1	H ₂ O	rt	2	— ^e	— ^e
2	DMF	rt	2	71	88:12
3	EtOH	rt	2	— ^e	— ^e
4	DCM	rt	2	— ^e	— ^e
5	THF	rt	2	— ^e	— ^e
6	DMF	50 °C (MW)	1	73	93:7
7	DMF	80 °C (MW)	1	49	64:36
8	DMF	100 °C (MW)	1	— ^e	— ^e
9	DMF	50 °C (MW)	4	86	92:8
10 ^b	DMF	50°C (MW)	4	89	92:8

^a Reaction conditions: Run on a 0.5 mmol scale of alkyne **2A** (1.2 equiv), bromide **1a** (1.0 equiv), NaN₃ (1.0 equiv), solvent (2 mL), Cp₂Ni (20 mol%), Xantphos (20 mol%), Cs₂CO₃ (1.0 equiv).

^b Run on a 0.5 mmol scale of alkyne **2A** (1.0 equiv), bromide **1a** (1.2 equiv), NaN₃ (1.5 equiv), solvent (2 mL), Cp₂Ni (20 mol%), xantphos (20 mol%), Cs₂CO₃ (1.0 equiv).

^c Calculated yield of **3aA** determined by LCMS analysis from the crude product.

^d Determined by LCMS analysis from the crude product.

^e No triazole formation. Cp, cyclopentadienyl; cYield, calculated yield; DCM, dichloromethane; DMF, dimethylformamide; MW, microwave irradiation; temp, temperature; rt, room temperature.

First, we performed the reaction using conditions, which are similar to those used in NiAAC reported by Kim *et al.*: bromide **1a** (1.0 equiv), sodium azide (1.0 equiv), alkyne **2A** (1.2 equiv), nickelocene (Cp₂Ni) precatalyst (20 mol%), xantphos as ligand (20 mol%) and cesium carbonate (1.0 equiv) in water at room temperature for 2 hours. Using these conditions, conversion of the bromide **1a** to azide was observed but not the cycloaddition (entry 1).

Then, in order to improve the triazole formation, we started to change the solvent. The reaction was first investigated with dimethylformamide (entry 2) because it showed efficacy

in the NiAAC. Interestingly, it facilitated the triazole formation contrary to other solvents like dichloromethane, ethanol or tetrahydrofuran (entries 3–5).

After demonstrating that dimethylformamide was efficient for the reaction, we continued with the modification of the temperature. Heating the reaction mixture to 50°C under microwave irradiations for 1 hour (entry 6) resulted in a higher regioselectivity (88:12 to 93:7) but did not impact the yield (73 to 71%).

Increasing the temperature (80 or 100°C) was deleterious for the yield and the regioselectivity (entries 7 and 8), probably due to the catalyst degradation. Then, the time of the reaction was investigated. When the reaction vessel was heated under microwave irradiations for 4 h (entry 9), the yield increased (86 vs 73%) without harmful effect on the regioselectivity (ratio 92:8 vs 93:7). Finally, the bromide **1a** and sodium azide were used as excess reagents (1.2 and 1.5 equiv respectively) (entry 10). Under those conditions, excellent yield (89%) and regioselectivity (ratio 92:8) were observed without the formation of by-products.

To investigate the mechanism of this one-pot reaction, 4-*tert*-butylbenzyl bromide **1a** and sodium azide were mixed at room temperature for 2 h in DMF in presence of or without the Cp₂Ni/Xantphos catalytic system. In both conditions, the azide was formed in quantitative yield. Thus, the Cp₂Ni/Xantphos catalytic system has no influence on the S_N2 reaction and only has beneficial effects for the azide-alkyne cycloaddition and its regioisomerism.

After optimizing the reaction conditions, we investigated the scope with various alkynes and bromides.

II. Substrate scope

1. With various alkynes

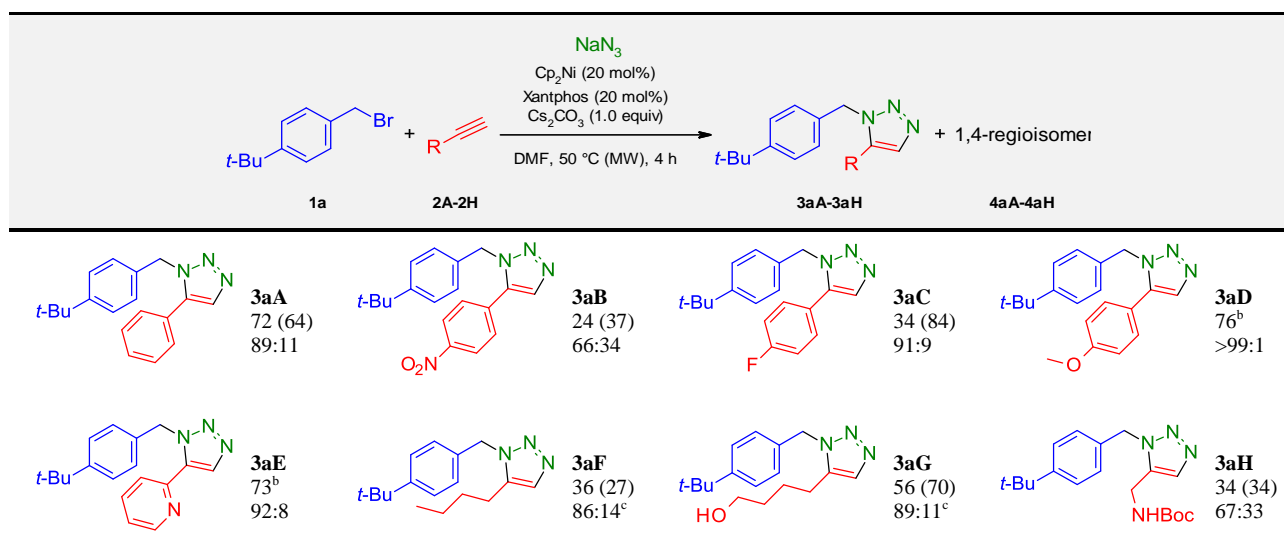
The use of aromatic (**2A–2E**) and aliphatic alkynes (**2F–2H**) in reaction with the bromide **1a** was explored, and the results are reported above (Table 30). Except for alkynes **2D** and **2E**, the attempts to separate and isolate the two regioisomers were not productive by classical flash column chromatography, or by C-18 reversed-phase flash column chromatography with the use of classical or pentafluorophenyl columns. However, due to the high regioselectivity rates associated with this reaction (from ratio 66:34 to > 99:1), flash

chromatography was still performed to afford the 1,5-triazole in mixture with the 1,4 in order to evaluate the efficiency of this one-pot multicomponent methodology.

Modest to excellent calculated yields ranging from 27% to 84% were obtained. Besides, with the aim of isolating and characterizing properly the 1,5–ring, the crude mixtures were also purified using semi-preparative supercritical fluid chromatography (SFC); with similar isolated yield (24% to 72%).

The regioselectivity of each reaction was measured by SFC analysis of the crude reaction mixtures obtained after the work-up of the reactions carried out with alkynes **2A–2E** and **2H**, or according to the ¹H-NMR spectra for reactions carried out with alkynes **2F** and **2G**, for which the separation of the two regioisomers by SFC was not optimal. Modest to excellent regioselectivities were observed. Given the regioselectivity obtained with the *para*-nitrophenylacetylene **2B** (ratio 66:34) compared to the phenylacetylene **2A** (ratio 89:11), the *para*-fluorophenylacetylene **2C** (ratio 91:9) and the *para*-methoxyphenylacetylene **2D** (ratio > 99:1), a positive mesomeric effect on the phenyl moiety seems to have a positive contribution on the regioselectivity without impacting the yield. Interestingly, heteroaryl (**2E**) and alkyl (**2F**) chains are tolerated in this methodology. Hydroxyl (**2G**) and carbamates (**H**) groups are also compatible.

Table 30 : Substrate scope with various alkynes.^a adapted from Camberlein *et al.*⁽¹³⁸⁾



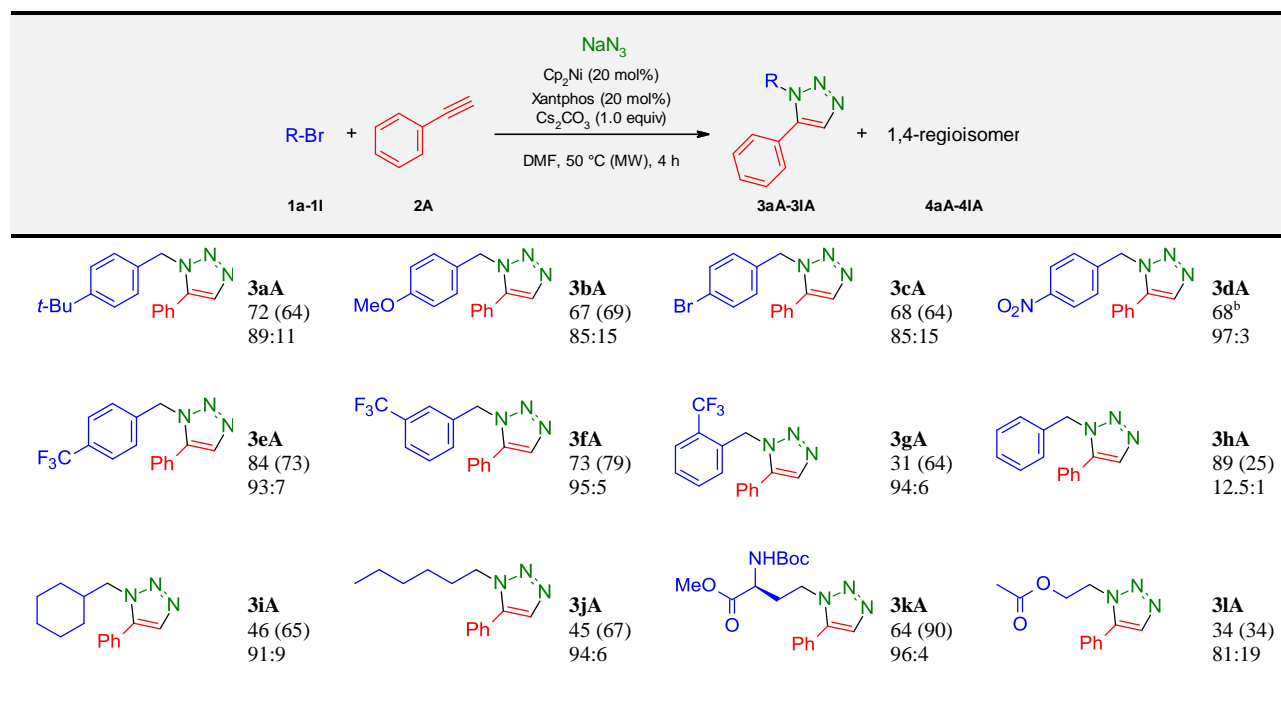
^aReaction conditions: Run on a 0.3–0.6 mmol scale of alkyne **2** with **1a** (1.2 equiv), NaN₃ (1.5 equiv), Cp₂Ni (20 mol%), Xantphos (20 mol%), Cs₂CO₃ (1.0 equiv), DMF (2.0 mL), 50 °C (MW), 4 h. Isolated yields (%) of **3** obtained after SFC purification; **3/4** ratio determined from the crude product by SFC analysis unless noted otherwise; in brackets: calculated yields (%) of **3** obtained after flash column chromatography purification (in mixture with **4**).^bIsolated yield (%) of **3** obtained after flash column chromatography purification; ^cDetermined by ¹H NMR. Boc, *tert*-butoxycarbonyl; Cp, cyclopentadienyl; *t*-Bu, *tert*-butyl.

2. With various bromides

The use of aromatic benzyl bromides possessing either electron-donating (**1a** and **1b**) or electron-withdrawing (**1c–1g**) and non-saturated bromides (**1i–1l**) in reaction with the alkyne **2A** was explored and the results are reported above (Table 31).

Concerning the aromatic benzyl bromide, modest to high yields both after flash chromatography purification (calculated yield: 64%–79%) and after semi-preparative SFC purification (isolated yield: 31%–84%) were obtained. The *ortho*-CF₃ bromide **1g** afforded the triazole **3gA** with the lowest yield in the series, probably due to steric effects. Besides, the position of the trifluoro group has demonstrated a minor influence on the yield without impacting the regioselectivity. Noteworthy, for these aromatic benzyl bromides, high to excellent regioselectivities were obtained (from 85:15 to 97:3 ratios). Regarding the non-saturated bromide (**1i–1l**), they could be efficient in this one-pot methodology. Interestingly, functional groups such as carbamate-protected amine (**1k**) and ester (**1l**) are also well-tolerated, affording the corresponding 1,5-regioisomers with high to excellent yields and regioselectivities. Moreover, no influence on enantiomerism for the triazole **3kA** was observed.

Table 31 : Substrate scope with various bromides.^a adapted from Camberlein *et al.*⁽¹³⁸⁾



^aReaction conditions: Run on a 0.49 mmol scale of alkyne **2A** with **1** (1.2 equiv), NaN₃ (1.5 equiv), Cp₂Ni (20 mol%), xantphos (20 mol%), Cs₂CO₃ (1.0 equiv), DMF (2.0 mL), 50 °C (MW), 4 h. Isolated yields (%) of **3** obtained after SFC purification; **3/4** ratio determined from the crude product by SFC analysis unless noted otherwise; in brackets: calculated yields (%) of **3** obtained after flash column chromatography purification (in mixture with **4**). ^bIsolated yield (%) of **3** obtained after flash column chromatography. Boc, *tert*-butoxycarbonyl; Cp, cyclopentadienyl; Me, methyl; Ph, phenyl; t-Bu, *tert*-butyl.

Conclusion

Thus, we managed to establish a methodology to efficiently access diverse 1,5-disubstituted 1,2,3-triazoles in a fast and simple manner, bypassing the encountered and known problems with the main reported procedures (Figure 68).

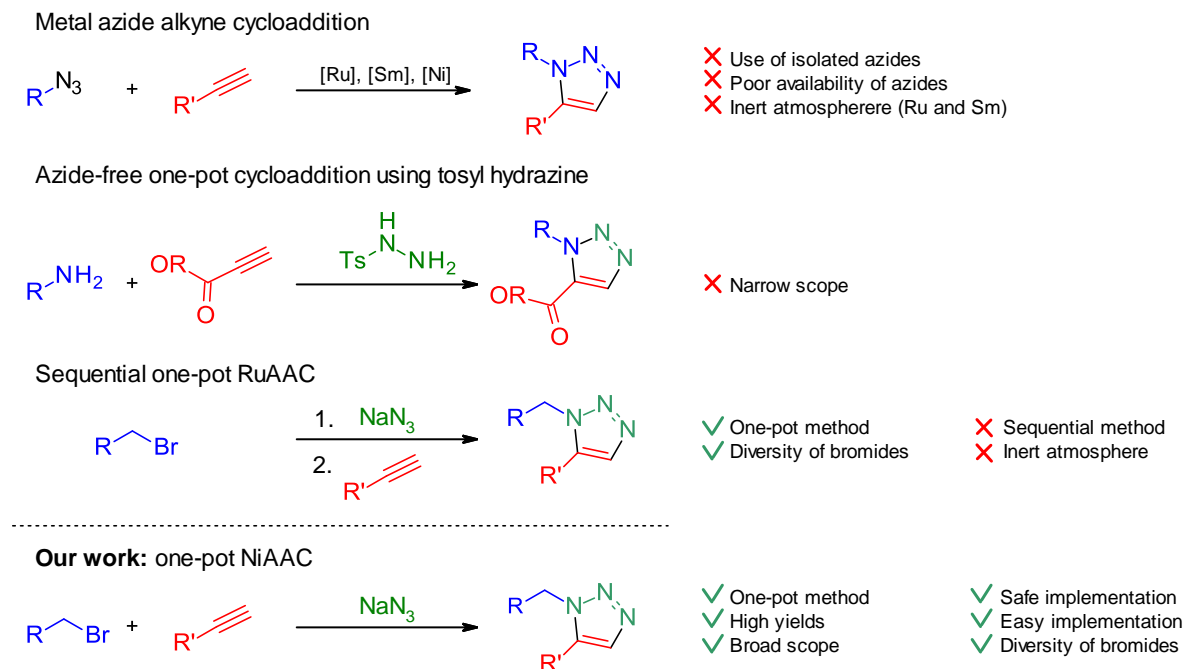


Figure 68 : Comparison between the main strategies for the synthesis of 1,5-disubstituted 1,2,3-triazole and our one-pot NiAAC strategy adapted from Camberlein *et al.*⁽¹³⁸⁾

Remarkably, one of the advantages of this one-pot reaction is the *in-situ* generation of azides from bromides, which are commercially available with a broad diversity. Thus, this one-pot method avoids the sequential and time-consuming synthesis and isolation of azides, which could be unstable and are rarely commercially available. It makes this procedure very useful, in particular when sensitive low-molecular weight azides are needed. A diverse range of functional groups including, *N*-protected amines, hydroxyls and esters are tolerated in this procedure. This method will enable the synthesis of libraries of functionalizable 1,5-regioisomers especially useful for drug discovery and chemical biology purposes.

General conclusion

The objectives of this work were to, first, identify new ligands of ERAP2 and LasB using the KTGS strategy and, secondly, to optimize the ligands into leads.

Regarding ERAP2, the KTGS strategy was initiated from 6 azides and 180 alkynes. The azides derived from β -amino acids containing a hydroxamate, which allowed us to coordinate the zinc ion of ERAP2 and therefore place the ligands in the active site. The alkynes were from the U1177 alkyne library and imported the diversity on the ligands. As for 85% of KTGS reports, mass spectrometry was used to identify the hits, allowing the identification of a micromolar compound (**Hit E1**, $IC_{50} = 3.0 \mu M$). The SAR studies enabled us to improve the potency and led to the identification of two new selective and submicromolar ERAP2 inhibitor families: the α -1,4 and the β -1,5 families. Strikingly, these inhibitors display good ADME properties and toxicity and selectivity profiles (Figure 69).

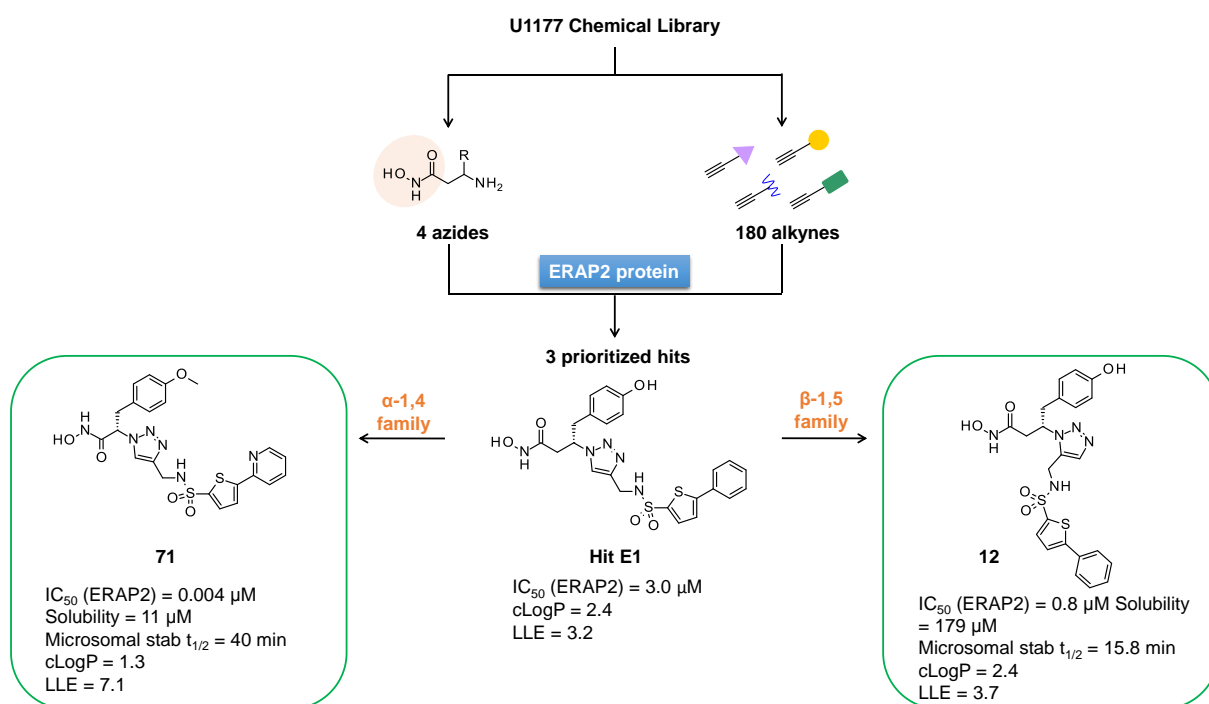


Figure 69 : ERAP2-templated formation of Hit E1 and optimization in 12 and 71 and their respective features. The warhead is highlighted in salmon.

Concerning LasB, the KTGS experiment was performed from 4 azides and 190 alkynes. As for ERAP2, the azides bore a hydroxamate to coordinate the zinc ion of LasB and were designed from known SARs. The alkynes were also from the U1177 alkyne library and introduced the diversity as previously. Mass spectrometry was also used to identify the ligands. As the templated ligands from the azides **Z7** and **Z8** (β -leucine and leucine) were

very structurally similar to those from the KTGS with ERAP2, we decided to stay focused on the hits from **Z9** and **Z10** (the two malonic derivatives).

Biological evaluation of the templated ligands from these two azides showed that the provided flexibility by the ethyl chain (**Z4**) was not very well tolerated, as the starting azide showed a higher IC₅₀ than the most potent hit. Even if, **Z9** displayed surprisingly a high potency (17 nM), the KTGS led to a seven-fold gain in the activity for the most potent templated ligand (**Hit L1**, IC₅₀ = 2.4 nM).

Strikingly, **LasB hit 1** has a promising profile: nanomolar potency, no off-target effects, no cytotoxicity and no antibacterial activity but demonstrates a limited solubility and metabolic stability. The SAR studies performed on this templated ligand did not lead to a significant increase in potency but allowed us to improve the solubility and the metabolic stability (142 μM to > 200 μM for the solubility and 30 min to > 120 min for the metabolic stability). The most promising analogs **160** and **169** with enhanced physicochemical properties are also potent, selective, non-cytotoxic and devoid of antibacterial activity, which makes them promising compounds (Figure 70).

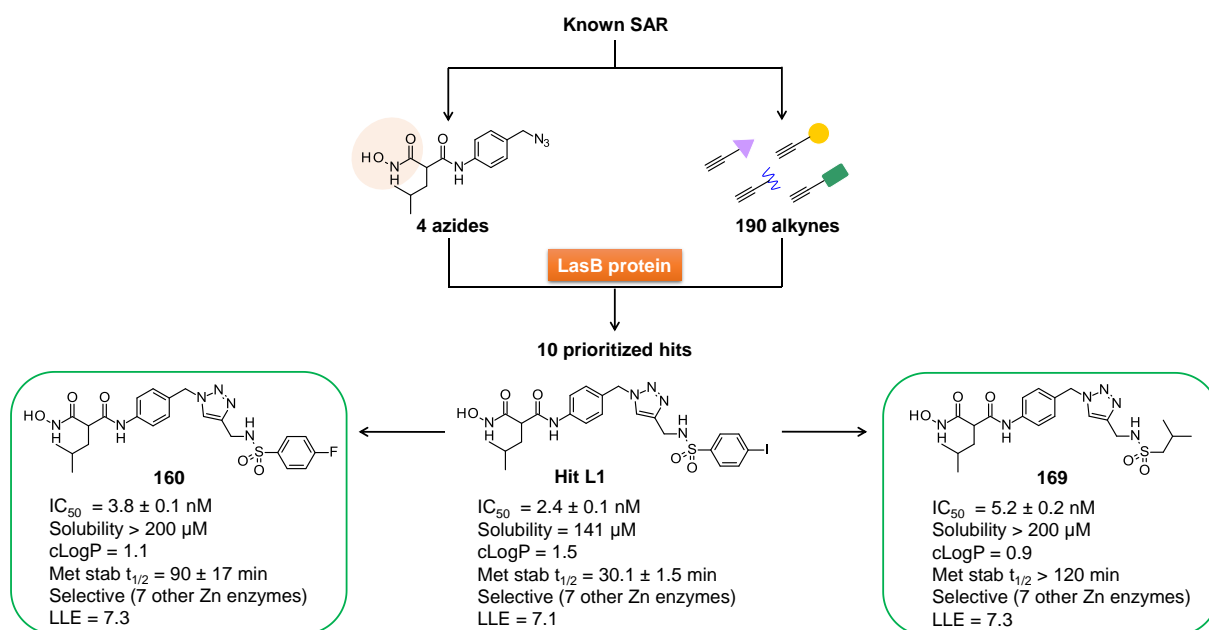


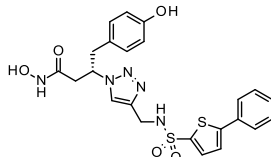
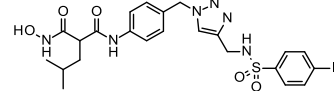
Figure 70 : LasB-templated formation of Hit L1 and optimization in 160 and 169 and their respective features. The warhead is highlighted in salmon.

Thus, these inhibitors have to be tested in model systems closer to reality such as in presence of pulmonary surfactant or in a *Galleria mellonella* infection model. Additionally, co-crystallization of **161** (4-chloro) with LasB was performed to elucidate the binding mode of the KTGS ligands and will help us to conduct further medchem optimization. Interestingly, it suggests the possibility of maximizing the pocket occupancy using a macrocycle.

As explained previously, the design and the selection of the warhead-bearing reagents are a crucial step for a successful KTGS. Several methods can help the design of these reagents such as computational methods (docking, crystal structure), known SARs or approved drugs. As we worked with zinc metalloenzymes, a ZBG (hydroxamate here) was introduced in our warheads to coordinate the zinc and therefore facilitate the binding of the templated ligands in the active sites. Noteworthy, besides providing diversity on the ligands, the alkynes can also bind protein pockets improving the pocket occupancy and therefore increasing the ligand potency. Thus, a large scope of reagents is also crucial to maximize the chances of success; more than 170 alkynes were used here thanks to the large library of the U1177's team.

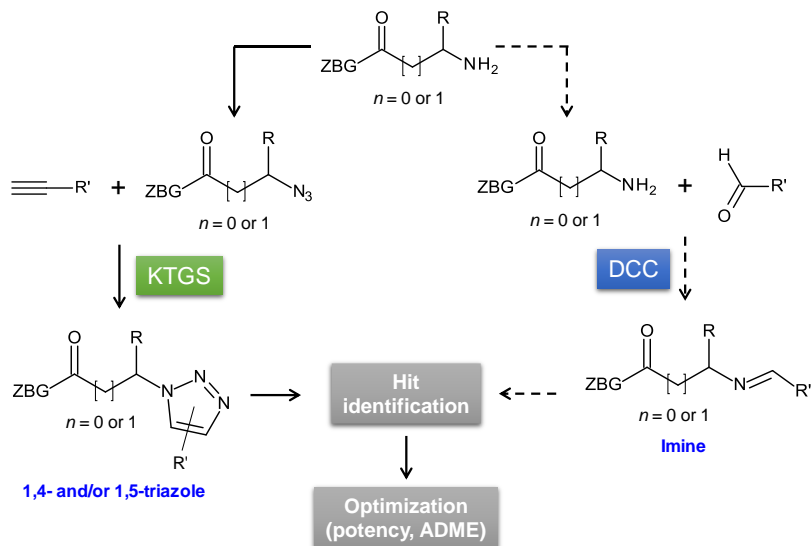
Thus, we applied the KTGS strategy with success thanks to a good design of our warhead-bearing reagents and the use of a large pool of reagents. Strikingly, the ERAP2 and LasB templated ligands display a LLE above 3 and comply with the Doak space (Table 32).

Table 32 : Structural features of ERAP2 and LasB KTGS ligands

Compound	Structure	MW (g/mol)	cLogP	Rotatable bonds	HBA	HBD	PSA (Å ²)	LLE
ERAP2 Hit 1		513.6	2.4	9	10	4	183	3.2
LasB Hit 1		626.5	1.5	10	11	4	164	7.1

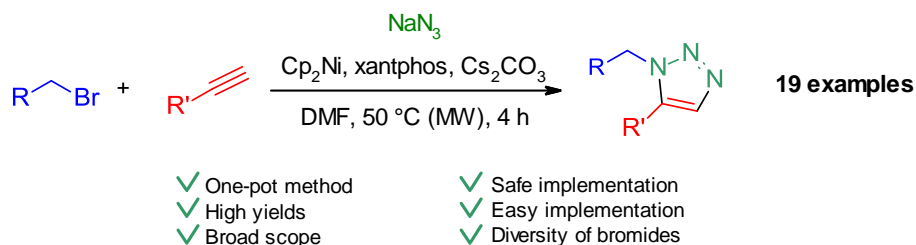
Then, we focused on our second objective, which was to optimize the templated ligands as we improved their potency and their physicochemical properties; making them promising leads in the field of cancer and autoimmune diseases for ERAP2 and in the fight against AMR for LasB.

As perspectives, it would be interesting to apply the DCC strategy with these two zinc metalloenzymes to compare the two protein-templated strategies. For example, the irreversible link through the triazole moiety could be replaced by a reversible link using an imine or an acylhydrazone (Scheme 44).



Scheme 44 : Protein-templated strategies with the enzyme ERAP2. The KTGS strategy was applied using the Huisgen 1,3-dipolar cycloaddition and led to the formation of the 1,2,3-triazole disubstituted. The DCC could also be applied, from amines and aldehydes leading to imine formations, to compare the two strategies. DCC strategy could be applied with LasB in modifying the starting amines.

Finally, additionally to the previous work, a one pot nickel-catalyzed methodology for the preparation of to 1,5-disubstituted 1,2,3-triazoles was developed (Scheme 45) and could be applied in the future for the synthesis of 1,5-regioisomers after a KTGS experiment using the Huisgen 1,3-dipolar cycloaddition.



Scheme 45 : Developed one pot nickel-catalyzed reaction for the synthesis of 1,5-disubstituted 1,2,3-triazoles

Experimental part

I. Chemistry

1. General information

Solvents for synthesis, analysis and purification were purchased as analytical grade from commercial suppliers and used directly without further purification. Chemical reagents were purchased as reagent grade and used without further purification.

➤ For compounds of chapters 2 and 4

Syntheses under microwave irradiation were performed using Biotage® Initiator+.

NMR spectra were recorded on a Bruker DRX-300 spectrometer. The results were calibrated to signals from the solvent as an internal reference [e.g., 2.50 (residual DMSO-*d*₆) and 39.52 (DMSO-*d*₆) ppm for ¹H and ¹³C NMR spectra, respectively]. Chemical shifts (δ) are reported in parts per million (ppm). NMR coupling constants (*J*) are reported in Hertz (Hz), and splitting patterns are indicated as follows: (s) for singlet, (d) for doublet, (t) for triplet, (q) for quartet, (quin) for quintet, (sext) for sextuplet, (sept) for septuplet, (dd) for doublet of doublet, (ddd) for doublet of doublet of doublet, (dt) for doublet of triplet, (qd) for quartet of doublet, (m) for multiplet, and (br) for broad, δ for chemical shift, *J* for coupling constant.

LC-MS Waters system was equipped with a 2747 sample manager, a 2695 separations module, a 2996 photodiode array detector (200–400 nm) and a Micromass ZQ2000 detector (scan 100–800). XBridge C₁₈ column (50 mm x 4.6 mm, 3.5 μ m, Waters) was used. Purity (%) was determined by LC-MS, using UV detection (215 or 254 nm), and all isolated compounds showed purity greater than 95%. HRMS analysis was performed on a LC-MS system equipped with a LCT Premier XE mass spectrometer (Waters), using a XBridge C₁₈ column (50 mm x 4.6 mm, 3.5 μ m, Waters). Flash chromatography was performed using an Interchim Puriflash® 430 with silica columns. UV and ELSD detection were used to collect the desired product. Reverse flash chromatography was performed using a CombiFlash® C₁₈ Rf200 with C₁₈ silica gel cartridges. UV detection (215 and 254 nm) was used to collect the desired product.

➤ For compounds of the chapter 3

NMR spectra were recorded on a Bruker UltraShield Plus 500 MHz device. The results were calibrated and presented as before.

LC-MS analysis were measured on a LC-MS system, consisting of a Thermo Scientific Dionex UltiMate 3000 pump, autosampler, column compartment, and detector (Thermo Fisher Scientific, Dreieich, Germany) and ESI quadrupole MS (MSQ Plus or ISQ EC, Thermo Fisher Scientific, Dreieich, Germany). High-resolution mass was determined by LCMS/MS using Thermo Scientific Q Exactive Focus Orbitrap LC-MS/MS system. Purity was determined as before. Flash chromatography

was performed using either a Teledyne ISCO CombiFlash Rf+ 150 or a Teledyne ISCO CombiFlash NEXTGEN 300+ equipped with RediSepRf silica columns. Preparative HPLC was performed on a Thermo Scientific Dionex Ultimate 3000 system.

➤ **For compounds of the chapter 4**

The chromatographic system used for SFC was a SFC-PICLAB hybrid 10-20 apparatus (PIC Solution, Avignon, France) equipped with an autosampler comprising a 48-vial plate (model Alias, Emmen, Netherlands), three model 40 P pumps: two for CO₂ and a third for the modifier (Knauer, Berlin, Germany), a column oven with a Valco ten-position column selection valve, and a Valco six-position solvent switching valve. The system was also composed of a Smartline 2600 diode array detector (DAD) (Knauer, Berlin, Germany). Detection wavelength was set at 215 nm. The system was controlled, and the data was acquired with the SFC PicLab Analytic Online v.3.1.2 software (PIC Solution, Avignon, France). Retention times were average values of two replicate determinations. The data were processed by SFC New Data Manager V.1.8.0 software (Pic Solution, Avignon, France). The stationary phases used for SFC, and purchased from Chiral Technologies Europe (Illkirch, France), are a Chiralcel OD-H, cellulose tris (3,5dimethylphenylcarbamate) used for the purification of all compounds excepted compound 3aE, and a Chiralpak IC, cellulose tris (3,5dichlorophenylcarbamate) used for the purification of 3aE. The two columns have dimensions of 4.6x250 mm with 5 μm particle size. All SFC analyses were run in isocratic mode. The column oven temperature was 40°C and the outlet pressure was maintained at 150 bar for all experiments. For the determinations of the regioselectivity rate and the purity of the purified fraction of 1,5-disubstituted 1,2,3-triazole, the injected volume was 20 μL, the used flow rate was 4 mL/min and the mobile phase was always CO₂- modifier mixture with 10% of ethanol as modifier excepted for compound 3aG where the used flow rate was 2 mL/min and the mobile phase was always CO₂-modifier mixture with 20% of ethanol as modifier.

2. General procedures

General procedure A: Azide formation

A suspension of amine (1 eq.), ZnCl₂ (0.06 eq.) and K₂CO₃ (2–4 eq.) in anhydrous methanol (0.18–0.25 M) under inert atmosphere was cooled down to 0 °C with an ice-bath. Besides, anhydrous *N,N*-diisopropylethylamine (1.1–2.1 eq.) was slowly added to a solution of 1*H*-imidazole-1-sulfonyl azide; hydrogen sulfate or hydrogen chloride (1.2 eq.) solubilized in anhydrous methanol (0.3 M) under inert atmosphere (solution A). The azide-containing solution A was immediately added dropwise to the first mixture at 0 °C. Then, the cooling bath was removed and the white mixture was stirred at room temperature overnight. The mixture was then cooled down to 0 °C, diluted with water and carefully acidified to pH = 2 with diluted aq. HCl (1N). It was finally extracted with ethyl acetate. Combined

organic layers were dried over MgSO₄, filtered and concentrated under reduced pressure or the residue was finally purified through flash chromatography to give the desired azide.

General procedure B: Amide formation

Carboxylic acid (1 eq.) and amine (1.1–1.6 eq.) were solubilized in *N,N*-dimethylformamide (0.28–0.45M) or CH₂Cl₂ (0.2 M). HBTU (1.1–1.7 eq.) or HOBt (0.1 eq.) and EDC·HCl (1.5 eq.), and trimethylamine or diisopropylethylamine (3–5 eq.) were then added and the mixture was stirred overnight. The mixture was then washed with diluted aq. HCl (1 M), sat. aq. NaHCO₃ and sat. aq. NaCl. Combined organic layers were dried over MgSO₄, filtered and concentrated under reduced pressure or the residue was finally purified through flash chromatography to give the desired amide.

General procedure C: Intramolecular click chemistry⁽⁶⁸⁾

The azido intermediate was dissolved in DMF (0.009–0.04 M) and refluxed overnight to allow cyclisation. After cooling down, the mixture was diluted in water and extracted with ethyl acetate. Combined organic layers were dried over MgSO₄, filtered and concentrated under reduced pressure. The crude product was finally purified through flash chromatography to furnish the desired cyclic 1,5-triazole.

General procedure D: Lactame hydrolysis⁽⁶⁸⁾

Pyrazinone or diazepinone 1,5-triazoles (1 eq.) was diluted in a 6 M aq. HCl solution (0.06–0.13 M) and heated under microwave irradiations at 85 °C for 1–3 hours. Then, solvents were evaporated under reduced pressure to give 1,5-triazoles as hydrochloric acid salts, which were used in the next step without further purification.

General procedure E: Esterification

Carboxylic acid (1 eq.) was dissolved in MeOH (0.1–0.5 M) and cooled down to 0 °C before thionyl chloride (2.0 eq.) was slowly added dropwise. The resulting solution was stirred overnight in the melting ice bath. Solvents were then evaporated under reduced pressure to give the desired products or residues were dissolved in a mixture of ethyl acetate and saturated aqueous NaHCO₃ and extracted twice. Combined organic layers were dried over MgSO₄, filtered and concentrated under reduced pressure to afford desired esters.

General procedure F: Sulfonamide formation⁽⁴⁾

The amine (1–1.5 eq.) was dissolved in *N,N*-dimethylformamide or dichloromethane (0.04–0.10 M) and cooled down to 0°C. R1-sulfonyl chloride (1–1.2 eq.) was then carefully added followed by *N,N*-diisopropylethylamine (1.2–3 eq.). The mixture was allowed to reach room temperature and was stirred overnight. Then, the crude was diluted in aq. HCl (0.5 M) and extracted with ethyl acetate. Combined organic layers were dried over MgSO₄, filtered and concentrated under reduced pressure. The residue was finally purified through flash chromatography to afford the desired sulfonamide.

General procedure G: Aminolysis

To an ester solution (1 eq.) in methanol (0.04-0.35M) was added aq. hydroxylamine (50% w/w in water, 0.04–0.35 M) and KCN (0.1–0.5 eq.). The mixture was stirred 16 to 72 h. Then, the solvents were removed under reduced pressure and the residue was purified through flash chromatography.

General procedure H: Copper-catalyzed click reaction

Azide (1 eq.) and alkyne (1.0–2.5 eq.) were dissolved in *N,N*-dimethylformamide (0.03–0.09 M) before an addition of copper sulfate pentahydrate (0.2–0.4 eq.) in water (0.05–0.09 M) and sodium ascorbate (0.5–1 eq.). The resulting mixture was stirred at room temperature overnight. The mixture was then diluted in water and extracted with ethyl acetate. Combined organic layers were dried over MgSO₄, filtered and concentrated under reduced pressure. The residue was finally purified through flash chromatography affording the desired 1,4-triazole.

General procedure I: Monosaponification

Malonate diester (1 eq.) was dissolved in a mixture of methanol/water or ethanol/water (9:1–8:2, 0.32–0.58M) and sodium hydroxide (1.2 eq.) or potassium hydroxide (1.0 eq.) was added. The reaction mixture was stirred at room temperature overnight. Then, solvents were evaporated under reduced pressure and the aqueous mixture remaining was diluted with sat. aq. NaHCO₃ and washed with CH₂Cl₂. The aqueous layer was then carefully acidified (pH~1) with aq. HCl and extracted with CH₂Cl₂. Combined organic layers were dried over MgSO₄, filtered and concentrated under reduced pressure affording the desired product.

General procedure J: Boc deprotection

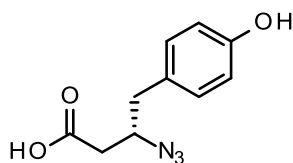
The Boc-protected intermediate was dissolved in a mixture of ethanol and dichloromethane (1:1, 0.09–0.11M) and the reaction was cooled down to 0 °C before an addition of 4 N HCl in dioxane (0.18–0.22M). The mixture was stirred at room temperature overnight. Then, solvents were evaporated to give the desired compound.

General procedure K: One-pot methodology for 1,5-triazole

To a solution of bromide derivative (1.2 eq.) in *N,N*-dimethylformamide (0.25 M) were successively added sodium azide (1.5 eq.), alkyne (1.0 eq.), di(cyclopenta-1,3-dien-1-yl)nickel (20 mol%), xantphos (20 mol%) and cesium carbonate (1.0 eq.). The brown mixture was heated under microwave irradiations (50 °C, 4 h). The dark purple mixture was filtered on a celite pad, diluted with water and extracted twice with ethyl acetate. The organic layer was dried over MgSO₄, filtered and concentrated under reduced pressure. The residue was divided into two fractions unless noted otherwise. One fraction was purified through flash silica gel column (cHex to cHex/EtOAc: 8:2) and the other fraction was purified by SFC to afford the desired 1,5-disubstituted 1,2,3-triazole.

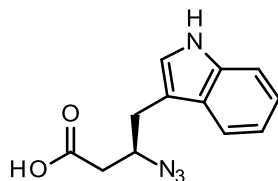
3. Synthesis of chapter 2 compounds (1–75)

(3*S*)-3-Azido-4-(4-hydroxyphenyl)butanoic acid (1)



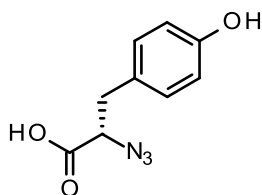
Compound **1** was synthesized according to the general procedure A, using *L*- β -homotyrosine (290 mg, 1.25 mmol), ZnCl_2 (10.2 mg, 0.07 mmol), K_2CO_3 (691 mg, 5.0 mmol), anhydrous *N,N*-diisopropylethylamine (240 μL , 1.38 mmol) and diazo transfer reagent (407 mg, 1.5 mmol) in anhydrous MeOH (5 mL) overnight. Compound **1** was obtained as light yellow oil (277 mg, 93%) and was used in the next step without further purification. LC tr = 1.97 min, MS (ESI-): m/z = 220 [M - H]⁻. ¹H NMR (300 MHz, MeOD-*d*₄) δ ppm: 7.10–7.05 (m, 2H), 6.76–6.72 (m, 2H), 3.99–3.90 (m, 1H), 2.80 (dd, J = 13.8 and 5.8 Hz, 1H), 2.71 (dd, J = 13.8 and 8.0 Hz, 1H), 2.53 (dd, J = 16.3 and 4.4 Hz, 1H), 2.36 (dd, J = 16.3 and 9.2 Hz, 1H). ¹³C NMR (75 MHz, MeOD-*d*₄) δ ppm: 174.5, 157.4, 131.5 (2C), 129.5, 116.3 (2C), 62.4, 40.7, 39.6.

(3*R*)-3-Azido-4-(1*H*-indol-3-yl)butanoic acid (2)



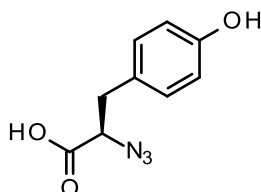
Compound **2** was synthesized according to the general procedure A, using *D*- β -homotryptophan (637 mg, 2.50 mmol), ZnCl_2 (20.4 mg, 0.15 mmol), K_2CO_3 (1380 mg, 10.0 mmol), anhydrous *N,N*-diisopropylethylamine (480 μL , 2.75 mmol) and diazo transfer reagent (814 mg, 3.0 mmol) in anhydrous MeOH (10 mL) overnight. Compound **2** was obtained as brown oil (611 mg, 95%) and was used in the next step without further purification. LC tr = 2.40 min, MS (ESI-): m/z = 243 [M - H]⁻. ¹H NMR (300 MHz, MeOD-*d*₄) δ ppm: 7.60–7.56 (m, 1H), 7.37–7.34 (m, 1H), 7.13 (s, 1H), 7.11–7.00 (m, 2H), 4.14–4.05 (m, 1H), 3.08–2.95 (m, 2H), 2.59 (dd, J = 16.3 and 4.5 Hz, 1H), 2.42 (dd, J = 16.3 and 9.0 Hz, 1H). ¹³C NMR (75 MHz, MeOD-*d*₄) δ ppm: 174.7, 138.1, 128.7, 124.7, 122.4, 119.9, 119.2, 112.3, 111.4, 61.4, 39.7, 31.3.

(2*S*)-2-Azido-3-(4-hydroxyphenyl)propanoic acid (23)



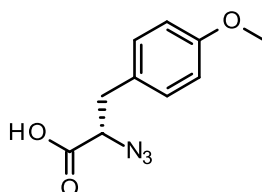
Compound **23** was synthesized according to the general procedure A, using *L*-tyrosine (226 mg, 1.25 mmol), ZnCl₂ (10.2 mg, 0.08 mmol), K₂CO₃ (691 mg, 5.0 mmol), anhydrous *N,N*-diisopropylethylamine (240 μL, 1.38 mmol) and diazo transfer reagent (407 mg, 1.5 mmol) in anhydrous MeOH (5mL) overnight. Compound **23** was obtained as pale brown oil (277 mg, 93%) and was used in the next step without further purification. LC tr = 1.40 min, MS (ESI-): *m/z* = 206 [M - H]⁻. ¹H NMR (300 MHz, MeOD-*d*₄) δ ppm: 7.10–7.06 (m, 2H), 6.75–6.70 (m, 2H), 4.08 (dd, *J* = 8.4 and 5.2 Hz, 1H), 3.07 (dd, *J* = 14.1 and 5.2 Hz, 1H), 2.89 (dd, *J* = 14.1 and 8.4 Hz, 1H). ¹³C NMR (75 MHz, MeOD-*d*₄) δ ppm: 173.3, 157.5, 131.4 (2C), 128.5, 116.3 (2C), 64.7, 37.8.

(2*R*)-2-Azido-3-(4-hydroxyphenyl)propanoic acid (37)



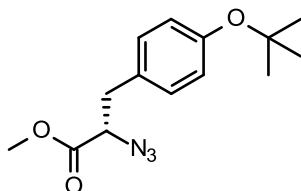
Compound **37** was synthesized according to the general procedure A, using *D*-tyrosine (226 mg, 1.25 mmol), ZnCl₂ (10.2 mg, 0.08 mmol), K₂CO₃ (691 mg, 5.0 mmol), anhydrous *N,N*-diisopropylethylamine (240 μL, 1.38 mmol) and diazo transfer reagent (407 mg, 1.5 mmol) in anhydrous MeOH (5mL) overnight. Compound **37** was obtained as pale brown oil (202 mg, 76%) and was used in the next step without further purification. LC tr = 1.42 min, MS (ESI-): *m/z* = 206 [M - H]⁻. ¹H NMR (300 MHz, MeOD-*d*₄) δ ppm: 7.10–7.06 (m, 2H), 6.75–6.70 (m, 2H), 4.08 (dd, *J* = 8.5 and 5.2 Hz, 1H), 3.07 (dd, *J* = 14.1 and 5.2 Hz, 1H), 2.89 (dd, *J* = 14.1 and 8.5 Hz, 1H). ¹³C NMR (75 MHz, MeOD-*d*₄) δ ppm: 173.4, 157.5, 131.4 (2C), 128.5, 116.3 (2C), 64.7, 37.8.

(2*S*)-2-Azido-3-(4-methoxyphenyl)propanoic acid (60)



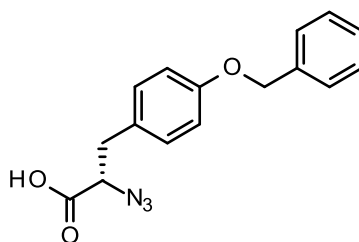
Compound **60** was synthesized according to the general procedure A, using *O*-methyl *L*-tyrosine analog (226 mg, 1.16 mmol), ZnCl₂ (9.5 mg, 0.07 mmol), K₂CO₃ (641 mg, 4.64 mmol), anhydrous *N,N*-diisopropylethylamine (222 μL, 1.28 mmol) and diazo transfer reagent (378 mg, 1.39 mmol) in anhydrous MeOH (5mL) overnight. Compound **60** was obtained as orange oil (257 mg, 96%) and was used in the next step without further purification. LC tr = 1.83 min, MS (ESI-): *m/z* = 220 [M - H]⁻. ¹H NMR (300 MHz, MeOD-*d*₄) δ ppm: 7.19–7.16 (m, 2H), 6.88–6.83 (m, 2H), 4.11 (dd, *J* = 8.4 and 5.2 Hz, 1H), 3.77 (s, 3H), 3.11 (dd, *J* = 14.1 and 5.2 Hz, 1H), 2.92 (dd, *J* = 14.1 and 8.4 Hz, 1H). ¹³C NMR (75 MHz, MeOD-*d*₄) δ ppm: 173.3, 160.2, 131.4 (2C), 129.8, 114.9 (2C), 64.7, 55.6, 37.7.

(2S)-2-Azido-3-(4-tert-butoxyphenyl)propanoic acid (63)



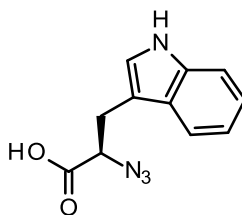
Compound **63** was synthesized according to the general procedure A, using *O*-tert-butyl *L*-tyrosine (360 mg, 1.25 mmol), ZnCl₂ (10.2 mg, 0.08 mmol), K₂CO₃ (691 mg, 5.0 mmol), anhydrous *N,N*-diisopropylethylamine (240 μL, 1.38 mmol) and diazo transfer reagent (407 mg, 1.5 mmol) in anhydrous MeOH (5mL) overnight. Compound **63** was obtained as yellow oil (337 mg, 50%) and was used in the next step without further purification. Purity: 51%, LC tr = 3.23 min, MS (ESI-): *m/z* = not visible [M - H]⁻, MS (ESI+): *m/z* = not visible [M + H]⁺. ¹H NMR (300 MHz, MeOD-*d*₄) δ ppm: 7.18–7.13 (m, 2H), 6.96–6.91 (m, 2H), 4.21 (dd, *J* = 8.4 and 5.7 Hz, 1H), 3.74 (s, 3H), 3.12 (dd, *J* = 14.1 and 5.7 Hz, 1H), 2.96 (dd, *J* = 14.1 and 8.4 Hz, 1H), 1.32 (s, 9H). ¹³C NMR (75 MHz, MeOD-*d*₄) δ ppm: 172.0, 155.7, 131.4, 130.9 (2C), 125.3 (2C), 79.6, 64.4, 53.0, 37.9, 29.2 (3C).

(2S)-2-azido-3-(4-benzyloxyphenyl)propanoic acid (62)



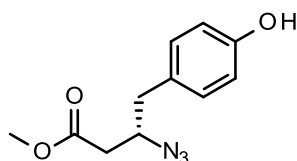
Compound **62** was synthesized according to the general procedure A, using *O*-benzyl *L*-tyrosine (339 mg, 1.25 mmol), ZnCl₂ (10.2 mg, 0.08 mmol), K₂CO₃ (691 mg, 5.0 mmol), anhydrous *N,N*-diisopropylethylamine (240 μL, 1.38 mmol) and diazo transfer reagent (407 mg, 1.5 mmol) in anhydrous MeOH (5mL) overnight. Compound **62** was obtained as brown oil (372 mg, 85%) and was used in the next step without further purification. LC tr = 2.57 min, MS (ESI-): *m/z* = 296 [M - H]⁻. ¹H NMR (300 MHz, MeOD-*d*₄) δ ppm: 7.43–7.27 (m, 5H), 7.19–7.13 (m, 2H), 6.96–6.90 (m, 2H), 5.05 (s, 2H), 4.20–4.10 (m, 1H), 3.10 (dd, *J* = 14.0 and 5.2 Hz, 1H), 2.92 (dd, *J* = 14.0 and 8.5 Hz, 1H). ¹³C NMR (75 MHz, MeOD-*d*₄) δ ppm: 173.3, 159.3, 138.7, 131.7, 131.4 (2C), 129.5 (2C), 128.8, 128.5 (2C), 116.0 (2C), 71.0, 64.6, 37.7.

(2R)-2-azido-3-(1H-indol-3-yl)propanoic acid (29)



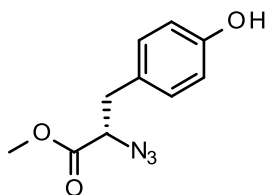
Compound **29** was synthesized according to the general procedure A, using D-tryptophan (255 mg, 1.25 mmol), ZnCl₂ (10.2 mg, 0.08 mmol), K₂CO₃ (691 mg, 5.0 mmol), anhydrous *N,N*-diisopropylethylamine (240 μL, 1.38 mmol) and diazo transfer reagent (407 mg, 1.5 mmol) in anhydrous MeOH (5mL) overnight. Compound **29** was obtained as brown oil (288 mg, 89%) and was used in the next step without further purification. LC tr = 1.95 min, MS (ESI-): *m/z* = 229 [M - H]⁻. ¹H NMR (300MHz, MeOD-*d*₄) δ ppm: 7.58 (1H, m, 1H), 7.34, (dt, *J* = 7.9 and 1.6 Hz, 1H), 7.14 (s, 1H), 7.12–7.07 (m, 1H), 7.04–6.99 (m, 1H) 4.19 (dd, *J* = 8.1 and 5.2 Hz, 1H), 3.34 (ddd, *J* = 14.5, 5.2 and 0.7 Hz, 1H) and 3.18 (ddd, *J* = 14.5, 8.1 and 0.4 Hz, 1H). ¹³C NMR (75MHz, MeOD-*d*₄) δ ppm: 173.9, 138.0, 128.6, 124.7, 122.4, 119.8, 119.1, 112.2, 110.5, 64.1, 28.7.

Methyl (3*S*)-3-azido-4-(4-hydroxyphenyl)butanoate (Z4-a)



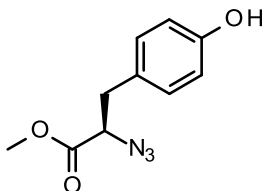
Compound **Z4-a** was synthesized according to the general procedure E, using carboxylic acid **1** (191 mg, 0.86 mmol) and thionyl chloride (126 μL, 1.73 mmol) in MeOH (0.07M) overnight. Compound **Z4-a** was obtained as orange oil (418 mg, quant. yield) and was used in the next step without further purification. LC tr = 2.37min. MS (ESI-): *m/z* = 234 [M - H]⁻. ¹H NMR (300MHz, MeOD-*d*₄) δ ppm: 7.08–7.05 (m, 2H), 6.76–6.72 (m, 2H), 4.01–3.92 (m, 1H), 3.67 (s, 3H), 2.82–2.66 (m, 2H), 2.60–2.53 (m, 1H), 2.45–2.36 (m, 1H). ¹³C NMR (75MHz, MeOD-*d*₄) δ ppm: 173.0, 157.4, 131.5 (2C), 129.3, 116.3 (2C), 62.4, 52.3, 40.7, 39.5.

Methyl (2*S*)-2-azido-3-(4-hydroxyphenyl)propanoate (30)



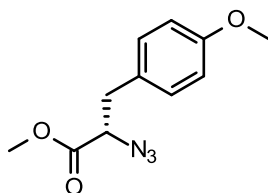
Compound **30** was synthesized according to the general procedure E, using carboxylic acid **23** (258 mg, 1.25 mmol) and thionyl chloride (182 μL, 2.49 mmol) in MeOH (5 mL) overnight. Compound **30** was obtained as brown oil (193 mg, 70%) and was used in the next step without further purification. LC tr = 2.40 min, MS (ESI-): *m/z* = 220 [M - H]⁻. ¹H NMR (300 MHz, MeOD-*d*₄) δ ppm: 7.07–7.02 (m, 2H), 6.74–6.70 (m, 2H), 4.13 (dd, *J* = 8.1 and 5.7 Hz, 1H), 3.73 (s, 3H), 3.04 (dd, *J* = 14.0 and 5.7 Hz, 1H), 2.90 (dd, *J* = 14.0 and 8.2 Hz, 1H). ¹³C NMR (75 MHz, MeOD-*d*₄) δ ppm: 172.2, 157.6, 131.3 (2C), 128.1, 116.3 (2C), 64.6, 52.9, 37.7.

Methyl (2R)-2-azido-3-(4-hydroxyphenyl)propanoate (**38**)



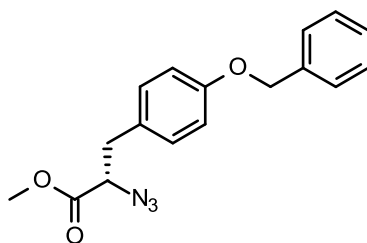
Compound **38** was synthesized according to the general procedure E, using carboxylic acid **37** (202 mg, 0.98 mmol) and thionyl chloride (142 μ L, 1.95 mmol) in MeOH (5 mL) overnight. Compound **38** was obtained as brown oil (130 mg, 60%) and was used in the next step without further purification. LC tr = 2.38 min, MS (ESI-): $m/z = 220$ [M - H]⁻. ¹H NMR (300 MHz, MeOD-*d*₄) δ ppm: 7.07–7.02 (m, 2H), 6.74–6.70 (m, 2H), 4.14 (dd, $J = 8.1$ and 5.7 Hz, 1H), 3.73 (s, 3H), 3.05 (dd, $J = 14.0$ and 5.7 Hz, 1H), 2.90 (dd, $J = 14.0$ and 8.1 Hz, 1H). ¹³C NMR (75 MHz, MeOD-*d*₄) δ ppm: 172.2, 157.6, 131.3 (2C), 128.1, 116.3 (2C), 64.6, 52.9, 37.7.

Methyl (2S)-2-azido-3-(4-methoxyphenyl)propanoate (**62**)



Compound **62** was synthesized according to the general procedure E, using carboxylic acid **60** (257 mg, 1.16 mmol) and thionyl chloride (169 μ L, 2.32 mmol) in MeOH (2.4 mL) overnight. Compound **62** was obtained as orange oil (251 mg, 83%) and was used in the next step without further purification. LC tr = 2.85 min, MS (ESI+), MS (ESI-): no ionization. ¹H NMR (300 MHz, MeOD-*d*₄) δ ppm: 7.16–7.13 (m, 2H), 6.87–6.84 (m, 2H), 4.18 (dd, $J = 8.1$ and 5.6 Hz, 1H), 3.77 (s, 3H), 3.74 (s, 3H), 3.08 (dd, $J = 14.0$ and 5.6 Hz, 1H), 2.92 (dd, $J = 14.0$ and 8.1 Hz, 1H). ¹³C NMR (75MHz, MeOD-*d*₄) δ ppm: 172.1, 160.3, 131.4 (2C), 129.4, 114.9 (2C), 64.5, 55.6, 52.9, 37.7.

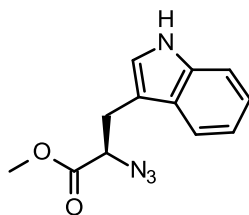
Methyl (2S)-2-azido-3-(4-benzyloxyphenyl)propanoate (**61**)



Compound **61** was synthesized according to the general procedure E, using carboxylic acid **59** (357 mg, 1.2 mmol) and thionyl chloride (175 μ L, 2.4 mmol) in MeOH (5 mL) overnight. Compound **61** was obtained as brown oil (339 mg, 77%) and was used in the next step without further purification. LC tr = 3.30 min, MS (ESI+): $m/z = 284$ [M - 2N + H]⁺. ¹H NMR (300 MHz, MeOD-*d*₄) δ ppm: 7.44–7.27 (m, 5H), 7.17–7.11 (m, 2H), 6.95–6.90 (m, 2H), 5.05 (s, 2H), 4.17 (dd, $J = 8.2$ and 5.6 Hz, 1H),

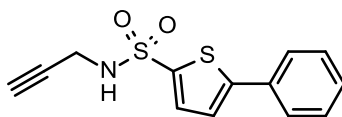
3.35 (s, 3H), 3.08 (dd, $J = 14.0$ and 5.6 Hz, 1H), 2.93 (dd, $J = 14.0$ and 8.2 Hz, 1H). ^{13}C NMR (75 MHz, MeOD- d_4) δ ppm: 171.9, 159.2, 138.5, 131.3 (2C), 129.6, 129.4 (2C), 128.8, 128.5 (2C), 115.9 (2C), 70.8, 64.3, 53.0, 37.5.

Methyl (2*R*)-2-azido-3-(1*H*-indol-3-yl)propanoate (**31**)



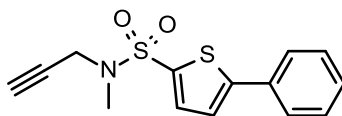
Compound **31** was synthesized according to the general procedure E, using carboxylic acid **29** (270 mg, 1.0 mmol) and thionyl chloride (145 μL , 2.0 mmol) in MeOH (2.5 mL) overnight. Compound **31** was obtained as orange oil (213 mg, 45%) and was used in the next step without further purification. Purity: 51%, LC tr = 2.78 min, MS (ESI -): $m/z = 243$ [M - H] $^-$. ^1H NMR (300 MHz, MeOD- d_4) δ ppm: 7.54 (ddd, $J = 7.8$, 1.2 and 0.7 Hz, 1H), 7.34, (dt, 7.8 and 1.2 Hz, 1H), 7.14 (s, 1H), 7.10–7.07 (m, 1H), 7.04–6.99 (m, 1H), 4.25 (dd, $J = 7.6$ and 5.9 Hz, 1H), 3.71 (s, 3H), 3.32 (ddd, $J = 14.6$, 5.9 and 0.7 Hz, 1H) and 3.20 (ddd, $J = 14.6$, 7.6 and 0.8 Hz, 1H). ^1H NMR (75MHz, MeOD- d_4) δ ppm: 172.5, 138.0, 128.5, 124.8, 122.5, 119.9, 119.1, 112.3, 110.1, 63.9, 52.9 and 28.6.

5-phenyl-*N*-prop-2-ynyl-thiophene-2-sulfonamide (**32**)



Compound **32** was synthesized according to the general procedure F, using propargylamine (82 μL , 1.28 mmol), 5-phenylthiophene-2-sulfonyl chloride (300 mg, 1.16 mmol) and *N,N*-diisopropylethylamine (242 μL , 1.39 mmol) in CH_2Cl_2 (5 mL) overnight. The crude product was filtered on silica gel (CH_2Cl_2 to $\text{CH}_2\text{Cl}_2/\text{MeOH}$: 9/1) affording compound **32** as a beige solid (309 mg, 97%). LC tr = 2.80 min, MS (ESI-): $m/z = 276$ [M - H] $^-$. ^1H NMR (300 MHz, CDCl_3) δ ppm: 7.63–7.58 (m, 3H), 7.46–7.38 (m, 3H), 7.25 (d, $J = 2.5$ Hz, 1H), 4.81 (br t, $J = 5.8$ Hz, 1H), 3.94 (dd, $J = 6.2$ and 2.7 Hz, 2H), 2.17 (t, $J = 2.6$ Hz, 1H). ^{13}C NMR (75 MHz, CDCl_3) δ ppm: 152.1, 138.3, 134.0, 132.8, 129.4 (2C), 126.5 (2C), 123.2, 77.8, 73.4, 33.4.

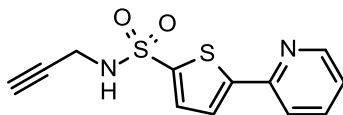
N-methyl-5-phenyl-*N*-prop-2-ynyl-thiophene-2-sulfonamide (**14**)



Compound **14** was synthesized according to the general procedure F, using *N*-methylpropargylamine (36 μL , 0.43 mmol), 5-phenylthiophene-2-sulfonyl chloride (100 mg, 0.39 mmol) and *N,N*-diisopropylethylamine (81 μL , 0.46 mmol) in CH_2Cl_2 (5 mL) overnight. The crude product was

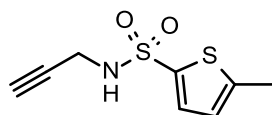
filtered on silica gel (cHex to cHex/EtOAc: 8/2) affording compound **14** as a beige powder (95 mg, 83%). LC tr = 3.08 min, MS (ESI+): $m/z = 292 [M + H]^+$. $^1\text{H NMR}$ (300 MHz, CDCl_3) δ ppm: 7.62–7.59 (m, 2H), 7.56 (d, $J = 3.9$ Hz, 1H), 7.46–7.38 (m, 3H), 7.29 (d, $J = 3.9$ Hz, 1H), 4.07 (d, $J = 2.6$ Hz, 2H), 2.94 (s, 3H), 2.15 (t, $J = 2.5$ Hz, 1H). $^{13}\text{C NMR}$ (75 MHz, CDCl_3) δ ppm: 151.6, 135.5, 133.7, 132.8, 129.4 (2C), 129.3, 126.4 (2C), 123.3, 76.0, 74.4, 40.1, 34.7.

***N*-prop-2-ynyl-5-(2-pyridyl)thiophene-2-sulfonamide (44)**



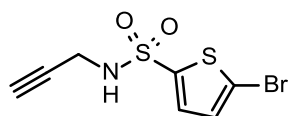
Compound **44** was synthesized according to the general procedure F, using propargylamine (81 μL , 1.27 mmol), 5-(2-pyridyl)thiophene-2-sulfonyl chloride (300 mg, 1.16 mmol) and *N,N*-diisopropylethylamine (241 μL , 1.39 mmol) in CH_2Cl_2 (5 mL) overnight. The crude product was filtered on silica gel (CH_2Cl_2 to $\text{CH}_2\text{Cl}_2/\text{MeOH}$: 9/1) affording compound **44** as a pale yellow solid (226 mg, 70%). LC tr = 2.42 min, MS (ESI+): $m/z = 279 [M + H]^+$. $^1\text{H NMR}$ (300 MHz, $\text{MeOD-}d_4$) δ ppm: 8.53 (ddd, $J = 4.9, 1.7$ and 1.1 Hz, 1H), 7.91–7.82 (m, 2H), 7.67 (d, $J = 4.0$ Hz, 1H), 7.61 (d, $J = 4.0$ Hz, 1H), 7.34 (ddd, $J = 7.0, 4.9$ and 1.7 Hz, 1H), 3.86 (d, $J = 2.5$ Hz, 2H), 2.53 (t, $J = 2.5$ Hz, 1H). $^{13}\text{C NMR}$ (75 MHz, $\text{MeOD-}d_4$) δ ppm: 152.4, 152.0, 150.6, 143.6, 138.7, 134.1, 125.5, 124.7, 120.7, 79.3, 73.6, 33.4.

5-methyl-*N*-prop-2-ynyl-thiophene-2-sulfonamide (43)



Compound **43** was synthesized according to the general procedure F, using propargylamine (107 μL , 1.68 mmol), 5-methylthiophene-2-sulfonyl chloride (210 μL , 1.53 mmol) and *N,N*-diisopropylethylamine (319 μL , 1.83 mmol) in CH_2Cl_2 (5 mL) overnight. The crude product was filtered on silica gel (CH_2Cl_2 to $\text{CH}_2\text{Cl}_2/\text{MeOH}$: 9/1) affording compound **43** as brown oil (309 mg, 94%). LC tr = 2.32 min, MS (ESI-): $m/z = 214 [M - H]^-$. $^1\text{H NMR}$ (300 MHz, $\text{MeOD-}d_4$) δ ppm: 7.42 (d, $J = 3.7$ Hz, 1H), 6.84–6.82 (m, 1H), 3.77 (d, $J = 2.6$ Hz, 2H), 2.54–2.52 (m, 4H). $^{13}\text{C NMR}$ (75 MHz, $\text{MeOD-}d_4$) δ ppm: 149.0, 139.2, 133.8, 126.9, 79.4, 73.5, 33.3, 15.3.

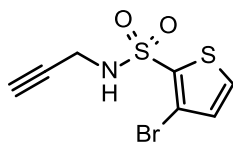
5-bromo-*N*-prop-2-ynyl-thiophene-2-sulfonamide (41)



Compound **41** was synthesized according to the general procedure F, using propargylamine (81 μL , 1.26 mmol), 5-bromothiophene-2-sulfonyl chloride (300 mg, 1.15 mmol) and *N,N*-

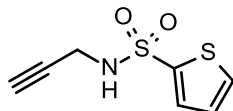
Diisopropylethylamine (240 μ L, 1.38 mmol) in CH_2Cl_2 (5 mL) overnight. The crude product was purified by flash chromatography on silica gel (cHex to cHex/EtOAc: 8/2) affording compound **41** as pale yellow oil (235 mg, 70%). LC tr = 2.55 min, MS (ESI⁻): m/z = 278 and 280 [M - H]⁻. ¹H NMR (300 MHz, CDCl_3) δ ppm: 7.42 (d, J = 4.0 Hz, 1H), 7.08 (d, J = 3.8 Hz, 1H), 4.95–4.91 (m, 1H), 3.92 (dd, J = 6.0 and 2.5 Hz, 2H), 2.20 (t, J = 2.6 Hz, 1H). ¹³C NMR (75 MHz, CDCl_3) δ ppm: 141.0, 133.1, 130.5, 120.5, 77.3, 73.4, 33.1.

3-bromo-*N*-prop-2-ynyl-thiophene-2-sulfonamide (**42**)



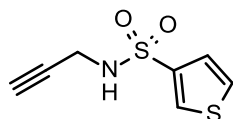
Compound **42** was synthesized according to the general procedure F, using propargylamine (81 μ L, 1.26 mmol), 3-bromothiophene-2-sulfonyl chloride (300 mg, 1.15 mmol) and *N,N*-diisopropylethylamine (240 μ L, 1.38 mmol) in CH_2Cl_2 (5 mL) overnight. The crude product was filtered on silica gel (CH_2Cl_2 to $\text{CH}_2\text{Cl}_2/\text{MeOH}$: 9/1) affording compound **42** as a beige solid (287 mg, 89%). LC tr = 2.32 min, MS (ESI⁻): m/z = 278 and 280 [M - H]⁻. ¹H NMR (300 MHz, $\text{MeOD-}d_4$) δ ppm: 7.74 (d, J = 5.3 Hz, 1H), 7.16 (d, J = 5.3 Hz, 1H), 3.86 (d, J = 2.3 Hz, 2H), 2.45 (t, J = 2.5 Hz, 1H). ¹³C NMR (75 MHz, $\text{MeOD-}d_4$) δ : 133.8, 133.7, 132.6, 114.8, 79.0, 73.2, 33.1.

N-prop-2-ynylthiophene-2-sulfonamide (**45**)



Compound **45** was synthesized according to the general procedure F, using propargylamine (264 μ L, 4.12 mmol), thiophene-2-sulfonyl chloride (500 mg, 2.74 mmol) and *N,N*-diisopropylethylamine (572 μ L, 3.29 mmol) in CH_2Cl_2 (15 mL) overnight. The crude product was purified by flash chromatography on silica gel (CH_2Cl_2 to $\text{CH}_2\text{Cl}_2/\text{MeOH}$: 95/5) affording compound **45** as yellow oil (430 mg, 78%). LC tr = 2.08 min, MS (ESI⁻): m/z = 200 [M - H]⁻. ¹H NMR (300 MHz, $\text{MeOH-}d_4$) δ ppm: 7.77 (dd, J = 1.4 and 5.0 Hz, 1H), 7.63 (dd, J = 1.4 and 3.8 Hz, 1H), 7.14 (dd, J = 3.0 and 5.0 Hz, 1H), 3.80 (d, J = 2.5 Hz, 2H), 2.50 (t, J = 2.5 Hz, 1H). ¹³C NMR (75 MHz, $\text{MeOH-}d_4$) δ ppm: 142.4, 133.4, 133.3, 128.4, 79.3, 73.5, 33.3.

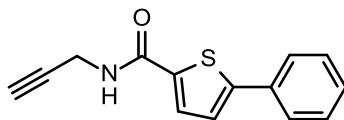
N-prop-2-ynylthiophene-3-sulfonamide (**46**)



Compound **46** was synthesized according to the general procedure F, using propargylamine (116 μ L, 1.81 mmol), thiophene-3-sulfonyl chloride (300 mg, 1.64 mmol) and *N,N*-diisopropylethylamine (343

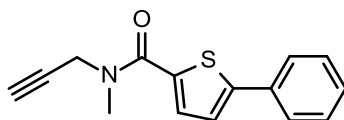
μL , 1.97 mmol) in CH_2Cl_2 (5 mL) overnight. The crude product was filtered on silica gel (CH_2Cl_2 to $\text{CH}_2\text{Cl}_2/\text{MeOH}$: 9/1) affording compound **46** as a beige solid (287 mg, 87%). LC tr = 2.02 min, MS (ESI-): $m/z = 200$ $[\text{M} - \text{H}]^-$. ^1H NMR (300 MHz, $\text{MeOD}-d_4$) δ ppm: 8.08 (dd, $J = 3.1$ and 1.3 Hz, 1H), 7.58 (dd, $J = 5.2$ and 3.1 Hz, 1H), 7.38 (dd, $J = 5.2$ and 1.3 Hz, 1H), 3.78 (dd, $J = 2.5$ Hz, 2H), 2.48 (t, $J = 2.5$ Hz, 1H). ^{13}C NMR (75 MHz, $\text{MeOD}-d_4$) δ ppm: 141.6, 131.8, 129.1, 126.7, 79.5, 73.4, 33.1.

5-phenyl-*N*-prop-2-ynyl-thiophene-2-carboxamide (15)



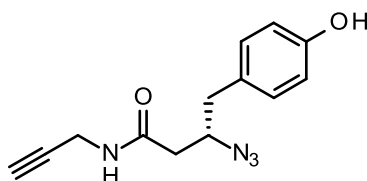
Compound **15** was synthesized according to the general procedure B, using 5-phenylthiophene-2-carboxylic acid (150 mg, 0.73 mmol), propargylamine (77 μL , 1.18 mmol), HBTU (456 mg, 1.18 mmol) and trimethylamine (307 μL , 2.2 mmol) in DMF (2 mL) 48h. The crude product was purified by flash chromatography on silica gel (cHex to cHex/EtOAc: 75/25) affording compound **15** as a white solid (134 mg, 76%). LC tr = 2.68 min, MS (ESI+): $m/z = 242$ $[\text{M} + \text{H}]^+$. ^1H NMR (300 MHz, $\text{DMSO}-d_6$) δ ppm: 8.99 (t, $J = 5.2$ Hz, 1H), 7.78 (d, $J = 4.0$ Hz, 1H), 7.73–7.70 (m, 2H), 7.55 (d, $J = 4.0$ Hz, 1H), 7.48–7.34 (m, 3H), 4.06 (dd, $J = 2.5$ and 5.6 Hz, 2H), 3.17 (t, $J = 2.5$ Hz, 1H). ^{13}C NMR (75 MHz, $\text{DMSO}-d_6$) δ ppm: 160.7, 147.7, 138.1, 133.0, 129.5, 129.2 (2C), 128.6, 125.7 (2C), 124.4, 81.1, 73.2, 28.4.

N-methyl-5-phenyl-*N*-prop-2-ynyl-thiophene-2-carboxamide (16)



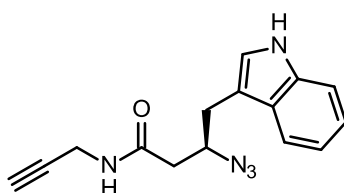
Compound **16** was synthesized according to the general procedure B, using 5-phenylthiophene-2-carboxylic acid (150 mg, 0.73 mmol), *N*-methylpropargylamine (102 μL , 1.18 mmol), HBTU (456 mg, 1.18 mmol) and trimethylamine (307 μL , 2.2 mmol) in DMF (2 mL) 48h. The crude product was purified by flash chromatography on C18 column ($\text{H}_2\text{O}/\text{MeOH}$: 9/1 to MeOH) affording compound **16** as a white solid (90 mg, 48%). LC tr = 2.87 min, MS (ESI+): $m/z = 256$ $[\text{M} + \text{H}]^+$. ^1H NMR (300 MHz, CDCl_3) δ ppm: 7.65–7.61 (m, 2H), 7.48–7.31 (m, 4H), 7.26 (d, $J = 5.7$ Hz, 1H), 4.36 (d, $J = 2.5$ Hz, 2H), 3.29 (s, 3H), 2.36 (t, $J = 2.3$ Hz, 1H). ^{13}C NMR (75 MHz, CDCl_3) δ ppm: 164.1, 148.6, 136.2, 133.5, 130.6, 129.1 (2C), 128.5, 126.2 (2C), 122.9, 78.6, 73.0, 39.6, 35.7.

(3*S*)-3-Azido-4-(4-hydroxyphenyl)-*N*-prop-2-ynyl-butanamide (3)



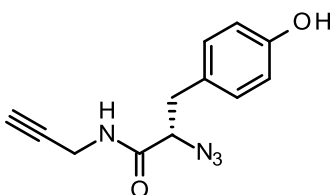
Compound **3** was synthesized according to the general procedure B, using azido carboxylic acid **1** (334 mg, 1.51 mmol), propargylamine (126 μ L, 1.96 mmol), HBTU (630 mg, 1.66 mmol) and trimethylamine (619 μ L, 4.53 mmol) in DMF (5 mL) overnight. Compound **3** was obtained as yellow oil (369 mg, 90%) and was used in the next step without further purification. LC tr = 2.07 min, MS (ESI-): m/z = 257 [M-H]⁻. ¹H NMR (300 MHz, MeOD-*d*₄) δ ppm: 7.09–7.04 (m, 2H), 6.76–6.71 (m, 2H), 4.03–3.97 (m, 1H), 3.96–3.94 (m, 2H), 2.79 (dd, J = 13.9 and 5.7 Hz, 1H), 2.70 (dd, J = 13.9 and 8.0 Hz, 1H), 2.58 (t, J = 2.6 Hz, 1H), 2.40 (dd, J = 14.8 and 5.0 Hz, 1H), 2.31 (dd, J = 14.7 and 8.9 Hz, 1H). ¹³C NMR (75 MHz, MeOD-*d*₄) δ ppm: 172.4, 157.4, 131.5 (2C), 129.4, 116.3 (2C), 80.4, 72.2, 62.6, 41.3, 40.9, 29.5.

(3R)-3-Azido-4-(1H-indol-3-yl)-N-prop-2-ynyl-butanamide (4)



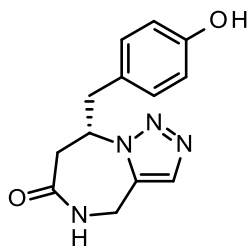
Compound **4** was synthesized according to the general procedure B, using azido carboxylic acid **2** (611 mg, 2.50 mmol), propargylamine (208 μ L, 3.3 mmol), HBTU (1040 mg, 2.8 mmol) and trimethylamine (1030 μ L, 7.5 mmol) in DMF (10 mL) overnight. Compound **4** was obtained as brown oil (487 mg, 57%) and was used in the next step without further purification. LC tr = 2.50 min, MS (ESI-): m/z = 280 [M - H]⁻. ¹H NMR (300 MHz, MeOD-*d*₄) δ ppm: 7.59–7.56 (m, 1H), 7.36–7.33 (m, 1H), 7.13 (s, 1H), 7.10–7.00 (m, 2H), 4.19–4.11 (m, 1H), 3.94–3.93 (m, 2H), 3.07–2.95 (m, 2H), 2.57 (t, J = 2.6 Hz, 1H), 2.46 (dd, J = 14.7 and 5.0 Hz, 1H), 2.36 (dd, J = 14.7 and 8.9 Hz, 1H). ¹³C NMR (75 MHz, MeOD-*d*₄) δ ppm: 172.6, 138.1, 128.8, 124.7, 122.4, 119.9, 119.3, 112.3, 111.4, 80.4, 72.2, 61.7, 41.5, 31.4, 29.4.

(2S)-2-Azido-3-(4-hydroxyphenyl)-N-prop-2-ynyl-propanamide (24)



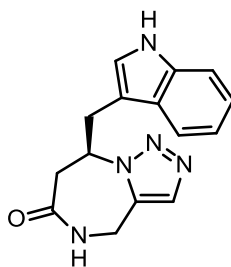
Compound **24** was synthesized according to the general procedure B, using azido carboxylic acid **23** (505 mg, 2.4 mmol), propargylamine (203 μ L, 3.2 mmol), HBTU (1020 mg, 2.7 mmol) and trimethylamine (1000 μ L, 7.3 mmol) in DMF (10 mL) overnight. Compound **24** was obtained as brown oil (345 mg, 50%) and was used in the next step without further purification. LC tr = 2.05 min, MS (ESI-): m/z = 243 [M - H]⁻. ¹H NMR (300 MHz, MeOD-*d*₄) δ ppm: 7.09–7.03 (m, 2H), 6.74–6.69 (m, 2H), 3.98–3.92 (m, 3H), 3.08 (dd, J = 13.8 and 6.1 Hz, 1H), 2.89 (dd, J = 13.8 and 7.9 Hz, 1H), 2.57 (t, J = 2.6 Hz, 1H). ¹³C NMR (75 MHz, MeOD-*d*₄) δ ppm: 171.6, 157.6, 131.4 (2C), 128.2, 116.3 (2C), 80.1, 72.3, 65.7, 38.1, 29.4.

(8S)-8-[(4-Hydroxyphenyl)methyl]-4,5,7,8-tetrahydrotriazolo[1,5-a][1,4]diazepin-6-one (5)



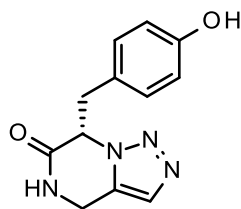
Compound **5** was synthesized according to the general procedure C, using **3** (1660 mg, 6.43 mmol) in DMF (200 mL) overnight. The crude product was purified by flash chromatography on silica gel (CH₂Cl₂ to CH₂Cl₂/MeOH: 9/1) affording compound **5** as a brown solid (1156 mg, 70%). LC tr = 1.48 min, MS (ESI+): $m/z = 259 [M + H]^+$. ¹H NMR (300 MHz, MeOD-*d*₄) δ ppm: 7.57 (s, 1H), 7.03–6.99 (m, 2H), 6.74–6.70 (m, 2H), 5.05–4.97 (m, 1H), 4.41 (dd, $J = 27.8$ and 17.0 Hz, 2H), 3.43 (dd, $J = 13.7$ and 3.5 Hz, 1H), 3.15 (dd, $J = 13.7$ and 9.1 Hz, 1H), 3.03 (dd, $J = 14.5$ and 4.4 Hz, 1H), 2.95 (dd, $J = 14.5$ and 8.3 Hz, 1H). ¹³C NMR (75 MHz, MeOD-*d*₄) δ ppm: 175.1, 157.7, 135.5, 131.9 (2C), 131.8, 127.6, 116.4 (2C), 59.8, 42.1, 36.1, 35.6.

(8R)-8-(1H-Indol-3-ylmethyl)-4,5,7,8-tetrahydrotriazolo[1,5-a][1,4]diazepin-6-one (6)



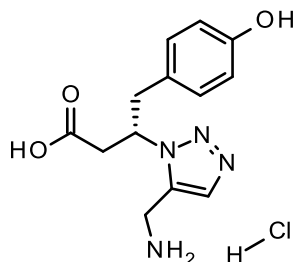
Compound **6** was synthesized according to the general procedure C, using **4** (487 mg, 1.73 mmol) in DMF (50 mL) overnight. The crude product was purified by flash chromatography on silica gel (CH₂Cl₂ to CH₂Cl₂/MeOH: 9/1) affording compound **6** as a brown oil (217 mg, 45%). LC tr = 1.90min, MS (ESI+): $m/z = 282 [M + H]^+$. ¹H NMR (300 MHz, MeOD-*d*₄) δ ppm: 7.56 (s, 1H), 7.54–7.51 (m, 1H), 7.36–7.32 (m, 1H), 7.12–6.99 (m, 3H), 5.13–5.05 (m, 1H), 4.39 (d, $J = 17.0$ Hz, 1H), 4.30 (d, $J = 17.0$ Hz, 1H), 3.69 (dd, $J = 14.3$ and 3.1 Hz, 1H), 3.43–3.38 (m, 1H), 3.08–2.95 (m, 2H). ¹³C NMR (75 MHz, MeOD-*d*₄) δ ppm: 175.4, 138.0, 135.5, 131.8, 128.7, 125.6, 122.6, 120.1, 119.1, 112.4, 109.6, 59.0, 36.6, 35.6, 33.1.

(7S)-7-[(4-Hydroxyphenyl)methyl]-5,7-dihydro-4H-triazolo[1,5-a]pyrazin-6-one (25)



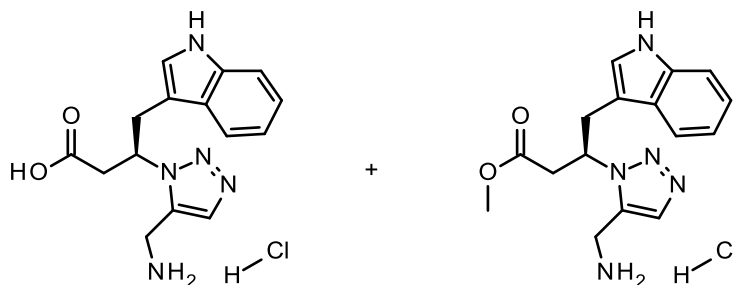
Compound **25** was synthesized according to the general procedure C, using **24** (330 mg, 1.35 mmol) in DMF (150 mL) overnight. The crude product was purified by flash chromatography on silica gel (CH₂Cl₂ to CH₂Cl₂/MeOH: 85/15) affording compound **25** as an orange solid (176 mg, 48%). LC tr = 1.42 min, MS (ESI+): m/z = 245 [M + H]⁺. ¹H NMR (300 MHz, DMSO-*d*₆) δ ppm: 9.31 (s, 1H), 8.42 (br d, *J* = 2.0 Hz, 1H), 7.53 (s, 1H), 6.52 (d, *J* = 8.5 Hz, 2H), 6.42 (d, *J* = 8.5 Hz, 2H), 5.38 (t, *J* = 3.9 Hz, 1H), 4.28 (dd, *J* = 16.7 and 2.7 Hz, 1H), 3.39–3.16 (m, 3H). ¹³C NMR (75 MHz, DMSO-*d*₆) δ ppm: 165.9, 156.6, 130.2 (2C), 129.2, 128.5, 124.2, 115.0 (2C), 60.0, 37.8, 35.4.

(3S)-3-[5-(Aminomethyl)triazol-1-yl]-4-(4-hydroxyphenyl)butanoic acid;hydrochloride (7)



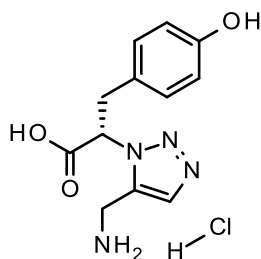
Compound **7** was synthesized according to the general procedure D, using diazepinone **5** (1150 mg, 4.45 mmol) in a 6M aq. HCl solution (30 mL) under MW irradiations (85°C, 1h). Compound **7** was obtained as brown solid (1390 mg, quant. yield) and was used in the next step without further purification. LC tr = 1.33 min, MS (ESI+): m/z = 277 [M + H]⁺. ¹H NMR (300 MHz, DMSO-*d*₆) δ ppm: 8.64 (t, *J* = 6.1 Hz, 2H), 7.70 (s, 1H), 6.79 (d, *J* = 8.5 Hz, 2H), 6.62 (d, *J* = 8.5 Hz, 2H), 4.96–4.86 (m, 1H), 3.85 (dd, *J* = 15.2 and 5.7 Hz, 1H), 3.68 (dd, *J* = 15.2 and 5.7 Hz, 1H), 3.17–3.08 (m, 2H), 3.02–2.93 (m, 2H). ¹³C NMR (75 MHz, DMSO-*d*₆) δ ppm: 171.9, 156.2, 132.6, 131.7, 130.0 (2C), 126.7, 115.2 (2C), 56.8, 40.2, 38.6, 31.2.

(3R)-3-[5-(Aminomethyl)triazol-1-yl]-4-(1H-indol-3-yl)butanoic acid;hydrochloride (not isolated)



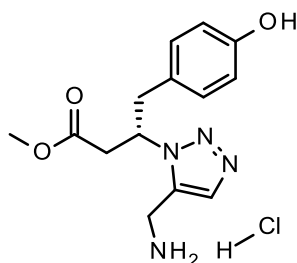
Diazepinone **6** (217 mg, 0.77 mmol) in a 6M aq. HCl solution (7.5 mL) and methanol (5 mL) was heated under MW irradiations (85°C 1+1h) in order to try the lactame hydrolysis-esterification tandem; a mixture of carboxylic acid/methyl ester was obtained (25/75%), the carboxylic acid was therefore not isolated and the mixture was dissolved in thionyl chloride and stirred at room temperature until total conversion in ester.

(2S)-2-[5-(Aminomethyl)triazol-1-yl]-3-(4-hydroxyphenyl)propanoic acid;hydrochloride (not isolated)



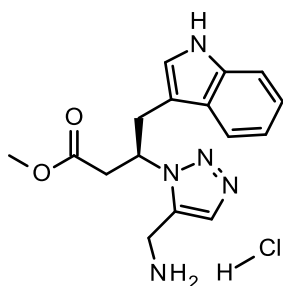
General procedure D was applied to pyrazinone **25** (1150 mg, 4.45 mmol) in a 6M aq. HCl solution (5 mL) under MW irradiations (1h at 85°C and 1h at 100°C). 70% of conversion was observed and the desired carboxylic acid was not therefore isolated.

Methyl (3S)-3-[5-(aminomethyl)triazol-1-yl]-4-(4-hydroxyphenyl)butanoate;hydrochloride (8)



Compound **8** was synthesized according to the general procedure E, using carboxylic acid **7** (1380 mg, 4.41 mmol) and thionyl chloride (644 μ L, 8.82 mmol) in MeOH (25 mL) overnight. Compound **8** was obtained as a brown solid (1302 mg, 90%) and was used in the next step without further purification. LC tr = 1.60 min, MS (ESI+): $m/z = 291$ [M + H]⁺. ¹H NMR (300 MHz, MeOD-*d*₄) δ ppm: 7.87 (s, 1H), 6.78 (d, $J = 8.5$ Hz, 2H), 6.63 (d, $J = 8.5$ Hz, 2H), 5.20–5.11 (m, 1H), 3.87 (dd, $J = 22.7$ and 15.3 Hz, 2H), 3.63 (s, 3H), 3.47 (dd, $J = 18.0$ and 10.5 Hz, 1H), 3.28–3.22 (m, 2H), 3.08 (dd, $J = 13.6$ and 10.6 Hz, 1H). ¹³C NMR (75 MHz, MeOD-*d*₄) δ ppm: 173.3, 158.0, 134.1, 133.3, 131.1 (2C), 128.0, 116.6 (2C), 60.3, 52.8, 41.8, 39.4, 32.4.

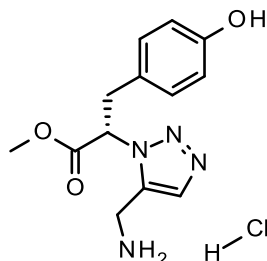
Methyl (3R)-3-[5-(aminomethyl)triazol-1-yl]-4-(1H-indol-3-yl)butanoate;hydrochloride (9)



Compound **9** was synthesized according to the general procedure E, using a mixture of carboxylic acid and methyl ester (259 mg, 0.77 mmol), and thionyl chloride (113 μ L, 1.54 mmol) in MeOH (3.5 mL) overnight. Compound **9** was obtained as a brown solid (270 mg, quant. yield) and was used in the next step without further purification. LC tr = 1.85 min, MS (ESI+): $m/z = 314$ [M + H]⁺. ¹H NMR (300

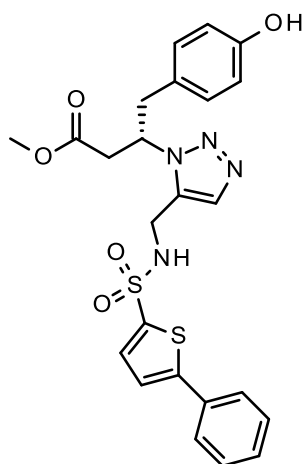
MHz, MeOD- d_4) δ ppm: 7.90 (s, 1H), 7.43 (d, J = 7.8 Hz, 1H), 7.33 (d, J = 8.0 Hz, 1H), 7.13–6.99 (m, 2H), 6.84 (s, 1H), 5.34–5.24 (m, 1H), 3.77–3.72 (m, 1H), 3.64 (s, 3H), 3.62–3.37 (m, 5H). ^{13}C NMR (75 MHz, MeOD- d_4) δ ppm: 173.3, 137.8, 134.4, 132.7, 127.9, 125.0, 122.9, 120.4, 118.6, 112.7, 109.9, 59.9, 52.8, 39.4, 32.5, 32.1.

Methyl (2S)-2-[5-(aminomethyl)triazol-1-yl]-3-(4-hydroxyphenyl)propanoate;hydrochloride (26)



Compound **26** was synthesized according to the general procedure E, using the corresponding carboxylic acid (194 mg, 0.45 mmol), and thionyl chloride (66 μL , 0.91 mmol) in MeOH (5.0 mL) overnight. Compound **26** was obtained as yellow oil (100 mg, 56%) and was used in the next step without further purification. LC tr = 1.55 min, MS (ESI+): m/z = 277 [$\text{M} + \text{H}$] $^+$. ^1H NMR (300 MHz, MeOD- d_4) δ ppm: 7.81 (s, 1H), 6.90–6.85 (m, 2H), 6.66–6.62 (m, 2H), 5.70 (dd, J = 10.9 and 4.8 Hz, 1H), 4.15–3.94 (m, 2H), 3.80 (s, 3H), 3.64 (dd, J = 14.3 and 4.8 Hz, 1H), 3.44 (dd, J = 14.3 and 10.9 Hz, 1H). ^{13}C NMR (75 MHz, MeOD- d_4) δ ppm: 169.6, 157.8, 134.2, 133.6, 131.2 (2C), 127.4, 116.5 (2C), 64.1, 53.8, 37.6, 32.9.

Methyl (3S)-4-(4-hydroxyphenyl)-3-[5-[[5-(phenyl-2-thienyl)sulfonylamino]methyl]triazol-1-yl]butanoate (10)

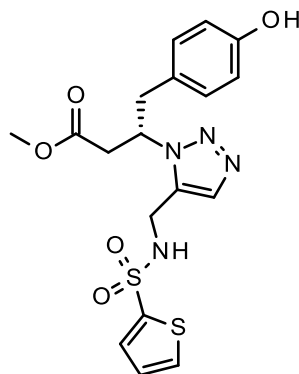


Compound **10** was synthesized according to the general procedure F, using amine **8** (77 mg, 0.24 mmol), 5-phenylthiophene-2-sulfonyl chloride (73.2 mg, 0.28 mmol) and N,N -diisopropylethylamine (82 μL , 0.47 mmol) in DMF (2.5 mL) overnight. The crude product was purified by flash chromatography on silica gel (CH_2Cl_2 to $\text{CH}_2\text{Cl}_2/\text{MeOH}$: 95/5) affording compound **10** as a white solid (100 mg, 65%). LC tr = 2.73 min, MS (ESI+): m/z = 513 [$\text{M} + \text{H}$] $^+$. ^1H NMR (300 MHz, MeOD- d_4) δ ppm: 7.71–7.67 (m, 2H), 7.52–7.40 (m, 5H), 7.37 (s, 1H), 6.77–6.74 (m, 2H), 6.64–6.61 (m, 2H),

4.99–4.91 (m, 1H), 3.87 (d, $J = 15.6$, 1H), 3.78 (d, $J = 15.6$ Hz, 1H), 3.59 (s, 3H), 3.35–3.26 (m, 1H), 3.16–3.02 (m, 3H). ^{13}C NMR (75 MHz, MeOD- d_4) δ ppm: 172.5, 161.0, 157.7, 152.5, 136.4, 134.5, 134.0, 133.2, 131.3 (2C), 130.4 (2C), 130.3, 128.5, 127.2 (2C), 124.5, 116.5 (2C), 59.2, 52.4, 42.1, 39.5, 36.7.

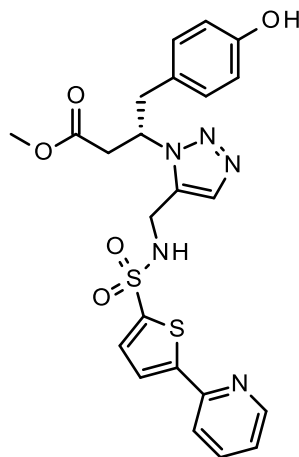
Methyl (3S)-4-(4-hydroxyphenyl)-3-[5-[(2-thienylsulfonylamino)methyl]triazol-1-yl]butanoate

(72)



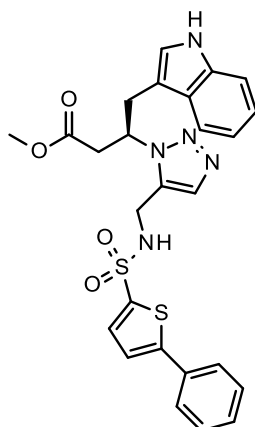
Compound **72** was synthesized according to the general procedure F, using amine **8** (55 mg, 0.17 mmol), thiophene-2-sulfonyl chloride (36.9 mg, 0.2 mmol) and *N,N*-diisopropylethylamine (59 μL , 0.34 mmol) in DMF (2 mL) overnight. The crude product was purified by flash chromatography on silica gel (CH_2Cl_2 to $\text{CH}_2\text{Cl}_2/\text{MeOH}$: 95/5) affording compound **72** as colorless oil (22 mg, 30%). LC $t_r = 2.23$ min, MS (ESI+): $m/z = 437$ [$\text{M} + \text{H}$] $^+$. ^1H NMR (300 MHz, MeOD- d_4) δ ppm: 7.81 (dd, $J = 5.0$ and 1.3 Hz, 1H), 7.56 (dd, $J = 3.8$ and 1.3 Hz, 1H), 7.33 (s, 1H), 7.17 (dd, $J = 5.0$ and 3.8 Hz, 1H), 6.77–6.72 (m, 2H), 6.64–6.60 (m, 2H), 4.97–4.89 (m, 1H), 3.84 (d, $J = 15.6$ Hz, 1H), 3.73 (d, $J = 15.8$ Hz, 1H), 3.59 (s, 3H), 3.35–3.26 (m, 1H), 3.16–3.10 (m, 2H), 3.05–3.02 (m, 1H). ^{13}C NMR (75 MHz, MeOD- d_4) δ ppm: 172.5, 157.7, 141.8, 136.4, 133.7, 133.6, 133.1, 131.2 (2C), 128.7, 128.5, 116.5 (2C), 59.2, 52.4, 42.0, 39.6, 36.7.

Methyl (3S)-4-(4-hydroxyphenyl)-3-[5-[[[5-(2-pyridyl)-2-thienyl]sulfonylamino]methyl]triazol-1-yl]butanoate (73)



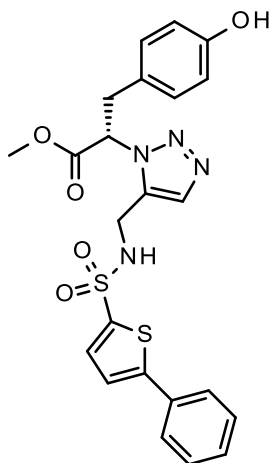
Compound **73** was synthesized according to the general procedure G, using amine **8** (80 mg, 0.25 mmol), 5-(2-pyridyl)thiophene-2-sulfonyl chloride (76.3 mg, 0.29 mmol) and *N,N*-diisopropylethylamine (85 μ L, 0.49 mmol) in DMF (2.5 mL) overnight. The crude product was purified by flash chromatography on silica gel (CH_2Cl_2 to $\text{CH}_2\text{Cl}_2/\text{MeOH}$: 9/1) affording compound **73** as colorless oil (69 mg, 54%). LC tr = 2.43 min, MS (ESI+): $m/z = 514$ $[\text{M} + \text{H}]^+$. ^1H NMR (300 MHz, $\text{DMSO-}d_6$) δ ppm: 9.43–9.04 (m, 1H), 8.60–8.56 (m, 2H), 8.09–7.92 (m, 2H), 7.88 (d, $J = 3.9$ Hz, 1H), 7.54 (d, $J = 3.9$ Hz, 1H), 7.42–7.38 (m, 2H), 6.81–6.78 (m, 2H), 6.63–6.61 (m, 2H), 4.91–4.82 (m, 1H), 3.96 (dd, $J = 15.6$ and 5.3 Hz, 1H), 3.79 (dd, $J = 15.6$ and 6.1 Hz, 1H), 3.16 (s, 3H), 3.11–2.89 (m, 4H). ^{13}C NMR (75 MHz, $\text{DMSO-}d_6$) δ ppm: 170.5, 156.3, 150.4, 150.3, 149.7, 141.1, 137.6, 134.0, 133.0, 132.1, 130.0 (2C), 126.5, 125.0, 123.9, 119.4, 115.2 (2C), 56.6, 51.6, 38.1, 35.5, 33.9.

Methyl (3R)-4-(1H-indol-3-yl)-3-[5-[(5-phenyl-2-thienyl)sulfonylamino]methyl]triazol-1-yl]butanoate (11)



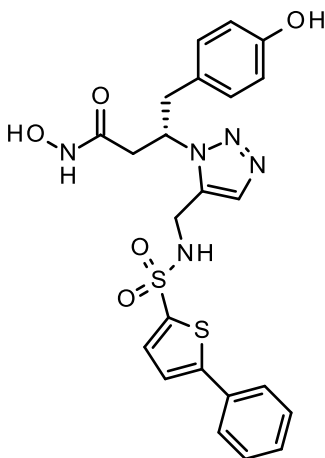
Compound **11** was synthesized according to the general procedure G, using amine **9** (135 mg, 0.39 mmol), 5-phenylthiophene-2-sulfonyl chloride (120 mg, 0.46 mmol) and *N,N*-Diisopropylethylamine (148 μ L, 0.85 mmol) in DMF (5 mL) overnight. The crude product was purified by flash chromatography on silica gel (CH_2Cl_2 to $\text{CH}_2\text{Cl}_2/\text{MeOH}$: 98/2) affording compound **11** as a brown solid (126 mg, 61%). LC tr = 2.98 min, MS (ESI+): $m/z = 536$ $[\text{M} + \text{H}]^+$. ^1H NMR (300 MHz, $\text{DMSO-}d_6$) δ ppm: 10.90–10.89 (m, 1H), 8.45 (t, $J = 5.9$ Hz, 1H), 7.75–7.71 (m, 2H), 7.55 (d, $J = 3.9$ Hz, 1H), 7.53–7.43 (m, 4H), 7.39 (s, 1H), 7.37 (d, $J = 3.9$ Hz, 1H), 7.32 (d, $J = 8.0$ Hz, 1H), 7.08–6.90 (m, 3H), 5.03–4.94 (m, 1H), 3.92 (dd, $J = 15.6$ and 5.4 Hz, 1H), 3.66 (dd, $J = 15.5$ and 6.3 Hz, 1H), 3.49 (s, 3H), 3.38–3.30 (m, 1H), 3.23 (dd, $J = 16.9$ and 9.2 Hz, 2H), 3.09 (dd, $J = 17.0$ and 4.8 Hz, 1H). ^{13}C NMR (75 MHz, $\text{DMSO-}d_6$) δ ppm: 170.7, 162.3, 149.5, 138.6, 136.0, 134.0, 133.0, 132.2, 132.1, 129.4 (2C), 129.2, 126.8, 125.9 (2C), 124.1, 121.1, 118.7, 118.0, 111.5, 108.9, 55.9, 51.6, 38.3, 35.6, 31.1.

Methyl (2*S*)-3-(4-hydroxyphenyl)-2-[5-[[5-phenyl-2-thienyl)sulfonylamino]methyl]triazol-1-yl]propanoate (27)



Compound **27** was synthesized according to the general procedure G, using amine **26** (100 mg, 0.26 mmol), 5-phenylthiophene-2-sulfonyl chloride (79.4 mg, 0.31 mmol) and N,N-Diisopropylethylamine (98 μ L, 0.57 mmol) in DMF (5 mL) overnight. The crude product was purified by flash chromatography on silica gel (CH_2Cl_2 to $\text{CH}_2\text{Cl}_2/\text{MeOH}$: 95/5) affording compound **27** as a yellow solid (37.7 mg, 29%). LC tr = 2.70 min, MS (ESI-): m/z = 497 [M - H]⁻. ¹H NMR (300 MHz, $\text{DMF-}d_7$) δ ppm: 9.51 (br s, 1H), 8.43 (br s, 1H), 7.82–7.78 (m, 2H), 7.64 (d, J = 3.9 Hz, 1H), 7.62 (d, J = 3.9 Hz, 1H), 7.57 (s, 1H), 7.55–7.44 (m, 3H), 7.00–6.95 (m, 2H), 6.73–6.68 (m, 2H), 5.72 (dd, J = 10.3 and 5.2 Hz, 1H), 4.18 (d, J = 16.0 Hz, 1H), 4.09 (d, J = 16.0 Hz, 1H), 3.74 (s, 3H), 3.63 (dd, J = 14.1 and 5.1 Hz, 1H), 3.50–3.41 (m, 1H). ¹³C NMR (75 MHz, $\text{DMF-}d_7$) δ ppm: 168.9, 157.2, 150.5, 139.6, 135.3, 133.6, 133.0, 130.4 (2C), 130.5, 129.7 (2C), 129.5, 126.6, 126.4 (2C), 124.3, 115.6 (2C), 62.1, 52.8, 36.6, 36.2.

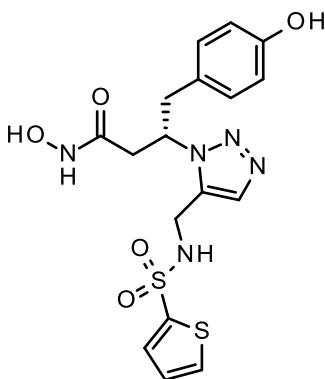
(3*S*)-4-(4-hydroxyphenyl)-3-[5-[[5-phenyl-2-thienyl)sulfonylamino]methyl]triazol-1-yl]butanehydroxamic acid (12)



Compound **12** was synthesized according to the general procedure D, using ester **10** (100 mg, 0.2 mmol), KCN (2.54 mg, 0.04 mmol) and aq. NH_2OH (2.6 mL, 50% w/w in water) in MeOH (2.6 mL)

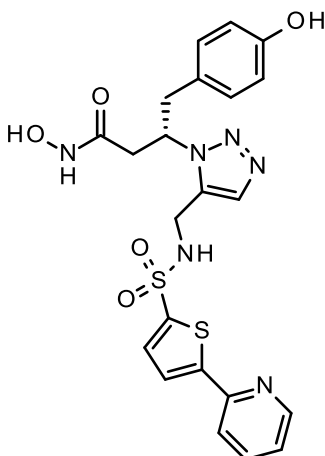
overnight. The crude product was purified by flash chromatography on silica gel (CH₂Cl₂ to CH₂Cl₂/MeOH: 95/5) affording compound **12** as a white solid after lyophilization (54 mg, 63%). Purity: 99%, LC tr = 2.37 min, MS (ESI+): m/z = 514 [M + H]⁺. ¹H NMR (300 MHz, MeOD-*d*₄) δ ppm: 7.71–7.67 (m, 2H), 7.53 (d, *J* = 3.9 Hz, 1H), 7.48–7.40 (m, 4H), 7.37 (s, 1H), 6.71 (d, *J* = 8.6 Hz, 2H), 6.61 (d, *J* = 8.6 Hz, 2H), 4.97–4.91 (m, 1H), 3.97–3.82 (m, 2H), 3.14–2.97 (m, 3H), 2.84 (dd, *J* = 15.3 and 4.9 Hz, 1H). ¹³C NMR (75 MHz, MeOD-*d*₄) δ ppm: 168.7, 157.7, 152.4, 140.0, 136.3, 134.7, 134.0, 133.2, 131.1 (2C), 130.4 (2C), 130.2, 128.6, 127.2 (2C), 124.6, 116.5 (2C), 59.3, 41.9, 38.4, 36.5. HRMS-ESI+ (m/z) calcd. for C₂₃H₂₄N₅O₅S₂ [M + H]⁺ 514.1226, found 514.1219.

(3*S*)-4-(4-Hydroxyphenyl)-3-[5-[(2-thienylsulfonylamino)methyl]triazol-1-yl]butanehydroxamic acid (74)



Compound **74** was synthesized according to the general procedure D, using ester **72** (22 mg, 0.05 mmol), KCN (0.66 mg, 0.01 mmol) and aq. NH₂OH (1 mL, 50% w/w in water) in MeOH (1 mL) overnight. The crude product was purified by flash chromatography on silica gel (CH₂Cl₂ to CH₂Cl₂/MeOH: 9/1) affording compound **74** as a white solid after lyophilization (14 mg, 62%). Purity: 99%, LC tr = 1.80 min, MS (ESI+): m/z = 437 [M + H]⁺. ¹H NMR (300 MHz, MeOD-*d*₄) δ ppm: 7.81 (dd, *J* = 5.0 and 1.1 Hz, 1H), 7.56 (dd, *J* = 3.7 and 1.1 Hz, 1H), 7.32 (s, 1H), 7.16 (dd, *J* = 4.9 and 3.8 Hz, 1H), 6.72–6.70 (m, 2H), 6.62–6.60 (m, 2H), 4.88–4.84 (m, 1H), 3.77 (s, 2H), 3.14–2.99 (m, 3H), 2.84 (dd, *J* = 15.3 and 4.7 Hz, 1H). ¹³C NMR (75 MHz, MeOD-*d*₄) δ ppm: 159.2, 148.2, 132.3, 126.8, 124.2, 124.1, 123.6, 121.6 (2C), 119.3, 119.1, 107.0 (2C), 49.8, 32.4, 28.9, 27.1. HRMS-ESI+ (m/z) calcd. for C₁₇H₂₀N₅O₅S₂ [M + H]⁺ 438.0906, found 438.0910.

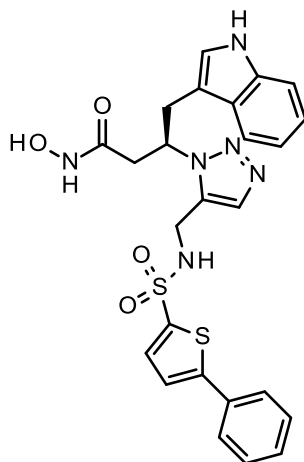
(3S)-4-(4-Hydroxyphenyl)-3-[5-[[[5-(2-pyridyl)-2-thienyl]sulfonylamino]methyl]triazol-1-yl]butanehydroxamic acid (75)



Compound **75** was synthesized according to the general procedure D, using ester **73** (57 mg, 0.1 mmol), KCN (1.45 mg, 0.02 mmol) and aq. NH_2OH (1.5 mL, 50% w/w in water) in MeOH (1.5 mL) overnight. The crude product was purified by flash chromatography on silica gel (CH_2Cl_2 to $\text{CH}_2\text{Cl}_2/\text{MeOH}$: 9/1) affording compound **75** as a white solid after lyophilization (20 mg, 34%).

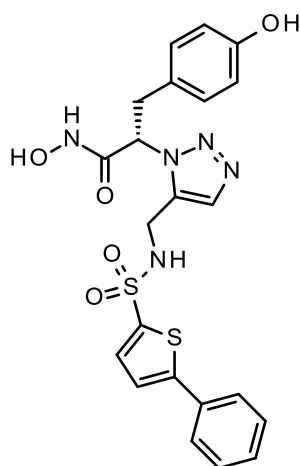
Purity: 99%, LC tr = 2.07 min, MS (ESI+): $m/z = 515$ $[\text{M} + \text{H}]^+$. ^1H NMR (300 MHz, $\text{DMSO}-d_6$) δ ppm: 10.54 (br s, 1H), 9.26 (s, 1H), 8.79 (br s, 1H), 8.60 (ddd, $J = 4.8, 1.7$ and 0.9 Hz, 1H), 8.38 (br s, 1H), 8.07 (dt, $J = 7.9$ and 1.0 Hz, 1H), 7.92 (td, $J = 11.5$ and 1.8 Hz, 1H), 7.85 (d, $J = 4.0$ Hz, 1H), 7.55 (d, $J = 4.0$ Hz, 1H), 7.41 (ddd, $J = 7.5, 4.8$ and 1.0 Hz, 1H), 6.75–6.72 (m, 2H), 6.59–6.57 (m, 2H), 4.86–4.76 (m, 1H), 3.92–3.82 (m, 2H), 3.03 (dd, $J = 13.6$ and 6.2 Hz, 1H), 2.93 (dd, $J = 13.6$ and 8.7 Hz, 1H), 2.85 (dd, $J = 15.5$ and 10.1 Hz, 1H), 2.65 (dd, $J = 15.5$ and 4.5 Hz, 1H). ^{13}C NMR (75 MHz, $\text{DMSO}-d_6$) δ ppm: 165.8, 156.1, 150.4, 150.3, 149.7, 141.0, 137.6, 133.7, 133.1, 131.9, 129.8 (2C), 126.8, 125.0, 123.9, 119.4, 115.2 (2C), 56.7, 40.2, 36.8, 35.4. HRMS-ESI+ (m/z) calcd. for $\text{C}_{22}\text{H}_{23}\text{N}_6\text{O}_5\text{S}_2$ $[\text{M} + \text{H}]^+$ 515.1171, found 515.1181.

(3R)-4-(1H-Indol-3-yl)-3-[5-[[[5-(phenyl-2-thienyl)sulfonylamino]methyl]triazol-1-yl]butanehydroxamic acid (13)



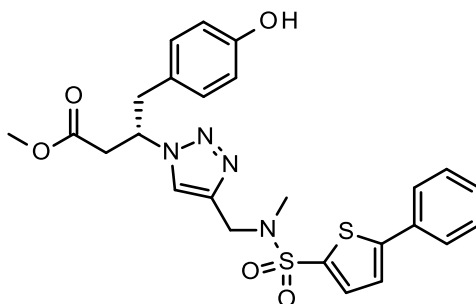
Compound **13** was synthesized according to the general procedure D, using ester **11** (116 mg, 0.22 mmol), KCN (2.82 mg, 0.04 mmol) and aq. NH₂OH (3 mL, 50% w/w in water) in MeOH (3 mL) overnight. The crude product was purified by flash chromatography on silica gel (CH₂Cl₂ to CH₂Cl₂/MeOH: 95/5) affording compound **13** as a white solid after lyophilization (99 mg, 84%). Purity: 99%, LC tr= 2.62 min, MS (ESI+): m/z = 537 [M + H]⁺. ¹H NMR (300 MHz, DMSO-*d*₆) δ ppm: 10.87 (br s, 1H), 8.79 (br s, 1H), 7.75–7.71 (m, 2H), 7.54–7.29 (m, 8H), 7.06–7.00 (m, 1H), 6.95–6.90 (m, 1H), 6.87 (d, *J* = 2.3 Hz, 1H), 5.03–4.92 (m, 1H), 3.85 (d, *J* = 15.4 Hz, 1H), 3.71 (d, *J* = 15.5 Hz, 1H), 3.20–3.12 (m, 2H), 2.94–2.71 (m, 2H). ¹³C NMR (75 MHz, DMSO-*d*₆) δ ppm: 166.0, 149.5, 138.6, 136.0, 133.8, 133.1, 132.2, 131.9, 129.4 (2C), 129.2, 126.8, 126.0 (2C), 124.1, 123.8, 121.1, 118.6, 117.9, 111.5, 109.2, 56.0, 37.1, 35.5, 31.0. HRMS-ESI+ (m/z) calcd. for C₂₅H₂₅N₆O₄S₂ [M + H]⁺ 537.1394, found 537.1379.

(2S)-3-(4-Hydroxyphenyl)-2-[5-[(5-phenyl-2-thienyl)sulfonylamino]methyl]triazol-1-yl]propanehydroxamic acid (28**)**



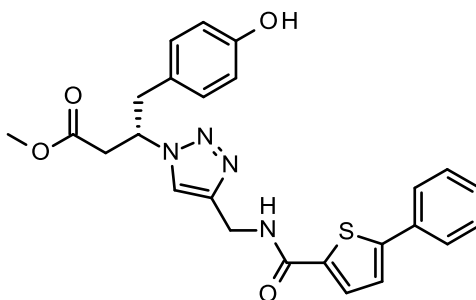
Compound **28** was synthesized according to the general procedure D, using ester **27** (75 mg, 0.15 mmol), KCN (1.96 mg, 0.02 mmol) and aq. NH₂OH (5.4 mL, 50% w/w in water) in MeOH (5.4 mL) overnight. The crude product was purified by flash chromatography on silica gel (CH₂Cl₂ to CH₂Cl₂/MeOH: 9/1) affording compound **28** as a white solid after lyophilization (19 mg, 25%). Purity: 100%, LC tr = 2.33 min, MS (ESI-): m/z = 498 [M - H]⁻. ¹H NMR (DMSO-*d*₆) δ ppm: 9.24-9.14 (m, 2H), 7.72 (dd, *J* = 8.3 and 1.5 Hz, 2H), 7.55 (dd, *J* = 6.2 and 3.9 Hz, 2H), 7.51-7.43 (m, 4H), 6.93 (d, *J* = 8.5 Hz, 2H), 6.60 (d, *J* = 8.5 Hz, 2H), 5.12 (t, *J* = 7.5 Hz, 1H), 4.21 (br s, 2H), 3.41 (dd, *J* = 13.9 and 7.4 Hz, 2H), 3.25-3.17 (m, 2H). ¹³C NMR (DMSO-*d*₆) δ ppm: 163.4, 156.1, 149.5, 139.0, 134.5, 133.0, 132.7, 132.1, 130.0 (2C), 129.4 (2C), 129.2, 126.1, 125.9 (2C), 124.1, 115.1 (2C), 60.9, 36.0, 35.6. HRMS-ESI+ (m/z) calcd. for C₂₂H₂₂N₅O₅S₂ [M + H]⁺ 500.1062, found 500.1068.

Methyl (3S)-4-(4-hydroxyphenyl)-3-[4-[[methyl-(5-phenyl-2-thienyl)sulfonyl]amino]methyl]triazol-1-yl]butanoate (17)



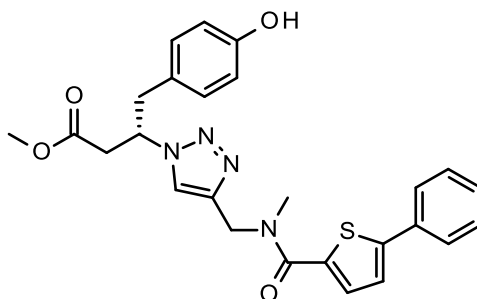
Compound **17** was synthesized according to the general procedure H, using azide **Z4-a** (84 mg, 0.36 mmol), alkyne **14** (104 mg, 0.36 mmol), copper (II) sulfate pentahydrate (16.2 mg, 0.07 mmol) and sodium ascorbate (32.1 mg, 0.18 mmol) in DMF (6 mL) and H₂O (5 mL) overnight. The crude product was purified by flash chromatography on silica gel (CH₂Cl₂ to CH₂Cl₂/EtOAc: 85/15) affording compound **17** as a white solid (69 mg, 37%). LC tr = 2.75 min, MS (ESI-): m/z = 525 [M - H]⁻. ¹H NMR (300 MHz, MeOD-*d*₄) δ ppm: 7.68–7.63 (m, 2H), 7.58 (s, 1H), 7.55 (d, *J* = 4.0 Hz, 1H), 7.45–7.34 (m, 4H), 6.78–6.73 (m, 2H), 6.63–6.58 (m, 2H), 5.08–4.99 (m, 1H), 4.36–4.26 (m, 2H), 3.55 (s, 3H), 3.15–2.95 (m, 4H), 2.65 (s, 3H). ¹³C NMR (75 MHz, MeOD-*d*₄) δ ppm: 172.0, 157.5, 152.5, 142.8, 136.9, 134.8, 133.9, 131.1 (2C), 130.4 (2C), 130.3, 128.3, 127.2 (2C), 125.6, 124.8, 116.3 (2C), 61.5, 52.4, 46.2, 41.6; 39.5, 35.2.

Methyl (3S)-4-(4-hydroxyphenyl)-3-[4-[[5-phenylthiophene-2-carbonyl]amino]methyl]triazol-1-yl]butanoate (18)



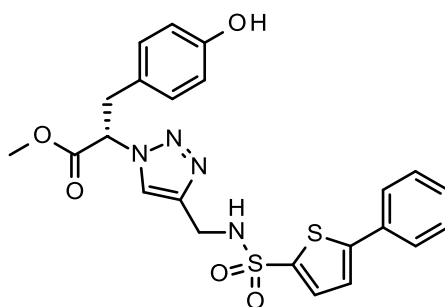
Compound **18** was synthesized according to the general procedure H, using azide **Z4-a** (52 mg, 0.22 mmol), alkyne **15** (53.3 mg, 0.22 mmol), copper (II) sulfate pentahydrate (10 mg, 0.04 mmol) and sodium ascorbate (20 mg, 0.11 mmol) in DMF (4 mL) and H₂O (3 mL) overnight. The crude product was purified by flash chromatography on silica gel (CH₂Cl₂ to CH₂Cl₂/EtOAc: 6/4) affording compound **18** as a white solid (21 mg, 37%). LC t_R = 2.52 min, MS (ESI-): m/z = 475 [M - H]⁻. ¹H NMR (300 MHz, DMSO-*d*₆) δ ppm: 9.22 (s, 1H), 9.09–9.05 (m, 1H), 8.00 (s, 1H), 7.78 (d, *J* = 4.0 Hz, 1H), 7.73–7.69 (m, 2H), 7.54 (d, *J* = 3.9 Hz, 1H), 7.48–7.34 (m, 3H), 6.85–6.83 (m, 2H), 6.60–6.57 (m, 2H), 5.09–5.00 (m, 1H), 4.45 (d, *J* = 6.0 Hz, 2H), 3.49 (s, 3H), 3.10–2.88 (m, 4H). ¹³C NMR (75 MHz, DMSO-*d*₆) δ ppm: 170.3, 160.8, 156.1, 147.5, 144.5, 138.7, 133.1, 130.0 (2C), 129.3, 129.2 (2C), 128.5, 126.7, 125.7 (2C), 124.3, 122.3, 115.1 (2C), 58.9, 51.5, 40.0, 38.1, 34.6.

Methyl (3*S*)-4-(4-hydroxyphenyl)-3-[4-[[methyl-(5-phenylthiophene-2-carbonyl)amino]methyl]triazol-1-yl]butanoate (19)



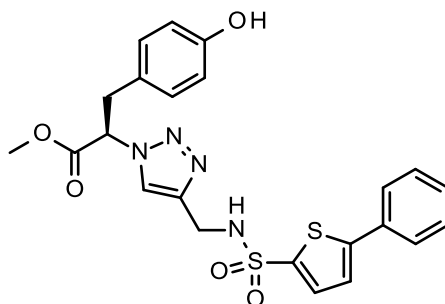
Compound **19** was synthesized according to the general procedure H, using azide **Z4-a** (82 mg, 0.35 mmol), alkyne **16** (89 mg, 0.35 mmol), copper (II) sulfate pentahydrate (15.8 mg, 0.06 mmol) and sodium ascorbate (31.4 mg, 0.16 mmol) in DMF (6 mL) and H₂O (5 mL) overnight. The crude product was purified by flash chromatography on silica gel (CH₂Cl₂ to CH₂Cl₂/EtOAc: 7/3) affording compound **19** as a white solid (28 mg, 16%). LC tr = 2.58 min, MS (ESI⁻): *m/z* = 489 [M - H]⁻. ¹H NMR (300 MHz, MeOD-*d*₄) δ ppm: 7.70–7.64 (m, 3H), 7.43–7.33 (m, 5H), 6.83–6.78 (m, 2H), 6.63–6.59 (m, 2H), 5.14–5.05 (m, 1H), 4.72 (br s, 2H), 4.60–4.59 (m, 1H), 3.58 (s, 3H), 3.24–3.02 (m, 6H). ¹³C NMR (75 MHz, MeOD-*d*₄) δ ppm: 172.1, 157.5, 137.0, 134.6, 132.4, 131.1 (2C), 130.2 (2C), 129.6, 129.3, 128.4, 128.3, 128.0, 127.0 (2C), 125.4, 124.3, 116.3 (2C), 65.2, 61.6, 52.4, 49.3, 41.7, 39.6.

Methyl (2*S*)-3-(4-hydroxyphenyl)-2-[4-[[5-phenyl-2-thienyl)sulfonylamino]methyl]triazol-1-yl]propanoate (33)



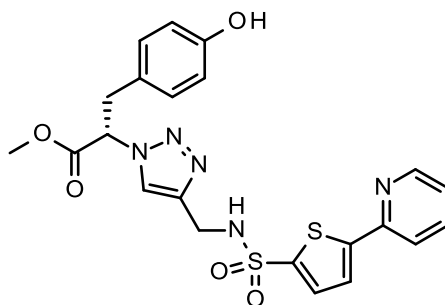
Compound **33** was synthesized according to the general procedure H, using azide **30** (65 mg, 0.29 mmol), alkyne **32** (82 mg, 0.29 mmol), copper (II) sulfate pentahydrate (13.4 mg, 0.05 mmol) and sodium ascorbate (26.4 mg, 0.15 mmol) in DMF (5 mL) and H₂O (4 mL) overnight. The crude product was purified by flash chromatography on silica gel (CH₂Cl₂ to CH₂Cl₂/EtOAc: 8/2) affording compound **33** as a white solid (65 mg, 44%). LC tr = 2.70 min, MS (ESI⁺): *m/z* = 499 [M + H]⁺. ¹H NMR (300 MHz, DMSO-*d*₆) δ ppm: 9.24 (s, 1H), 8.45 (s, 1H), 8.02 (s, 1H), 7.74–7.69 (m, 2H), 7.58–7.53 (m, 2H), 7.50–7.38 (m, 3H), 6.88–6.85 (m, 2H), 6.60–6.55 (m, 2H), 5.71–5.65 (m, 1H), 4.15 (s, 2H), 3.64 (s, 3H), 3.40–3.25 (m, 2H). ¹³C NMR (75 MHz, DMSO-*d*₆) δ ppm: 168.7, 156.2, 149.1, 143.2, 139.6, 132.7, 132.2, 129.9 (2C), 129.4 (2C), 129.1, 125.9 (2C), 125.6, 124.0, 123.5, 115.1 (2C), 63.3, 52.8, 38.3, 36.0.

Methyl (2R)-3-(4-hydroxyphenyl)-2-[4-[[5-(phenyl-2-thienyl)sulfonylamino]methyl]triazol-1-yl]propanoate (39)



Compound **39** was synthesized according to the general procedure H, using azide **38** (65 mg, 0.29 mmol), alkyne **32** (82 mg, 0.29 mmol), copper (II) sulfate pentahydrate (13.4 mg, 0.05 mmol) and sodium ascorbate (26.4 mg, 0.15 mmol) in DMF (5 mL) and H₂O (4 mL) overnight. The crude product was purified by flash chromatography on silica gel (CH₂Cl₂ to CH₂Cl₂/MeOH: 95/5) affording compound **39** as a white solid (107 mg, 73%). LC tr = 2.70 min, MS (ESI+): m/z = 499 [M + H]⁺. ¹H NMR (300 MHz, DMSO-*d*₆) δ ppm: 9.25 (s, 1H), 8.46 (s, 1H), 8.03 (s, 1H), 7.74–7.71 (m, 2H), 7.58 (d, *J* = 3.9 Hz, 1H), 7.55 (d, *J* = 3.9 Hz, 1H), 7.50–7.38 (m, 3H), 6.87 (d, *J* = 8.6 Hz, 2H), 6.58 (d, *J* = 8.6 Hz, 2H), 5.71–5.66 (m, 1H), 4.15 (s, 2H), 3.63 (s, 3H), 3.42–3.26 (m, 2H). ¹³C NMR (75 MHz, DMSO-*d*₆) δ ppm: 168.7, 156.2, 149.1, 143.2, 139.6, 132.8, 132.2, 129.9 (2C), 129.4 (2C), 129.1, 125.9 (2C), 125.6, 124.0, 123.5, 115.1 (2C), 63.3, 52.7, 38.3, 36.0.

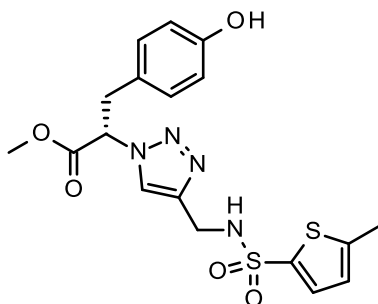
Methyl (2S)-3-(4-hydroxyphenyl)-2-[4-[[[5-(2-pyridyl)-2-thienyl]sulfonylamino]methyl]triazol-1-yl]propanoate (50)



Compound **50** was synthesized according to the general procedure H, using azide **30** (40 mg, 0.18 mmol), alkyne **44** (50 mg, 0.18 mmol), copper (II) sulfate pentahydrate (9 mg, 0.04 mmol) and sodium ascorbate (18 mg, 0.09 mmol) in DMF (5.5 mL) and H₂O (4.5 mL) overnight. The crude product was purified by flash chromatography on silica gel (CH₂Cl₂ to CH₂Cl₂/MeOH: 9/1) affording compound **50** as a white powder (107 mg, 73%). LC tr = 2.43 min, MS (ESI+): m/z = 500 [M + H]⁺. ¹H NMR (300 MHz, DMSO-*d*₆) δ ppm: 9.25 (s, 1H), 8.57 (ddd, *J* = 4.8, 1.7 and 1.0 Hz, 1H), 8.46 (br s, 1H), 8.04 (dt, *J* = 8.0 and 1.0 Hz, 1H), 8.03 (s, 1H), 7.89 (td, *J* = 11.5 and 1.7 Hz, 1H), 7.82 (d, *J* = 3.9 Hz, 1H), 7.59 (d, *J* = 3.9 Hz, 1H), 7.38 (ddd, *J* = 7.5, 4.8 and 1.0 Hz, 1H), 6.89–6.84 (m, 2H), 6.60–6.55 (m, 2H), 5.68 (dd, *J* = 9.9 and 5.8 Hz, 1H), 4.14 (s, 2H), 3.64 (s, 3H), 3.38 (dd, *J* = 14.5 and 5.8 Hz, 1H), 3.28 (dd, *J* = 14.3 and 9.9 Hz, 1H). ¹³C NMR (75 MHz, DMSO-*d*₆) δ ppm: 168.7, 156.2, 150.4, 150.0,

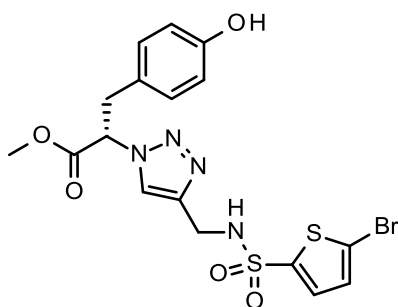
149.7, 143.2, 142.0, 137.5, 132.6, 129.9 (2C), 125.6, 124.9, 123.8, 123.5, 119.3, 115.1 (2C), 63.3, 52.7, 38.3, 36.0.

Methyl (2*S*)-3-(4-hydroxyphenyl)-2-[4-[[5-methyl-2-thienyl)sulfonylamino]methyl]triazol-1-yl]propanoate (49)



Compound **49** was synthesized according to the general procedure H, using azide **30** (70 mg, 0.32 mmol), alkyne **43** (68.1 mg, 0.32 mmol), copper (II) sulfate pentahydrate (15.8 mg, 0.06 mmol) and sodium ascorbate (31.3 mg, 0.16 mmol) in DMF (5.5 mL) and H₂O (4.5 mL) overnight. The crude product was purified by flash chromatography on silica gel (CH₂Cl₂ to CH₂Cl₂/MeOH: 95/5) affording compound **49** as colorless oil (109 mg, 78%). LC tr = 2.27 min, MS (ESI+): *m/z* = 437 [M + H]⁺. ¹H NMR (300 MHz, MeOD-*d*₄) δ ppm: 7.80 (s, 1H), 7.37 (d, *J* = 3.7 Hz, 1H), 6.90–6.86 (m, 2H), 6.77 (dq, *J* = 3.7 and 1.2 Hz, 1H), 6.66–6.61 (m, 2H), 5.58 (dd, *J* = 9.9 and 5.5 Hz, 1H), 4.19 (s, 2H), 3.72 (s, 3H), 3.46 (dd, *J* = 14.3 and 5.5 Hz, 1H), 3.33 (dd, *J* = 14.0 and 10.2 Hz, 1H), 2.48 (d, *J* = 1.2 Hz, 3H). ¹³C NMR (75 MHz, MeOD-*d*₄) δ ppm: 170.0, 157.6, 149.0, 145.2, 139.1, 133.6, 131.1 (2C), 127.2, 127.0, 124.8, 116.4 (2C), 65.6, 53.5, 39.3, 38.1, 15.4.

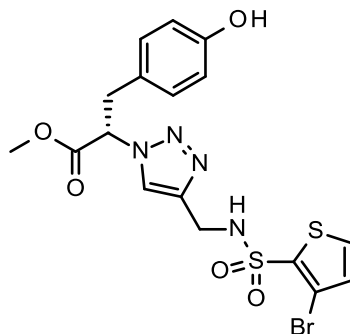
Methyl (2*S*)-2-[4-[[5-bromo-2-thienyl)sulfonylamino]methyl]triazol-1-yl]-3-(4-hydroxyphenyl)propanoate (47)



Compound **47** was synthesized according to the general procedure H, using azide **30** (63 mg, 0.29 mmol), alkyne **41** (79.8 mg, 0.29 mmol), copper (II) sulfate pentahydrate (12.9 mg, 0.05 mmol) and sodium ascorbate (25.6 mg, 0.14 mmol) in DMF (5 mL) and H₂O (4 mL) overnight. The crude product was purified by flash chromatography on silica gel (CH₂Cl₂ to CH₂Cl₂/MeOH: 98/2) affording compound **47** as pale yellow oil (140 mg, 91%). LC tr = 2.52 min, MS (ESI+): *m/z* = 501 and 503 [M + H]⁺. ¹H NMR (300 MHz, DMSO-*d*₆) δ ppm: 9.25 (s, 1H), 8.52 (br t, *J* = 5.8 Hz, 1H), 8.03 (s, 1H), 7.40 (d, *J* = 4.0 Hz, 1H), 7.31 (d, *J* = 4.0 Hz, 1H), 6.89 (d, *J* = 8.5 Hz, 2H), 6.59 (d, *J* = 8.5 Hz, 2H),

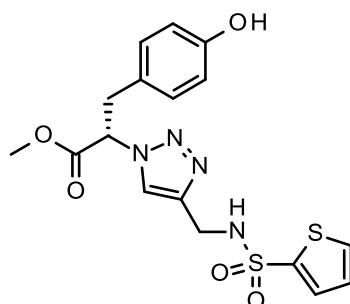
5.72–5.67 (m, 1H), 4.12–4.10 (m, 2H), 3.68 (s, 3H), 3.44–3.28 (m, 2H). ¹³C NMR (75 MHz, DMSO-*d*₆) δ ppm: 168.7, 156.2, 142.9, 142.3, 132.3, 131.3, 129.9 (2C), 125.6, 123.5, 118.2, 115.1 (2C), 63.3, 52.8, 38.2, 36.0.

Methyl (2*S*)-2-[4-[[3-bromo-2-thienyl)sulfonylamino]methyl]triazol-1-yl]-3-(4-hydroxyphenyl)propanoate (48)



Compound **48** was synthesized according to the general procedure H, using azide **30** (100 mg, 0.45 mmol), alkyne **42** (127 mg, 0.45 mmol), copper (II) sulfate pentahydrate (22.6 mg, 0.09 mmol) and sodium ascorbate (44.8 mg, 0.23 mmol) in DMF (5.5 mL) and H₂O (4.5 mL) overnight. The crude product was purified by flash chromatography on silica gel (CH₂Cl₂ to CH₂Cl₂/MeOH: 95/5) affording compound **48** as colorless oil (165 mg, 72%). LC tr = 2.35 min, MS (ESI⁺): *m/z* = 501 and 503 [M + H]⁺. ¹H NMR (300 MHz, MeOD-*d*₄) δ ppm: 7.79 (br s, 1H), 7.65 (d, *J* = 5.2 Hz, 1H), 7.06 (d, *J* = 5.2 Hz, 1H), 6.89 (d, *J* = 8.1 Hz, 2H), 6.64 (d, *J* = 8.1 Hz, 2H), 5.57 (dd, *J* = 9.4 and 5.3 Hz, 1H), 4.29 (s, 2H), 3.71 (s, 3H), 3.46 (dd, *J* = 14.2 and 5.3 Hz, 1H), 3.32 (dd, *J* = 14.0 and 10.1 Hz, 1H). ¹³C NMR (75 MHz, MeOD-*d*₄) δ ppm: 170.0, 157.5, 145.1 (br), 137.6, 133.8, 132.6, 131.1 (2C), 127.2, 124.9 (br), 116.4 (2C), 114.2, 65.6, 53.5, 39.0, 38.1.

Methyl (2*S*)-3-(4-hydroxyphenyl)-2-[4-[(2-thienyl)sulfonylamino]methyl]triazol-1-yl]propanoate (51)

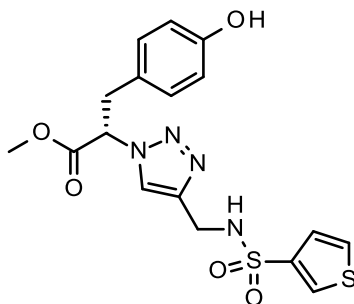


Compound **51** was synthesized according to the general procedure H, using azide **30** (63 mg, 0.29 mmol), alkyne **45** (57.3 mg, 0.29 mmol), copper (II) sulfate pentahydrate (12.9 mg, 0.05 mmol) and sodium ascorbate (25.6 mg, 0.14 mmol) in DMF (5 mL) and H₂O (4 mL) overnight. The crude product was purified by flash chromatography on silica gel (CH₂Cl₂) affording compound **51** as brown oil (110 mg, 86%). LC tr = 2.25 min, MS (ESI⁺): *m/z* = 423 [M + H]⁺. ¹H NMR (300 MHz, DMSO-*d*₆) δ ppm: 9.25 (s, 1H), 8.36 (t, *J* = 6.0 Hz, 1H), 8.00 (s, 1H), 7.91 (dd, *J* = 1.3 and 5.0 Hz, 1H), 7.58 (dd, *J* = 1.3

and 3.7 Hz, 1H), 7.16 (dd, $J = 3.7$ and 5.0 Hz, 1H), 6.89 (d, $J = 8.5$ Hz, 2H), 6.59 (d, $J = 8.4$ Hz, 2H), 5.72–5.67 (m, 1H), 4.08 (d, $J = 5.9$ Hz, 2H), 3.67 (s, 3H), 3.44–3.28 (m, 2H). ^{13}C NMR (75 MHz, $\text{DMSO-}d_6$) δ ppm: 168.8, 156.2, 143.2, 141.1, 132.5, 131.7, 129.9 (2C), 127.7, 125.7, 123.5, 115.1 (2C), 63.3, 52.8, 38.2, 36.0.

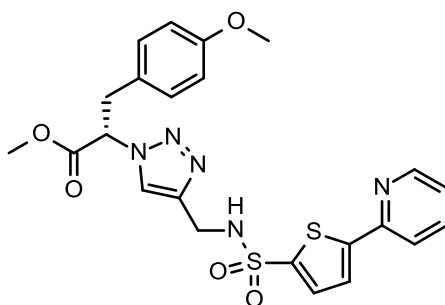
Methyl (2*S*)-3-(4-hydroxyphenyl)-2-[4-[(3-thienylsulfonylamino)methyl]triazol-1-yl]propanoate

(52)



Compound **52** was synthesized according to the general procedure H, using azide **30** (70 mg, 0.32 mmol), alkyne **46** (63.7 mg, 0.32 mmol), copper (II) sulfate pentahydrate (15.8 mg, 0.06 mmol) and sodium ascorbate (31.3 mg, 0.16 mmol) in DMF (5.5 mL) and H_2O (4.5 mL) overnight. The crude product was purified by flash chromatography on silica gel (CH_2Cl_2 to $\text{CH}_2\text{Cl}_2/\text{MeOH}$: 95/5) affording compound **52** as brown oil (90 mg, 62%). LC tr = 2.22 min, MS (ESI+): $m/z = 423$ [$\text{M} + \text{H}$] $^+$. ^1H NMR (300 MHz, $\text{MeOD-}d_4$) δ ppm: 8.01 (dd, $J = 3.1$ and 1.3 Hz, 1H), 7.77 (s, 1H), 7.51 (dd, $J = 5.1$ and 3.1 Hz, 1H), 7.29 (dd, $J = 5.1$ and 1.3 Hz, 1H), 6.91–6.84 (m, 2H), 6.66–6.62 (m, 2H), 5.57 (dd, $J = 10.0$ and 5.6 Hz, 1H), 4.18 (s, 2H), 3.72 (s, 3H), 3.47 (dd, $J = 14.3$ and 5.6 Hz, 1H), 3.33 (dd, $J = 14.3$ and 10.0 Hz, 1H). ^{13}C NMR (75 MHz, $\text{MeOD-}d_4$) δ ppm: 170.1, 157.6, 145.3, 141.5, 131.6, 131.1 (2C), 129.5, 127.2, 126.4, 124.8, 116.4 (2C), 65.6, 53.5, 39.1, 38.0.

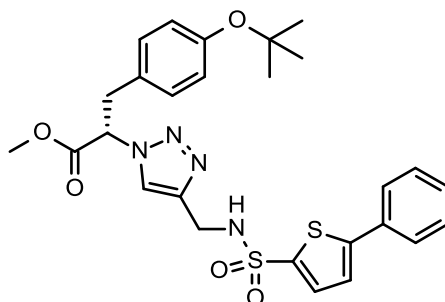
Methyl (2*S*)-3-(4-methoxyphenyl)-2-[4-[[[5-(2-pyridyl)-2-thienyl]sulfonylamino]methyl]triazol-1-yl]propanoate (67)



Compound **67** was synthesized according to the general procedure H, using azide **62** (128 mg, 0.48 mmol), alkyne **44** (134.2 mg, 0.48 mmol), copper (II) sulfate pentahydrate (24.1 mg, 0.1 mmol) and sodium ascorbate (47.8 mg, 0.24 mmol) in DMF (9 mL) and H_2O (8 mL) overnight. The crude product was purified by flash chromatography on silica gel (cHex/EtOAc : 95/5 to 3/7) affording compound **67** as a white solid (160 mg, 65%). LC tr = 2.70 min, MS (ESI-): $m/z = 512$ [$\text{M} - \text{H}$] $^-$. ^1H NMR (300MHz,

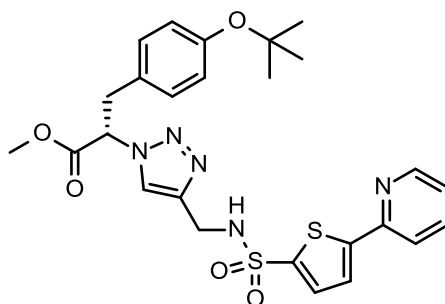
DMSO-*d*₆) δ ppm: 8.57 (ddd, $J = 4.9, 1.7$ and 1.0 Hz, 1H), 8.46 (br s, 1H), 8.04 (s, 1H), 8.02 (dt, $J = 8.0$ and 1.0 Hz, 1H), 7.90 (td, $J = 8.0$ and 1.7 Hz, 1H), 7.83 (d, $J = 4.0$ Hz, 1H), 7.60 (d, $J = 4.0$ Hz, 1H), 7.37 (ddd, $J = 7.5, 4.9$ and 1.0 Hz, 1H), 7.01–6.97 (m, 2H), 6.77–6.73 (m, 2H), 5.73 (dd, $J = 9.9$ and 5.7 Hz, 1H), 4.14 (s, 2H), 3.67 (m, 3H), 3.65 (m, 3H), 3.44 (dd, $J = 14.3$ and 5.7 Hz, 1H), 3.34 (dd, $J = 14.3$ and 9.9 Hz, 1H). ¹³C NMR (75 MHz, DMSO-*d*₆) δ ppm: 168.7, 158.1, 150.4, 150.0, 149.7, 143.2, 142.0, 137.5, 132.6, 129.9 (2C), 127.5, 124.9, 123.8, 123.5, 119.3, 113.7 (2C), 63.1, 54.9, 52.8, 38.3, 35.9.

Methyl (2*S*)-3-(4-*tert*-butoxyphenyl)-2-[4-[[5-phenyl-2-thienyl]sulfonylamino]methyl]triazol-1-yl]propanoate (65)



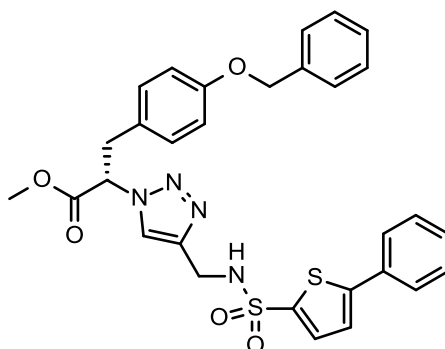
Compound **65** was synthesized according to the general procedure H, using azide **63** (150 mg, 0.27 mmol), alkyne **32** (75 mg, 0.27 mmol), copper (II) sulfate pentahydrate (13.5 mg, 0.05 mmol) and sodium ascorbate (26.8 mg, 0.14 mmol) in DMF (5.5 mL) and H₂O (4.5 mL) overnight. The crude product was purified by flash chromatography on silica gel (cHex/EtOAc: 9/1 to 6/4) affording compound **65** as a white solid (88 mg, 56%). LC *tr* = 3.25 min, MS (ESI+): $m/z = 555$ [M + H]⁺. ¹H NMR (300 MHz, DMSO-*d*₆) δ ppm: 8.45 (t, $J = 5.9$ Hz, 1H), 8.02 (s, 1H), 7.74–7.70 (m, 2H), 7.57 (d, $J = 3.9$ Hz, 1H), 7.55 (d, $J = 3.9$ Hz, 1H), 7.50–7.38 (m, 3H), 7.00–6.95 (m, 2H), 6.80–6.76 (m, 2H), 5.76 (dd, $J = 9.9$ and 5.9 Hz, 1H), 4.13 (d, $J = 5.9$ Hz, 2H), 3.64 (s, 3H), 3.46 (dd, $J = 14.3$ and 5.9 Hz, 1H), 3.36 (dd, $J = 14.3$ and 9.9 Hz, 1H), 1.22 (s, 9H). ¹³C NMR (75 MHz, DMSO-*d*₆) δ ppm: 168.7, 153.9, 149.1, 143.2, 139.6, 132.8, 132.2, 130.2, 129.5 (2C), 129.4 (2C), 129.1, 125.9 (2C), 124.0, 123.6, 123.5 (2C), 77.8, 63.0, 52.8, 38.3, 36.2, 28.5 (3C).

Methyl (2*S*)-3-(4-*tert*-butoxyphenyl)-2-[4-[[5-(2-pyridyl)-2thienyl]sulfonylamino]methyl]triazol-1-yl]propanoate (66)



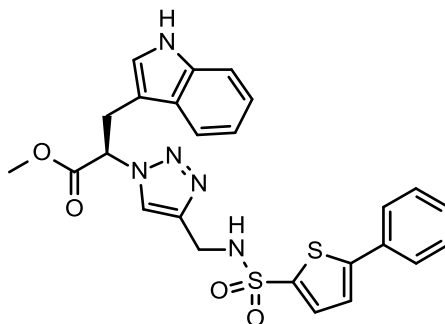
Compound **66** was synthesized according to the general procedure H, using azide **63** (99.6 mg, 0.18 mmol), alkyne **44** (50 mg, 0.18 mmol), copper (II) sulfate pentahydrate (9 mg, 0.04 mmol) and sodium ascorbate (17.8 mg, 0.09 mmol) in DMF (5.5 mL) and H₂O (4.5 mL) overnight. The crude product was purified by flash chromatography on silica gel (CH₂Cl₂ to CH₂Cl₂/MeOH: 9/1) affording compound **66** as a white powder (32 mg, 32%). LC tr = 2.98 min, MS (ESI-): m/z = 554 [M-H]⁻. ¹H NMR (300 MHz, DMSO-*d*₆) δ ppm: 8.57 (ddd, *J* = 4.8, 1.7 and 1.0 Hz, 1H), 8.45 (t, *J* = 6.0 Hz, 1H), 8.04 (dt, *J* = 8.0 and 1.0 Hz, 1H), 8.01 (s, 1H), 7.88 (td, *J* = 11.5 and 1.7 Hz, 1H), 7.82 (d, *J* = 4.0 Hz, 1H), 7.59 (d, *J* = 4.0 Hz, 1H), 7.37 (ddd, *J* = 7.5, 4.8 and 1.0 Hz, 1H), 6.99–6.95 (m, 2H), 6.80–6.76 (m, 2H), 5.75 (dd, *J* = 9.8 and 6.0 Hz, 1H), 4.12 (d, *J* = 5.9 Hz, 2H), 3.64 (s, 3H), 3.45 (dd, *J* = 14.2 and 5.9 Hz, 1H), 3.35 (dd, *J* = 14.2 and 9.8 Hz, 1H), 1.22 (s, 9H). ¹³C NMR (75 MHz, DMSO-*d*₆) δ ppm: 168.6, 153.8, 150.4, 150.0, 149.6, 143.2, 142.0, 137.5, 132.6, 130.2, 129.5 (2C), 124.9, 123.7, 123.6, 123.5 (2C), 119.3, 77.8, 62.9, 52.7, 38.2, 36.2, 28.5.

Methyl (2*S*)-3-(4-benzyloxyphenyl)-2-[4-[(5-phenyl-2-thienyl)sulfonylamino]methyl]triazol-1-yl]propanoate (64**)**



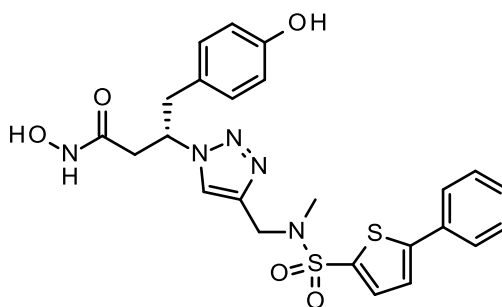
Compound **64** was synthesized according to the general procedure H, using azide **61** (70 mg, 0.23 mmol), alkyne **32** (62.4 mg, 0.23 mmol), copper (II) sulfate pentahydrate (11.2 mg, 0.05 mmol) and sodium ascorbate (22.3 mg, 0.11 mmol) in DMF (5.5 mL) and H₂O (4.5 mL) overnight. The crude product was purified by flash chromatography on silica gel (CH₂Cl₂ to CH₂Cl₂/MeOH: 9/1) affording compound **64** as a white solid (100 mg, 72%). LC tr = 3.32 min, MS (ESI+): m/z = 589 [M+H]⁺. ¹H NMR (300 MHz, DMSO-*d*₆) δ ppm: 8.47 (br t, *J* = 5.4 Hz, 1H), 8.05 (s, 1H), 7.74–7.70 (m, 2H), 7.59 (d, *J* = 3.9 Hz, 1H), 7.55 (d, *J* = 3.9 Hz, 1H), 7.49–7.30 (m, 8H), 7.03–6.98 (m, 2H), 6.86–6.81 (m, 2H), 5.75 (dd, *J* = 9.9 and 5.7 Hz, 1H), 5.01 (s, 2H), 4.15 (d, *J* = 5.4 Hz, 2H), 3.65 (s, 3H), 3.45 (dd, *J* = 14.3 and 5.7 Hz, 1H), 3.36 (dd, *J* = 14.3 and 9.9 Hz, 1H). ¹³C NMR (75 MHz, DMSO-*d*₆) δ ppm: 168.7, 157.2, 149.1, 143.2, 139.6, 137.0, 132.8, 132.2, 130.0 (2C), 129.4 (2C), 129.1, 128.4 (2C), 127.8, 127.8, 127.7 (2C), 125.9 (2C), 124.0, 123.6, 114.6 (2C), 69.1, 63.1, 52.8, 38.3, 35.9.

Methyl (2R)-3-(1H-indol-3-yl)-2-[4-[[5-(phenyl-2-thienyl)sulfonylamino]methyl]triazol-1-yl]propanoate (34)



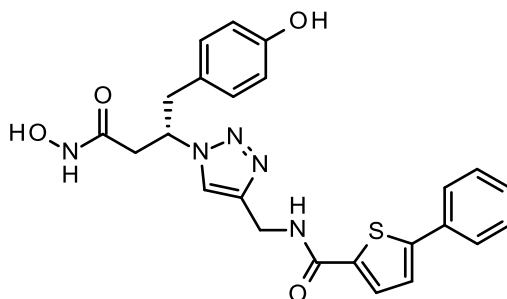
Compound **34** was synthesized according to the general procedure H, using azide **31** (144 mg, 0.3 mmol), alkyne **32** (98 mg, 0.3 mmol), copper (II) sulfate pentahydrate (15 mg, 0.06 mmol) and sodium ascorbate (29.7 mg, 0.06 mmol) in DMF (6 mL) and H₂O (5 mL) overnight. The crude product was purified by flash chromatography on silica gel (cHex/EtOAc: 95/5 to 4/6) affording compound **34** as an orange solid (127 mg, 77%). LC tr = 2.19 min, MS (ESI⁻): m/z = 520 [M - H]⁻. ¹H NMR (300MHz, DMSO-*d*₆) δ ppm: 10.84 (d, *J* = 1.4 Hz, 1H), 8.45 (br s, 1H), 8.10 (s, 1H), 7.72–7.68 (m, 2H), 7.55 (d, *J* = 3.9 Hz, 1H), 7.49–7.40 (m, 5H), 7.31–7.29 (m, 1H), 7.09–7.04 (m, 1H), 7.01–6.87 (m, 1H), 6.90 (d, *J* = 2.3 Hz, 1H), 5.75 (dd, *J* = 9.3 and 5.9 Hz, 1H), 4.14 (s, 2H), 3.67–3.53 (5H, m). ¹³C NMR (75MHz, DMSO-*d*₆) δ ppm: 168.9, 149.0, 143.1, 139.5, 135.9, 132.7, 132.2, 129.3 (2C), 129.1, 126.7, 125.9 (2C), 123.9, 123.8, 123.4, 121.1, 118.6, 117.9, 111.5, 108.0, 62.5, 52.8, 38.3, 27.3.

(3S)-4-(4-Hydroxyphenyl)-3-[4-[[methyl-[(5-phenyl-2-thienyl)sulfonyl]amino]methyl]triazol-1-yl]butanehydroxamic acid (20)



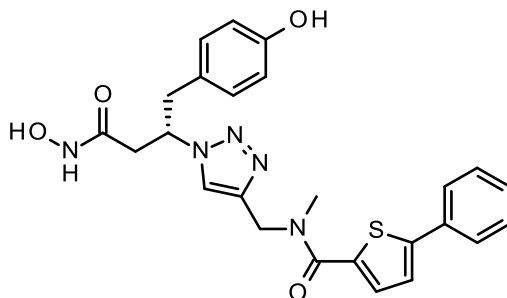
Compound **20** was synthesized according to the general procedure G, using ester **17** (69 mg, 0.13 mmol), KCN (0.9 mg, 0.01 mmol) and aq. NH₂OH (1 mL, 50% w/w in water) in MeOH (1 mL) overnight. The crude product was purified by flash chromatography on silica gel (CH₂Cl₂ to CH₂Cl₂/MeOH: 9/1) affording compound **20** as a white solid after lyophilization (64 mg, 53%). Purity: 100%, LC tr = 2.37 min, MS (ESI⁻): m/z = 526 [M - H]⁻. ¹H NMR (300 MHz, DMSO-*d*₆) δ ppm: 10.49 (s, 1H), 9.22 (s, 1H), 8.80 (s, 1H), 7.85 (s, 1H), 7.77–7.74 (m, 2H), 7.68–7.65 (m, 2H), 7.50–7.42 (m, 3H), 6.72–6.70 (m, 2H), 6.57–6.54 (m, 2H), 5.07–4.98 (m, 1H), 4.24 (m, 2H), 3.05–2.89 (m, 2H), 2.75–2.62 (m, 2H), 2.58 (s, 3H). ¹³C NMR (75 MHz, DMSO-*d*₆) δ ppm: 165.5, 156.0, 150.0, 140.4, 134.7, 133.8, 132.0, 129.8, 129.4, 129.3, 126.8, 126.0, 124.5, 124.0, 115.1, 59.5, 45.0, 40.1, 37.0, 34.4. HRMS-ESI⁺ (m/z) calcd. for C₂₄H₂₆N₅O₅S₂ [M + H]⁺ 528.1375, found 528.1376.

***N*-[[1-[(1*S*)-3-(hydroxyamino)-1-[(4-hydroxyphenyl)methyl]-3-oxo-propyl]triazol-4-yl]methyl]-5-phenyl-thiophene-2-carboxamide (**21**)**



Compound **21** was synthesized according to the general procedure G, using ester **18** (18 mg, 0.04 mmol), KCN (0.2 mg, 0.004 mmol) and aq. NH₂OH (0.5 mL, 50% w/w in water) in MeOH (0.5 mL) overnight. The crude product was purified by flash chromatography on silica gel (CH₂Cl₂ to CH₂Cl₂/MeOH: 9/1) affording compound **21** as a white solid after lyophilization (11 mg, 61%). Purity: 99%, LC tr = 2.18 min, MS (ESI-): m/z = 476 [M - H]⁻. ¹H NMR (300 MHz, DMSO-*d*₆) δ ppm: 10.51 (s, 1H), 9.24 (s, 1H), 9.08 (t, *J* = 5.7 Hz, 1H), 8.79 (s, 1H), 7.87 (s, 1H), 7.79 (d, *J* = 4.0 Hz, 1H), 7.72-7.70 (m, 2H), 7.54 (d, *J* = 4.0 Hz, 1H), 7.47-7.42 (m, 2H), 7.39-7.33 (m, 1H), 6.85-6.77 (m, 2H), 6.59-6.57 (m, 2H), 5.12-5.02 (m, 1H), 4.44 (d, *J* = 5.7 Hz, 2H), 3.01-2.98 (m, 2H), 2.74-2.54 (m, 2H). ¹³C NMR (75 MHz, DMSO-*d*₆) δ ppm: 165.6, 160.9, 156.0, 147.5, 144.2, 138.7, 133.1, 129.9, 129.4, 129.3, 128.5, 126.9, 125.7, 124.4, 122.5, 115.1, 62.8, 59.1, 36.9, 34.6. HRMS-ESI+ (m/z) calcd for C₂₄H₂₄N₅O₄S [M + H]⁺ 478.1549, found 478.1545.

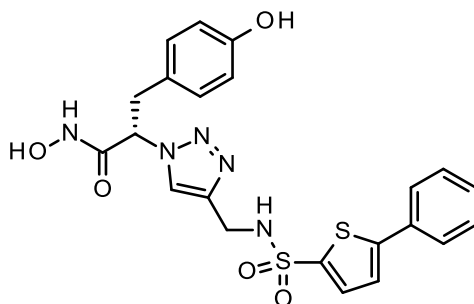
***N*-[[1-[(1*S*)-3-(hydroxyamino)-1-[(4-hydroxyphenyl)methyl]-3-oxo-propyl]triazol-4-yl]methyl]-*N*-methyl-5-phenyl-thiophene-2-carboxamide (**22**)**



Compound **22** was synthesized according to the general procedure G, using ester **19** (26 mg, 0.05 mmol), KCN (0.3 mg, 0.005 mmol) and aq. NH₂OH (0.7 mL, 50% w/w in water) in MeOH (0.7 mL) overnight. The crude product was purified by flash chromatography on silica gel (CH₂Cl₂ to CH₂Cl₂/MeOH: 9/1) affording compound **22** as a white solid after lyophilization (13 mg, 50%). Purity: 99%, LC t_R = 2.22 min, MS (ESI+): m/z = 492 [M + H]⁺. ¹H NMR (300 MHz, DMSO-*d*₆) δ ppm: 10.50 (s, 1H), 9.21 (s, 1H), 8.80 (s, 1H), 7.90 (s, 1H), 7.73-7.70 (m, 2H), 7.55-7.35 (m, 5H), 6.76-6.73 (m, 2H), 6.58-6.55 (m, 2H), 5.09-5.06 (m, 1H), 4.68-4.67 (m, 2H), 3.09-2.94 (m, 5H), 2.78-2.63 (m, 2H). ¹³C NMR (75 MHz, DMSO-*d*₆) δ ppm: 165.5, 162.7, 156.0, 146.7, 142.1, 137.0,

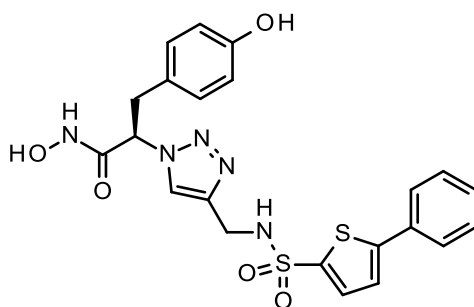
132.9, 130.7, 129.8 (2C), 129.2 (2C), 128.5, 126.9, 125.7 (2C), 123.7, 123.2, 115.0 (2C), 59.4, 39.5, 37.2. HRMS-ESI+ (m/z) calcd. for C₂₅H₂₆N₅O₄S [M + H]⁺ 492.1706, found 492.1702.

(2S)-3-(4-Hydroxyphenyl)-2-[4-[(5-phenyl-2-thienyl)sulfonylamino]methyl]triazol-1-yl]propanehydroxamic acid (35)



Compound **35** was synthesized according to the general procedure G, using ester **33** (65 mg, 0.13 mmol), KCN (0.8 mg, 0.01 mmol) and aq. NH₂OH (0.5 mL, 50% w/w in water) in MeOH (0.5 mL) overnight. The crude product was purified by flash chromatography on silica gel (CH₂Cl₂ to CH₂Cl₂/MeOH: 95/5) affording compound **35** as a white solid after lyophilization (46 mg, 71%). Purity: 99%, LC t_R = 2.47 min, MS (ESI+): m/z = 500 [M + H]⁺. ¹H NMR (300 MHz, DMSO-*d*₆) δ ppm: 8.09 (s, 1H), 7.73–7.71 (m, 2H), 7.57–7.53 (m, 2H), 7.49–7.38 (m, 3H), 7.91–7.89 (m, 2H), 6.62–6.59 (m, 2H) 5.20 (t, *J* = 7.9 Hz, 1H), 4.17 (s, 2H), 3.25–3.18 (m, 1H), 3.13–3.05 (m, 1H). ¹³C NMR (75 MHz, DMSO-*d*₆) δ ppm: 163.8, 156.2, 149.1, 143.2, 139.7, 132.8, 132.3, 130.0 (2C), 129.4 (2C), 129.1, 125.9 (2C), 125.8, 124.0, 122.2, 115.1 (2C), 62.0, 38.3, 36.8. HRMS-ESI+ (m/z) calcd. for C₂₂H₂₂N₅O₅S₂ [M + H]⁺ 500.1062, found 500.1064.

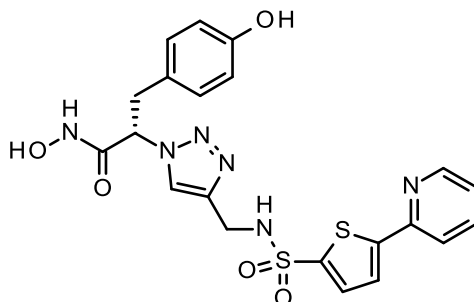
(2R)-3-(4-Hydroxyphenyl)-2-[4-[(5-phenyl-2-thienyl)sulfonylamino]methyl]triazol-1-yl]propanehydroxamic acid (40)



Compound **40** was synthesized according to the general procedure G, using ester **39** (97 mg, 0.19 mmol), KCN (2.5 mg, 0.04 mmol) and aq. NH₂OH (2.5 mL, 50% w/w in water) in MeOH (2.5 mL) overnight. The crude product was purified by flash chromatography on silica gel (CH₂Cl₂ to CH₂Cl₂/MeOH: 95/5) affording compound **40** as a white solid after lyophilization (73 mg, 74%). Purity: 99%, LC t_R = 2.37 min, MS (ESI+): m/z = 500 [M + H]⁺. ¹H NMR (300 MHz, DMSO-*d*₆) δ ppm: 9.32 (br s, 3H), 8.09 (s, 1H), 7.72 (br d, *J* = 6.9 Hz, 2H), 7.57–7.53 (m, 2H), 7.49–7.39 (m, 3H), 6.90 (br d, *J* = 8.3 Hz, 2H), 6.60 (br d, *J* = 8.3 Hz, 2H), 5.20 (t, *J* = 7.6 Hz, 1H), 4.17 (s, 2H), 3.22 (dd,

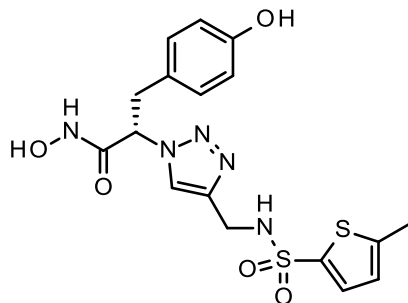
$J = 13.8$ and 7.6 Hz, 1H), 3.09 (dd, $J = 13.8$ and 8.3 Hz, 1H). ^{13}C NMR (75 MHz, $\text{DMSO-}d_6$) δ ppm: 163.8, 156.2, 149.0, 143.2, 139.7, 132.8, 132.2, 129.9 (2C), 129.3 (2C), 129.1, 125.9 (2C), 125.7, 124.0, 122.2, 115.1 (2C), 62.0, 38.3, 36.7. HRMS-ESI+ (m/z) calcd. for $\text{C}_{22}\text{H}_{22}\text{N}_5\text{O}_5\text{S}_2$ [$\text{M} + \text{H}$] $^+$ 500.1042, found 500.1062.

(2S)-3-(4-Hydroxyphenyl)-2-[4-[[[5-(2-pyridyl)-2-thienyl]sulfonylamino]methyl]triazol-1-yl]propanehydroxamic acid (56)



Compound **56** was synthesized according to the general procedure G, using ester **50** (50 mg, 0.1 mmol), KCN (1.3 mg, 0.02 mmol) and aq. NH_2OH (2.5 mL, 50% w/w in water) in MeOH (2.5 mL) overnight. The crude product was purified by flash chromatography on silica gel (CH_2Cl_2 to $\text{CH}_2\text{Cl}_2/\text{MeOH}$: 9/1) affording compound **56** as a white solid after lyophilization (32 mg, 63%). Purity: 99%, LC tr = 2.08 min, MS (ESI-): $m/z = 499$ [$\text{M} - \text{H}$] $^-$. ^1H NMR (300 MHz, $\text{DMSO-}d_6$) δ ppm: 9.27 (s, 2H), 8.09 (s, 1H), 7.74–7.71 (m, 2H), 7.57 (d, $J = 3.9$ Hz, 1H), 7.54 (d, $J = 3.9$ Hz, 1H), 7.49–7.38 (m, 3H), 6.91–6.88 (m, 2H), 6.62–6.59 (m, 2H), 5.20 (t, $J = 7.8$ Hz, 1H), 4.17 (s, 2H), 3.21 (dd, $J = 13.8$ and 7.5 Hz, 1H), 3.09 (dd, $J = 13.8$ and 8.2 Hz, 1H). ^{13}C NMR (75 MHz, $\text{DMSO-}d_6$) δ ppm: 163.8, 156.2, 149.1, 143.2, 139.6, 132.8, 132.2, 130.0, 129.3 (2C), 129.1, 125.9 (2C), 125.7, 124.0, 122.2, 115.1 (2C), 62.0, 38.3, 36.7. HRMS-ESI+ (m/z) calcd. for $\text{C}_{21}\text{H}_{21}\text{N}_6\text{O}_5\text{S}_2$ [$\text{M} + \text{H}$] $^+$ 501.0996, found 501.1015.

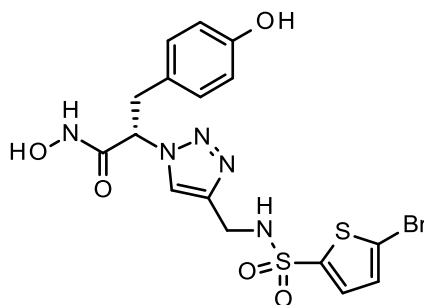
(2S)-3-(4-Hydroxyphenyl)-2-[4-[[[5-methyl-2-thienyl]sulfonylamino]methyl]triazol-1-yl]propanehydroxamic acid (55)



Compound **55** was synthesized according to the general procedure G, using ester **49** (109 mg, 0.25 mmol), KCN (3.2 mg, 0.05 mmol) and aq. NH_2OH (2.5 mL, 50% w/w in water) in MeOH (2.5 mL) overnight. The crude product was purified by flash chromatography on silica gel (CH_2Cl_2 to $\text{CH}_2\text{Cl}_2/\text{MeOH}$: 95/5) affording compound **55** as a white solid after lyophilization (64 mg, 59%).

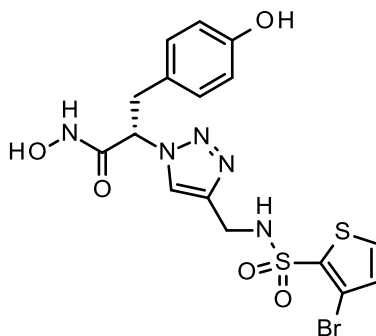
Purity: 99%, LC tr = 1.97 min, MS (ESI+): $m/z = 438 [M + H]^+$. $^1\text{H NMR}$ (300 MHz, $\text{DMSO-}d_6$) δ ppm: 9.27 (br s, 1H), 9.13 (br s, 1H), 8.04 (s, 1H), 7.39 (d, $J = 3.7$ Hz, 1H), 6.96–6.93 (m, 2H), 6.88 (dd, $J = 3.7$ and 1.0 Hz, 1H), 6.64–6.61 (m, 2H), 5.21 (t, $J = 7.8$ Hz, 1H), 4.08 (s, 2H), 3.24 (dd, $J = 13.9$ and 7.3 Hz, 1H), 3.13 (dd, $J = 13.9$ and 8.3 Hz, 1H), 2.49 (s, 3H). $^{13}\text{C NMR}$ (75 MHz, $\text{DMSO-}d_6$) δ ppm: 163.8, 156.2, 146.7, 143.3, 138.0, 132.0, 130.0 (2C), 126.2, 125.8, 122.1, 115.2 (2C), 62.0, 38.3, 36.8, 15.1. HRMS-ESI+ (m/z) calcd. for $\text{C}_{17}\text{H}_{20}\text{N}_5\text{O}_5\text{S}_2 [M + H]^+$ 438.0904, found 438.0906.

(2S)-2-[4-[[5-(5-Bromo-2-thienyl)sulfonylamino]methyl]triazol-1-yl]-3-(4-hydroxyphenyl)propanehydroxamic acid (53)



Compound **53** was synthesized according to the general procedure G, using ester **47** (124 mg, 0.25 mmol), KCN (3.2 mg, 0.05 mmol) and aq. NH_2OH (3 mL, 50% w/w in water) in MeOH (3 mL) overnight. The crude product was purified by flash chromatography on silica gel (CH_2Cl_2 to $\text{CH}_2\text{Cl}_2/\text{MeOH}$: 9/1) affording compound **53** as a white solid after lyophilization (50 mg, 38%). Purity: 95%, LC tr = 2.13 min, MS (ESI-): $m/z = 500$ and $502 [M - H]^-$. $^1\text{H NMR}$ (300 MHz, $\text{DMSO-}d_6$) δ ppm: 10.98 (br s, 1H), 9.28–9.17 (m, 2H), 8.10 (s, 1H), 7.39 (d, $J = 3.9$ Hz, 1H), 7.30 (d, $J = 3.9$ Hz, 1H), 6.97–6.94 (m, 2H), 6.64–6.61 (m, 2H), 5.22 (t, $J = 7.8$ Hz, 1H), 4.13 (s, 2H), 3.24 (dd, $J = 14.1$ and 7.4 Hz, 1H), 3.14 (dd, $J = 13.7$ and 8.4 Hz, 1H). $^{13}\text{C NMR}$ (75 MHz, $\text{DMSO-}d_6$) δ ppm: 163.8, 156.2, 143.0, 142.3, 132.4, 131.3, 130.0 (2C), 125.8, 122.3, 118.3, 115.2 (2C), 62.0, 38.2, 36.8. HRMS-ESI+ (m/z) calcd. for $\text{C}_{16}\text{H}_{17}\text{N}_5\text{O}_5\text{S}_2\text{Br} [M + H]^+$ 501.9854, found 501.9839.

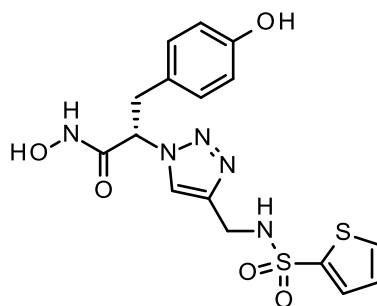
(2S)-2-[4-[[3-(3-Bromo-2-thienyl)sulfonylamino]methyl]triazol-1-yl]-3-(4-hydroxyphenyl)propanehydroxamic acid (54)



Compound **54** was synthesized according to the general procedure G, using ester **48** (75 mg, 0.15 mmol), KCN (1.9 mg, 0.03 mmol) and aq. NH_2OH (2 mL, 50% w/w in water) in MeOH (2 mL) overnight. The crude product was purified by flash chromatography on silica gel (CH_2Cl_2 to

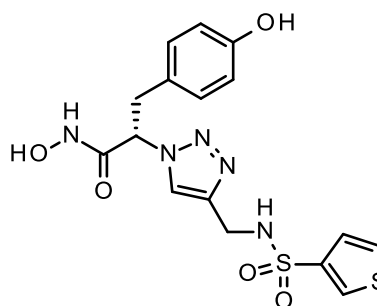
CH₂Cl₂/MeOH: 9/1) affording compound **54** as a white solid after lyophilization (50 mg, 51%). Purity: 99%, LC tr = 1.95min, MS (ESI+): m/z = 502 and 504 [M + H]⁺. ¹H NMR (300 MHz, DMSO-*d*₆) δ ppm: 11.07 (br s, 1H), 9.27–9.19 (m, 2H), 8.71 (br s, 1H), 8.00 (s, 1H), 7.91 (d, *J* = 5.2 Hz, 1H), 7.23 (d, *J* = 5.2 Hz, 1H), 6.96–6.93 (m, 2H), 6.64–6.61 (m, 2H), 5.19 (t, *J* = 7.7 Hz, 1H), 4.21 (s, 2H), 3.23 (dd, *J* = 14.0 and 7.4 Hz, 1H), 3.11 (dd, *J* = 14.0 and 8.2 Hz, 1H). ¹³C NMR (DMSO-*d*₆) δ ppm: 163.7, 156.2, 143.4, 136.8, 132.6, 132.3, 130.0 (2C), 125.7, 121.9, 115.2 (2C), 112.6, 61.9, 38.1, 36.8. HRMS-ESI+ (m/z) calcd. for C₁₆H₁₇N₅O₅S₂Br [M + H]⁺ 501.9854, found 501.9827.

(2S)-3-(4-Hydroxyphenyl)-2-[4-[(2-thienylsulfonylamino)methyl]triazol-1-yl]propanehydroxamic acid (57)



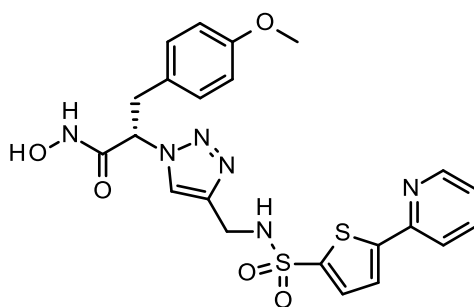
Compound **57** was synthesized according to the general procedure G, using ester **51** (94 mg, 0.22 mmol), KCN (2.9 mg, 0.04 mmol) and aq. NH₂OH (2.5 mL, 50% w/w in water) in MeOH (2.5 mL) overnight. The crude product was purified by flash chromatography on silica gel (CH₂Cl₂ to CH₂Cl₂/MeOH: 95/5) affording compound **57** as a white solid after lyophilization (67 mg, 70%). Purity: 99%, LC tr = 1.82 min, MS (ESI+): m/z = 424 [M + H]⁺. ¹H NMR (300 MHz, DMSO-*d*₆) δ ppm: 11.03 (br s, 1H), 9.27 (s, 1H), 9.19 (br s, 1H), 8.33 (br s, 1H), 8.06 (s, 1H), 7.91 (dd, *J* = 5.0 and 1.3 Hz, 1H), 7.58 (dd, *J* = 3.7 and 1.3 Hz, 1H), 7.16 (dd, *J* = 5.0 and 3.7 Hz, 1H), 6.97–6.93 (m, 2H), 6.65–6.60 (m, 2H), 5.22 (t, *J* = 7.8 Hz, 1H), 4.10 (s, 2H), 3.24 (dd, *J* = 13.9 and 7.3 Hz, 1H), 3.14 (dd, *J* = 13.9 and 8.3 Hz, 1H). ¹³C NMR (75 MHz, DMSO-*d*₆) δ ppm: 163.8, 156.2, 143.2, 141.2, 132.5, 131.7, 130.0 (2C), 127.7, 125.8, 122.1, 115.2 (2C), 62.0, 38.3, 36.7. HRMS-ESI+ (m/z) calcd for C₁₆H₁₈N₅O₅S₂ [M + H]⁺ 424.0719, found 424.0749.

(2S)-3-(4-Hydroxyphenyl)-2-[4-[(3-thienylsulfonylamino)methyl]triazol-1-yl]propanehydroxamic acid (58)



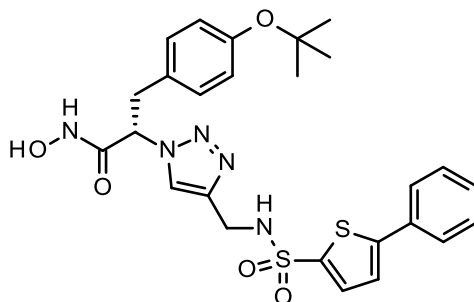
Compound **58** was synthesized according to the general procedure G, using ester **52** (90 mg, 0.21 mmol), KCN (2.8 mg, 0.04 mmol) and aq. NH₂OH (2.5 mL, 50% w/w in water) in MeOH (2.5 mL) overnight. The crude product was purified by flash chromatography on silica gel (CH₂Cl₂ to CH₂Cl₂/MeOH: 95/5) affording compound **58** as a white solid after lyophilization (35 mg, 38%). Purity: 99%, LC tr = 1.78 min, MS (ESI+): *m/z* = 424 [M + H]⁺. ¹H NMR (300 MHz, DMSO-*d*₆) δ ppm: 9.27 (br s, 1H), 9.14 (br s, 1H), 8.14 (dd, *J* = 3.0 and 1.3 Hz, 1H), 8.04 (s, 1H), 7.71 (dd, *J* = 5.1 and 3.0 Hz, 1H), 7.31 (dd, *J* = 5.1 and 1.3 Hz, 1H), 6.97–6.92 (m, 2H), 6.65–6.60 (m, 2H), 5.21 (t, *J* = 7.8 Hz, 1H), 4.06 (s, 2H), 3.24 (dd, *J* = 13.9 and 7.3 Hz, 1H), 3.14 (dd, *J* = 13.9 and 8.4 Hz, 1H). ¹³C NMR (75 MHz, DMSO-*d*₆) δ ppm: 163.8, 156.2, 143.4, 140.3, 130.5, 130.0 (2C), 129.0, 125.8, 125.3, 122.1, 115.2 (2C), 62.0, 38.1, 36.7. HRMS-ESI+ (*m/z*) calcd. for C₁₆H₁₈N₅O₅S₂ [M + H]⁺ 424.0728, found 424.0749.

(2S)-3-(4-Methoxyphenyl)-2-[4-[[[5-(2-pyridyl)-2-thienyl]sulfonylamino]methyl]triazol-1-yl]propanehydroxamic acid (71)



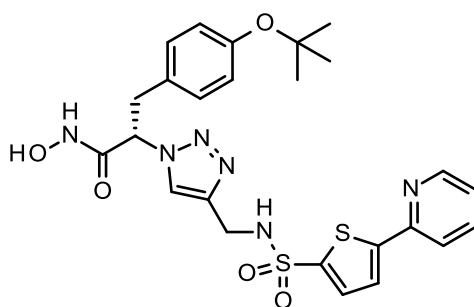
Compound **71** was synthesized according to the general procedure G, using ester **67** (150 mg, 0.29 mmol), KCN (3.8 mg, 0.06 mmol) and aq. NH₂OH (2.9 mL, 50% w/w in water) in MeOH (2.9 mL) overnight. The crude product was purified by flash chromatography on silica gel (CH₂Cl₂ to CH₂Cl₂/MeOH: 95/5) affording compound **71** as a white solid after lyophilization (106 mg, 69%). Purity: 98%, LC tr = 2.30 min, MS (ESI-): *m/z* = 513 [M - H]⁻. ¹H NMR (300 MHz, DMSO-*d*₆) δ ppm: 11.6 (br s, 1H), 9.19 (br s, 1H), 8.56 (ddd, *J* = 4.8, 1.7 and 0.9 Hz, 1H), 8.46 (br s, 1H), 8.09 (s, 1H), 8.02 (dt, *J* = 8.0 and 1.0 Hz, 1H), 7.88 (td, *J* = 7.5 and 1.7 Hz, 1H), 7.82 (d, *J* = 4.0 Hz, 1H), 7.59 (d, *J* = 4.0 Hz, 1H), 7.37 (ddd, *J* = 7.5, 4.8 and 1.0 Hz, 1H), 7.04–7.00 (m, 2H), 6.81–6.77 (m, 2H), 5.22 (t, *J* = 7.9 Hz, 1H), 4.15 (s, 2H), 3.69 (m, 3H) 3.44 (dd, *J* = 13.8 and 7.5 Hz, 1H), 3.14 (dd, *J* = 13.8 and 8.2 Hz, 1H). ¹³C NMR (75 MHz, DMSO-*d*₆) δ ppm: 163.7, 158.1, 150.4, 150.0, 149.7, 143.2, 142.1, 137.5, 132.6, 130.0 (2C), 127.5, 124.9, 123.7, 122.2, 119.3, 113.7 (2C), 61.9, 59.9, 38.3, 36.6. HRMS-ESI+ (*m/z*) calcd. for C₂₂H₂₃N₆O₅S₂ [M + H]⁺ 515.1178, found: 515.1178.

(2S)-3-(4-*tert*-Butoxyphenyl)-2-[4-[[5-(2-thienyl)sulfonylamino]methyl]triazol-1-yl]propanehydroxamic acid (69)



Compound **69** was synthesized according to the general procedure G, using ester **65** (75 mg, 0.13 mmol), KCN (1.7 mg, 0.03 mmol) and aq. NH₂OH (2.5 mL, 50% w/w in water) in MeOH (2.5 mL) overnight. The crude product was purified by flash chromatography on silica gel (CH₂Cl₂ to CH₂Cl₂/MeOH: 9/1) affording compound **69** as a white solid after lyophilization (67 mg, 90%). Purity: 99%, LC tr = 2.85 min, MS (ESI-): *m/z* = 554 [M - H]⁻. ¹H NMR (300 MHz, DMSO-*d*₆) δ ppm: 8.11 (s, 1H), 7.75–7.72 (m, 2H), 7.58 (d, *J* = 3.9 Hz, 1H), 7.55 (d, *J* = 3.9 Hz, 1H), 7.50–7.38 (m, 3H), 7.03–6.99 (m, 2H), 6.85–6.81 (m, 2H), 5.26 (t, *J* = 7.8 Hz, 1H), 4.18 (s, 2H), 3.30 (dd, *J* = 13.8 and 7.4 Hz, 1H), 3.18 (dd, *J* = 13.8 and 8.1 Hz, 1H), 1.25 (s, 9H). ¹³C NMR (75 MHz, DMSO-*d*₆) δ ppm: 163.7, 153.9, 149.1, 143.3, 139.7, 132.8, 132.2, 130.2, 129.5 (2C), 129.4 (2C), 129.1, 125.9 (2C), 124.0, 123.4 (2C), 122.2, 77.8, 61.7, 38.3, 36.8, 28.5 (3C). HRMS-ESI+ (*m/z*) calcd. for C₂₆H₃₀N₅O₅S₂ [M + H]⁺ 556.1680, found 556.1688.

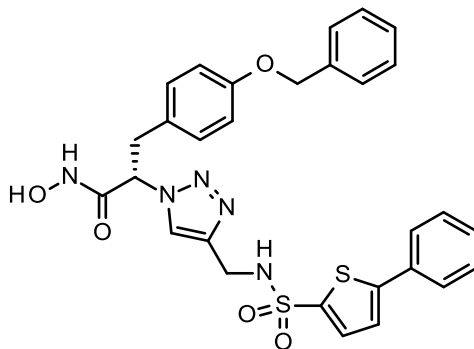
(2S)-3-(4-*tert*-Butoxyphenyl)-2-[4-[[[5-(2-pyridyl)-2-thienyl]sulfonylamino]methyl]triazol-1-yl]propanehydroxamic acid (70)



Compound **70** was synthesized according to the general procedure G, using ester **66** (60 mg, 0.11 mmol), KCN (1.4 mg, 0.02 mmol) and aq. NH₂OH (1.5 mL, 50% w/w in water) in MeOH (1.5 mL) overnight. The crude product was purified by flash chromatography on silica gel (CH₂Cl₂ to CH₂Cl₂/MeOH: 9/1) affording compound **70** as a white solid after lyophilization (52 mg, 86%). Purity: 99%, LC tr = 2.57 min, MS (ESI+): *m/z* = 557 [M + H]⁺; 501 [M + H - tBu]⁺. ¹H NMR (300 MHz, DMSO-*d*₆) δ ppm: 11.09 (s, 1H), 9.21 (s, 1H), 8.56 (ddd, *J* = 4.9, 1.7 and 0.9 Hz, 1H), 8.47 (t, *J* = 5.9 Hz, 1H), 8.09 (s, 1H), 8.02 (dt, *J* = 7.9 and 1.0 Hz, 1H), 7.88 (td, *J* = 7.8 and 1.7 Hz, 1H), 7.82 (d, *J* = 4.0 Hz, 1H), 7.58 (d, *J* = 4.0 Hz, 1H), 7.36 (ddd, *J* = 7.5, 4.9 and 1.0 Hz, 1H), 7.02–6.99 (m, 2H), 6.83–6.80 (m, 2H), 5.24 (t, *J* = 7.8 Hz, 1H), 4.16 (d, *J* = 4.8 Hz, 2H), 3.28 (dd, *J* = 14.1 and 7.4 Hz,

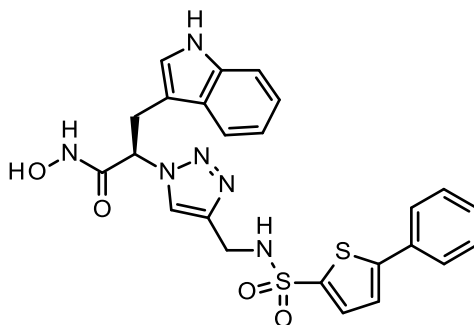
1H), 3.15 (dd, $J = 14.0$ and 8.0 Hz, 1H), 1.24 (s, 9H). ^{13}C NMR (75 MHz, $\text{DMSO-}d_6$) δ ppm: 163.7, 153.9, 150.4, 150.0, 149.7, 143.3, 142.1, 137.5, 132.6, 130.2, 129.5 (2C), 124.9, 123.7, 123.4 (2C), 122.2, 119.4, 77.8, 61.7, 38.3, 36.8, 28.5 (3C). HRMS-ESI+ (m/z) calcd. for $\text{C}_{25}\text{H}_{29}\text{N}_6\text{O}_5\text{S}_2$ [$\text{M} + \text{H}$] $^+$ 557.1641, found 557.1669.

(2S)-3-(4-Benzyloxyphenyl)-2-[4-[(5-phenyl-2-thienyl)sulfonylamino]methyl]triazol-1-yl]propanehydroxamic acid (68)



Compound **68** was synthesized according to the general procedure G, using ester **64** (80 mg, 0.14 mmol), KCN (1.8 mg, 0.03 mmol) and aq. NH_2OH (2.5 mL, 50% w/w in water) in MeOH (2.5 mL) overnight. The crude product was purified by flash chromatography on silica gel (CH_2Cl_2 to $\text{CH}_2\text{Cl}_2/\text{MeOH}$: 9/1) affording compound **68** as a white solid after lyophilization (74 mg, 92%). Purity: 99%, LC tr = 2.95 min, MS (ESI-): $m/z = 588$ [$\text{M} - \text{H}$] $^-$. ^1H NMR (300 MHz, $\text{DMSO-}d_6$) δ ppm: 11.10 (s, 1H), 9.22 (s, 1H), 8.47 (br t, $J = 6.0$ Hz, 1H), 8.12 (s, 1H), 7.75–7.71 (m, 2H), 7.58 (d, $J = 3.9$ Hz, 1H), 7.56 (d, $J = 3.9$ Hz, 1H), 7.50–7.30 (m, 8H), 7.06–7.03 (m, 2H), 6.89–6.86 (m, 2H), 5.25 (t, $J = 7.8$ Hz, 1H), 5.04 (s, 2H), 4.18 (br d, $J = 4.2$ Hz, 2H), 3.28 (dd, $J = 13.8$ and 7.3 Hz, 1H), 3.17 (dd, $J = 13.8$ and 8.2 Hz, 1H). ^{13}C NMR (75 MHz, $\text{DMSO-}d_6$) δ ppm: 163.7, 157.3, 149.1, 143.2, 139.6, 137.1, 132.8, 132.2, 130.0 (2C), 129.8, 129.4 (2C), 129.1, 128.4 (2C), 127.8, 127.7 (2C), 125.9 (2C), 124.0, 122.2, 114.6 (2C), 69.1, 61.8, 38.3, 36.6. HRMS-ESI+ (m/z) calcd. for $\text{C}_{29}\text{H}_{28}\text{N}_5\text{O}_5\text{S}_2$ [$\text{M} + \text{H}$] $^+$ 590.1531, found 590.1532.

(2R)-3-(1H-Indol-3-yl)-2-[4-[(5-phenyl-2-thienyl)sulfonylamino]methyl]triazol-1-yl]propanehydroxamic acid (36)

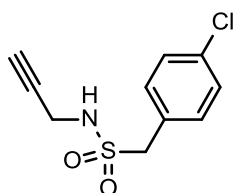


Compound **36** was synthesized according to the general procedure G, using ester **34** (115 mg, 0.22 mmol), KCN (2.8 mg, 0.04 mmol) and aq. NH_2OH (2.1 mL, 50% w/w in water) in MeOH (2.1 mL)

overnight. The crude product was purified by flash chromatography on silica gel (CH₂Cl₂ to CH₂Cl₂/MeOH: 95/5) affording compound **36** as a white solid after lyophilization (64 mg, 53%). Purity: 95%, LC tr = 2.58 min, MS (ESI-): m/z = 521 [M - H]⁻. ¹H NMR (300 MHz, DMSO-*d*₆) δ ppm: 11.17 (br s, 1H), 10.85 (br s, 1H), 9.21 (br s, 1H), 8.45 (br s, 1H), 8.18 (s, 1H), 7.71–7.69 (m, 2H), 7.57 (d, *J* = 7.7 Hz, 1H), 7.54–7.39 (m, 5H), 7.31 (d, *J* = 7.7 Hz, 1H), 7.09–7.04 (m, 1H), 7.09–6.96 (m, 3H), 5.40–5.35 (m, 1H), 4.16 (s, 2H), 3.47 (dd, *J* = 14.4 and 7.4 Hz, 1H), 3.36 (dd, *J* = 14.4 and 8.4 Hz, 1H). ¹³C NMR (75 MHz, DMSO-*d*₆) δ ppm: 164.2, 149.0, 143.1, 139.6, 136.0, 132.9, 132.3, 129.4 (2C), 126.9, 125.9, 124.0 (2C), 123.9, 122.1, 121.1, 118.5, 118.3, 111.4, 108.0, 60.9, 38.3, 20.0. HRMS-ESI+ (m/z) calcd. for C₂₄H₂₂N₆O₄S₂ [M + H]⁺ 523.1222, found 523.1223.

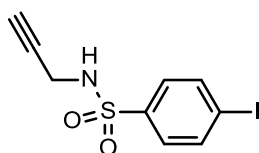
4. Synthesis of chapter 3 compounds (**Z7–Z10** and **76–196**)

1-(4-Chlorophenyl)-*N*-prop-2-ynyl-methanesulfonamide (**147**)



Compound **147** was synthesized according to the general procedure F, using propargylamine (94 μL, 1.47 mmol), (4-chlorophenyl)methanesulfonyl chloride (300 mg, 1.33 mmol) and *N,N*-diisopropylethylamine (464 μL, 2.67 mmol) in CH₂Cl₂ (5 mL) overnight. The crude product was purified by flash chromatography on silica gel (cHex to cHex/EtOAc: 7/3) affording compound **147** as a light yellow solid (187 mg, 45%). LC tr = 3.88 min, MS (ESI-): m/z = 242 and 244 [M - H]⁻. ¹H NMR (500 MHz, DMSO-*d*₆) δ ppm: 7.68 (t, *J* = 5.8 Hz, 1H), 7.46–7.45 (m, 2H), 7.42–7.40 (m, 2H), 4.40 (s, 2H), 3.79 (dd, *J* = 5.8 and 2.4 Hz, 2H), 3.34 (t, *J* = 2.4 Hz, 1H). ¹³C NMR (126 MHz, DMSO-*d*₆) δ ppm: 133.0, 132.7 (2C), 129.2, 128.4 (2C), 80.5, 74.8, 57.0, 31.8.

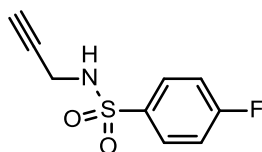
4-Iodo-*N*-prop-2-ynyl-benzenesulfonamide (**93**)



Compound **93** was synthesized according to the general procedure F, using propargylamine (70 μL, 1.09 mmol), 4-iodobenzenesulfonyl chloride (300 mg, 0.99 mmol) and *N,N*-diisopropylethylamine (345 μL, 1.98 mmol) in CH₂Cl₂ (5 mL) overnight. The crude product was purified by flash chromatography on silica gel (cHex to cHex/EtOAc: 7/3) affording compound **93** as a white solid (207 mg, 64%). LC tr = 4.04 min, MS (ESI-): m/z = 320 [M - H]⁻. ¹H NMR (500 MHz, DMSO-*d*₆) δ ppm:

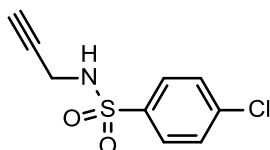
8.23 (br s, 1H), 7.98–7.97 (m, 2H), 7.56–7.55 (m, 2H), 3.71 (s, 2H), 3.06 (t, $J = 2.5$ Hz, 1H). ^{13}C NMR (126 MHz, $\text{DMSO-}d_6$) δ ppm: 140.2, 138.0 (2C), 128.5 (2C), 100.6, 79.2, 74.9, 31.9.

4-Fluoro-*N*-prop-2-ynyl-benzenesulfonamide (141)



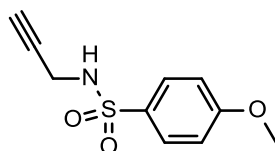
Compound **141** was synthesized according to the general procedure F, using propargylamine (217 μL , 3.39 mmol), 4-fluorobenzenesulfonyl chloride (600 mg, 3.08 mmol) and *N,N*-diisopropylethylamine (1070 μL , 6.17 mmol) in CH_2Cl_2 (10 mL) overnight. The crude product was purified by flash chromatography on silica gel (cHex to cHex/EtOAc: 7/3) affording compound **141** as a white solid (263 mg, 39%). LC tr = 3.40 min, MS (ESI+): $m/z = 214$ $[\text{M} + \text{H}]^+$. ^1H NMR (500 MHz, $\text{DMSO-}d_6$) δ ppm: 8.18 (br s, 1H), 7.88–7.85 (m, 2H), 7.44–7.41 (m, 2H), 3.71 (d, $J = 2.5$ Hz, 2H), 3.03 (t, $J = 2.5$ Hz, 1H). ^{13}C NMR (126 MHz, $\text{DMSO-}d_6$) δ ppm: 164.2 (d, $J = 250.3$ Hz), 137.0 (d, $J = 2.8$ Hz), 129.8 (d, $J = 9.2$ Hz, 2C), 116.2 (d, $J = 22.8$ Hz, 2C), 79.2, 74.8, 31.9.

4-Chloro-*N*-prop-2-ynyl-benzenesulfonamide (142)



Compound **142** was synthesized according to the general procedure F, using propargylamine (100 μL , 1.56 mmol), 4-chlorobenzenesulfonyl chloride (300 mg, 1.42 mmol) and *N,N*-diisopropylethylamine (495 μL , 2.84 mmol) in CH_2Cl_2 (5 mL) overnight. The crude product was purified by flash chromatography on silica gel (cHex to cHex/EtOAc: 7/3) affording compound **142** as a white solid (283 mg, 85%). LC tr = 3.81 min, MS (ESI+): $m/z = 230$ $[\text{M} + \text{H}]^+$. ^1H NMR (500 MHz, $\text{DMSO-}d_6$) δ ppm: 8.25 (br s, 1H), 7.82–7.80 (m, 2H), 7.67–7.66 (m, 2H), 3.73 (d, $J = 2.5$ Hz, 2H), 3.05 (t, $J = 2.5$ Hz, 1H). ^{13}C NMR (126 MHz, $\text{DMSO-}d_6$) δ ppm: 139.5, 137.4, 129.2 (2C), 128.7 (2C), 79.1, 74.9, 31.9.

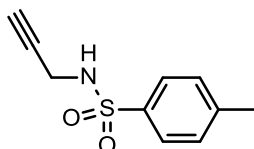
4-Methoxy-*N*-prop-2-ynyl-benzenesulfonamide (143)



Compound **143** was synthesized according to the general procedure F, using propargylamine (205 μL , 3.19 mmol), 4-methoxybenzenesulfonyl chloride (600 mg, 2.90 mmol) and *N,N*-diisopropylethylamine (1010 μL , 5.81 mmol) in CH_2Cl_2 (10 mL) overnight. The crude product was purified by flash

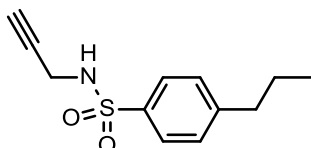
chromatography on silica gel (cHex to cHex/EtOAc: 5/5) affording compound **143** as a yellowish solid (528 mg, 76%). LC tr = 3.35 min, MS (ESI+): $m/z = 226 [M + H]^+$. $^1\text{H NMR}$ (500 MHz, $\text{DMSO-}d_6$) δ ppm: 7.95 (br s, 1H), 7.74–7.71 (m, 2H), 7.11–7.08 (m, 2H), 3.83 (s, 3H), 3.64 (d, $J = 2.5$ Hz, 2H), 3.04 (t, $J = 2.5$ Hz, 1H). $^{13}\text{C NMR}$ (126 MHz, $\text{DMSO-}d_6$) δ ppm: 162.0, 132.1, 128.9 (2C), 114.2 (2C), 79.5, 74.6, 55.6, 31.9.

4-Methyl-*N*-prop-2-ynyl-benzenesulfonamide (**107**)



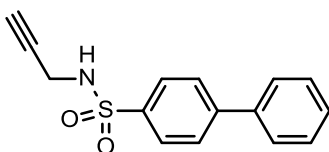
Compound **107** was synthesized according to the general procedure F, using propargylamine (111 μL , 1.73 mmol), 4-methylbenzenesulfonyl chloride (300 mg, 1.57 mmol) and *N,N*-diisopropylethylamine (548 μL , 3.15 mmol) in CH_2Cl_2 (5 mL) overnight. Compound **107** was obtained as a white solid (302 mg, 89%) and used in the next step without further purifications. LC tr = 3.58 min, MS (ESI+): $m/z = 210 [M + H]^+$. $^1\text{H NMR}$ (500 MHz, $\text{DMSO-}d_6$) δ ppm: 8.04 (t, $J = 5.9$ Hz, 1H), 7.69–7.68 (m, 2H), 7.39–7.38 (m, 2H), 3.65 (dd, $J = 5.9$ and 2.5 Hz, 2H), 3.05 (t, $J = 2.5$ Hz, 1H), 2.38 (s, 3H). $^{13}\text{C NMR}$ (126 MHz, $\text{DMSO-}d_6$) δ ppm: 142.8, 137.6, 129.5 (2C), 126.7 (2C), 79.4, 74.6, 31.9, 21.0.

4-Propyl-*N*-prop-2-ynyl-benzenesulfonamide (**108**)



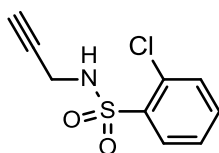
Compound **108** was synthesized according to the general procedure F, using propargylamine (97 μL , 1.51 mmol), 4-propylbenzenesulfonyl chloride (300 mg, 1.37 mmol) and *N,N*-diisopropylethylamine (478 μL , 2.74 mmol) in CH_2Cl_2 (5 mL) overnight. The crude product was purified by flash chromatography on silica gel (cHex to cHex/EtOAc: 7/3) affording compound **108** as a white solid (149 mg, 45%). LC tr = 4.31 min, MS (ESI+): $m/z = 238 [M + H]^+$. $^1\text{H NMR}$ (500 MHz, $\text{DMSO-}d_6$) δ ppm: 8.04 (t, $J = 5.1$ Hz, 1H), 7.71–7.70 (m, 2H), 7.40–7.38 (m, 2H), 3.67–3.65 (m, 2H), 3.02 (t, $J = 2.5$ Hz, 1H), 2.63 (t, $J = 7.4$ Hz, 2H), 1.60 (sep, $J = 7.4$ Hz, 2H), 0.88 (t, $J = 7.3$ Hz, 3H). $^{13}\text{C NMR}$ (126 MHz, $\text{DMSO-}d_6$) δ ppm: 147.3, 137.8, 129.0 (2C), 126.8 (2C), 79.4, 74.6, 37.0, 31.9, 23.8, 13.5.

4-Phenyl-*N*-prop-2-ynyl-benzenesulfonamide (**95**)



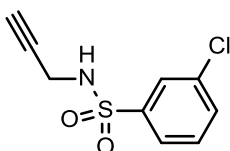
Compound **95** was synthesized according to the general procedure F, using propargylamine (83.6 μL , 1.31 mmol), 4-phenylbenzenesulfonyl chloride (300 mg, 1.19 mmol) and *N,N*-diisopropylethylamine (414 μL , 2.37 mmol) in CH_2Cl_2 (5 mL) overnight. Compound **95** was obtained as a white solid (298 mg, 91%) and used in the next step without further purifications. LC tr = 4.39 min, MS (ESI+): $m/z = 272$ $[\text{M} + \text{H}]^+$. ^1H NMR (500 MHz, $\text{DMSO-}d_6$) δ ppm: 8.20 (t, $J = 5.7$ Hz, 1H), 7.89 (s, 4H), 7.74 (d, $J = 7.5$ Hz, 2H), 7.51 (t, $J = 7.4$ Hz, 2H), 7.44 (t, $J = 7.2$ Hz, 1H), 3.73 (dd, $J = 6.3$ and 2.6 Hz, 2H), 3.06 (t, $J = 2.6$ Hz, 1H). ^{13}C NMR (126 MHz, $\text{DMSO-}d_6$) δ ppm: 144.0, 139.2, 138.6, 129.1 (2C), 128.5, 127.4 (2C), 127.3 (2C), 127.1 (2C), 79.4, 74.8, 32.0.

2-Chloro-*N*-prop-2-ynyl-benzenesulfonamide (**144**)



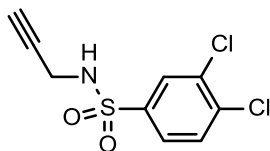
Compound **144** was synthesized according to the general procedure F, using propargylamine (167 μL , 2.21 mmol), 2-chlorobenzenesulfonyl chloride (500 mg, 2.37 mmol) and *N,N*-diisopropylethylamine (825 μL , 4.74 mmol) in CH_2Cl_2 (10 mL) overnight. The crude product was purified by flash chromatography on silica gel (cHex to cHex/EtOAc: 7/3) affording compound **144** as a white solid (478 mg, 87%). LC tr = 3.49 min, MS (ESI+): $m/z = 230$ $[\text{M} + \text{H}]^+$. ^1H NMR (500 MHz, $\text{DMSO-}d_6$) δ ppm: 8.33 (br s, 1H), 7.99–7.97 (m, 1H), 7.66–7.62 (m, 2H), 7.54–7.51 (m, 1H), 3.78 (d, $J = 2.5$ Hz, 2H), 2.96 (t, $J = 2.5$ Hz, 1H). ^{13}C NMR (126 MHz, $\text{DMSO-}d_6$) δ ppm: 138.1, 134.1, 131.6, 130.9, 130.5, 127.5, 79.1, 74.3, 31.8.

3-Chloro-*N*-prop-2-ynyl-benzenesulfonamide (**145**)



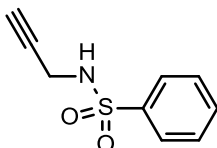
Compound **145** was synthesized according to the general procedure F, using propargylamine (167 μL , 2.21 mmol), 3-chlorobenzenesulfonyl chloride (500 mg, 2.37 mmol) and *N,N*-diisopropylethylamine (825 μL , 4.74 mmol) in CH_2Cl_2 (10 mL) overnight. The crude product was purified by flash chromatography on silica gel (cHex to cHex/EtOAc: 7/3) affording compound **145** as a white solid (300 mg, 54%). LC tr = 3.81 min, MS (ESI-): $m/z = 228$ $[\text{M} - \text{H}]^-$. ^1H NMR (500 MHz, $\text{DMSO-}d_6$) δ ppm: 8.30 (br s, 1H), 7.83–7.82 (m, 1H), 7.78–7.72 (m, 2H), 7.64–7.61 (m, 1H), 3.76 (d, $J = 2.4$ Hz, 2H), 3.05 (t, $J = 2.4$ Hz, 1H). ^{13}C NMR (126 MHz, $\text{DMSO-}d_6$) δ ppm: 142.5, 133.6, 132.5, 131.2, 126.4, 125.4, 79.1, 74.9, 31.9.

3,4-Dichloro-*N*-prop-2-ynylbenzenesulfonamide (146)



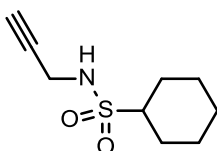
Compound **146** was synthesized according to the general procedure F, using propargylamine (172 μ L, 2.69 mmol), 3,4-chlorobenzenesulfonyl chloride (600 mg, 2.44 mmol) and *N,N*-diisopropylethylamine (851 μ L, 4.89 mmol) in CH_2Cl_2 (10 mL) overnight. The crude product was purified by flash chromatography on silica gel (cHex to cHex/EtOAc: 7/3) affording compound **146** as a white solid (436 mg, 66%). LC tr = 4.22 min, MS (ESI-): $m/z = 262, 264$ and 266 $[\text{M} - \text{H}]^-$. ^1H NMR (500 MHz, $\text{DMSO}-d_6$) δ ppm: 8.38 (br s, 1H), 8.00–7.99 (m, 1H), 7.89–7.88 (m, 1H), 7.77–7.76 (m, 1H), 3.78 (d, $J = 2.3$ Hz, 2H), 3.09 (t, $J = 2.3$ Hz, 1H). ^{13}C NMR (126 MHz, $\text{DMSO}-d_6$) δ ppm: 141.0, 135.6, 131.9, 131.5, 128.6, 127.0, 79.0, 75.1, 31.9.

N-Prop-2-ynylbenzenesulfonamide (148)



Compound **148** was synthesized according to the general procedure F, using propargylamine (239 μ L, 3.74 mmol), benzenesulfonyl chloride (600 mg, 3.4 mmol) and *N,N*-diisopropylethylamine (1180 μ L, 6.79 mmol) in CH_2Cl_2 (10 mL) overnight. The crude product was purified by flash chromatography on silica gel (cHex to cHex/EtOAc: 7/3) affording compound **148** as light yellow oil (527 mg, 78%). LC tr = 3.17 min, MS (ESI+): $m/z = 196$ $[\text{M} + \text{H}]^+$. ^1H NMR (500 MHz, $\text{DMSO}-d_6$) δ ppm: 8.16 (br s, 1H), 7.82–7.80 (m, 2H), 7.66–7.63 (m, 1H), 7.60–7.57 (m, 2H), 3.69 (d, $J = 2.5$ Hz, 2H), 3.04 (t, $J = 2.5$ Hz, 1H). ^{13}C NMR (126 MHz, $\text{DMSO}-d_6$) δ ppm: 140.5, 132.6, 129.1 (2C), 126.7 (2C), 79.3, 74.6, 31.9.

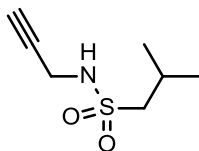
N-Prop-2-ynylcyclohexanesulfonamide (149)



Compound **149** was synthesized according to the general procedure F, using propargylamine (193 μ L, 3.01 mmol), cyclohexanesulfonyl chloride (500 mg, 2.74 mmol) and *N,N*-diisopropylethylamine (954 μ L, 5.47 mmol) in CH_2Cl_2 (10 mL) overnight. The crude product was purified by flash chromatography on silica gel (cHex to cHex/EtOAc: 4/6) affording compound **149** as yellow oil (116 mg, 20%). LC tr = not visible (254 nm), MS (ESI+): no ionization $[\text{M} + \text{H}]^+$; MS (ESI-): no ionization $[\text{M} - \text{H}]^-$. ^1H NMR (500 MHz, $\text{DMSO}-d_6$) δ ppm: 7.57 (t, $J = 6.0$ Hz, 1H), 3.77 (dd, $J = 6.0$ and 2.5 Hz,

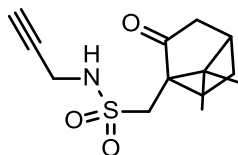
2H), 3.29 (t, $J = 2.5$ Hz, 1H), 2.95 (tt, $J = 17.6$ and 3.4 Hz, 1H), 2.07–2.05 (m, 2H), 1.79 (dt, $J = 12.7$ and 2.9 Hz, 2H), 1.63 (dt, $J = 12.7$ and 3.4 Hz, 1H), 1.38–1.08 (m, 5H). ^{13}C NMR (126 MHz, DMSO- d_6) δ ppm: 80.6, 74.3, 59.7, 31.6, 25.9 (2C), 24.8, 24.6 (2C).

2-Methyl-*N*-prop-2-ynyl-propane-1-sulfonamide (106)



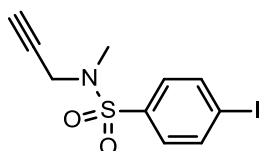
Compound **106** was synthesized according to the general procedure F, using propargylamine (135 μL , 2.11 mmol), 2-methylpropane-1-sulfonyl chloride (300 mg, 1.92 mmol) and *N,N*-diisopropylethylamine (667 μL , 3.83 mmol) in CH_2Cl_2 (10 mL) overnight. The crude product was purified by flash chromatography on silica gel (cHex to cHex/EtOAc: 4/6) affording compound **106** as yellow oil (271 mg, 79%). LC tr = not visible (254 nm), MS (ESI+): no ionization $[\text{M} + \text{H}]^+$; MS (ESI-): no ionization $[\text{M} - \text{H}]^-$. ^1H NMR (500 MHz, DMSO- d_6) δ ppm: 7.58 (t, $J = 5.9$ Hz, 1H), 3.78 (dd, $J = 5.9$ and 2.5 Hz, 2H), 3.30 (t, $J = 2.5$ Hz, 1H), 2.97 (d, $J = 6.4$ Hz, 2H), 2.12 (sep, $J = 6.8$ Hz, 1H), 1.03–1.01 (m, 6H). ^{13}C NMR (126 MHz, DMSO- d_6) δ ppm: 80.5, 74.6, 59.6, 31.5, 24.2, 22.2 (2C).

1-(7,7-Dimethyl-2-oxo-norbornan-1-yl)-*N*-prop-2-ynyl-methanesulfonamide (94)



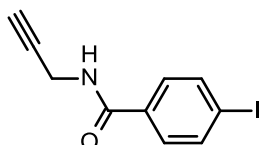
Compound **94** was synthesized according to the general procedure F, using propargylamine (84.3 μL , 1.32 mmol), (7,7-dimethyl-2-oxo-norbornan-1-yl)methanesulfonyl chloride (300 mg, 1.2 mmol) and *N,N*-diisopropylethylamine (417 μL , 2.39 mmol) in CH_2Cl_2 (5 mL) overnight. Compound **94** was obtained as a white solid (210 mg, 64%) and used in the next step without further purifications. LC tr = 3.59 min, MS (ESI+): $m/z = 270$ $[\text{M} + \text{H}]^+$. ^1H NMR (500 MHz, DMSO- d_6) δ ppm: 7.57 (t, $J = 6.0$ Hz, 1H), 3.84 (dd, $J = 6.0$ and 2.5 Hz, 2H), 3.42 (d, $J = 14.9$ Hz, 1H), 3.04 (d, $J = 14.9$ Hz, 1H), 2.37–2.32 (m, 2H), 2.05 (t, $J = 4.5$ Hz, 1H), 1.99–1.90 (m, 2H), 1.54–1.48 (m, 1H), 1.42–1.37 (m, 1H), 1.03 (s, 3H), 0.80 (s, 3H). ^{13}C NMR (126 MHz, DMSO- d_6) δ ppm: 215.0, 80.5, 75.0, 58.0, 49.2, 47.6, 42.1, 42.0, 31.9, 26.3, 24.6, 19.6, 19.4.

4-Iodo-*N*-methyl-*N*-prop-2-ynyl-benzenesulfonamide (115)



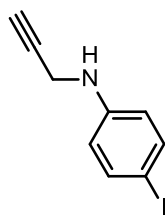
Compound **115** was synthesized according to the general procedure F, using *N*-methylpropargylamine (92 μ L, 1.09 mmol), 4-iodobenzenesulfonyl chloride (300 mg, 0.99 mmol) and *N,N*-diisopropylethylamine (345 μ L, 1.98 mmol) in CH_2Cl_2 (5 mL) overnight. Compound **94** was obtained as a white solid (327 mg, 97%) and used in the next step without further purifications. LC tr = 4.55 min, MS (ESI+): $m/z = 336$ $[\text{M} + \text{H}]^+$. ^1H NMR (500 MHz, $\text{DMSO-}d_6$) δ ppm: 8.01–7.99 (m, 2H), 7.57–7.54 (m, 2H), 4.03 (d, $J = 2.4$ Hz, 2H), 3.16 (t, $J = 2.4$ Hz, 1H), 2.73 (s, 3H). ^{13}C NMR (126 MHz, $\text{DMSO-}d_6$) δ ppm: 138.1 (2C), 136.3, 129.2 (2C), 101.6, 76.8, 76.6, 39.3, 34.1.

4-Iodo-*N*-prop-2-ynyl-benzamide (116)



Propargylamine (79.3 μ L, 1.24 mmol) and triethylamine (308 μ L, 2.25 mmol) were solubilized in CH_2Cl_2 (5 mL). The reaction media was cooled at 0°C and 4-iodobenzoyl chloride (300 mg, 1.13 mmol) was added. The mixture was allowed to reach room temperature and was stirred overnight. Then, it was diluted in water and washed twice with 0.25 M aq. HCl, with sat. aq. NaHCO_3 and brine. The organic layer was dried over MgSO_4 , filtered and concentrated under reduced pressure affording compound **116** as an orange powder (159 mg, 49%). LC tr = 3.71 min, MS (ESI+): $m/z = 286$ $[\text{M} + \text{H}]^+$. ^1H NMR (500 MHz, $\text{DMSO-}d_6$) δ ppm: 9.01 (t, $J = 5.4$ Hz, 1H), 7.87–7.85 (m, 2H), 7.64–7.62 (m, 2H), 4.04 (dd, $J = 5.4$ and 2.4 Hz, 2H), 3.12 (t, $J = 2.4$ Hz, 1H). ^{13}C NMR (126 MHz, $\text{DMSO-}d_6$) δ ppm: 165.3, 137.3 (2C), 133.2, 129.3 (2C), 99.2, 81.1, 73.0, 28.5.

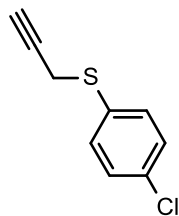
4-Iodo-*N*-prop-2-ynyl-aniline (118)



To a solution of 4-iodoaniline (300 mg, 1.37 mmol) in DMF (3 mL) were added K_2CO_3 (379 mg, 2.74 mmol) and propargylbromide (143 μ L, 1.51 mmol). The resulting solution was stirred at room temperature for 48h. After 48h, the conversion was not complete and propargylbromide (195 μ L, 2.05 mmol) was added and the mixture was stirred overnight at 60°C . The conversion was not significantly increased and the reaction was therefore stopped at 50% of conversion (LC-MS monitoring). The mixture was then diluted in water and extracted three times with ethyl acetate. Combined organic layers were dried over MgSO_4 , filtered and concentrated under reduced pressure. Finally, the residue was purified through two successive flash chromatographies on silica gel (cHex to cHex/EtOAc: 6/4) and (cHex/ CH_2Cl_2 to cHex/ CH_2Cl_2 : 7/3 to 5/5) affording compound **118** as brown oil (100 mg, 28%). LC tr = 3.61 min, MS (ESI+): $m/z = 258$ $[\text{M} + \text{H}]^+$. ^1H NMR (500 MHz, $\text{DMSO-}d_6$)

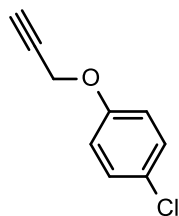
δ : 7.39–7.37 (m, 2H), 6.49–6.48 (m, 2H), 6.22 (t, $J = 6.1$ Hz, 1H), 3.83 (dd, $J = 6.1$ and 2.4 Hz, 2H), 3.08 (t, $J = 2.4$ Hz, 1H). ^{13}C NMR (126 MHz, DMSO- d_6) δ : 147.5, 137.1 (2C), 115.5 (2C), 81.8, 77.4, 73.2, 31.9.

1-Chloro-4-prop-2-ynylsulfanyl-benzene (120)



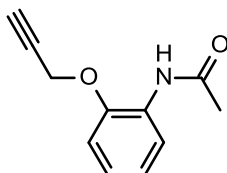
To a solution of 4-chlorobenzenethiol (300 mg, 2.07 mmol) in DMF (3 mL) were added K_2CO_3 (573 mg, 4.15 mmol) and propargylbromide (216 μL , 2.28 mmol). The resulting solution was heated at 60°C and stirred overnight. The mixture was then diluted in water and extracted three times with ethyl acetate. Combined organic layers were dried over MgSO_4 , filtered and concentrated under reduced pressure affording the desired product as a brown solid (352 mg, 92%). LC tr = 4.81 min, MS (ESI+): $m/z = \text{no ionisation } [\text{M} + \text{H}]^+$, (ESI-): $m/z = \text{no ionisation } [\text{M} - \text{H}]^-$. ^1H NMR (500 MHz, DMSO- d_6) δ ppm: 7.41 (s, 4H), 3.87 (d, $J = 2.6$ Hz, 2H), 3.16 (t, $J = 2.6$ Hz, 1H). ^{13}C NMR (126 MHz, DMSO- d_6) δ ppm: 134.0, 131.0, 130.2 (2C), 128.9 (2C), 80.1, 74.0, 20.6.

1-Chloro-4-prop-2-ynoxy-benzene (119)



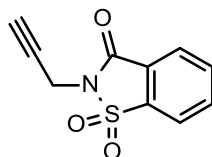
To a solution of 4-chlorophenol (300 mg, 2.33 mmol) in DMF (3 mL) were added K_2CO_3 (645 mg, 4.67 mmol) and propargylbromide (243 μL , 2.57 mmol). The resulting solution was heated at 60°C and stirred overnight. The mixture was then diluted in water and extracted three times with ethyl acetate. Organic layers were combined and solvents were evaporated under reduced pressure and the residue was purified through flash chromatography on silica gel (cHex to cHex/EtOAc: 8/2) affording compound **119** as a brown solid (376 mg, 96%). LC tr = 4.55 min, MS (ESI+): $m/z = \text{no ionisation } [\text{M} + \text{H}]^+$, (ESI-): $m/z = \text{no ionisation } [\text{M} - \text{H}]^-$. ^1H NMR (500 MHz, DMSO- d_6) δ ppm: 7.37–7.34 (m, 2H), 7.03–6.99 (m, 2H), 4.80 (d, $J = 2.4$ Hz, 2H), 3.59 (t, $J = 2.3$ Hz, 1H). ^{13}C NMR (126 MHz, DMSO- d_6) δ ppm: 156.0, 129.2 (2C), 125.0, 116.7 (2C), 78.9, 78.5, 55.7.

N-(2-Prop-2-ynoxyphenyl)acetamide (100)



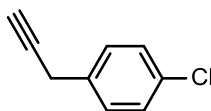
To a solution of N-(2-hydroxyphenyl)acetamide (150 mg, 0.99 mmol) in DMF (5 mL) were added K_2CO_3 (274 mg, 1.98 mmol) and propargylbromide (103 μ L, 1.09 mmol). The resulting solution was heated at 60°C and stirred overnight. The mixture was then diluted in water and extracted three times with ethyl acetate. Organic layers were combined and solvents were evaporated under reduced pressure affording compound **100** as a brown solid (182 mg, 96%). LC tr = 3.03 min, MS (ESI+): m/z = 190 $[M + H]^+$. 1H NMR (500 MHz, DMSO- d_6) δ ppm: 9.13 (s, 1H), 7.91 (d, J = 7.5 Hz, 1H), 7.12–7.11 (m, 1H), 7.06 (t, J = 7.5 Hz, 1H), 6.93 (t, J = 7.5 Hz, 1H), 4.86 (d, J = 2.0 Hz, 2H), 3.60 (t, J = 2.2 Hz, 1H), 2.08 (s, 3H). ^{13}C NMR (126 MHz, DMSO- d_6) δ ppm: 168.5, 147.6, 127.9, 124.1, 122.6, 121.0, 112.9, 79.2, 78.6, 56.0, 23.8.

1,1-Dioxo-2-prop-2-ynyl-1,2-benzothiazol-3-one (117)⁽¹³⁹⁾



Saccharin (500 mg, 2.73 mmol) was dissolved in dry DMF (3 mL). Sodium carbonate (289 mg, 2.73 mmol) was added portion wise followed by propargyl bromide (441 μ L, 80 wt% in toluene, 4.09 mmol). The reaction media was stirred overnight at 80°C. The mixture was then diluted in ethyl acetate and washed with brine. The organic layer was dried over $MgSO_4$, filtered and concentrated under reduced pressure affording compound **117** as a brown solid (548 mg, 89%). LC tr = 3.47 min, MS (ESI+): m/z = 222 $[M + H]^+$. 1H NMR (500 MHz, DMSO- d_6) δ ppm: 8.34 (dt, J = 7.7 and 0.8 Hz, 1H), 8.14 (dt, J = 7.7 and 0.8 Hz, 1H), 8.07 (td, J = 11.4 and 1.1 Hz, 1H), 8.01 (td, J = 11.4 and 0.9 Hz, 1H), 4.58 (d, J = 2.5 Hz, 2H), 3.40 (t, J = 2.5 Hz, 1H). ^{13}C NMR (126 MHz, DMSO- d_6) δ ppm: 157.9, 136.9, 136.1, 135.4, 126.0, 125.3, 121.7, 77.0, 75.2, 27.5.

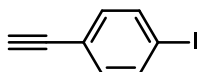
1-Chloro-4-prop-2-ynyl-benzene (121)



2-(4-chlorophenyl)acetaldehyde (500 mg, 3.23 mmol) and potassium carbonate (894 mg, 6.47 mmol) were mixed in anhydrous methanol (7 mL) followed by a dropwise addition of the Ohira-Bestmann reagent (647 μ L, 4.31 mmol) and the reaction media was stirred overnight at room temperature overnight. The mixture was then diluted in CH_2Cl_2 and washed with 5% aq. $NaHCO_3$. The organic

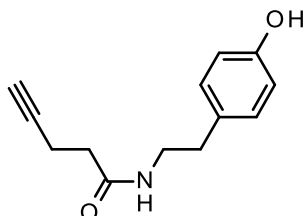
layer was concentrated under reduced pressure and the residue was purified through flash silica gel column (cH to cH/EtOAc 9:1), affording compound **121** as yellow oil (169 mg, 32%). LC tr = 5.14 min, MS (ESI+): m/z = no ionization $[M + H]^+$; MS (ESI-): m/z = no ionization $[M - H]^-$. ^1H NMR (500 MHz, DMSO- d_6) δ ppm: 7.30 (s, 4H), 3.59 (d, $J = 2.7$ Hz, 2H), 2.21 (t, $J = 2.7$ Hz, 1H). ^{13}C NMR (126 MHz, DMSO- d_6) δ ppm: 134.7, 132.7, 129.3 (2C), 128.8 (2C), 81.5, 71.0, 24.4.

1-Ethynyl-4-iodo-benzene (122)



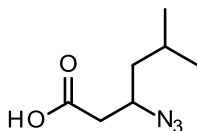
4-iodobenzaldehyde (600 mg, 2.59 mmol, 1 eq) and potassium carbonate (715 mg, 5.17 mmol, 2 eq) were mixed in anhydrous methanol (7.0 mL) followed by a dropwise addition of Ohira-Bestmann reagent (466 μL , 3.10 mmol, 1.2 eq). The resulting mixture was stirred overnight at room temperature. The mixture was then diluted with CH_2Cl_2 and washed with 5% aq. NaHCO_3 . The organic layer was dried over MgSO_4 , filtered and concentrated under reduced pressure. Finally, the residue was purified through flash silica gel column (cH to cH/EtOAc: 9:1) affording the desired product as a white solid (256 mg, 43%). LC tr = 4.96 min, MS (ESI+): m/z= no ionization $[M + H]^+$; MS (ESI-): m/z= no ionization $[M - H]^-$. ^1H NMR (500 MHz, CDCl_3) δ ppm: 7.68–7.66 (m, 2H), 7.22–7.20 (m, 2H), 3.13 (s, 1H). ^{13}C NMR (126 MHz, CDCl_3) δ ppm: 137.6 (2C), 133.6 (2C), 121.6, 94.9, 82.7, 78.6.

N-[2-(4-Hydroxyphenyl)ethyl]pent-4-ynamide (109)



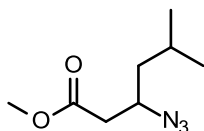
Pentynoic acid (100 mg, 1.02 mmol), tyramine (210.0 mg, 1.53 mmol, 1.5 eq) and HBTU (464 mg, 1.22 mmol, 1.2 eq) were put in solution in DMF (5.0 mL) and triethylamine (424 μL , 3.06 mmol, 3 eq) and the mixture was stirred overnight at room temperature. The resulting mixture was then diluted with water and extracted with EtOAc (three times). Organic layers were combined and solvents were evaporated in vacuo. The residue was then purified through flash silica gel column (cH/EtOAc: 9:1 to 5:5), affording compound **109** as a colorless oil (107 mg, 47%). LC tr = 2.57 min, MS (ESI+): m/z= 218 $[M + H]^+$. ^1H NMR (500 MHz, DMSO- d_6) δ ppm: 9.19 (s, 1H), 7.95 (t, $J = 5.5$ Hz, 1H), 6.99–6.97 (m, 2H), 6.68–6.65 (m, 2H), 3.20–3.16 (m, 2H), 2.78 (t, $J = 2.6$ Hz, 1H), 2.58–2.55 (m, 2H), 2.35–2.31 (m, 2H), 2.25–2.22 (m, 2H). ^{13}C NMR (126 MHz, DMSO- d_6) δ ppm: 170.1, 155.7, 129.6 (2C), 129.5, 115.1 (2C), 83.9, 71.4, 40.7, 34.4, 34.2, 14.3.

3-Azido-5-methyl-hexanoic acid (**76**)



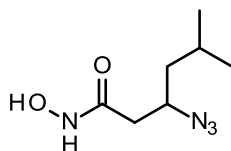
Compound **76** was synthesized according to the general procedure A, using β -homo leucine (363 mg, 2.50 mmol), ZnCl_2 (20.4 mg, 0.15 mmol), K_2CO_3 (1380 mg, 10.0 mmol), anhydrous *N,N*-diisopropylethylamine (479 μL , 2.75 mmol) and diazo transfer reagent (814 mg, 3.0 mmol) in anhydrous MeOH (10 mL) overnight. Compound **76** was obtained as light yellow oil (428 mg, 99%) and was used in the next step without further purification. LC tr = 2.52min. MS (ESI-): $m/z = 170.15$ $[\text{M} - \text{H}]^-$. ^1H NMR (300 MHz, $\text{MeOD-}d_4$) δ ppm: 3.87–3.84 (m, 1H), 2.54 (dd, $J = 16.2$ and 4.7 Hz, 1H), 2.42 (dd, $J = 16.2$ and 8.7 Hz, 1H), 1.81–1.74 (m, 1H), 1.53–1.43 (m, 1H), 1.38–1.29 (m, 1H), 0.97 (d, $J = 3.5$ Hz, 3H), 0.95 (d, $J = 3.5$ Hz, 3H). ^{13}C NMR (75 MHz, $\text{MeOD-}d_4$) δ ppm: 174.7, 58.9, 44.4, 40.6, 26.2, 23.4, 22.0.

Methyl 3-azido-5-methyl-hexanoate (**77**)



Compound **77** was synthesized according to the general procedure E, using carboxylic acid **76** (405 mg, 2.37 mmol) and thionyl chloride (345 μL , 4.73 mmol) in MeOH (8 mL) overnight. Compound **77** was obtained as yellow oil (345 mg, 77%) and was used in the next step without further purification. LC tr = 3.03 min, MS (ESI+): $m/z = 158$ $[\text{M} - 2\text{N} + \text{H}]^+$. ^1H NMR (300MHz, $\text{MeOD-}d_4$) δ ppm: 3.89–3.80 (m, 1H), 3.71 (s, 3H), 2.59 (dd, $J = 16.1$ and 4.6 Hz, 1H), 2.47 (dd, $J = 16.1$ and 8.9 Hz, 1H), 1.85–1.71 (m, 1H), 1.53–1.43 (m, 1H), 1.36–1.27 (m, 1H), 0.97 (d, $J = 3.8$ Hz, 3H), 0.95 (d, $J = 3.9$ Hz, 3H). ^{13}C NMR (75MHz, $\text{MeOD-}d_4$) δ ppm: 173.0, 58.8, 52.3, 44.3, 40.5, 26.2, 23.4, 22.0.

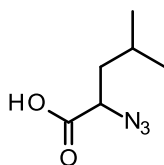
3-Azido-5-methyl-hexanehydroxamic acid (**Z7**)



Compound **Z7** was synthesized according to the general procedure G, using ester **77** (330 mg, 1.76 mmol), KCN (23 mg, 0.35 mmol) and aq. NH_2OH (5 mL, 50% w/w in water) in MeOH (5 mL) overnight. The crude product was purified by flash chromatography on silica gel (CH_2Cl_2 to $\text{CH}_2\text{Cl}_2/\text{MeOH}$: 9/1) affording compound **Z7** as a white solid after lyophilization (160 mg, 48%). Purity: 99%, LC tr = 2.02 min, MS (ESI-): $m/z = 185$ $[\text{M} - \text{H}]^-$. ^1H NMR ($\text{DMSO-}d_6$) δ ppm: 10.51 (br s, 1H), 8.86 (br s, 1H), 3.84–3.75 (m, 1H), 2.24 (dd, $J = 14.6$ and 5.1 Hz, 1H), 2.15 (dd, $J = 14.6$ and

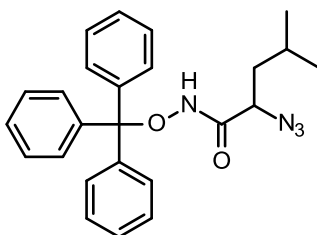
8.5 Hz, 1H), 1.77–1.64 (m, 1H), 1.45–1.36 (m, 1H), 1.34–1.25 (m, 1H), 0.90 (d, $J = 6.6$ Hz, 6H). ^{13}C NMR (DMSO- d_6) δ ppm: 166.0, 57.5, 42.5, 37.8, 24.6, 22.9, 21.5.

2-Azido-4-methyl-pentanoic acid (**78**)



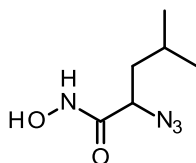
Compound **78** was synthesized according to the general procedure A, using leucine (328 mg, 2.50 mmol), ZnCl_2 (20.4 mg, 0.15 mmol), K_2CO_3 (1380 mg, 10.0 mmol), anhydrous N,N -diisopropylethylamine (479 μL , 2.75 mmol) and diazo transfer reagent (814 mg, 3.0 mmol) in anhydrous MeOH (10 mL) overnight. Compound **78** was obtained as light yellow oil (393 mg, quant. yield) and was used in the next step without further purification. LC tr = 2.00 min, MS (ESI-): $m/z = 156$ [M - H] $^-$. ^1H NMR (MeOD- d_4) δ ppm: 3.91 (t, $J = 7.3$ Hz, 1H), 1.79 (sep, $J = 6.7$ Hz, 1H), 1.67–1.62 (m, 2H), 0.98 (d, $J = 4.4$ Hz, 3H), 0.96 (d, $J = 4.4$ Hz, 3H). ^{13}C NMR (MeOD- d_4) δ ppm: 174.3, 61.5, 41.1, 26.3, 23.2, 21.8.

2-Azido-4-methyl- N -trityloxy-pentanamide (**79**)



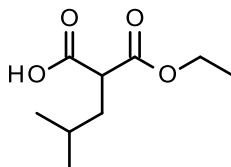
Carboxylic acid **78** (200 mg, 1.27 mmol) was dissolved in DMF (5 mL) and EDCI (610 mg, 3.18 mmol, 2.5 eq), HOBt (604 mg, 3.94 mmol), N -methylmorpholine (1.47 mL, 13.35 mmol) were added. The mixture was stirred at room temperature for 10 min, and O -tritylhydroxylamine (876 mg, 3.18 mmol) was added. The mixture was stirred at room temperature during 48h. Then, DMF was evaporated under reduced pressure and the residue was dissolved in EtOAc and washed with sat. aq. NaHCO_3 (three times) and with water (once). The organic layer was dried over MgSO_4 , filtered and concentrated under reduced pressure. The crude product was purified by flash chromatography on silica gel (cHex to cHex/ CH_2Cl_2 5:5) to give **79** as a white solid (103 mg, 19%). LC tr = 3.58 min, MS (ESI-): $m/z = 413$ [M - H] $^-$. ^1H NMR (DMSO- d_6) δ ppm: 10.78 (s, 1H), 7.36–7.27 (m, 15H), 3.44–3.38 (m, 1H), 1.30–1.15 (m, 2H), 1.11–1.03 (m, 1H), 0.75 (d, $J = 6.4$ Hz, 3H), 0.73 (d, $J = 6.4$ Hz, 3H). ^{13}C NMR (DMSO- d_6) δ ppm: 167.7, 142.0 (3C), 128.8 (6C), 127.7 (6C), 126.6 (3C), 92.3, 56.5, 52.0, 24.1, 22.32, 21.8.

2-Azido-4-methyl-pentanehydroxamic acid (**Z8**)



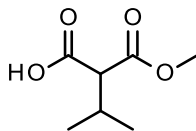
The O-trityl hydroxamate intermediate **79** (220 mg, 0.53 mmol) was dissolved in CH₂Cl₂ (5 mL) and cooled down to 0°C before an addition of TFA (0.25 mL) and triisopropylsilane (0.25 mL) were added. The mixture was stirred at room temperature for 20 min. Solvents were removed under reduced pressure and the residue was purified by flash chromatography on silica gel (CH₂Cl₂ to CH₂Cl₂/MeOH: 9:1) to give **Z8** as a brownish oil (36 mg, 39%). Purity: 100%, LC tr = 1.90 min, MS (ESI-): m/z = 171 [M - H]⁻ ¹H NMR (CDCl₃) δ ppm: 9.14 (br s, 2H), 3.95–3.90 (m, 1H), 1.82–1.76 (m, 1H), 1.72–1.69 (m, 2H), 0.96 (d, J = 6.0 Hz, 6H). ¹³C NMR (CDCl₃) δ ppm: 168.5, 60.6, 40.8, 25.0, 23.0, 21.7.

2-Ethoxycarbonyl-4-methyl-pentanoic acid (**80**)



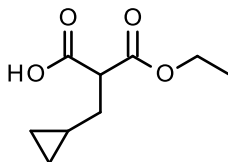
Compound **80** was synthesized according to the general procedure I, using diethylmalonate (1000 mg, 4.62 mmol) and NaOH (222 mg, 5.55 mmol) in EtOH/H₂O (10 mL, 8:2 v/v) overnight. Compound **80** was obtained as colorless oil (711 mg, 80%) and was used in the next step without further purification. LC tr = 2.10 min, MS (ESI+): m/z = 189 [M + H]⁺. ¹H NMR (MeOD-*d*₄) δ ppm: 4.18 (q, J = 7.1 Hz, 2H), 3.41 (t, J = 7.6 Hz, 1H), 1.77–1.72 (m, 2H), 1.64–1.50 (m, 1H), 1.26 (t, J = 7.1 Hz, 3H), 0.93 (d, J = 6.5 Hz, 6H). ¹³C NMR (MeOD-*d*₄) δ ppm: 173.0, 171.6, 62.3, 51.4, 38.8, 27.4, 22.7, 22.5, 14.4.

2-Methoxycarbonyl-3-methyl-butanoic acid (**174-a**)



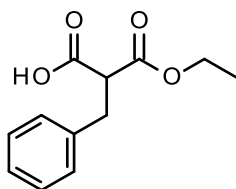
Compound **174-a** was synthesized according to the general procedure I, using dimethylmalonate (745 mg, 4.28 mmol) and KOH (240 mg, 4.28 mmol) in MeOH/H₂O (11 mL, 10:1 v/v) overnight. Compound **174-a** was obtained as colorless oil (711 mg, 80%) and was used in the next step without further purification. LC tr = 2.71 min, MS (ESI+): m/z = 161 [M + H]⁺. ¹H NMR (500 MHz, DMSO-*d*₆) δ ppm: 12.85 (s, 1H), 3.63 (s, 3H), 3.11 (d, J = 8.6 Hz, 1H), 2.23–2.14 (m, 1H), 0.93 (d, J = 6.7 Hz, 3H), 0.91 (d, J = 6.7 Hz, 3H). ¹³C NMR (126 MHz, DMSO-*d*₆) δ ppm: 169.7, 169.2, 58.2, 51.9, 28.0, 20.1, 20.0.

2-(Cyclopropylmethyl)-3-ethoxy-3-oxo-propanoic acid (**175-a**)



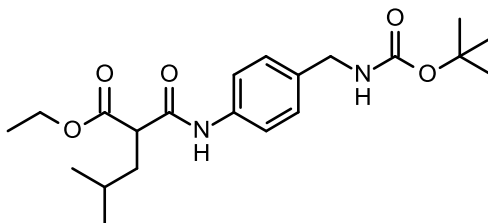
Compound **175-a** was synthesized according to the general procedure I, using dimethylmalonate (550 mg, 2.57 mmol) and KOH (144 mg, 2.57 mmol) in EtOH/H₂O (9 mL, 8:1 v/v) overnight. Compound **175-a** was obtained as colorless oil (347 mg, 71%) and was used in the next step without further purification. LC tr = not visible, MS (ESI+): m/z= 187 [M + H]⁺. ¹H NMR (500 MHz, DMSO-*d*₆) δ ppm: 12.80 (br s, 1H), 4.11 (q, *J* = 7.1 Hz, 2H), 3.40–3.35 (m, 1H), 1.69–1.60 (m, 2H), 1.18 (t, *J* = 7.1 Hz, 3H), 0.71–0.63 (m, 1H), 0.39–0.37 (m, 2H), 0.09–0.03 (m, 2H). ¹³C NMR (126 MHz, DMSO-*d*₆) δ ppm: 170.4, 169.5, 60.6, 51.9, 33.2, 14.0, 8.7, 4.4, 4.2.

2-Benzyl-3-ethoxy-3-oxo-propanoic acid (**173-a**)



Compound **173-a** was synthesized according to the general procedure I, using dimethylmalonate (1070 mg, 4.28 mmol) and KOH (240 mg, 4.28 mmol) in EtOH/H₂O (11 mL, 10:1 v/v) overnight. Compound **173-a** was obtained as colorless oil (694 mg, 72%) and was used in the next step without further purification. LC tr = 3.72 min, MS (ESI+): m/z= no ionization [M + H]⁺. ¹H NMR (500 MHz, CDCl₃) δ ppm: 10.23 (br s, 1H), 7.36–7.31 (m, 2H), 7.30–7.26 (m, 3H), 4.22 (q, *J* = 7.1 Hz, 2H), 3.76 (t, *J* = 7.7 Hz, 1H), 3.30 (dd, *J* = 7.7 and 2.8 Hz, 2H), 1.26 (t, *J* = 7.1 Hz, 3H). ¹³C NMR (126 MHz, CDCl₃) δ ppm: 174.3, 168.9, 137.4, 128.9 (2C), 128.7 (2C), 127.1, 62.0, 53.6, 34.9, 14.1.

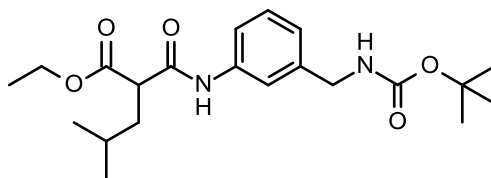
Ethyl 2-[[4-[(*tert*-butoxycarbonylamino)methyl]phenyl]carbamoyl]-4-methyl-pentanoate (**81**)



Compound **81** was synthesized according to the general procedure B, using carboxylic acid **80** (450 mg, 2.39 mmol), *tert*-butyl *N*-[(4-aminophenyl)methyl]carbamate (638 mg, 2.87 mmol), HBTU (1540 mg, 4.06 mmol) and trimethylamine (981 μL, 7.17 mmol) in DMF (8 mL) overnight. The crude product was purified by flash chromatography on silica gel (cHex/EtOAc: 9/1 to 7/3) affording compound **81** as an off-white solid (456 mg, 47%). LC tr = 3.03 min, MS (ESI-): m/z= 391 [M - H]⁻. ¹H NMR (DMSO-*d*₆) δ ppm: 10.18 (s, 1H), 7.52–7.49 (m, 2H), 7.33 (t, *J* = 6.0 Hz, 1H), 7.18–7.15 (m,

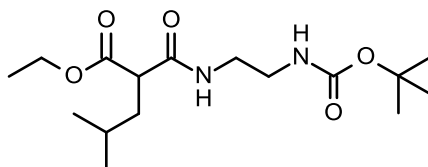
2H), 4.15–4.02 (m, 4H), 3.56 (dd, $J = 8.6$ Hz and 6.3 Hz, 1H), 1.80–1.60 (m, 2H), 1.57–1.45 (m, 1H), 1.39 (s, 9H), 1.16 (t, $J = 7.1$ Hz, 3H), 0.90 (d, $J = 6.6$ Hz, 3H), 0.87 (d, $J = 6.6$ Hz, 3H). ^{13}C NMR (DMSO- d_6) δ ppm: 169.8, 166.9, 155.7, 137.4, 135.4, 127.4 (2C), 119.2 (2C), 77.7, 60.6, 50.9, 43.0, 37.4, 28.2 (3C), 25.6, 22.6, 21.9, 14.0.

Ethyl 2-[[3-[(*tert*-butoxycarbonylamino)methyl]phenyl]carbamoyl]-4-methyl-pentanoate (110)



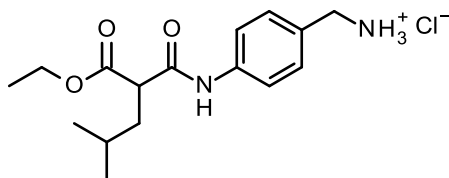
Compound **110** was synthesized according to the general procedure B, using carboxylic acid **80** (320 mg, 1.7 mmol), *tert*-butyl *N*-[(3-aminophenyl)methyl]carbamate (416 mg, 1.87 mmol), HBTU (967 mg, 2.55 mmol) and trimethylamine (697 μL , 5.10 mmol) in DMF (5 mL) overnight. The crude product was purified by flash chromatography on silica gel (cHex/EtOAc: 9/1 to 7/3) affording compound **110** as a yellowish solid (507 mg, 74%). LC tr = 4.77 min, MS (ESI+): $m/z = 393$ [M + H] $^+$, 337 [M - tBu] $^+$. ^1H NMR (500 MHz, DMSO- d_6) δ ppm: 10.24 (s, 1H), 7.47–7.45 (m, 2H), 7.42 (t, $J = 6.1$ Hz, 1H), 7.24 (t, $J = 8.0$ Hz, 1H), 6.93 (d, $J = 7.6$ Hz, 1H), 4.13–4.04 (m, 4H), 3.57 (dd, $J = 8.9$ and 6.0 Hz, 1H), 1.78–1.72 (m, 1H), 1.66–1.60 (m, 1H), 1.48 (sep, $J = 6.7$ Hz, 1H), 1.39 (s, 9H), 1.18–1.14 (m, 3H), 0.89 (d, $J = 6.6$ Hz, 3H), 0.87 (d, $J = 6.6$ Hz, 3H). ^{13}C NMR (126 MHz, DMSO- d_6) δ ppm: 169.9, 167.1, 155.8, 141.0, 138.8, 128.7, 122.3, 117.8, 117.7, 77.9, 60.7, 50.9, 43.4, 37.5, 28.3 (3C), 25.7, 22.8, 21.9, 14.1.

Ethyl 2-[2-(*tert*-butoxycarbonylamino)ethylcarbamoyl]-4-methyl-pentanoate (84)



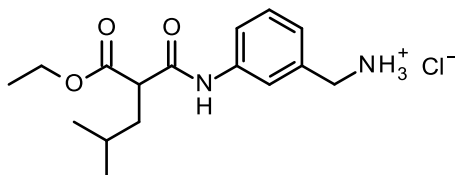
Compound **84** was synthesized according to the general procedure B, using carboxylic acid **80** (300 mg, 1.59 mmol), *tert*-butyl *N*-(2-aminoethyl)carbamate (281 mg, 1.75 mmol), HOBt (24.4 mg, 0.16 mmol), EDC.HCl (458 mg, 2.39 mmol) and diisopropylethylamine (833 μL , 4.78 mmol) in CH_2Cl_2 (8 mL) overnight. The crude product was purified by flash chromatography on silica gel (cHex to cHex/EtOAc: 6/4) affording compound **84** as a yellowish solid (423 mg, 80%). LC tr = 2.67 min, MS (ESI-): $m/z = 329$ [M - H] $^-$. ^1H NMR (DMSO- d_6) δ ppm: 8.13 (t, $J = 5.3$ Hz, 1H), 6.71 (t, $J = 5.2$ Hz, 1H), 4.08 (dd, $J = 7.1$ and 1.7 Hz, 1H), 4.03 (dd, $J = 7.1$ and 1.7 Hz, 1H), 3.30–3.25 (m, 1H), 3.15–3.04 (m, 2H), 3.01–2.94 (m, 2H), 1.65–1.40 (m, 3H), 1.37 (s, 9H), 1.15 (t, $J = 7.1$ Hz, 3H), 0.85 (d, $J = 6.5$ Hz, 3H), 0.84 (d, $J = 6.5$ Hz, 3H). ^{13}C NMR (DMSO- d_6) δ ppm: 170.0, 168.3, 155.6, 77.7, 60.3, 50.2, 39.52, 38.8, 37.4, 28.2 (3C), 25.5, 22.6, 22.0, 14.0.

[4-[(2-Ethoxycarbonyl-4-methyl-pentanoyl)amino]phenyl]methylammonium;chloride (82)



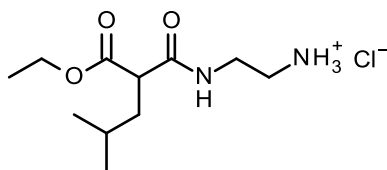
Compound **82** was synthesized according to the general procedure J, using the Boc-protected intermediate **81** (440 mg, 1.12 mmol), 4 N HCl in dioxane (5 mL) in a mixture CH₂Cl₂/EtOH (10 mL, 5:5 v/v) overnight. Compound **82** was obtained as yellow oil (369 mg, quant. yield) and was used in the next step without further purification. LC tr = 2.15 min, MS (ESI-): m/z = 291 [M - H]⁻. ¹H NMR (DMSO-*d*₆) δ ppm: 10.55 (s, 1H), 8.44 (br s, 3H), 7.65–7.60 (m, 2H), 7.44–7.41 (m, 2H), 4.13–4.04 (m, 2H), 3.96–3.91 (m, 2H), 3.68–3.63 (m, 1H), 1.79–1.61 (m, 2H), 1.50 (sep, *J* = 6.7 Hz, 1H), 1.15 (t, *J* = 7.1 Hz, 3H), 0.89 (d, *J* = 6.7 Hz, 3H), 0.87 (d, *J* = 6.7 Hz, 3H). ¹³C NMR (DMSO-*d*₆) δ ppm: 169.8, 167.4, 139.1, 129.6 (2C), 129.0, 119.2 (2C), 60.6, 50.9, 41.8, 37.5, 25.7, 22.7, 22.1, 14.1.

[3-[(2-Ethoxycarbonyl-4-methyl-pentanoyl)amino]phenyl]methylammonium;chloride (111)



Compound **111** was synthesized according to the general procedure J, using the Boc-protected intermediate **110** (495 mg, 1.26 mmol), 4 N HCl in dioxane (7 mL) in a mixture CH₂Cl₂/EtOH (14 mL, 7:7 v/v) overnight. Compound **111** was obtained as yellow oil (415 mg, quant. yield) and was used in the next step without further purification. LC tr = 2.82 min, MS (ESI+): m/z = 293 [M + H]⁺, 585 [2M + H]⁺. ¹H NMR (500 MHz, DMSO-*d*₆) δ ppm: 10.54 (s, 1H), 8.39 (br s, 3H), 7.79–7.78 (m, 1H), 7.54–7.53 (m, 1H), 7.36 (t, *J* = 7.9 Hz, 1H), 7.21–7.20 (m, 1H), 4.13–4.05 (m, 2H), 3.72–3.65 (m, 2H), 3.51–3.46 (m, 1H), 1.79–1.73 (m, 1H), 1.67–1.61 (m, 1H), 1.49 (sep, *J* = 6.6 Hz, 1H), 1.16 (t, *J* = 7.1 Hz, 3H), 0.90 (d, *J* = 6.6 Hz, 3H), 0.88 (d, *J* = 6.6 Hz, 3H). ¹³C NMR (126 MHz, DMSO-*d*₆) δ ppm: 169.9, 167.4, 139.2, 134.7, 129.2, 124.2, 119.9, 119.4, 60.7, 53.6, 50.9, 37.5, 25.7, 22.9, 22.0, 14.1.

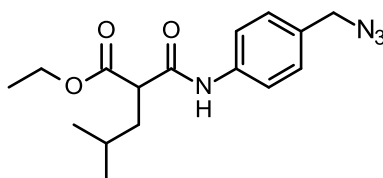
2-[(2-Ethoxycarbonyl-4-methyl-pentanoyl)amino]ethylammonium;chloride (85)



Compound **85** was synthesized according to the general procedure J, using the Boc-protected intermediate **84** (403 mg, 1.22 mmol), 4 N HCl in dioxane (6 mL) in a mixture CH₂Cl₂/EtOH (12 mL, 6:6 v/v) overnight. Compound **85** was obtained as colorless oil (325 mg, quant. yield) and was used in

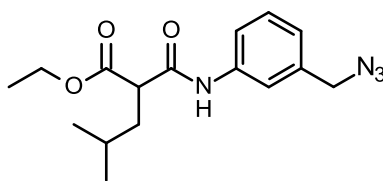
the next step without further purification. LC tr = 1.87 min, MS (ESI+): $m/z = 231 [M + H]^+$. ^1H NMR (300 MHz, $\text{DMSO-}d_6$) δ ppm: 8.53 (t, $J = 5.5$ Hz, 1H), 8.13 (br s, 3H), 4.09 (dd, $J = 7.2$ and 1.8 Hz, 1H), 4.04 (dd, $J = 7.2$ and 1.8 Hz, 1H), 3.35–3.28 (m, 3H), 2.89–2.77 (m, 2H), 1.65–1.59 (m, 2H), 1.44 (sep, $J = 6.7$ Hz, 1H), 1.16 (t, $J = 7.1$ Hz, 3H), 0.86 (d, $J = 6.5$ Hz, 3H), 0.85 (d, $J = 6.5$ Hz, 3H). ^{13}C NMR (75 MHz, $\text{DMSO-}d_6$) δ ppm: 169.9, 168.8, 60.5, 50.2, 38.2, 37.3, 36.6, 25.6, 22.4, 22.2, 14.0.

Ethyl 2-[[4-(azidomethyl)phenyl]carbamoyl]-4-methyl-pentanoate (83)



Compound **83** was synthesized according to the general procedure A, using amine **82** (350 mg, 0.93 mmol), ZnCl_2 (7.6 mg, 0.05 mmol), K_2CO_3 (512 mg, 3.7 mmol), anhydrous *N,N*-diisopropylethylamine (177 μL , 1.02 mmol) and diazo transfer reagent (301 mg, 1.11 mmol) in anhydrous MeOH (5 mL) overnight. The crude product was purified by flash chromatography on silica gel (cHex to cHex/EtOAc: 8/2) affording compound **84** as a yellowish solid (176 mg, 58%). LC tr = 3.02 min, MS (ESI-): $m/z = 317 [M - H]^-$. ^1H NMR (300 MHz, $\text{CDCl}_3 + \text{TMS}$) δ ppm: 8.75 (s, 1H), 7.58–7.56 (m, 2H), 7.28–7.24 (m, 2H), 4.28 (br s, 2H), 4.26–4.19 (m, 2H), 3.46 (t, $J = 7.7$ Hz, 1H), 1.90–1.85 (m, 2H), 1.64 (sep, $J = 6.7$ Hz, 1H), 1.30 (t, $J = 7.1$ Hz, 3H), 0.95 (d, $J = 6.7$ Hz, 6H). ^{13}C NMR (75 MHz, $\text{CDCl}_3 + \text{TMS}$) δ ppm: 172.8, 166.9, 137.8, 131.3, 129.0 (2C), 120.2 (2C), 61.8, 54.3, 52.4, 40.5, 26.4, 22.4, 22.1, 14.1.

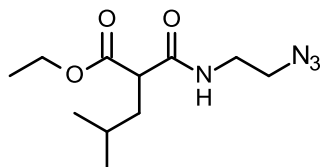
Ethyl 2-[[3-(azidomethyl)phenyl]carbamoyl]-4-methyl-pentanoate (112)



Compound **112** was synthesized according to the general procedure A, using amine **111** (405 mg, 1.07 mmol), ZnCl_2 (8.8 mg, 0.06 mmol), K_2CO_3 (296 mg, 2.14 mmol), anhydrous *N,N*-diisopropylethylamine (392 μL , 2.25 mmol) and diazo transfer reagent (270 mg, 1.29 mmol) in anhydrous MeOH (5 mL) overnight. The crude product was purified by flash chromatography on silica gel (cHex to cHex/EtOAc: 8/2) affording compound **112** as white crystals (121 mg, 31%). LC tr = 4.75 min, MS (ESI+): $m/z = 319 [M + H]^+$. ^1H NMR (500 MHz, $\text{DMSO-}d_6$) δ ppm: 10.31 (s, 1H), 7.65–7.64 (m, 1H), 7.55–7.53 (m, 1H), 7.34 (t, $J = 7.8$ Hz, 1H), 7.07–7.06 (m, 1H), 4.44 (s, 2H), 4.16–4.06 (m, 2H), 3.58 (dd, $J = 8.8$ and 6.2 Hz, 1H), 1.78–1.74 (m, 1H), 1.69–1.63 (m, 1H), 1.50 (sep, $J = 6.7$ Hz, 1H), 1.16 (t, $J = 7.0$ Hz, 3H), 0.90 (d, $J = 6.7$ Hz, 3H), 0.88 (d, $J = 6.7$ Hz, 3H). ^{13}C NMR (126

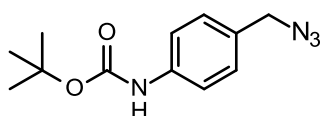
MHz, DMSO-*d*₆) δ ppm: 169.7, 167.2, 139.2, 136.4, 129.2, 123.5, 119.0, 118.9, 60.7, 53.6, 51.0, 37.4, 25.6, 22.7, 21.9, 14.0.

Ethyl 2-(2-azidoethylcarbamoyl)-4-methyl-pentanoate (86)



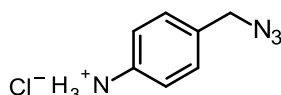
Compound **86** was synthesized according to the general procedure A, using amine **85** (325 mg, 1.22 mmol), ZnCl₂ (10.0 mg, 0.07 mmol), K₂CO₃ (674 mg, 4.87 mmol), anhydrous *N,N*-diisopropylethylamine (177 μ L, 1.02 mmol) and diazo transfer reagent (424 mg, 2.44 mmol) in anhydrous MeOH (5 mL) overnight. The crude product was purified by flash chromatography on silica gel (cHex/EtOAc: 9/1 to 6/4) affording compound **86** as colorless oil (72 mg, 19%). LC tr = 2.50 min, MS (ESI+): $m/z = 257$ [M + H]⁺. ¹H NMR (300 MHz, CDCl₃) δ ppm: 6.92–6.88 (m, 1H), 4.18 (dd, $J = 7.1$ and 1.2 Hz, 1H), 4.13 (dd, $J = 7.1$ and 1.1 Hz, 1H), 3.44–3.35 (m, 4H), 3.31–3.25 (m, 1H), 1.82–1.66 (m, 2H), 1.53 (sep, $J = 6.7$ Hz, 1H), 1.24 (t, $J = 7.1$ Hz, 3H), 0.89 (d, $J = 6.6$ Hz, 3H), 0.88 (d, $J = 6.6$ Hz, 3H). ¹³C NMR (75 MHz, CDCl₃) δ ppm: 172.3, 169.2, 61.6, 51.6, 50.7, 40.1, 39.2, 26.3, 22.4, 22.1, 14.1.

***Tert*-butyl *N*-[4-(azidomethyl)phenyl]carbamate (170)**



Compound **170** was synthesized according to the general procedure A, using *tert*-butyl *N*-[4-(aminomethyl)phenyl]carbamate (500 mg, 2.25 mmol), ZnCl₂ (18.4 mg, 0.14 mmol), K₂CO₃ (1240 mg, 9.0 mmol), anhydrous *N,N*-Diisopropylethylamine (240 μ L, 2.47 mmol) and diazo transfer reagent (566 mg, 2.7 mmol) in anhydrous MeOH (5 mL) overnight. Compound **170** was obtained as orange oil (558 mg, quant. yield) and was used in the next step without further purification. LC tr = 4.72 min, MS (ESI+): $m/z =$ no ionization [M + H]⁺. ¹H NMR (500 MHz, DMSO-*d*₆) δ ppm: 9.42 (s, 1H), 7.48–7.45 (m, 2H), 7.26–7.24 (m, 2H), 4.33 (s, 2H), 1.47 (s, 9H). ¹³C NMR (126 MHz, DMSO-*d*₆) δ ppm: 152.7, 139.5, 129.1 (3C), 128.8, 118.2, 79.1, 53.3, 28.1 (3C).

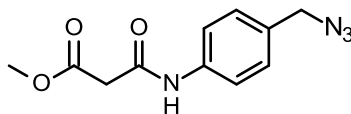
[4-(Azidomethyl)phenyl]ammonium;chloride (171)



Compound **171** was synthesized according to the general procedure J, using the Boc-protected intermediate **170** (550 mg, 2.22 mmol), 4 N HCl in dioxane (10 mL) in a mixture CH₂Cl₂/EtOH (20 mL, 10:10 v/v) overnight. Compound **171** was obtained as an orange solid (409 mg, quant. yield) and was used in the next step without further purification. LC tr = 1.40 min, MS (ESI+): $m/z = 149$ [M +

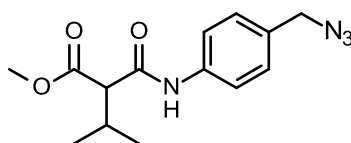
H]⁺. ¹H NMR (500 MHz, DMSO-*d*₆) δ ppm: 9.88 (br s, 3H), 7.45–7.43 (m, 2H), 7.33–7.32 (m, 2H), 4.46 (s, 2H).

Methyl 3-[4-(azidomethyl)anilino]-3-oxo-propanoate (172)



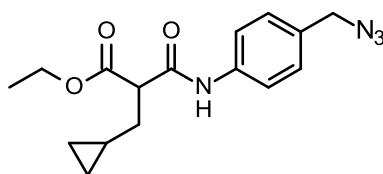
To a solution of **171** (400 mg, 2.17 mmol) in CH₂Cl₂ (8 mL) was added triethylamine (1190 μL, 8.67 mmol) and the reaction mixture was cooled down to 0°C. Methyl 3-chloro-3-oxo-propanoate (349 μL, 3.25 mmol) was added and the mixture was stirred overnight at room temperature. The mixture was then washed with sat. aq. NH₄Cl and the combined organic layers were dried over MgSO₄, filtered and concentrated under reduced pressure. Finally, the residue was purified through flash chromatography on silica gel column (cHex to cHex/EtOAc: 5:5) affording compound **172** as a yellowish oil (156 mg, 28%). LC tr = 3.43 min, MS (ESI⁺): *m/z* = 249 [M + H]⁺. ¹H NMR (500 MHz, DMSO-*d*₆) δ ppm: 10.27 (s, 1H), 7.60–7.58 (m, 2H), 7.33–7.31 (m, 2H), 4.38 (s, 2H), 3.65 (s, 3H), 3.48 (s, 2H). ¹³C NMR (126 MHz, DMSO-*d*₆) δ ppm: 168.1, 164.1, 138.7, 130.5, 129.2 (2C), 119.2 (2C), 53.2, 52.0, 43.5.

Methyl 2-[[4-(azidomethyl)phenyl]carbamoyl]-3-methyl-butanoate (174)



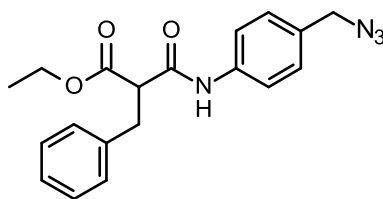
Compound **174** was synthesized according to the general procedure B, using carboxylic acid **174-a** (300 mg, 1.87 mmol), aniline **171** (415 mg, 2.27 mmol), HBTU (1070 mg, 2.81 mmol) and trimethylamine (1020 μL, 7.49 mmol) in DMF (5 mL) overnight. The crude product was purified by flash chromatography on silica gel (cHex to cHex/EtOAc: 6/4) affording compound **174** as a white solid (203 mg, 37%). LC tr = 4.18 min, MS (ESI⁺): *m/z* = 291 [M + H]⁺. ¹H NMR (500 MHz, DMSO-*d*₆) δ ppm: 10.28 (s, 1H), 7.62–7.60 (m, 2H), 7.33–7.31 (m, 2H), 4.38 (s, 2H), 3.64 (s, 3H), 3.24 (d, *J* = 9.7 Hz, 1H), 2.36–2.28 (m, 1H), 0.95 (d, *J* = 6.7 Hz, 3H), 0.92 (d, *J* = 6.7 Hz, 3H). ¹³C NMR (126 MHz, DMSO-*d*₆) δ ppm: 169.4, 166.3, 138.6, 130.6, 129.2 (2C), 119.4 (2C), 60.0, 53.2, 51.9, 28.4, 20.6, 19.8.

Ethyl 3-[4-(azidomethyl)anilino]-2-(cyclopropylmethyl)-3-oxo-propanoate (175)



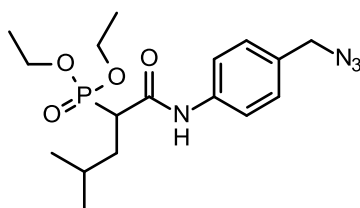
Compound **175** was synthesized according to the general procedure B, using carboxylic acid **175-a** (340 mg, 1.83 mmol), aniline **171** (405 mg, 2.19 mmol), HBTU (1040 mg, 2.74 mmol) and trimethylamine (1250 μ L, 9.13 mmol) in DMF (5 mL) overnight. The crude product was purified by flash chromatography on silica gel (cHex to cHex/EtOAc: 5/5) affording compound **175** as a pale yellow solid (277 mg, 43%). LC tr = 4.49 min, MS (ESI+): $m/z = 317 [M + H]^+$. $^1\text{H NMR}$ (500 MHz, DMSO- d_6) δ ppm: 10.30 (s, 1H), 7.62–7.61 (m, 2H), 7.33–7.31 (m, 2H), 4.38 (s, 2H), 4.12–4.09 (m, 2H), 3.59 (dd, $J = 8.6$ and 6.8 Hz, 1H), 1.81–1.63 (m, 2H), 1.17 (t, $J = 7.1$ Hz, 3H), 0.74–0.65 (m, 1H), 0.44–0.34 (m, 2H), 0.11–0.04 (m, 2H). $^{13}\text{C NMR}$ (126 MHz, DMSO- d_6) δ ppm: 169.5, 167.2, 138.8, 130.5, 129.2 (2C), 119.4 (2C), 60.6, 53.2, 53.2, 33.5, 14.0, 8.8, 4.4, 4.3.

Ethyl 3-[4-(azidomethyl)anilino]-2-benzyl-3-oxo-propanoate (**173**)



Compound **173** was synthesized according to the general procedure B, using carboxylic acid **173-a** (300 mg, 1.35 mmol), aniline **171** (299 mg, 1.62 mmol), HBTU (768 mg, 2.02 mmol) and trimethylamine (738 μ L, 5.4 mmol) in DMF (3 mL) overnight. The crude product was purified by flash chromatography on silica gel (cHex to cHex/EtOAc: 7/3) affording compound **173** as a white solid (152 mg, 31%). LC tr = 4.69 min, MS (ESI+): $m/z = 353 [M + H]^+$. $^1\text{H NMR}$ (500 MHz, DMSO- d_6) δ ppm: 10.25(s, 1H), 7.54–7.53 (m, 2H), 7.30–7.29 (m, 2H), 7.26–7.15 (m, 5H), 4.36 (s, 2H), 4.11–4.04 (m, 2H), 3.84 (dd, $J = 8.5$ and 6.8 Hz, 1H), 3.14–3.12 (m, 2H), 1.13 (t, $J = 7.1$ Hz, 3H). $^{13}\text{C NMR}$ (126 MHz, DMSO- d_6) δ ppm: 169.0, 166.4, 138.5, 138.4, 130.6, 129.1 (2C), 128.8 (2C), 128.3 (2C), 126.4, 119.4 (2C), 60.8, 54.3, 53.2, 34.2, 14.0.

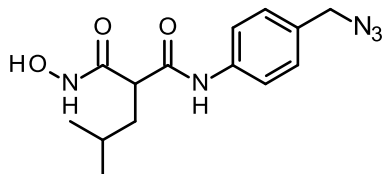
N-[4-(Azidomethyl)phenyl]-2-diethoxyphosphoryl-4-methyl-pentanamide (**194**)



A mixture of 2-diethoxyphosphoryl-4-methyl-pentanoic acid (328 mg, 1.3 mmol) and TBTU (522 mg, 1.6 mmol) in DMF (3 mL) was cooled to 0 $^{\circ}\text{C}$ and *N*-Methylmorpholine (298 μ L, 2.7 mmol) was added. The reaction mixture was stirred for 30 min and aniline **171** (200 mg, 1.1 mmol) was dissolved in DMF (2 mL) and added dropwise at 0 $^{\circ}\text{C}$. The mixture was stirred overnight at room temperature. Then, it was diluted in water and extracted with ethyl acetate. Combined organic layers were subsequently washed with 1 N aq. HCl, sat. aq. NaHCO_3 and brine, dried over MgSO_4 , filtered and concentrated under reduced pressure. The residue was finally purified through flash chromatography

on silica gel column (cHex to cHex/EtOAc: 6/4) to give compound **194** as a white solid (277 mg, 66%). LC tr = 4.39 min, MS (ESI+): $m/z = 383$ $[M + H]^+$. $^1\text{H NMR}$ (500 MHz, $\text{DMSO-}d_6$) δ ppm: 10.20 (s, 1H), 7.61–7.59 (m, 2H), 7.33–7.31 (m, 2H), 4.38 (s, 2H), 4.09–3.98 (m, 4H), 3.24–3.17 (m, 1H), 2.01–1.93 (m, 1H), 1.53–1.36 (m, 2H), 1.23–1.19 (m, 6H), 0.88 (d, $J = 6.6$ Hz, 3H), 0.86 (d, $J = 6.6$ Hz, 3H). $^{13}\text{C NMR}$ (126 MHz, $\text{DMSO-}d_6$) δ ppm: 166.5 (d, $J = 4.6$ Hz), 138.9, 130.4, 129.2 (2C), 119.2 (2C), 62.0 (d, $J = 6.4$ Hz), 61.8 (d, $J = 6.4$ Hz), 53.2, 44.5 (d, $J = 129.9$ Hz), 35.4 (d, $J = 5.5$ Hz), 26.3 (d, $J = 14.7$ Hz), 22.7, 21.2, 16.3, 16.2.

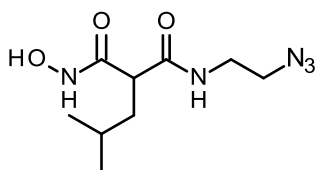
***N*-[4-(Azidomethyl)phenyl]-2-(hydroxycarbamoyl)-4-methyl-pentanamide (Z9)**



Compound **Z9** was synthesized according to the general procedure G, using ester **83** (176 mg, 0.55 mmol), KCN (7.13 mg, 0.11 mmol) and aq. NH_2OH (2.5 mL, 50% w/w in water) in MeOH (2.5 mL) overnight. The crude product was purified by flash chromatography on silica gel (CH_2Cl_2 to $\text{CH}_2\text{Cl}_2/\text{MeOH}$: 95/5) affording compound **Z9** as a white solid after lyophilization (65 mg, 38%).

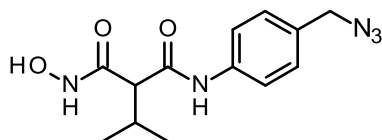
Purity: 100%, LC tr = 2.35 min, MS (ESI-): $m/z = 304$ $[M - H]^-$. $^1\text{H NMR}$ (300 MHz, $\text{DMSO-}d_6$) δ ppm: 10.52 (s, 1H), 9.82 (s, 1H), 8.97 (s, 1H), 7.62–7.59 (m, 2H), 7.32–7.30 (m, 2H), 4.37 (s, 2H), 3.22 (t, $J = 7.6$ Hz, 1H), 1.69 (t, $J = 7.3$ Hz, 2H), 1.49 (sep, $J = 6.7$ Hz, 1H), 0.89 (d, $J = 2.0$ Hz, 3H), 0.87 (d, $J = 2.0$ Hz, 3H). $^{13}\text{C NMR}$ (75 MHz, $\text{DMSO-}d_6$) δ ppm: 167.8, 166.3, 138.7, 130.4, 129.1 (2C), 119.5 (2C), 53.2, 50.0, 38.0, 25.7, 22.4, 22.3.

***N*-(2-Azidoethyl)-2-(hydroxycarbamoyl)-4-methyl-pentanamide (Z10)**



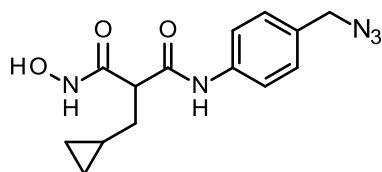
Compound **Z10** was synthesized according to the general procedure G, using ester **86** (72 mg, 0.28 mmol), KCN (3.6 mg, 0.06 mmol) and aq. NH_2OH (2.5 mL, 50% w/w in water) in MeOH (2.5 mL) overnight. The crude product was purified by flash chromatography on silica gel (CH_2Cl_2 to $\text{CH}_2\text{Cl}_2/\text{MeOH}$: 9/1) affording compound **Z10** as a white solid after lyophilization (65 mg, 38%). Purity: 100%, LC tr = 1.75 min, MS (ESI-): $m/z = 242$ $[M - H]^-$. $^1\text{H NMR}$ (300 MHz, $\text{DMSO-}d_6$) δ ppm: 10.50 (s, 1H), 8.93 (s, 1H), 7.84 (t, $J = 5.6$ Hz, 1H), 3.37–3.34 (m, 2H), 3.27–3.21 (m, 2H), 3.00–2.96 (m, 1H), 1.66–1.38 (m, 3H), 0.84 (d, $J = 6.4$ Hz, 6H). $^{13}\text{C NMR}$ ($\text{DMSO-}d_6$) δ ppm: 169.4, 166.6, 49.9, 49.0, 38.6, 38.3, 25.5, 22.5, 22.1.

***N*-[4-(Azidomethyl)phenyl]-2-(hydroxycarbonyl)-3-methyl-butanamide (180)**



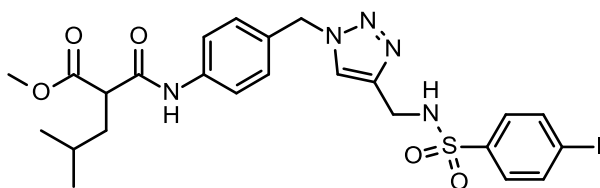
Compound **180** was synthesized according to the general procedure G, using ester **174** (100 mg, 0.34 mmol), KCN (4.44 mg, 0.07 mmol) and aq. NH_2OH (2.5 mL, 50% w/w in water) in MeOH (2.5 mL) overnight. The crude product was purified by flash chromatography on silica gel (CH_2Cl_2 to $\text{CH}_2\text{Cl}_2/\text{MeOH}$: 95/5) affording compound **180** as a white solid after lyophilization (43 mg, 43%). LC tr = 3.24 min, MS (ESI+): $m/z = 292$ $[\text{M} + \text{H}]^+$. ^1H NMR (500 MHz, $\text{DMSO}-d_6$) δ ppm: 10.55 (s, 1H), 9.78 (s, 1H), 9.02 (s, 1H), 7.62–7.60 (m, 2H), 7.32–7.30 (m, 2H), 4.37 (s, 2H), 2.73 (d, $J = 10.5$ Hz, 1H), 2.40–2.33 (m, 1H), 0.90 (d, $J = 6.6$ Hz, 3H), 0.89 (d, $J = 6.6$ Hz, 3H). ^{13}C NMR (126 MHz, $\text{DMSO}-d_6$) δ ppm: 167.3, 165.9, 138.6, 130.5, 129.1 (2C), 119.6 (2C), 59.7, 53.2, 29.7, 20.4, 20.3.

***N*-[4-(Azidomethyl)phenyl]-2-(cyclopropylmethyl)-3-(hydroxyamino)-3-oxo-propanamide (181)**



Compound **181** was synthesized according to the general procedure G, using ester **175** (135 mg, 0.42 mmol), KCN (5.5 mg, 0.08 mmol) and aq. NH_2OH (3.2 mL, 50% w/w in water) in MeOH (3.2 mL) overnight. The crude product was purified by flash chromatography on silica gel (CH_2Cl_2 to $\text{CH}_2\text{Cl}_2/\text{MeOH}$: 95/5) affording compound **181** as a white solid after lyophilization (58 mg, 44%). LC tr = 3.41 min, MS (ESI+): $m/z = 304$ $[\text{M} + \text{H}]^+$. ^1H NMR (500 MHz, $\text{DMSO}-d_6$) δ ppm: 10.51 (br s, 1H), 9.86 (s, 1H), 8.96 (s, 1H), 7.62–7.60 (m, 2H), 7.32–7.30 (m, 2H), 4.37 (s, 2H), 3.23 (t, $J = 7.5$ Hz, 1H), 1.72–1.69 (m, 2H), 0.68–0.61 (m, 1H), 0.40–0.34 (m, 2H), 0.09–0.08 (m, 2H). ^{13}C NMR (126 MHz, $\text{DMSO}-d_6$) δ ppm: 167.8, 166.2, 138.8, 130.3, 129.1 (2C), 119.4 (2C), 53.3, 52.0, 34.1, 9.0, 4.3, 4.3.

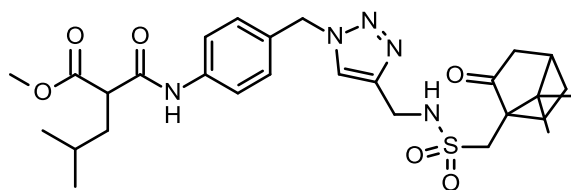
Methyl 2-[[4-[[4-[[4-(4-iodophenyl)sulfonylamino]methyl]triazol-1-yl]methyl]phenyl]carbonyl]-4-methyl-pentanoate (88)



Compound **88** was synthesized according to the general procedure H, using azide **87** (100 mg, 0.33 mmol), alkyne **93** (106 mg, 0.33 mmol), copper (II) sulfate pentahydrate (16.4 mg, 0.07 mmol) and sodium ascorbate (32.5 mg, 0.16 mmol) in DMF (5.5 mL) and H_2O (4.5 mL) overnight. The crude

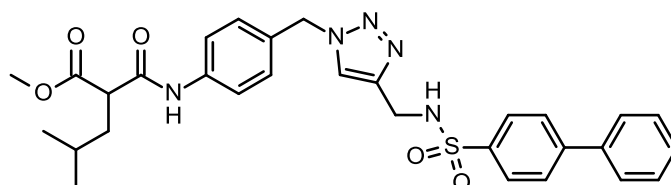
product was purified by flash chromatography on silica gel (CH₂Cl₂ to CH₂Cl₂/MeOH: 95/5) affording compound **88** as a white powder (119 mg, 51%). LC tr = 4.48 min, MS (ESI+): m/z = 626 [M + H]⁺. ¹H NMR (500 MHz, DMSO-*d*₆) δ ppm: 10.32 (s, 1H), 8.19 (t, *J* = 5.9 Hz, 1H), 7.93–7.91 (m, 2H), 7.85 (s, 1H), 7.59–7.57 (m, 2H), 7.51–7.50 (m, 2H), 7.27–7.25 (m, 2H), 5.45 (s, 2H), 4.03 (d, *J* = 5.9 Hz, 2H), 3.63 (s, 3H), 3.58 (dd, *J* = 8.9 and 6.1 Hz, 1H), 1.78–1.73 (m, 1H), 1.68–1.62 (m, 1H), 1.48 (sep, *J* = 6.6 Hz, 1H), 0.89 (d, *J* = 6.6 Hz, 3H), 0.87 (d, *J* = 6.6 Hz, 3H). ¹³C NMR (126 MHz, DMSO-*d*₆) δ ppm: 170.2, 167.1, 143.4, 140.0, 138.7, 138.0 (2C), 130.9, 128.8 (2C), 128.3 (2C), 123.2, 119.4 (2C), 100.4, 52.4, 52.1, 50.8, 38.0, 37.4, 25.6, 22.7, 21.9.

Methyl 2-[[4-[[4-[[[(7,7-dimethyl-2-oxo-norbornan-1-yl)methylsulfonylamino]methyl]triazol-1-yl]methyl]phenyl]carbamoyl]-4-methyl-pentanoate (89**)**



Compound **89** was synthesized according to the general procedure H, using azide **87** (100 mg, 0.33 mmol), alkyne **94** (88.5 mg, 0.33 mmol), copper (II) sulfate pentahydrate (16.4 mg, 0.07 mmol) and sodium ascorbate (32.5 mg, 0.16 mmol) in DMF (5.5 mL) and H₂O (4.5 mL) overnight. The crude product was purified by flash chromatography on silica gel (CH₂Cl₂ to CH₂Cl₂/MeOH: 95/5) affording compound **89** as colorless oil (137 mg, 64%). LC tr = 4.29 min, MS (ESI-): m/z = 572 [M - H]⁻. ¹H NMR (500 MHz, DMSO-*d*₆) δ ppm: 10.31 (s, 1H), 8.01 (s, 1H), 7.58–7.56 (m, 2H), 7.29–7.28 (m, 2H), 5.52 (s, 2H), 4.26–4.24 (m, 2H), 3.62 (s, 3H), 3.58 (dd, *J* = 8.9 and 6.0 Hz, 1H), 3.21 (d, *J* = 14.9 Hz, 1H), 3.17 (d, *J* = 5.2 Hz, 1H), 2.84 (d, *J* = 14.9 Hz, 1H), 2.32–2.27 (m, 2H), 2.01 (t, *J* = 4.5 Hz, 1H), 1.89 (d, *J* = 18.3 Hz, 2H), 1.78–1.73 (m, 1H), 1.67–1.62 (m, 1H), 1.50–1.44 (m, 2H), 1.38–1.33 (m, 1H), 0.95 (s, 3H), 0.88 (d, *J* = 6.6 Hz, 3H), 0.87 (d, *J* = 6.6 Hz, 3H), 0.70 (s, 3H). ¹³C NMR (126 MHz, DMSO-*d*₆) δ ppm: 214.6, 170.2, 167.1, 144.6, 138.7, 131.1, 128.8 (2C), 123.2, 119.4 (2C), 57.9, 52.4, 52.1, 50.8, 48.7, 47.6, 42.0, 41.9, 38.0, 37.4, 26.3, 25.6, 24.5, 22.7, 21.9, 19.4, 19.2.

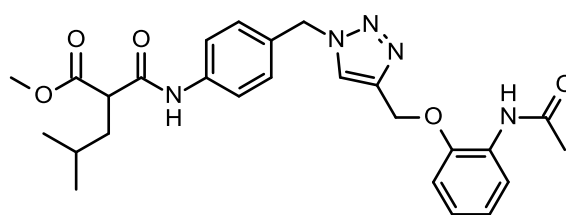
Methyl 4-methyl-2-[[4-[[4-[[[(4-phenylphenyl)sulfonylamino]methyl]triazol-1-yl]methyl]phenyl]carbamoyl]pentanoate (90**)**



Compound **90** was synthesized according to the general procedure H, using azide **87** (100 mg, 0.33 mmol), alkyne **95** (89.2 mg, 0.33 mmol), copper (II) sulfate pentahydrate (16.4 mg, 0.07 mmol) and sodium ascorbate (32.5 mg, 0.16 mmol) in DMF (5.5 mL) and H₂O (4.5 mL) overnight. The crude product was purified by flash chromatography on silica gel (CH₂Cl₂ to CH₂Cl₂/MeOH: 95/5) affording

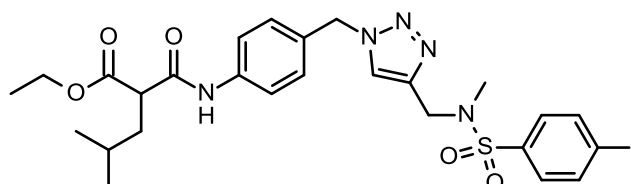
compound **90** as a greenish powder (139 mg, 62%). LC tr = 4.69 min, MS (ESI-): $m/z = 574$ [M - H]⁻. ¹H NMR (500 MHz, DMSO-*d*₆) δ ppm: 10.31 (s, 1H), 8.15 (t, $J = 5.9$ Hz, 1H), 7.89 (s, 1H), 7.84 (s, 4H), 7.74–7.72 (m, 2H), 7.57–7.55 (m, 2H), 7.53–7.50 (m, 2H), 7.46–7.43 (m, 1H), 7.26–7.24 (m, 2H), 5.45 (s, 2H), 4.06 (d, $J = 5.9$ Hz, 2H), 3.62 (s, 3H), 3.58 (dd, $J = 8.9$ and 6.0 Hz, 1H), 1.78–1.72 (m, 1H), 1.68–1.62 (m, 1H), 1.48 (sep, $J = 6.7$ Hz, 1H), 0.88 (d, $J = 6.7$ Hz, 3H), 0.87 (d, $J = 6.7$ Hz, 3H). ¹³C NMR (126 MHz, DMSO-*d*₆) δ ppm: 170.1, 167.1, 143.9, 143.7, 139.1, 138.7, 138.5, 131.0, 129.1 (2C), 128.8 (2C), 128.5, 127.3 (2C), 127.2 (2C), 127.1 (2C), 123.2, 119.4 (2C), 52.4, 52.1, 50.8, 38.1, 37.4, 25.6, 22.6, 21.9.

Methyl 2-[[4-[[4-[(2-acetamidophenoxy)methyl]triazol-1-yl]methyl]phenyl]carbamoyl]-4-methyl-pentanoate (92**)**



Compound **92** was synthesized according to the general procedure H, using azide **87** (100 mg, 0.33 mmol), alkyne **100** (62.2 mg, 0.33 mmol), copper (II) sulfate pentahydrate (16.4 mg, 0.07 mmol) and sodium ascorbate (32.5 mg, 0.16 mmol) in DMF (5.5 mL) and H₂O (4.5 mL) overnight. The crude product was purified by flash chromatography on silica gel (CH₂Cl₂ to CH₂Cl₂/MeOH: 95/5) affording compound **92** as a beige powder (139 mg, 62%). LC tr = 4.05 min, MS (ESI-): $m/z = 492$ [M - H]⁻. ¹H NMR (500 MHz, DMSO-*d*₆) δ ppm: 10.32 (s, 1H), 9.01 (s, 1H), 8.22 (s, 1H), 7.87 (d, $J = 7.7$ Hz, 1H), 7.59–7.57 (m, 2H), 7.29–7.27 (m, 2H), 7.20 (d, $J = 7.9$ Hz, 1H), 7.04 (t, $J = 7.4$ Hz, 1H), 6.90 (t, $J = 7.4$ Hz, 1H), 5.55 (s, 2H), 5.20 (s, 2H), 3.62 (s, 3H), 3.58 (dd, $J = 8.9$ and 6.1 Hz, 1H), 2.03 (s, 3H), 1.78–1.73 (m, 1H), 1.68–1.62 (m, 1H), 1.48 (sep, $J = 6.7$ Hz, 1H), 0.89 (d, $J = 6.7$ Hz, 3H), 0.87 (d, $J = 6.7$ Hz, 3H). ¹³C NMR (126 MHz, DMSO-*d*₆) δ ppm: 170.2, 168.3, 167.1, 148.5, 143.2, 138.7, 131.0, 128.7 (2C), 127.9, 124.4, 124.2, 122.5, 120.8, 119.4 (2C), 113.3, 62.3, 52.5, 52.1, 50.8, 37.4, 25.6, 23.8, 22.7, 21.9.

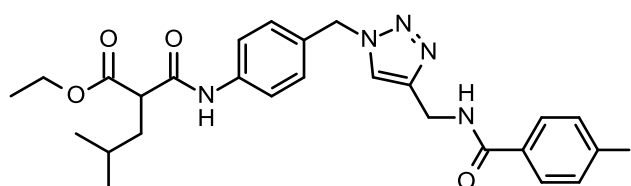
Methyl 2-[[4-[[4-[(4-iodophenyl)sulfonyl-methyl-amino]methyl]triazol-1-yl]methyl]phenyl]carbamoyl]-4-methyl-pentanoate (123**)**



Compound **123** was synthesized according to the general procedure H, using azide **83** (100 mg, 0.31 mmol), alkyne **115** (105 mg, 0.31 mmol), copper (II) sulfate pentahydrate (15.7 mg, 0.06 mmol) and sodium ascorbate (31.1 mg, 0.16 mmol) in DMF (5.5 mL) and H₂O (4.5 mL) overnight. The crude

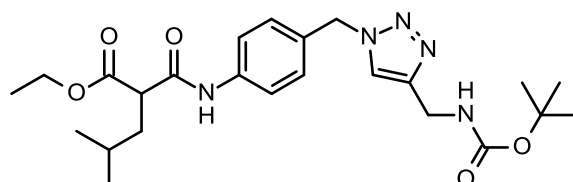
product was purified by flash chromatography on silica gel (CH₂Cl₂ to CH₂Cl₂/MeOH: 95/5) affording compound **123** as a white powder (132 mg, 59%). LC tr = 4.93 min, MS (ESI+): m/z = 654 [M + H]⁺. ¹H NMR (500 MHz, DMSO-*d*₆) δ ppm: 10.29 (s, 1H), 8.04 (s, 1H), 7.96–7.94 (m, 2H), 7.59–7.57 (m, 2H), 7.52–7.51 (m, 2H), 7.28–7.26 (m, 2H), 5.49 (s, 2H), 4.26 (s, 2H), 4.13–4.05 (m, 2H), 3.56 (dd, *J* = 8.7 and 6.2 Hz, 1H), 2.64 (s, 3H), 1.77–1.72 (m, 1H), 1.67–1.62 (m, 1H), 1.49 (sep, *J* = 6.7 Hz, 1H), 1.15 (t, *J* = 7.1 Hz, 3H), 0.88 (d, *J* = 6.7 Hz, 3H), 0.87 (d, *J* = 6.7 Hz, 3H). ¹³C NMR (126 MHz, DMSO-*d*₆) δ ppm: 169.7, 167.2, 141.8, 138.8, 138.2 (2C), 136.5, 130.9, 128.9 (2C), 128.7 (2C), 124.0, 119.5 (2C), 101.3, 60.7, 52.5, 50.9, 44.7, 37.4, 34.7, 25.7, 22.7, 21.9, 14.0.

Ethyl 2-[[4-[[4-[(4-iodobenzoyl)amino]methyl]triazol-1-yl]methyl]phenyl]carbamoyl]-4-methyl-pentanoate (124**)**



Compound **124** was synthesized according to the general procedure H, using azide **83** (100 mg, 0.31 mmol), alkyne **116** (89.5 mg, 0.31 mmol), copper (II) sulfate pentahydrate (15.7 mg, 0.06 mmol) and sodium ascorbate (31.1 mg, 0.16 mmol) in DMF (5.5 mL) and H₂O (4.5 mL) overnight. The crude product was purified by flash chromatography on silica gel (CH₂Cl₂ to CH₂Cl₂/MeOH: 98/2) affording compound **124** as a white solid (141 mg, 60%). LC tr = 4.61 min, MS (ESI+): m/z = 604 [M+H]⁺. ¹H NMR (500 MHz, DMSO-*d*₆) δ ppm: 10.28 (s, 1H), 9.05 (t, *J* = 5.6 Hz, 1H), 7.98 (s, 1H), 7.85–7.83 (m, 2H), 7.65–7.63 (m, 2H), 7.57–7.55 (m, 2H), 7.30–7.28 (m, 2H), 5.49 (s, 2H), 4.47 (d, *J* = 5.7 Hz, 2H), 4.12–4.05 (m, 2H), 3.55 (dd, *J* = 8.7 and 6.2 Hz, 1H), 1.77–1.71 (m, 1H), 1.67–1.62 (m, 1H), 1.48 (sep, *J* = 6.7 Hz, 1H), 1.15 (t, *J* = 7.1 Hz, 3H), 0.88 (d, *J* = 6.7 Hz, 3H), 0.87 (d, *J* = 6.7 Hz, 3H). ¹³C NMR (126 MHz, DMSO-*d*₆) δ ppm: 169.7, 167.1, 165.4, 145.1, 138.7, 137.2 (2C), 133.5, 131.1, 129.3 (2C), 128.8 (2C), 122.9, 119.4 (2C), 98.9, 60.6, 52.4, 50.9, 37.4, 34.9, 25.6, 22.6, 21.9, 14.0.

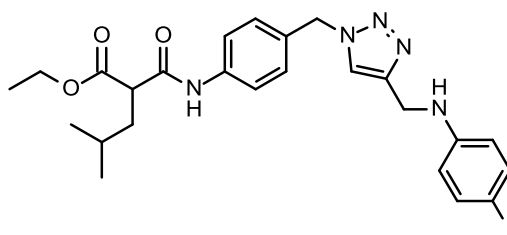
Ethyl 2-[[4-[[4-[(tert-butoxycarbonylamino)methyl]triazol-1-yl]methyl]phenyl]carbamoyl]-4-methyl-pentanoate (125**)**



Compound **125** was synthesized according to the general procedure H, using azide **83** (100 mg, 0.31 mmol), *N*-*boc*-propargylamine (48.7 mg, 0.31 mmol), copper (II) sulfate pentahydrate (15.7 mg, 0.06 mmol) and sodium ascorbate (31.1 mg, 0.16 mmol) in DMF (5.5 mL) and H₂O (4.5 mL) overnight. The crude product was purified by flash chromatography on silica gel (CH₂Cl₂ to CH₂Cl₂/MeOH:

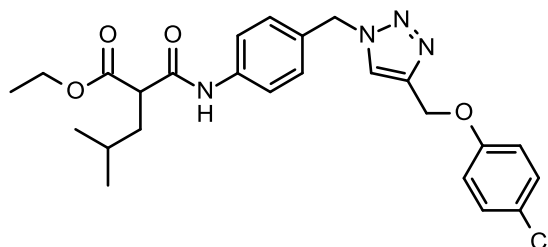
95/5) affording compound **125** as a colorless solid (115 mg, 72%). LC tr = 4.35 min, MS (ESI+): m/z = 474 $[M + H]^+$, 418 $[M + H - tBu]^+$, 374 $[M + H - boc]^+$. 1H NMR (500 MHz, DMSO- d_6) δ ppm: 10.31 (s, 1H), 7.87 (s, 1H), 7.57–7.56 (m, 2H), 7.31–7.27 (m, 3H), 5.49 (s, 2H), 4.13 (d, J = 5.7 Hz, 2H), 4.10–4.07 (m, 2H), 3.55 (dd, J = 8.7 and 6.2 Hz, 1H), 1.77–1.71 (m, 1H), 1.66–1.61 (m, 1H), 1.47 (sep, J = 6.7 Hz, 1H), 1.36 (s, 9H), 1.14 (t, J = 7.1 Hz, 3H), 0.88 (d, J = 6.7 Hz, 3H), 0.86 (d, J = 6.7 Hz, 3H). ^{13}C NMR (126 MHz, DMSO- d_6) δ ppm: 169.8, 167.2, 155.6, 145.9, 138.7, 131.2, 128.8 (2C), 122.6, 119.4 (2C), 78.0, 60.7, 52.3, 51.0, 37.4, 35.7, 28.3 (3C), 25.7, 22.7, 22.0, 14.1.

Ethyl 2-[[4-[[4-[(4-iodoanilino)methyl]triazol-1-yl]methyl]phenyl]carbamoyl]-4-methyl-pentanoate (126)



Compound **126** was synthesized according to the general procedure H, using azide **83** (100 mg, 0.31 mmol), alkyne **118** (80.7 mg, 0.31 mmol), copper (II) sulfate pentahydrate (15.7 mg, 0.06 mmol) and sodium ascorbate (31.1 mg, 0.16 mmol) in DMF (5.5 mL) and H₂O (4.5 mL) overnight. The crude product was purified by flash chromatography on silica gel (CH₂Cl₂ to CH₂Cl₂/MeOH: 98/2) affording compound **126** as yellow oil (170 mg, 85%). LC tr = 4.96 min, MS (ESI+): m/z = 576 $[M + H]^+$. 1H NMR (500 MHz, DMSO- d_6) δ ppm: 10.31 (s, 1H), 7.96 (s, 1H), 7.56–7.55 (m, 2H), 7.33–7.31 (m, 2H), 7.27–7.25 (m, 2H), 6.48–6.46 (m, 2H), 6.29 (t, J = 8.1 Hz, 1H), 5.49 (s, 2H), 4.23 (d, J = 5.4 Hz, 2H), 4.12–4.08 (m, 2H), 3.55 (dd, J = 8.8 and 6.2 Hz, 1H), 1.77–1.71 (m, 1H), 1.66–1.61 (m, 1H), 1.47 (sep, J = 6.7 Hz, 1H), 1.15 (t, J = 7.1 Hz, 3H), 0.88 (d, J = 6.7 Hz, 3H), 0.86 (d, J = 6.7 Hz, 3H). ^{13}C NMR (126 MHz, DMSO- d_6) δ ppm: 169.8, 167.2, 148.1, 145.6, 138.7, 137.1 (2C), 131.2, 128.8 (2C), 122.8, 119.5 (2C), 115.0 (2C), 76.6, 60.7, 52.4, 50.9, 38.3, 37.4, 25.7, 22.7, 22.0, 14.1.

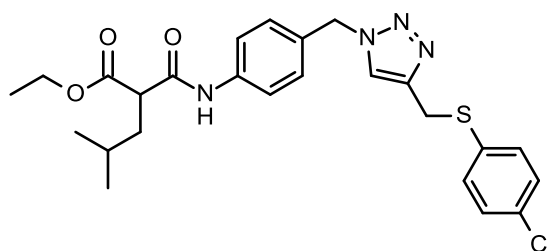
Ethyl 2-[[4-[[4-[(4-chlorophenoxy)methyl]triazol-1-yl]methyl]phenyl]carbamoyl]-4-methyl-pentanoate (127)



Compound **127** was synthesized according to the general procedure H, using azide **83** (70 mg, 0.22 mmol), alkyne **119** (36.6 mg, 0.22 mmol), copper (II) sulfate pentahydrate (11 mg, 0.04 mmol) and sodium ascorbate (21.8 mg, 0.11 mmol) in DMF (5 mL) and H₂O (4 mL) overnight. The crude product was purified by flash chromatography on silica gel (CH₂Cl₂ to CH₂Cl₂/MeOH: 95/5) affording

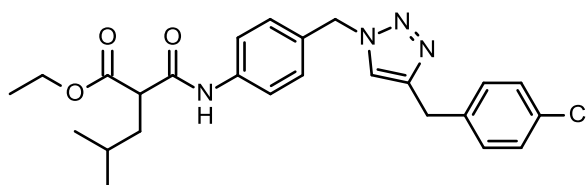
compound **127** as a white solid (59 mg, 54%). LC tr = 4.99 min, MS (ESI+): $m/z = 485$ and 487 $[M + H]^+$. 1H NMR (500 MHz, DMSO- d_6) δ ppm: 10.30 (s, 1H), 8.23 (s, 1H), 7.59–7.57 (m, 2H), 7.33–7.29 (m, 4H), 7.07–7.02 (m, 2H), 5.54 (s, 2H), 5.12 (s, 2H), 4.13–4.05 (m, 2H), 3.56 (dd, $J = 8.7$ and 6.2 Hz, 1H), 1.77–1.72 (m, 1H), 1.67–1.62 (m, 1H), 1.48 (sep, $J = 6.7$ Hz, 1H), 1.15 (t, $J = 7.1$ Hz, 3H), 0.89 (d, $J = 6.7$ Hz, 3H), 0.87 (d, $J = 6.7$ Hz, 3H). ^{13}C NMR (126 MHz, DMSO- d_6) δ ppm: 169.7, 167.2, 156.9, 142.7, 138.8, 130.9, 129.2 (3C), 128.8 (2C), 124.6, 119.5 (2C), 116.5 (2C), 61.4, 60.7, 52.5, 50.9, 37.4, 25.6, 22.6, 21.9, 14.0.

Ethyl 2-[[4-[[4-[(4-chlorophenyl)sulfanylmethyl]triazol-1-yl]methyl]phenyl]carbamoyl]-4-methyl-pentanoate (128)



Compound **128** was synthesized according to the general procedure H, using azide **83** (70 mg, 0.22 mmol), alkyne **120** (40.2 mg, 0.22 mmol), copper (II) sulfate pentahydrate (11 mg, 0.04 mmol) and sodium ascorbate (21.8 mg, 0.11 mmol) in DMF (5 mL) and H₂O (4 mL) overnight. The crude product was purified by flash chromatography on silica gel (CH₂Cl₂ to CH₂Cl₂/MeOH: 95/5) affording compound **128** as a white solid (77 mg, 69%). LC tr = 5.01 min, MS (ESI+): $m/z = 501$ and 503 $[M + H]^+$. 1H NMR (500 MHz, DMSO- d_6) δ ppm: 10.28 (s, 1H), 7.92 (s, 1H), 7.57–7.55 (m, 2H), 7.36–7.31 (m, 4H), 7.21–7.19 (m, 2H), 5.47 (s, 2H), 4.27 (s, 2H), 4.13–4.05 (m, 2H), 3.56 (dd, $J = 8.7$ and 6.2 Hz, 1H), 1.77–1.72 (m, 1H), 1.68–1.62 (m, 1H), 1.49 (sep, $J = 6.7$ Hz, 1H), 1.15 (t, $J = 7.1$ Hz, 3H), 0.89 (d, $J = 6.7$ Hz, 3H), 0.87 (d, $J = 6.7$ Hz, 3H). ^{13}C NMR (126 MHz, DMSO- d_6) δ ppm: 169.7, 167.1, 143.5, 138.7, 134.7, 131.0, 130.7, 130.2 (2C), 128.8 (2C), 128.5 (2C), 123.3, 119.4 (2C), 60.6, 52.4, 50.9, 37.4, 27.3, 25.6, 22.6, 21.9, 14.0.

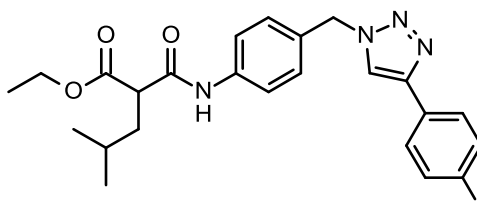
Ethyl 2-[[4-[[4-[(4-chlorophenyl)methyl]triazol-1-yl]methyl]phenyl]carbamoyl]-4-methyl-pentanoate (129)



Compound **129** was synthesized according to the general procedure H, using azide **83** (100 mg, 0.31 mmol), alkyne **121** (47.3 mg, 0.31 mmol), copper (II) sulfate pentahydrate (15.7 mg, 0.06 mmol) and sodium ascorbate (31.1 mg, 0.16 mmol) in DMF (5.5 mL) and H₂O (4.5 mL) overnight. The crude product was purified by flash chromatography on silica gel (cHex to cHex/EtOAc: 5/5) affording compound **129** as a white solid (85 mg, 54%). LC tr = 4.92 min, MS (ESI+): $m/z = 469$ and 471

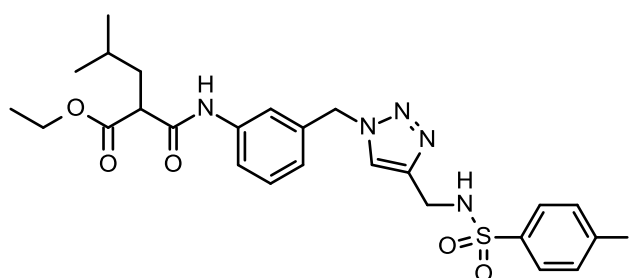
[M+H]⁺. ¹H NMR (500 MHz, DMSO-*d*₆) δ ppm: 10.29 (s, 1H), 7.85 (s, 1H), 7.57–7.55 (m, 2H), 7.34–7.33 (m, 2H), 7.28–7.24 (m, 4H), 5.47 (s, 2H), 4.13–4.05 (m, 2H), 3.96 (s, 2H), 3.55 (dd, *J* = 8.7 and 6.2 Hz, 1H), 1.77–1.71 (m, 1H), 1.67–1.62 (m, 1H), 1.48 (sep, *J* = 6.7 Hz, 1H), 1.15 (t, *J* = 7.1 Hz, 3H), 0.88 (d, *J* = 6.7 Hz, 3H), 0.87 (d, *J* = 6.7 Hz, 3H). ¹³C NMR (126 MHz, DMSO-*d*₆) δ ppm: 169.7, 167.1, 145.9, 138.7, 138.6, 131.1, 130.8, 130.4 (2C), 128.7 (2C), 128.3 (2C), 122.5, 119.4 (2C), 60.7, 52.4, 50.9, 37.4, 30.5, 25.6, 22.6, 21.9, 14.0.

Ethyl 2-[[4-[[4-(4-iodophenyl)triazol-1-yl]methyl]phenyl]carbamoyl]-4-methyl-pentanoate (130)



Compound **130** was synthesized according to the general procedure H, using azide **83** (100 mg, 0.31 mmol), alkyne **122** (71.6 mg, 0.31 mmol), copper (II) sulfate pentahydrate (15.7 mg, 0.06 mmol) and sodium ascorbate (31.1 mg, 0.16 mmol) in DMF (5.5 mL) and H₂O (4.5 mL) overnight. The crude product was purified by flash chromatography on silica gel (cHex to cHex/EtOAc: 7/3) affording compound **130** as a white solid (151 mg, 82%). LC tr = 5.21 min, MS (ESI⁺): *m/z* = 547 [M + H]⁺. ¹H NMR (500 MHz, DMSO-*d*₆) δ ppm: 10.33 (s, 1H), 8.64 (s, 1H), 7.80–7.78 (m, 2H), 7.66–7.64 (m, 2H), 7.60–7.59 (m, 2H), 7.34–7.32 (m, 2H), 5.58 (s, 2H), 4.12–4.05 (m, 2H), 3.56 (dd, *J* = 8.8 and 6.1 Hz, 1H), 1.77–1.71 (m, 1H), 1.66–1.61 (m, 1H), 1.47 (sep, *J* = 6.7 Hz, 1H), 1.14 (t, *J* = 7.1 Hz, 3H), 0.88 (d, *J* = 6.7 Hz, 3H), 0.86 (d, *J* = 6.7 Hz, 3H). ¹³C NMR (126 MHz, DMSO-*d*₆) δ ppm: 169.7, 167.2, 145.7, 138.8, 137.7 (2C), 130.8, 130.2, 128.8 (2C), 127.2 (2C), 121.7, 119.5 (2C), 93.7, 60.7, 52.7, 50.9, 37.4, 25.6, 22.6, 21.9, 14.0.

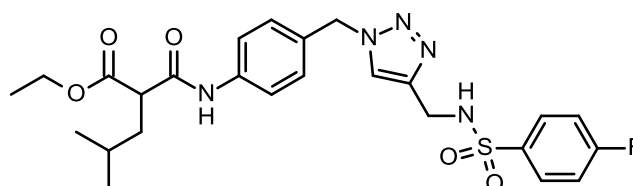
Ethyl 2-[[3-[[4-[(4-iodophenyl)sulfonylamino]methyl]triazol-1-yl]methyl]phenyl]carbamoyl]-4-methyl-pentanoate (113)



Compound **113** was synthesized according to the general procedure H, using azide **112** (110 mg, 0.35 mmol), alkyne **93** (111 mg, 0.35 mmol), copper (II) sulfate pentahydrate (17.3 mg, 0.07 mmol) and sodium ascorbate (34.2 mg, 0.17 mmol) in DMF (5.5 mL) and H₂O (4.5 mL) overnight. The crude product was purified by flash chromatography on silica gel (CH₂Cl₂ to CH₂Cl₂/MeOH: 98/2) affording compound **113** as yellow oil (218 mg, 86%). LC tr = 4.71 min, MS (ESI⁺): *m/z* = 640 [M + H]⁺. ¹H

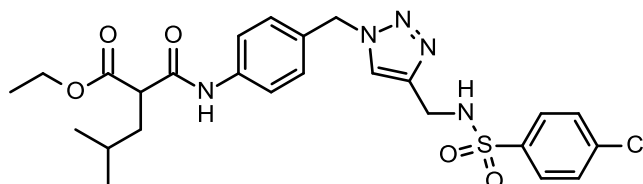
NMR (500 MHz, DMSO-*d*₆) δ ppm: 10.30 (s, 1H), 8.21 (br s, 1H), 7.93–7.92 (m, 2H), 7.90 (s, 1H), 7.56–7.55 (m, 2H), 7.52–7.50 (m, 2H), 7.33–7.30 (m, 1H), 6.97–6.96 (m, 1H), 5.50 (s, 2H), 4.13–4.06 (m, 2H), 4.05–4.04 (m, 2H), 3.56 (dd, *J* = 8.7 and 6.2 Hz, 1H), 1.78–1.72 (m, 1H), 1.67–1.62 (m, 1H), 1.48 (sep, *J* = 6.7 Hz, 1H), 1.15 (t, *J* = 7.1 Hz, 3H), 0.89 (d, *J* = 6.7 Hz, 3H), 0.87 (d, *J* = 6.7 Hz, 3H). ¹³C NMR (126 MHz, DMSO-*d*₆) δ ppm: 169.7, 167.2, 143.5, 140.0, 139.2, 138.0 (2C), 136.6, 129.3, 128.3 (2C), 123.5, 123.2, 119.0, 118.7, 100.4, 60.7, 52.7, 50.9, 38.0, 37.4, 25.7, 22.7, 21.9, 14.1.

Ethyl 2-[[4-[[4-[(4-fluorophenyl)sulfonylamino]methyl]triazol-1-yl]methyl]phenyl]carbamoyl]-4-methyl-pentanoate (150)



Compound **150** was synthesized according to the general procedure H, using azide **83** (100 mg, 0.31 mmol), alkyne **141** (67 mg, 0.31 mmol), copper (II) sulfate pentahydrate (15.7 mg, 0.06 mmol) and sodium ascorbate (31.1 mg, 0.16 mmol) in DMF (5.5 mL) and H₂O (4.5 mL) overnight. The crude product was purified by flash chromatography on silica gel (CH₂Cl₂ to CH₂Cl₂/MeOH: 95/5) affording compound **150** as a pale yellow solid (137 mg, 76%). LC tr = 4.38 min, MS (ESI+): *m/z* = 532 [M+H]⁺. ¹H NMR (500 MHz, DMSO-*d*₆) δ ppm: 10.29 (s, 1H), 8.15 (t, *J* = 5.8 Hz, 1H), 7.85 (s, 1H), 7.82–7.79 (m, 2H), 7.58–7.56 (m, 2H), 7.37–7.33 (m, 2H), 7.25–7.23 (m, 2H), 5.45 (s, 2H), 4.13–4.06 (m, 2H), 4.04 (d, *J* = 5.8 Hz, 2H), 3.56 (dd, *J* = 8.7 and 6.2 Hz, 1H), 1.77–1.72 (m, 1H), 1.68–1.62 (m, 1H), 1.49 (sep, *J* = 6.7 Hz, 1H), 1.15 (t, *J* = 7.1 Hz, 3H), 0.89 (d, *J* = 6.7 Hz, 3H), 0.87 (d, *J* = 6.7 Hz, 3H). ¹³C NMR (126 MHz, DMSO-*d*₆) δ ppm: 169.7, 167.2, 164.1 (d, *J* = 250.8 Hz), 143.5, 138.7, 136.8 (d, *J* = 2.9 Hz), 130.9, 129.6 (d, *J* = 9.2 Hz, 2C), 128.8 (2C), 123.2, 119.4 (2C), 116.2 (d, *J* = 22.1 Hz, 2C), 60.7, 52.4, 51.0, 38.0, 37.4, 25.7, 22.7, 21.9, 14.0.

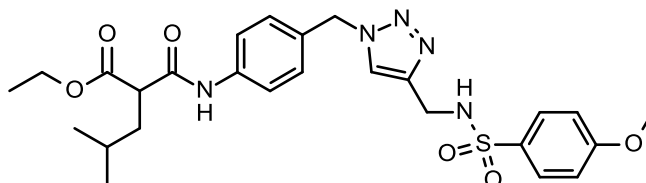
Ethyl 2-[[4-[[4-[(4-chlorophenyl)sulfonylamino]methyl]triazol-1-yl]methyl]phenyl]carbamoyl]-4-methyl-pentanoate (151)



Compound **151** was synthesized according to the general procedure H, using azide **83** (100 mg, 0.31 mmol), alkyne **142** (72.1 mg, 0.31 mmol), copper (II) sulfate pentahydrate (15.7 mg, 0.06 mmol) and sodium ascorbate (31.1 mg, 0.16 mmol) in DMF (5.5 mL) and H₂O (4.5 mL) overnight. The crude product was purified by flash chromatography on silica gel (CH₂Cl₂ to CH₂Cl₂/MeOH: 98/2) affording compound **151** as a colorless wax (138 mg, 73%). LC tr = 4.55 min, MS (ESI+): *m/z* = 548 and 550

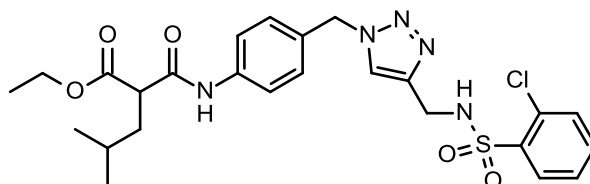
[M + H]⁺. ¹H NMR (500 MHz, DMSO-*d*₆) δ ppm: 10.29 (s, 1H), 8.22 (t, *J* = 5.9 Hz, 1H), 7.86 (s, 1H), 7.75–7.73 (m, 2H), 7.59–7.57 (m, 4H), 7.25–7.24 (m, 2H), 5.45 (s, 2H), 4.11–4.05 (m, 4H), 3.56 (dd, *J* = 8.7 and 6.2 Hz, 1H), 1.78–1.72 (m, 1H), 1.68–1.62 (m, 1H), 1.49 (sep, *J* = 6.7 Hz, 1H), 1.15 (t, *J* = 7.1 Hz, 3H), 0.89 (d, *J* = 6.7 Hz, 3H), 0.87 (d, *J* = 6.7 Hz, 3H). ¹³C NMR (126 MHz, DMSO-*d*₆) δ ppm: 169.7, 167.1, 143.4, 139.3, 138.7, 137.2, 130.9, 129.2 (2C), 128.8 (2C), 128.5 (2C), 123.2, 119.4 (2C), 60.7, 52.3, 50.9, 38.0, 37.4, 25.6, 22.6, 21.9, 14.0.

Ethyl 2-[[4-[[4-[(4-methoxyphenyl)sulfonylamino]methyl]triazol-1-yl]methyl]phenyl]carbamoyl]-4-methyl-pentanoate (152)



Compound **152** was synthesized according to the general procedure H, using azide **83** (100 mg, 0.31 mmol), alkyne **143** (70.8 mg, 0.31 mmol), copper (II) sulfate pentahydrate (15.7 mg, 0.06 mmol) and sodium ascorbate (31.1 mg, 0.16 mmol) in DMF (5.5 mL) and H₂O (4.5 mL) overnight. The crude product was purified by flash chromatography on silica gel (CH₂Cl₂ to CH₂Cl₂/MeOH: 95/5) affording compound **152** as a white solid (141 mg, 76%). LC tr = 4.34 min, MS (ESI⁺): *m/z* = 544 [M + H]⁺. ¹H NMR (500 MHz, DMSO-*d*₆) δ ppm: 10.29 (s, 1H), 7.92 (t, *J* = 5.8 Hz, 1H), 7.85 (s, 1H), 7.70–7.69 (m, 2H), 7.58–7.56 (m, 2H), 7.25–7.24 (m, 2H), 7.07–7.05 (m, 2H), 5.46 (s, 2H), 4.13–4.05 (m, 2H), 3.98 (d, *J* = 5.9 Hz, 2H), 3.82 (s, 3H), 3.56 (dd, *J* = 8.9 and 6.5 Hz, 1H), 1.77–1.72 (m, 1H), 1.68–1.62 (m, 1H), 1.48 (sep, *J* = 6.7 Hz, 1H), 1.15 (t, *J* = 7.1 Hz, 3H), 0.89 (d, *J* = 6.7 Hz, 3H), 0.87 (d, *J* = 6.7 Hz, 3H). ¹³C NMR (126 MHz, DMSO-*d*₆) δ ppm: 169.7, 167.1, 162.1, 143.7, 138.7, 131.9, 131.0, 128.7 (4C), 123.2, 119.4 (2C), 114.3 (2C), 60.7, 55.6, 52.4, 51.0, 38.1, 37.4, 25.7, 22.7, 21.9, 14.0.

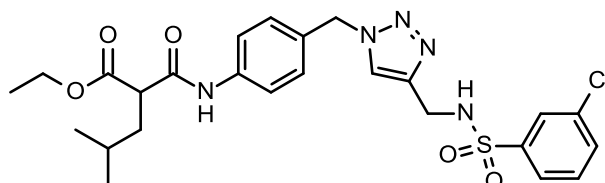
Ethyl 2-[[4-[[4-[(2-chlorophenyl)sulfonylamino]methyl]triazol-1-yl]methyl]phenyl]carbamoyl]-4-methyl-pentanoate (153)



Compound **153** was synthesized according to the general procedure H, using azide **83** (100 mg, 0.31 mmol), alkyne **144** (72.1 mg, 0.31 mmol), copper (II) sulfate pentahydrate (15.7 mg, 0.06 mmol) and sodium ascorbate (31.1 mg, 0.16 mmol) in DMF (5.5 mL) and H₂O (4.5 mL) overnight. The crude product was purified by flash chromatography on silica gel (CH₂Cl₂ to CH₂Cl₂/MeOH: 98/2) affording compound **153** as colorless oil (170 mg, 82%). LC tr = 4.40 min, MS (ESI⁺): *m/z* = 548 and 550 [M + H]⁺. ¹H NMR (500 MHz, DMSO-*d*₆) δ ppm: 10.31 (s, 1H), 8.37 (br s, 1H), 7.88 (dd, *J* = 7.9 and 1.6 Hz, 1H), 7.73 (s, 1H), 7.59–7.57 (m, 2H), 7.53 (td, *J* = 11.5 and 1.6 Hz, 1H), 7.48 (dd, *J* = 7.9 and 1.3

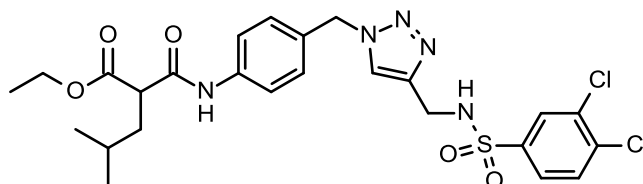
Hz, 1H), 7.42 (td, $J = 11.3$ and 1.3 Hz, 1H), 7.23–7.22 (m, 2H), 5.42 (s, 2H), 4.15 (br s, 2H), 4.11–4.08 (m, 2H), 3.56 (dd, $J = 9.0$ and 6.4 Hz, 1H), 1.78–1.73 (m, 1H), 1.68–1.63 (m, 1H), 1.49 (sep, $J = 6.6$ Hz, 1H), 1.15 (t, $J = 7.0$ Hz, 3H), 0.89 (d, $J = 6.6$ Hz, 3H), 0.87 (d, $J = 6.6$ Hz, 3H). ^{13}C NMR (126 MHz, DMSO- d_6) δ ppm: 169.7, 167.2, 143.6, 138.7, 138.0, 133.8, 131.5, 130.9, 130.5, 130.3, 128.8 (2C), 127.4, 123.0, 119.5 (2C), 60.7, 52.3, 51.0, 37.8, 37.4, 25.7, 22.6, 21.9, 14.0.

Ethyl 2-[[4-[[4-[(3-chlorophenyl)sulfonylamino]methyl]triazol-1-yl]methyl]phenyl]carbamoyl]-4-methyl-pentanoate (154)



Compound **154** was synthesized according to the general procedure H, using azide **83** (100 mg, 0.31 mmol), alkyne **145** (72.1 mg, 0.31 mmol), copper (II) sulfate pentahydrate (15.7 mg, 0.06 mmol) and sodium ascorbate (31.1 mg, 0.16 mmol) in DMF (5.5 mL) and H₂O (4.5 mL) overnight. The crude product was purified by flash chromatography on silica gel (CH₂Cl₂ to CH₂Cl₂/MeOH: 98/2) affording compound **154** as a white solid (136 mg, 74%). LC tr = 4.55 min, MS (ESI+): $m/z = 548$ and 550 [$M + H$]⁺. ^1H NMR (500 MHz, DMSO- d_6) δ ppm: 10.30 (s, 1H), 8.28 (br s, 1H), 7.82 (s, 1H), 7.74 (t, $J = 1.7$ Hz, 1H), 7.70–7.68 (m, 1H), 7.66–7.64 (m, 1H), 7.58–7.56 (m, 2H), 7.53 (t, $J = 7.9$ Hz, 1H), 7.25–7.23 (m, 2H), 5.44 (s, 2H), 4.13–4.06 (m, 4H), 3.56 (dd, $J = 8.7$ and 6.2 Hz, 1H), 1.78–1.72 (m, 1H), 1.68–1.62 (m, 1H), 1.49 (sep, $J = 6.7$ Hz, 1H), 1.15 (t, $J = 7.1$ Hz, 3H), 0.89 (d, $J = 6.7$ Hz, 3H), 0.87 (d, $J = 6.7$ Hz, 3H). ^{13}C NMR (126 MHz, DMSO- d_6) δ ppm: 169.7, 167.2, 143.3, 142.4, 138.7, 133.7, 132.3, 131.1, 130.9, 128.8 (2C), 126.1, 125.2, 123.1, 119.5 (2C), 60.7, 52.4, 50.9, 38.0, 37.4, 25.7, 22.6, 21.9, 14.0.

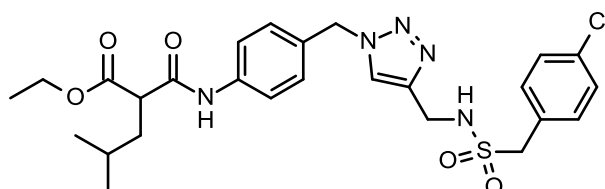
Ethyl 2-[[4-[[4-[(3,4-dichlorophenyl)sulfonylamino]methyl]triazol-1-yl]methyl]phenyl]carbamoyl]-4-methyl-pentanoate (155)



Compound **155** was synthesized according to the general procedure H, using azide **83** (70 mg, 0.22 mmol), alkyne **146** (58.1 mg, 0.22 mmol), copper (II) sulfate pentahydrate (11 mg, 0.04 mmol) and sodium ascorbate (21.8 mg, 0.11 mmol) in DMF (5.5 mL) and H₂O (4.5 mL) overnight. The crude product was purified by flash chromatography on silica gel (CH₂Cl₂ to CH₂Cl₂/MeOH: 95/5) affording compound **155** as a white powder (108 mg, 77%). LC tr = 4.76 min, MS (ESI+): $m/z = 582$, 584 and 586 [$M + H$]⁺. ^1H NMR (500 MHz, DMSO- d_6) δ ppm: 10.29 (s, 1H), 8.36 (br s, 1H), 7.91 (d, $J = 2.1$ Hz, 1H), 7.88 (s, 1H), 7.77 (d, $J = 8.4$ Hz, 1H), 7.67 (dd, $J = 8.4$ and 2.1 Hz, 1H), 7.58–7.57 (m, 2H),

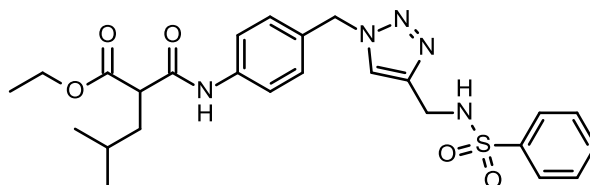
7.25–7.23 (m, 2H), 5.45 (s, 2H), 4.11–4.05 (m, 4H), 3.56 (dd, $J = 8.8$ and 6.2 Hz, 1H), 1.78–1.72 (m, 1H), 1.68–1.62 (m, 1H), 1.49 (sep, $J = 6.6$ Hz, 1H), 1.15 (t, $J = 7.1$ Hz, 3H), 0.89 (d, $J = 6.6$ Hz, 3H), 0.87 (d, $J = 6.6$ Hz, 3H). ^{13}C NMR (126 MHz, $\text{DMSO-}d_6$) δ ppm: 169.7, 167.1, 143.2, 140.9, 138.7, 135.4, 131.9, 131.4, 130.8, 128.7 (2C), 128.4, 126.6, 123.2, 119.5 (2C), 60.7, 52.4, 50.9, 38.0, 37.4, 25.6, 22.6, 21.9, 14.0.

Ethyl 2-[[4-[[4-[(4-chlorophenyl)methylsulfonylamino]methyl]triazol-1-yl]methyl]phenyl]carbamoyl]-4-methyl-pentanoate (156)



Compound **156** was synthesized according to the general procedure H, using azide **83** (70 mg, 0.22 mmol), alkyne **147** (53.6 mg, 0.22 mmol), copper (II) sulfate pentahydrate (11 mg, 0.04 mmol) and sodium ascorbate (21.8 mg, 0.11 mmol) in DMF (5.5 mL) and H_2O (4.5 mL) overnight. The crude product was purified by flash chromatography on silica gel (CH_2Cl_2 to $\text{CH}_2\text{Cl}_2/\text{MeOH}$: 95/5) affording compound **156** as colorless oil (65 mg, 45%). LC tr = 4.60 min, MS (ESI+): $m/z = 562$ and 564 [$\text{M} + \text{H}$] $^+$. ^1H NMR (500 MHz, $\text{DMSO-}d_6$) δ ppm: 10.29 (s, 1H), 7.99 (s, 1H), 7.63 (t, $J = 5.9$ Hz, 1H), 7.59–7.57 (m, 2H), 7.37–7.36 (m, 2H), 7.32–7.30 (m, 2H), 7.28–7.27 (m, 2H), 5.53 (s, 2H), 4.34 (s, 2H), 4.17 (d, $J = 5.9$ Hz, 2H), 4.13–4.05 (m, 2H), 3.55 (dd, $J = 8.6$ and 6.2 Hz, 1H), 1.77–1.71 (m, 1H), 1.68–1.62 (m, 1H), 1.48 (sep, $J = 6.7$ Hz, 1H), 1.15 (t, $J = 7.1$ Hz, 3H), 0.88 (d, $J = 6.7$ Hz, 3H), 0.87 (d, $J = 6.7$ Hz, 3H). ^{13}C NMR (126 MHz, $\text{DMSO-}d_6$) δ ppm: 169.7, 167.1, 144.7, 138.8, 132.9, 132.5 (2C), 131.1, 129.3, 128.8 (2C), 128.3 (2C), 123.2, 119.4 (2C), 60.7, 56.7, 52.4, 50.9, 38.0, 37.4, 25.6, 22.6, 21.9, 14.0.

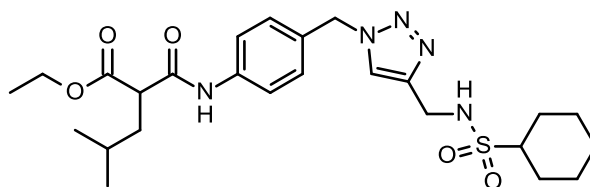
Ethyl 2-[[4-[[4-(benzenesulfonamidomethyl)triazol-1-yl]methyl]phenyl]carbamoyl]-4-methyl-pentanoate (157)



Compound **157** was synthesized according to the general procedure H, using azide **83** (100 mg, 0.31 mmol), alkyne **148** (61.3 mg, 0.31 mmol), copper (II) sulfate pentahydrate (15.7 mg, 0.06 mmol) and sodium ascorbate (31.1 mg, 0.17 mmol) in DMF (5.5 mL) and H_2O (4.5 mL) overnight. The crude product was purified by flash chromatography on silica gel (CH_2Cl_2 to $\text{CH}_2\text{Cl}_2/\text{MeOH}$: 95/5) affording compound **157** as colorless wax (123 mg, 68%). LC tr = 4.32 min, MS (ESI+): $m/z = 514$ [$\text{M} + \text{H}$] $^+$. ^1H NMR (500 MHz, $\text{DMSO-}d_6$) δ ppm: 10.33 (s, 1H), 8.13 (t, $J = 5.9$ Hz, 1H), 7.81 (s, 1H), 7.76–7.74 (m, 2H), 7.61–7.51 (m, 5H), 7.25–7.23 (m, 2H), 5.44 (s, 2H), 4.12–4.05 (m, 2H), 4.03 (d, $J = 5.9$ Hz,

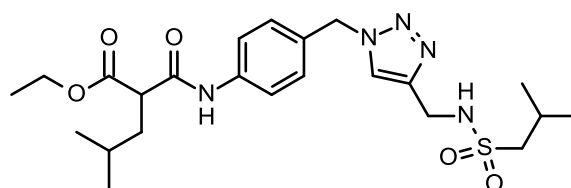
2H), 3.56 (dd, $J = 9.0$ and 6.1 Hz, 1H), 1.78–1.72 (m, 1H), 1.67–1.62 (m, 1H), 1.48 (sep, $J = 6.7$ Hz, 1H), 1.15 (t, $J = 7.1$ Hz, 3H), 0.89 (d, $J = 6.7$ Hz, 3H), 0.87 (d, $J = 6.7$ Hz, 3H). ^{13}C NMR (126 MHz, $\text{DMSO-}d_6$) δ ppm: 170.2, 167.6, 141.1, 140.8, 139.2, 132.8, 131.4, 129.5 (2C), 129.2 (2C), 126.9 (2C), 123.6, 119.9 (2C), 61.1, 52.8, 51.4, 38.6, 37.8, 26.1, 23.1, 22.4, 14.5.

Ethyl 2-[[4-[[4-[(cyclohexylsulfonylamino)methyl]triazol-1-yl]methyl]phenyl]carbamoyl]-4-methyl-pentanoate (158)



Compound **158** was synthesized according to the general procedure H, using azide **83** (70 mg, 0.22 mmol), alkyne **149** (44.3 mg, 0.22 mmol), copper (II) sulfate pentahydrate (11 mg, 0.04 mmol) and sodium ascorbate (21.8 mg, 0.11 mmol) in DMF (5.5 mL) and H_2O (4.5 mL) overnight. The crude product was purified by flash chromatography on silica gel (CH_2Cl_2 to $\text{CH}_2\text{Cl}_2/\text{MeOH}$: 9/1) affording compound **158** as colorless oil (58 mg, 47%). LC tr = 4.39 min, MS (ESI+): $m/z = 520$ [$\text{M} + \text{H}$] $^+$. ^1H NMR (500 MHz, $\text{DMSO-}d_6$) δ ppm: 10.28 (s, 1H), 8.01 (s, 1H), 7.58–7.56 (m, 2H), 7.50 (t, $J = 5.4$ Hz, 1H), 7.31–7.29 (m, 2H), 5.52 (s, 2H), 4.18 (d, $J = 4.6$ Hz, 2H), 4.10–4.07 (m, 2H), 3.56–3.53 (m, 1H), 2.71–2.64 (m, 1H), 1.89–1.87 (m, 2H), 1.77–1.71 (m, 1H), 1.67–1.64 (m, 3H), 1.53–1.52 (m, 1H), 1.49–1.46 (m, 1H), 1.23–1.21 (m, 2H), 1.15 (t, $J = 6.8$ Hz, 3H), 1.03–1.00 (m, 3H), 0.89–0.86 (m, 6H). ^{13}C NMR (126 MHz, $\text{DMSO-}d_6$) δ ppm: 169.7, 167.1, 144.9, 138.7, 131.1, 128.7 (2C), 123.1, 119.4 (2C), 60.6, 59.4, 52.4, 50.9, 37.7, 37.4, 25.9 (2C), 25.6, 24.8, 24.4 (2C), 22.6, 21.9, 14.0.

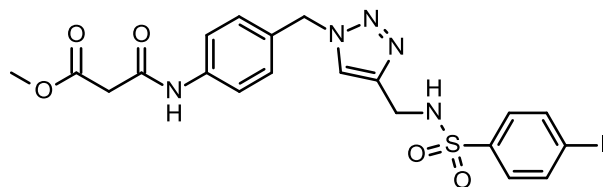
Ethyl 2-[[4-[[4-[(isobutylsulfonylamino)methyl]triazol-1-yl]methyl]phenyl]carbamoyl]-4-methyl-pentanoate (159)



Compound **159** was synthesized according to the general procedure H, using azide **83** (100 mg, 0.31 mmol), alkyne **106** (55 mg, 0.31 mmol), copper (II) sulfate pentahydrate (15.7 mg, 0.06 mmol) and sodium ascorbate (31.1 mg, 0.17 mmol) in DMF (5.5 mL) and H_2O (4.5 mL) overnight. The crude product was purified by flash chromatography on silica gel (CH_2Cl_2 to $\text{CH}_2\text{Cl}_2/\text{MeOH}$: 95/5) affording compound **159** as colorless oil (85 mg, 51%). LC tr = 4.29 min, MS (ESI+): $m/z = 494$ [$\text{M} + \text{H}$] $^+$. ^1H NMR (500 MHz, $\text{DMSO-}d_6$) δ ppm: 10.29 (s, 1H), 8.01 (s, 1H), 7.58–7.56 (m, 2H), 7.53 (t, $J = 5.9$ Hz, 1H), 7.30–7.28 (m, 2H), 5.52 (s, 2H), 4.18 (d, $J = 5.9$ Hz, 2H), 4.10–4.07 (m, 2H), 3.55 (dd, $J = 8.6$ and 6.3 Hz, 1H), 2.80 (d, $J = 6.4$ Hz, 2H), 1.97 (sep, $J = 6.7$ Hz, 1H), 1.77–1.71 (m, 1H), 1.67–1.62 (m, 1H), 1.48 (sep, $J = 6.7$ Hz, 1H), 1.15 (t, $J = 7.1$ Hz, 3H), 0.91 (d, $J = 6.7$ Hz, 6H), 0.88 (d, $J =$

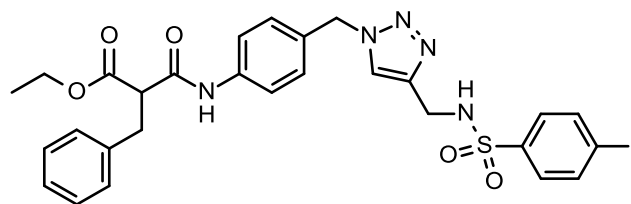
6.7 Hz, 3H), 0.87 (d, $J = 6.7$ Hz, 3H). ^{13}C NMR (126 MHz, $\text{DMSO-}d_6$) δ ppm: 169.7, 167.2, 144.6, 138.7, 131.1, 128.7 (2C), 123.2, 119.4 (2C), 60.7, 59.2, 52.4, 50.9, 37.6, 37.4, 25.6, 24.1, 22.7, 22.1 (2C), 21.9, 14.0.

Methyl 3-[4-[[4-[[[4-iodophenyl)sulfonylamino]methyl]triazol-1-yl]methyl]anilino]-3-oxo-propanoate (176)



Compound **176** was synthesized according to the general procedure H, using azide **172** (70 mg, 0.28 mmol), alkyne **93** (90.6 mg, 0.28 mmol), copper (II) sulfate pentahydrate (14.1 mg, 0.06 mmol) and sodium ascorbate (27.9 mg, 0.14 mmol) in DMF (5 mL) and H_2O (4 mL) overnight. The crude product was purified by flash chromatography on silica gel (CH_2Cl_2 to $\text{CH}_2\text{Cl}_2/\text{MeOH}$: 95/5) affording compound **176** as pale yellow oil (140 mg, 86%). LC tr = 3.72 min, MS (ESI+): $m/z = 570$ [$\text{M} + \text{H}$] $^+$. ^1H NMR (500 MHz, $\text{DMSO-}d_6$) δ ppm: 10.25 (s, 1H), 8.19 (t, $J = 5.9$ Hz, 1H), 7.93–7.91 (m, 2H), 7.85 (s, 1H), 7.57–7.55 (m, 2H), 7.51–7.50 (m, 2H), 7.26–7.24 (m, 2H), 5.45 (s, 2H), 4.03 (d, $J = 5.9$ Hz, 2H), 3.64 (s, 3H), 3.47 (s, 2H). ^{13}C NMR (126 MHz, $\text{DMSO-}d_6$) δ ppm: 168.1, 164.1, 143.4, 140.0, 138.7, 138.0 (2C), 130.8, 128.8 (2C), 128.3 (2C), 123.2, 119.3 (2C), 100.4, 52.4, 52.0, 43.4, 38.0.

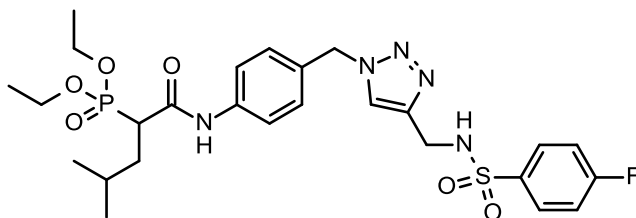
Ethyl 2-benzyl-3-[4-[[4-[[[4-iodophenyl)sulfonylamino]methyl]triazol-1-yl]methyl]anilino]-3-oxo-propanoate (177)



Compound **177** was synthesized according to the general procedure H, using azide **173** (65 mg, 0.18 mmol), alkyne **93** (59.2 mg, 0.18 mmol), copper (II) sulfate pentahydrate (9.21 mg, 0.04 mmol) and sodium ascorbate (18.3 mg, 0.09 mmol) in DMF (5 mL) and H_2O (4 mL) overnight. The crude product was purified by flash chromatography on silica gel (CH_2Cl_2 to $\text{CH}_2\text{Cl}_2/\text{MeOH}$: 95/5) affording compound **176** as a colorless solid (94 mg, 74%). LC tr = 4.59 min, MS (ESI+): $m/z = 674$ [$\text{M} + \text{H}$] $^+$. ^1H NMR (500 MHz, $\text{DMSO-}d_6$) δ ppm: 10.20 (s, 1H), 8.18 (t, $J = 5.6$ Hz, 1H), 7.93–7.91 (m, 2H), 7.84 (s, 1H), 7.51–7.49 (m, 4H), 7.26–7.22 (m, 6H), 7.18–7.15 (m, 1H), 5.44 (s, 2H), 4.08 (q, $J = 7.0$ Hz, 2H), 4.02 (d, $J = 5.5$ Hz, 2H), 3.82 (dd, $J = 8.2$ and 7.1 Hz, 1H), 3.16–3.08 (m, 2H), 1.12 (t, $J = 7.0$ Hz, 3H). ^{13}C NMR (126 MHz, $\text{DMSO-}d_6$) δ ppm: 169.0, 166.4, 143.4, 140.0, 138.5, 138.4, 138.0

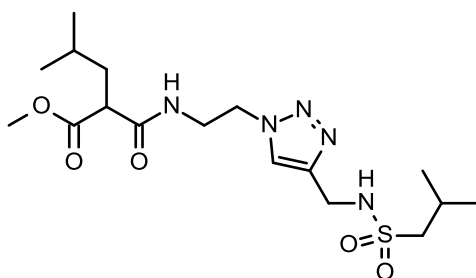
(2C), 130.9, 128.8 (2C), 128.7 (2C), 128.3 (2C), 128.2 (2C), 126.4, 123.2, 119.5 (2C), 100.4, 60.8, 54.3, 52.3, 38.0, 34.2, 14.0.

2-Diethoxyphosphoryl-N-[4-[[4-[(4-fluorophenyl)sulfonylamino]methyl]triazol-1-yl]methyl]phenyl]-4-methyl-pentanamide (195)



Compound **195** was synthesized according to the general procedure H, using azide **194** (100 mg, 0.26 mmol), alkyne **141** (55.8 mg, 0.26 mmol), copper (II) sulfate pentahydrate (13.1 mg, 0.05 mmol) and sodium ascorbate (25.9 mg, 0.13 mmol) in DMF (5.5 mL) and H₂O (4.5 mL) overnight. The crude product was purified by flash chromatography on silica gel (CH₂Cl₂ to CH₂Cl₂/MeOH: 95/5) affording compound **195** as a white solid (129 mg, 77%). LC tr = 4.07 min, MS (ESI+): m/z = 596 [M + H]⁺. ¹H NMR (500 MHz, DMSO-*d*₆) δ ppm: 10.20 (s, 1H), 8.15 (t, *J* = 6.0 Hz, 1H), 7.85 (s, 1H), 7.81–7.79 (m, 2H), 7.57–7.55 (m, 2H), 7.36–7.33 (m, 2H), 7.25–7.23 (m, 2H), 5.45 (s, 2H), 4.05–3.98 (m, 6H), 3.22–3.15 (m, 1H), 1.99–1.92 (m, 1H), 1.49–1.38 (m, 2H), 1.22–1.17 (m, 6H), 0.87–0.85 (m, 6H). ¹³C NMR (126 MHz, DMSO-*d*₆) δ ppm: 166.6 (d, *J* = 4.9 Hz), 164.1 (d, *J* = 250.4 Hz), 143.5, 138.9, 136.8 (d, *J* = 2.8 Hz), 130.9, 129.6 (d, *J* = 9.3 Hz, 2C), 128.8 (2C), 123.2, 119.3 (2C), 116.3 (d, *J* = 23.0 Hz, 2C), 62.1 (d, *J* = 6.4 Hz), 61.9 (d, *J* = 6.4 Hz), 52.4, 44.5 (d, *J* = 130.1 Hz), 38.1, 35.4 (d, *J* = 4.7 Hz), 26.4 (*J* = 14.7 Hz), 23.0, 21.3, 16.3, 16.3.

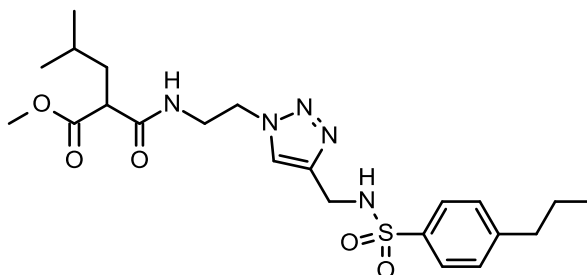
Methyl 2-[2-[4-[(isobutylsulfonylamino)methyl]triazol-1-yl]ethylcarbamoyl]-4-methyl-pentanoate (102)



Compound **102** was synthesized according to the general procedure H, using azide **101** (100 mg, 0.41 mmol), alkyne **106** (72.3 mg, 0.41 mmol), copper (II) sulfate pentahydrate (20.6 mg, 0.08 mmol) and sodium ascorbate (40.9 mg, 0.21 mmol) in DMF (6 mL) and H₂O (5 mL) overnight. The crude product was purified by flash chromatography on silica gel (CH₂Cl₂ to CH₂Cl₂/MeOH: 95/5) affording compound **102** as a white solid (54 mg, 31%). LC tr = 3.20 min, MS (ESI+): m/z = 418 [M + H]⁺. ¹H NMR (500 MHz, DMSO-*d*₆) δ ppm: 8.35 (t, *J* = 5.6 Hz, 1H), 7.93 (s, 1H), 7.54 (t, *J* = 6.1 Hz, 1H), 4.43–4.40 (m, 2H), 4.18 (d, *J* = 6.1 Hz, 2H), 3.59 (s, 3H), 3.56–3.46 (m, 2H), 3.29 (dd, *J* = 8.6 and 6.5

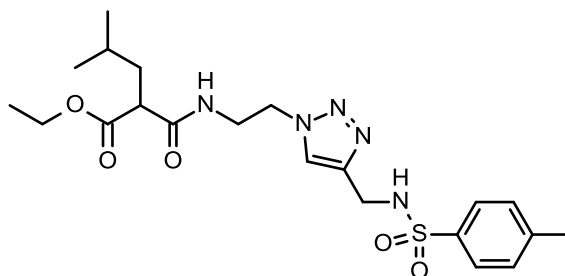
Hz, 1H), 2.89 (d, $J = 6.4$ Hz, 2H), 2.04 (sep, $J = 6.6$ Hz, 1H), 1.62–1.57 (m, 1H), 1.55–1.49 (m, 1H), 1.34 (sep, $J = 6.7$ Hz, 1H), 0.97 (d, $J = 6.7$ Hz, 6H), 0.83–0.80 (m, 6H). ^{13}C NMR (126 MHz, $\text{DMSO-}d_6$) δ ppm: 170.4, 168.6, 144.2, 123.4, 59.1, 51.9, 49.8, 48.4, 39.1, 37.7, 37.3, 25.3, 24.2, 22.7, 22.2 (2C), 21.8.

Methyl 4-methyl-2-[2-[4-[(4-propylphenyl)sulfonylamino]methyl]triazol-1-yl]ethylcarbamoyl]pentanoate (104)



Compound **104** was synthesized according to the general procedure H, using azide **101** (100 mg, 0.41 mmol), alkyne **108** (98 mg, 0.41 mmol), copper (II) sulfate pentahydrate (20.6 mg, 0.08 mmol) and sodium ascorbate (40.9 mg, 0.21 mmol) in DMF (6 mL) and H_2O (5 mL) overnight. The crude product was purified by flash chromatography on silica gel (CH_2Cl_2 to $\text{CH}_2\text{Cl}_2/\text{MeOH}$: 95/5) affording compound **104** as a white solid (135 mg, 57%). LC tr = 4.24 min, MS (ESI+): $m/z = 480$ $[\text{M} + \text{H}]^+$. ^1H NMR (500 MHz, $\text{DMSO-}d_6$) δ ppm: 8.33 (t, $J = 5.6$ Hz, 1H), 8.04 (t, $J = 6.1$ Hz, 1H), 7.78 (s, 1H), 7.70–7.68 (m, 2H), 7.40–7.38 (m, 2H), 4.35–4.33 (m, 2H), 3.99 (d, $J = 6.1$ Hz, 2H), 3.58 (s, 3H), 3.55–3.41 (m, 2H), 3.28 (dd, $J = 8.7$ and 6.4 Hz, 1H), 2.63 (t, $J = 7.6$ Hz, 2H), 1.65–1.56 (m, 3H), 1.54–1.48 (m, 1H), 1.33 (sep, $J = 6.7$ Hz, 1H), 0.89 (t, $J = 7.3$ Hz, 3H), 0.81–0.79 (m, 6H). ^{13}C NMR (126 MHz, $\text{DMSO-}d_6$) δ ppm: 170.4, 168.3, 147.1, 143.2, 137.7, 129.0 (2C), 126.6 (2C), 123.4, 51.9, 49.8, 48.3, 38.2, 37.3, 36.9, 25.3, 23.7, 22.7, 21.8, 21.6, 13.6.

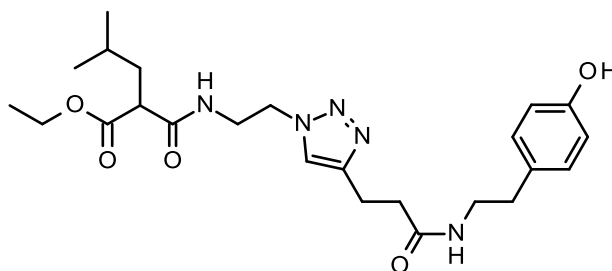
Ethyl 4-methyl-2-[2-[4-[(p-tolyl)sulfonylamino]methyl]triazol-1-yl]ethylcarbamoyl]pentanoate (103)



Compound **103** was synthesized according to the general procedure H, using azide **86** (100 mg, 0.39 mmol), alkyne **107** (81.6 mg, 0.39 mmol), copper (II) sulfate pentahydrate (19.5 mg, 0.08 mmol) and sodium ascorbate (38.6 mg, 0.2 mmol) in DMF (5.5 mL) and H_2O (4.5 mL) overnight. The crude product was purified by flash chromatography on silica gel (CH_2Cl_2 to $\text{CH}_2\text{Cl}_2/\text{MeOH}$: 95/5) affording compound **103** as colorless oil (123 mg, 58%). LC tr = 3.93 min, MS (ESI+): $m/z = 466$ $[\text{M} + \text{H}]^+$. ^1H

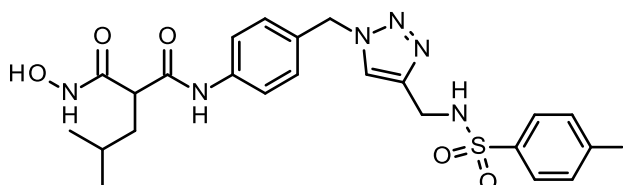
NMR (500 MHz, DMSO-*d*₆) δ ppm: 8.34 (t, *J* = 5.6 Hz, 1H), 8.06 (t, *J* = 5.2 Hz, 1H), 7.78 (s, 1H), 7.67–7.66 (m, 2H), 7.38–7.37 (m, 2H), 4.39–4.31 (m, 2H), 4.08–4.00 (m, 2H), 3.97 (d, *J* = 5.2 Hz, 2H), 3.50–3.42 (m, 2H), 3.26 (dd, *J* = 8.6 and 6.5 Hz, 1H), 2.37 (s, 3H), 1.61–1.55 (m, 1H), 1.53–1.47 (m, 1H), 1.32 (sep, *J* = 6.7 Hz, 1H), 1.13 (t, *J* = 7.0 Hz, 3H), 0.81–0.78 (m, 6H). ¹³C NMR (126 MHz, DMSO-*d*₆) δ ppm: 170.0, 168.7, 143.3, 142.8, 137.4, 129.7 (2C), 126.7 (2C), 123.5, 60.6, 50.0, 48.4, 39.1, 38.2, 37.3, 25.4, 22.8, 21.9, 21.0, 14.1.

Ethyl 2-[2-[4-[3-[2-(4-hydroxyphenyl)ethylamino]-3-oxo-propyl]triazol-1-yl]ethylcarbamoyl]-4-methyl-pentanoate (105)



Compound **105** was synthesized according to the general procedure H, using azide **86** (100 mg, 0.39 mmol), alkyne **109** (84.8 mg, 0.39 mmol), copper (II) sulfate pentahydrate (19.5 mg, 0.08 mmol) and sodium ascorbate (38.6 mg, 0.2 mmol) in DMF (5.5 mL) and H₂O (4.5 mL) overnight. The crude product was purified by flash chromatography on silica gel (CH₂Cl₂ to CH₂Cl₂/MeOH: 95/5) affording compound **105** as colorless oil (116 mg, 45%). LC tr = 3.30 min, MS (ESI+): *m/z* = 474 [M + H]⁺. ¹H NMR (500 MHz, DMSO-*d*₆) δ ppm: 9.19 (s, 1H), 8.34 (t, *J* = 5.6 Hz, 1H), 7.94 (t, *J* = 5.6 Hz, 1H), 7.71 (s, 1H), 6.96–6.95 (m, 2H), 6.66–6.65 (m, 2H), 4.37–4.34 (m, 2H), 4.08–4.00 (m, 2H), 3.56–3.44 (m, 2H), 3.26 (dd, *J* = 8.7 and 6.4 Hz, 1H), 3.20–3.16 (m, 2H), 2.79 (t, *J* = 7.8 Hz, 2H), 2.56 (t, *J* = 7.5 Hz, 2H), 2.37 (t, *J* = 7.8 Hz, 3H), 1.61–1.55 (m, 1H), 1.52–1.47 (m, 1H), 1.31 (sep, *J* = 6.7 Hz, 1H), 1.14 (t, *J* = 7.1 Hz, 3H), 0.81 (d, *J* = 6.7 Hz, 2H), 0.79 (d, *J* = 6.7 Hz, 3H). ¹³C NMR (126 MHz, DMSO-*d*₆) δ ppm: 170.9, 170.0, 168.7, 155.6, 145.9, 129.6, 129.5 (2C), 122.1, 115.1 (2C), 60.5, 50.0, 48.3, 40.6, 39.1, 37.3, 35.0, 34.4, 25.4, 22.8, 21.8, 21.4, 14.0.

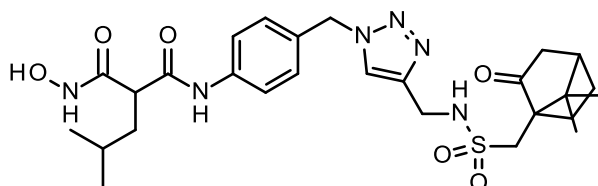
2-(Hydroxycarbamoyl)-N-[4-[4-[[4-(4-iodophenyl)sulfonylamino]methyl]triazol-1-yl]methyl]phenyl]-4-methyl-pentanamide (Hit L1)



Hit L1 was synthesized according to the general procedure G, using ester **88** (110 mg, 0.17 mmol), KCN (2.27 mg, 0.03 mmol) and NH₂OH (1.5 mL, 50% w/w in water) in MeOH (1.5 mL) overnight. The crude product was purified by flash chromatography on silica gel (CH₂Cl₂ to CH₂Cl₂/MeOH: 95/5) affording compound **Hit L1** as a white solid after lyophilization (96 mg, 85%). Purity: 97%, LC

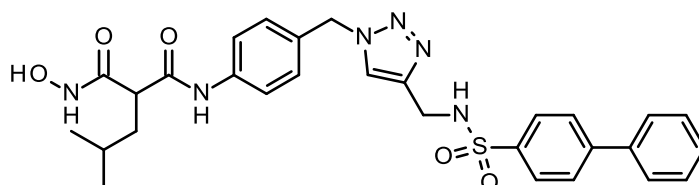
tr = 3.77 min, MS (ESI+): m/z = 627 [M + H]⁺. ¹H NMR (300 MHz, DMSO-*d*₆) δ ppm: 10.54 (br s, 1H), 9.92 (s, 1H), 8.96 (br s, 1H), 8.34–8.08 (m, 1H), 7.93–7.91 (m, 2H), 7.83 (s, 1H), 7.58–7.57 (m, 2H), 7.51–7.49 (m, 2H), 7.24–7.23 (m, 2H), 5.44 (s, 2H), 4.03 (s, 2H), 3.23 (t, *J* = 7.5 Hz, 1H), 1.67 (t, *J* = 7.1 Hz, 2H), 1.46 (sep, *J* = 6.6 Hz, 1H), 0.85–0.87 (m, 6H). ¹³C NMR (126 MHz, DMSO-*d*₆) δ ppm: 167.9, 166.3, 143.5, 140.1, 138.8, 138.0 (2C), 130.7, 128.7 (2C), 128.3 (2C), 123.2, 119.6 (2C), 100.4, 52.4, 49.9, 38.1, 38.0, 25.7, 22.4, 22.3. HRMS-ESI+ (m/z): calcd. for C₂₃H₂₈IN₆O₅S [M + H]⁺ 627.0887, found 627.0877.

***N*-[4-[[4-[(7,7-Dimethyl-2-oxo-norbornan-1-yl)methylsulfonylamino]methyl]triazol-1-yl]methyl]phenyl]-2-(hydroxycarbamoyl)-4-methyl-pentanamide (Hit L2)**



Hit L2 was synthesized according to the general procedure G, using ester **89** (127 mg, 0.22 mmol), KCN (2.85 mg, 0.04 mmol) and NH₂OH (2 mL, 50% w/w in water) in MeOH (2 mL) overnight. The crude product was purified by flash chromatography on silica gel (CH₂Cl₂ to CH₂Cl₂/MeOH: 95/5) followed by preparative HPLC (H₂O+0.05%FA / ACN+0.05%FA: 95:5 to 5:95) affording compound **Hit L2** as a white solid after lyophilization (13 mg, 10%). Purity: 100%, LC tr = 3.57 min, MS (ESI+): m/z = 575 [M + H]⁺. ¹H NMR (500 MHz, DMSO-*d*₆) δ ppm: 10.52 (br s, 1H), 9.81 (s, 1H), 8.96 (s, 1H), 8.00 (s, 1H), 7.57–7.55 (m, 3H), 7.28–7.26 (m, 2H), 5.51 (s, 2H), 4.26–4.24 (m, 2H), 3.24–3.18 (m, 2H), 2.87–2.84 (m, 1H), 2.33–2.28 (m, 2H), 2.01 (t, *J* = 4.4 Hz, 1H), 1.91–1.87 (m, 2H), 1.69–1.65 (m, 2H), 1.50–1.46 (m, 2H), 1.39–1.34 (m, 1H), 0.96 (s, 3H), 0.87 (d, *J* = 6.6 Hz, 3H), 0.86 (d, *J* = 6.6 Hz, 3H), 0.71 (s, 3H). ¹³C NMR (126 MHz, DMSO-*d*₆) δ ppm: 214.6, 167.8, 168.3, 144.6, 138.7, 130.9, 128.6 (2C), 123.2, 119.5 (2C), 57.9, 52.4, 50.0, 48.6, 47.6, 42.0, 41.9, 38.0, 38.0, 26.3, 25.7, 24.5, 22.4, 22.3, 19.4, 19.2. HRMS-ESI+ (m/z): calcd. for C₂₇H₃₉N₆O₆S [M + H]⁺: 575.2652, found 575.2645.

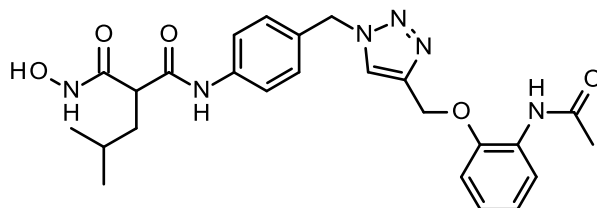
2-(Hydroxycarbamoyl)-4-methyl-N-[4-[[4-[(4-phenylphenyl)sulfonylamino]methyl]triazol-1-yl]methyl]phenyl]pentanamide (Hit L3)



Hit L3 was synthesized according to the general procedure G, using ester **90** (129 mg, 0.22 mmol), KCN (2.85 mg, 0.04 mmol) and NH₂OH (2 mL, 50% w/w in water) in MeOH (2 mL) overnight. The crude product was purified by flash chromatography on silica gel (CH₂Cl₂ to CH₂Cl₂/MeOH: 95/5) affording compound **Hit L3** as a white solid after lyophilization (42 mg, 32%). Purity: 100%, LC tr =

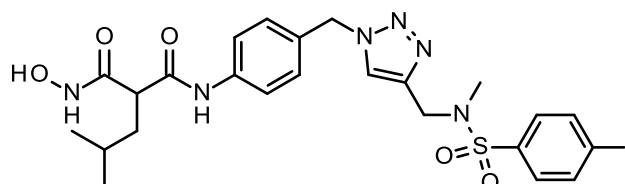
4.02 min, MS (ESI+): $m/z = 577$ $[M + H]^+$. $^1\text{H NMR}$ (500 MHz, $\text{DMSO-}d_6$) δ ppm: 10.52 (s, 1H), 9.82 (s, 1H), 8.97 (s, 1H), 7.62–7.59 (m, 2H), 7.32–7.30 (m, 2H), 4.37 (s, 2H), 3.22 (t, $J = 7.6$ Hz, 1H), 1.69 (t, $J = 7.3$ Hz, 2H), 1.49 (sep, $J = 6.7$ Hz, 1H), 0.89 (d, $J = 2.0$ Hz, 3H), 0.87 (d, $J = 2.0$ Hz, 3H). $^{13}\text{C NMR}$ (126 MHz, $\text{DMSO-}d_6$) δ ppm: 167.9, 166.2, 143.9, 143.6, 139.1, 138.8, 138.5, 130.7, 129.2 (2C), 128.6 (2C), 128.5, 127.3 (2C), 127.3 (2C), 127.1 (2C), 123.2, 119.5 (2C), 52.4, 49.8, 38.2, 37.9, 25.7, 22.4, 22.3. HRMS-ESI+ (m/z): calcd. for $\text{C}_{29}\text{H}_{33}\text{N}_6\text{O}_5\text{S}$ $[M + H]^+$ 577.2233, found 577.2221.

***N*-[4-[[4-[(2-Acetamidophenoxy)methyl]triazol-1-yl]methyl]phenyl]-2-(hydroxycarbamoyl)-4-methyl-pentanamide (Hit L5)**



Hit L5 was synthesized according to the general procedure G, using ester **92** (66 mg, 0.13 mmol), KCN (1.7 mg, 0.03 mmol) and NH_2OH (1.3 mL, 50% w/w in water) in MeOH (1.3 mL) overnight. The crude product was purified by preparative HPLC ($\text{H}_2\text{O} + 0.05\% \text{FA} / \text{ACN} + 0.05\% \text{FA}$: 95:5 to 5:95) affording compound **Hit L5** as a white solid after lyophilization (18 mg, 27%). Purity: 100%, LC tr = 3.30 min, MS (ESI+): $m/z = 495$ $[M + H]^+$. $^1\text{H NMR}$ (500 MHz, $\text{DMSO-}d_6$) δ ppm: 10.51 (br s, 1H), 9.83 (s, 1H), 9.01 (s, 1H), 8.97 (br s, 1H), 8.22 (s, 1H), 7.86 (d, $J = 7.6$ Hz, 1H), 7.57–7.56 (m, 2H), 7.27–7.25 (m, 2H), 7.20 (d, $J = 8.1$ Hz, 1H), 7.04 (t, $J = 7.6$ Hz, 1H), 6.90 (t, $J = 7.5$ Hz, 1H), 5.54 (s, 2H), 5.20 (s, 2H), 3.21 (t, $J = 7.6$ Hz, 1H), 2.03 (s, 3H), 1.67 (t, $J = 7.0$ Hz, 2H), 1.47 (sep, $J = 6.6$ Hz, 1H), 0.87 (d, $J = 6.5$ Hz, 3H), 0.86 (d, $J = 6.5$ Hz, 3H). $^{13}\text{C NMR}$ (126 MHz, $\text{DMSO-}d_6$) δ ppm: 168.4, 167.8, 166.2, 148.5, 143.1, 138.7, 130.8, 128.6 (2C), 127.9, 124.5, 124.3, 122.5, 120.8, 119.6 (2C), 113.3, 62.3, 52.5, 49.9, 38.0, 25.7, 23.9, 22.4, 22.3. HRMS-ESI+ (m/z): calcd. for $\text{C}_{25}\text{H}_{31}\text{N}_6\text{O}_5$ $[M + H]^+$ 495.2278, found 495.2352.

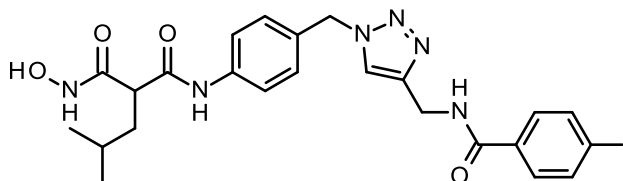
2-(Hydroxycarbamoyl)-*N*-[4-[[4-[(4-iodophenyl)sulfonyl-methyl-amino]methyl]triazol-1-yl]methyl]phenyl]-4-methyl-pentanamide (131)



Compound **131** was synthesized according to the general procedure G, using ester **123** (120 mg, 0.18 mmol), KCN (3.55 mg, 0.05 mmol) and NH_2OH (2.5 mL, 50% w/w in water) in MeOH (2.5 mL) for 72h. The crude product was purified by flash chromatography on silica gel (CH_2Cl_2 to $\text{CH}_2\text{Cl}_2/\text{MeOH}$: 95/5) affording compound **131** as a white solid after lyophilization (64 mg, 55%). Purity: 100%, LC tr = 4.07 min, MS (ESI+): $m/z = 641$ $[M + H]^+$. $^1\text{H NMR}$ (500 MHz, $\text{DMSO-}d_6$) δ ppm: 10.52 (s, 1H),

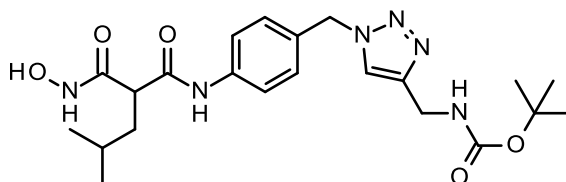
9.81 (s, 1H), 8.97 (s, 1H), 8.03 (s, 1H), 7.96–7.94 (m, 2H), 7.59–7.57 (m, 2H), 7.52–7.51 (m, 2H), 7.26–7.24 (m, 2H), 5.48 (s, 2H), 4.26 (s, 2H), 3.20 (t, $J = 7.6$ Hz, 1H), 2.63 (s, 3H), 1.68 (t, $J = 7.3$ Hz, 2H), 1.47 (sep, $J = 6.6$ Hz, 1H), 0.87 (d, $J = 6.5$ Hz, 3H), 0.86 (d, $J = 6.5$ Hz, 3H). ^{13}C NMR (126 MHz, DMSO- d_6) δ ppm: 167.8, 166.3, 141.8, 138.7, 138.2 (2C), 136.5, 130.7, 128.9 (2C), 128.6 (2C), 124.0, 119.6 (2C), 101.3, 52.5, 50.0, 44.7, 38.0, 34.7, 25.7, 22.4, 22.3. HRMS-ESI+ (m/z): calcd. for $\text{C}_{24}\text{H}_{30}\text{IN}_6\text{O}_5\text{S}$ $[\text{M}+\text{H}]^+$ 641.1043, found 641.1033.

***N*-[[1-[[4-[[2-(Hydroxycarbamoyl)-4-methyl-pentanoyl]amino]phenyl]methyl]triazol-4-yl]methyl]-4-iodo-benzamide (132)**



Compound **132** was synthesized according to the general procedure G, using ester **124** (132 mg, 0.22 mmol), KCN (4.23 mg, 0.07 mmol) and NH_2OH (2 mL, 50% w/w in water) in MeOH (2 mL) for 72h. The crude product was purified by flash chromatography on silica gel (CH_2Cl_2 to $\text{CH}_2\text{Cl}_2/\text{MeOH}$: 9/1) affording compound **132** as a white solid after lyophilization (53 mg, 41%). Purity: 100%, LC tr = 3.73 min, MS (ESI+): m/z = 591 $[\text{M} + \text{H}]^+$. ^1H NMR (500 MHz, DMSO- d_6) δ ppm: 10.52 (s, 1H), 9.80 (s, 1H), 9.05 (t, $J = 7.1$ Hz, 1H), 8.97 (s, 1H), 7.97 (s, 1H), 7.85–7.83 (m, 2H), 7.64–7.63 (m, 2H), 7.56–7.54 (m, 2H), 7.28–7.26 (m, 2H), 5.48 (s, 2H), 4.47 (d, $J = 4.3$ Hz, 2H), 3.20 (t, $J = 6.6$ Hz, 1H), 1.67 (t, $J = 7.3$ Hz, 2H), 1.49–1.44 (m, 1H), 0.88–0.85 (m, 6H). ^{13}C NMR (126 MHz, DMSO- d_6) δ ppm: 167.8, 166.3, 165.5, 145.1, 138.7, 137.2 (2C), 133.5, 131.0, 129.3 (2C), 128.7 (2C), 122.9, 119.6 (2C), 99.0, 52.4, 49.9, 38.0, 34.9, 25.7, 22.4, 22.3. HRMS-ESI+ (m/z): calcd. for $\text{C}_{24}\text{H}_{28}\text{IN}_6\text{O}_4$ $[\text{M} + \text{H}]^+$ 591.1217, found 591.1208.

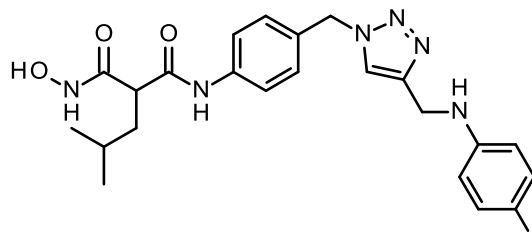
***Tert*-butyl *N*-[[1-[[4-[[2-(hydroxycarbamoyl)-4-methyl-pentanoyl]amino]phenyl]methyl]triazol-4-yl]methyl]carbamate (133)**



Compound **133** was synthesized according to the general procedure G, using ester **125** (105 mg, 0.22 mmol), KCN (4.29 mg, 0.07 mmol) and NH_2OH (2.3 mL, 50% w/w in water) in MeOH (2.3 mL) for 48h. The crude product was purified by preparative HPLC ($\text{H}_2\text{O}+0.05\%\text{FA}$ / $\text{ACN}+0.05\%\text{FA}$: 95:5 to 5:95) affording compound **133** as a white solid after lyophilization (36 mg, 35%). Purity: 100%, LC tr = 3.41 min, MS (ESI+): m/z = 921 $[2\text{M} + \text{H}]^+$, 461 $[\text{M} + \text{H}]^+$, 405 $[\text{M} - \text{tBu} + \text{H}]^+$, 361 $[\text{M} - \text{Boc} + \text{H}]^+$. ^1H NMR (500 MHz, DMSO- d_6) δ ppm: 10.54 (s, 1H), 9.83 (s, 1H), 8.99 (s, 1H), 7.87 (s, 1H), 7.57–7.55 (m, 2H), 7.31 (t, $J = 5.8$ Hz, 1H), 7.26–7.25 (m, 2H), 5.49 (s, 2H), 4.13 (d, $J = 5.9$ Hz, 2H),

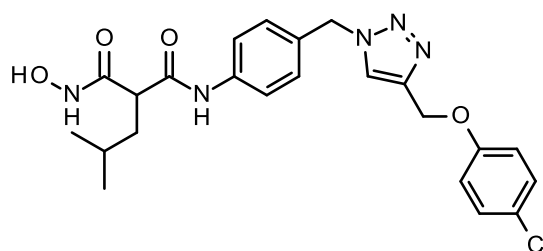
3.20 (t, $J = 7.6$ Hz, 1H), 1.67 (t, $J = 7.3$ Hz, 2H), 1.46 (sep, $J = 6.6$ Hz, 1H), 1.36 (s, 9H), 0.87 (d, $J = 6.5$ Hz, 3H), 0.86 (d, $J = 6.5$ Hz, 3H). ^{13}C NMR (126 MHz, $\text{DMSO-}d_6$) δ ppm: 167.9, 166.3, 155.6, 145.9, 138.7, 131.0, 128.6 (2C), 122.6, 119.5 (2C), 77.9, 52.3, 50.0, 38.0, 35.7, 28.3 (3C), 25.7, 22.4, 22.3. HRMS-ESI+ (m/z): calcd. for $\text{C}_{22}\text{H}_{33}\text{N}_6\text{O}_5$ [$\text{M} + \text{H}$] $^+$ 461.2512, found 461.2480.

2-(Hydroxycarbamoyl)-*N*-[4-[[4-(4-iodoanilino)methyl]triazol-1-yl]methyl]phenyl]-4-methyl-pentanamide (134)



Compound **134** was synthesized according to the general procedure G, using ester **126** (158 mg, 0.27 mmol), KCN (5.31 mg, 0.08 mmol) and NH_2OH (2.5 mL, 50% w/w in water) in MeOH (2.5 mL) for 72h. The crude product was purified by flash chromatography on silica gel (CH_2Cl_2 to $\text{CH}_2\text{Cl}_2/\text{MeOH}$: 9/1) affording compound **134** as a white solid after lyophilization (31 mg, 20%). Purity: 100%, LC tr = 4.13 min, MS (ESI+): $m/z = 563$ [$\text{M} + \text{H}$] $^+$. ^1H NMR (500 MHz, $\text{DMSO-}d_6$) δ ppm: 10.52 (s, 1H), 9.80 (s, 1H), 8.97 (s, 1H), 7.94 (s, 1H), 7.56–7.54 (m, 2H), 7.33–7.31 (m, 2H), 7.26–7.24 (m, 2H), 6.49–6.47 (m, 2H), 6.27 (t, $J = 5.8$ Hz, 1H), 5.48 (s, 2H), 4.24 (d, $J = 5.8$ Hz, 2H), 3.20 (t, $J = 7.6$ Hz, 1H), 1.67 (t, $J = 7.2$ Hz, 2H), 1.47 (sep, $J = 6.7$ Hz, 1H), 0.87 (d, $J = 6.6$ Hz, 3H), 0.86 (d, $J = 6.6$ Hz, 3H). ^{13}C NMR (126 MHz, $\text{DMSO-}d_6$) δ ppm: 167.8, 166.1, 148.1, 145.5, 138.6, 137.1 (2C), 131.0, 128.6 (2C), 122.7, 119.6 (2C), 115.0 (2C), 76.5, 52.4, 49.9, 38.3, 38.0, 25.7, 22.4, 22.3. HRMS-ESI+ (m/z): calcd. for $\text{C}_{23}\text{H}_{28}\text{IN}_6\text{O}_3$ [$\text{M} + \text{H}$] $^+$ 563.1268, found 563.1232.

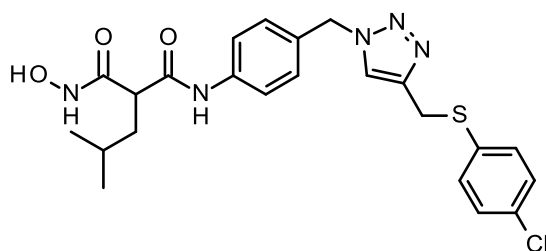
***N*-[4-[[4-(4-Chlorophenoxy)methyl]triazol-1-yl]methyl]phenyl]-2-(hydroxycarbamoyl)-4-methyl-pentanamide (135)**



Compound **135** was synthesized according to the general procedure G, using ester **127** (50 mg, 0.1 mmol), KCN (2.0 mg, 0.03 mmol) and NH_2OH (1.5 mL, 50% w/w in water) in MeOH (1.5 mL) for 72h. The crude product was purified by preparative HPLC ($\text{H}_2\text{O}+0.05\%\text{FA}$ / $\text{ACN}+0.05\%\text{FA}$: 95:5 to 5:95) affording compound **135** as a white solid after lyophilization (21 mg, 43%). Purity: 100%, LC tr = 4.13 min, MS (ESI+): $m/z = 472$ and 474 [$\text{M} + \text{H}$] $^+$. ^1H NMR (500 MHz, $\text{DMSO-}d_6$) δ ppm: 10.53 (s, 1H), 9.83 (s, 1H), 8.97 (s, 1H), 8.23 (s, 1H), 7.58–7.56 (m, 2H), 7.33–7.32 (m, 2H), 7.29–7.27 (m,

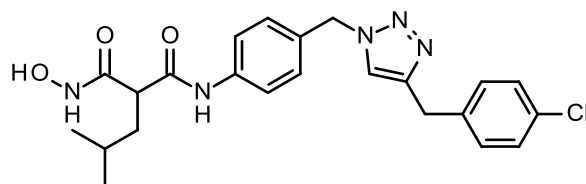
2H), 7.06–7.04 (m, 2H), 5.53 (s, 2H), 5.11 (s, 2H), 3.21 (t, $J = 7.6$ Hz, 1H), 1.69–1.67 (m, 2H), 1.47 (sep, $J = 6.7$ Hz, 1H), 0.87 (d, $J = 6.6$ Hz, 3H), 0.86 (d, $J = 6.6$ Hz, 3H). ^{13}C NMR (126 MHz, $\text{DMSO-}d_6$) δ ppm: 167.8, 166.3, 156.9, 142.7, 138.7, 130.8, 129.2 (2C), 128.7 (2C), 124.6, 124.6, 119.6 (2C), 116.5 (2C), 61.4, 52.5, 49.9, 38.0, 25.7, 22.4, 22.3. HRMS-ESI+ (m/z): calcd. for $\text{C}_{23}\text{H}_{27}\text{ClN}_5\text{O}_4$ [$\text{M} + \text{H}$] $^+$ 472.1752, found 472.1718.

***N*-[4-[[4-[(4-Chlorophenyl)sulfanylmethyl]triazol-1-yl]methyl]phenyl]-2-(hydroxycarbamoyl)-4-methyl-pentanamide (136)**



Compound **136** was synthesized according to the general procedure G, using ester **128** (70 mg, 0.14 mmol), KCN (2.7 mg, 0.04 mmol) and NH_2OH (1.5 mL, 50% w/w in water) in MeOH (1.5 mL) for 72h. The crude product was purified by preparative HPLC ($\text{H}_2\text{O}+0.05\%\text{FA} / \text{ACN}+0.05\%\text{FA}$: 95:5 to 5:95) affording compound **136** as a white solid after lyophilization (11 mg, 15%). Purity: 95%, LC tr = 4.13 min, MS (ESI+): $m/z = 488$ and 490 [$\text{M} + \text{H}$] $^+$. ^1H NMR (500 MHz, $\text{DMSO-}d_6$) δ ppm: 10.55 (s, 1H), 9.83 (s, 1H), 8.97 (br s, 1H), 7.93 (s, 1H), 7.56–7.54 (m, 2H), 7.36–7.32 (m, 4H), 7.19–7.18 (m, 2H), 5.46 (s, 2H), 4.27 (s, 2H), 3.21 (t, $J = 7.6$ Hz, 1H), 1.69–1.66 (m, 2H), 1.47 (sep, $J = 6.6$ Hz, 1H), 0.87 (d, $J = 6.6$ Hz, 3H), 0.86 (d, $J = 6.6$ Hz, 3H). ^{13}C NMR (126 MHz, $\text{DMSO-}d_6$) δ ppm: 167.8, 166.3, 143.5, 138.7, 134.7, 130.8, 130.6, 130.2 (2C), 128.8 (2C), 128.4 (2C), 123.3, 119.5 (2C), 52.4, 49.9, 38.0, 27.3, 25.7, 22.4, 22.3. HRMS-ESI+ (m/z): calcd. for $\text{C}_{23}\text{H}_{27}\text{ClN}_5\text{O}_3\text{S}$ [$\text{M} + \text{H}$] $^+$ 488.1523, found 488.1490.

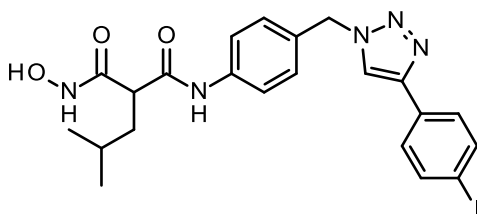
***N*-[4-[[4-[(4-Chlorophenyl)methyl]triazol-1-yl]methyl]phenyl]-2-(hydroxycarbamoyl)-4-methyl-pentanamide (137)**



Compound **137** was synthesized according to the general procedure G, using ester **129** (75 mg, 0.16 mmol), KCN (3.1 mg, 0.05 mmol) and NH_2OH (1.5 mL, 50% w/w in water) in MeOH (1.5 mL) for 72h. The crude product was purified by preparative HPLC ($\text{H}_2\text{O}+0.05\%\text{FA} / \text{ACN}+0.05\%\text{FA}$: 95:5 to 5:95) affording compound **137** as a white solid after lyophilization (11 mg, 15%). Purity: 100%, LC tr = 4.04 min, MS (ESI+): $m/z = 456$ and 458 [$\text{M} + \text{H}$] $^+$. ^1H NMR (500 MHz, $\text{DMSO-}d_6$) δ ppm: 10.53 (br s, 1H), 9.81 (s, 1H), 8.97 (br s, 1H), 7.84 (s, 1H), 7.56–7.54 (m, 2H), 7.34–7.32 (m, 2H), 7.26–7.24 (m, 4H), 5.46 (s, 2H), 3.96 (s, 2H), 3.20 (t, $J = 7.6$ Hz, 1H), 1.67 (t, $J = 7.0$ Hz, 2H), 1.47 (sep, $J = 6.7$

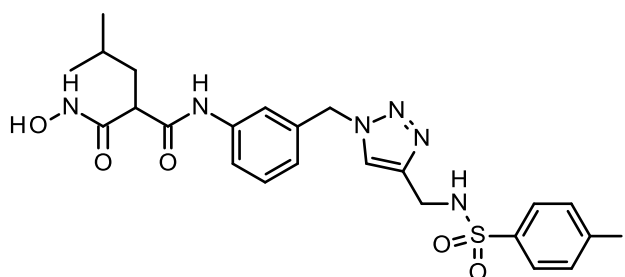
Hz, 1H), 0.87 (d, $J = 6.6$ Hz, 3H), 0.86 (d, $J = 6.6$ Hz, 3H). ^{13}C NMR (126 MHz, $\text{DMSO-}d_6$) δ ppm: 167.8, 166.3, 146.0, 138.7, 138.6, 130.9, 130.8, 130.4 (2C), 128.6 (2C), 128.3 (2C), 122.5, 119.5 (2C), 52.4, 49.9, 38.0, 30.5, 25.7, 22.4, 22.3. HRMS-ESI+ (m/z): calcd. for $\text{C}_{23}\text{H}_{27}\text{ClN}_5\text{O}_3$ [$\text{M} + \text{H}$] $^+$ 456.1802, found 456.1773.

2-(Hydroxycarbamoyl)-*N*-[4-[[4-(4-iodophenyl)triazol-1-yl]methyl]phenyl]-4-methyl-pentanamide (138)



Compound **138** was synthesized according to the general procedure G, using ester **130** (140 mg, 0.25 mmol), KCN (4.96 mg, 0.08 mmol) and NH_2OH (2.5 mL, 50% w/w in water) in MeOH (2.5 mL) for 72h. The crude product was purified by flash chromatography on silica gel (CH_2Cl_2 to $\text{CH}_2\text{Cl}_2/\text{MeOH}$: 95/5) affording compound **138** as a white solid after lyophilization (28 mg, 20%). Purity: 100%, LC tr = 4.31 min, MS (ESI+): $m/z = 534$ [$\text{M} + \text{H}$] $^+$. ^1H NMR (500 MHz, $\text{DMSO-}d_6$) δ ppm: 10.52 (br s, 1H), 9.83 (s, 1H), 8.98 (br s, 1H), 8.63 (s, 1H), 7.81–7.79 (m, 2H), 7.67–7.59 (m, 4H), 7.33–7.32 (m, 2H), 5.58 (s, 2H), 3.20 (t, $J = 7.3$ Hz, 1H), 1.67 (t, $J = 6.9$ Hz, 2H), 1.51–1.43 (m, 1H), 0.88–0.85 (m, 6H). ^{13}C NMR (126 MHz, $\text{DMSO-}d_6$) δ ppm: 167.9, 166.3, 145.7, 138.8, 137.7 (2C), 130.6, 130.3, 128.7 (2C), 127.2 (2C), 121.7, 119.6 (2C), 93.8, 52.7, 50.0, 38.0, 25.7, 22.4, 22.3. HRMS-ESI+ (m/z): calcd. for $\text{C}_{22}\text{H}_{25}\text{IN}_5\text{O}_3$ [$\text{M} + \text{H}$] $^+$ 534.1002, found 534.0970.

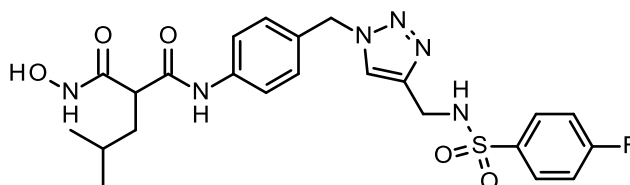
2-(Hydroxycarbamoyl)-*N*-[3-[[4-[[4-(4-iodophenyl)sulfonylamino]methyl]triazol-1-yl]methyl]phenyl]-4-methyl-pentanamide (114)



Compound **114** was synthesized according to the general procedure G, using ester **113** (206 mg, 0.32 mmol), KCN (4.15 mg, 0.06 mmol) and NH_2OH (3.5 mL, 50% w/w in water) in MeOH (3.5 mL) for 96h. The crude product was purified by flash chromatography on silica gel (CH_2Cl_2 to $\text{CH}_2\text{Cl}_2/\text{MeOH}$: 95/5) affording compound **114** as a white solid after lyophilization (13 mg, 6%). Purity: 95%, LC tr = 3.84 min, MS (ES+): $m/z = 627$ [$\text{M} + \text{H}$] $^+$. ^1H NMR (500 MHz, $\text{DMSO-}d_6$) δ ppm: 10.52 (br s, 1H), 9.83 (s, 1H), 8.96 (s, 1H), 8.21 (br s, 1H), 7.94–7.92 (m, 2H), 7.89 (s, 1H), 7.56–7.51 (m, 4H), 7.32–7.29 (m, 1H), 6.96–6.95 (m, 1H), 5.49 (s, 2H), 4.04 (s, 2H), 3.21 (t, $J = 7.5$ Hz, 1H), 1.70–1.64 (m,

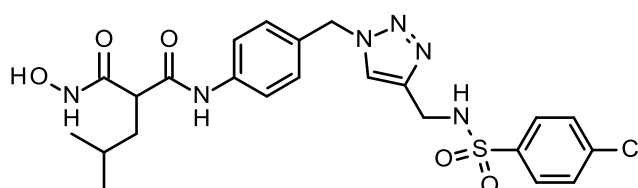
2H), 1.47 (sep, $J = 6.6$ Hz, 1H), 0.87 (d, $J = 6.4$ Hz, 3H), 0.86 (d, $J = 6.4$ Hz, 3H). ^{13}C NMR (126 MHz, $\text{DMSO-}d_6$) δ ppm: 167.8, 166.3, 143.5, 140.0, 139.1, 138.0 (2C), 136.4, 129.2, 128.3 (2C), 123.4, 123.0, 119.1, 118.9, 100.4, 52.7, 49.9, 38.0, 37.9, 25.7, 22.4, 22.3. HRMS-ESI+ (m/z): calcd. for $\text{C}_{23}\text{H}_{28}\text{N}_6\text{O}_5\text{S}$ [$\text{M} + \text{H}$] $^+$ 627.0887, found 627.0879.

***N*-[4-[[4-[(4-Fluorophenyl)sulfonylamino]methyl]triazol-1-yl]methyl]phenyl]-2-(hydroxycarbamoyl)-4-methyl-pentanamide (150)**



Compound **160** was synthesized according to the general procedure G, using ester **150** (127 mg, 0.23 mmol), KCN (4.62 mg, 0.07 mmol) and NH_2OH (3 mL, 50% w/w in water) in MeOH (3 mL) for 72h. The crude product was purified by flash chromatography on silica gel (CH_2Cl_2 to $\text{CH}_2\text{Cl}_2/\text{MeOH}$: 95/5) affording compound **160** as a white solid after lyophilization (96 mg, 78%). Purity: 100%, LC tr = 3.46 min, MS (ESI+): $m/z = 519$ [$\text{M} + \text{H}$] $^+$. ^1H NMR (500 MHz, $\text{DMSO-}d_6$) δ ppm: 10.51 (br s, 1H), 9.83 (s, 1H), 8.97 (br s, 1H), 8.19 (br s, 1H), 7.84 (s, 1H), 7.82–7.79 (m, 2H), 7.57–7.56 (m, 2H), 7.38–7.34 (m, 2H), 7.23–7.22 (m, 2H), 5.45 (s, 2H), 4.04 (s, 2H), 3.21 (t, $J = 7.5$ Hz, 1H), 1.68 (t, $J = 7.2$ Hz, 2H), 1.47 (sep, $J = 6.6$ Hz, 1H), 0.87 (d, $J = 6.3$ Hz, 3H), 0.86 (d, $J = 6.3$ Hz, 3H). ^{13}C NMR (126 MHz, $\text{DMSO-}d_6$) δ ppm: 167.8, 166.3, 164.1 (d, $J = 250.8$ Hz), 143.5, 138.7, 136.8 (d, $J = 2.8$ Hz), 130.7, 129.6 (d, $J = 9.2$ Hz, 2C), 128.6 (2C), 123.2, 119.6 (2C), 116.2 (d, $J = 22.8$ Hz, 2C), 52.4, 49.9, 38.1, 38.0, 25.7, 22.4, 22.3. HRMS-ESI+ (m/z): calcd. for $\text{C}_{23}\text{H}_{28}\text{FN}_6\text{O}_5\text{S}$ [$\text{M} + \text{H}$] $^+$: 519.1826, found 519.1819.

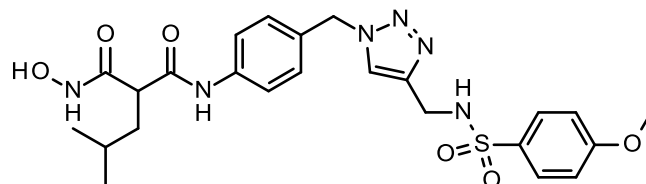
***N*-[4-[[4-[(4-Chlorophenyl)sulfonylamino]methyl]triazol-1-yl]methyl]phenyl]-2-(hydroxycarbamoyl)-4-methyl-pentanamide (161)**



Compound **161** was synthesized according to the general procedure G, using ester **151** (128 mg, 0.23 mmol), KCN (4.52 mg, 0.07 mmol) and NH_2OH (2.8 mL, 50% w/w in water) in MeOH (2.8 mL) for 72h. The crude product was purified by flash chromatography on silica gel (CH_2Cl_2 to $\text{CH}_2\text{Cl}_2/\text{MeOH}$: 9/1) affording compound **161** as a white solid after lyophilization (59 mg, 47%). Purity: 100%, LC tr = 3.64 min, MS (ESI+): $m/z = 535$ and 537 [$\text{M} + \text{H}$] $^+$. ^1H NMR (500 MHz, $\text{DMSO-}d_6$) δ ppm: 10.53 (s, 1H), 9.81 (s, 1H), 8.98 (s, 1H), 8.22 (t, $J = 6.0$ Hz, 1H), 7.85 (s, 1H), 7.75–7.73 (m, 2H), 7.60–7.56 (m, 4H), 7.24–7.22 (m, 2H), 5.44 (s, 2H), 4.05 (d, $J = 3.6$ Hz, 2H), 3.21 (t, $J = 7.5$ Hz, 1H), 1.68 (t, $J = 6.9$ Hz, 2H), 1.47 (sep, $J = 6.6$ Hz, 1H), 0.88–0.86 (m, 6H). ^{13}C NMR (126 MHz, $\text{DMSO-}d_6$) δ

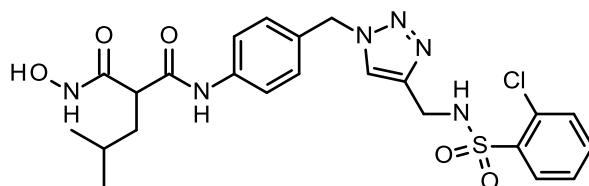
ppm: 169.7, 167.1, 143.4, 139.3, 138.7, 137.2, 130.9, 129.2 (2C), 128.8 (2C), 128.5 (2C), 123.2, 119.4 (2C), 52.3, 50.9, 38.0, 37.4, 25.6, 22.6, 21.9. HRMS-ESI+ (m/z): calcd. for C₂₃H₂₈ClN₆O₅S [M + H]⁺ 535.1530, found 535.1526.

2-(Hydroxycarbamoyl)-N-[4-[[4-[[4-methoxyphenyl)sulfonylamino]methyl]triazol-1-yl]methyl]phenyl]-4-methyl-pentanamide (162)



Compound **162** was synthesized according to the general procedure G, using ester **152** (131 mg, 0.24 mmol), KCN (4.66 mg, 0.07 mmol) and NH₂OH (3 mL, 50% w/w in water) in MeOH (3 mL) for 72h. The crude product was purified by flash chromatography on silica gel (CH₂Cl₂ to CH₂Cl₂/MeOH: 9/1) affording compound **162** as a white solid after lyophilization (34 mg, 26%). Purity: 100%, LC tr = 3.43 min, MS (ESI+): m/z = 531 [M + H]⁺. Purity: 100%, LC tr = 3.43 min, MS (ESI+): m/z = 531 [M + H]⁺. ¹H NMR (500 MHz, DMSO-*d*₆) δ ppm: 10.53 (br s, 1H), 9.83 (s, 1H), 8.97 (br s, 1H), 7.92 (br s, 1H), 7.84 (s, 1H), 7.71–7.69 (m, 2H), 7.57–7.56 (m, 2H), 7.24–7.22 (m, 2H), 7.07–7.05 (m, 2H), 5.45 (s, 2H), 3.98 (s, 2H), 3.82 (s, 3H), 3.21 (t, *J* = 7.6 Hz, 1H), 1.68 (t, *J* = 7.2 Hz, 2H), 1.47 (sep, *J* = 6.6 Hz, 1H), 0.88–0.86 (m, 6H). ¹³C NMR (126 MHz, DMSO-*d*₆) δ ppm: 167.8, 166.3, 162.1, 143.7, 138.7, 131.9, 130.8, 128.7 (2C), 128.6 (2C), 123.2, 119.5 (2C), 114.3 (2C), 55.6, 52.4, 49.9, 38.1, 38.0, 25.7, 22.4, 22.3. HRMS-ESI+ (m/z): calcd. for C₂₄H₃₁N₆O₆S [M + H]⁺: 531.2026, found 531.1997.

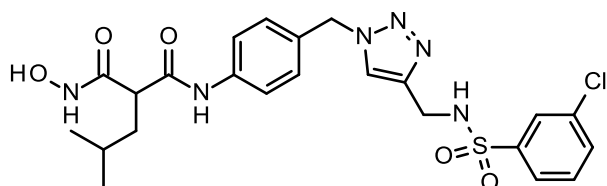
N-[4-[[4-[[2-Chlorophenyl)sulfonylamino]methyl]triazol-1-yl]methyl]phenyl]-2-(hydroxycarbamoyl)-4-methyl-pentanamide (163)



Compound **163** was synthesized according to the general procedure G, using ester **153** (160 mg, 0.29 mmol), KCN (5.65 mg, 0.09 mmol) and NH₂OH (3 mL, 50% w/w in water) in MeOH (3 mL) for 72h. The crude product was purified by flash chromatography on silica gel (CH₂Cl₂ to CH₂Cl₂/MeOH: 9/1) affording compound **163** as a white solid after lyophilization (12 mg, 7%). Purity: 100%, LC tr = 3.43 min, MS (ESI+): m/z = 535 and 537 [M + H]⁺. ¹H NMR (DMSO-*d*₆) δ ppm: 10.55 (br s, 1H), 9.84 (s, 1H), 8.99 (br s, 1H), 8.37 (br s, 1H), 7.90–7.89 (m, 1H), 7.74 (s, 1H), 7.59–7.57 (m, 2H), 7.55–7.49 (m, 2H), 7.45–7.42 (m, 1H), 7.22–7.21 (m, 2H), 5.42 (s, 2H), 4.16 (s, 2H), 3.22 (t, *J* = 7.6 Hz, 1H), 1.69 (t, *J* = 7.0 Hz, 2H), 1.49 (sep, *J* = 6.6 Hz, 1H), 0.89 (d, *J* = 6.4 Hz, 3H), 0.88 (d, *J* = 6.4 Hz, 3H). ¹³C NMR (126 MHz, DMSO-*d*₆) δ ppm: 167.9, 166.3, 143.7, 138.7, 138.0, 133.9, 131.6, 130.8,

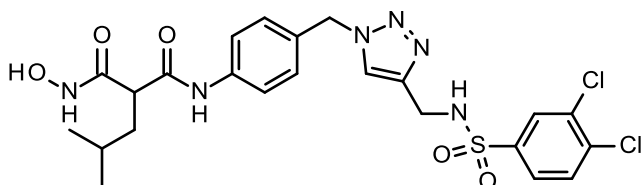
130.6, 130.4, 128.7 (2C), 127.5, 123.1, 119.6 (2C), 52.3, 50.0, 38.0, 37.9, 25.8, 22.5, 22.3. HRMS-ESI+ (m/z): calcd. for C₂₃H₂₈ClN₆O₅S [M+H]⁺ 535,1530, found 535.1500.

***N*-[4-[[4-[(3-Chlorophenyl)sulfonylamino]methyl]triazol-1-yl]methyl]phenyl]-2-(hydroxycarbamoyl)-4-methyl-pentanamide (164)**



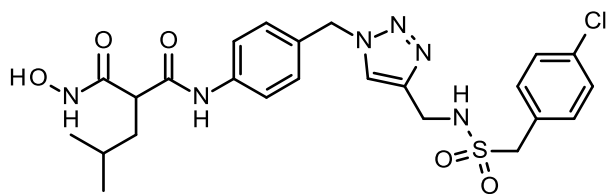
Compound **164** was synthesized according to the general procedure G, using ester **154** (125 mg, 0.23 mmol), KCN (4.41 mg, 0.07 mmol) and NH₂OH (2.5 mL, 50% w/w in water) in MeOH (2.5 mL) for 72h. The crude product was purified by flash chromatography on silica gel (CH₂Cl₂ to CH₂Cl₂/MeOH: 9/1) affording compound **164** as a white solid after lyophilization (67 mg, 55%). Purity: 100%, LC tr = 3.66 min, MS (ESI+): m/z = 535 and 537 [M + H]⁺. ¹H NMR (500 MHz, DMSO-*d*₆) δ ppm: 10.53 (br s, 1H), 9.82 (s, 1H), 8.98 (s, 1H), 8.29 (br s, 1H), 7.84 (s, 1H), 7.75–7.74 (m, 1H), 7.70–7.66 (m, 2H), 7.58–7.55 (m, 3H), 7.24–7.22 (m, 2H), 5.45 (s, 2H), 4.09 (s, 2H), 3.21 (t, *J* = 7.6 Hz, 1H), 1.71–1.67 (m, 2H), 1.48 (sep, *J* = 6.7 Hz, 1H), 0.88 (d, *J* = 6.6 Hz, 3H), 0.87 (d, *J* = 6.6 Hz, 3H). ¹³C NMR (126 MHz, DMSO-*d*₆) δ ppm: 167.9, 166.3, 143.3, 142.4, 138.8, 133.7, 132.4, 131.2, 130.7, 128.7 (2C), 126.2, 125.2, 123.2, 119.6 (2C), 52.4, 50.0, 38.1, 38.0, 25.8, 22.4, 22.3. HRMS-ESI+ (m/z): calcd. for C₂₃H₂₈ClN₆O₅S [M + H]⁺ 535,1530, found 535.1496.

***N*-[4-[[4-[(3,4-Dichlorophenyl)sulfonylamino]methyl]triazol-1-yl]methyl]phenyl]-2-(hydroxycarbamoyl)-4-methyl-pentanamide (165)**



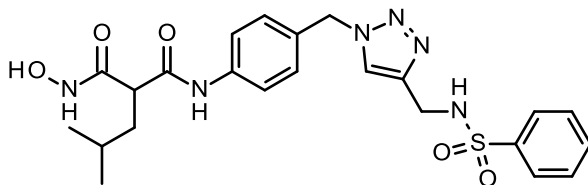
Compound **165** was synthesized according to the general procedure G, using ester **155** (108 mg, 0.18 mmol), KCN (3.59 mg, 0.06 mmol) and NH₂OH (1.8 mL, 50% w/w in water) in MeOH (1.8 mL) for 72h. The crude product was purified by flash chromatography on silica gel (CH₂Cl₂ to CH₂Cl₂/MeOH: 95/5) affording compound **165** as a white solid after lyophilization (19 mg, 18%). Purity: 95%, LC tr = 3.94 min, MS (ESI-): m/z = 569, 571 and 573 [M + H]⁺. ¹H NMR (500 MHz, DMSO-*d*₆) δ ppm: 10.54 (br s, 1H), 9.82 (s, 1H), 8.97 (s, 1H), 8.35 (br s, 1H), 7.91–7.90 (m, 1H), 7.88 (s, 1H), 7.79–7.78 (m, 1H), 7.68–7.67 (m, 1H), 7.58–7.56 (m, 2H), 7.24–7.22 (m, 2H), 5.44 (s, 2H), 4.10 (s, 2H), 3.21 (t, *J* = 7.6 Hz, 1H), 1.69–1.66 (m, 2H), 1.47 (sep, *J* = 6.7 Hz, 1H), 0.87 (d, *J* = 6.6 Hz, 3H), 0.86 (d, *J* = 6.6 Hz, 3H). ¹³C NMR (126 MHz, DMSO-*d*₆) δ ppm: 167.8, 166.3, 143.2, 140.9, 138.7, 135.4, 131.9, 131.5, 130.7, 128.6 (2C), 128.4, 126.7, 123.3, 119.9 (2C), 52.4, 50.0, 38.0, 38.0, 25.7, 22.4, 22.3. HRMS-ESI+ (m/z): calcd. for C₂₃H₂₇Cl₂N₆O₅S [M + H]⁺ 569.1141, found 569.1099.

***N*-[4-[[4-[[4-(4-Chlorophenyl)methylsulfonylamino]methyl]triazol-1-yl]methyl]phenyl]-2-(hydroxycarbamoyl)-4-methyl-pentanamide (166)**



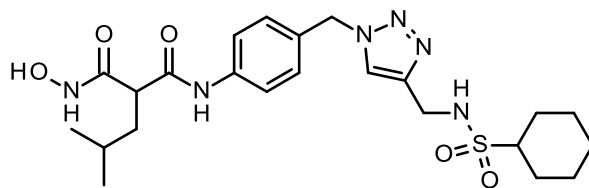
Compound **166** was synthesized according to the general procedure G, using ester **156** (58 mg, 0.1 mmol), KCN (2 mg, 0.03 mmol) and NH₂OH (1.2 mL, 50% w/w in water) in MeOH (1.2 mL) for 72h. The crude product was purified by flash chromatography on silica gel (CH₂Cl₂ to CH₂Cl₂/MeOH: 9/1) affording compound **166** as a white solid after lyophilization (13 mg, 23%). Purity: 100%, LC tr = 3.74 min, MS (ESI+): *m/z* = 549 and 551 [M + H]⁺. ¹H NMR (500 MHz, DMSO-*d*₆) δ ppm: 10.52 (s, 1H), 9.81 (s, 1H), 8.97 (s, 1H), 7.97 (s, 1H), 7.64 (t, *J* = 5.9 Hz, 1H), 7.58–7.56 (m, 2H), 7.38–7.37 (m, 2H), 7.30–7.28 (m, 4H), 5.52 (s, 2H), 4.34 (s, 2H), 4.17 (d, *J* = 5.8 Hz, 2H), 3.20 (t, *J* = 7.6 Hz, 1H), 1.67 (t, *J* = 6.2 Hz, 2H), 1.47 (sep, *J* = 6.6 Hz, 1H), 0.87 (d, *J* = 6.4 Hz, 3H), 0.86 (d, *J* = 6.4 Hz, 3H). ¹³C NMR (126 MHz, DMSO-*d*₆) δ ppm: 167.8, 166.3, 148.7, 138.7, 132.9, 132.5 (2C), 130.9, 129.3, 128.7 (2C), 128.3 (2C), 123.2, 119.5 (2C), 56.7, 52.4, 49.9, 38.0, 38.0, 25.7, 22.4, 22.2. HRMS-ESI+ (*m/z*): calcd. for C₂₄H₃₀ClN₆O₅S [M + H]⁺ 549.1687, found 549.1653.

***N*-[4-[[4-(Benzenesulfonamidomethyl)triazol-1-yl]methyl]phenyl]-2-(hydroxycarbamoyl)-4-methyl-pentanamide (167)**



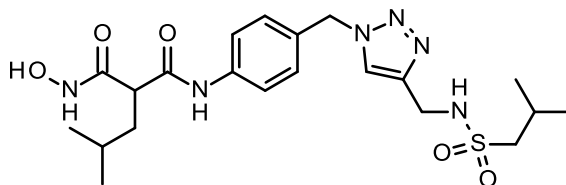
Compound **167** was synthesized according to the general procedure G, using ester **157** (113 mg, 0.22 mmol), KCN (4.25 mg, 0.07 mmol) and NH₂OH (2.5 mL, 50% w/w in water) in MeOH (2.5 mL) for 72h. The crude product was purified by flash chromatography on silica gel (CH₂Cl₂ to CH₂Cl₂/MeOH: 9/1) affording compound **167** as a white solid after lyophilization (19 mg, 17%). Purity: 100%, LC tr = 3.36 min, MS (ESI+): *m/z* = 501 [M + H]⁺. ¹H NMR (500 MHz, DMSO-*d*₆) δ ppm: 10.50 (br s, 1H), 9.83 (s, 1H), 8.96 (br s, 1H), 8.13 (br s, 1H), 7.80 (s, 1H), 7.76–7.75 (m, 2H), 7.61–7.51 (m, 5H), 7.23–7.21 (m, 2H), 5.44 (s, 2H), 4.03 (s, 2H), 3.21 (t, *J* = 7.6 Hz, 1H), 1.68 (t, *J* = 7.2 Hz, 2H), 1.47 (sep, *J* = 6.6 Hz, 1H), 0.88 (d, *J* = 6.5 Hz, 3H), 0.87 (d, *J* = 6.5 Hz, 3H). ¹³C NMR (126 MHz, DMSO-*d*₆) δ ppm: 167.9, 166.3, 143.6, 140.4, 138.7, 132.4, 130.7, 129.1 (2C), 128.7 (2C), 126.5 (2C), 123.1, 119.6 (2C), 52.4, 50.0, 38.1, 38.0, 25.7, 22.4, 22.3. HRMS-ESI+ (*m/z*): calcd. for C₂₃H₂₉N₆O₅S [M + H]⁺ 501.1920, found 501.1889.

***N*-[4-[[4-[(Cyclohexylsulfonylamino)methyl]triazol-1-yl]methyl]phenyl]-2-(hydroxycarbamoyl)-4-methyl-pentanamide (168)**



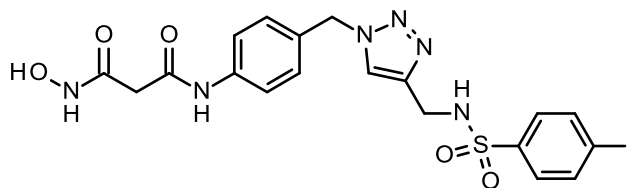
Compound **168** was synthesized according to the general procedure G, using ester **158** (50 mg, 0.1 mmol), KCN (1.9 mg, 0.03 mmol) and NH₂OH (1.2 mL, 50% w/w in water) in MeOH (1.2 mL) for 48h. The crude product was purified by flash chromatography on silica gel (CH₂Cl₂ to CH₂Cl₂/MeOH: 9/1) affording compound **168** as a white solid after lyophilization (7 mg, 14%). Purity: 100%, LC tr = 3.36 min, MS (ESI+): *m/z* = 501 [M + H]⁺. ¹H NMR (500 MHz, DMSO-*d*₆) δ ppm: 10.53 (br s, 1H), 9.83 (s, 1H), 8.96 (br s, 1H), 7.99 (s, 1H), 7.58–7.56 (m, 2H), 7.50 (t, *J* = 5.8 Hz, 1H), 7.28–7.27 (m, 2H), 5.52 (s, 2H), 4.18 (d, *J* = 5.8 Hz, 2H), 3.20 (t, *J* = 7.6 Hz, 1H), 2.75–2.70 (m, 1H), 1.90–1.88 (m, 2H), 1.69–1.66 (m, 4H), 1.55–1.54 (m, 1H), 1.47 (sep, *J* = 6.6 Hz, 1H), 1.27–1.20 (m, 2H), 1.07–1.03 (m, 3H), 0.87–0.86 (m, 6H). ¹³C NMR (126 MHz, DMSO-*d*₆) δ ppm: 167.8, 166.2, 144.9, 138.7, 130.9, 128.6 (2C), 123.1, 119.5 (2C), 59.4, 52.4, 49.9, 38.0, 37.7, 25.9 (2C), 25.7, 24.8, 24.5 (2C), 22.4, 22.3. HRMS-ESI+ (*m/z*): calcd. for C₂₃H₃₅N₆O₅S [M + H]⁺ 507.2390, found 507.2356.

2-(Hydroxycarbamoyl)-*N*-[4-[[4-[(isobutylsulfonylamino)methyl]triazol-1-yl]methyl]phenyl]-4-methyl-pentanamide (169)



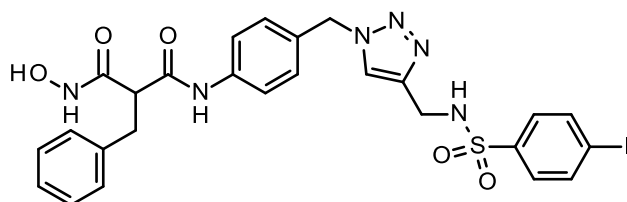
Compound **169** was synthesized according to the general procedure G, using ester **159** (75 mg, 0.15 mmol), KCN (2.94 mg, 0.05 mmol) and NH₂OH (1.5 mL, 50% w/w in water) in MeOH (1.5 mL) overnight. The crude product was purified by flash chromatography on silica gel (CH₂Cl₂ to CH₂Cl₂/MeOH: 95/5) affording compound **169** as a white solid after lyophilization (35 mg, 48%). Purity: 100%, LC tr = 3.33 min, MS (ESI+): *m/z* = 481 [M + H]⁺. ¹H NMR (500 MHz, DMSO-*d*₆) δ ppm: 10.52 (s, 1H), 9.80 (s, 1H), 8.97 (s, 1H), 8.00 (s, 1H), 7.57–7.55 (m, 2H), 7.53 (t, *J* = 6.0 Hz, 1H), 7.28–7.26 (m, 2H), 5.52 (s, 2H), 4.18 (d, *J* = 6.0 Hz, 2H), 3.20 (t, *J* = 7.6 Hz, 1H), 2.82 (d, *J* = 6.4 Hz, 2H), 1.97 (sep, *J* = 6.7 Hz, 1H), 1.68–1.66 (m, 2H), 1.47 (sep, *J* = 6.7 Hz, 1H), 0.92 (d, *J* = 6.6 Hz, 6H), 0.87 (d, *J* = 6.6 Hz, 3H), 0.86 (d, *J* = 6.6 Hz, 3H). ¹³C NMR (126 MHz, DMSO-*d*₆) δ ppm: 167.9, 166.3, 144.6, 138.7, 130.9, 128.6 (2C), 123.2, 119.5 (2C), 59.2, 52.4, 50.0, 38.0, 37.6, 25.7, 24.2, 22.4, 22.3, 22.2 (2C). HRMS-ESI+ (*m/z*): calcd. for C₂₁H₃₃N₆O₅S [M + H]⁺ 481.2233, found 481.2202.

3-(Hydroxyamino)-N-[4-[[4-[[[(4-iodophenyl)sulfonylamino]methyl]triazol-1-yl]methyl]phenyl]-3-oxo-propanamide (178)



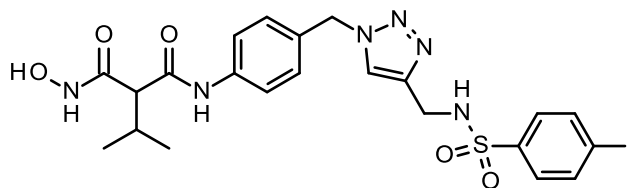
Compound **178** was synthesized according to the general procedure G, using ester **176** (130 mg, 0.23 mmol), KCN (2.94 mg, 0.05 mmol) and NH_2OH (2.5 mL, 50% w/w in water) in MeOH (2.5 mL) overnight. The crude product was purified by flash chromatography on silica gel (CH_2Cl_2 to $\text{CH}_2\text{Cl}_2/\text{MeOH}$: 9/1) affording compound **178** as a white solid after lyophilization (18 mg, 14%). Purity: 100%, LC tr = 3.25 min, MS (ESI+): $m/z = 571$ $[\text{M} + \text{H}]^+$. ^1H NMR (500 MHz, $\text{DMSO}-d_6$) δ ppm: 10.62 (br s, 1H), 10.21 (s, 1H), 8.96 (br s, 1H), 8.32 (br s, 1H), 7.93–7.91 (m, 2H), 7.84 (s, 1H), 7.59–7.57 (m, 2H), 7.51–7.49 (m, 2H), 7.25–7.23 (m, 2H), 5.45 (s, 2H), 4.03 (s, 2H), 3.11 (s, 2H). ^{13}C NMR (126 MHz, $\text{DMSO}-d_6$) δ ppm: 165.4, 163.3, 143.4, 140.0, 138.9, 138.0 (2C), 130.6, 128.7 (2C), 128.3 (2C), 123.2, 119.2 (2C), 100.4, 52.4, 42.0, 38.0. HRMS-ESI+ (m/z): calcd. for $\text{C}_{19}\text{H}_{20}\text{IN}_6\text{O}_5\text{S}$ $[\text{M} + \text{H}]^+$ 571.0261, found 571.0225.

2-Benzyl-3-(hydroxyamino)-N-[4-[[4-[[[(4-iodophenyl)sulfonylamino]methyl]triazol-1-yl]methyl]phenyl]-3-oxo-propanamide (179)



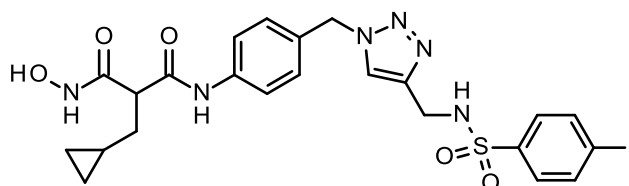
Compound **179** was synthesized according to the general procedure G, using ester **177** (85 mg, 0.13 mmol), KCN (2.44 mg, 0.04 mmol) and NH_2OH (1.8 mL, 50% w/w in water) in MeOH (1.8 mL) for 96h. The crude product was purified by flash chromatography on silica gel (CH_2Cl_2 to $\text{CH}_2\text{Cl}_2/\text{MeOH}$: 9/1) affording compound **179** as a white solid after lyophilization (67 mg, 81%). Purity: 100%, LC tr = 3.85 min, MS (ESI+): $m/z = 661$ $[\text{M} + \text{H}]^+$. ^1H NMR (500 MHz, $\text{DMSO}-d_6$) δ ppm: 10.50 (br s, 1H), 9.86 (s, 1H), 8.97 (br s, 1H), 8.17 (br s, 1H), 7.93–7.91 (m, 2H), 7.83 (s, 1H), 7.55–7.50 (m, 4H), 7.27–7.23 (m, 6H), 7.18–7.15 (m, 1H), 5.44 (s, 2H), 4.03 (s, 2H), 3.46 (t, $J = 7.5$ Hz, 1H), 3.16–3.06 (m, 2H). ^{13}C NMR (126 MHz, $\text{DMSO}-d_6$) δ ppm: 167.0, 165.4, 143.4, 140.0, 138.9, 138.7, 138.0 (2C), 130.7, 128.8 (2C), 128.7 (2C), 128.3 (2C), 128.2 (2C), 126.3, 123.2, 119.5 (2C), 100.4, 53.1, 52.4, 38.0, 34.4. HRMS-ESI+ (m/z): calcd. for $\text{C}_{26}\text{H}_{26}\text{IN}_6\text{O}_5\text{S}$ $[\text{M} + \text{H}]^+$ 661.0730, found 661.0683.

2-(Hydroxycarbamoyl)-N-[4-[[4-[(4-iodophenyl)sulfonylamino]methyl]triazol-1-yl]methyl]phenyl]-3-methyl-butanamide (182)



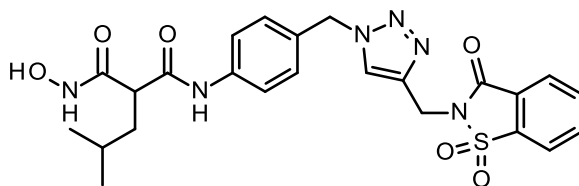
Compound **182** was synthesized according to the general procedure H, using azide **180** (35 mg, 0.12 mmol), alkyne **93** (38.6 mg, 0.12 mmol), copper (II) sulfate pentahydrate (6.0 mg, 0.02 mmol) and sodium ascorbate (11.9 mg, 0.06 mmol) in DMF (2.5 mL) and H₂O (1.5 mL) overnight. The crude product was purified by flash chromatography on silica gel (CH₂Cl₂ to CH₂Cl₂/MeOH: 95/5) affording compound **182** as a white solid after lyophilization (41 mg, 55%). Purity: 100%, LC tr = 3.51 min, MS (ESI+): *m/z* = 613 [M + H]⁺. ¹H NMR (500 MHz, DMSO-*d*₆) δ ppm: 10.56 (s, 1H), 9.77 (s, 1H), 9.02 (s, 1H), 8.19 (t, *J* = 5.8 Hz, 1H), 7.93–7.91 (m, 2H), 7.84 (s, 1H), 7.59–7.57 (m, 2H), 7.51–7.49 (m, 2H), 7.25–7.23 (m, 2H), 5.44 (s, 2H), 4.03 (d, *J* = 5.7 Hz, 2H), 2.71 (d, *J* = 10.5 Hz, 1H), 2.39–2.32 (m, 1H), 0.89–0.87 (m, 6H). HRMS-ESI+ (*m/z*): calcd. for C₂₂H₂₆IN₆O₅S [M + H]⁺ 613.0730, found 613.0689.

2-(Cyclopropylmethyl)-3-(hydroxyamino)-N-[4-[[4-[(4-iodophenyl)sulfonylamino]methyl]triazol-1-yl]methyl]phenyl]-3-oxo-propanamide (183)



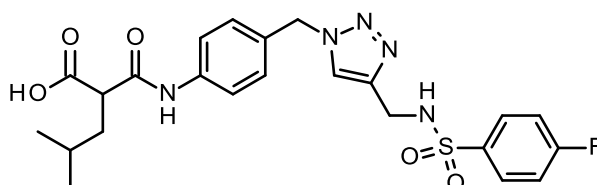
Compound **183** was synthesized according to the general procedure H, using azide **181** (50 mg, 0.17 mmol), alkyne **93** (52.9 mg, 0.12 mmol), copper (II) sulfate pentahydrate (8.2 mg, 0.03 mmol) and sodium ascorbate (16.3 mg, 0.08 mmol) in DMF (3 mL) and H₂O (2 mL) overnight. The crude product was purified by flash chromatography on silica gel (CH₂Cl₂ to CH₂Cl₂/MeOH: 95/5) affording compound **183** as a white solid after lyophilization (49 mg, 47%). Purity: 100%, LC tr = 3.64 min, MS (ESI+): *m/z* = 625 [M + H]⁺. ¹H NMR (500 MHz, DMSO-*d*₆) δ ppm: 10.51 (s, 1H), 9.85 (s, 1H), 8.96 (s, 1H), 8.20–8.17 (m, 1H), 7.93–7.91 (m, 2H), 7.84 (s, 1H), 7.58–7.50 (m, 4H), 7.25–7.23 (m, 2H), 5.44 (s, 2H), 4.03–4.02 (m, 2H), 3.21 (t, *J* = 6.9 Hz, 1H), 1.69 (t, *J* = 6.7 Hz, 2H), 0.65–0.62 (m, 1H), 0.37–0.35 (m, 2H), 0.08–0.07 (m, 2H). ¹³C NMR (126 MHz, DMSO-*d*₆) δ ppm: 167.8, 166.2, 143.4, 140.0, 138.8, 138.0 (2C), 130.7, 128.7 (2C), 128.3 (2C), 123.2, 119.5 (2C), 100.4, 52.4, 52.0, 38.0, 34.1, 9.0, 4.3, 4.3. HRMS-ESI+ (*m/z*): calcd. for C₂₃H₂₆IN₆O₅S [M + H]⁺ 625.0730, found 625.0691.

2-(Hydroxycarbamoyl)-4-methyl-N-[4-[[4-[(1,1,3-trioxo-1,2-benzothiazol-2-yl)methyl]triazol-1-yl]methyl]phenyl]pentanamide (139)



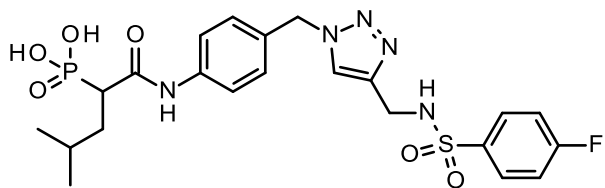
Compound **139** was synthesized according to the general procedure H, using azide **Z9** (50 mg, 0.26 mmol), alkyne **117** (145 mg, 0.66 mmol), copper (II) sulfate pentahydrate (8.2 mg, 0.03 mmol) and sodium ascorbate (51.9 mg, 0.26 mmol) in DMF (5.5 mL) and H₂O (4.5 mL) for 72h. The crude product was purified by preparative HPLC (H₂O+0.05%FA / ACN+0.05%FA 95:5 to 5:95) affording compound **139** as a white solid after lyophilization (21 mg, 15%). Purity: 100%, LC tr = 2.55 min, MS (ESI+): $m/z = 527 [M + H]^+$. ¹H NMR (500 MHz, DMSO-*d*₆) δ ppm: 10.53 (s, 1H), 9.81 (s, 1H), 8.96 (s, 1H), 8.32–8.30 (m, 1H), 8.14–8.12 (m, 2H), 8.07–7.99 (m, 2H), 7.56–7.54 (m, 2H), 7.25–7.24 (m, 2H), 5.51 (s, 2H), 4.97 (s, 2H), 3.20 (t, $J = 7.6$ Hz, 1H), 1.67 (t, $J = 7.2$ Hz, 2H), 1.46 (sep, $J = 6.6$ Hz, 1H), 0.87 (d, $J = 6.6$ Hz, 3H), 0.86 (d, $J = 6.6$ Hz, 3H). ¹³C NMR (126 MHz, DMSO-*d*₆) δ ppm: 167.8, 166.3, 158.3, 141.4, 138.7, 136.9, 136.0, 135.3, 130.8, 128.6 (2C), 126.2, 125.2, 124.0, 121.6, 119.5 (2C), 52.5, 49.9, 38.0, 33.5, 25.7, 22.4, 22.3. HRMS-ESI+ (m/z): calcd. for C₂₄H₂₇N₆O₆S [M + H]⁺ 527.1712, found 527.1619.

2-[[4-[[4-[(4-Fluorophenyl)sulfonylamino]methyl]triazol-1-yl]methyl]phenyl]carbamoyl]-4-methyl-pentanoic acid (193)



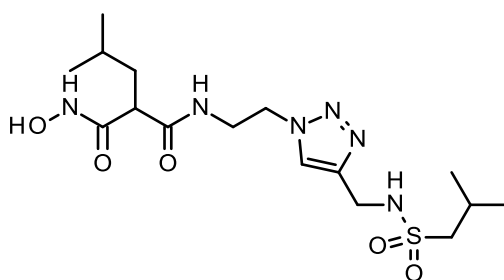
To a solution of ethyl ester **150** (70 mg, 0.13 mmol) in THF (1.2 mL) was added sodium hydroxide (10.5 mg, 0.26 mmol) in water (1.2 mL) and the mixture was stirred overnight at room temperature. Then, solvents were evaporated under reduced pressure and the crude was purified through preparative HPLC (H₂O+0.05%FA / ACN+0.05%FA 95:5 to 5:95) to give compound **193** as a white solid after lyophilization (36 mg, 54%). Purity: 100%, LC tr = 3.82 min, MS (ESI+): $m/z = 504 [M + H]^+$. ¹H NMR (500 MHz, DMSO-*d*₆) δ ppm: 12.71 (br s, 1H), 10.28 (s, 1H), 8.15 (t, $J = 5.6$ Hz, 1H), 7.84 (s, 1H), 7.82–7.79 (m, 2H), 7.59–7.57 (m, 2H), 7.37–7.34 (m, 2H), 7.24–7.22 (m, 2H), 5.45 (s, 2H), 4.04 (d, $J = 5.4$ Hz, 2H), 3.46 (dd, $J = 8.9$ and 6.0 Hz, 1H), 1.75–1.69 (m, 1H), 1.64–1.59 (m, 1H), 1.49 (sep, $J = 6.7$ Hz, 1H), 0.88 (d, $J = 6.6$ Hz, 3H), 0.86 (d, $J = 6.6$ Hz, 3H). ¹³C NMR (126 MHz, DMSO-*d*₆) δ ppm: 171.4, 167.8, 164.1 (d, $J = 250.6$ Hz), 143.4, 138.9, 136.8 (d, $J = 3.1$ Hz), 130.7, 129.5 (d, $J = 9.2$ Hz, 2C), 128.7 (2C), 123.2, 119.3 (2C), 116.2 (d, $J = 22.1$ Hz, 2C), 52.4, 51.2, 38.0, 37.5, 25.7, 22.7, 22.0. HRMS-ESI+ (m/z): calcd. for C₂₃H₂₇FN₅O₅S [M + H]⁺ 504.1717, found 504.1680.

[1-[[4-[[4-[(4-Fluorophenyl)sulfonylamino]methyl]triazol-1-yl]methyl]phenyl]carbamoyl]-3-methyl-butyl]phosphonic acid (196)



To a solution of diethyl phosphonate **195** (120 mg, 0.2 mmol) in dichloromethane (2 mL), bromotrimethylsilane (266 μ L, 2.0 mmol) was added dropwise over a period of 15 min. The reaction mixture was stirred at room temperature overnight. The conversion was not complete, a new addition of bromotrimethylsilane (266 μ L, 2.0 mmol) was done and the mixture was stirred overnight again. Then, methanol was added and the mixture stirred for 30 min at room temperature to cleave the previously formed TMS ester. The solvents were removed under reduced pressure and the crude product was finally purified through preparative HPLC (H₂O+0.05%FA/ ACN+0.05%FA: 95:5 to 5:95) to give compound **196** as a white solid after lyophilization (41 mg, 35%). Purity: 95%, LC tr = 3.16 min, MS (ESI⁺): m/z = 540 [M + H]⁺. ¹H NMR (500 MHz, DMSO-*d*₆) δ ppm: 10.08 (s, 1H), 8.14 (t, *J* = 6.0 Hz, 1H), 7.82–7.79 (m, 3H), 7.60–7.59 (m, 2H), 7.38–7.35 (m, 2H), 7.22–7.20 (m, 2H), 5.43 (s, 2H), 4.03 (d, *J* = 5.9 Hz, 2H), 3.00–2.94 (m, 1H), 1.98–1.91 (m, 1H), 1.51–1.39 (m, 2H), 0.85 (d, *J* = 6.2 Hz, 6H). ¹³C NMR (126 MHz, DMSO-*d*₆) δ ppm: 168.2, 164.1 (d, *J* = 250.9 Hz), 143.5, 139.5, 136.8 (d, *J* = 2.8 Hz), 130.1, 129.6 (d, *J* = 9.8 Hz, 2C), 128.6 (2C), 123.1, 119.1 (2C), 116.2 (d, *J* = 23.0 Hz, 2C), 52.5, 46.2 (d, *J* = 126.9 Hz), 38.1, 35.8, 26.5 (d, *J* = 14.5 Hz), 23.2, 21.4. HRMS-ESI⁺ (m/z): calcd. for C₂₂H₂₈FN₅O₆P [M + H]⁺ 540.1082, found 540.1158.

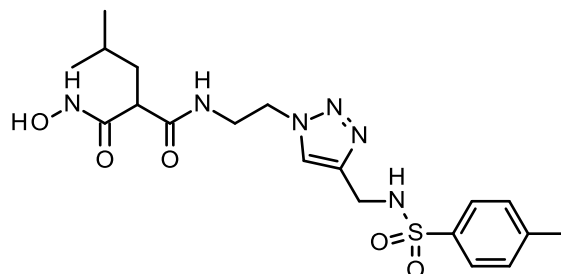
2-(Hydroxycarbamoyl)-N-[2-[4-[(isobutylsulfonylamino)methyl]triazol-1-yl]ethyl]-4-methylpentanamide (Hit L6)



Hit L6 was synthesized according to the general procedure G, using ester **102** (47 mg, 0.11 mmol), KCN (1.45 mg, 0.02 mmol) and NH₂OH (1.5 mL, 50% w/w in water) in MeOH (1.5 mL) overnight. The crude product was purified by flash chromatography on silica gel (CH₂Cl₂ to CH₂Cl₂/MeOH: 9/1) affording **Hit L6** as a white solid after lyophilization (24 mg, 51%). Purity: 100%, LC tr = not visible, MS (ESI⁺): m/z = 419 [M + H]⁺. ¹H NMR (500 MHz, DMSO-*d*₆) δ ppm: 10.48 (br s, 1H), 8.94 (br s, 1H), 7.92 (s, 1H), 7.81 (t, *J* = 5.4 Hz, 1H), 7.50 (br s, 1H), 4.40 (t, *J* = 6.2 Hz, 2H), 4.18 (s, 2H), 3.52–3.44 (m, 2H), 2.94 (t, *J* = 7.6 Hz, 1H), 2.88 (d, *J* = 6.3 Hz, 2H), 2.03 (sep, *J* = 6.6 Hz, 1H), 1.58–1.48 (m, 2H), 1.38–1.33 (m, 1H), 0.97 (d, *J* = 6.7 Hz, 6H), 0.82 (d, *J* = 6.4 Hz, 6H). ¹³C NMR (126 MHz,

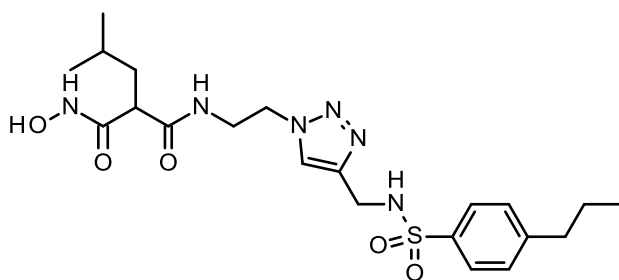
DMSO-*d*₆) δ ppm: 169.4, 166.6, 144.1, 123.5, 59.2, 48.9, 48.5, 39.1, 38.4, 37.7, 25.5, 24.2, 22.4, 22.2 (2C), 22.1. HRMS-ESI+ (*m/z*): calcd for C₁₆H₃₁N₆O₅S [M + H]⁺: 419.2077, found 419.2067.

2-(Hydroxycarbamoyl)-4-methyl-N-[2-[4-[(*p*-tolylsulfonylamino)methyl]triazol-1-yl]ethyl]pentanamide (Hit L7)



Hit L7 was synthesized according to the general procedure G, using ester **103** (113 mg, 0.24 mmol), KCN (3.13 mg, 0.05 mmol) and NH₂OH (2.5 mL, 50% w/w in water) in MeOH (2.5 mL) overnight. The crude product was purified by flash chromatography on silica gel (CH₂Cl₂ to CH₂Cl₂/MeOH: 9/1) affording **Hit L7** as a white solid after lyophilization (37 mg, 34%). Purity: 100%, LC tr = 3.08 min, MS (ESI+): *m/z* = 453 [M + H]⁺. ¹H NMR (500 MHz, DMSO-*d*₆) δ ppm: 10.50 (br s, 1H), 8.94 (br s, 1H), 8.00 (br s, 1H), 7.80 (t, *J* = 5.1 Hz, 1H), 7.76 (s, 1H), 7.68–7.66 (m, 2H), 7.38–7.36 (m, 2H), 4.33 (t, *J* = 6.0 Hz, 2H), 3.98 (s, 2H), 3.45–3.42 (m, 2H), 2.93 (t, *J* = 7.5 Hz, 1H), 2.38 (s, 3H), 1.57–1.46 (m, 2H), 1.37–1.32 (m, 1H), 0.82–0.80 (m, 6H). ¹³C NMR (126 MHz, DMSO-*d*₆) δ ppm: 169.4, 166.6, 143.1, 142.7, 137.4, 129.6 (2C), 126.7 (2C), 123.5, 48.9, 48.4, 39.0, 38.4, 38.1, 25.5, 22.4, 22.1, 21.0. HRMS-ESI+ (*m/z*): calcd for C₁₉H₂₉N₆O₅S [M + H]⁺ 453.1920, found 453.1912.

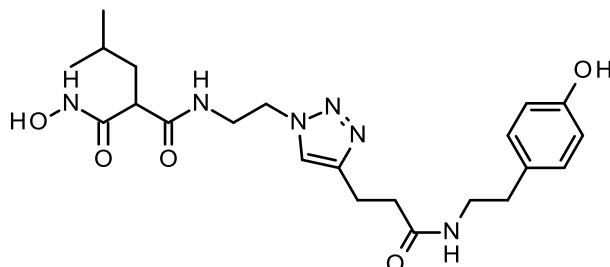
2-(Hydroxycarbamoyl)-4-methyl-N-[2-[4-[(4-propylphenyl)sulfonylamino]methyl]triazol-1-yl]ethyl]pentanamide (Hit L8)



Hit L8 was synthesized according to the general procedure G, using ester **104** (120 mg, 0.25 mmol), KCN (3.23 mg, 0.05 mmol) and NH₂OH (2.5 mL, 50% w/w in water) in MeOH (2.5 mL) overnight. The crude product was purified by flash chromatography on silica gel (CH₂Cl₂ to CH₂Cl₂/MeOH: 9/1) affording **Hit L8** as a white solid after lyophilization (81 mg, 68%). Purity: 100%, LC tr = 3.65 min, MS (ESI+): *m/z* = 481 [M + H]⁺. ¹H NMR (500 MHz, DMSO-*d*₆) δ ppm: 10.49 (br s, 1H), 8.93 (br s, 1H), 8.00 (br s, 1H), 7.79–7.69 (m, 4H), 7.39–7.38 (m, 2H), 4.33 (s, 2H), 4.00 (s, 2H), 3.60–3.43 (m, 2H), 2.94–2.91 (m, 1H), 2.64–2.61 (m, 2H), 1.61–1.50 (m, 4H), 1.34 (br s, 1H), 0.90–0.88 (m, 3H), 0.81–0.80 (m, 6H). ¹³C NMR (126 MHz, DMSO-*d*₆) δ ppm: 169.4, 166.6, 147.1, 143.2, 137.7, 129.0

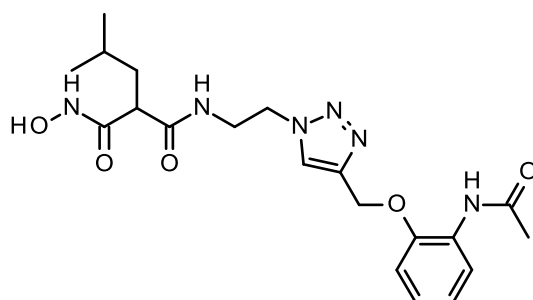
(2C), 126.7 (2C), 123.5, 48.9, 48.4, 39.0, 38.4, 38.1, 36.9, 25.5, 23.7, 22.4, 22.1, 13.6. HRMS-ESI+ (m/z): calcd. for C₂₁H₃₃N₆O₅S [M + H]⁺ 481.2233, found 481.2227.

2-(Hydroxycarbamoyl)-N-[2-[4-[3-[2-(4-hydroxyphenyl)ethylamino]-3-oxo-propyl]triazol-1-yl]ethyl]-4-methyl-pentanamide (Hit L10)



Hit L10 was synthesized according to the general procedure G, using ester **105** (106 mg, 0.22 mmol), KCN (2.9 mg, 0.04 mmol) and NH₂OH (2.5 mL, 50% w/w in water) in MeOH (2.5 mL) for 48h. The crude product was purified by flash chromatography on silica gel (CH₂Cl₂ to CH₂Cl₂/MeOH: 9/1) affording **Hit L10** as a white solid after lyophilization (54 mg, 52%). Purity: 100%, LC tr = 2.55 min, MS (ESI+): m/z = 461 [M + H]⁺. ¹H NMR (500 MHz, DMSO-*d*₆) δ ppm: 10.50 (br s, 1H), 9.16 (br s, 1H), 8.95 (br s, 1H), 7.91 (t, *J* = 5.5 Hz, 1H), 7.81 (t, *J* = 5.7 Hz, 1H), 7.70 (s, 1H), 6.97–6.95 (m, 2H), 6.67–6.65 (m, 2H), 4.36–4.33 (m, 2H), 3.48–3.44 (m, 2H), 3.21–3.17 (m, 2H), 2.94 (t, *J* = 7.7 Hz, 1H), 2.82–2.78 (m, 2H), 2.58–2.55 (m, 2H), 2.40–2.37 (m, 2H), 1.56–1.46 (m, 2H), 1.34 (sep, *J* = 6.6 Hz, 1H), 0.82 (d, *J* = 6.6 Hz, 3H), 0.81 (d, *J* = 6.6 Hz, 3H). ¹³C NMR (126 MHz, DMSO-*d*₆) δ ppm: 171.0, 169.4, 166.6, 155.6, 145.9, 129.5, 129.5 (2C), 122.2, 115.1 (2C), 48.9, 48.3, 40.6, 39.1, 38.4, 34.9, 34.4, 25.5, 22.4, 22.2, 21.4. HRMS-ESI+ (m/z): calcd. for C₂₂H₃₃N₆O₅ [M + H]⁺ 461.2512, found 461.2502.

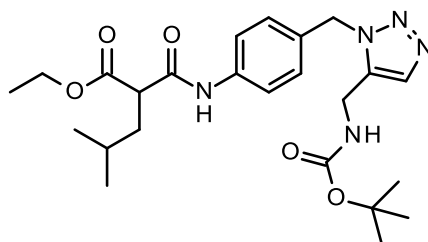
N-[2-[4-[(2-Acetamidophenoxy)methyl]triazol-1-yl]ethyl]-2-(hydroxycarbamoyl)-4-methyl-pentanamide (Hit L9)



Hit L9 was synthesized according to the general procedure H, using azide **Z10** (88 mg, 0.36 mmol), alkyne **100** (68.4 mg, 0.36 mmol), copper (II) sulfate pentahydrate (18.1 mg, 0.07 mmol) and sodium ascorbate (35.8 mg, 0.18 mmol) in DMF (5.5 mL) and H₂O (4.5 mL) overnight. The crude product was purified by preparative HPLC (H₂O+0.05%FA / ACN+0.05%FA: 95:5 to 5:95) affording **Hit L9** as a white solid after lyophilization (82 mg, 51%). Purity: 100%, LC tr = 2.77 min, MS (ESI+): m/z = 433 [M + H]⁺. ¹H NMR (500 MHz, DMSO-*d*₆) δ ppm: 10.52 (s, 1H), 9.01 (s, 1H), 8.95 (s, 1H), 8.15

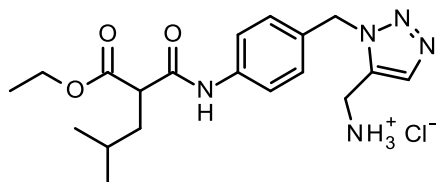
(s, 1H), 7.91–7.90 (m, 1H), 7.84 (t, $J = 5.7$ Hz, 1H), 7.24–7.23 (m, 1H), 7.07–7.04 (m, 1H), 6.92–6.89 (m, 1H), 5.20 (s, 2H), 4.44 (t, $J = 6.1$ Hz, 2H), 3.52–3.50 (m, 2H), 2.94 (t, $J = 7.7$ Hz, 1H), 2.07 (s, 3H), 1.57–1.46 (m, 2H), 1.35 (sep, $J = 6.6$ Hz, 1H), 0.80 (d, $J = 6.6$ Hz, 3H), 0.79 (d, $J = 6.6$ Hz, 3H). ^{13}C NMR (126 MHz, $\text{DMSO-}d_6$) δ ppm: 169.4, 168.4, 166.6, 148.5, 142.7, 127.9, 124.8, 124.2, 122.3, 120.8, 113.2, 62.3, 49.0, 48.6, 39.0, 38.4, 25.5, 23.9, 22.4, 22.1.

Ethyl 2-[[4-[[5-[(*tert*-butoxycarbonylamino)methyl]triazol-1-yl]methyl]phenyl]carbonyl]-4-methyl-pentanoate (184**)**



To a microwave tube filled with dioxane (6.0 mL) and degassed with N_2 during 10 min was added $\text{Cp}^*\text{RuCl}(\text{COD})$ (16.7 mg, 0.04 mmol, 0.05 eq) and the mixture was stirred under N_2 at room temperature during 2 min. Then, **83** (280 mg, 0.88 mmol) and *N*-*boc*-propargylamine (136 mg, 0.88 mmol) were added, the tube was sealed and the reaction media was heated at 80°C and stirred overnight. After, dioxane was evaporated under reduced pressure and the crude was purified through flash chromatography on silica gel column (CH_2Cl_2 to $\text{CH}_2\text{Cl}_2/\text{MeOH}$: 95/5) affording compound **184** as brown oil (295 mg, 70%). LC tr = 4.40 min, MS (ESI+): $m/z = 947$ [$2\text{M} + \text{H}$] $^+$, 474 [$\text{M} + \text{H}$] $^+$, 418 [$\text{M} - \text{tBu} + \text{H}$] $^+$, 374 [$\text{M} - \text{Boc} + \text{H}$] $^+$. ^1H NMR (500 MHz, $\text{DMSO-}d_6$) δ ppm: 10.28 (s, 1H), 7.58–7.56 (m, 2H), 7.53 (s, 1H), 7.46 (t, $J = 5.5$ Hz, 1H), 7.17–7.16 (m, 2H), 5.54 (s, 2H), 4.18 (d, $J = 5.7$ Hz, 2H), 4.13–4.06 (m, 2H), 3.56 (dd, $J = 8.7$ and 6.1 Hz, 1H), 1.78–1.72 (m, 1H), 1.68–1.62 (m, 1H), 1.53–1.44 (m, 1H), 1.36 (s, 9H), 1.16 (t, $J = 7.1$ Hz, 3H), 0.89 (d, $J = 6.7$ Hz, 3H), 0.87 (d, $J = 6.7$ Hz, 3H). ^{13}C NMR (126 MHz, $\text{DMSO-}d_6$) δ ppm: 169.7, 167.1, 155.5, 138.5, 135.7, 132.7, 130.7, 128.0 (2C), 119.4 (2C), 78.4, 60.6, 50.9, 50.2, 37.4, 32.9, 28.1 (3C), 25.6, 22.7, 21.9, 14.0.

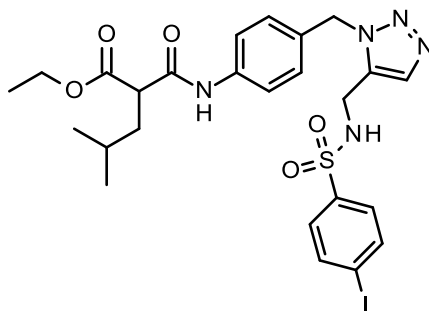
[3-[[4-[(2-Ethoxycarbonyl-4-methyl-pentanoyl)amino]phenyl]methyl]triazol-4-yl]methylammonium;chloride (186**)**



Compound **184** (290 mg, 0.61 mmol) was dissolved in ethanol and dichloromethane (5 mL, 2.5:2.5 v/v) and 4 N HCl in dioxane (2.5 mL) was added. The mixture was stirred overnight at room temperature. Then, solvents were evaporated to give compound **186** as a yellowish oil (251 mg, yield considered quantitative). LC tr = 3.04 min, MS (ESI+): $m/z = 374$ [$\text{M} + \text{H}$] $^+$. ^1H NMR (500 MHz, $\text{DMSO-}d_6$) δ : 10.47 (s, 1H), 8.74 (br s, 3H), 7.89 (s, 1H), 7.61–7.59 (m, 2H), 7.21–7.19 (m, 2H), 5.68

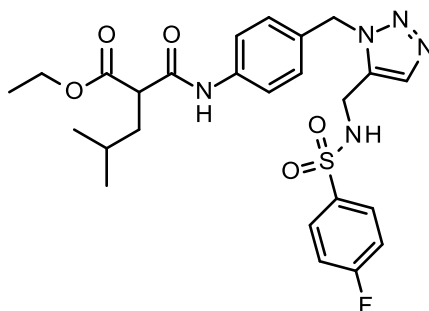
(s, 2H), 4.15–4.05 (m, 4H), 1.76–1.71 (m, 1H), 1.67–1.61 (m, 1H), 1.48 (sep, $J = 6.7$ Hz, 1H), 1.15 (t, $J = 7.1$ Hz, 3H), 0.88 (d, $J = 6.6$ Hz, 3H), 0.86 (d, $J = 6.6$ Hz, 3H). ^{13}C NMR (126 MHz, $\text{DMSO-}d_6$) δ : 169.8, 167.3, 138.8, 134.3, 131.1, 130.3, 128.2 (2C), 119.5 (2C), 60.6, 50.9, 50.6, 37.4, 31.1, 25.7, 22.7, 22.0, 14.0.

Ethyl 2-[[4-[[5-[[4-(4-iodophenyl)sulfonylamino]methyl]triazol-1-yl]methyl]phenyl]carbamoyl]-4-methyl-pentanoate (187)



Compound **187** was synthesized according to the general procedure F, using **186** (70 mg, 0.17 mmol), 4-iodobenzenesulfonyl chloride (62 mg, 0.21 mmol) and *N,N*-diisopropylethylamine (89 μL , 0.51 mmol) in DMF (2 mL) overnight. The crude product was purified by flash chromatography on silica gel (CH_2Cl_2 to $\text{CH}_2\text{Cl}_2/\text{MeOH}$: 95/5) affording compound **187** as brown oil (71 mg, 64%). LC tr = 4.68 min, MS (ESI+): $m/z = 640$ $[\text{M} + \text{H}]^+$. ^1H NMR (500 MHz, $\text{DMSO-}d_6$) δ ppm: 10.30 (s, 1H), 8.39 (t, $J = 5.5$ Hz, 1H), 7.96–7.94 (m, 2H), 7.57–7.55 (m, 2H), 7.50 (s, 1H), 7.48–7.46 (m, 2H), 7.13–7.11 (m, 2H), 5.48 (s, 2H), 4.14–4.04 (m, 4H), 3.56 (dd, $J = 8.7$ and 6.2 Hz, 1H), 1.78–1.73 (m, 1H), 1.68–1.62 (m, 1H), 1.49 (sep, $J = 6.7$ Hz, 1H), 1.15 (t, $J = 7.1$ Hz, 3H), 0.89 (d, $J = 6.7$ Hz, 3H), 0.87 (d, $J = 6.7$ Hz, 3H). ^{13}C NMR ($\text{DMSO-}d_6$) δ ppm: 169.7, 167.1, 139.4, 138.6, 138.2 (2C), 133.5, 133.4, 130.3, 128.2 (2C), 128.2 (2C), 119.4 (2C), 100.9, 60.7, 50.9, 50.3, 37.4, 35.3, 25.6, 22.7, 21.9, 14.0.

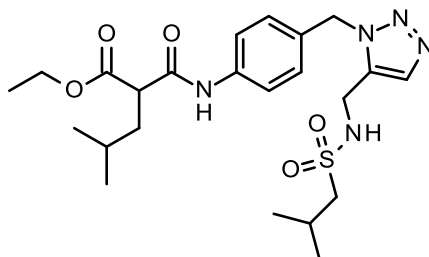
Ethyl 2-[[4-[[5-[[4-(4-fluorophenyl)sulfonylamino]methyl]triazol-1-yl]methyl]phenyl]carbamoyl]-4-methyl-pentanoate (188)



Compound **188** was synthesized according to the general procedure F, using **186** (70 mg, 0.17 mmol), 4-fluorobenzenesulfonyl chloride (39.9 mg, 0.21 mmol) and *N,N*-diisopropylethylamine (89 μL , 0.51 mmol) in DMF (2 mL) overnight. The crude product was purified by flash chromatography on silica gel (CH_2Cl_2 to $\text{CH}_2\text{Cl}_2/\text{MeOH}$: 95/5) affording compound **188** as pale yellow oil (65 mg, 70%). LC tr = 4.41 min, MS (ESI+): $m/z = 532$ $[\text{M} + \text{H}]^+$. ^1H NMR (500 MHz, $\text{DMSO-}d_6$) δ ppm: 10.29 (s, 1H),

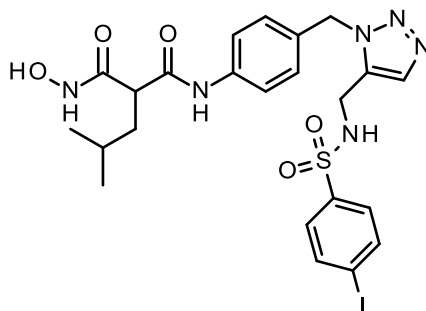
8.35 (s, 1H), 7.78–7.75 (m, 2H), 7.56–7.55 (m, 2H), 7.49 (s, 1H), 7.41–7.38 (m, 2H), 7.13–7.12 (m, 2H), 5.48 (s, 2H), 4.12–4.06 (m, 4H), 3.56 (dd, $J = 8.7$ and 6.2 Hz, 1H), 1.78–1.72 (m, 1H), 1.68–1.62 (m, 1H), 1.49 (sep, $J = 6.7$ Hz, 1H), 1.15 (t, $J = 7.1$ Hz, 3H), 0.89 (d, $J = 6.7$ Hz, 3H), 0.87 (d, $J = 6.7$ Hz, 3H). ^{13}C NMR (126 MHz, DMSO- d_6) δ ppm: 169.7, 167.2, 164.2 ($J = 251.4$ Hz), 138.6, 136.2 ($J = 2.8$ Hz), 133.5, 133.2, 130.3, 129.6 ($J = 9.2$ Hz, 2C), 128.2 (2C), 119.4 (2C), 116.4 ($J = 23.0$ Hz, 2C), 60.7, 50.9, 50.3, 37.4, 35.3, 25.6, 22.6, 21.9, 14.0.

Ethyl 2-[[4-[[5-[(isobutylsulfonylamino)methyl]triazol-1-yl]methyl]phenyl]carbonyl]-4-methyl-pentanoate (189)



Compound **189** was synthesized according to the general procedure F, using **186** (100 mg, 0.24 mmol), 4-fluorobenzenesulfonyl chloride (45.9 mg, 0.29 mmol) and *N,N*-diisopropylethylamine (127 μL , 0.73 mmol) in DMF (2 mL) overnight. The crude product was purified by flash chromatography on silica gel (CH_2Cl_2 to $\text{CH}_2\text{Cl}_2/\text{MeOH}$: 95/5) affording compound **189** as yellow oil (80 mg, 65%). LC tr = 4.30 min, MS (ESI+): $m/z = 494$ [$\text{M} + \text{H}$] $^+$. ^1H NMR (500 MHz, DMSO- d_6) δ ppm: 10.29 (s, 1H), 7.72 (t, $J = 5.2$ Hz, 1H), 7.67 (s, 1H), 7.58–7.56 (m, 2H), 7.21–7.19 (m, 2H), 5.56 (s, 2H), 4.22 (d, $J = 5.2$ Hz, 2H), 4.14–4.04 (m, 2H), 3.55 (dd, $J = 8.8$ and 6.2 Hz, 1H), 2.82 (d, $J = 6.5$ Hz, 2H), 2.01 (sep, $J = 6.7$ Hz, 1H), 1.77–1.71 (m, 1H), 1.67–1.61 (m, 1H), 1.48 (sep, $J = 6.7$ Hz, 1H), 1.15 (t, $J = 7.1$ Hz, 3H), 0.96 (d, $J = 6.7$ Hz, 6H), 0.88 (d, $J = 6.7$ Hz, 3H), 0.87 (d, $J = 6.7$ Hz, 3H). ^{13}C NMR (126 MHz, DMSO- d_6) δ ppm: 169.7, 167.1, 138.6, 134.4, 133.4, 130.5, 128.2 (2C), 119.4 (2C), 60.7, 58.9, 50.9, 50.3, 37.4, 34.9, 25.6, 24.2, 22.7, 22.2 (2C), 21.9, 14.0.

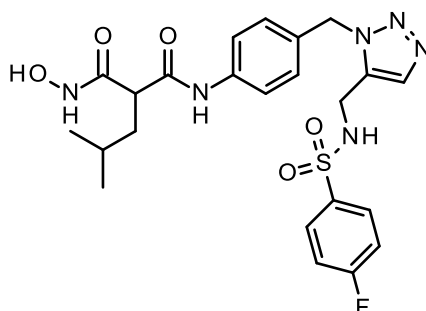
2-(Hydroxycarbonyl)-*N*-[4-[[5-[[4-iodophenyl]sulfonylamino]methyl]triazol-1-yl]methyl]phenyl]-4-methyl-pentanamide (190)



Compound **190** was synthesized according to the general procedure G, using ester **187** (64 mg, 0.1 mmol), KCN (1.94 mg, 0.03 mmol) and NH_2OH (1.2 mL, 50% w/w in water) in MeOH (1.2 mL) for 48h. The crude product was purified through preparative HPLC ($\text{H}_2\text{O}+0.05\%\text{FA}$ / $\text{ACN}+0.05\%\text{FA}$:

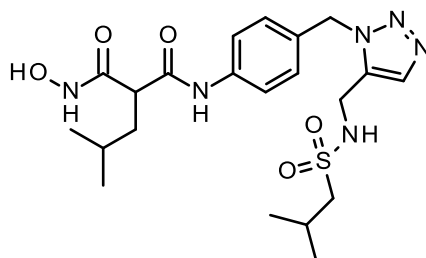
95:5 to 5:95) to give compound **190** as a white solid after lyophilization (18 mg, 29%). Purity: 100%, LC tr = 3.82 min, MS (ESI+): $m/z = 627 [M + H]^+$. $^1\text{H NMR}$ (500 MHz, $\text{DMSO-}d_6$) δ ppm: 10.54 (br s, 1H), 9.82 (s, 1H), 8.97 (s, 1H), 8.39 (br s, 1H), 7.97–7.95 (m, 2H), 7.56–7.54 (m, 2H), 7.49–7.47 (m, 3H), 7.11–7.10 (m, 2H), 5.47 (s, 2H), 4.05 (s, 2H), 3.21 (t, $J = 7.6$ Hz, 1H), 1.70–1.66 (m, 2H), 1.48 (sep, $J = 6.6$ Hz, 1H), 0.87 (d, $J = 6.6$ Hz, 3H), 0.86 (d, $J = 6.6$ Hz, 3H). $^{13}\text{C NMR}$ (126 MHz, $\text{DMSO-}d_6$) δ ppm: 167.9, 166.3, 139.4, 138.6, 138.2 (2C), 133.5, 133.4, 130.2, 128.2 (2C), 128.1 (2C), 119.6 (2C), 100.9, 50.3, 50.0, 38.0, 35.3, 25.7, 22.4, 22.3. HRMS-ESI+ (m/z): calcd. for $\text{C}_{23}\text{H}_{28}\text{N}_6\text{O}_5\text{S}$ $[M + H]^+$: 627.0887, found 627.0881.

***N*-[4-[[5-[(4-Fluorophenyl)sulfonylamino]methyl]triazol-1-yl]methyl]phenyl]-2-(hydroxycarbamoyl)-4-methyl-pentanamide (**191**)**



Compound **191** was synthesized according to the general procedure G, using ester **188** (58 mg, 0.11 mmol), KCN (2.11 mg, 0.03 mmol) and NH_2OH (1.2 mL, 50% w/w in water) in MeOH (1.2 mL) for 48h. The crude product was purified through preparative HPLC ($\text{H}_2\text{O}+0.05\%\text{FA} / \text{ACN}+0.05\%\text{FA}$: 95:5 to 5:95) to give compound **191** as a white solid after lyophilization (21 mg, 37%). Purity: 100%, LC tr = 3.50 min, MS (ESI+): $m/z = 519 [M + H]^+$. $^1\text{H NMR}$ (500 MHz, $\text{DMSO-}d_6$) δ ppm: 10.53 (br s, 1H), 9.82 (s, 1H), 8.96 (s, 1H), 8.35 (br s, 1H), 7.79–7.76 (m, 2H), 7.56–7.54 (m, 2H), 7.48 (s, 1H), 7.42–7.39 (m, 2H), 7.12–7.10 (m, 2H), 5.48 (s, 2H), 4.06 (s, 2H), 3.21 (t, $J = 7.6$ Hz, 1H), 1.70–1.66 (m, 2H), 1.47 (sep, $J = 6.7$ Hz, 1H), 0.87 (d, $J = 6.7$ Hz, 3H), 0.86 (d, $J = 6.7$ Hz, 3H). $^{13}\text{C NMR}$ (126 MHz, $\text{DMSO-}d_6$) δ ppm: 167.9, 166.3, 164.2 (d, $J = 251.1$ Hz), 138.6, 136.2 (d, $J = 2.7$ Hz), 133.5, 133.3, 130.1, 129.6 (d, $J = 9.6$ Hz, 2C), 128.1 (2C), 119.5 (2C), 116.4 (d, $J = 22.5$ Hz, 2C), 50.3, 50.0, 38.0, 35.3, 25.7, 22.4, 22.3. HRMS-ESI+ (m/z): calcd. for $\text{C}_{23}\text{H}_{28}\text{FN}_6\text{O}_5\text{S}$ $[M + H]^+$ 519.1826, found 519.1821.

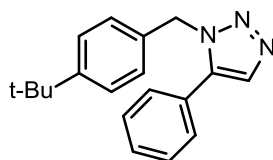
2-(Hydroxycarbamoyl)-*N*-[4-[[5-[(isobutylsulfonylamino)methyl]triazol-1-yl]methyl]phenyl]-4-methyl-pentanamide (192**)**



Compound **192** was synthesized according to the general procedure G, using ester **189** (70 mg, 0.14 mmol), KCN (2.74 mg, 0.04 mmol) and NH₂OH (1.5 mL, 50% w/w in water) in MeOH (1.5 mL) for 48h. The crude product was purified through preparative HPLC (H₂O+0.05%FA / ACN+0.05%FA: 95:5 to 5:95) to give compound **192** as a white solid after lyophilization (34 mg, 50%). Purity: 100%, LC tr = 3.36 min, MS (ESI+): m/z= 481 [M + H]⁺. ¹H NMR (DMSO-*d*₆) δ ppm: 10.52 (s, 1H), 9.81 (s, 1H), 8.96 (s, 1H), 7.72 (t, *J* = 5.4 Hz, 1H), 7.67 (s, 1H), 7.57–7.55 (m, 2H), 7.19–7.17 (m, 2H), 5.55 (s, 2H), 4.22 (d, *J* = 5.1 Hz, 2H), 3.20 (t, *J* = 7.6 Hz, 1H), 2.84 (d, *J* = 6.4 Hz, 2H), 2.02 (sep, *J* = 6.7 Hz, 1H), 1.69–1.65 (m, 2H), 1.47 (sep, *J* = 6.7 Hz, 1H), 0.97 (d, *J* = 6.7 Hz, 6H), 0.87 (d, *J* = 6.7 Hz, 3H), 0.86 (d, *J* = 6.7 Hz, 3H). ¹³C NMR (126 MHz, DMSO-*d*₆) δ ppm: 167.8, 166.3, 138.6, 134.4, 133.4, 130.4, 128.1 (2C), 119.5 (2C), 58.9, 50.3, 50.0, 38.0, 35.0, 25.7, 24.2, 22.4, 22.3, 22.2 (2C). HRMS-ESI (m/z): calcd. for C₂₁H₃₁N₆O₅S [M - H]⁻ 479.2077, found 479.2083.

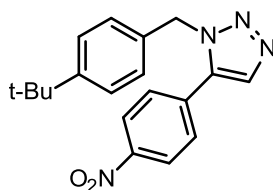
5. Synthesis of chapter 4 compounds (3aA–3aH and 3bA–3I)

1-[(4-*Tert*-butylphenyl)methyl]-5-phenyl-triazole (3aA)



Compound **3aA** was synthesized according to the general procedure K, from ethynylbenzene (0.49 mmol) and 1-(bromomethyl)-4-*tert*-butyl-benzene. Purification of 56% of crude by flash chromatography (58 mg, **3aA/4aA** ratio = 8.3:1, 64% yield). Injection of 29% of crude for semi-preparative SFC purification (injected volume: 20 μL, flow rate: 2 mL/min, mobile phase: CO₂-modifier mixture with 20% of ethanol as modifier) afforded compound **3aA** as a yellow oil (30 mg, 72% yield). Purity = 96%, tr = 3.76 min. ¹H NMR (300 MHz, CDCl₃) δ ppm: 7.71 (s, 1H), 7.44–7.39 (m, 3H), 7.30–7.24 (m, 4H), 7.04–7.00 (m, 2H), 2.48 (s, 2H), 1.26 (s, 9H). ¹³C NMR (75 MHz, CDCl₃) δ ppm: 151.3, 138.2, 133.3, 132.5, 129.6, 129.1 (2C), 129.0 (2C), 127.1 (3C), 125.8 (2C), 51.6, 34.6, 31.4 (3C). HRMS (ESI+) m/z: [M + H]⁺ calcd for. C₁₉H₂₂N₃ 292.1814; Found 292.1814.

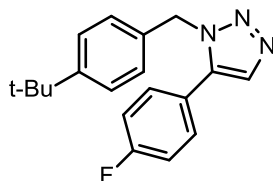
1-[(4-*Tert*-butylphenyl)methyl]-5-(4-nitrophenyl)triazole (3aB)



Compound **3aB** was synthesized according to the general procedure K, from 1-ethynyl-4-nitrobenzene (0.34 mmol) and 1-(bromomethyl)-4-*tert*-butyl-benzene. Purification of 50% of crude by flash chromatography (33 mg, **3aB/4aB** ratio = 1.9:1, 37% yield). Injection of 33% of crude for

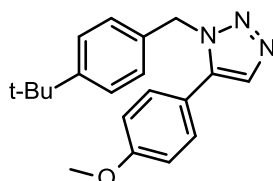
semipreparative SFC purification (injected volume: 250 μ L, flow rate: 6 mL/min, mobile phase: CO₂-modifier mixture with 5% of ethanol as modifier) afforded compound **3aB** as a colorless oil (9 mg, 24% yield). Purity >99%, tr = 8.87 min. ¹H NMR (300 MHz, CDCl₃) δ ppm: 8.29–8.24 (m, 2H), 7.83 (s, 1H), 7.48–7.43 (m, 2H), 7.34–7.29 (m, 2H), 7.02–6.99 (m, 2H), 5.56 (s, 2H), 1.28 (s, 9H). ¹³C NMR (CDCl₃) δ ppm: 151.9, 148.4, 136.1, 134.1, 133.6, 131.9, 129.9 (2C), 127.0 (2C), 126.1 (2C), 124.2 (2C), 52.2, 34.7, 31.3 (3C). HRMS (ESI+) m/z: [M + H]⁺ calcd for C₁₉H₂₁N₄O₂ 337.1665; Found 337.1668.

1-[(4-*Tert*-butylphenyl)methyl]-5-(4-fluorophenyl)triazole (**3aC**)



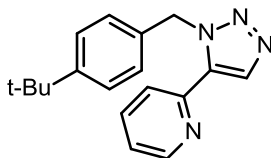
Compound **3aC** was synthesized according to the general procedure K, from 1-ethynyl-4-fluorobenzene (0.42 mmol) and 1-(bromomethyl)-4-*tert*-butylbenzene. Purification of 59% of crude by flash chromatography (71 mg, **3aC/4aC** ratio = 10.2:1, 84% yield). Injection of 27% of crude for semipreparative SFC purification (injected volume: 250 μ L, flow rate: 3 mL/min, mobile phase: CO₂-modifier mixture with 5% of ethanol as modifier) afforded compound **3aC** as a white solid (12 mg, 34% yield). Purity = 97%, tr = 3.33 min. ¹H NMR (300 MHz, CDCl₃) δ ppm: 7.69 (s, 1H), 7.32–7.27 (m, 2H), 7.25–7.20 (m, 2H), 7.14–7.07 (m, 2H), 7.03–6.98 (m, 2H), 5.47 (s, 2H), 1.27 (s, 9H). ¹³C NMR (75 MHz, CDCl₃) δ ppm: 163.5 (d, *J* = 250.8 Hz), 151.5, 137.2, 133.4, 132.4, 131.1 (d, *J* = 8.4 Hz, 2C), 127.1 (2C), 125.9 (2C), 123.2 (d, *J* = 3.3 Hz), 116.2 (d, *J* = 22.1 Hz, 2C), 51.7, 34.7, 31.3 (3C). HRMS (ESI+) m/z: [M + H]⁺ calcd for C₁₉H₂₁N₃F 310.1720; found 310.1716.

1-[(4-*Tert*-butylphenyl)methyl]-5-(4-methoxyphenyl)triazole (**3aD**)



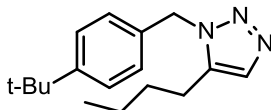
Compound **3aD** was synthesized according to the general procedure K, from 1-ethynyl-4-methoxybenzene (0.38 mmol) and 1-(bromomethyl)-4-*tert*-butylbenzene. Purification by flash chromatography afforded compound **3aD** as a white solid (94 mg, **3aD/4aD** ratio = 99:1, 76% yield). Purity >99%, tr = 5.11 min. ¹H NMR (300 MHz, CDCl₃) δ ppm: 7.67 (s, 1H), 7.32–7.28 (m, 2H), 7.22–7.17 (m, 2H), 7.05–7.02 (m, 2H), 6.96–6.91 (m, 2H), 5.47 (s, 2H), 3.84 (s, 3H), 1.28 (s, 9H). ¹³C NMR (75 MHz, CDCl₃) δ ppm: 160.6, 151.3, 138.1, 133.0, 132.7, 130.4 (2C), 127.1 (2C), 125.8 (2C), 119.2, 114.5 (2C), 55.5, 51.5, 34.6, 31.4 (3C). HRMS (ESI+) m/z: [M + H]⁺ calcd for C₂₀H₂₄N₃O 322.1923; found 322.1919.

2-[3-[(4-*Tert*-butylphenyl)methyl]triazol-4-yl]pyridine (3aE)



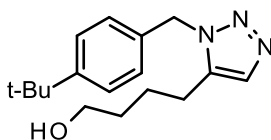
Compound **3aE** was synthesized according to the general procedure K, from 2-ethynylpyridine (0.49 mmol) and 1-(bromomethyl)-4-*tert*-butyl-benzene. **3aE/4aE** ratio = 11.5:1 Purification by flash chromatography afforded compound **3aE** as a colorless oil (104 mg, 73% yield). Purity = 96%, tr = 16.27 min. ¹H NMR (300 MHz, CDCl₃) δ ppm: 8.70 (qd, *J* = 4.9 and 0.9 Hz, 1H), 7.98 (s, 1H), 7.74 (dt, *J* = 7.8 and 1.8 Hz, 1H), 7.54 (td, *J* = 7.9 and 1.0 Hz, 1H), 7.30–7.23 (m, 3H), 7.20–7.16 (m, 2H), 6.12 (s, 2H), 1.24 (s, 9H). ¹³C NMR (75 MHz, CDCl₃) δ ppm: 150.9, 149.6, 147.2, 137.2, 135.7, 133.7, 133.2, 127.8 (2C), 125.5 (2C), 123.4, 123.0, 52.8, 34.6, 31.4 (3C). HRMS (ESI+) *m/z*: [M + H]⁺ calcd for C₁₈H₂₁N₄ 293.1766; found 293.1765.

5-Butyl-1-[(4-*tert*-butylphenyl)methyl]triazole (3aF)



Compound **3aF** was synthesized according to the general procedure K, from hex-1-yne (0.61 mmol) and 1-(bromomethyl)-4-*tert*-butyl-benzene. Purification of 74% of crude by flash chromatography (38 mg, **3aF/4aF** ratio = 5.9:1, 27% yield). Injection of 17% of crude for semi-preparative SFC purification (injected volume: 250 μL, flow rate: 4 mL/min, mobile phase: CO₂-modifier mixture with 10% of ethanol as modifier) afforded compound **3aF** as a white solid (12 mg, 36% yield). Purity = 86% (determined by ¹H NMR). tr = 2.95 min. ¹H NMR (300 MHz, CDCl₃) δ ppm: 7.49 (s, 1H), 7.38–7.34 (m, 2H), 7.13–7.10 (m, 2H), 5.48 (s, 2H), 2.61–2.40 (m, 2H), 1.56–1.46 (m, 2H), 1.38–1.26 (m, 11H), 0.87 (t, *J* = 7.5 Hz, 2H). ¹³C NMR (75 MHz, CDCl₃) δ ppm: 151.5, 132.6, 132.1, 127.9, 127.1 (2C), 125.9 (2C), 51.5, 34.7, 31.4 (3C), 30.1, 23.0, 22.3, 13.7. HRMS (ESI+) *m/z*: [M + H]⁺ calcd for C₁₇H₂₆N₃ 272.2127; found 272.2129.

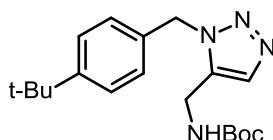
4-[3-[(4-*Tert*-butylphenyl)methyl]triazol-4-yl]butan-1-ol (3aG)



Compound **3aG** was synthesized according to the general procedure K, from hex-5-yn-1-ol (0.51 mmol) and 1-(bromomethyl)-4-*tert*-butyl-benzene. Purification of 58% of crude by flash chromatography (67 mg, **3aG/4aG** ratio = 7.8:1, 70% yield). Injection of 28% of crude for semi-preparative SFC purification (injected volume: 250 μL, flow rate: 2 mL/min, mobile phase: CO₂-modifier mixture with 20% of ethanol as modifier) afforded compound **3aG** as a colorless oil (26 mg,

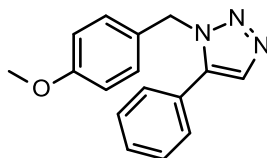
56% yield). Purity = 89% (determined by ^1H NMR). t_r = 9.27 min. ^1H NMR (300 MHz, CDCl_3) δ ppm: 7.46 (s, 1H), 7.36–7.31 (m, 2H), 7.10–7.07 (m, 2H), 5.45 (s, 2H), 3.60 (t, J = 6.0 Hz, 2H), 2.57–2.52 (m, 2H), 2.26 (br s, 1H), 1.66–1.48 (m, 4H), 1.28 (s, 9H). ^{13}C NMR (75 MHz, CDCl_3) δ ppm: 151.5, 137.3, 132.5, 132.0, 127.0 (2C), 125.9 (2C), 62.0, 51.5, 34.6, 32.0, 31.3 (3C), 24.3, 23.0. HRMS (ESI+) m/z : $[\text{M} + \text{H}]^+$ calcd for $\text{C}_{17}\text{H}_{26}\text{N}_3\text{O}$ 288.2076; found 288.2073.

***Tert*-butyl *N*-[[3-[(4-*tert*-butylphenyl)methyl]triazol-4-yl]methyl]carbamate (**3aH**)**



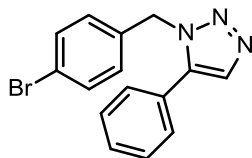
Compound **3aH** was synthesized according to the general procedure K, from *tert*-butyl *N*prop-2-ynylcarbamate (0.32 mmol) and 1-(bromomethyl)-4-*tert*-butylbenzene. Purification of 32% of crude by flash chromatography (18 mg, **3aH/4aH** ratio = 2:1, 34% yield). Injection of 22% of crude for semi-preparative SFC purification (injected volume: 20 μL , flow rate: 5 mL/min, mobile phase: CO_2 -modifier mixture with 5% of ethanol as modifier) afforded compound **3aH** as a white solid (8 mg, 34% yield). Purity = 98%, t_r = 4.61 min. ^1H NMR (500 MHz, CDCl_3) δ ppm: 7.61 (s, 1H), 7.28–7.34 (m, 2H), 7.17–7.14 (m, 2H), 5.56 (s, 2H), 4.50 (br s, 1H), 4.28 (br d, J = 5.0 Hz, 2H), 1.41 (s, 9H), 1.30 (s, 9H). ^{13}C NMR (125 MHz, CDCl_3) δ ppm: 155.5, 151.8, 134.9, 133.7, 131.7, 127.4 (2C), 126.2 (2C), 80.6, 52.1, 33.5, 31.4 (3C), 29.8, 28.4 (3C). HRMS (ESI+) m/z : $[\text{M} + \text{H}]^+$ calcd for $\text{C}_{19}\text{H}_{29}\text{N}_4\text{O}_2$ 345.2291; found 345.2291.

1-[(4-Methoxyphenyl)methyl]-5-phenyl-triazole (3bA**)**



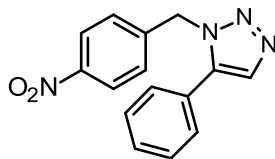
Compound **3bA** was synthesized according to the general procedure K, from ethynylbenzene (0.49 mmol) and 1-(bromomethyl)-4-methoxybenzene. Purification of 71% of crude by flash chromatography (74 mg, **3bA/4bA** ratio = 5.8:1, 69% yield). Injection of 20% of crude for semi-preparative SFC purification (injected volume: 485 μL , flow rate: 4 mL/min, mobile phase: CO_2 -modifier mixture with 10% of ethanol as modifier) afforded compound **3bA** as a colorless oil (17 mg, 67% yield). Purity = 86%, t_r = 5.20 min. ^1H NMR (300 MHz, CDCl_3) δ ppm: 7.69 (s, 1H), 7.44–7.38 (m, 3H), 7.27–7.23 (m, 2H), 7.02–6.97 (m, 2H), 6.80–6.75 (m, 2H), 5.46 (s, 2H), 3.74 (s, 3H). ^{13}C NMR (75 MHz, CDCl_3) δ ppm: 159.5, 138.0, 133.4, 129.6, 129.04 (2C), 129.01 (2C), 128.8 (2C), 127.6, 127.1, 114.2 (2C), 55.3, 51.5. HRMS (ESI+) m/z : $[\text{M} + \text{H}]^+$ calcd for $\text{C}_{16}\text{H}_{13}\text{N}_3\text{O}$ 266.1293; found 266.1302. The analytical data are in accordance with those reported in the literature.⁽¹⁴⁰⁾

1-[(4-Bromophenyl)methyl]-5-phenyl-triazole (3cA)



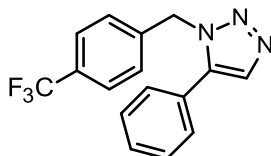
Compound **3cA** was synthesized according to the general procedure K, from ethynylbenzene (0.49 mmol) and 1-bromo4-(bromomethyl)benzene. Purification of 60% of crude by flash chromatography (70 mg, **3cA/4cA** ratio = 5.6:1, 64% yield). Injection of 27% of crude for semi-preparative SFC purification (injected volume: 250 μ L, flow rate: 2 mL/min, mobile phase: CO₂-modifier mixture with 20% of ethanol as modifier) afforded compound **3cA** as a yellow oil (28 mg, 68% yield). Purity = 97%, tr = 5.86 min. ¹H NMR (300 MHz, CDCl₃) δ ppm: 7.72 (s, 1H), 7.44–7.37 (m, 5H), 7.24–7.20 (m, 2H), 6.95–6.92 (m, 2H), 5.48 (s, 2H). ¹³C NMR (75 MHz, CDCl₃) δ ppm: 138.3, 134.5, 133.5, 132.1 (2C), 129.8 (2C), 129.2 (2C), 129.0 (2C), 128.9, 126.8, 122.4, 51.3. HRMS (ESI+) m/z: [M + H]⁺ calcd for C₁₅H₁₃N₃Br₂ 314.0293; found 314.0297. The analytical data are in accordance with those reported in the literature.⁽¹⁴¹⁾

1-[(4-Nitrophenyl)methyl]-5-phenyl-triazole (3dA)



Compound **3dA** was synthesized according to the general procedure K, from ethynylbenzene (0.49 mmol) and 1-(bromomethyl)-4-nitro-benzene. Purification of 51% of crude by flash chromatography afforded compound **3dA** as a brown solid (49 mg, **3dA/4dA** ratio = 31.1:1, 68% yield). Purity = 96%, tr = 8.29 min. ¹H NMR (300 MHz, CDCl₃) δ ppm: 8.14–8.11 (m, 2H), 7.77 (s, 1H), 7.47–7.39 (m, 3H), 7.24–7.21 (m, 4H), 5.65 (s, 2H). ¹³C NMR (75 MHz, CDCl₃) δ ppm: 147.8, 142.5, 138.4, 133.5, 130.0, 129.3 (2C), 128.8 (2C), 128.1 (2C), 126.4, 124.1 (2C), 51.1. HRMS (ESI+) m/z: [M + H]⁺ calcd for C₁₅H₁₃N₄O₂ 281.1039; found 281.1049. The analytical data are in accordance with those reported in the literature.⁽¹⁴⁰⁾

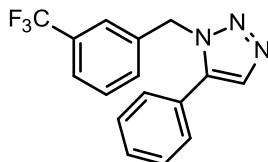
5-Phenyl-1-[[4-(trifluoromethyl)phenyl]methyl]triazole (3eA)



Compound **3eA** was synthesized according to the general procedure K, from ethynylbenzene (0.49 mmol) and 1-(bromomethyl)-4-(trifluoromethyl)benzene. Purification of 55% of crude by flash chromatography (65 mg, **3eA/4eA** ratio = 12.8:1, 73% yield). Injection of 30% of crude for semi-preparative SFC purification (injected volume: 250 μ L, flow rate: 4 mL/min, mobile phase: CO₂-

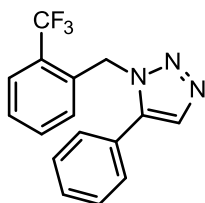
modifier mixture with SI8 10% of ethanol as modifier) afforded compound **3eA** as a white solid (37 mg, 84% yield). Purity >99%, tr = 2.71 min. ^1H NMR (300 MHz, CDCl_3) δ ppm: 7.77 (s, 1H), 7.57–7.54 (m, 2H), 7.48–7.41 (m, 3H), 7.27–7.24 (m, 2H), 7.22–7.17 (m, 2H) 5.61 (s, 2H). ^{13}C NMR (75 MHz, CDCl_3) δ ppm: 139.4, 138.4, 133.5, 130.6 (q, $J = 32.6$ Hz), 129.8 (2C), 129.2, 128.9 (2C), 127.6 (2C), 126.7, 125.9 (q, $J = 3.6$ Hz, 2C), 124.1 (q, $J = 269.0$ Hz), 51.3. HRMS (ESI+) m/z : $[\text{M} + \text{H}]^+$ calcd for $\text{C}_{16}\text{H}_{13}\text{N}_3\text{F}_3$ 304.1062; found 304.1062. The analytical data are in accordance with those reported in the literature.⁽¹²⁸⁾

5-Phenyl-1-[[3-(trifluoromethyl)phenyl]methyl]triazole (**3fA**)



Compound **3fA** was synthesized according to the general procedure K, from ethynylbenzene (0.49 mmol) and 1-(bromomethyl)-3-(trifluoromethyl)benzene. Purification of 56% of crude by flash chromatography (69 mg, **3fA/4fA** ratio = 18.7:1, 79% yield). Injection of 29% of crude for semi-preparative SFC purification (injected volume: 250 μL , flow rate: 2 mL/min, mobile phase: CO_2 -modifier mixture with 20% of ethanol as modifier) afforded compound **3fA** as a white solid (32 mg, 73% yield). Purity >99%, tr = 2.61 min. ^1H NMR (300 MHz, CDCl_3) δ ppm: 7.72 (s, 1H), 7.53–7.50 (m, 1H), 7.45–7.37 (m, 4H), 7.27–7.23 (m, 2H), 7.22–7.18 (m, 2H) 5.57 (s, 2H). ^{13}C NMR (75 MHz, CDCl_3) δ ppm: 138.3, 136.4, 133.5, 131.3 (q, $J = 32.3$ Hz), 130.8, 129.9, 129.6, 129.2 (2C), 129.0 (2C), 126.7, 125.2 (q, $J = 3.4$ Hz), 124.4 (q, $J = 3.7$ Hz), 123.8 (q, $J = 272.4$ Hz), 51.4. HRMS (ESI+) m/z : $[\text{M} + \text{H}]^+$ calcd for $\text{C}_{16}\text{H}_{13}\text{N}_3\text{F}_3$ 304.1062; found 304.1064.

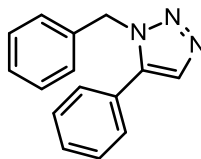
5-Phenyl-1-[[2-(trifluoromethyl)phenyl]methyl]triazole (**3gA**)



Compound **3gA** was synthesized according to the general procedure K, from ethynylbenzene (0.49 mmol) and 1-(bromomethyl)-2-(trifluoromethyl)benzene. Purification of 61% of crude by flash chromatography (62 mg, **3gA/4gA** ratio = 15.1:1, 64% yield). Injection of 26% of crude for semi-preparative SFC purification (injected volume: 250 μL , flow rate: 4 mL/min, mobile phase: CO_2 -modifier mixture with 5% of ethanol as modifier) afforded compound **3gA** as a colorless oil (12 mg, 31% yield). Purity >99%, tr = 2.31 min. ^1H NMR (300 MHz, CDCl_3) δ ppm: 7.84 (s, 1H), 7.69–7.66 (m, 1H), 7.49–7.44 (m, 1H), 7.44–7.33 (m, 4H), 7.22–7.18 (m, 2H), 6.77–6.75 (m, 1H) 5.79 (s, 2H). ^{13}C NMR (75 MHz, CDCl_3) δ ppm: 138.8, 134.5, 133.5, 132.7, 129.8, 129.2 (2C), 128.5 (2C), 128.2,

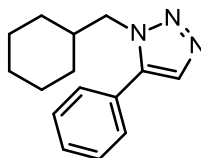
127.6, 127.2, 126.8, 126.3 (q, $J = 5.8$ Hz), 124.3 (q, $J = 273.8$ Hz), 48.4 (q, $J = 3.5$ Hz). HRMS (ESI+) m/z : $[M + H]^+$ calcd for $C_{16}H_{13}N_3F_3$ 304.1062; found 304.1065.

1-Benzyl-5-phenyl-triazole (3hA)



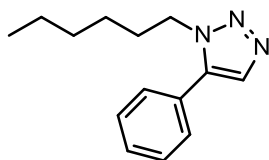
Compound **3hA** was synthesized according to the general procedure K, from ethynylbenzene (0.49 mmol) and bromomethylbenzene. Purification of 68% of crude by flash chromatography (21 mg, **3hA/4hA** ratio = 12.5:1, 25% yield). Injection of 21% of crude for semi-preparative SFC purification (injected volume: 250 μ L, flow rate: 2 mL/min, mobile phase: CO₂-modifier mixture with 20% of ethanol as modifier) afforded compound **3hA** as a pale brown solid (22 mg, 89% yield). Purity = 98%, $t_r = 3.96$ min. ¹H NMR (300 MHz, CDCl₃) δ ppm: 7.72 (s, 1H), 7.43–7.36 (m, 3H), 7.28–7.21 (m, 5H), 7.08–7.03 (m, 2H), 5.53 (s, 2H). ¹³C NMR (75 MHz, CDCl₃) δ ppm: 138.3, 135.6, 133.4, 129.6, 129.04 (2C), 128.97 (2C), 128.9 (2C), 128.2, 127.2 (2C), 127.0, 51.9. HRMS (ESI+) m/z : $[M + H]^+$ calcd for $C_{15}H_{20}N_3$ 236.1188; found 236.1190. The analytical data are in accordance with those reported in the literature.⁽¹⁴⁰⁾

1-(Cyclohexylmethyl)-5-phenyl-triazole (3iA)



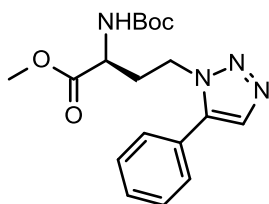
Compound **3iA** was synthesized according to the general procedure K, from ethynylbenzene (0.49 mmol) and bromomethylcyclohexane. Purification of 47% of crude by flash chromatography (40 mg, **3iA/4iA** ratio = 10.1:1, 65% yield). Injection of 35% of crude for semi-preparative SFC purification (injected volume: 250 μ L, flow rate: 4 mL/min, mobile phase: CO₂-modifier mixture with 10% of ethanol as modifier) afforded compound **3iA** as a pale brown solid (19 mg, 46% yield). Purity = 97%, $t_r = 2.89$ min. ¹H NMR (300 MHz, CDCl₃) δ ppm: 7.67 (s, 1H), 7.51–7.45 (m, 3H), 7.38–7.33 (m, 2H), 4.16 (d, $J = 7.4$ Hz, 2H), 1.95–1.80 (m, 1H), 1.68–1.56 (m, 3H), 1.56–1.46 (m, 2H), 1.21–1.03 (m, 3H), 0.90–0.78 (m, 2H). ¹³C NMR (75 MHz, CDCl₃) δ ppm: 138.3, 133.1, 129.4, 129.1 (2C), 129.0 (2C), 127.6, 54.3, 38.6, 30.5 (2C), 26.1, 25.6 (2C). HRMS (ESI+) m/z : $[M + H]^+$ calcd for $C_{15}H_{20}N_3$ 242.1657; found 242.1648.

1-Hexyl-5-phenyl-triazole (3jA)



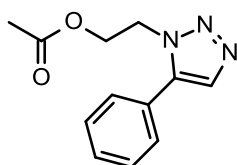
Compound **3jA** was synthesized according to the general procedure K, from ethynylbenzene (0.49 mmol) and bromomethylhexane. Purification of 70% of crude by flash chromatography (56 mg, **3jA/4jA** ratio = 15.4:1, 67% yield). Injection of 20% of crude for semi-preparative SFC purification (injected volume: 250 μ L, flow rate: 4 mL/min, mobile phase: CO₂-modifier mixture with 5% of ethanol as modifier) afforded compound **3jA** as a colorless oil (10 mg, 45% yield). Purity = 99%, *tr* = 2.29 min. ¹H NMR (300 MHz, CDCl₃) δ ppm: 7.68 (s, 1H), 7.52–7.46 (m, 3H), 7.40–7.35 (m, 2H), 4.33 (t, *J* = 7.2 Hz, 2H), 1.87–1.77 (m, 2H), 1.28–1.17 (m, 6H), 0.86–0.78 (m, 3H). ¹³C NMR (75 MHz, CDCl₃) δ ppm: 137.8, 133.2, 129.5, 129.2 (2C), 128.9 (2C), 127.5, 48.4, 31.2, 30.2, 26.2, 22.5, 14.0. HRMS (ESI+) *m/z*: [M + H]⁺ calcd for C₁₄H₂₀N₃ 230.1657; found 230.1659. The analytical data are in accordance with those reported in the literature.⁽¹⁴¹⁾

Methyl (2S)-2-(tert-butoxycarbonylamino)-4-(5-phenyltriazol-1-yl)butanoate (3kA)



Compound **3kA** was synthesized according to the general procedure K, from ethynylbenzene (0.29 mmol) and methyl (2S)-4-bromo-2-(tert-butoxycarbonylamino)butanoate. Purification of 49% of crude by flash chromatography (48 mg, **3kA/4kA** ratio = 22.5:1, 90% yield). Injection of 34% of crude for semi-preparative SFC purification (injected volume: 250 μ L, flow rate: 4 mL/min, mobile phase: CO₂-modifier mixture with 10% of ethanol as modifier) afforded compound **3kA** as a colorless oil (23 mg, 64% yield). Purity = 97%, *tr* = 3.10 min. ¹H NMR (300 MHz, CDCl₃) δ ppm: 7.68 (s, 1H), 7.52–7.46 (m, 3H), 7.40–7.35 (m, 2H), 5.79 (br d, *J* = 6.6 Hz, 1H), 4.44–4.39 (m, 2H), 4.37–4.28 (m, 1H), 3.66 (s, 3H), 2.52–2.41 (m, 1H), 2.33–2.21 (m, 1H), 1.40 (s, 9H). ¹³C NMR (75 MHz, CDCl₃) δ ppm: 171.9, 155.4, 138.1, 133.3, 129.7, 129.3 (2C), 128.9 (2C), 127.0, 80.4, 52.8, 51.3, 44.7, 32.8, 28.4 (3C). HRMS (ESI+) *m/z*: [M + H]⁺ calcd for C₁₈H₂₄N₄O₄ 361.1876; found 361.1877.

2-(5-Phenyltriazol-1-yl)ethyl acetate (3lA)



Compound **3IA** was synthesized according to the general procedure K, From ethynylbenzene (0.49 mmol) and 2-bromoethyl acetate. Purification of one crude by flash chromatography (81 mg, **3IA/4IA** ratio = 4.2:1, 58% yield). Injection of 67% of the other crude for semi-preparative SFC purification (injected volume: 100 μ L, flow rate: 6 mL/min, mobile phase: CO₂-modifier mixture with 5% of ethanol as modifier) afforded compound **3IA** as a yellow oil (12 mg, 16% yield). Purity = 96%, tr = 2.67 min. ¹H NMR (300 MHz, CDCl₃) δ ppm: 7.72 (s, 1H), 7.53–7.48 (m, 3H), 7.44–7.40 (m, 2H), 4.62 (t, *J* = 5.4 Hz, 2H), 4.44 (t, *J* = 5.4 Hz, 2H), 1.89 (s, 3H). ¹³C NMR (75 MHz, CDCl₃) δ ppm: 170.5, 138.7, 133.4, 129.8, 129.3 (2C), 129.0 (2C), 127.0, 62.5, 47.0, 20.6. HRMS (ESI+) *m/z*: [M + H]⁺ calcd for C₁₂H₁₄N₃O₃ 232.1086; found 232.1085.

II. Biology

General protocole for Kinetic Target-guided synthesis:

Three experiments were performed, one in presence of the target enzyme, one without the target enzyme (only with the buffer solution, azides and alkynes = “blank” plate) and one using copper catalysis for the formation of the 1,4-disubstituted 1,2,3-triazoles which were used as controls (“chemical catalysis” plate).

In a 96-well plate, were mixed 0.5 μ L of azide solution (10.2 mM), 0.5 μ L of a given mixture of alkynes solution (each alkyne at 10.2 mM) and 50 μ L of the enzyme (1.02 μ M for ERAP2, 4.08 μ M for LasB) in a buffer solution (Hepes.NaCl for ERAP2, 50 mM Tris + 2.5 mM CaCl₂ for LasB, pH = 7.4). The 96-well plate was sealed and shaken at 37°C for 7 days for ERAP2 experiment and 6 days for LasB experiment. For the copper catalysis plate, the enzyme solution was replaced by a mixture of *t*-BuOH/H₂O (1/1, 49 μ L), 0.5 μ L of a copper sulfate solution (5.1 mM) and 0.5 μ L of a sodium ascorbate (51 mM).

Samples of the reactions (15 μ L) were diluted in MeOH (15 μ L) and injected for UPLC–MS–MS analysis using a multi MRM-method (after 3 and 7 days for ERAP2, 3 and 6 days for LasB). The hits were identified in each cluster by mass and retention time and compared to both incubation with buffer in place of the enzyme (blank plate) and synthetically prepared triazoles obtained in mixtures (chemical catalysis plate). An additional analysis by LC–HRMS using a time of flight method was performed to search for the exact mass (*m/z* +/- 10 ppm) of the expected triazoles and therefore refine the hits selection.

Solubility assay (compounds of the chapter 2):

5.0 μ L of the compound (10mM solution in DMSO) is mixed with 245.0 μ L of PBS pH 7.4 (in triplicate) or to 245.0 μ L of MeOH (triplicate*2). The tubes are shaken for 24 hours at room temperature. The solutions are centrifuged (4000 rpm, 5 min) and filtered (except three of the 6

'MeOH' tubes). Then, 10.0 μ L of each solution is diluted in 490 μ L of methanol before LC-MS/MS analysis.

LogD determination assay (compounds of the chapter 2):

20.0 μ L of the compound (in 10mM solution in DMSO) is mixed with 980.0 μ L of a noctanol (pre-saturated with PBS) / PBS pH 7.4 (pre-saturated with n-octanol) mixture, in a 1:1 ratio. The tubes are shaken for 2h at room temperature. Then, 20.0 μ L of each phase is diluted in 480.0 μ L of diluted in 480.0 μ L of methanol before LC-MS/MS analysis. Each compound is tested in triplicate.

Kinetic Turbidimetric solubility assay (compounds of the chapter 3):

The desired compounds were sequentially diluted in DMSO in a 96-well plate. 1.5 μ L of each well were transferred into another 96-well plate and mixed with 148.5 μ L of PBS. Plates were shaken for 5 min at 600 rpm at room temperature, and the absorbance at 620 nm was measured. Absorbance values were normalized by blank subtraction and plotted using GraphPad Prism 8.4.2 (GraphPad Software, San Diego, CA, USA). Solubility (S) was determined based on the First X value of AUC function using a threshold of 0.005.

Metabolic stability in Mouse Liver S9 Fraction assay:

For the evaluation of combined phase I and phase II metabolic stability, the compound (1 μ M) was incubated with 1 mg/mL pooled liver S9 fraction (Xenotech), 2 mM NADPH, 1 mM UDPGA, 10 mM MgCl₂, 5 mM GSH and 0.1 mM PAPS at 37 °C for 0, 5, 15, 30 and 60 min. The metabolic stability of Testosterone (1 μ M), verapamil (1 μ M) and ketoconazol (1 μ M) were determined in parallel to confirm the enzymatic activity of the S9 fraction. The incubation was stopped by precipitation of S9 enzymes with 2 volumes of cold acetonitrile containing internal standard (150 nM Diphenhydramine). Samples were stored on ice for 10 min and precipitated protein was removed by centrifugation (15 min, 4°C, 4,000 rpm). The remaining test compound at different time points was analyzed by LC-MS/MS (TSQ Quantum Access MAX, Thermo Fisher, Dreieich, Germany) and used to determine half-life (t_{1/2}).

In vitro ERAP2, ERAP1 and IRAP activity assay (compounds of the chapter 2):

ERAP2 was prepared as previously described.⁽¹⁴²⁾

The enzymatic activity of ERAP2 was assayed using R-AMC (L-Arginine-7-amido-4-methylcoumarin hydrochloride, Sigma). Hepes at 50 mM with 100 mM NaCl at pH 7 was used as buffer. Briefly, 60 nL of test compounds were added in 384-wells plates (dark, non-binding surface) by acoustic dispensing with Echo (Labcyte) and preincubated 30 min at ambient temperature with 10 μ L of ERAP2 1 mg/mL or vehicle. The reaction was then started with the addition of 10 μ L of substrate at 10 mM. The final concentration of ERAP2, substrate and DMSO was 0.5 mg/mL, 5 mM and 0.4% respectively. For the kinetic readout a Victor 3V (PerkinElmer) was used with excitation at 380 nm and emission at 450 nm. The fluorescence was measured each 3 min during 1 h.

In vitro ERAP1 and IRAP activity assays were performed as for ERAP2 using L-AMC (L-Leucine-7-Amido-4-Methylcoumarin, from Sigma) as the substrate, recombinant human ERAP1 (PILS/ARTS1 from R&D Systems, ref 2334-ZN-010) at 0.8 mg/mL final concentration or recombinant human IRAP (prepared as previously described)⁽¹⁴³⁾ at 0.2 mg/mL final concentration respectively.

All measurements were carried out as 8-point dose response curves and reported as the average of at least three independent measurements. Bestatin was used as a reference inhibitor (100% inhibition at 2 mM). Data analysis was performed using Xlfit® v 5.0 or GraphPad Prism® v 4.0. Nonlinear curve fitting and statistical analysis was done using built-in functions.

In vitro LasB activity assay (compounds of the chapter 3):

The LasB activity assay was performed as described previously⁽¹²³⁾ using the fluorogenic substrate 2-Aminobenzoyl-Ala-GlyLeu-Ala-4 Nitrobenzylamide, purchased from Peptides International (Louisville, KY, USA).

Fluorescence intensity was measured for 60 min at 37 °C in black 384-well microtiter plates (Greiner BioOne, Kremsmünster, Austria) using a CLARIOstar microplate reader (BMG Labtech, Ortenberg, Germany) with an excitation wavelength of 340 ± 15 nm and an emission wavelength of 415 ± 20 nm. The assay was performed in a final volume of 50 μ L of assay buffer (50 mM Tris, pH 7.2, 2.5 mM CaCl_2 , 0.075% Pluronic F-127, 5% DMSO) containing LasB at a final concentration of 10 nM (commercial batch, from Merck or Elastin Products Company) or 0.3 nM (purified batch) and the substrate at 150 μ M. Before substrate addition, compounds were preincubated with the enzyme for 15 min at 37 °C. Experiments were performed in duplicates and repeated for at least two times. Blank controls without enzyme were performed. After blank subtraction, the slope of samples containing inhibitors (v) was divided by the slope of a simultaneously started uninhibited enzymatic reaction (v0). IC50 values were determined with nonlinear regression using GraphPad Prism 5 (Graph Pad Software, San Diego, CA, USA) and are given as mean values \pm standard deviation (SD). The slope factor was constrained to 1.

MIC determination assay (compounds of the chapter 3):

Assays regarding the determination of the minimum inhibitory concentration (MIC) were performed as described previously.⁽¹⁴⁴⁾ The experiments were based on the *P. aeruginosa* strain PA14. For the case that no MIC value could be determined due to activity reasons, percentage (%) inhibition at 100 μ M (or lower, depending on the solubility of the compounds) was calculated. The OD at 600 nm was measured 16 h after inhibitor addition in a CLARIOstar Platereader (BMG Labtech, Ortenberg, Germany).

Selectivity assay:

➤ MMPs inhibition

MMP -1, -2, -3, -7, -8 and -14 Inhibitor Screening Assay kits were purchased from AnaSpec

(Fremont, CA, USA). The assay was performed as described previously⁽¹⁴⁵⁾ using batimastat as a positive control according to the guidelines of the manufacturer.

➤ HDACs inhibition

HDAC3 and HDAC8 Inhibitor Screening Assay kits were purchased from Sigma-Aldrich. The assay was performed according to the guidelines of the manufacturer using trichostatin. Fluorescence signals were measured in a CLARIOstar plate reader (BMG Labtech).

➤ TACE

ADAM-17 (TACE) Inhibitor Screening Assay Kit was purchased from Sigma-Aldrich. The assay was performed according to the guidelines of the manufacturer using ilomastat as a positive control. Fluorescence signals were measured in a CLARIOstar plate reader (BMG Labtech).

➤ COX-1

COX-1 Inhibitor Screening Assay Kit was purchased from Abcam. The assay was performed according to the guidelines of the manufacturer. Fluorescence signals were measured in a CLARIOstar plate reader (BMG Labtech).

Cytotoxicity assay (compounds of the chapter 3):

Hep G2, HEK293 or A549 cells (2×10^5 cells per well) were seeded in 24-well, flat-bottomed plates. Culturing of cells, incubations, and OD measurements were performed as described previously (Int. J. Cancer 2007, 121, 206–210). Twenty-four hours after seeding the cells, the incubation was started by the addition of test compound in a final DMSO concentration of 1%. The living cell mass was determined after 48 h. At least two independent measurements were performed for each compound.

References

1. Chen AY, Adamek RN, Dick BL, Credille CV, Morrison CN, Cohen SM. Targeting Metalloenzymes for Therapeutic Intervention. *Chem Rev.* 2019 Jan 23;119(2):1323–455.
2. Schaal JB, Marezky T, Tran DQ, Tran PA, Tongaonkar P, Blobel CP, et al. Macrocyclic θ -defensins suppress tumor necrosis factor- α (TNF- α) shedding by inhibition of TNF- α -converting enzyme. *J Biol Chem.* 2018 Feb 23;293(8):2725–34.
3. Boyd SE, Livermore DM, Hooper DC, Hope WW. Metallo- β -Lactamases: Structure, Function, Epidemiology, Treatment Options, and the Development Pipeline. *Antimicrob Agents Chemother.* 2020 Sep 21;64(10):e00397-20.
4. Deprez-Poulain R, Hennuyer N, Bosc D, Liang WG, Enée E, Marechal X, et al. Catalytic site inhibition of insulin-degrading enzyme by a small molecule induces glucose intolerance in mice. *Nat Commun.* 2015 Sep 23;6:8250.
5. Kany AM, Sikandar A, Haupenthal J, Yahiaoui S, Maurer CK, Proschak E, et al. Binding Mode Characterization and Early in Vivo Evaluation of Fragment-Like Thiols as Inhibitors of the Virulence Factor LasB from *Pseudomonas aeruginosa*. *ACS Infect Dis.* 2018 Jun 8;4(6):988–97.
6. Kany AM, Sikandar A, Yahiaoui S, Haupenthal J, Walter I, Empting M, et al. Tackling *Pseudomonas aeruginosa* Virulence by a Hydroxamic Acid-Based LasB Inhibitor. *ACS Chem Biol.* 2018 Sep 21;13(9):2449–55.
7. Konstantinović J, Yahiaoui S, Alhayek A, Haupenthal J, Schönauer E, Andreas A, et al. N-Aryl-3-mercaptosuccinimides as Antivirulence Agents Targeting *Pseudomonas aeruginosa* Elastase and *Clostridium* Collagenases. *J Med Chem.* 2020 Aug 13;63(15):8359–68.
8. Jaegle M, Wong EL, Tauber C, Nawrotzky E, Arkona C, Rademann J. Protein-Templated Fragment Ligations-From Molecular Recognition to Drug Discovery. *Angew Chem Int Ed Engl.* 2017 Jun 19;56(26):7358–78.
9. Bosc D, Jakhlal J, Deprez B, Deprez-Poulain R. Kinetic target-guided synthesis in drug discovery and chemical biology: a comprehensive facts and figures survey. *Future Med Chem.* 2016;8(4):381–404.
10. Cheeseman JD, Corbett AD, Gleason JL, Kazlauskas RJ. Receptor-assisted combinatorial chemistry: thermodynamics and kinetics in drug discovery. *Chem Weinh Bergstr Ger.* 2005 Mar 4;11(6):1708–16.
11. Hartman AM, Gierse RM, Hirsch AKH. Protein-Templated Dynamic Combinatorial Chemistry: Brief Overview and Experimental Protocol. *Eur J Org Chem.* 2019 Jun 16;2019(22):3581–90.
12. Frei P, Hevey R, Ernst B. Dynamic Combinatorial Chemistry: A New Methodology Comes of Age. *Chem Weinh Bergstr Ger.* 2019 Jan 2;25(1):60–73.
13. Bosc D, Camberlein V, Gealageas R, Castillo-Aguilera O, Deprez B, Deprez-Poulain R. Kinetic Target-Guided Synthesis: Reaching the Age of Maturity. *J Med Chem.* 2020 Apr 23;63(8):3817–33.

14. Nguyen R, Huc I. Using an Enzyme's Active Site To Template Inhibitors This work was supported by the Centre National de la Recherche Scientifique and by the Ecole Polytechnique (predoctoral fellowship to R.N.). We thank Prof. Jean-Marie Lehn for stimulating discussions. *Angew Chem Int Ed Engl.* 2001 May 4;40(9):1774–6.
15. Inglese J, Benkovic SJ. Multisubstrate adduct inhibitors of glycinamide ribonucleotide transformylase: Synthetic and enzyme-assembled. *Tetrahedron.* 1991 Jan 1;47(14):2351–64.
16. Lewis WG, Green LG, Grynszpan F, Radić Z, Carlier PR, Taylor P, et al. Click chemistry in situ: acetylcholinesterase as a reaction vessel for the selective assembly of a femtomolar inhibitor from an array of building blocks. *Angew Chem Int Ed Engl.* 2002 Mar 15;41(6):1053–7.
17. Kulkarni SS, Hu X, Doi K, Wang H-G, Manetsch R. Screening of protein-protein interaction modulators via sulfo-click kinetic target-guided synthesis. *ACS Chem Biol.* 2011 Jul 15;6(7):724–32.
18. Oueis E, Nachon F, Sabot C, Renard P-Y. First enzymatic hydrolysis/thio-Michael addition cascade route to synthesis of AChE inhibitors. *Chem Commun Camb Engl.* 2014 Feb 25;50(16):2043–5.
19. Jaegle M, Steinmetzer T, Rademann J. Protein-Templated Formation of an Inhibitor of the Blood Coagulation Factor Xa through a Background-Free Amidation Reaction. *Angew Chem Int Ed Engl.* 2017 Mar 20;56(13):3718–22.
20. Wong EL, Nawrotzky E, Arkona C, Kim BG, Beligny S, Wang X, et al. The transcription factor STAT5 catalyzes Mannich ligation reactions yielding inhibitors of leukemic cell proliferation. *Nat Commun.* 2019 Jan 8;10(1):66.
21. Mancini F, Unver MY, Elgaher WAM, Jumde VR, Alhayek A, Lukat P, et al. Protein-Templated Hit Identification through an Ugi Four-Component Reaction*. *Chem Weinh Bergstr Ger.* 2020 Nov 17;26(64):14585–93.
22. Congreve M, Carr R, Murray C, Jhoti H. A 'rule of three' for fragment-based lead discovery? *Drug Discov Today.* 2003 Oct 1;8(19):876–7.
23. Krasieński A, Radić Z, Manetsch R, Raushel J, Taylor P, Sharpless KB, et al. In situ selection of lead compounds by click chemistry: target-guided optimization of acetylcholinesterase inhibitors. *J Am Chem Soc.* 2005 May 11;127(18):6686–92.
24. Unver MY, Gierse RM, Ritchie H, Hirsch AKH. Druggability Assessment of Targets Used in Kinetic Target-Guided Synthesis. *J Med Chem.* 2018 Nov 8;61(21):9395–409.
25. Willand N, Desroses M, Toto P, Dirie B, Lens Z, Villeret V, et al. Exploring drug target flexibility using in situ click chemistry: application to a mycobacterial transcriptional regulator. *ACS Chem Biol.* 2010 Nov 19;5(11):1007–13.
26. Pollastri MP. Overview on the Rule of Five. *Curr Protoc Pharmacol.* 2010 Jun;Chapter 9:Unit 9.12.
27. Doak BC, Zheng J, Dobritzsch D, Kihlberg J. How Beyond Rule of 5 Drugs and Clinical Candidates Bind to Their Targets. *J Med Chem.* 2016 Mar 24;59(6):2312–27.

28. Mondal M, Unver MY, Pal A, Bakker M, Berrier SP, Hirsch AKH. Fragment-Based Drug Design Facilitated by Protein-Templated Click Chemistry: Fragment Linking and Optimization of Inhibitors of the Aspartic Protease Endothiapepsin. *Chem Weinh Bergstr Ger*. 2016 Oct 10;22(42):14826–30.
29. Köster H, Craan T, Brass S, Herhaus C, Zentgraf M, Neumann L, et al. A small nonrule of 3 compatible fragment library provides high hit rate of endothiapepsin crystal structures with various fragment chemotypes. *J Med Chem*. 2011 Nov 24;54(22):7784–96.
30. Riera Romo M, Pérez-Martínez D, Castillo Ferrer C. Innate immunity in vertebrates: an overview. *Immunology*. 2016 Jun;148(2):125–39.
31. Paludan SR, Pradeu T, Masters SL, Mogensen TH. Constitutive immune mechanisms: mediators of host defence and immune regulation. *Nat Rev Immunol*. 2020 Aug 11;1–14.
32. Jain A, Pasare C. Innate control of adaptive immunity: Beyond the three-signal paradigm. *J Immunol Baltim Md 1950*. 2017 May 15;198(10):3791–800.
33. Turvey SE, Broide DH. Innate immunity. *J Allergy Clin Immunol*. 2010 Feb;125(2 Suppl 2):S24–32.
34. Biedermann T, Röcken M, Carballido JM. TH1 and TH2 lymphocyte development and regulation of TH cell-mediated immune responses of the skin. *J Investig Dermatol Symp Proc*. 2004 Jan;9(1):5–14.
35. Zhang N, Bevan MJ. CD8(+) T cells: foot soldiers of the immune system. *Immunity*. 2011 Aug 26;35(2):161–8.
36. Shapiro-Shelef M, Lin K-I, McHeyzer-Williams LJ, Liao J, McHeyzer-Williams MG, Calame K. Blimp-1 is required for the formation of immunoglobulin secreting plasma cells and pre-plasma memory B cells. *Immunity*. 2003 Oct;19(4):607–20.
37. Choo SY. The HLA system: genetics, immunology, clinical testing, and clinical implications. *Yonsei Med J*. 2007 Feb 28;48(1):11–23.
38. Kisselev AF, Akopian TN, Woo KM, Goldberg AL. The sizes of peptides generated from protein by mammalian 26 and 20 S proteasomes. Implications for understanding the degradative mechanism and antigen presentation. *J Biol Chem*. 1999 Feb 5;274(6):3363–71.
39. Falk K, Rötzschke O, Stevanović S, Jung G, Rammensee HG. Allele-specific motifs revealed by sequencing of self-peptides eluted from MHC molecules. *Nature*. 1991 May 23;351(6324):290–6.
40. Serwold T, Gonzalez F, Kim J, Jacob R, Shastri N. ERAAP customizes peptides for MHC class I molecules in the endoplasmic reticulum. *Nature*. 2002 Oct 3;419(6906):480–3.
41. Vitulano C, Tedeschi V, Paladini F, Sorrentino R, Fiorillo MT. The interplay between HLA-B27 and ERAP1/ERAP2 aminopeptidases: from anti-viral protection to spondyloarthritis. *Clin Exp Immunol*. 2017 Dec;190(3):281–90.
42. de Castro JAL, Stratikos E. Intracellular antigen processing by ERAP2: Molecular mechanism and roles in health and disease. *Hum Immunol*. 2019 May;80(5):310–7.

43. Peng G, McEwen AG, Olieric V, Schmitt C, Albrecht S, Cavarelli J, et al. Insight into the remarkable affinity and selectivity of the aminobenzosuberone scaffold for the M1 aminopeptidases family based on structure analysis. *Proteins*. 2017 Aug;85(8):1413–21.
44. Babaie F, Hosseinzadeh R, Ebrazeh M, Seyfizadeh N, Aslani S, Salimi S, et al. The roles of ERAP1 and ERAP2 in autoimmunity and cancer immunity: New insights and perspective. *Mol Immunol*. 2020 May;121:7–19.
45. Wang J, Cooper MD. Histidine residue in the zinc-binding motif of aminopeptidase A is critical for enzymatic activity. *Proc Natl Acad Sci U S A*. 1993 Feb 15;90(4):1222–6.
46. Vazeux G, Wang J, Corvol P, Llorens-Cortès C. Identification of glutamate residues essential for catalytic activity and zinc coordination in aminopeptidase A. *J Biol Chem*. 1996 Apr 12;271(15):9069–74.
47. Hermant P. Endoplasmic Reticulum AminoPeptidase 1 & 2: Cibles thérapeutiques émergentes pour lamodulation de la présentation antigénique. 2016.
48. Vazeux G, Iturrioz X, Corvol P, Llorens-Cortés C. A glutamate residue contributes to the exopeptidase specificity in aminopeptidase A. *Biochem J*. 1998 Sep 1;334 (Pt 2):407–13.
49. Addlagatta A, Gay L, Matthews BW. Structure of aminopeptidase N from *Escherichia coli* suggests a compartmentalized, gated active site. *Proc Natl Acad Sci U S A*. 2006 Sep 5;103(36):13339–44.
50. Chang S-C, Momburg F, Bhutani N, Goldberg AL. The ER aminopeptidase, ERAP1, trims precursors to lengths of MHC class I peptides by a ‘molecular ruler’ mechanism. *Proc Natl Acad Sci U S A*. 2005 Nov 22;102(47):17107–12.
51. Mpakali A, Giastas P, Mathioudakis N, Mavridis IM, Saridakis E, Stratikos E. Structural Basis for Antigenic Peptide Recognition and Processing by Endoplasmic Reticulum (ER) Aminopeptidase 2. *J Biol Chem*. 2015 Oct 23;290(43):26021–32.
52. Haroon N, Inman RD. Endoplasmic reticulum aminopeptidases: biology and pathogenic potential. *Nat Rev Rheumatol*. 2010 Aug;6(8):461–7.
53. Stratikos E, Stamogiannos A, Zervoudi E, Fruci D. A role for naturally occurring alleles of endoplasmic reticulum aminopeptidases in tumor immunity and cancer pre-disposition. *Front Oncol*. 2014;4:363.
54. Compagnone M, Cifaldi L, Fruci D. Regulation of ERAP1 and ERAP2 genes and their dysfunction in human cancer. *Hum Immunol*. 2019 May;80(5):318–24.
55. Kuo I-C, Kao H-K, Huang Y, Wang C-I, Yi J-S, Liang Y, et al. Endoplasmic reticulum aminopeptidase 2 involvement in metastasis of oral cavity squamous cell carcinoma discovered by proteome profiling of primary cancer cells. *Oncotarget*. 2017 Sep 22;8(37):61698–708.
56. Cifaldi L, Lo Monaco E, Forloni M, Giorda E, Lorenzi S, Petrini S, et al. Natural killer cells efficiently reject lymphoma silenced for the endoplasmic reticulum aminopeptidase associated with antigen processing. *Cancer Res*. 2011 Mar 1;71(5):1597–606.

57. Lim YW, Chen-Harris H, Mayba O, Lianoglou S, Wuster A, Bhangale T, et al. Germline genetic polymorphisms influence tumor gene expression and immune cell infiltration. *Proc Natl Acad Sci U S A*. 2018 Dec 11;115(50):E11701–10.
58. Evans DM, Spencer CCA, Pointon JJ, Su Z, Harvey D, Kochan G, et al. Interaction between ERAP1 and HLA-B27 in ankylosing spondylitis implicates peptide handling in the mechanism for HLA-B27 in disease susceptibility. *Nat Genet*. 2011 Jul 10;43(8):761–7.
59. Kirino Y, Bertias G, Ishigatsubo Y, Mizuki N, Tugal-Tutkun I, Seyahi E, et al. Genome-wide association analysis identifies new susceptibility loci for Behçet’s disease and epistasis between HLA-B*51 and ERAP1. *Nat Genet*. 2013 Feb;45(2):202–7.
60. Kuiper JJW, Van Setten J, Ripke S, Van ’T Slot R, Mulder F, Missotten T, et al. A genome-wide association study identifies a functional ERAP2 haplotype associated with birdshot chorioretinopathy. *Hum Mol Genet*. 2014 Nov 15;23(22):6081–7.
61. Wong AHM, Zhou D, Rini JM. The X-ray crystal structure of human aminopeptidase N reveals a novel dimer and the basis for peptide processing. *J Biol Chem*. 2012 Oct 26;287(44):36804–13.
62. Papakyriakou A, Zervoudi E, Theodorakis EA, Saveanu L, Stratikos E, Vourloumis D. Novel selective inhibitors of aminopeptidases that generate antigenic peptides. *Bioorg Med Chem Lett*. 2013 Sep 1;23(17):4832–6.
63. Zervoudi E, Saridakis E, Birtley JR, Seregin SS, Reeves E, Kokkala P, et al. Rationally designed inhibitor targeting antigen-trimming aminopeptidases enhances antigen presentation and cytotoxic T-cell responses. *Proc Natl Acad Sci U S A*. 2013 Dec 3;110(49):19890–5.
64. Zervoudi E, Papakyriakou A, Georgiadou D, Evnouchidou I, Gajda A, Poreba M, et al. Probing the S1 specificity pocket of the aminopeptidases that generate antigenic peptides. *Biochem J*. 2011 Apr 15;435(2):411–20.
65. Laura M, Ronan G, Vy LB, Valentin G, Omar C-A, Virgyl C, et al. Modulators of hERAP2 discovered by high-throughput screening. *Eur J Med Chem*. 2021 Feb 5;211:113053.
66. Gupta SP. QSAR studies on hydroxamic acids: a fascinating family of chemicals with a wide spectrum of activities. *Chem Rev*. 2015 Jul 8;115(13):6427–90.
67. Harris JL, Backes BJ, Leonetti F, Mahrus S, Ellman JA, Craik CS. Rapid and general profiling of protease specificity by using combinatorial fluorogenic substrate libraries. *Proc Natl Acad Sci U S A*. 2000 Jul 5;97(14):7754–9.
68. Balducci E, Bellucci L, Petricci E, Taddei M, Tafi A. Microwave-assisted intramolecular Huisgen cycloaddition of azido alkynes derived from alpha-amino acids. *J Org Chem*. 2009 Feb 6;74(3):1314–21.
69. European Food Safety Authority, European Centre for Disease Prevention and Control. The European Union Summary Report on Antimicrobial Resistance in zoonotic and indicator bacteria from humans, animals and food in 2018/2019. *EFSA J Eur Food Saf Auth*. 2021 Apr;19(4):e06490.
70. European Centre for Disease Prevention and Control. Antimicrobial resistance in the EU/EEA (EARS-Net) - Annual Epidemiological Report 2019. Stockholm: ECDC; 2020. 2020.

71. Antimicrobial resistance in the EU/EEA (EARS-Net) - Annual Epidemiological Report for 2019 [Internet]. European Centre for Disease Prevention and Control. 2020 [cited 2021 Oct 11]. Available from: <https://www.ecdc.europa.eu/en/publications-data/surveillance-antimicrobial-resistance-europe-2019>
72. O'Neill J. Antimicrobial Resistance:Tackling a crisis for the health and wealth of nations. 2014.
73. Moradali MF, Ghods S, Rehm BHA. *Pseudomonas aeruginosa* Lifestyle: A Paradigm for Adaptation, Survival, and Persistence. *Front Cell Infect Microbiol*. 2017;7:39.
74. Ramphal R, Vishwanath S. Why is *Pseudomonas* the colonizer and why does it persist? *Infection*. 1987 Aug;15(4):281–7.
75. European Cystic Fibrosis Society Patient Registry Annual Reports 2017 [Internet]. Available from: <https://www.ecfs.eu/projects/ecfs-patient-registry/annual-reports>
76. Cystic Fibrosis Foundation Patient Registry Annual Report 2019 [Internet]. 2019. Available from: <https://www.cff.org/>
77. Balasubramanian D, Schneper L, Kumari H, Mathee K. A dynamic and intricate regulatory network determines *Pseudomonas aeruginosa* virulence. *Nucleic Acids Res*. 2013 Jan 7;41(1):1–20.
78. LaSarre B, Federle MJ. Exploiting quorum sensing to confuse bacterial pathogens. *Microbiol Mol Biol Rev MMBR*. 2013 Mar;77(1):73–111.
79. Lee J, Zhang L. The hierarchy quorum sensing network in *Pseudomonas aeruginosa*. *Protein Cell*. 2015 Jan;6(1):26–41.
80. Everett MJ, Davies DT. *Pseudomonas aeruginosa* elastase (LasB) as a therapeutic target. *Drug Discov Today*. 2021 Sep;26(9):2108–23.
81. Yang J, Zhao H-L, Ran L-Y, Li C-Y, Zhang X-Y, Su H-N, et al. Mechanistic insights into elastin degradation by pseudolysin, the major virulence factor of the opportunistic pathogen *Pseudomonas aeruginosa*. *Sci Rep*. 2015 Apr 23;5:9936.
82. Heck LW, Morihara K, Abrahamson DR. Degradation of soluble laminin and depletion of tissue-associated basement membrane laminin by *Pseudomonas aeruginosa* elastase and alkaline protease. *Infect Immun*. 1986 Oct;54(1):149–53.
83. Beaufort N, Corvazier E, Hervieu A, Choqueux C, Dussiot M, Louedec L, et al. The thermolysin-like metalloproteinase and virulence factor LasB from pathogenic *Pseudomonas aeruginosa* induces anoikis of human vascular cells. *Cell Microbiol*. 2011 Aug;13(8):1149–67.
84. Beaufort N, Corvazier E, Mlanaoindrou S, de Bentzmann S, Pidard D. Disruption of the endothelial barrier by proteases from the bacterial pathogen *Pseudomonas aeruginosa*: implication of matrilysin and receptor cleavage. *PLoS One*. 2013;8(9):e75708.
85. Diebel LN, Liberati DM, Amin PB, Diglio CA. Cleavage of SIgA by gram negative respiratory pathogens enhance neutrophil inflammatory potential. *J Trauma*. 2009 May;66(5):1336–42; discussion 1342.

86. Krylov VN, Smirnova TA, Minenkova IB, Plotnikova TG, Zhazikov IZ, Khrenova EA. Pseudomonas bacteriophage contains an inner body in its capsid. *Can J Microbiol.* 1984 Jun 1;30(6):758–62.
87. Parmely M, Gale A, Clabaugh M, Horvat R, Zhou WW. Proteolytic inactivation of cytokines by *Pseudomonas aeruginosa*. *Infect Immun.* 1990 Sep;58(9):3009–14.
88. Pedersen BK, Kharazmi A, Theander TG, Odum N, Andersen V, Bendtzen K. Selective modulation of the CD4 molecular complex by *Pseudomonas aeruginosa* alkaline protease and elastase. *Scand J Immunol.* 1987 Jul;26(1):91–4.
89. Sun J, LaRock DL, Skowronski EA, Kimmey JM, Olson J, Jiang Z, et al. The *Pseudomonas aeruginosa* protease LasB directly activates IL-1 β . *EBioMedicine.* 2020 Oct;60:102984.
90. Theander TG, Kharazmi A, Pedersen BK, Christensen LD, Tvede N, Poulsen LK, et al. Inhibition of human lymphocyte proliferation and cleavage of interleukin-2 by *Pseudomonas aeruginosa* proteases. *Infect Immun.* 1988 Jul;56(7):1673–7.
91. Matheson NR, Potempa J, Travis J. Interaction of a novel form of *Pseudomonas aeruginosa* alkaline protease (aeruginolysin) with interleukin-6 and interleukin-8. *Biol Chem.* 2006 Jul;387(7):911–5.
92. Leidal KG, Munson KL, Johnson MC, Denning GM. Metalloproteases from *Pseudomonas aeruginosa* degrade human RANTES, MCP-1, and ENA-78. *J Interferon Cytokine Res Off J Int Soc Interferon Cytokine Res.* 2003 Jun;23(6):307–18.
93. Schultz DR, Miller KD. Elastase of *Pseudomonas aeruginosa*: inactivation of complement components and complement-derived chemotactic and phagocytic factors. *Infect Immun.* 1974 Jul;10(1):128–35.
94. Kuang Z, Hao Y, Walling BE, Jeffries JL, Ohman DE, Lau GW. *Pseudomonas aeruginosa* elastase provides an escape from phagocytosis by degrading the pulmonary surfactant protein-A. *PloS One.* 2011;6(11):e27091.
95. Alcorn JF, Wright JR. Degradation of pulmonary surfactant protein D by *Pseudomonas aeruginosa* elastase abrogates innate immune function. *J Biol Chem.* 2004 Jul 16;279(29):30871–9.
96. Schmidtchen A, Frick I-M, Andersson E, Tapper H, Björck L. Proteinases of common pathogenic bacteria degrade and inactivate the antibacterial peptide LL-37. *Mol Microbiol.* 2002 Oct;46(1):157–68.
97. Morihara K, Tsuzuki H, Oda K. Protease and elastase of *Pseudomonas aeruginosa*: inactivation of human plasma alpha 1-proteinase inhibitor. *Infect Immun.* 1979 Apr;24(1):188–93.
98. Cosgrove S, Chotirmall SH, Greene CM, McElvaney NG. Pulmonary proteases in the cystic fibrosis lung induce interleukin 8 expression from bronchial epithelial cells via a heme/meprip/epidermal growth factor receptor/Toll-like receptor pathway. *J Biol Chem.* 2011 Mar 4;286(9):7692–704.
99. Britigan BE, Hayek MB, Doebbeling BN, Fick RB. Transferrin and lactoferrin undergo proteolytic cleavage in the *Pseudomonas aeruginosa*-infected lungs of patients with cystic fibrosis. *Infect Immun.* 1993 Dec;61(12):5049–55.

100. Miller RA, Rasmussen GT, Cox CD, Britigan BE. Protease cleavage of iron-transferrin augments pyocyanin-mediated endothelial cell injury via promotion of hydroxyl radical formation. *Infect Immun*. 1996 Jan;64(1):182–8.
101. Komori Y, Nonogaki T, Nikai T. Hemorrhagic activity and muscle damaging effect of *Pseudomonas aeruginosa* metalloproteinase (elastase). *Toxicol Off J Int Soc Toxicology*. 2001 Sep;39(9):1327–32.
102. van der Plas MJA, Bhongir RKV, Kjellström S, Siller H, Kassetty G, Mörgelin M, et al. *Pseudomonas aeruginosa* elastase cleaves a C-terminal peptide from human thrombin that inhibits host inflammatory responses. *Nat Commun*. 2016 May 16;7:11567.
103. Okamoto T, Akaike T, Suga M, Tanase S, Horie H, Miyajima S, et al. Activation of human matrix metalloproteinases by various bacterial proteinases. *J Biol Chem*. 1997 Feb 28;272(9):6059–66.
104. Cowell BA, Twining SS, Hobden JA, Kwong MSF, Fleiszig SMJ. Mutation of *lasA* and *lasB* reduces *Pseudomonas aeruginosa* invasion of epithelial cells. *Microbiol Read Engl*. 2003 Aug;149(Pt 8):2291–9.
105. Casilag F, Lorenz A, Krueger J, Klawonn F, Weiss S, Häussler S. The *LasB* Elastase of *Pseudomonas aeruginosa* Acts in Concert with Alkaline Protease *AprA* To Prevent Flagellin-Mediated Immune Recognition. *Infect Immun*. 2016 Jan;84(1):162–71.
106. Kamath S, Kapatral V, Chakrabarty AM. Cellular function of elastase in *Pseudomonas aeruginosa*: role in the cleavage of nucleoside diphosphate kinase and in alginate synthesis. *Mol Microbiol*. 1998 Dec;30(5):933–41.
107. Gi M, Jeong J, Lee K, Lee K-M, Toyofuku M, Yong DE, et al. A drug-repositioning screening identifies pentetic acid as a potential therapeutic agent for suppressing the elastase-mediated virulence of *Pseudomonas aeruginosa*. *Antimicrob Agents Chemother*. 2014 Dec;58(12):7205–14.
108. Cigana C, Castandet J, Sprynski N, Melessike M, Beyria L, Ranucci S, et al. *Pseudomonas aeruginosa* Elastase Contributes to the Establishment of Chronic Lung Colonization and Modulates the Immune Response in a Murine Model. *Front Microbiol*. 2020;11:620819.
109. Bianconi I, Jeukens J, Freschi L, Alcalá-Franco B, Facchini M, Boyle B, et al. Comparative genomics and biological characterization of sequential *Pseudomonas aeruginosa* isolates from persistent airways infection. *BMC Genomics*. 2015 Dec 29;16:1105.
110. Kam CM, Nishino N, Powers JC. Inhibition of thermolysin and carboxypeptidase A by phosphoramidates. *Biochemistry*. 1979 Jul 10;18(14):3032–8.
111. Kessler E, Israel M, Landshman N, Chechick A, Blumberg S. In vitro inhibition of *Pseudomonas aeruginosa* elastase by metal-chelating peptide derivatives. *Infect Immun*. 1982 Nov;38(2):716–23.
112. Cathcart GR, Gilmore BF, Greer B, Harriott P, Walker B. Inhibitor profiling of the *Pseudomonas aeruginosa* virulence factor *LasB* using N-alpha mercaptoamide template-based inhibitors. *Bioorg Med Chem Lett*. 2009 Nov 1;19(21):6230–2.
113. Cathcart GRA, Quinn D, Greer B, Harriott P, Lynas JF, Gilmore BF, et al. Novel inhibitors of the *Pseudomonas aeruginosa* virulence factor *LasB*: a potential therapeutic approach for the attenuation

of virulence mechanisms in pseudomonal infection. *Antimicrob Agents Chemother.* 2011 Jun;55(6):2670–8.

114. Kany AM, Sikandar A, Haupenthal J, Yahiaoui S, Maurer CK, Proschak E, et al. Binding Mode Characterization and Early in Vivo Evaluation of Fragment-Like Thiols as Inhibitors of the Virulence Factor LasB from *Pseudomonas aeruginosa*. *ACS Infect Dis.* 2018 Jun 8;4(6):988–97.
115. Konstantinović J, Yahiaoui S, Alhayek A, Haupenthal J, Schönauer E, Andreas A, et al. N-Aryl-3-mercaptosuccinimides as Antivirulence Agents Targeting *Pseudomonas aeruginosa* Elastase and *Clostridium* Collagenases. *J Med Chem.* 2020 Aug 13;63(15):8359–68.
116. Hydroxamic acid based collagenase inhibitors.
117. Kany AM, Sikandar A, Yahiaoui S, Haupenthal J, Walter I, Empting M, et al. Tackling *Pseudomonas aeruginosa* Virulence by a Hydroxamic Acid-Based LasB Inhibitor. *ACS Chem Biol.* 2018 Sep 21;13(9):2449–55.
118. Leiris S, Davies DT, Sprynski N, Castandet J, Beyria L, Bodnarchuk MS, et al. Virtual Screening Approach to Identifying a Novel and Tractable Series of *Pseudomonas aeruginosa* Elastase Inhibitors. *ACS Med Chem Lett.* 2021 Feb 11;12(2):217–27.
119. Garner AL, Struss AK, Fullagar JL, Agrawal A, Moreno AY, Cohen SM, et al. 3-Hydroxy-1-alkyl-2-methylpyridine-4(1H)-thiones: Inhibition of the *Pseudomonas aeruginosa* Virulence Factor LasB. *ACS Med Chem Lett.* 2012 Aug 9;3(8):668–72.
120. Fullagar JL, Garner AL, Struss AK, Day JA, Martin DP, Yu J, et al. Antagonism of a zinc metalloprotease using a unique metal-chelating scaffold: tropolones as inhibitors of *P. aeruginosa* elastase. *Chem Commun Camb Engl.* 2013 Apr 21;49(31):3197–9.
121. Galdino ACM, Viganor L, de Castro AA, da Cunha EFF, Mello TP, Mattos LM, et al. Disarming *Pseudomonas aeruginosa* Virulence by the Inhibitory Action of 1,10-Phenanthroline-5,6-Dione-Based Compounds: Elastase B (LasB) as a Chemotherapeutic Target. *Front Microbiol.* 2019;10:1701.
122. Inhibitors of *Pseudomonas aeruginosa* virulence factor LasB. EP20192608.6.
123. Nishino N, Powers JC. *Pseudomonas aeruginosa* elastase. Development of a new substrate, inhibitors, and an affinity ligand. *J Biol Chem.* 1980 Apr 25;255(8):3482–6.
124. Buysse K, Farard J, Nikolaou A, Vanderheyden P, Vauquelin G, Pedersen DS, et al. Amino triazolo diazepines (Ata) as constrained histidine mimics. *Org Lett.* 2011 Dec 16;13(24):6468–71.
125. Winum J-Y, Scozzafava A, Montero J-L, Supuran CT. New zinc binding motifs in the design of selective carbonic anhydrase inhibitors. *Mini Rev Med Chem.* 2006 Aug;6(8):921–36.
126. Worrell BT, Malik JA, Fokin VV. Direct evidence of a dinuclear copper intermediate in Cu(I)-catalyzed azide-alkyne cycloadditions. *Science.* 2013 Apr 26;340(6131):457–60.
127. Boren BC, Narayan S, Rasmussen LK, Zhang L, Zhao H, Lin Z, et al. Ruthenium-catalyzed azide-alkyne cycloaddition: scope and mechanism. *J Am Chem Soc.* 2008 Jul 16;130(28):8923–30.
128. Kim WG, Kang ME, Lee JB, Jeon MH, Lee S, Lee J, et al. Nickel-Catalyzed Azide-Alkyne Cycloaddition To Access 1,5-Disubstituted 1,2,3-Triazoles in Air and Water. *J Am Chem Soc.* 2017 Sep 6;139(35):12121–4.

129. Maiuolo L, Russo B, Algieri V, Nardi M, Di Gioia ML, Tallarida MA, et al. Regioselective synthesis of 1,5-disubstituted 1,2,3-triazoles by 1,3-dipolar cycloaddition: Role of Er(OTf)₃, ionic liquid and water. *Tetrahedron Lett.* 2019 Feb 28;60(9):672–4.
130. Cheng G, Zeng X, Shen J, Wang X, Cui X. A metal-free multicomponent cascade reaction for the regioselective synthesis of 1,5-disubstituted 1,2,3-triazoles. *Angew Chem Int Ed Engl.* 2013 Dec 9;52(50):13265–8.
131. Bräse S, Gil C, Knepper K, Zimmermann V. Organic azides: an exploding diversity of a unique class of compounds. *Angew Chem Int Ed Engl.* 2005 Aug 19;44(33):5188–240.
132. Johansson JR, Lincoln P, Nordén B, Kann N. Sequential one-pot ruthenium-catalyzed azide-alkyne cycloaddition from primary alkyl halides and sodium azide. *J Org Chem.* 2011 Apr 1;76(7):2355–9.
133. Dey S, Pathak T. A general route to 1,5-disubstituted 1,2,3-triazoles with alkyl/alkyl, alkyl/aryl, aryl/aryl combinations: a metal-free, regioselective, one-pot three component approach. *RSC Adv.* 2014 Jan 28;4(18):9275–8.
134. Bai H-W, Cai Z-J, Wang S-Y, Ji S-J. Aerobic Oxidative Cycloaddition of α -Chlorotosylhydrazones with Arylamines: General Chemoselective Construction of 1,4-Disubstituted and 1,5-Disubstituted 1,2,3-Triazoles under Metal-Free and Azide-Free Conditions. *Org Lett.* 2015 Jun 19;17(12):2898–901.
135. Wan J-P, Cao S, Liu Y. A Metal- and Azide-Free Multicomponent Assembly toward Regioselective Construction of 1,5-Disubstituted 1,2,3-Triazoles. *J Org Chem.* 2015 Sep 18;80(18):9028–33.
136. Huang W, Zhu C, Li M, Yu Y, Wu W, Tu Z, et al. TBAI or KI-Promoted Oxidative Coupling of Enamines and N-Tosylhydrazine: An Unconventional Method toward 1,5- and 1,4,5-Substituted 1,2,3-Triazoles. *Adv Synth Catal.* 2018;360(16):3117–23.
137. Cao S, Liu Y, Hu C, Wen C, Wan J-P. Alkyl Propiolates Participated [3+2] Annulation for the Switchable Synthesis of 1,5- and 1,4-Disubstituted 1,2,3-Triazoles Containing Ester Side Chain. *ChemCatChem.* 2018;10(21):5007–11.
138. Camberlein V, Kraupner N, Bou Karroum N, Lipka E, Deprez-Poulain R, Deprez B, et al. Multi-component reaction for the preparation of 1,5-disubstituted 1,2,3-triazoles by in-situ generation of azides and nickel-catalyzed azide-alkyne cycloaddition. *Tetrahedron Lett.* 2021 Jun 8;73:153131.
139. Gutekunst WR, Hawker CJ. A General Approach to Sequence-Controlled Polymers Using Macrocyclic Ring Opening Metathesis Polymerization. *J Am Chem Soc.* 2015 Jul 1;137(25):8038–41.
140. Gangaprasad D, Paul Raj J, Kiranmye T, Sasikala R, Karthikeyan K, Kutti Rani S, et al. A tunable route to oxidative and eliminative [3+2] cycloadditions of organic azides with nitroolefins: CuO nanoparticles catalyzed synthesis of 1,2,3-triazoles under solvent-free condition. *Tetrahedron Lett.* 2016 Jul 20;57(29):3105–8.
141. Wang D, Salmon L, Ruiz J, Astruc D. A recyclable ruthenium(II) complex supported on magnetic nanoparticles: a regioselective catalyst for alkyne-azide cycloaddition. *Chem Commun Camb Engl.* 2013 Aug 11;49(62):6956–8.

142. Mpakali A, Giastas P, Deprez-Poulain R, Papakyriakou A, Koumantou D, Gealageas R, et al. Crystal Structures of ERAP2 Complexed with Inhibitors Reveal Pharmacophore Requirements for Optimizing Inhibitor Potency. *ACS Med Chem Lett.* 2017 Mar 9;8(3):333–7.
143. Kokkala P, Mpakali A, Mauvais F-X, Papakyriakou A, Daskalaki I, Petropoulou I, et al. Optimization and Structure-Activity Relationships of Phosphinic Pseudotriptide Inhibitors of Aminopeptidases That Generate Antigenic Peptides. *J Med Chem.* 2016 Oct 13;59(19):9107–23.
144. Elgaher WAM, Fruth M, Groh M, Haupenthal J, Hartmann RW. Expanding the scaffold for bacterial RNA polymerase inhibitors: design, synthesis and structure–activity relationships of ureido-heterocyclic-carboxylic acids. *RSC Adv.* 2013 Dec 3;4(5):2177–94.
145. Schönauer E, Kany AM, Haupenthal J, Hüsecken K, Hoppe IJ, Voos K, et al. Discovery of a Potent Inhibitor Class with High Selectivity toward Clostridial Collagenases. *J Am Chem Soc.* 2017 Sep 13;139(36):12696–703.